The engineering behaviour of the tropical clay soils of Dhaka, Bangladesh

A T M. Shakhawat Hossain

THE ENGINEERING BEHAVIOUR OF THE TROPICAL CLAY SOILS OF DHAKA, BANGLADESH

A thesis submitted to the School of Engineering, University of Durham

for the degree of Doctor of Philosophy

by

A.T.M. Shakhawat Hossain

July, 2001

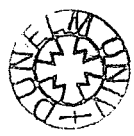

STATEMENT OF COPYRIGHT

DECLARATION

I hereby declare that no part of the work reported in this thesis has previously been submitted by me for any degree in this university or any other university.

CONTENTS

ABSTRACT

This research has evaluated the engineering behaviour of the tropical clay soils of Dhaka, Bangladesh. Attempts have been made to show the relationship of mineralogy and fabric with engineering properties. The engineering behaviour has been investigated by comparing the soil properties in a natural and destructured state at the same void ratio. Consolidation behaviour of the soils are discussed, based on oedometer and triaxial tests. Undrained and drained mechanical behaviour have been evaluated from triaxial tests in terms of stress-strain curves, stress paths, bonding effects, critical state conditions, stiffness and yielding behaviour. A framework for the tropical clay soils of Dhaka is presented.

The tropical clay soils of Dhaka are intermediate to high plasticity inorganic clay. These soils are mainly composed of illite,. kaolinite, chlorite and some non clay minerals mainly quartz and feldspar. It was observed that these soils showed a random open microfabric of silt and clay. There was also some evidence that aluminosilicates, iron compounds and silica formed bonds between and within the grains.

An apparent preconsolidation pressure of 170 kPa to 250 kPa was estimated for the natural soils, which is likely to be due to the bonded structure of the soils. The compressibility of the soil is very low to medium. The consolidation results are consistent with the mineralogy of the soils.

It is established that the tropical clay soils of Dhaka are bonded. Bonding has an influence on the development of stress-strain and stiffness of these soils.. Under undrained shearing, samples initially showed peak positive values of excess pore water pressure followed by negative values at higher strains due to the tendency of the samples to dilate. No negative pore water pressures were observed at high

confining pressures. Only a few samples at low confining pressures reach the critical state at very large strains approximately in excess of 20%. High confining pressure samples may not have reached the critical state due to the formation of distinct shear surfaces.

A significant difference between the natural and destructured failure surfaces was observed due to the presence of bonds in the natural soils. Differences in failure type were observed between the natural and destructured soils of three boreholes. It was observed that stiffness values gradually decreased with increasing strain. For the natural soils, two yield points could be identified at low confining pressures below the final yield. It was also observed that bond breakdown would occur in isotropic compression for tests at high confining pressures. At the final yield, the soil looses almost all of its stiffness due to bonding. After final yield, a soil's behaviour is controlled only by friction. It was observed that three zones of behaviour could be identified for these soils in the stress space.

ACKNOWLEDGEMENTS

This research work has been carried out in the Geotechnical Engineering division of the School of Engineering, University of Durham. I would like to express my heartiest gratitude and thanks to my supervisors Dr. D.G. Toll and Dr. A.R. Selby for their supervision to carry out this research work. Their friendly manner, encouragement, guidance and helpful suggestions throughout the work inspired me in many ways and made it possible for me to complete the work. The efforts of my supervisors are gratefully acknowledged.

Financial assistance to carry out this research work provided by the Commonwealth Scholarship Commission is gratefully acknowledged.

The author would like to thank all teaching members of the Department of Geological Sciences, Jahangirnagar University, Savar, Dhaka, Bangladesh and Department of Geology, University of Dhaka, Bangladesh for their cooperation during field work and sample collection in Bangladesh.

Assistance provided by Dr. Bryn Jones, X-ray diffraction laboratory, University of Newcastle for access to their X-ray diffraction unit is duly acknowledged. I would also like to express my thanks to Mr. Andrew Yates of the Scanning Electron Microscope unit, School of Engineering, University of Durham for his suggestions on Scanning Electron Microscope.

My appreciation goes to Bernard MacEleavey and Steve Richardson of the Geotechnical Engineering laboratories for their continuous support during laboratory work. I am thankful to them. Thanks are also due to Michael for some computational support during data acquisition.

My thanks are also due to all my friends and especially to John Martin, Illias, Eva and Kanan for their support in many occasions.

I am very much grateful to my parents for their constant encouragement and support over the years. I must express my appreciation to my wife Sabrina, who not only tolerated many late nights and working weekends, but also encouraged me continuously in various ways to complete this work successfully. Thanks to my daughter Oloka Shushupti for adjusting herself with the situation when I was terribly busy with my thesis writing.

NOTATION

e	void ratio
c_v	coefficient of consolidation
m_v	coefficient of volume compressibility
C_c	compression index
p'_c	apparent preconsolidation pressure
λ	slope of the normal consolidation line (negative)
k	coefficient of permeability
ε_a	axial strain
ε_s	shear strain
ε_v	volumetric strain
c'	effective cohesion
q	deviatoric stress ($\sigma_1' - \sigma_3'$)
σ_1'	effective major principal stress
σ_3'	effective minor principal stress
p'	mean effective stress $(\sigma_1' + 2\sigma_3')/3$
Γ	specific volume of the soil at critical state with $p' = 1$ kPa.
M	critical state stress ratio
G_{tan}	tangential shear modulus
v	specific volume (1+e)

LIST OF FIGURES

CHAPTER 1

INTRODUCTION

1.1 General

Dhaka is the capital of Bangladesh, which is expanding rapidly. Rapid urbanization in the city area has led to an increased interest in the engineering behaviour of the soils which are present within the city area. Geotechnical information of the subsoil in an urban area is important for various civil engineering works. Lack of sophisticated laboratory facilities and non-availability of the proper geotechnical information of the subsoil makes foundation and engineering works expensive, difficult and sometimes hazardous.

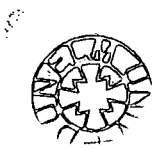

The soils within the city area are formed under a warm to hot and humid to subtropical climatic conditions and derived from a residual soil horizon. In addition, these red clay soils are of different nature from the other sedimentary soils of Bangladesh. The red colours indicate the presence of iron oxide common in well-oxidized soil. Therefore the present research was performed with a view to evaluate the mineralogy, fabric, mechanical behaviour of the tropical clay soils of Dhaka to establish the stress strain characteristics at small and large strains, stiffness and yielding behaviour and finally to establish a framework of behaviour based on stress history and bonding (physical linkage between particles) for these soils.

1.2 Objectives

The main aim of this research work was to attain the following objectives for the tropical clay soils of Dhaka, Bangladesh.

i. To evaluate the mineralogy of the soil.
ii. To study the fabric of the soil.
iii. To identify and evaluate the basic geotechnical parameters.
iv. To show the relationship of basic geotechnical parameters with mineralogy.
v. To evaluate the consolidation characteristics viz. the coefficient of volume compressibility, the coefficient of consolidation and compression index.
vi. To identify the stress-strain characteristics of the soil.
vii. To derive stress paths for these soils.
viii. To understand yield behaviour of the tropical clay soil of Dhaka.
ix. To evaluate the small strain behaviour of the soil.
x. To measure the stiffness of the soil and to see the changes in stiffness with increasing strain.
xi. To compare the results of natural and destructured soils to understand bonding effects of the soils.

xii. To observe the critical state behaviour at large strains and

xiii. Finally to establish a framework of behaviour for the tropical clay soils of Dhaka based on stress history and bonding.

To achieve the above objectives an extensive experimental laboratory testing programme was carried out on undisturbed natural and destructured samples of the tropical clay soils of Dhaka. Basic geotechnical parameters were determined in accordance with standard test procedures. A series of undrained and drained triaxial tests was also carried out on natural and destructured samples using a range of effective confining pressures. In addition, X-Ray Diffraction (XRD) and Scanning Electron Micrograph (SEM) were also done on some samples to evaluate the mineralogy and fabric of the soil.

1.3 Thesis Layout

The thesis is arranged in nine chapters. Chapter 1 describes the background and objectives of the thesis. Apart from this introduction chapter a brief review of previous literature relating to the general aspects of tropical soils has been made in Chapter 2. In Chapter 2 some previous research on the engineering behaviour of natural and artificial soils are also discussed in terms of strength, stiffness and yielding.

In Chapter 3, geology, the site locations, borehole descriptions, a brief description of undisturbed sample collection and preparation of natural and destructured samples are discussed.

Chapter 4 describes the experimental methods of testing to carry out all the laboratory tests. The basic principle of the computer control system used in the testing is discussed.

The results of the testing programme carried out on samples collected from three boreholes are presented in Chapters 5,6,7 and 8. Mineralogy, fabric and other basic geotechnical parameters of the soils are discussed in chapter 5. The relationship between mineralogy and some basic geotechnical parameters are also discussed in this chapter.

Chapter 6 mainly deals with the triaxial consolidation results. The volume change during consolidation and the measured values of coefficient of volume compressibilty, the coefficient of consolidation and the compression index are discussed. Some oedometer test results are also presented in this chapter.

Results of undrained triaxial tests are discussed in Chapter 7. Results on samples taken from two boreholes at different sites are discussed in terms of stress strain curves, stress paths, stress ratios and excess pore water pressures with increasing strains. Stiffness and yielding characteristics are also discussed in Chapter 7. Small strain characteristics are evaluated. Critical state conditions are discussed. Undrained triaxial test results of natural and destructured soils are also compared and evaluated in Chapter 7. Comparisons between the results of samples from two boreholes are also presented in this chapter. Finally a framework for the tropical clay soils of Dhaka, Bangladesh is discussed.

Chapter 8 presents the results of drained triaxial tests on both natural and destructured samples taken from a third borehole from the same geologic formation.

Drained stress strain behaviour of the soils is discussed in terms of stress strain curves, stress paths and volumetric strains. Small strain drained test results are also presented. A comparison has been made in Chapter 8 between the drained test results of natural and destructured soils. Zones of behaviour under drained shearing are also discussed.

Graphical results are grouped at the end of each chapter. The thesis ends with Chapter 9, which contains the main conclusions of the research work carried out. Some future recommendations are also made in Chapter 9.

CHAPTER 2

LITERATURE REVIEW

2.1. Introduction

A literature review was undertaken on the engineering characteristics of tropical soils from different parts of the world. Bonding in tropical soils plays an important role in the stress-strain development, strength, stiffness and yielding characteristics of these natural soils. Therefore a review was also done for the stress-strain, strength, stiffness and yielding characteristics of natural and artificially bonded soils. Previous work carried out both on natural and destructured samples to interpret the mechanical behaviour of the bonded soils are discussed in this chapter. Mineralogy and fabric of some of the natural soils and their relationship with engineering properties are also discussed.

2.2. General aspects of tropical soils

In this section a brief review of the general aspects including the classification, basic geotechnical properties, mineralogy and fabric of tropical soils from different parts of the world are discussed. There is a huge literature on tropical soils, which has been variously defined. However, from an engineering point of view, there is a little confusion in defining tropical soils, their formations and properties. Much has been written on various tropical residual soils, in pedological, geological, geomorphological and engineering literature (Fookes, 1997).

Blight (1988) pointed out that generally the soils which are formed in the tropics under a warm to hot and humid to subtropical climate and derived from a residual soil horizon are considered as tropical soils. He discussed the origin and formation of tropical and residual soils. Tropical soils are formed by in situ weathering of rocks, the three major agencies of weathering being physical, chemical and biological processes. In the weathering process the parent rock and rock minerals break down, releasing internal energy and forming substances having a lower internal energy which are therefore more stable. He also mentioned chemical processes; chiefly hydrolysis, cation exchange and oxidation alter the original rock minerals to more stable clay minerals. Residual soils form from igneous, sedimentary or metamorphic parent rocks. Chemical processes tend to predominate in the weathering of igneous rocks whereas physical processes dominate the weathering of sedimentary and metamorphic rocks. He also pointed out that presence of iron oxide in these soils has an influence on the specific gravity and void ratio results.

Smith (1985) pointed out that meaningful research into the engineering properties of natural lateritic soils should be multidisciplinary and include geotechnical engineering, mineralogy, geology and fabric of the soils. He also suggested some

modus operandi for research into natural lateritic soils. Some of these viz. site investigation, drilling and sampling, classification tests, oedometer and triaxial tests are common in any engineering investigation. In addition, he emphasized the importance of studying mineralogy and fabric of the residual soils, which have an influence on the engineering properties.

Fookes (1997) noted that in tropical regions weathering of primary minerals is more intense and occurs at greater depths. The alteration of minerals is often so intense that the soil materials behave, in an engineering sense, quite differently from the parent materials from which they were derived. He also noted that iron oxide is crystallized as haematite when the soil is seasonally desiccated, or as goethite in a constantly humid environment; haematite giving the soil a red colour, goethite a brown or ochreous colour. Gibbsite is the main aluminium oxide formed. He also noted that silica is lost in solution or combines with other weathering products to form silicate clay minerals (mainly smectite) or silica deficient clay minerals (mainly kaolinite). Bases (K, Na, Ca, and Mg) are either lost in solution or are incorporated into silicate clay minerals. Kaolinite accommodates little or no bases. Fookes (1997) mentioned that the engineering behaviour of the tropical residual soils cannot be so easily predicted because:

i. The weathering products that result under certain tropical conditions may contain minerals with unusual properties.

ii. Weathering of a material in situ implies the presence of a relict structure, which may persist as a form of weak bonding even in the most extremely weathered products. Such a bonding can influence metastable behaviour.

Fookes (1997) noted that tropical soils differ from transported soils, which are principally derived from coastal, alluvial, wind blown or glacial processes. He pointed out that these soils have particular characteristics, which distinguish them

from material deposited from a fluid medium such as wind or water. He proposed a formal classification of residual soils. The major subdivisions of the formal classification of residual soils are listed in Table 1.

Table 1: Major subdivisions of formal classification of residual soils (Fookes, 1997)

RESIDUAL SOILS	
A. DURICRUSTS	B. MATURE SOILS
Silcrete	Vertisols
Calcrete	Fersiallitic (andosols)
Gypcrete	Fersiallitic (senso stricto)
Ferricrete	Ferruginous (senso stricto)
Alcrete (alucrete)	Ferrallitic

Fookes (1997) mentioned the following characteristics of insitu residual soils to show the influence of these characteristics on the engineering behaviour.

i. Mineralogy.
ii. Variable structure and the presence of bonding between particles.
iii. Variable void ratio unconnected with stress history.
iv. Permeability often unrelated to particle size and grading.
v. Discontinuities of low strength.
vi. Partial saturation, which frequently occurs to considerable depth in these soils.

Fookes (1997) discussed the problems of measuring index properties of tropical residual soils. He noted that even partial drying at moderate temperatures might change the structure and physical behaviour of tropical residual soils. Oven-drying from 105^0 to 110^0C frequently has a substantial effect on soil properties but drying at a lower temperature (e.g. 50^0C), and even partial air-drying at ambient laboratory temperature can also produce significant changes. He also discussed that as a general rule it should be assumed that all tropical residual soils would be affected in some way by drying. Classification tests should therefore be applied to natural soil with as little drying as possible, at least until it can be established from comparative tests that drying has no significant effect on the test results. The method of preparation should always be reported.

Wesley (1973) discussed some basic engineering properties of halloysite and allophane clays of Java, Indonesia. He noted that engineering properties of these soils are more closely related to mineralogical composition than to pedological grouping. He points out that air or oven drying of the halloysite samples produces a small, although quite significant, changes in properties, but air or oven drying of the allophane samples completely alters the nature of the materials.

Sridharan (1988) mentioned that residual soil from insitu weathering of parent rock in a tropical climate could be defined as tropical soil. He discussed the importance of structure and microfabric of fine grained tropical soils. He concluded that microfabric and associated interparticle forces could play an important role in controlling the strength and volume change behaviour of fine grained tropical soils. The macrofabric features such as stratification, fissuring, voids and large scale inhomogenities can also play an important role in affecting the shearing resistance and volume change behaviour of the fine grained tropical soils (Sridharan, 1988).

Duchaufour (1982) distinguished three phases of residual soil development in tropical areas, which is summarised in Table 2. They are characterized by increasing weathering of primary minerals, increasing loss of silica and increasing dominance of new clay minerals formed from dissolved materials.

Table 2: Different residual soil phases in relation to climatic factors (Duchaufour (1982)

Phase	Soil type	Zone	Mean annual temp. (^{0}C)	Annual rainfall (m)	Dry season
1	fersiallitic	Mediterranean, subtropical	13-20	0.5-1.0	yes
2	ferruginous ferrisols (transitional)	subtropical	20-25	1.0-1.5	some-times
3	ferrallitic	tropical	>25	>1.5	no

Wesley (1988) mentioned three bases for classification of residual soils, which are at present in use for grouping residual soils. These are listed below.

1. Methods based on the weathering profile
2. Methods based on pedological groups
3. Method intended for local use on specific soil type only.

On the basis of degree of weathering he mentioned six categories of soil type. These are fresh rock, slightly weathered, moderately weathered, highly weathered, and completely weathered and soil. Based on pedology, Wesley (1988) classified tropical soil groups as Lateritic soils, Latsols and Red clay in the first group, Volcanic ash soils and Andosols in the second group and Black cotton soils, Black clays, Tropical black earths and Grumusols in the third group. He also noted that halloysite and kaolinite are the dominant clay minerals of Lateritic soils, Latsols and Red clay. Allophane and minor halloysite are common in Volcanic ash soils and Andosols. Smectite is common in black cotton soils, black clays and Grumusols.

Based on the influences of composition and structure on soils, Wesley (1988) grouped residual soils as Group A, Group B and Group C for local use. In Group A soils are without a strong mineralogical influence but these are soils in which macro

or micro structure plays important role on the engineering behaviour of the soil. The most important form of microstructure is the inter-particle bonding or cementation. Group B type of residual soils is strongly influenced by conventional clay minerals such as are common in sedimentary soils. Group C type of residual soils are strongly influenced by the presence of clay minerals which are not found in sedimentary clays viz. Halloysite and Allophane. In addition to these silicate minerals, tropical soils may contain non-silicate minerals (or 'oxide' minerals), in particular the hydrated forms of aluminium and iron oxide (the sesquioxides), gibbsite and goethite. The main role of sesquioxides appears to be to act as cementing agents, which bind the other mineral constituents into clusters or aggregations.

Wesley (1988) also-mentioned that with residual soils the position which a soil occupies on the conventional plasticity chart provides a good indication of soil properties, possibly just as good as for sedimentary soils. He reported that soils which plot well below A-line behave as silts while those which plot well above the A-line behave as clays (Figure 1). He emphasized the position above or below the A-line, which is of most significance, especially with tropical residual soils. The lines drawn parallel to A-line (Figure 1) divide soils into three labelled clay, silty clay and silt and would be more relevant to residual soils. He also mentioned many residual soils behave as silty clays for engineering purposes, and rightly fall into the category of silty clay on this chart.

Fookes (1997) and Cook & Newill (1988) mentioned a framework for the field description, examination, identification of soils. This framework links soil material characteristics of the soil profile to the soil mass characteristics. The main elements of describing this framework are listed in Table 3.

Table 3: Main elements for field description, examination and identification of tropical residual soils (after Newill and Cook, 1988 and Fookes, 1997)

Site characteristics	Soil material characteristics	Soil mass characteristics
Location Landform Geology Current climate Hydrology Vegetation	Moisture Colour Strength Fabric Texture Density and relative density Apparent behaviour Mineralogy Classification	Composition Geological structure Behaviour Nomenclature

Vargas (1988) pointed out that soil identification and classification must be done on the basis of index properties only. The purpose of a classification system is only to group a sample of soil in a class with common index properties. He also pointed out that preparation of tropical soil samples, for identification tests must be done with appropriate methods in order to completely destroy any aggregation of their grains or any structure imposed on their fabric by any eventual state that occurred to the soil.

Newill (1961) studied the basic engineering properties of two red clays from Kenya. He mentioned that kaolinite clays (which include halloysites) are commonly associated in the tropics with high iron oxide contents. He observed an increase in liquid and plastic limit values by removing free iron from the red clay soils and noted that the presence of halloysite influences the engineering properties of red clay soils. He suggested that oven drying causes the clay particles to aggregate into clusters that could partially be broken down by the dispersion process.

Rao et al. (1988) pointed out that iron oxide has a significant influence on the index and compressibility characteristics of kaolinite rich red tropical soils. They observed a decrease in liquid and plastic limits of the kaolinite rich red soils, despite an increase in fines content on iron oxide removal. In comparison, iron oxide removal from the montmorillonitic soil leads to an increase in liquid and plastic limits of the soil specimen. They mentioned that iron oxide present in the kaolinitic soil binds individual soil particles into coarser aggregates and contributes to the development of a random soil structure. The flocculated structure in turn exerts an important influence on the liquid limit and compressibility behaviour of the kaolinitic soil.

Sabba Rao et al. (1988) discussed the influence of climate specially the effect of humidity and temperature on the index properties of tropical soils. They concluded that the liquid limit of Na, Ca-montmorillonite is significantly affected by humidity changes owing to changes in the adsorbed water layers. The liquid limits of black cotton soil and kaolinite are unaffected by humidity changes. The plastic limit is unaffected by humidity and temperature. The shrinkage limit of black cotton soil increases with humidity (Sabba Rao et al., 1988).

Tropical residual soils are formed by quite different processes from other sedimentary soils. Weathering has a strong influence on the formation of tropical residual soils. Vaughan and Kwan (1984) pointed out that the initial structure and porosity are the important parameters for residual soil characteristics. The initial structure and porosity are a product of the weathering process rather than insitu stress history. They emphasised that the structure is modified from that of the parent rock by chemical alteration and the leaching or precipitation of soluble material.

Vaughan (1988) and Vaughan et al. (1988) mentioned that there are clear differences between the factors influencing transported and residual soils. In transported soils

the particles are 'pre-formed', delivered by some transporting agency and deposited in a certain way. Residual soils are developed in place without transportation. The particles and their arrangement evolve progressively as a consequence of chemical weathering, with widely varying mineralogy and void ratio. Most residual soils are weakly bonded and the bonding may be broken by loading and strain. Once broken, it is irrecoverable. They also pointed out that some factors (namely the particles, mineralogy and stress history) control the engineering behaviour of residual soils. They mentioned that mineralogy of a residual soil is partly inherited from the parent rock and partly generated by weathering.

Smectites are often present in vertisols. They are active clay minerals and their presence in quantity can cause large volume changes in response to small changes in effective stress. Kaolinites occur in many residual soils particularly in fersiallitic, ferruginous and ferralitic profiles. A soil containing kaolinite has higher strength and a lower compressibility than a soil of the same clay fraction containing smectite. Vaughan (1988) also mentioned that typically a soil with less than 15% clay content behaves much like a granular material. A soil with more than 40% clay content has properties dominated by the presence of the clay. In such a soil the platy clay minerals can orientate and a continuous shear surface can form. Clay minerals present are sometimes coated with other minerals, which change their behaviour.

2.3 Research on bonded soils

2.3.1 General on bonded soils

A review of the previous work shows that bonding or cementation is common in a large range of materials viz. soft and stiff clays, sands, residual soils and weak rocks. Bonding in natural soils plays an important role in the stress-strain development, strength, stiffness and yielding characteristics of natural soils. All these materials show similarities in their mechanical behaviour. A review on the mechanical

behaviour of naturally and artificially bonded soils are discussed in the following sections. Stress-strain, strength, stiffness and yielding characteristics of some natural soils from different parts of the world are also reviewed.

Vaughan (1985) noted that bonding and porosity entirely control the properties of residual soils. He explained the necessity for developing a general framework for describing and clarifying the engineering properties of residual soils. He concluded that the framework for a weakly bonded, particulate material, in which the yielding of the bonds is represented by a yield locus in stress space, is a potentially relevant and helpful one for a wide range of residual soils. Vaughan et al. (1988) confirmed that yield of the bonded structure can be mapped as a yield surface in deviatoric stress/ mean effective stress/void ratio space in a manner similar to the yield of sedimentary clays. In the classical soil mechanics of sedimentary clays, porosity is a function of stress history, and bonding is ignored.

Vaughan (1985) also suggested that the behaviour of soils with bonded structure can be best understood through comparing their properties with those of the same soils in a remoulded and destructured state. Bonded structure, as used by Vaughan (1988) indicated a component of strength and stiffness and which behaved as if it was due to physical connections between particles. He noted that the bonded structure is destroyed by remoulding and destructuring even if the porosity of the soil is unaltered.

Vaughan (1985, 1988) mentioned the effects of bonded structure in residual soils. He pointed out that residual soils typically exhibit a yield stress. This yield stress (the apparent pre-consolidation pressure) is related to structure and bonding and not to stress history. A bonded soil exhibits a peak shear strength envelope in terms of effective stress, which has a cohesion intercept, c'. This is due to bonded structure rather than dilation (although the latter may also be present) and is thus unrelated to

density. In bonded soils this component of strength is destroyed by yield. He also mentioned that if the cohesion intercept were due to overconsolidation and dilation during shear it would not exist at a normal stress in excess of the yield stress.

Many soils have been subject to bonding agencies during their geological history; such as deposition of carbonate and iron salts which physically bond particles together. Vaughan (1988) and Leroueil and Vaughan (1990) described possible causes of bonding, which are listed below:

i. Cementation through the deposition of carbonates, hydroxides, organic matter, etc.
ii. Deposition of silica at particle contacts after dissolution from sand particles.
iii. Cold welding at interparticle contacts in soils subjected to high pressure.
iv. Growth of bonds during the chemical alteration of minerals accompanying weathering.

Leroueil and Vaughan (1990) also discussed the role of structure in many naturally structured soils (including soft clays, stiff over-consolidated clays, clay-shales, sand, weak and porous rock and residual soil). They noted that a soil from which the structure has been removed or destroyed by straining and remoulding would be referred to as destructured. They also noted that the interparticle bonding plays an important role in the case of weakly bonded natural soils. The weakly bonded soils have components of tensile and shear strength and stiffness which will have a strong influence on the engineering behaviour. The strength and stiffness behaviour of a weakly bonded soil can be explained by means of yield stress. They also noted that structuring has similar effects in all these materials. Stiff behaviour, followed by yield above certain stress levels, is mainly observed in each case. They also noted that structuring increases strength and enlarges the stress domain in which the soil shows stiff behaviour.

2.3.2 Stress-strain, strength, stiffness and yielding in bonded soils

Vargas (1953) discussed the influence of structure in residual soils. He pointed out that bonding within the soil structure gives the well known 'quasi-preconsolidation pressure''. He observed from Oedometer tests the presence of additional strength in natural samples, when compared to remoulded samples, and defined this as ''apparent or virtual-preconsolidation pressure''. Wesley (1974) also presented one-dimensional compression test results on undisturbed and remoulded residual soils from Java. He observed that undisturbed soil is initially stiffer than the remoulded one and it can show much larger strength than the remoulded soil at the same void ratios.

Sangrey (1972) discussed typical results of some naturally cemented clays of Canada. He mentioned that although the causes of cementation may vary, they all exhibit some common mechanical characteristics. He discussed the drained stress-strain curves of Labrador Clay (figure 2) and noted that at low confining pressure (test LA7) the cementation dominates and little frictional resistance is left once the bonding is destroyed by shear failure. At low stresses, these soils appear to be stronger than expected, with less strain being required prior to yield and they show brittle behaviour (test LA7). However, higher stresses (test LA8) enable sufficient frictional resistance to be built up after the cementation bonds are broken and the behaviour changes to ductile (test LA8 in figure 2).

Uriel and Serrano (1973) presented drained stress-strain behaviour of two porous volcanic soils of different bulk densities from Canary Island (Spain). They noted that these volcanic soils are strongly dependent on bonding and their conclusions were similar to those previously presented by Sangrey (1972). They noted that at low confining pressures the behaviour of the samples was brittle while at higher stresses it changed to ductile.

Jardine et al. (1984) discussed the undrained stress-strain, stiffness characteristics for London Clay, Ham River Sand and chalk. These soils owe their stiffness to bonding, density, strength and initial effective stresses in various degrees, and exhibit different post-yield behaviour pattern. The stress paths for Ham River Sand are marked by HRS1 and HRS2 and those of chalk are marked by C1 and C2 respectively (figure 3). The figure also shows the strain levels at appropriate intervals. They observed that sand samples show a stiff response to loading over the initial portions of each test but the samples rapidly lost stiffness as the stress paths approached the dilatant part of their state boundary surface. After yield the stress paths curved to the right and climbed the state boundary surface until, at large strains, peak strengths are developed. The samples did not reach an undrained critical state condition. The stress paths of the chalk tests C1 and C2 are presented in the same figure. They observed that these two tests show stiff behaviour up to brittle failure. The failure strains for tests C1 and C2 were both around 0.075%. The post-failure behaviour can be seen to be characterized by a progressive weakening with the effective stresses roughly following the unloading paths. The stress paths for London Clay marked by LC1 and LC2 are shown in figure 4. They observed stiff response of the stress paths up to axial strains of around 0.1%. They also observed that stress paths deviated to the right after attaining an axial strain of 1% until peak strengths were mobilized at strains of 4.5% and 3.5% respectively. They also reported that the samples had formed polished shear surfaces within the specimens. They observed that the stiffness curves are non-linear and showed a reduction of stiffness with increasing strain.

Burland (1989) discussed the stiffness of soils at small strains. He presented results of a typical unconsolidated undrained test on an undisturbed sample of London Clay. The measured effective stress path is shown in figure 5.a, with locally measured values of axial strain indicated. A comparison between the externally and locally measured stress-strain curves are shown in figure 5.b. It can be seen that the initial part of the externally measured stress-strain curve at very small strain is apparently linear but the local measurements show much stiffer non-linear behaviour. At axial

strains less than about 0.1% local measurements give much higher stiffness than those determined from traditional external measurements. Stiffness measured from internal measurements versus strain curve (in log scale) are shown in figure 5.c. The strongly non-linear nature of the sample response is evident in figure 5.c, with a decrease of stiffness value from 1700 kPa at 0.003% to about 150 kPa at 1.0% strain. He noted that this small strain region requires more study.

Vaughan (1985) pointed out that in order to study the effects of bonding on soil behaviour, artificially bonded samples should be used. He defined a yield stress as a stress state at which a material shows a discontinuity in stress-strain behaviour. He also suggested that yield is best identified from the stress-strain curve plotted to a natural or log-log scale. Vaughan (1985) also noted that in drained tests, samples continue to contract after a constant shear stress has been reached. At low confining stresses, yield and failure nearly coincide (figure 6). At higher confining stresses yield is much more gradual. The stress paths for saturated undrained tests on the bonded soil end on the critical state line CSL at virtually the same points as the paths for the same tests on unbonded soil tested at the same density. He also noted that the soil when loaded beyond the initial yield surface without failure, the current state of soil involves the combined influences of both the remaining bonding and plastic strains imposed by stress history.

Vaughan (1988) suggested the existence of two yields and identified that once the soil has exceeded its yield stress its bonding is progressively destroyed as large strains develop. He explained that post yield deformation depends on yield stress and initial porosity, rather than on the intrinsic compressibility of the 'destructured' soil. In figure 7, there is an initial stage [a] where no bonds break. This is followed by an initial yield and some bonds start to break progressively [stage (b)] with increasing yield. A much more dramatic second yield produces large subsequent strains [stage (c)]. At first yield some of the bonds starts to yield, and the total bond strength in the soil reduces. However, the bond strength is still greater than the

average stress carried by the bonds, and the soil remains stiff (figure 7). Therefore, before second yield a bonded soil will be stiff and deformation will be small. At second yield the increasing average bond stress becomes equal to the decreasing average bond strength and general bond failure and large strains follow. The bond strength is not completely destroyed immediately after second yield, but is destroyed progressively by increasing strain. Deformation will always be small unless the second yield stress is exceeded. If the bond strength is significant, second yield will not occur until the stress/void ratio path has moved to a point which is impossible for the destructured soil (Vaughan, 1988). He also mentioned that after yield, as the bonded structure is destroyed by increasing strain, the stress path translates towards that for the destructured soil (figure 8). He reviewed the results of many residual soils and concluded that the compression curve for the weak soil converges with that of the destructured soil. Convergence of the path for the strong soil might occur at much higher stresses. Vaughan (1988) pointed out that tangential stiffness versus strain might give a clearer indication of yield.

Vaughan et al. (1988) discussed the yield behaviour of different bonded residual soils and artificially bonded soils. They observed two consistent yield surfaces for both the natural and artificial soils. Two examples of the observed yield surfaces in volcanic agglomerate and in a residual soil from basalt are shown in figures 9 and 10 respectively. They observed a sharp yield in the line plot of strain versus stress from drained tests under isotropic stress. A more gradual yield from (a) to (b) (figure 9) was observed at high confining pressures. Yield was then followed by plastic behaviour and failure at a much higher shear stress (c). At lower confining stress, yield is abrupt and is very close to the failure surface (figure 9). It can be seen from these figures that the yield behaviour observed for these natural soils are similar to the yield behaviour observed in artificially bonded soils as shown in figure 11.

Vaughan et al. (1988) also noted that first yield may only involve a slight change in stiffness. It is often indistinct, and it can only be observed if precise measurements of strain are made. They also noted that second yield does not coincide with the complete destruction of bonds. This occurs at much larger strains. They also mentioned that at low effective confining pressures, first, second and final failure occur close together, with second yield and failure coinciding (figure 11).

Maccarini (1987) in his study of an artificially bonded soil (made up of quartz sand, a kaolin sand (cfk) and a small quantity of kaolin slurry) defined the first and second yield of the bonds, which are shown in figure 12. He defined first yield of the bonds at the end of the linear part of the curve of deviator stress versus axial strain plotted on natural scale (figure 12), the second yield at the maximum point of curvature of the same graph (figure 12). Bressani (1990) also used the same graph to interpret the first and second yield of the bonds plotted on a log-log scale to show the clearer change in behaviour.

Bressani and Vaughan (1989) carried out drained triaxial compression tests on artificial bonded soil (the same as Maccarini, 1987). The results are shown in figure 13. As can be seen in figure 13, yield at low mean stress occurs only slightly before peak deviator stress is reached (test 'n' of figure 13). At higher mean stress yield occurs well before failure (test 'o' of figure 13). Failure coincides with critical state and the complete destruction of bonding by large strains. They also concluded that the bond strength would decrease with increasing strain (figure 13) and the stress path can have a marked influence on the strength observed at low effective stresses in weakly bonded materials, even when the path does not approach yield prior to failure.

Leroueil and Vaughan (1990) pointed out that the yield curve could be divided into three zones, as shown in figure 14. These are:

i. Compression yield, where yield occurs remote from the eventual failure envelope.

ii. Shearing yield, where yield and shear failure more or less coincide at low confining stresses and

iii. Swelling yield, in which yield occurs remote from the failure envelope due to swelling. The swelling yield may not be present in some materials if their swelling is not large enough to break the bonds.

The complete yield curve represented in figure 14 may not be present in all soils and the orientation and shape of it may change.

Leroueil and Vaughan (1990) also discussed the stress strain curves obtained in undrained triaxial compression tests carried out on the intact and destructured natural clays after consolidation under the same overconsolidation ratio (figure 15). They showed that destructured clay presents lower strength, lower stiffness and reaches a smaller peak at a larger strain than an intact clay due to the destruction of bonds in the destructured clay. They also compared the strength envelopes of the intact soil with that from the same soil which was allowed to swell under zero stress and then reconsolidated before undrained triaxial testing. They observed that the strength envelope for the swelled soil was lower than the envelope of the intact soil, due to destructuring (figure 16).

Toll and Malandraki (1993) carried out undrained triaxial compression tests on artificially bonded and destructured samples at effective confining stresses ranging between 5 and 600 kPa. They used the technique developed by Maccarini (1987), but without the c.f.k.(crushed fired kaolin) sand. The stress paths for undrained tests on bonded samples are shown in figure 17. They prepared the samples in a relatively dense condition (void ratio = 0.6). Based on the analysed samples they concluded the following remarks:

1. For confining stress below 400 kPa the bonded soil can sustain higher stress ratios than the destructured soil, showing that the bond does affect the failure surface at low stresses (figure 18).
2. At confining stresses above 400 kPa the failure surfaces for the bonded and destructured soil coincide (figure 18), suggesting that sufficient straining occurs before reaching the surface so that all the bonding is destroyed.
3. A consistent yield surface can be observed for the bonded soil (defined by a change in stiffness).

They identified the position of the two yield surfaces in the q-p′ space and showed their relationship with the failure surfaces as shown in figure 19.

Leddra et al. (1993) studied the deformation characteristics of a weakly bonded chalk, from two different sites with a wide variation in porosity. They carried out undrained triaxial experiments following isotropic and K_0 consolidation to define the failure line for chalks subject to different consolidation pressures with different degrees of pore filling cementation. They suggested that chalk behaves as an elastic material at low stresses, but as the applied stress increases the cementation progressively breaks down and the material undergoes yield and the structure begins to deform in a ductile manner. Yield is followed by strain softening and/or strain hardening. They also observed that as the void ratio decreases the yield stress increases and the importance of strain softening decreases (figure 20 and 21). It was also observed that deformation proceeds through a decrease in void ratio as the effective stress increases (figure 21).

They presented the undrained stress paths for isotropically consolidated chalk samples as shown in figure 22. From these stress paths they indicated that undrained behaviour is dependent upon the magnitude of the consolidation stress (p′) at the onset of undrained shear (figure 22). They also noted that the stress path for an experiment conducted at a low mean effective stress (i.e. below the yield stress)

climbed above the projection of the failure line, yielded and then rapidly strain softened with little excess pore pressure generation (figure 22 and 23) until it reached the failure line. It then continued to strain soften whilst following the failure line. Samples subject to mean effective stresses within the yield and immediate post yield regime underwent severe strain softening as they followed the projection of the failure line. Samples consolidated into a strain hardening regime continue to strain harden once their stress paths have reached the failure line (Leddra et. al. 1993).

Gens and Nova (1993) noted that there is a clear need to include the effects of bonding (among other factors) in order to model soil behaviour realistically. They noted that most bonded soils with increasing confining pressure show a transition from a brittle/dilatant behaviour to a ductile/compressive behaviour (as shown in figure 24). They also noted that initial stiffness and deviator stress at yield might also decrease at high confining stresses. After yield, bond degradation occurs in a gradual manner.

Hobbs et al. (1988) discussed isotropically consolidated, undrained (CIU) triaxial tests on single, 100mm diameter and 200mm high, cylindrical specimens to investigate the insitu stress-strain characteristics of some undisturbed tropical red clay soils from west Java, Indonesia. These red clay soils achieved a peak strength at low strains. From the observed effective stress paths they concluded that the clay showed a transition from pseudo-overconsolidated to normally consolidated behaviour. A series of stress paths for some of the samples is shown in figure 25. From the e-log p curves they identified two yield points as the soil structure deforms under different levels of effective stress (figure 26). A first yield point occurred under effective loads of 100-200 kPa (interpreted as reflecting failure of inter-ped bonding as the soil destructures) and a second yield point at higher stress levels of 500-600 kPa (interpreted as further destructuring of the ped clusters due to failure of intra-ped bonds).

Sridharan (1988) presented some typical stress-strain curves of undisturbed and remoulded samples for a desiccated lateritic soil (figure 27). He observed that the undisturbed soil exhibits larger shear strength and a stiffer stress-strain response. He also noted that strains at failure were larger for remoulded soils than for undisturbed soils. By removing the chemical bonds they observed a reduction in strength in these tropical soils.

Hight et al. (1992) discussed the stress-strain, strength and stiffness characteristics of the Bothkennar clay. From the undrained triaxial test results they discussed that the Bothkennar soil showed pronounced brittleness in triaxial compression, with the effective stress path progressively collapsing inside the initial bounding surface but not reaching a well defined critical state. It was also observed that reconstituted samples showed lower strength, lower stiffness, less brittleness and larger strains to peak than the natural samples due to the presence of structure in natural soils (figure 28). They also mentioned that the Bothkennar Clay has a high, non-linear pre-yield stiffness and a low pre-yield compressibility. They noted that the clay showed recoverable behaviour up to strains of 0.02%. They observed that the resistance of the soil due to its bonded structure was reduced progressively by shear and volumetric strains. They also observed that undrained strengths are highest in triaxial compression and least in triaxial extension.

Allman and Atkinson (1992) discussed triaxial test results, comparing the behaviour of reconstituted samples and intact samples of Bothkennar clay soil. They observed that in undrained compression tests most samples reached a reasonably well defined constant stress ratio state at strains above about 15%; only the samples at the higher overconsolidation ratio showed any well-defined peak stress ratios. They also noted that the undrained strength of intact samples is significantly greater than that of reconstituted samples at the same water content. From the observed stiffness characteristics they noted that the stiffness and strain curves are non-linear. They

observed a decrease in stiffness values with increasing strain and with increasing confining pressures.

Paul et al. (1992) mentioned that the increased strength and apparent preconsolidation of the Bothkennar clay may be due in part to bonding between silt particles by aluminosilicates, iron compounds and silica. They mentioned that two levels of bonding might occur. One providing a link between aggregates called inter-aggregate bonds and the other providing a link between particles within an aggregate called intra-aggregate bonds.

Clayton et al. (1992) pointed out that in Bothkennar Clay, bonds formed by aluminosilicates, iron compounds and silica are observed between aggregates and silt grains. They suggested that there is a progressive breakdown of inter-aggregate pores, proceeding from the largest to the smallest pores. Strains in inter-aggregate bonds are likely to be directly related to inter-aggregate pore size and the soil would be expected to fail first between those aggregates having the largest inter-aggregate pore size. They observed a progressive degradation in stiffness with increasing amplitude of the strain cycle above 0.5%

Taylor and Coop (1993) studied the undrained stress strain and strength characteristics of Boom Clay from Mol, Belgium. They observed initially a very stiff response of the samples and after an axial strain of about 2% the samples were close to the peak strength with the formation of a polished slip planes. Some samples (tests G and B in figure 29) showed a sudden drop in strength at an axial strain of 2%. They discussed an irregular reduction in stiffness with increasing strain and observed the close similarity of stiffness values for undisturbed samples at strain levels greater than 0.1%.

Little and Hataf (1990) studied the undrained stress-strain behaviour of weathered undisturbed and reconstituted Keuper Marl. They observed that the reconstituted samples did not show any maximum stress level even at high values of shear strain. For undisturbed specimens the peak stresses are identifiable and brittle behaviour can be seen in some cases (figure 30). The effective stress paths showed the characteristics of isotropically normally consolidated and overconsolidated soils (figure 31). They also discussed that the higher stress ratio value for the undisturbed specimens might be related to larger grain size of the undisturbed soil due to aggregation of the clay particle into larger silt-size units by some cementing or aggregating agent. This bonding was broken down in the process of reconstitution and reconstituted samples showed lower strength than the undisturbed samples.

Atkinson et al. (1993) worked on the measurement of stiffness of soils and weak rocks in the laboratory. They concluded that the stress-strain behaviour of many stiff soils and weak rocks is highly non-linear and to obtain parameters for calculation of ground movements it is necessary to take account of changing stiffness with strain. They discussed the results of stiffness of undisturbed London Clay during drained shearing. They mentioned that the stress strain curve appears to be non-linear (figure 32.a) and it is very difficult to determine this clearly near the start of the test where the strains were very small. The non-linear stress-strain behaviour of stiff soils and weak rocks can be examined more easily by plotting the stress-strain curve with strains in logarithmic scale as in figure 32.b. They observed large changes in shear modulus (G′) over relatively small ranges of strain (figure 32.c). It was observed that the shear modulus falls from about G′= 56 MPa at a shear strain (ε_s) = 0.005% to about G′= 30 MPa at a shear strain ε_s = 0.05%. In their study they also compared the stiffness values for uncemented and artificially cemented carbonate sands. They noted that cementing increases the stiffness substantially at small strains, but after modest straining the stiffness reduces to values comparable to those for the uncemented sand. It can be seen from figure 33 that the value of shear modulus for cemented samples is about G′= 95 MPa at a shear strain ε_s = 0.1% and

reduces to values comparable to those for uncemented samples at a shear strain ε_s = 0.6%.

Based on small strain behaviour on reconstituted soil, Jardine et al. (1991) and Jardine (1992) suggested that three yield conditions could be identified. These are: Y1 indicating the limit of linear elastic behaviour (i.e. the end of the elastic region); Y2 indicating the limit of recoverable behaviour (The behaviour up to Y2 may be non-linear but no significant plastic strains are generated); Y3 indicating the complete destruction of any structure within the soil when the stiffness has dropped to comparatively low values. The zones represented by Y1 and Y2 are kinematic and move according to the current stress path direction. Y3 is static and independent of stress history.

Smith et al. (1992) from triaxial stress path tests discussed the yielding characteristics of undisturbed Bothkennar Clay. They mentioned that the stress space within the initial bounding surface may be divided into three zones separated by yield surfaces of different types. These zones are shown in figure 34. They noted that yielding is classically associated with a sharp change from elastic to plastic behaviour. They identified two kinematic sub-yield surfaces existing within an initial bounding surface. They also pointed out that within the innermost zone (zone 1) the soil's behaviour is linear elastic. The first elastic zone (before Y1) could not be mapped accurately (figure 34) and the zone 1 was located at very small strains. The second zone (before Y2), where the soil behaviour changed to become non-linear and the behaviour of the soil under shear was recoverable, was found at axial strain (ε_a) = 0.02%. They mentioned that it is also more difficult to map the zone 2 (Y2) than the Y3 envelope. In summary they stated that irrecoverable straining starts when the stress path enters zone 3 (Y3). This third zone (before Y3) determined the onset of large strain yielding. They discussed that stiffness behaviour is stiff and non-linear before large scale yielding.

A conceptual picture of yield for bonded structured materials is given by Malandraki and Toll (2001), which is shown in figure 35. There are various proposals in the literature for identifing yield in natural and artificial soils. Some of which are discussed earlier of this section. Different definitions of yield for bonded materials have been reviewed by Malandraki and Toll (1996). They pointed out that traditionally 'yield' has been described as a clear change in behaviour. Atkinson (1990) described yield as the end of the elastic range, which is the classical meaning of yielding in mechanics. Malandraki and Toll (1994, 1996) defined yield for a weakly bonded artificial soil based on changes in the tangential stiffness (E_{tan}) versus axial strain plotted to log-log scale. They mentioned that a first loss in stiffness defines the 'first yield' (figure 36). They mentioned that in final yield, the bonded soil losses all of its stiffness due to bonding. Malandraki and Toll (1994,1996) also identified an additional yield point called 'second yield' for an artificially bonded soil between the first and the final yield points. The term 'second yield' was used by Vaughan (1988) and Malandraki and Toll (1994, 1996). To avoid confusion between the term 'second yield' and 'Y2' as used by other researchers, Malandraki and Toll (2000) introduced the term 'bond yield' to represent the point where a major change in tangential stiffness occurs between the first and the final yield condition (figure 36).

Two modes of failure for bonded soils have been identified by Malandraki and Toll (1996). They mentioned that a first mode of failure is defined when shearing a bonded soil at low confining stresses. Here the bonded soil exhibits greater strengths than those of the destructured soil and yield (bond yield) coincides with failure. The second mode of failure is defined when shearing at high confining stresses, and bond yield occurs under shear or isotropic compression. In this case, the soil's strength coincides with that of the destructured soil.

Malandraki and Toll (1994, 1996) observed that bonded soils showed higher stifffness values than the destructured soils up to 1% strain and after that stiffness values of both the natural and destructured soils are close to each other. They also pointed out that E_{tan} increases almost linearly with an increase in p´ for the low stress levels (figure 37). Similarly the strain contours for the bonded soil are also approximately linear in the same region (figure 38).

A model of yield behaviour was proposed by Malandraki and Toll (1996) using Vaughan's ideas about yield (Vaughan, 1985, 1988; Vaughan et al., 1988). They identified four zones of behaviour from the relative positions of the failure surface and the second yield surface for an artificially bonded soil under shear in triaxial compression (figure 39). They found that in the first zone the bonds entirely control the soil's behaviour at failure. In the second zone, the bonds only partially control the soil's behaviour at failure. In the third and fourth zone, the soil's behaviour at failure is independent of bonding and its behaviour is governed by that of the destructured material. However, bond yield occurs under shear in the third zone and under isotropic compression in the fourth zone (figure 39).

2.4 Summary

In this chapter a literature review was undertaken of the general aspects of tropical soils from different parts of the world. Weathering has a strong influence on the formation of the tropical residual soils. Mineralogy and fabric of these soils play an important role on the engineering behaviour of these soils. In addition, the presence of cementation or bonding in tropical residual soils also plays an important role on the mechanical behaviour of these soils. Therefore, a review was also undertaken on bonded soil behaviour.

Most of the previous research work on tropical soil behaviour has focused on the formation, classification and basic geotechnical properties. But a multidisiplinary approach to research on tropical soil behaviour is very limited. It is discussed that soil's mechanical behaviour can be best explained by comparing their properties in a natural and destructured state at the same grading and at the same void ratio to understand the effects of bonding on the soil's behaviour, in respect of the peak strength and stiffness. However, only a small amount of data from triaxial tests on undisturbed samples of natural tropical residual soils has been published, which emphasized the need to carry out research on the tropical clay soils of Dhaka.

Research on various bonded soils suggests that although bonding of these materials has arisen from different reasons their mechanical behaviour is very similar. These bonded materials initially show stiff behaviour followed by yield. Yield of the bonds can be represented in the stress space by a yield curve. Defining yield from the stress-strain curve has caused some confusion in the past. There are various suggestions in the literature to define yield of the bonded structure in bonded soils. Some of the researchers suggested an initial yield surface, followed by a final yield surface at higher stresses close to the failure surface. Some of the researchers also pointed out that there might be an additional yield point between the initial and the final yield points.

Bonding in tropical residual soils has a special significance in the stress-strain development, strength, stiffness and yielding characteristics of these soils. No attempt has yet been made to study the mineralogy, fabric and the effects of bonding on the tropical clay soils of Dhaka. This is the first attempt to take an integrated multidisciplinary approach to evaluate the engineering behaviour of the tropical clay soils of Dhaka and to show the influence of mineralogy and fabric on the engineering behaviour. The work carried out in this study clarifies the stress-strain behaviour, stress paths, bonding effects at low and high confining pressures, peak strength, critical state condition, stiffness and yielding behaviour within which test data for the tropical clay soils of Dhaka, Bangladesh can be interpreted.

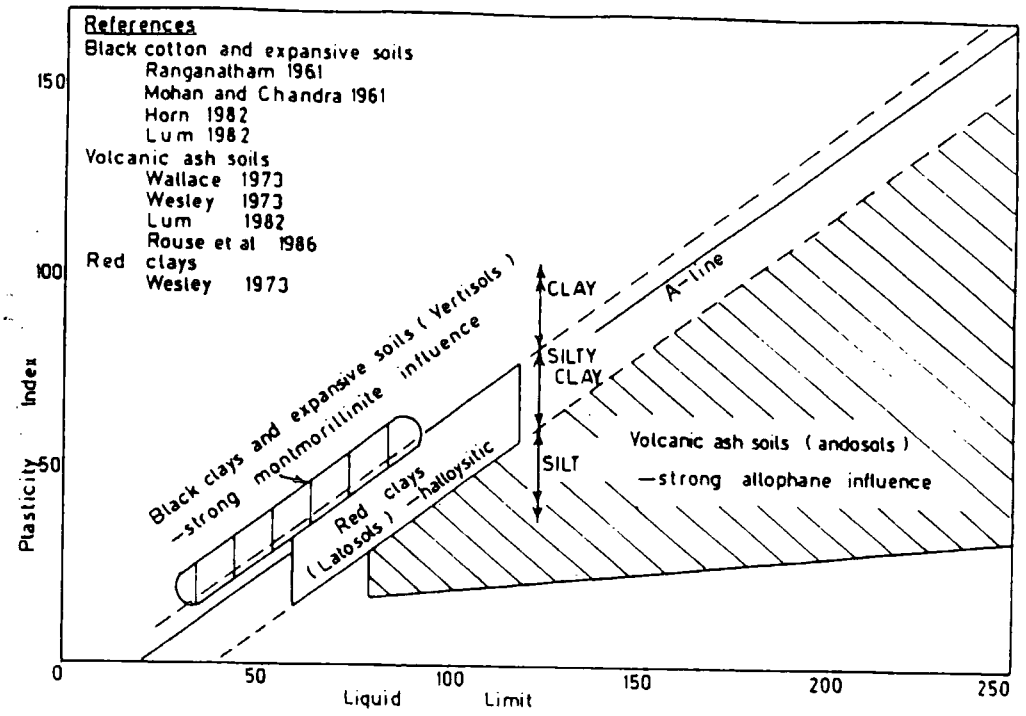

Fig. 1 Possible division of plasticity chart for use with residual soils (Wesley, 1988)

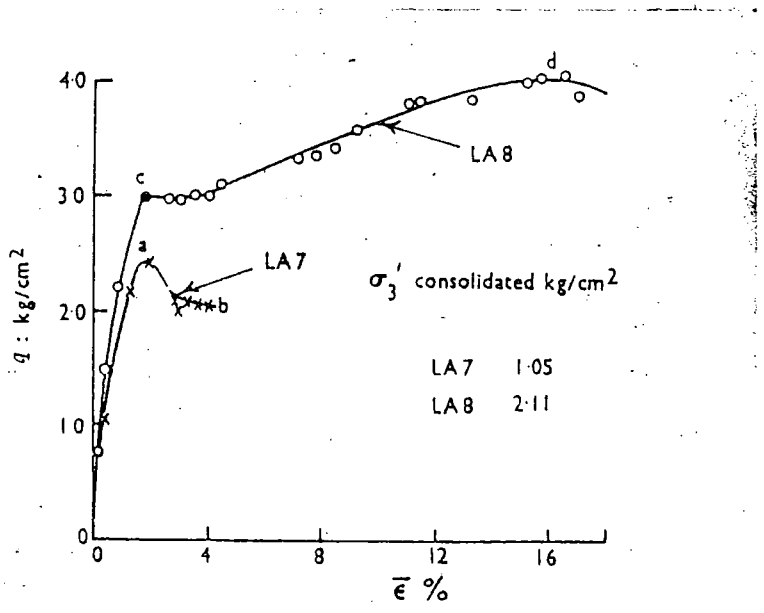

Fig.2 Two stress-strain curves for Labrador clay (Sangrey, 1972)

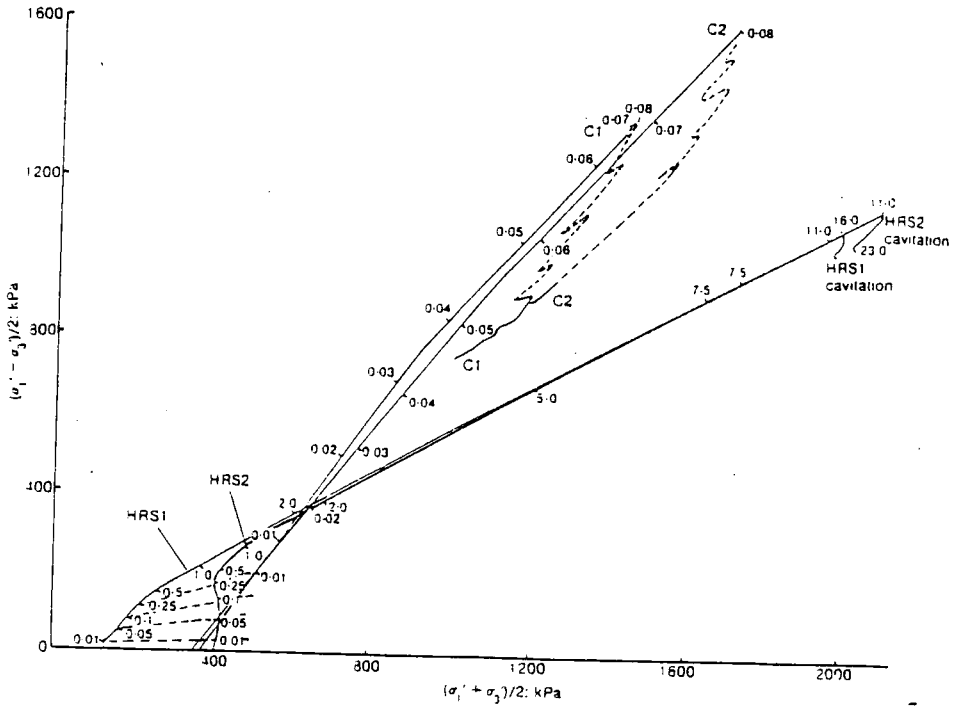

Fig. 3 Stress paths for Ham river sand (HRS) and Chalk (C) samples (Jardine et al.; 1984)

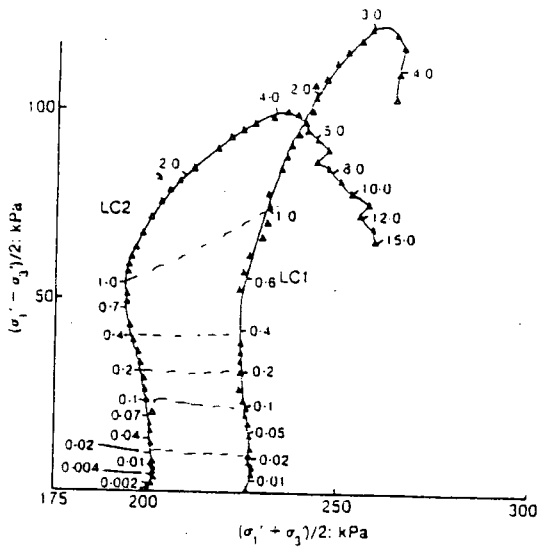

Fig. 4 Stress paths for London clay (LC) (Jardine et al.; 1984)

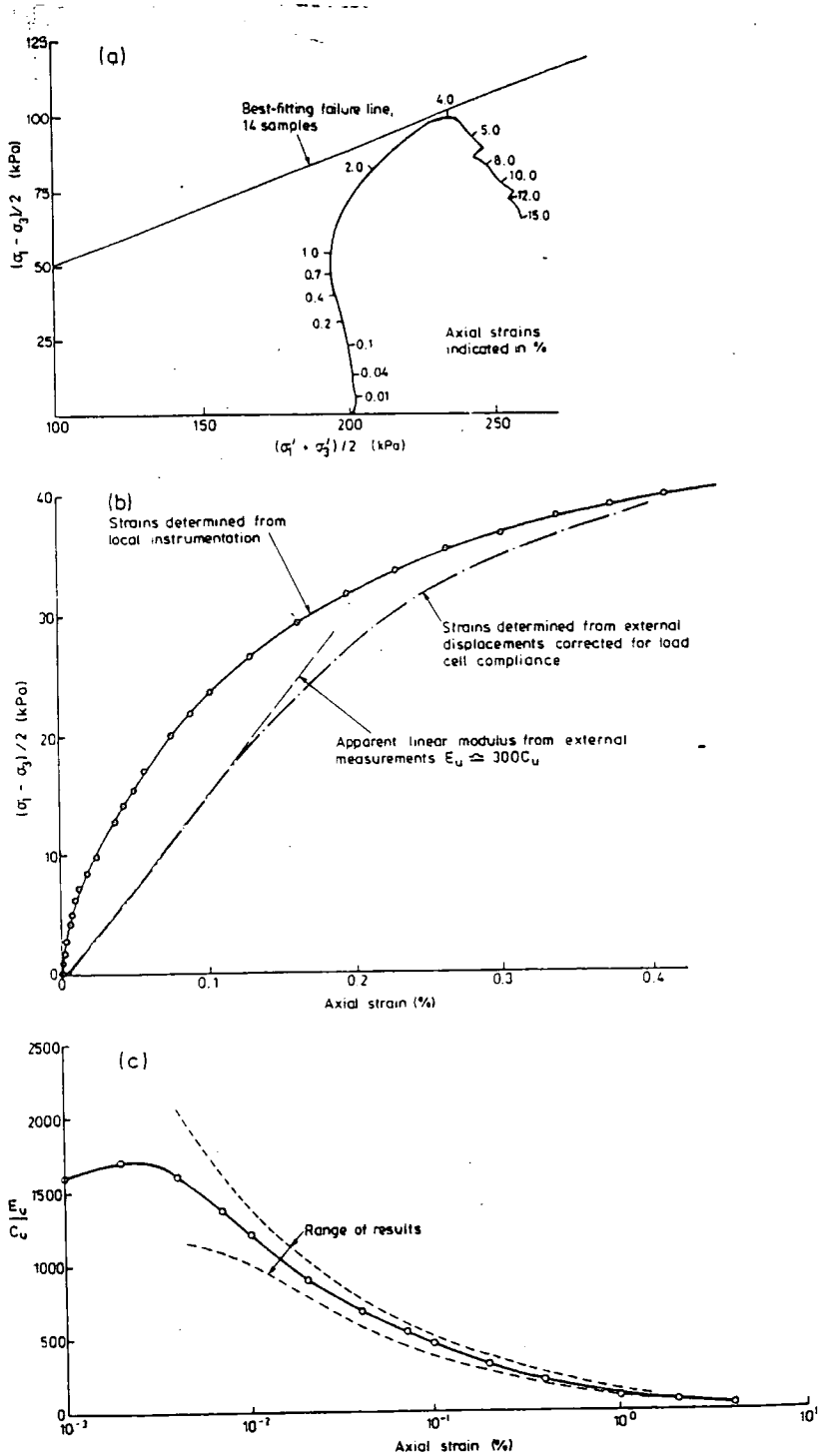

Fig.5. a. Undrained stress paths b. Initial stress strain behaviour and c. Stiffness-strain results on an undisturbed London clay (Burland, 1989)

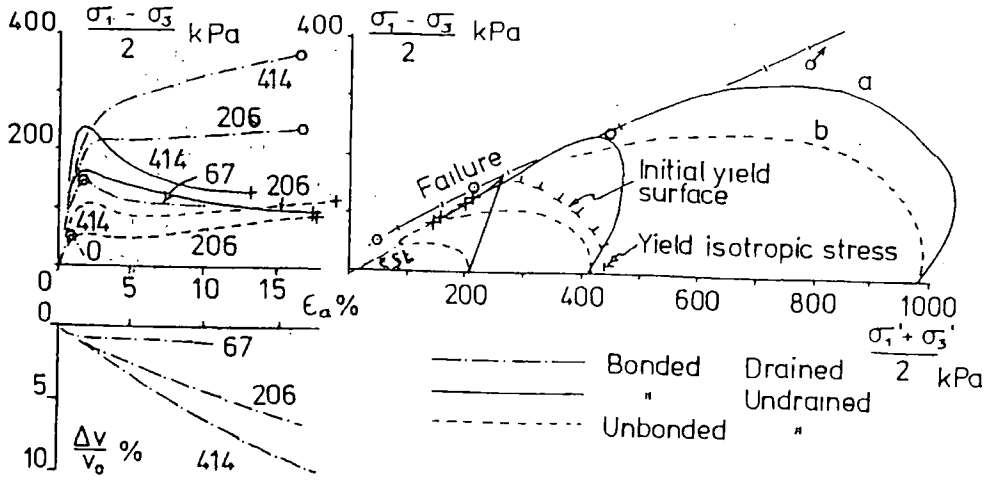

Fig.6 Triaxial test results on artificially bonded soil (Vaughan, 1985)

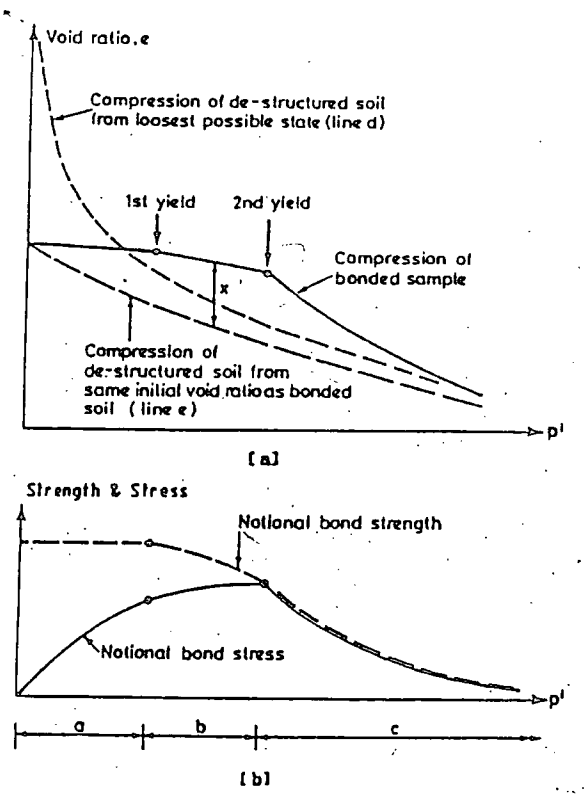

Fig.7 Yield of the soil with bonded structure when loaded at constant stress ratio (Vaughan, 1988)

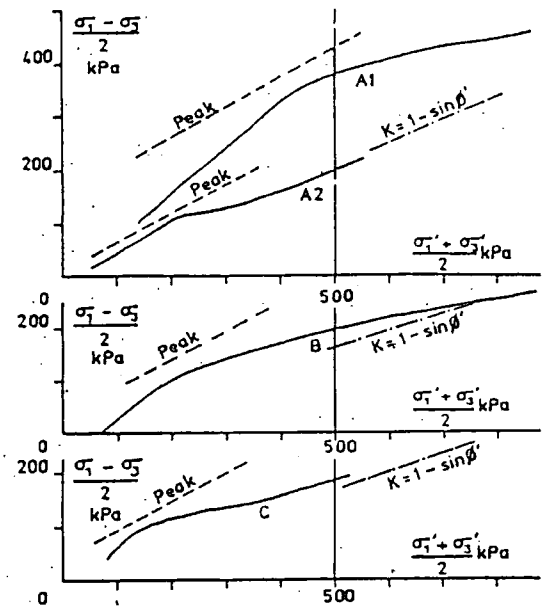

Fig.8 Convergence of failure surface for various bonded natural soils (Vaughan, 1988)

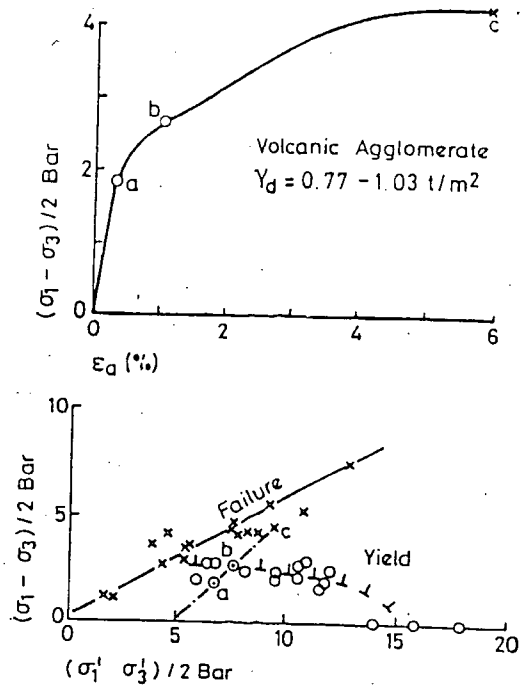

Fig.9 Yield surface observed in volcanic agglomerate (Vaughan et al.; 1988)

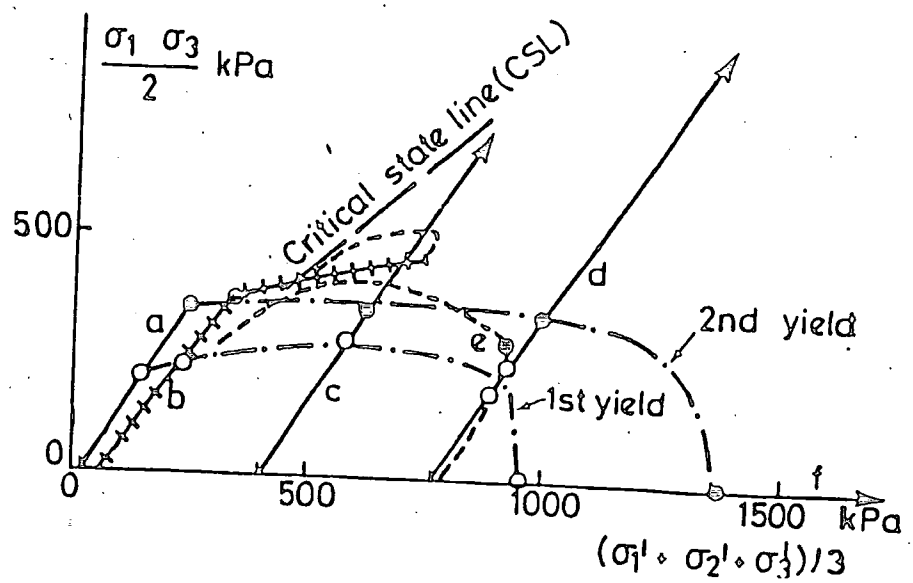

Fig.10 Yield observed in residual soil from basalt (Vaughan et al., 1988)

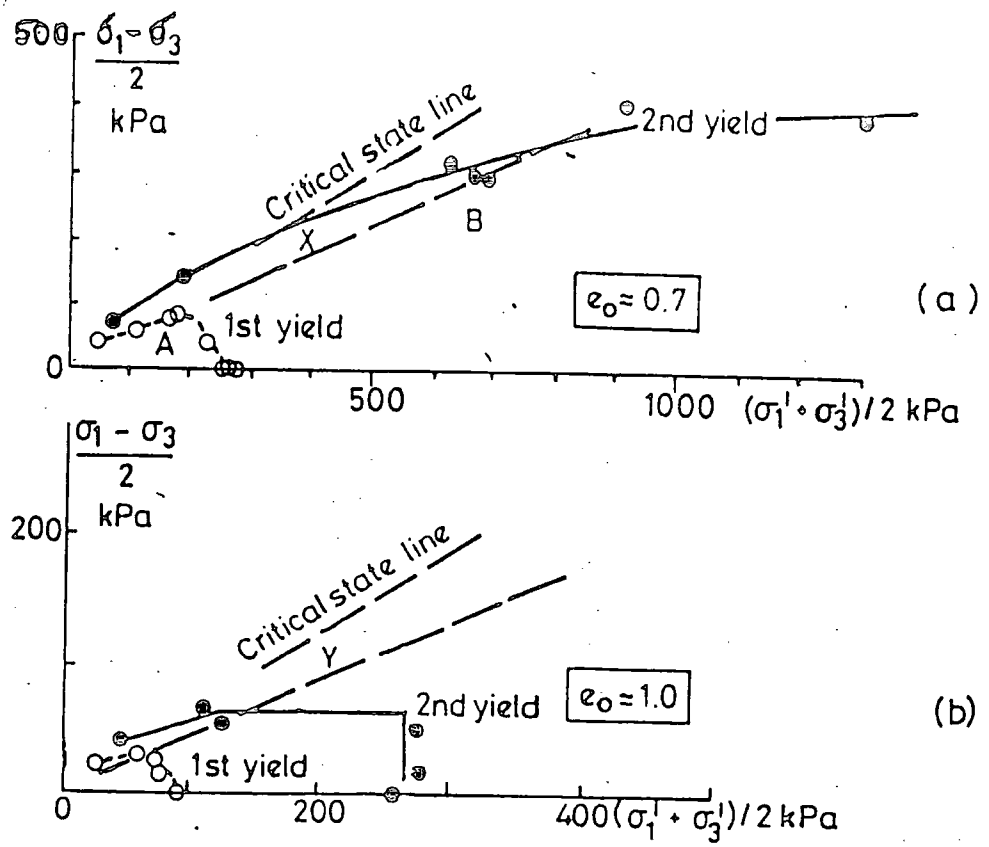

Fig.11 Yield observed in artificial soils (Vaughan et al., 1988)

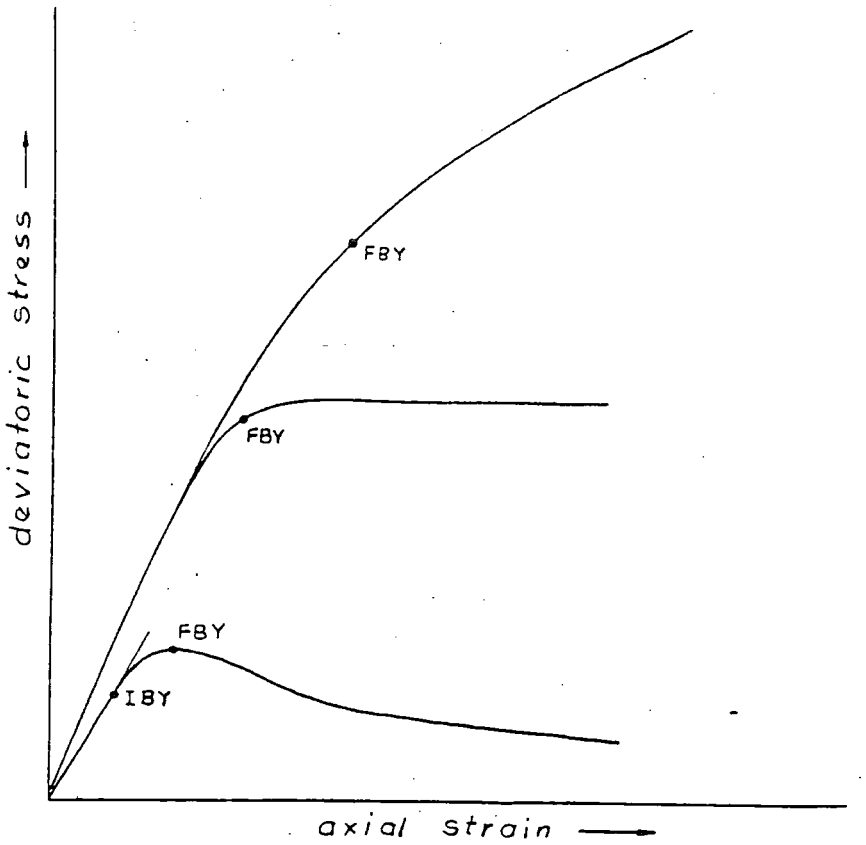

Fig.12 Definition of initial and second bond yields on deviator stress versus axial strain space (Maccarini, 1987)

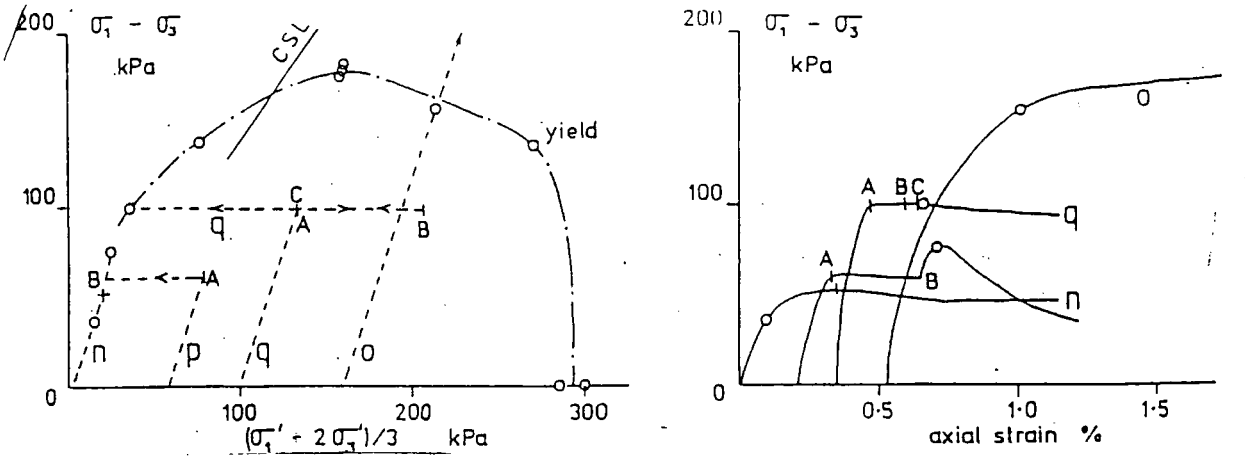

Fig.13 Effect of stress path on yield and failure of artificially bonded soils (Bressani and Vaughan, 1989)

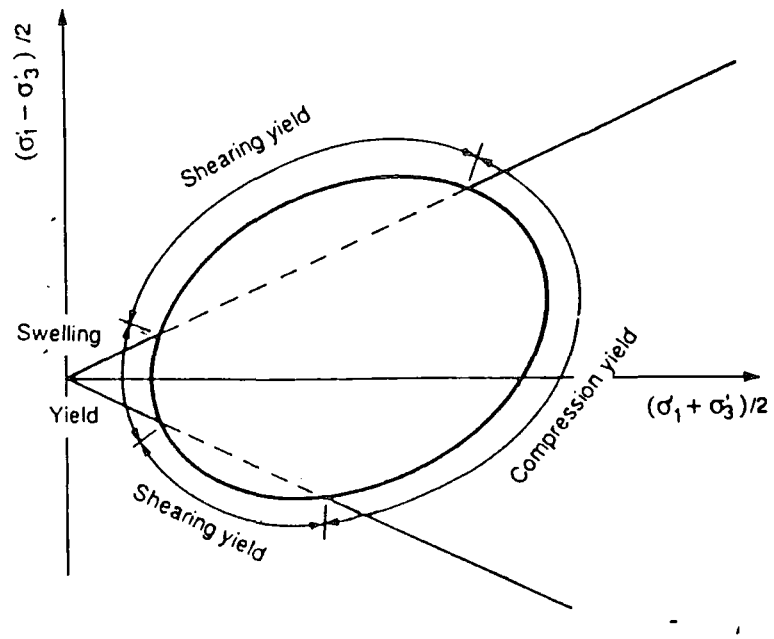

Fig. 14 Schematic figure showing different zones of yielding (Leroueil and Vaughan; 1990)

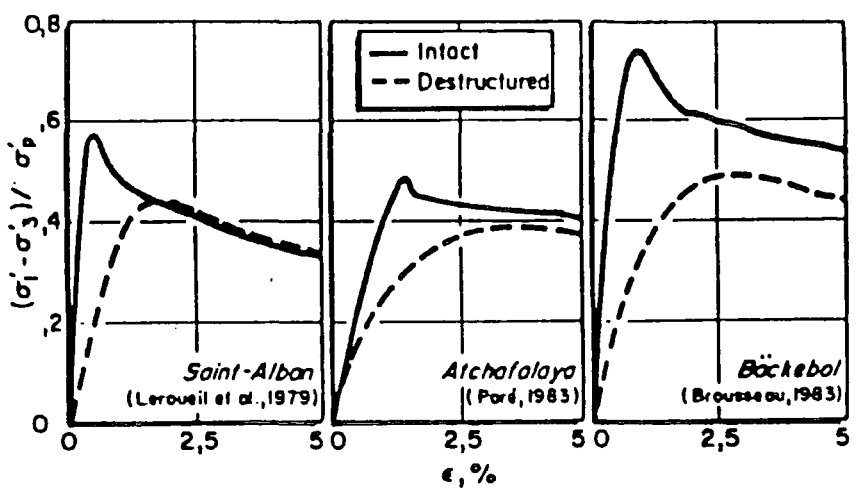

Fig. 15 Undrained stress strain relations on natural and destructured natural clays (Leroueil and Vaughan; 1990)

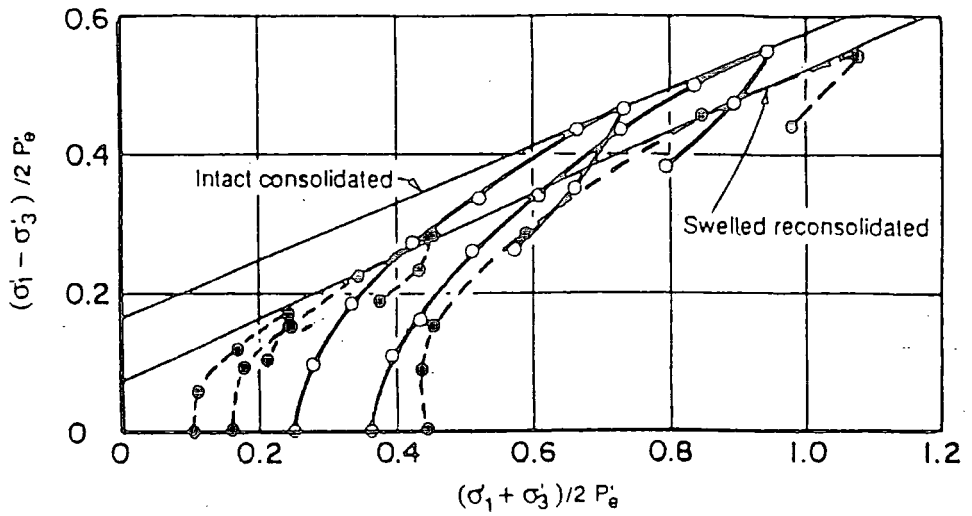

Fig.16 Strength envelopes for undrained triaxial compression tests on Todi clay (Leroueil and Vaughan; 1990)

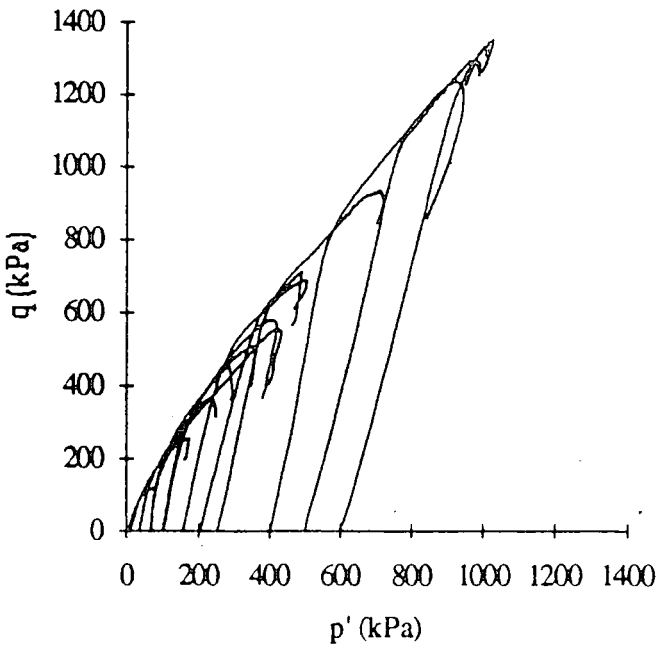

Fig.17 Stress paths for undrained tests on bonded samples (Toll and Malandraki, 1993)

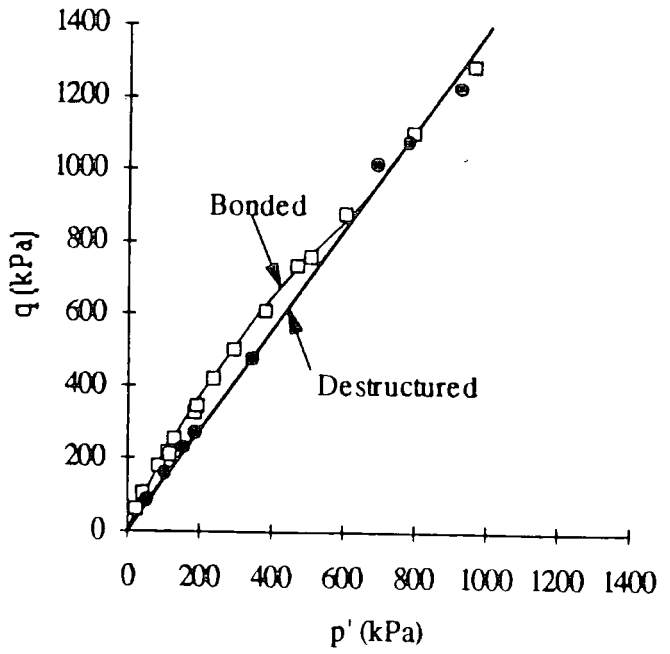

Fig. 18 A comparison of bounding surfaces for bonded and destructured samples (Toll and Malandraki, 1993)

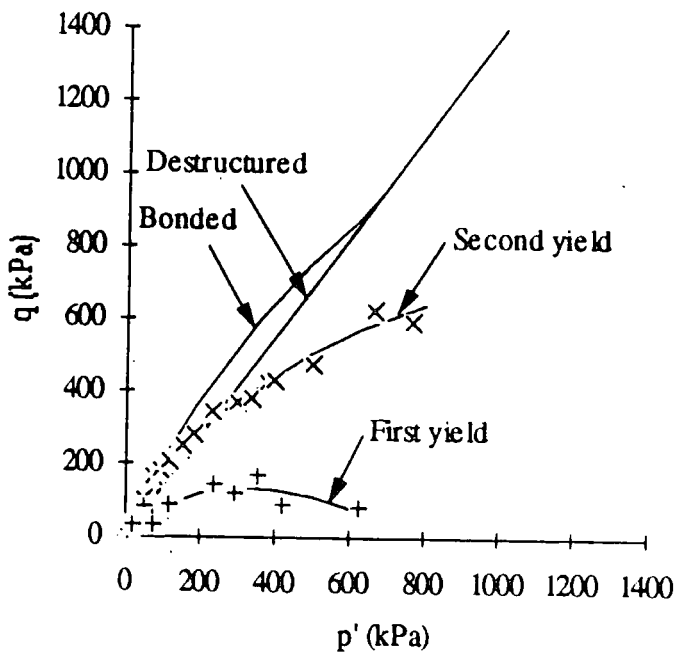

Fig. 19 Yield surfaces for bonded soil (Toll and Malandraki, 1993)

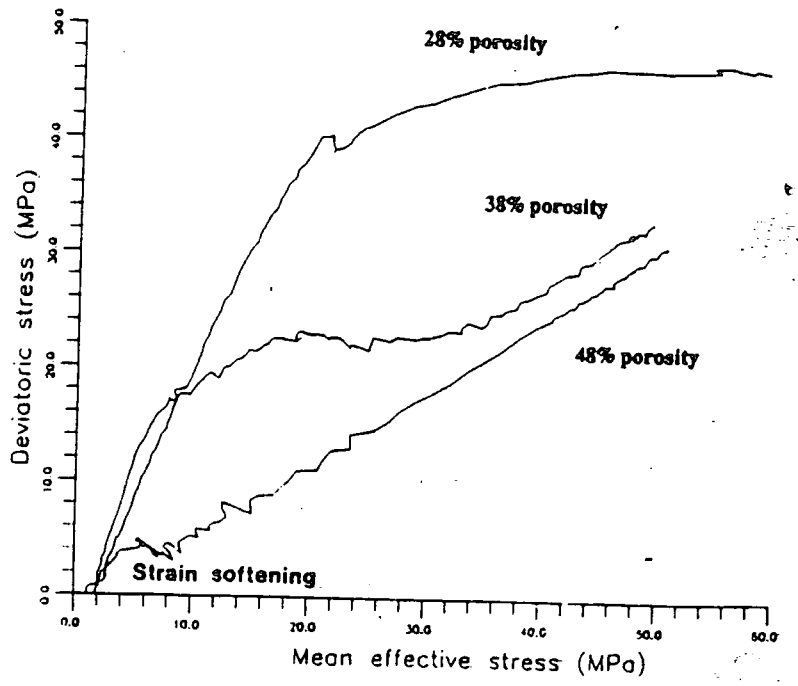

Fig.20 Deviatoric stress versus mean effective stress for three different chalk samples (Leddra et al., 1993)

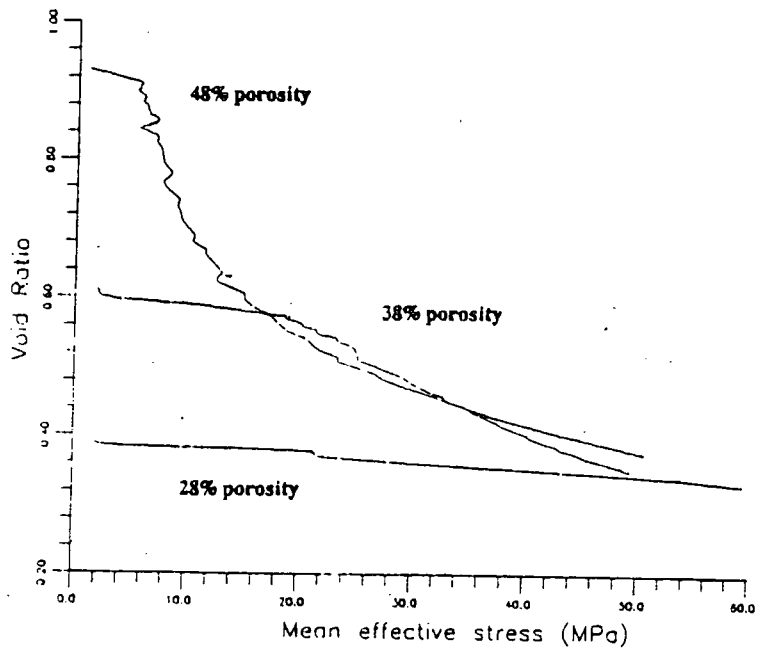

Fig.21 Void ratio versus mean effective stress for three chalk samples (Leddra et al., 1993)

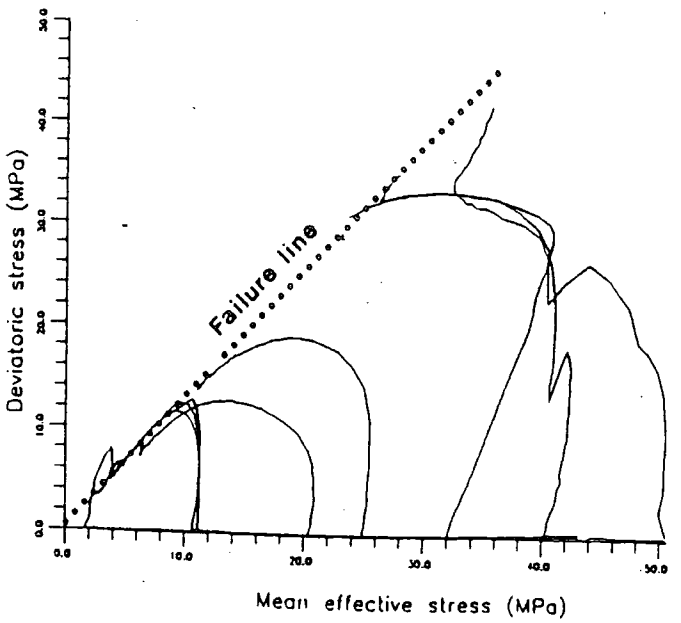

Fig.22 Undrained stress paths on chalk samples (Leddra et al., 1993)

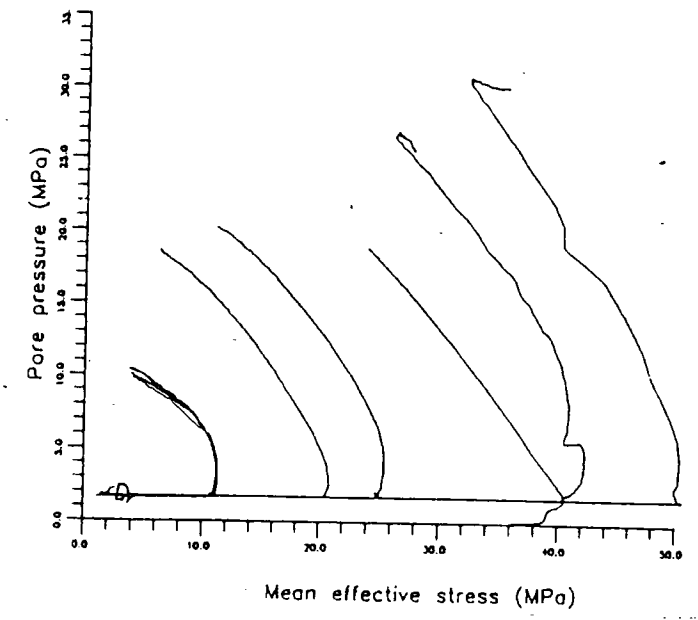

Fig.23 Pore pressure/ mean effective stress for isotropically consolidated undrained tests on chalk samples (Leddra et al., 1993)

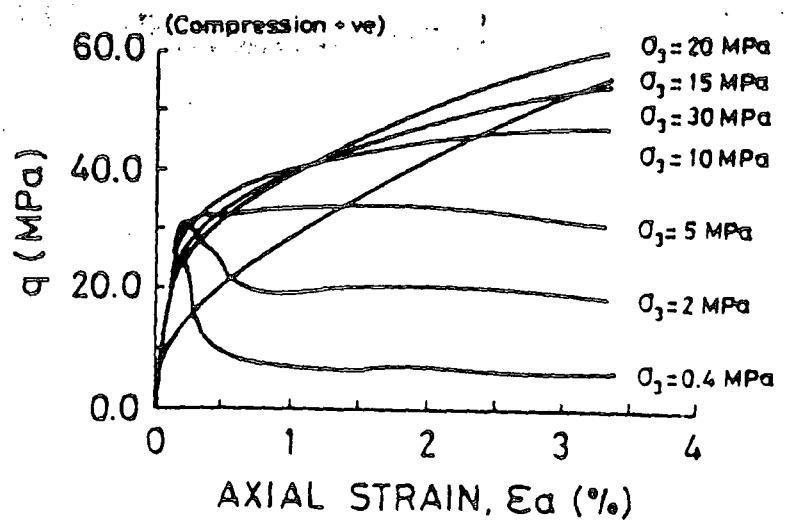

Fig.24 Stress-strain results on Oolitic limestone (Gens & Nova, 1993)

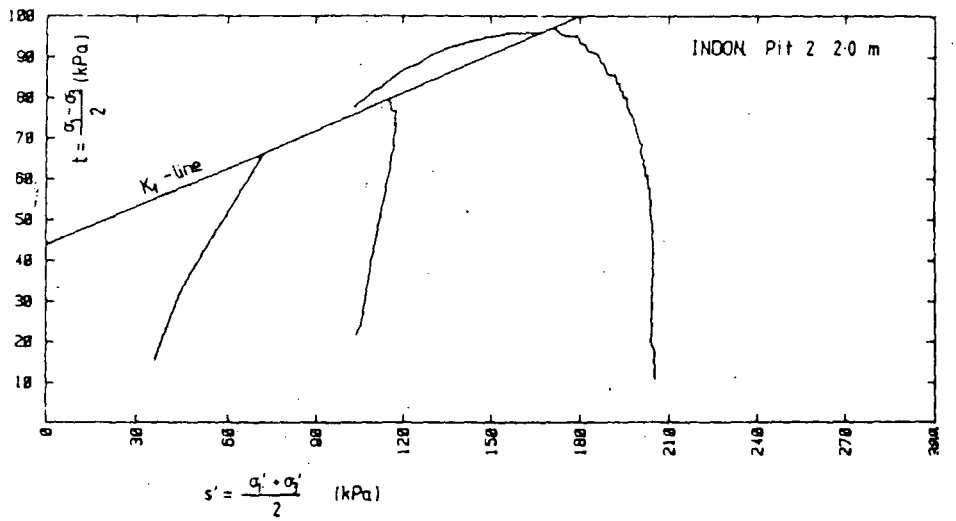

Fig. 25 Stress paths for some tropical clay soils of Java, Indonesia (Hobbs et al.; 1988)

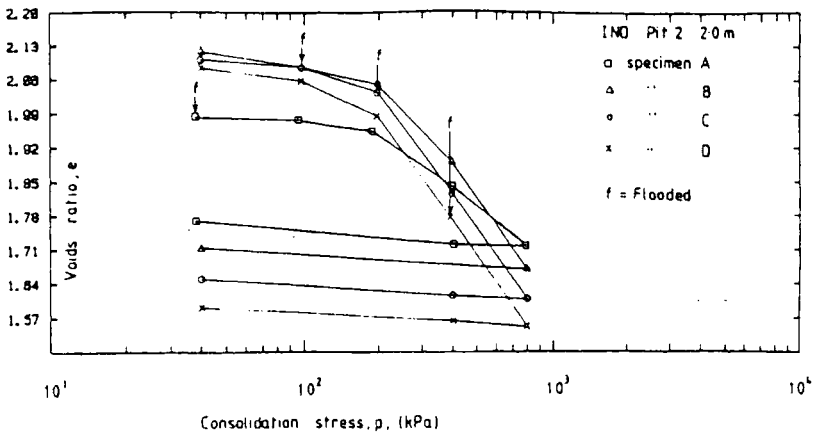

Fig. 26 e vs logp curves for some tropical clay soils of Java, Indonesia (Hobbs et al.; 1988)

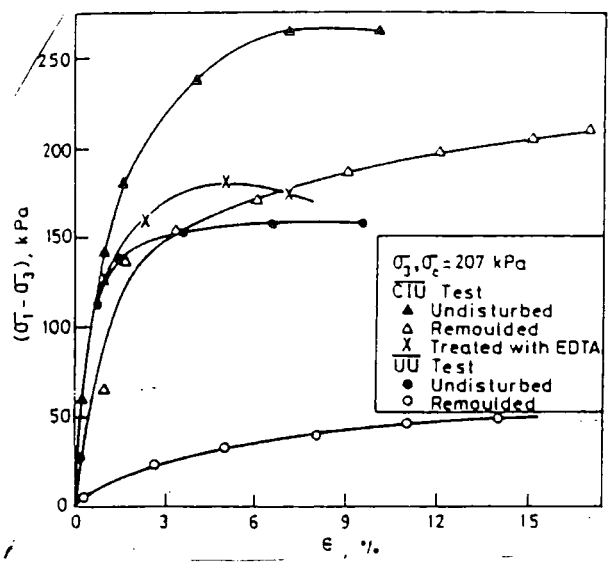

Fig. 27 Typical stress-strain curves for a desiccated tropical lateritic soil (Sridharan, 1988)

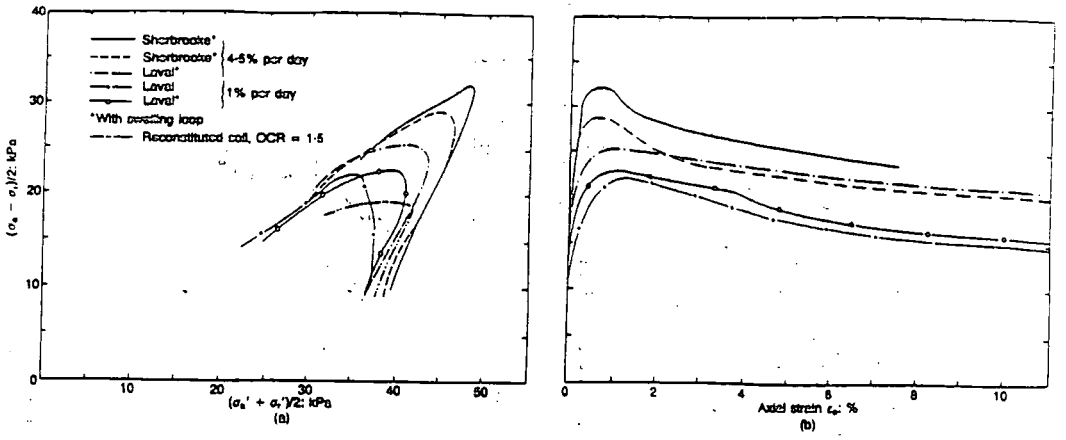

Fig.28 Effective stress paths and stress-strain curves of Bothkennar clay under triaxial compression (Hight et al.; 1992)

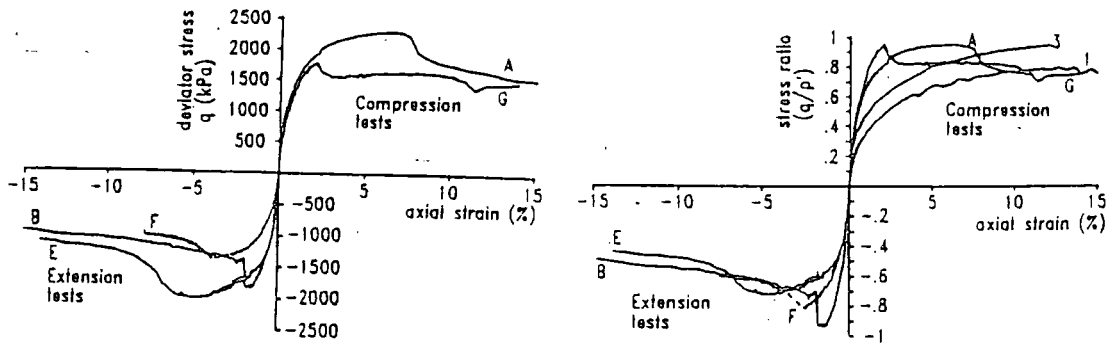

Fig.29 Stress strain curves for Boom clay (Taylor and Coop, 1993)

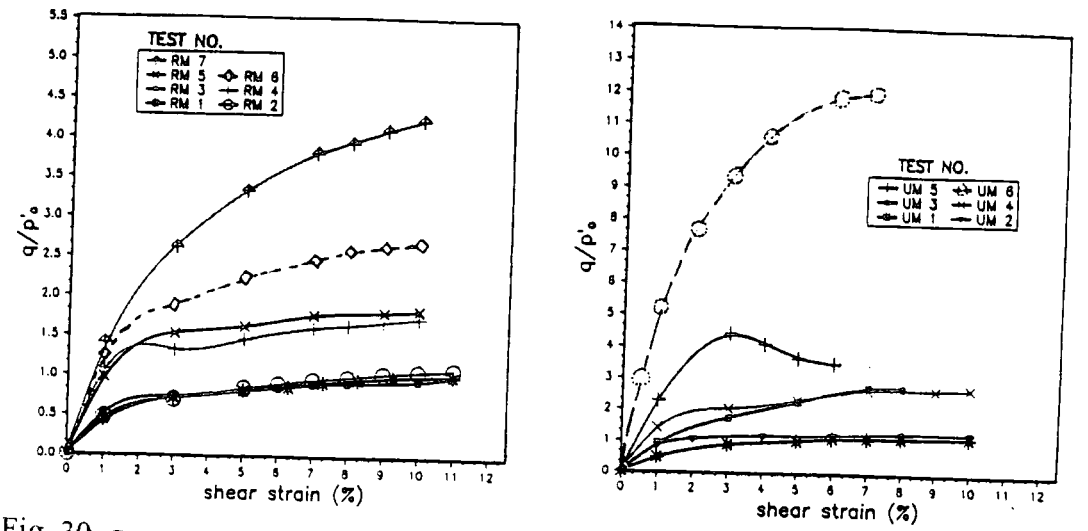

Fig. 30. Stress strain behaviour on reconstituted (a) and undisturbed (b) specimens of Keuper Marl (Little and Hataf, 1993)

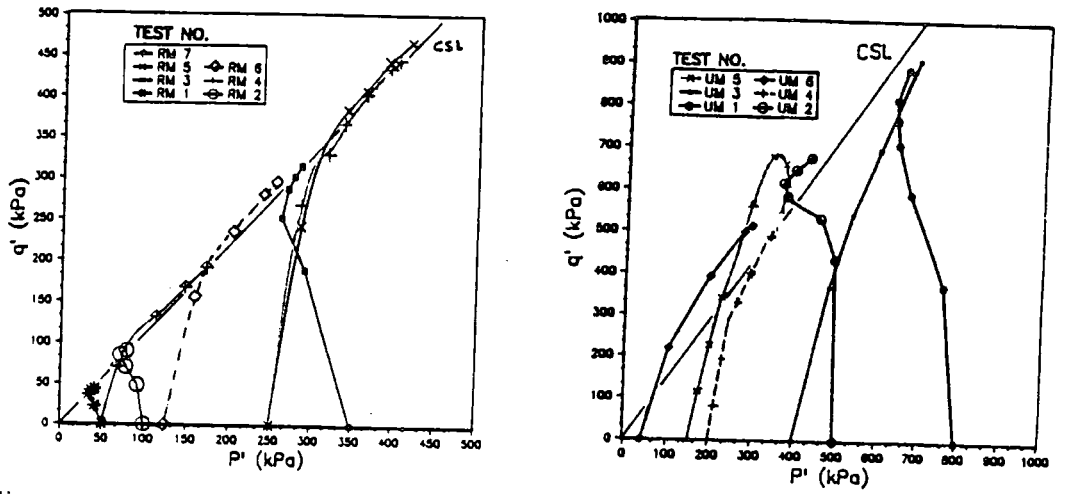

Fig. 31 Effective stress paths for reconstituted (a) and undisturbed (b) specimens of Keuper Marl (Little and Hataf, 1993)

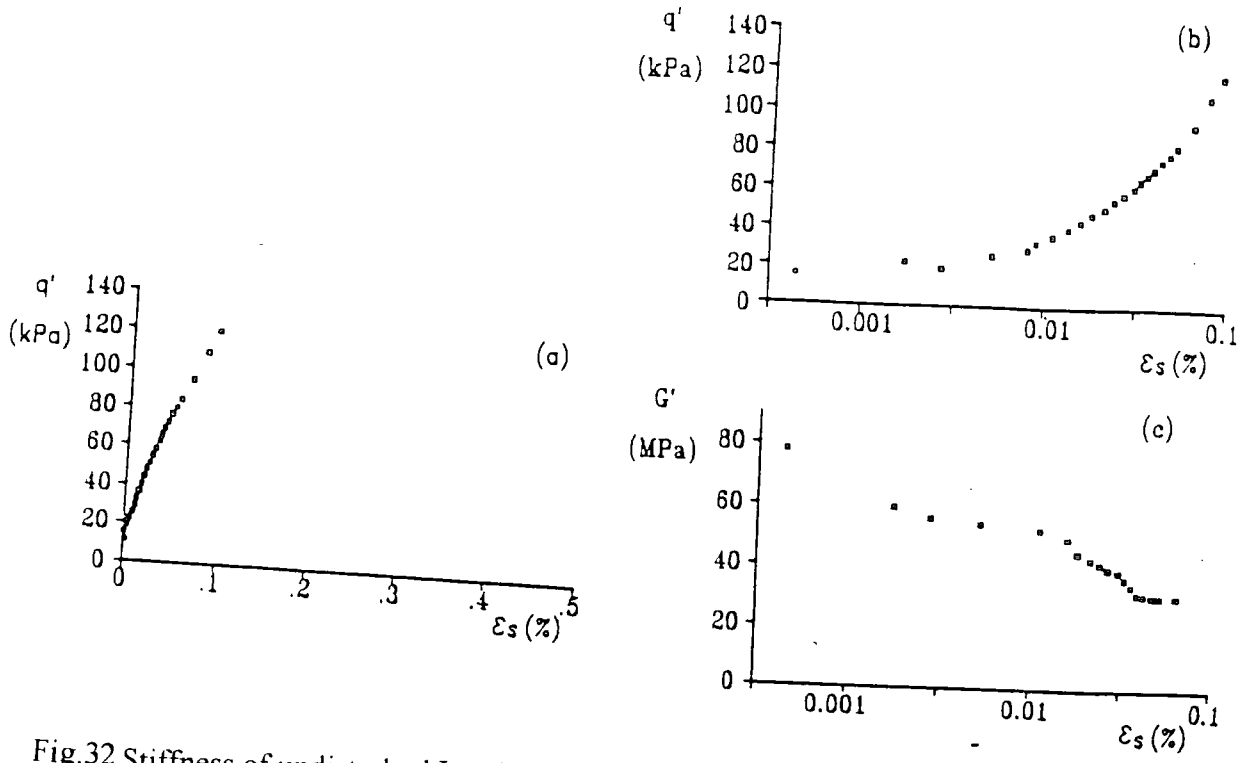

Fig.32 Stiffness of undisturbed London clay during drained shearing (Atkinson et al.; 1993)

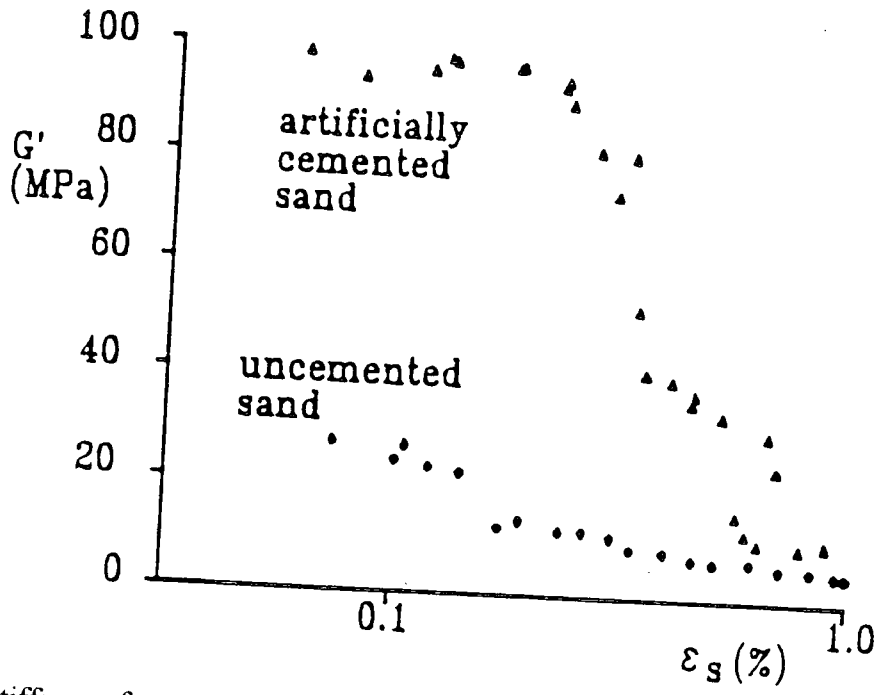

Fig. 33 Stiffness of cemented and uncemented carbonate sands in drained triaxial compression tests (Atkinson et al., 1993)

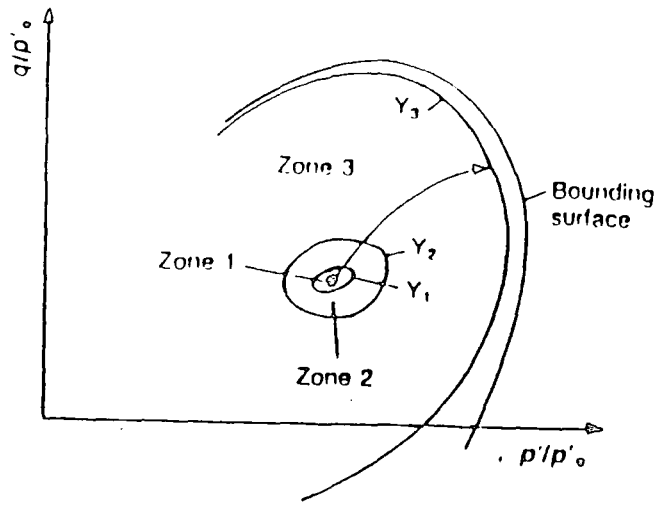

Fig.34 Three zones of yield surfaces (Smith et al.; 1992)

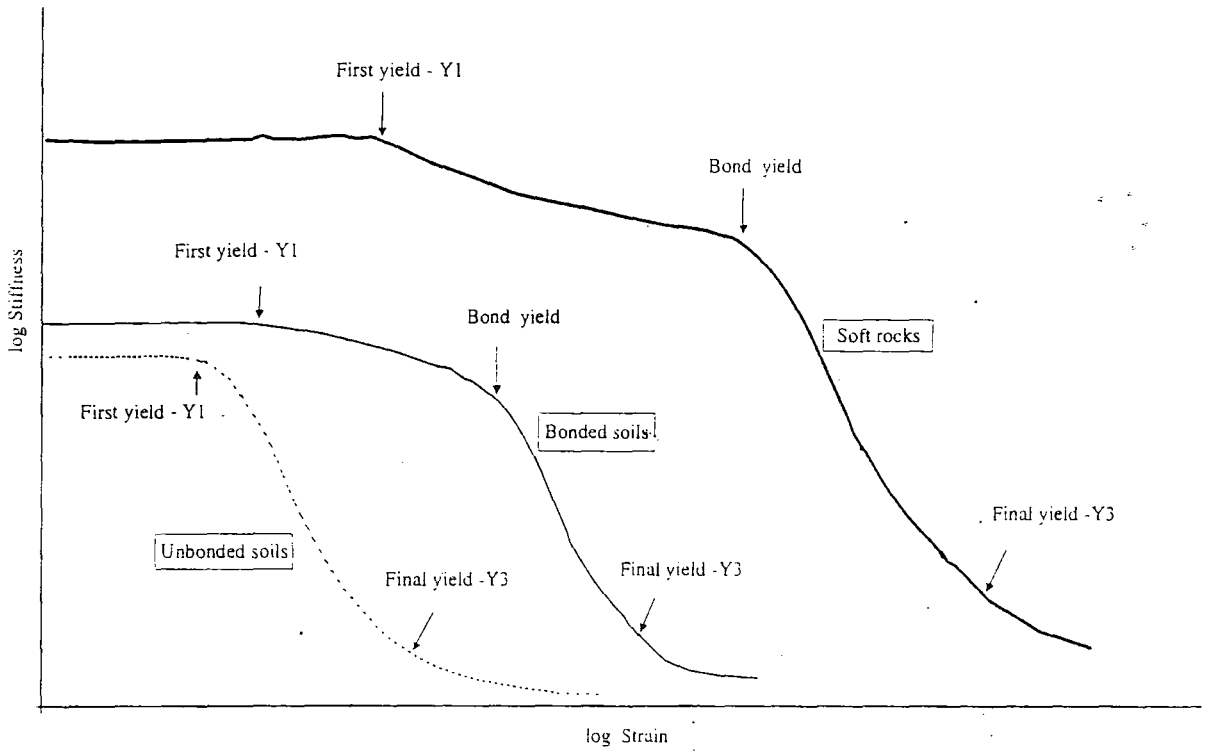

Fig. 35 Conceptual picture of yield for bonded structured materials (Malandraki and Toll, 2001)

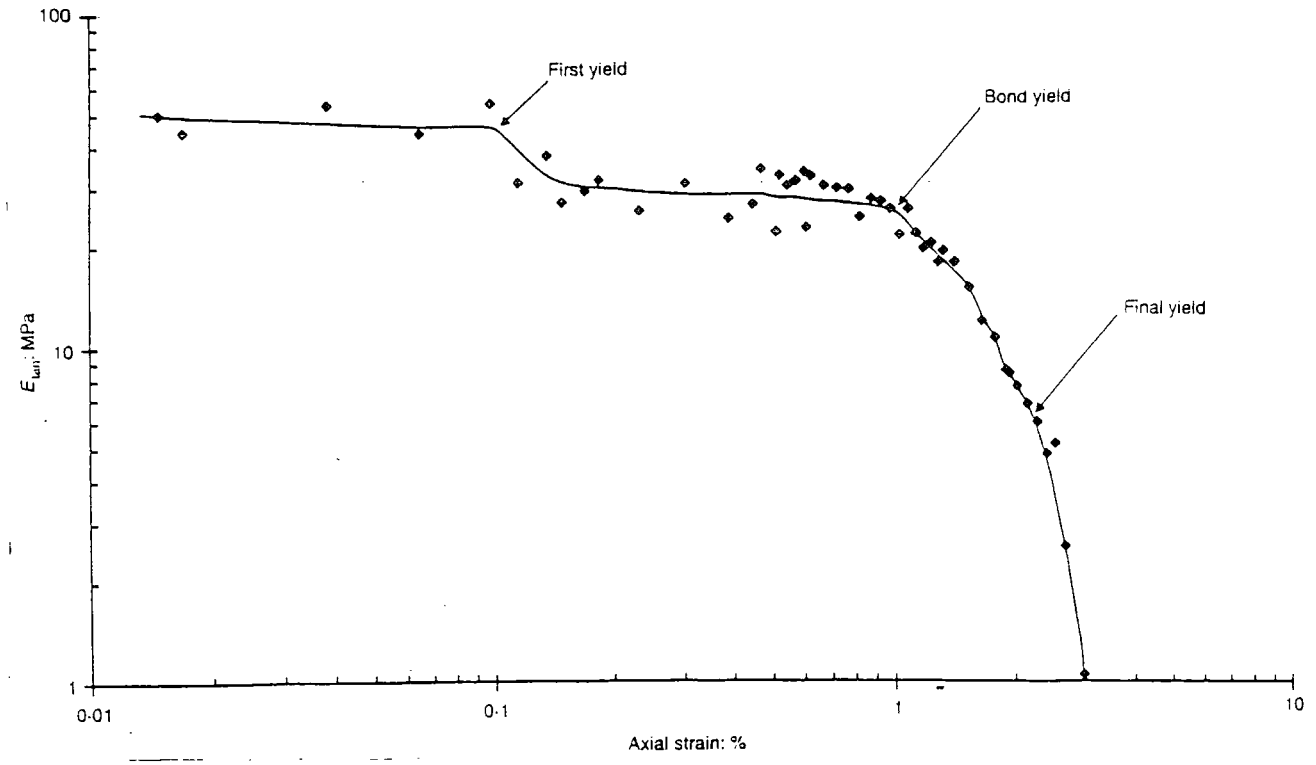

Fig. 36 Definition of three yield conditions for bonded soils (Malandraki and Toll, 2000)

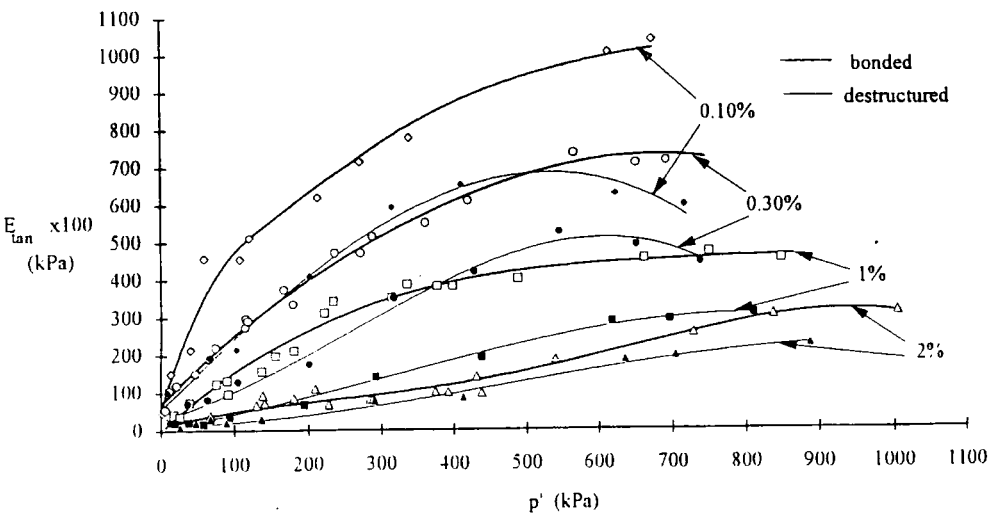

Fig.37 Tangential stiffness versus mean effective stress for the bonded and destructured soils at different percentages of strain (Malandraki and Toll, 1994)

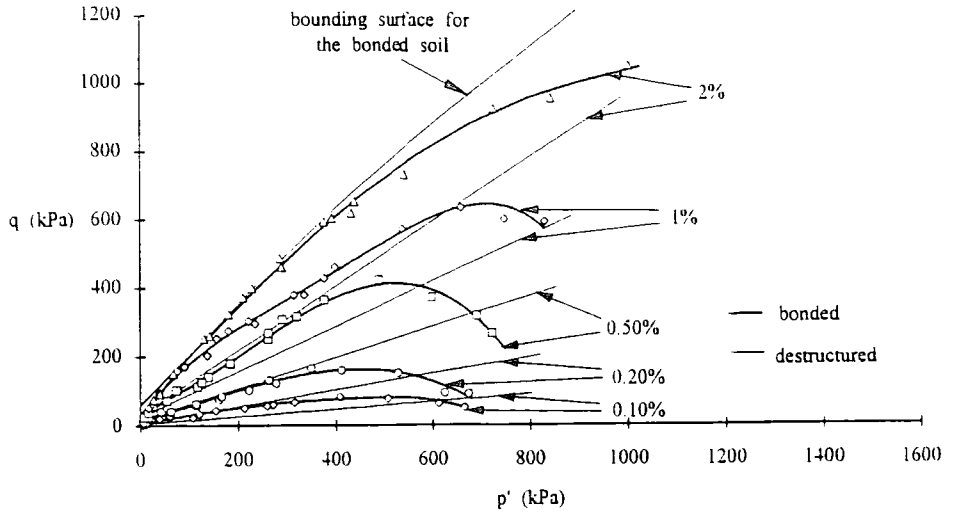

Fig. 38 Strain contours for the bonded and destructured soils plotted in the q-p′ space (Malandraki and Toll, 1994)

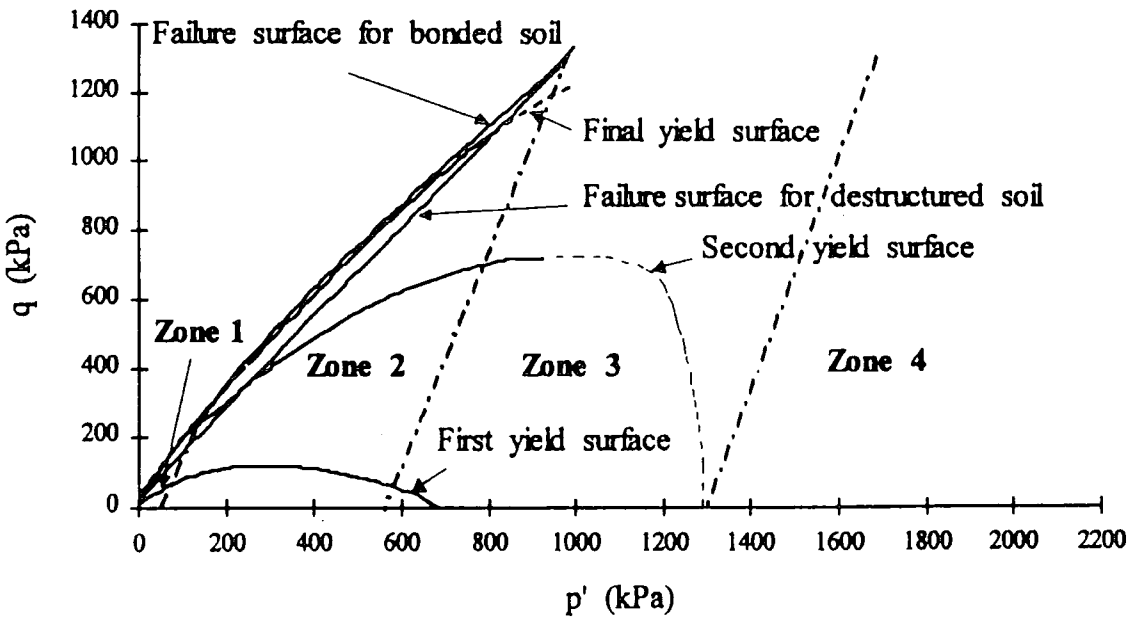

Fig.39 Four zones of behaviour for an artificially bonded soil (Malandraki and Toll, 1996)

CHAPTER 3

GEOLOGY, SAMPLE COLLECTION AND PREPARATION

3.1 Introduction

In this chapter a brief description of the geology of the study area, borehole locations and collection of undisturbed natural samples are described. Sample preparation for both natural and destructured samples is also described.

3.2 General Geology

Dhaka city is located in the central part of Bangladesh, which is situated in the southern tip of a Pleistocene terrace, the Madhupur Tract. Dhaka is characterized by

tropical, humid climatic conditions. This is marked by cool and short winters, long and wet hot summers with high rainfall. The mean annual rainfall is 2238mm. (Source: Bangladesh Meteorological Department). The city is bounded by the Turag River in the north-west, the Buriganga River in the south and southeast, the Balu River in the east and the Buriganga and the Turag River in the west (figure 3.1). Most of the streams and rivers are seasonal, ill-drained and fed by monsoon water.

Dhaka city occupies land of low relief with many low depressions. The city shows significant variation in the ground surface. The surface elevation of the city ranges from 1.5m to 15m above Mean sea level, reaching a maximum in the Mirpur Area and a minimum at the periphery of the city. The average elevation of the city is about 6m above Mean sea level (M.S.L.).

The reddish brown clayey deposits which outcrop over the land surface of Madhupur Tract is the oldest exposed rock in the study area (figure 3.2). These reddish brown soils contain ferruginous cements, concretions and nodules. It is unconformably underlain by Dupi Tila Formation and overlain by the recent Alluvium. Islam (1974) and Bakr (1977) named these reddish brown deposits the Madhupur Clay without giving a proper lithostratigraphical rank. Alam and Khan (1980) subdivided the Madhupur Clay into two lithologic sub units: the Lower Mottled Clay sub unit and the Upper Red Clay sub unit. Monsur (1990) renamed the Madhupur Clay Formation as the Madhupur Clay and Sand Formation and produced a formal stratigraphical classification. The alluvial deposits that overlie the Madhupur Clay has also been given new nomenclature by Monsur (1990) and called the Basabo Silty Clay Formation. Alam et al. (1990) of the Geological Survey of Bangladesh renamed the Madhupur Clay Formation as a Madhupur Clay Residuum (a residual soil horizon).

Monsur (1995) noted that the reddish brown colour of the Madhupur formations is clearly related to iron compounds. Monsur (1995) also mentioned that these are insitu developed soil and do not represent transported or re-deposited soil materials. He also mentioned that these soils have undergone intensive weathering processes that released Fe ions in a free state and appeared in the form of nodules or in association with clay. The well oxygenated upper members of these formations favoured the formation of haematite. The abundance of haematite and goethite minerals in Madhupur clay soils is also reported by Monsur. A generalized stratigraphical succession of the Madhupur area (after Monsur, 1990) is set out in Table 3.1.

Table: 3.1 Stratigraphic succession of the Madhupur area (after Monsur, 1990).

Chrono-stratigraphy		Formation	Member	Bed		Lithologic description	Thickness (m)
Series	Sub series/ Stage						
HOLOCENE	Sub Atlantic	Basabo Silty Clay	Matuail Clay	Silty clay		Pale olive (5Y 6/4) very sticky silty clay with modern soil on top. _____ Unconformity_____ Light yellowish brown (10 YR 6/4) very sticky clayey silt, containing plenty of plant roots and iron concretions. _____Unconformity_____ Yellowish red silty clay _____Unconformity_____ Pale yellow (5Y 7/3) clayey silt, containing wood fragments and iron concretions. _____Unconformity_____ Light bluish gray (5B 7/1) sand-silt-clay to sand. It contains plant roots, wood fragments and Iron concretions. _____Unconformity_____	5
	Sub Boreal			Clayey silt			
	Atlantic		Gul shan Sand	Silty clay			
	Boreal			Clayey silt			
	Pre Boreal			Sand			
PLEISTOCENE	Middle	Madhupur Clay and Sand		Kalsi bed	1	Pale yellowish brown with light brown spotted sandy clay _____Unconformity_____	2
	Lower				2	Yellowish brown silty clay, containing iron concretions. _____Unconformity_____	4
			Dhaka Clay			Red (2.5 YR 4/6) with reddish yellow (7.5 YR 6/6) spots. It is highly weathered , containing iron concretions, pipe stems. Calcareous nodules, plant roots and manganese spots. _____Unconformity_____	5
			Mirpur Silty Clay			Light brown (5YR 5/6) sandy clay to clayey sand with moderate reddish brown (10 R 4/6) spots, containing iron concretions, pipe stems, plant roots and manganese spots. _____Unconformity_____	4
			Bhaluka Sand			Pale yellowish brown (10 YR 6/2) silty sand to sand with light brown (5YR 5/6) reduction spots. It is highly micaceous and cross bedded. It contains some intraformational clayey beds. _____Unconformity_____	4
PLIO-CENE		Dupi Tila				Quartz chalcedony gravel bed oxidized sands with intraformational clay beds. It contains large silicified wood fragments.	

3.3 Borehole Locations

The area investigated is located between latitudes $23^0$42′N to $23^0$50′N and longitudes from $90^0$22′E to $90^0$26′E. Three boreholes were drilled in the area to collect undisturbed natural samples. The borehole locations are shown in figure 3.1 and the borehole information is listed in Table 3.2. The detailed description of soils from the three boreholes is given in Tables 3.3, 3.4 and 3.5.

Table 3.2 Borehole information

Borehole number	Location	Latitudes	Longitudes
One	Mirpur (site 1)	$23^0$49.5′N to $23^0$49.8′N	$90^0$22.5′E to $90^0$22.8′E
Two	Curzon Hall	$23^0$43.6′N to $23^0$43.8′N	$90^0$24.5′E to $90^0$24.8′E
Three	Mirpur (site 2)	$23^0$48.3′N to $23^0$48.5′N	$90^0$21.7′E to $90^0$21.9′E

Table: 3.3 Description of soils of borehole one

Depth (m)	**Soil description**
0-0.91	Firm to stiff, light grey to reddish mottled fine CLAY with SILT
0.91-1.37	Firm to stiff, highly oxidized, reddish mottled, plastic fine CLAY with SILT.
1.37-2.13	Stiff, reddish, containing some ferruginous concretions, highly oxidized, SILT with CLAY.
2.13-5.08	Stiff, mostly reddish, occasionally reddish brown, mottled, some ferruginous concretions and iron nodules are present, highly oxidized, SILTS with CLAY.
5.08-6.40	Stiff, reddish brown, mottled SILTS with CLAY.
6.40-8.83	Stiff, contain some ferruginous concretions and some mica particles, mostly reddish brown to yellowish brown SILTS with CLAY.
8.83-10.0	Stiff, grains are of different sizes, some mica and sand particles present, less oxidized, mainly reddish brown to yellowish brown deposits of SILT with CLAY.

Table: 3.4 Description of soils of borehole two

Depth (m)	Soil description
0-1.05	Firm to stiff, plastic, light grey to reddish mottled fine CLAY with SILT. Some carbonaceous matter present.
1.05-1.98	Firm to stiff, plastic, highly oxidized, reddish grey to yellowish brown mottled CLAY with SILT.
1.98-2.59	Firm to stiff, reddish, plastic and containing ferruginous concretions, highly oxidized deposits of SILTS and CLAY.
2.59-3.20	Stiff, reddish, SILTS with CLAY. Some ferruginous concretions present.
3.20-4.11	Stiff, mostly reddish, sometimes grey and reddish brown, mottled, some ferruginous concretions and iron nodules are present, highly oxidized deposits of SILTS with CLAY.
4.11-4.50	Stiff, some ferruginous concretions are present, mainly reddish to reddish brown deposits of SILT with CLAY.
4.50-5.33	Stiff, contain ferruginous concretions and iron nodules, mainly reddish to reddish brown SILTS with CLAY.
5.33-5.94	Stiff , contain some mica & ferruginous concretions, reddish brown to yellowish brown SILTS with CLAY
5.94-6.40	Stiff, reddish to yellowish brown deposits of SILT with CLAY. Some sand and mica.particles present,
6.40-7.16	Yelowish brown to reddish brown, mainly medium dense to loose SANDS, SILTS and CLAYare also present.

Table: 3.5 Description of soils of borehole three

Depth (m)	Soil description
0-0.87	Firm to stiff, light grey to reddish mottled fine CLAY with SILT.
0.87-1.50	Firm to stiff, light grey to reddish mottled fine CLAY with SILT.
1.50-2.94	Firm to stiff, highly oxidized, reddish mottled CLAY with SILT.
2.94-4.53	Stiff, mostly reddish, containing some ferruginous concretions and iron nodules, highly oxidized, SILTS with CLAY.
4.53-5.55	Stiff, mainly reddish brown to yellowish brown SILTS with CLAY.
5.55-6.19	Stiff, mostly reddish to reddish brown deposits, some iron nodules present, highly oxidized, SILTS with CLAY.
6.19-7.95	Stiff, contain some ferruginous concretions and iron nodules, some mica are also present, reddish brown to yellowish brown SILTS with CLAY.
7.95-9.38	Stiff, some mica and sand particles are present, less oxidized, reddish brown to yellowish brown deposits of SILT with CLAY.
9.38-10.80	Stiff, brownish to reddish brown deposits of SILT with CLAY. Some sand and mica.particles present.

3.4 Sampling

Undisturbed natural samples were collected in the field from three different boreholes within the same geologic formation at three different locations. The borehole information is given in Table 3.2. The samples were recovered using a standard 100mm diameter (U100) open tube drive sampler (of length approximately 450 mm) with the technical assistance of a local engineering firm.

Boreholes were advanced by a cable tool percussion rig. Before a sample was taken, the bottom of the borehole was cleared of loose or disturbed material as far as possible. When borehole advancement proceeded, the hole was supported by using a steel liner. After reaching the desired sampling depth the boring tools were detached and replaced with rods equipped with a drop hammer. The open tube U100 sampler (with an area ratio of about 30%) was attached at the bottom of the drilling rod. It was equipped with a hard steel cutting shoe at the front end, and a driving shoe at the other. The sampler was then pushed into the ground with the drop hammer. When the sampler reached the required depth, it is then withdrawn from the ground to the surface where both shoes were removed. The whole process was repeated several times to collect samples at different depths.

Approximately 50 mm thickness of soil material was removed from each end of the recovered samples. The sample recovered from the sampler were initially coated with a layer of 'cling film' and then sealed immediately with paraffin wax. The top and bottom end of each sample was marked. The samples were then tightly packed with two layers of aluminium foil. All samples, after sampling, were kept upright both during storage and transportation.

3.5 Preparation of undisturbed natural sample for triaxial testing

Before each test, undisturbed natural samples were trimmed carefully with the help of very sharp knife. Cylindrical test specimens of length 76 mm. and diameter 38 mm. were prepared vertically from the central core part of the U100 tube. A rotary soil trimmer apparatus was used during trimming. After removing the sample from the aluminium foil and cutting its ends parallel to each other, the sample was placed between the plattens of the rotary trimmer. The sample was then trimmed approximately to the required shape and dimension (38x76 mm) with a sharp knife. A brass mould, 38 mm in internal diameter and 76 mm long, split along its axis was used to hold the sample while its ends were being trimmed. It was also used for setting the height of the specimen.

Immediately after trimming, the sample was then weighed accurately to an accuracy of 0.01 gm. The height and diameter of each sample was measured at a number of points with a slide caliper. The sample was then placed immediately in the triaxial apparatus. The trimmings were then placed in a airtight plastic bag to prepare destructured samples from the same material.

3.6 Destructured sample preparation

Vaughan (1988) mentioned that the behaviour of soils with bonded structure is best understood through comparing their properties with those of the same soils in a remoulded and destructured condition. In this study the destructured samples were prepared from the trimmed materials cut from around the natural samples.

The trimmed material of each sample was first mixed with sufficient distilled water in a bucket to loosen the sample and to separate all the particles of the sample without loosing or breaking any particles. For mixing with distilled water the bucket was placed in a mechanical shaker for half an hour. The trimmed material was than completely separated and a water slurry was produced. This slurry was then air dried. The air dried material was then mixed with distilled water to produce a paste with the same water content as in the natural sample. The paste was then wrapped in 'cling film' and sealed in a air tight plastic bag and kept in a sealed container for 3 to 5 days to allow equlibration. After attaining the desired moisture content the material was then used to prepare a sample of dimension 38x 76 mm in a cylindrical mould in six layers with the same void ratio and dry density. The weight, length and diameter of the prepared sample were measured and the sample was then placed in the triaxial cell.

3.7 Summary

In this chapter a brief description of the geology of the study area is given. The undisturbed natural sample collection and sample preparation technique is discussed. A description of destructured sample preparation is also given.

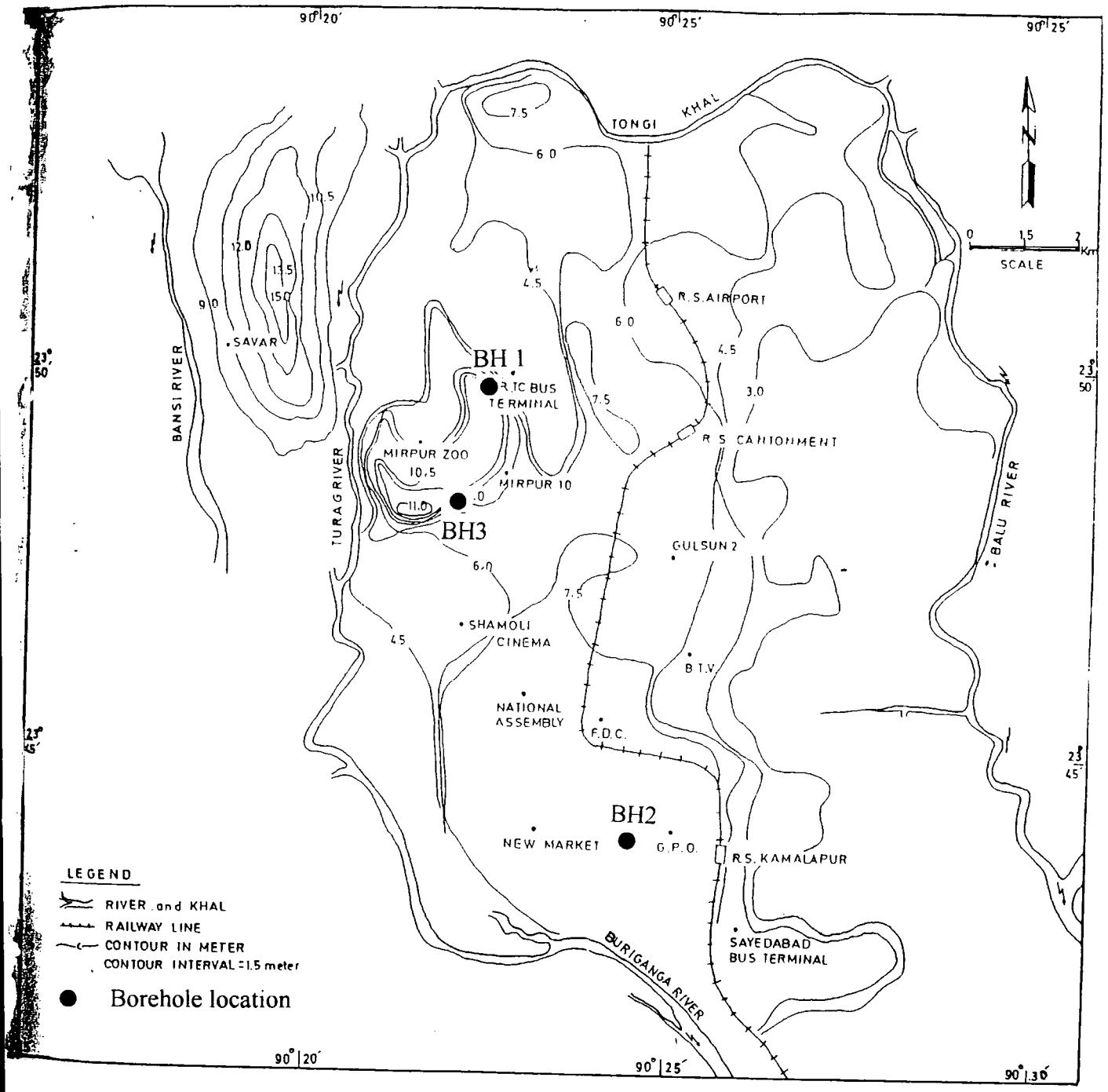

Fig.3.1 Map showing borehole locations of the study area

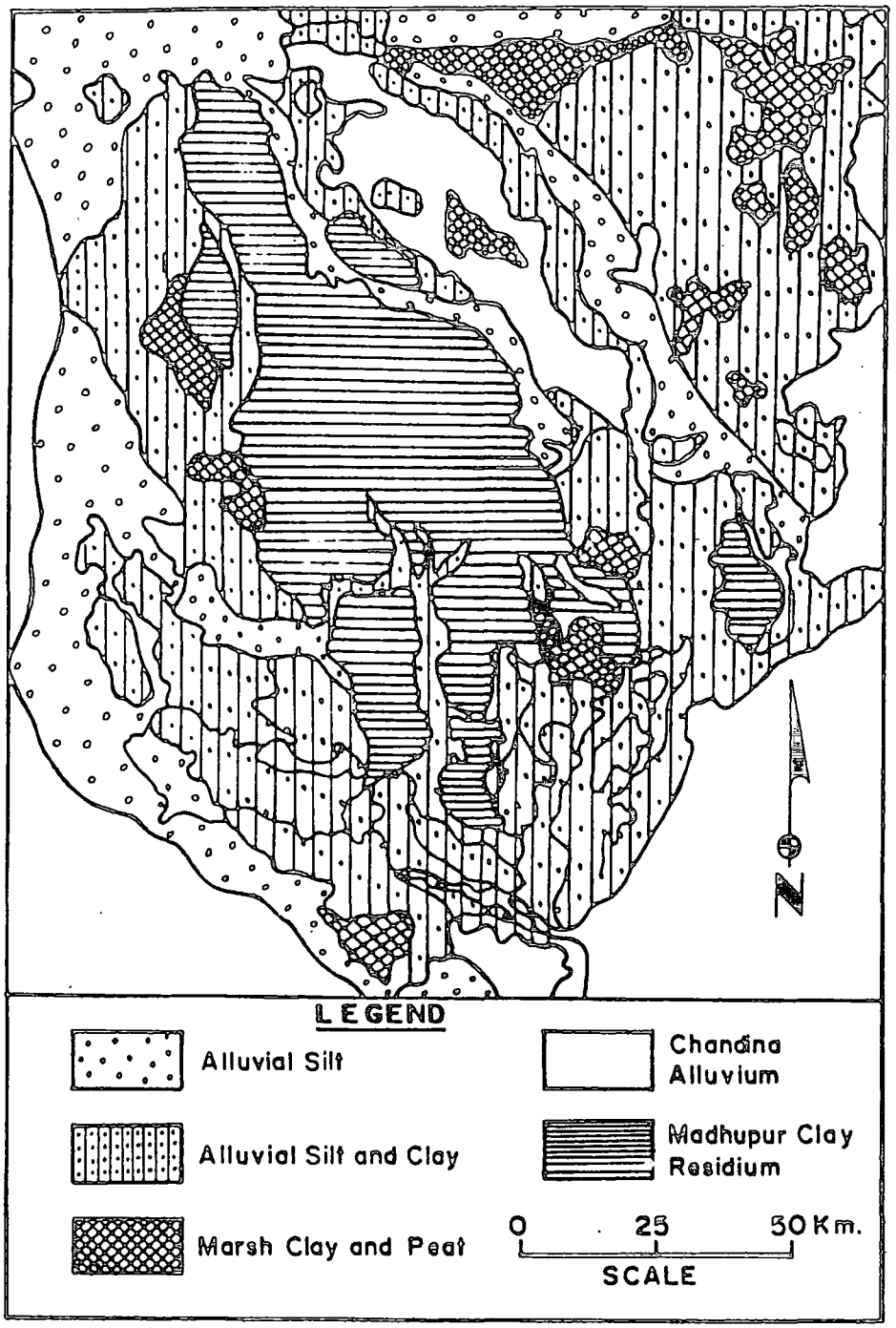

Modified after Alam et.al (1990)

Fig.3.2 Geological Map of Dhaka Region.

CHAPTER 4

Experimental Methods

4.1 Introduction

This chapter describes in brief, the experimental methods of different laboratory investigations carried out on the tropical clay soils of Dhaka, Bangladesh. The experimental programme is shown in figure 4.1. Basic classification test procedures are described and X-ray diffraction (X.R.D.) and Scanning electron microscope (S.E.M.) methods to evaluate mineralogy and fabric of the soils are discussed. Oedometer test procedures are then outlined before the procedures used in triaxial testsing are described in detail.

4.2 Basic Geotechnical parameters

All the basic geotechnical parameters including moisture content tests, particle size distribution, specific gravity tests, Atterberg consistency limits were determined in accordance with the British Standards BS1377 (1990).

The moisture content test is detailed in BS1377 (1990): Part 2.3.2 to determine the moisture content, w of a sample. In this method all the samples were dried in an oven at a temperature of 105^0 C for 24 hours.

Particle size distribution was evaluated by using both the dry and wet sieving method. Particles larger than 63μm retained on the 63μm sieve were air dried and sieved by using different BS test sieves as mentioned in BS1377 (1990) part 2.9.3. After washing, pipette method was used for grain size analysis (size less than 63 μm) by using their settling velocity according to Stoke's Law. This method is described in BS 1377: Part 2:9:4. Sodium hexametaphosphate dispersant solution was used for wet sieving.

Specific gravity measurements of the samples were performed by the pyknometer method in accordance with the British Standard as mentioned in BS1377 (1990): Part 2:8:3.

The Atterberg Limit tests on the natural- and air- dried samples were carried out after first sieving the soil on a 425 μm. sieve. The weight of the soil used for the natural- and air- dried states was determined by taking a second sample of similar

size each time and measuring water content. The natural samples were prepared in an undried state. The air-dry samples were prepared by spreading the material out in trays in the laboratory and leaving it open to the air for at least 6 days. The room temperature was 25° C. Before commencing testing each sample was mixed thoroughly with water and storing it in an airtight plastic bag overnight. Liquid Limits of the selected samples were determined by using the cone penetrometer method. Plastic Limits were also performed by the rolling thread method. The Liquid Limit, Plastic Limit and Plasticity Index methods are described in BS1377 (1990): Part 2.4.3, 2.5.3 and 2.5.4.

4.3 X-Ray Diffraction (X.R.D.).

X-ray Diffraction technique is the most satisfactory method for the identification of clay minerals (Grim, 1962). Mineralogy of the tropical clay soils of Dhaka was evaluated by using X-ray Diffraction technique.

The samples were analysed by detecting a stream of X-rays projected onto the samples placed on a glass slide, whilst it was rotated at a set of speeds. The beam was directed onto the particle lattice of the various crystals, which gave characteristic peaks when diverted to a receiver. The analysis of the samples were carried out on randomly oriented powder specimens in circular aluminium backfilled cavity mounts, with each sample being scanned from 2.5-80^0 2θ at a speed of 0.02^0/s. In this study, the X-ray diffraction was performed by a x-ray radiation tube with a detecting recording system. Two types of random powder sample, one from whole soil and the other from clay size fraction, were mounted in the circular cavity mounts for identification of minerals. All the whole samples were first air dried at room temperature and then ground to fine powder. Clay size fine fractions obtained

from pipette analysis were also air dried at room temperature before mounting. Copper radiation (CuKα) was used for the analysis. The spacing between the phases of atoms in the crystals (d-spacings) based on the corresponding diffraction angle (2θ) were used to identify individual minerals. The angle 2θ is available from the diffractogram. The interplanar spacings (d-spacings) for each peak corresponding to each value of 2θ are read directly from the standard table for copper radiation. The results are discussed in chapter 5.

4.4 Scanning Electron Microscope (S.E.M.).

Microfabric can be observed by using the Scanning Electron Microscope (SEM). The main aim of the SEM study was to evaluate the fabric of the soil. Some selected specimens from three boreholes were examined by using a Scanning Electron Microscope to study the fabric of the soil. The Scanning Electron Microscope was linked with an energy dispersive spectrometer system, which was used to identify the elemental composition of the soil by using energy dispersive x-ray spectrum (EDX). The SEM images were taken with an accelerating voltage of 20 kV.

In this study very thin prismatic specimens approximately 0.2 cm cross section and 1cm in length were first trimmed from the bulk sample with the help of a sharp knife. The samples were then air dried and secured to the 10mm holding stub using silver dag solution. The silver dag solution holds the samples securely on the stub. Before coating, the trimmed samples were cleaned by a jet of air to remove loose material from the top of the samples. The specimens were then sputter coated with a thin layer of gold to ensure good conduction across the stub. Applying a thin coat of gold on the specimen allows a clearer image to be obtained. After coating, the sample was then placed in the specimen holding chamber of the Scanning Electron

Microscope for viewing. The identified images were saved with a help of a computer. The elemental composition of soils of a particular area of the image was also observed by studying the EDX spectra. The SEM and EDX results are discussed in chapter 5.

4.5 Oedometer consolidation tests

One dimensional multi stage Oedometer consolidation tests were performed by using an Oedometer according to BS1377 (1990): Part 5.3. Cylindrical undisturbed samples were used for the test. The undisturbed samples were trimmed with a cutting ring and placed in the consolidation pot. Two porous plates were placed at the top and bottom of the samples. Loads of 50, 100, 200, 400, 800 and 1600 kPa were applied to the beam. The amount of each load increment was carried out as mentioned in BS1377 (1990).

4.6 Triaxial testing

4.6.1 Testing details

Consolidated undrained triaxial tests with pore water pressure measurements and drained triaxial tests were carried out on the undisturbed natural and destructured samples collected from three different boreholes. A computer controlled conventional Triaxial Cell with the usual electronic transducers (volume gauge, load cell, external displacement transducer and cell and pore pressure transducers) was used to carry out all the triaxial tests. The tests were monitored using the TRIAX program developed by Toll (1993). A pair of electrolevels (as described by Jardine et al.1984) for local measurement of axial strain (up to 2%) was used in all the tests. A pore water pressure probe (as described by Hight, 1982) was also used at the mid

height of the specimen for measuring the pore pressure within the samples in addition to the standard base measurement. All samples were initially saturated and were subjected to isotropic consolidation before shearing.

The computer control system runs on an IBM compatible PC and provides data acquisition and calibration facilities. Stepper motor driven air valves were used for controlling the cell and back pressures. They are able to be controlled in increments of 0.1 kPa, in the range of 10-800 kPa. A Measurement Systems Ltd. Datascan 7020 was used for data logging, which provides a resolution of 0.6μV. The unit can handle up to 16 transducers on different channels. The user specifies the control parameters in the form of equations. All commands from the user are given through the function keys and thus full flexibility of the system is given to the user.

The software can display up to four units. These are:

i. A clock window displays time, date and the stage of the test

ii. A monitor window displays output from the selected transducers.

iii. A plot window displaying a continuous plot of user selected variables.

iv. A calculation window provides continuously updated values of the user selected variables.

The system can deal with a test which comprises up to 100 different stages. The test proceeds from stage to stage by a series of alarms. These alarms are specified by the user in the form of equations (Toll, 1993). An example of the stage editor (in which the control variables are defined) is shown in figure 4.2.

In figure 4.2, box number 1 controls the back pressure and it is maintained constant at a value of 300 kPa, box number 2 controls the effective cell pressure (cell') and which is held constant at a value of 5kPa. Boxes 3 and 4 which can be used to control the ram pressure or a constant rate of strain pump (CRSP) are not used in this saturation stage. No alarms are needed since user intervention is used to decide when to proceed to the next stage of the test.

A tolerance band of 0.5 was used on each side of the hold value within which no control is necessary. Only if the calculated value falls outside the tolerance are pressures increased or decreased. The maximum number of pulses provides both a 'safety net' to avoid large numbers of pulses being sent to one controller without adjusting others, and also a means of specifying the number of pulses required to bring variables back within tolerance. In figure 4.2, the maximum number of pulses selected for box 1 and 2 are 10 and 20 respectively.

The computer controlled Triaxial Cell running with the TRIAX program is capable of taking readings for all aspects of the specimens from the different transducers through a data logger linked to the computer. Pressure transducers (of resolution 0.1 kPa) were used to measure the cell and back pressures with a capacity of 1000 kPa. External vertical displacements were measured with an external displacement transducer (of resolution 0.005mm) which had a range of 25 mm. An Imperial College Load Cell (resolution 0.1N) of capacity 4413 N was used to measure the axial load. An Imperial College Bellofram type volume gauge (of resolution 0.01 cm^3) having 100 cm^3 capacity was used to measure the volume change and was connected into the back pressure line. A miniature pore water probe of resolution 0.1 kPa (as described by Hight, 1982) was also used at the mid height of the specimen (as shown in figure 4.3) to measure the pore water pressure within the samples. For

this type of probe, a hole is cut in the membrane and a rubber holder for the transducer is inserted. As a result the pore water transducer has direct contact with the specimen. The pore water transducer sits in a holder installed within the membrane surrounding the sample. Liquid latex rubber is used to seal everything. Two internal strain gauges as described by Jardine et al. (1984) for local measurement of axial strain (up to 2%) was used to measure the internal strain and initial stiffness of the soil (figure 4.4). These gauges can resolve axial strains of ± 0.001%.

All the transducers were calibrated before testing. A Budenberg Dead Weight Tester was used for the calibration of the cell and back pressure transducers. The external vertical displacement transducer and the two internal electrolevels were bench calibrated using a Vernier Micrometer. The volume gauge was calibrated using a $25cm^3$ burette.

Polynomial regression curves (up to 2nd order) were then fitted to the calibration data. The regression coefficients were then stored in the computer and used to convert from voltages to engineering units.

4.6.2. Saturation of the samples

The saturation stage of the samples involves the increase of pore water pressure (p.w.p.) so that air in the voids is eliminated. The prepared samples were placed on to the bottom pedestal of the triaxial apparatus. Two porous disks (kept under de-aired water until required) were used at the top and bottom of the sample. After setting up samples in the triaxial apparatus, the cell was filled with water and the samples were flushed through with the deaired water under a small pressure gradient (10 kPa) for 24 hours. In this study, after initially flushing out air by flowing water

through the sample, the pore water pressure was increased in a controlled manner by the application of back pressure, so that air in the voids is forced into solution.

It was ensured that the back pressure does not by itself change the effective stress. To maintain this, the cell and the back pressures were raised simultaneously by maintaining a constant difference between them. The back pressure was always a little less than the cell pressure to ensure that the effective stress remains positive. The effective stress of the sample was always maintained constant at a value of 5 kPa. A back pressure of 300 kPa was then applied to the samples for twenty four hours, before testing the pore pressure coefficient (B) value. The parameter B was calculated by increasing the cell pressure by 50 kPa with the back pressure line closed to measure the change in pore water pressure. The pore pressure coefficient B was calculated from the equation $B = \Delta u / \Delta\sigma_3$. In this equation, Δu is the change in pore pressure and $\Delta\sigma_3$ is the change in cell pressure. If the B value was not as high as required then the cell pressure was reduced to its original value and the back pressure reapplied. The back pressure was maintained until a value of B of at least 0.98 was achieved. Most of the samples attained a value of B = 0.98 within 2-3 days when a back pressure of 300 kPa was applied. However, due to stress limitations of the system, samples which were consolidated at a stresses higher than 400 kPa were saturated by applying a back pressure of 200 kPa. In that case, saturation time was extended. These samples required 4-5 days to achieve a B value of 0.98.

4.6.3. Triaxial consolidation

In the consolidation stage the sample was consolidated isotropically under a confining pressure by allowing water to drain out into the back pressure system, so that the pore water pressure gradually falls until it equals the back pressure. This was done by adjusting the cell pressure and back pressure so that their difference was equal to the required effective confining pressure of the test. The resulting pore pressure in the sample was allowed to dissipate by the process of consolidation.

Drainage of water results in a decrease in volume and an increase in the effective stress, which after consolidation was taken to be equal to the difference between the confining pressure and the mean pore pressure remaining in the sample (an average of the base and probe measurements). Consolidation was allowed to continue until a steady value of volume change was obtained. It was monitored continuously in the plot window of the computer controlled system. When the time versus volume change curve on the computer screen showed a steady value, it was assumed that consolidation was complete. At the same time the back pressure and pore water pressure readings were also checked from the monitor window. It was observed that when consolidation was finished the p.w.p. reading from the probe was almost equal (± 1 kPa) to the back pressure reading. Samples were consolidated up to 24 hours at a range of confining pressures from 50 kPa up to 800 kPa before shearing.

4.6.4 Triaxial shearing

All the samples under undrained and drained shearing were sheared up to 30% of strain under a constant rate of strain of 1.25%/hr. No significant differences between base and mid hight pore water probe were observed at this rate of shear showing that there was equalization of pore water pressure throughout the sample during undrained shearing. The mid hight pore water probe under drained shearing showed a low gradient of pore water pressure in the sample. Each test on an average took 5 to 6 days to complete. The computer controlled system was used both to control the tests and to take data for different aspects of the test. Readings from the different transducers were taken initially for every second up to five minutes, and after that a scan interval of five seconds for an hour and finally every three minutes after 1% of strain up to twenty-four hours.

4.7. Summary

In this chapter all experimental methods used to carry out the laboratory tests are briefly discussed. The basic principle of the computer control system for triaxial testing is given. A brief review of the TRIAX software is also discussed.

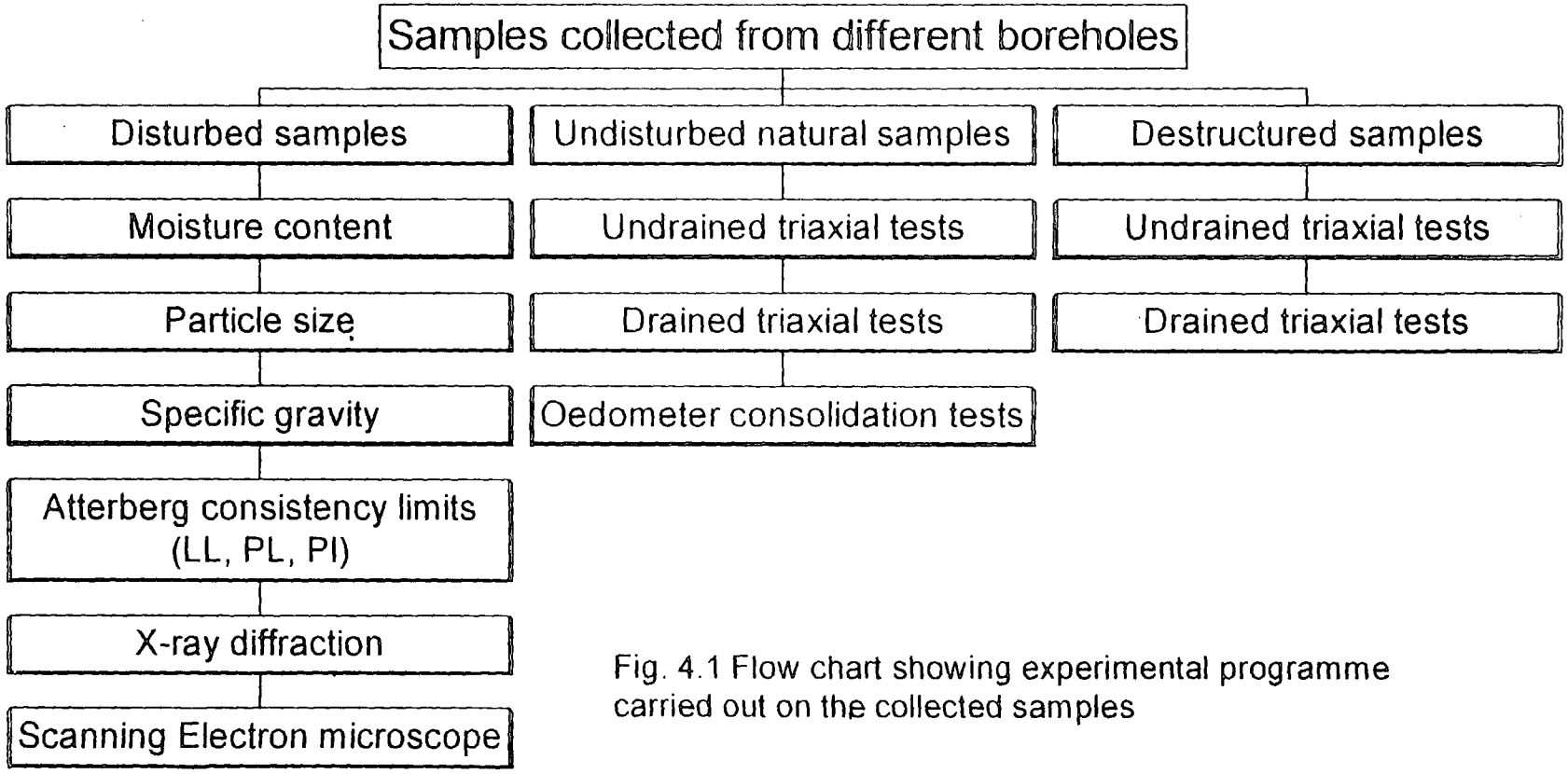

Fig. 4.1 Flow chart showing experimental programme carried out on the collected samples

STAGE 1
Stage description : SATURATION

No trigger for stage 1

Box	1 BACK	2 CELL	3 RAM	4 CRSP
Status	ON	ON	OFF	OFF
Control equation	back	cell'	Undefined	Undefined
Hold value	300	5	0	0
Tolerance	0.5	0.5	0	0
Increment	0	0	0	0
Maximum pulses	10	20	0	0

	Condition	Action
Alarm 1	Undefined	Undefined
Alarm 2	Undefined	Undefined
Alarm 3	Undefined	Undefined
Alarm 4	Undefined	Undefined
Alarm 5	Undefined	Undefined

Use Arrowed Cursor Keys to move, continue Key to leave (f10)

Fig. 4.2 A stage for controlling saturation

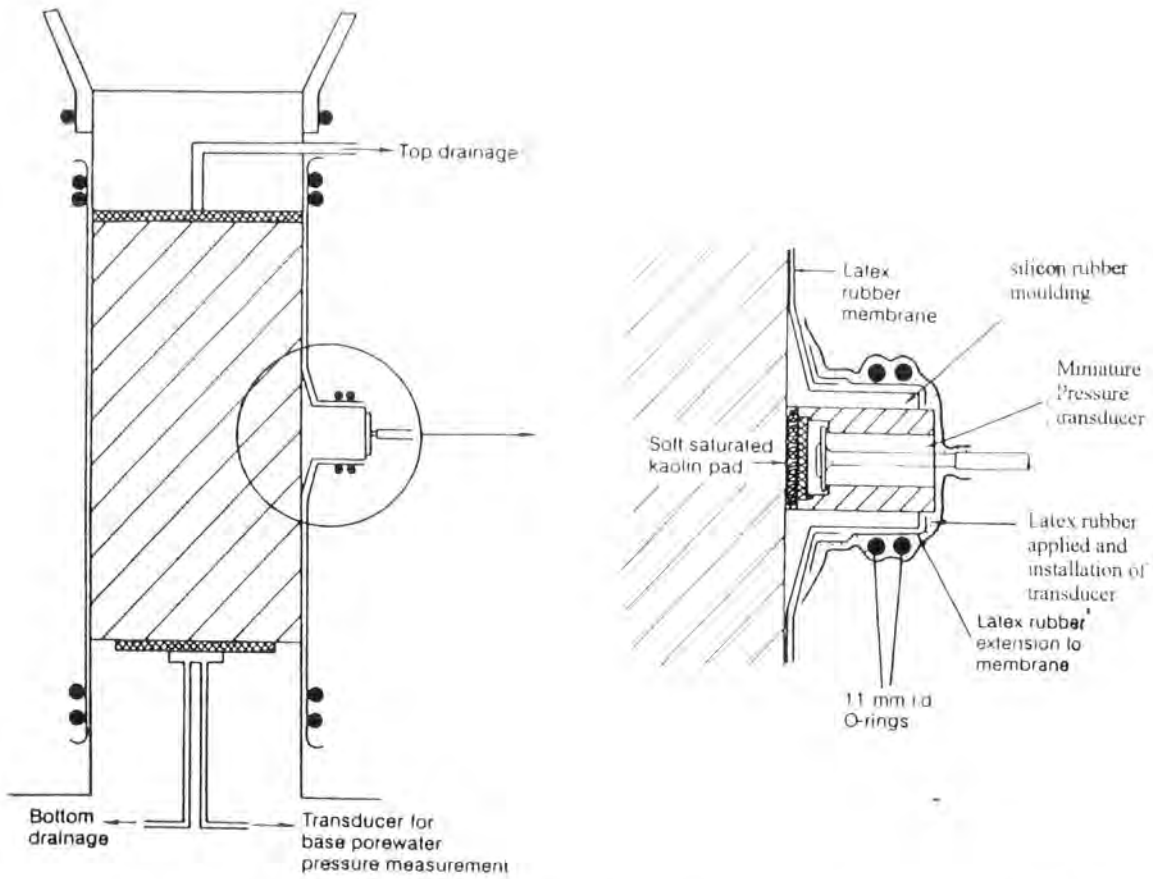

Fig. 4.3 Installation details of miniature pore water probe (after Hight, 1982)

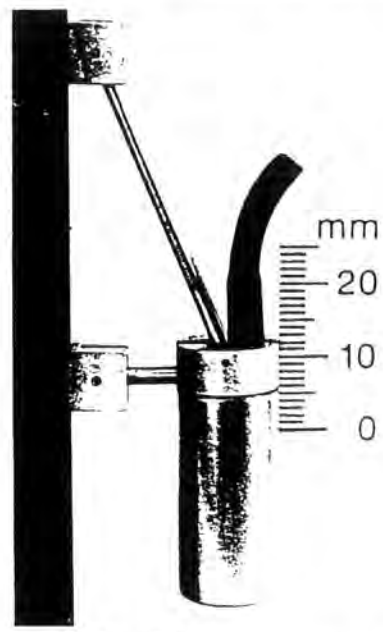

Fig. 4 4.An inclinometer gauge (after Burland 1989)

CHAPTER 5

MINERALOGY, FABRIC AND BASIC GEOTECHNICAL PARAMETERS

5.1 Introduction

In this chapter results are presented for the tropical clay soils of Dhaka in terms of mineralogy, fabric and basic geotechnical parameters. Relationships between mineralogy and basic geotechnical parameters are also discussed.

5.2 X-Ray Diffraction (X.R.D.) results

X-ray Diffraction method is one of the most important and widely used techniques for clay mineral identification. Qualitative bulk mineralogy of seven whole soil samples and five clay size fraction (less than 2μ) samples collected from three

different boreholes were determined and the results are listed in table 5.1. The principle of X-ray Diffraction and the methods of sample preparation are discussed in Chapter 4. The X-ray diffractograms of the analyzed samples are illustrated in figures 5.1 to 5.6. From the XRD results it is evident that the analyzed samples do not differ greatly in their mineral types.

Table 5.1. List of minerals identified from XRD analysis

Location (borehole nos.)	Sample numbers	Depth (m)	Identified minerals
Mirpur (borehole one)	$1S_1$ (clay fraction)	1.5-1.8	Chlorite, Kaolinite, Illite, Quartz, Illite-Quartz, Feldspar
	$1S_2$ (whole sample)	2.0-2.4	Illite, Feldspar, Kaolinite-Chlorite, Quartz, Illite-Quartz
	$1S_3$ (clay fraction)	5-5-5.9	Illite, Quartz, Orthoclase Feldspars, Chlorite, Kaolinite, Illite-Quartz
	$1S_4$ (whole sample	6.5-6.8	Illite, Quartz, Feldspar, Chlorite, Kaolinite, Illite-Quartz
Curzon Hall (borehole two)	$2S_1$ (clay fraction)	1.3-1.5	Chlorite, Illite, Quartz, Kaolinite, Feldspar, Illite-Quartz
	$2S_2$ (whole sample)	1.8-2.0	Kaolinite-Chlorite, Illite, Quartz, Feldspar, Illite-Quartz
	$2S_3$ (clay fraction)	4.5-4.8	Kaolinite-Chlorite, Illite, Quartz, Illite-Quartz
	$2S_4$ (whole sample)	6.0-6.4	Illite, Orthoclase Feldspars, Kaolinite, Quartz, Illite-Quartz
Mirpur (borehole three)	$3S_1$ (whole sample)	2.0-2.4	Chlorite-Kaolinite, Illite, Kaolinite, Quartz, Feldspar, Illite-Quartz
	$3S_2$ (whole sample)	3.5-3.8	Illite, Kaolinite, Orthoclase Feldspars, Chlorite, Illite-Quartz
	$3S_3$ (whole sample)	4.0-4.3	Illite, Muscovite, Kaolinite, Feldspars, Quartz, Illite-Quartz
	$3S_4$ (clay fraction)	5.5-5.8	Illite, Chlorite, Kaolinite, Orthoclase Feldspars, Quartz, , Illite-Quartz

Gillott (1987) mentioned that the proper estimation of clay minerals and quantitative evaluation by the X.R.D. method depends on the type of X.R.D. techniques. For

identification and estimation of clay minerals the basal plane reflections of a soil sample can be best studied by treating samples with chemicals to get a better peak width and hight ratios for estimation. The only accessible technique, which is used for this study, is not suitable for proper estimation because of coincidence of some peaks. Therefore no estimates were made to determine the percentage of each mineral and only qualitative results are given.

The diffractograms were studied for identifying minerals by comparing the observed 2-theta value for a particular peak in the diffractograms with the corresponding values of interplanar spacings (d-spacings) (figures 5.1-5.6). A list of the identified peaks with the corresponding d-spacings and 2-theta angle is given in Tables 5.2, 5.3 and 5.4. From the observed diffractograms, it was found that quartz is present in each sample and that it is quartz which is the source of most of the strong peaks visible including the largest peaks in most of the diffractograms at 3.34 Å and 4.26Å. The 3.34 Å peak of quartz is more intense than the other peaks including the peak 4.26 Å. Such increased intensity at 3.34 Å might be due to the presence of chlorite, illite and feldspar minerals. The coincidence with a strong reflection of illite or chlorite at 3.30 Å, 3.31Å would not permit it to be used as a scale of relative abundance in the samples. Therefore, the 4.26 Å peak was used to understand any relative change in quartz abundance in samples. Orthoclase feldspar appeared in several of the specimens, giving rise to the (usually small) reflection at about 3.24 Å, but is much less abundant than quartz.

The clay minerals which were identified in the samples include illite, kaolinite and chlorite. Illite, which is characterized by peaks mainly at 10, 5, 4.48 Å appeared in all samples. Kaolinite mineral was also identified which is characterized by 7.15 Å.

Table 5.2. Identification of some major peaks of different minerals from X-ray diffraction (borehole one)

Sample number	Peak number	2-Theta Angle	d-space (Å)	Identified mineral
$1S_1$	1	6.04	14.633	Chlorite
	2	8.88	9.958	Illite
	3	12.36	7.161	Kaolinite
	4	17.76	4.994	Illite
	5	19.96	4.448	Illite
	6	20.88	4.254	Quartz
	13	26.68	3.341	Illite-Quartz
	14	27.0	3.302	Illite
	15	27.48	3.246	Feldspar
	19	35.0	2.564	Quartz
	27	39.48	2.282	Quartz
	28	40.32	2.237	Quartz
	29	42.48	2.128	Quartz
	33	50.16	1.819	Quartz
	38	59.96	1.543	Quartz
$1S_2$	1	8.92	9.914	Illite
	2	12.08	7.327	Kaolinite-Chlorite
	3	17.8	4.983	Illite
	4	19.88	4.466	Kaolinite-Chlorite
	14	26.68	3.341	Illite-Quartz
	15	26.88	3.317	Illite
	16	27.04	3.298	Feldspar
	17	27.48	3.246	Feldspar
	18	27.88	3.2	Feldspar
	36	60	1.542	Quartz
$1S_3$	1	5.96	14.829	Chlorite
	2	8.8	10.049	Illite
	3	12.16	7.279	Kaolinite
	5	17.76	4.994	Illite
	7	19.92	4.457	Illite
	13	23.84	3.732	Feldspar
	15	25.28	3.523	Chlorite
	17	26.68	3.341	Illite-Quartz
	19	27.04	3.298	Feldspar
	20	27.52	3.241	Feldspar
	21	27.88	3.2	Feldspar
$1S_4$	1	8.96	9.87	Illite
	2	12.4	7.138	Kaolinite
	3	19.96	4.448	Illite
	9	25.44	3.501	Chlorite
	10	26.68	3.341	Illite-Quartz
	11	26.92	3.312	Illite
	12	27.08	3.293	Feldspar

Table 5.3. Identification of some major peaks of different minerals from X-ray diffraction (borehole two)

Sample number	Peak number	2-Theta Angle	d-space (Å)	Identified mineral
$2S_1$	1	8.88	9.958	Illite
	2	12.16	7.279	Kaolinite
	3	17.8	4.983	Illite
	4	19.84	4.475	Illite
	5	20.88	4.254	Quartz
	9	25.36	3.512	Chlorite
	10	26.64	3.346	Illite-Quartz
	11	26.88	3.317	Illite
	12	27.04	3.298	Feldspar
	13	27.52	3.241	Orthoclase
	19	34.96	2.567	Quartz
	20	36.56	2.458	Quartz
	21	36.8	2.442	Quartz
	24	39.48	2.282	Quartz
	32	59.96	1.543	Quartz
$2S_2$	1	8.84	10.003	Illite
	2	12.12	7.302	Kaolinite
	3	17.72	5.005	Illite
	6	20.88	4.254	Quartz
	9	23.88	3.726	Feldspar
	10	25.32	3.518	Kaolinite-Chlorite
	11	26.64	3.346	Illite-Quartz
	12	26.88	3.317	Illite
	13	27.04	3.298	Feldspar
	16	27.84	3.205	Feldspar
$2S_3$	1	9.02	9.804	Illite
	2	12.3	7.196	Kaolinite-Chlorite
	12	26.78	3.329	Illite-Quartz
	13	27.02	3.3	Illite
	23	35.1	2.557	Quartz
	26	36.7	2.449	Quartz
	32	39.58	2.277	Quartz
	34	40.42	2.232	Quartz
	37	42.58	2.123	Quartz
	40	50.26	1.815	Quartz
	46	60.1	1.54	Quartz
$2S_4$	1	8.84	10.003	Illite
	2	12.12	7.302	Kaolinite
	6	17.8	4.983	Illite
	7	19.88	4.466	Illite
	13	26.64	3.346	Illite-Quartz
	15	27.04	3.298	Feldspar
	16	27.52	3.241	0rthoclase

Table 5.4. Identification of some major peaks of different minerals from X-ray diffraction (borehole three)

Sample number	Peak number	2-Theta Angle	d-space (Å)	Identified mineral
$3S_1$	1	8.92	9.914	Illite
	2	12.32	7.184	Kaolinite
	3	17.84	4.972	Illite
	4	19.92	4.457	Illite
	6	20.88	4.254	Quartz
	8	25.32	3.518	Kaolinite-Chlorite
	9	26.68	3.341	Quartz-Illite
	10	27.04	3.298	Feldspar
	11	27.52	3.241	Orthoclase
	12	27.84	3.205	Feldspar
	14	34.96	2.567	Quartz
	16	36.56	2.458	Quartz
	26	42.44	2.13	Quartz
	29	50.16	1.819	Quartz
	39	59.96	1.543	Quartz
$3S_2$	1	5.72	15.451	Chlorite
	2	8.92	9.914	Illite
	3	12.36	7.161	Kaolinite
	5	17.84	4.972	Illite
	6	19.84	4.475	Illite
	14	23.8	3.739	Feldspar
	15	25.24	3.528	Chlorite
	17	26.64	3.346	Illite-Quartz
	19	27.04	3.298	Feldspar
	20	27.52	3.241	Orthoclase
$3S_3$	1	8.92	9.914	Illite
	3	17.84	4.972	Illite
	4	19.92	4.457	Illite
	9	23.92	3.72	Feldspar
	10	25.44	3.501	Kaolinite
	11	26.68	3.341	Quartz-Illite
	12	26.88	3.317	Illite
	21	35.04	2.561	Muscovite
	27	40.32	2.237	Quartz
	31	50.16	1.819	Quartz
	35	59.96	1.543	Quartz
$3S_4$	1	8.92	9.914	Illite
	2	12.4	7.138	Kaolinite
	3	17.76	4.994	Illite
	4	19.92	4.457	Illite
	7	25.36	3.512	Chlorite
	8	26.68	3.341	Quartz-Illite
	10	27.04	3.298	Feldspar

In general, the clay quartz ratio appeared higher in samples from borehole one and three than in borehole two samples. A description of the identified minerals is given below.

Non clay minerals

Quartz: Quartz is one of the most abundant minerals in all samples. The strong peaks of quartz were identified by distinctive reflections at 3.34 Å and 4.26 Å. These higher intensities might be due to the presence of muscovite and feldspar minerals. The other quartz peaks are smaller than these two largest peaks which are characterized by distinctive reflections at 2.13 Å, 1.819 Å, 1.543 Å, 2.458 Å, 2.282 Å, 2.13 Å, 2.449 Å, 2.232 Å, 2.459 Å, 2.455 Å and 2.46 Å.

Feldspars: Feldspar is present in minor amounts in all samples. K-feldspar (Orthoclase) was identified by weak reflections at 3.302 Å, 3.241 Å. Feldspar peaks were also identified at 3.72 Å, 3.73 Å and 3.26 Å.

Clay minerals

The clay minerals identified in the samples include Illite, Kaolinite and Chlorite.

Illite: Illite is the most common clay mineral present in all the samples. The identified sharp peak of Illite in all the samples indicate that they are well crystallized. Illite peaks were characterized by distinctive deflections at 10 Å, 4.48 Å, 9.93 Å, 4.98 Å, 4..994 Å, 5.01 Å, 3.30 Å and 3.329 Å.

Kaolinite: Kaolinite was also identified in the soil samples. In the diffractograms, Kaolinites were found to be poorly crystallized which is reflected in the diffraction patterns by the broadening and weakening of the peaks and a tendency for adjacent reflections to fuse together. The peaks characterized by deflection at 7.15 Å

establishes the presence of kaolinite mineral in the soil samples. Kaolinitic peaks were also identified by deflection at 3.501 Å. The presence of chlorite in some samples made the identification of kaolinite more complex. This is due to the similar d-spacing of kaolinite and chlorite at 3.5 Å.

Chlorite : Chlorite minerals identified in some samples are characterized by deflections at 14.633 Å, 14.829 Å, 15.45 Å and 3.50-3.53 Å. The interference of the chlorite peak with kaolinite sometimes made it difficult to identify chlorite minerals.

In borehole one samples, illite is the most dominant clay mineral (figures 5.1-5.2). Quartz peaks was found in all the samples of borehole one. A small amount of chlorite and kaolinite were also identified in some samples. Although there might be some variations in the relative percentages of clay minerals with respect to depth, a consistency was observed in the case of the minerals identified. A chlorite peak was clearly identified in sample $1S_1$ (figure 5.1). Samples $1S_2$ and $1S_4$ did not show any prominent peak of chlorite, which might be due to coincidence of the chlorite peak with kaolinite. There is no significant variation in illite peak intensities in the analyzed samples at different depths.

The common minerals found in the borehole two samples are illite, quartz, kaolinite and feldspar (figures 5.3-5.4). Although no individual chlorite peak was identified in borehole two samples, a peak of kaolinite-chlorite was observed for samples $2S_2$ and $2S_3$. Chlorite minerals may be confused with the kaolinite minerals because of their similar reflections.

Illite is the dominant mineral in all the samples of borehole three (figures 5.5-5.6) Next in predominance is quartz, feldspar etc. Kaolinite peaks are comparatively less. Chlorite is absent in most of the samples, which might be due to the destruction of chlorite due to weathering or the chlorite peaks may be confused with kaolinite

because of their similar reflections. Although no estimates were made regarding the percentages of clay minerals, there might have some variations in the relative percentages of clay minerals with respect to depth.

From the diffractograms for the three boreholes it was found that the samples broadly showed a consistency of identified minerals. Illite and kaolinite peak intensities did not show any significant variation in their reflection intensities with respect to depth and also at different sites. Although the samples were collected from the same geological formation, there might be some differences in the relative percentages of each mineral with respect to depth. Proper estimation of relative percentages of each mineral can only be determined by using other X.R.D. techniques (Gillott, 1987). As the present investigation to evaluate mineralogy had some limitations because of the accessibility of the X.R.D. techniques, it needs further investigation.

5.3. Scanning Electron Microscope (S.E.M.) results

The fabric of the tropical clay soils of Dhaka was studied by using Scanning Electron Microscope photographs. Five samples were selected from three different boreholes of the same geological formation to study the microfabric of the soil. Several photomicrographs of each sample were studied to evaluate the microstructure of the soil. All the photomicrographs were taken to study microfabric with a magnification of 'x1000'. It was found difficult to get the surface contrast of the intergranular spaces of the analyzed samples with other magnifications. It was observed that the intergranular spaces were distinguishable with certainty with the magnification used (x1000). Therefore, this magnification was used throughout to study the microfabric of the soils. E.D.X. (Energy Dispersive X-ray spectrum) of some selected areas of each sample was also studied in combination with the S.E.M. micrographs to identify the nature of linkage between grains. Some E.D.X. spectra are presented to understand the elemental composition of the near surface of the

samples. Samples are named by using letters and numbers. For example $1SEM_1$ indicates a photomicrograph of borehole one sample. The initial number indicates borehole number and the subscript after the three letters indicates the number of photomicrographs of each sample. All other samples are named similarly. The Scanning Electron Micrographs of a sample from borehole one are shown in figures 5.7 and 5.8. Two different images of the same sample $1SEM_1$ are shown in these figures. Sample $1SEM_1$ was collected from a depth of 2.0 m from the surface.

It can be seen from figure 5.7 that the micrographs showed a random mixture of silt and clay flakes. The fabric of the soil showed a generally open structure of silt and clay. Silt sized grains are coated with clay. The fabric is more random due to the presence of silt grains. A few larger silt grains are present on the right side of the micrograph. A large silt size grain marked by 'X' is shown in the right bottom corner of the micrograph (figure 5.7). EDX on this grain (figure 5.9) showed mainly peaks of silicon (Si) and aluminium (Al). Iron (Fe) peak was also identified on this grain. This suggests the silt grain is coated with iron and clay, which can be justified by the identified peaks of Fe, K, Al and Si in EDX analysis. Concentrations of Si, Al and K peaks are associated with clay. Si peaks might also appear due to the deposition of silica. Fe peaks appear due to the presence of iron coating in the samples, which might be associated with the deposition of hydroxides or other chemical alteration of minerals. Other silt grains observed throughout the specimen showed similar patterns of EDX. Clay flakes appeared as clusters was observed in many parts of the micrograph and some individual platelets of clay were also observed in figure 5.7. One of the clay-encrusted areas marked by 'Z' in figure 5.7 was also analyzed. The EDX spectrum on area 'Z' of figure 5.7 showed the presence of Si, Al, K and Fe, which are the constituents of clay and iron bearing compounds (figure 5.11). As clays are aluminosilicates and silt grains generally contains silica, it was difficult to decide whether the clay flakes present between the grains are the clay alone or whether they might consist of fine silt and clay as described by Collins and McGown (1974).

Several intra and inter granular spaces which appeared as pores in figure 5.7 were also identified. In many areas of the micrograph (figure 5.7) the intra and inter granular spaces appeared as black colour. The firing of EDX in a black area marked by 'Y' (in figure 5.7) was analyzed. This EDX spectrum shown in figure 5.10 showed strong peaks of Si. Al and Fe peaks were also identified. The identified K peak is relatively weak. These peaks might be derived either by EDX firing onto material behind or from the surrounding materials of the inter and intra granular spaces, which might be associated with clay, silica or iron compounds. Therefore these aluminosilicates, silica and iron compounds derived from clay might be acted as connectors between grains. Iron compounds derived from the deposition of hydroxides at particle contacts or other chemical alteration of minerals might be acted as cementing materials to form physical linkage between grains. Other intra and inter granular spaces also showed a similar EDX pattern. In some parts of the micrograph very thin intra granular micro fracture was observed. The inter particle bonding of these materials might have an influence on the engineering behaviour of the soils.

The second image on sample $1SEM_1$ is shown in figure 5.8. It can be seen from figure 5.8 that the micrograph showed a random open microfabric and the overall fabric is similar to figure 5.7. The randomly oriented clay platelets are intermixed with large silt size grains. Most of the silt grains are coated with clay and iron. Intra and inter granular spaces are common throughout the fabric. A large inter granular pore space was observed at the left bottom side of the micrograph. EDX firing on the intra and inter granular spaces showed peaks of Fe, Si and Al from the material behind or the surrounding material. The clay cluster also showed the presence of Si, Al, K and Fe between them.

Scanning electron micrograph of two samples of borehole two is shown in figures 5.12 and 5.13. Sample $2SEM_1$ was collected from a depth of 2.5 m and the sample

$2SEM_2$ was collected from a depth of 5 m. The microfabric of figure 5.12 is characterized by numerous silt size grains intermixed by a matrix of randomly oriented clay flakes. The silt grains showed strong Si and Al peaks in EDX. Because of iron coating a Fe peak is also detected on silt grains. Randomness of clay flakes was observed throughout the specimens. Clay platelets showed K, Si, Al and Fe peaks. The EDX of clay platelets of an area marked by 'Y' in figure 5.12 is shown in figure 5.15. The intra and inter granular spaces appeared as pores were also analyzed. EDX of such an area marked by 'X' in figure 5.12 is shown in figure 5.14. EDX of area 'X' showed strong peak of silicon with peaks of Al and Fe. The presence of Fe peaks is associated with iron coating of silt grains These materials were randomly oriented throughout the specimen in between clay flakes and between grains. They can act as binding materials within the soils.

The micrograph of another sample $2SEM_2$ from the same borehole is shown in figure 5.13. This sample revealed a random, open microfabric. Clay platelets are oriented at various angles in this random fabric. Silt grains are abundant and some of them are surrounded by a matrix of randomly oriented clay flakes. The silt grains showed Si, Al and Fe peaks in EDX. The intra and inter granular spaces were also analyzed. EDX of an area marked by 'X' in figure 5.13 is shown in figure 5.16. The EDX of area 'X' showed strong Si peak with Al, K and Fe peaks. Concentrations of Al, K and Fe with silicon are due to clay and iron coating appeared from the material behind or the surrounding material.

The micrographs of borehole three samples are shown in figures 5.17 to 5.20. Some of the selected energy dispersive X-ray spectrum of these samples is shown in figures 5.21 to 5.23. Sample $3SEM_1$ was collected from a depth of 4-m and the sample $3SEM_2$ from a depth of 1.5 m. It can be seen from figure 5.17 that the sample $3SEM_1$ showed a random, open microfabric of silt and clay flakes. The silt grains and clay flakes formed inter granular spaces between them, which appeared as pores. Some intra granular pore spaces were also observed. Large silt grains are clothed by

a skin of clay flakes oriented parallel to the surface of the large particles. Clay flakes are randomly oriented in different directions in the different parts of the micrograph. One of the clay clusters marked by 'X' in figure 5.17 was analyzed by using EDX. The EDX spectrum of area 'X' in figure 5.21 showed major concentrations of Si, Al and K and Fe. Concentrations of Si, Al, and K are associated with clay and Fe concentration is due to iron coating. The iron and clay coated silt is randomly orientated throughout the fabric and formed a patchy network of bonds between grains. An area marked by 'Y' in figure 5.17 showed strong peak of Si (figure 5.22) Al, K and Fe.

Two other microfabric views of the sample $3SEM_1$ are shown in figures 5.18 and 5.19. It can be seen from figure 5.18 that the random, open microfabric is a common feature of this sample. The randomly oriented clay flakes are intermixed with silt size grains. Most of the silt grains are coated with clay and iron. In the left bottom corner of the micrograph a small part of the display showed clay flakes in almost parallel alignment which was rarely observed in other parts of the fabric. This might be due to the lower abundance of silt grains in this particular area. The third micrograph from the same sample also showed a random fabric of silt and clay flakes (figure 5.19). The silt grains are coated with iron and clay. Silt grains in some areas are surrounded by a matrix of randomly oriented clay flakes.

The micrograph of another sample ($3SEM_2$) from the same borehole is shown in figure 5.20. The clay flakes and silt grains are randomly oriented in this figure. In some parts clay flakes are intermixed with large silt size grains. The silt grains are coated with clay and iron. The clay flakes showed the concentrations of Si, Al and K peaks as observed in other samples. Several intra and inter granular spaces appeared as pores were observed throughout the samples. An area marked by 'X' in figure 5.20 showed strong peaks of Si in EDX (figure 5.23). Fe, Al and K peaks were also identified. These peaks on area 'X' mainly derived from the materials behind or the surrounding materials.

5.4 Basic geotechnical parameters

In this section some basic geotechnical parameters for the tropical clay soils of Dhaka are discussed in terms of particle size distribution, specific gravity and Atterberg consistency limits. All the test procedures were discussed in chapter 4 and the results obtained from three boreholes are presented, compared and evaluated.

5.4.1 Particle size distribution

The particle size distribution of some samples from three different boreholes is listed in Table 5.5. The graphical presentations are shown in figures 5.24 to 5.26. The percentages obtained from sedimentation and sieving are plotted on a particle size distribution curve and the relative percentages of sand-silt-clay in the samples are tabulated in Table 5.5.

Table 5.5. Particle size distribution of the tropical clay soils of Dhaka

Location/ borehole no.	Sample no.	Depth (m)	Sand (%) (0.06-2.0 mm)	Silt (%) (0.002-0.06 mm)	Clay (%) (0-0.002mm)
Borehole one/ Mirpur	1	3- 3.5	14	56	30
	2	5-5.5	17	56	27
	3	6.5-7	19	59	22
Borehole two/Curzon Hall	1	4-4.5	8	61	31
	2	5-5.5	8	59	33
	3	6-6.5	9	63	28
Borehole three/ Mirpur	1	3-3.5	12	56	32
	2	5-5.5	16	59	25
	3	6.5-7	15	63	22

From the particle size distribution results, it is observed that there is a range of variation of the particle sizes. Silts and clays constitute over 80% of particles. Silt size particles are dominant in each case. Each sample contains a higher percentage of clay than the sand fractions. It can be seen from Table 5.5 that the clay percentages are highest in borehole two samples than the other boreholes and sand percentages are higher in borehole one and three samples compared to borehole two samples. Mineralogical results suggested that these soils are composed of illite, kaolinite, quartz and feldspar minerals.

In each borehole the proportion of clay generally decreased with increasing depth except one sample in borehole two. A small variation of silt and sand size fractions at different depths was also observed in each borehole due to the natural variability of the samples. The variations of sand, silt and clay percentage with respect to depth for samples of three different boreholes are listed in Table 5.5. It is to be noted here that the particle size distribution curves for different samples showed a variation in the silt range (at 0.02 mm). Newill (1961) suggested that oven drying can cause clay particles to aggregate into clusters that may only partially be broken down by the dispersion process. Therefore the variation in the silt size grain for different samples might be due to the differences in sample dispersion.

5.4.2 Specific gravity

The specific gravity of samples from the three boreholes was determined in accordance with BS1377 (1990). Test results are presented in Table 5.6. The specific gravity of all the samples lie between 2.59 to 2.65. The specific gravity values showed a variation within a limited range at different depths and at different locations. The specific gravity values obtained are near to that for quartz and clay minerals as mentioned by Lambe and Whitman (1969). The small variations may be due to the size range, the type of clay minerals and degree of dessication or drying

(Gidigasu, 1976). Taylor (1972) pointed out that the presence of the high organic content would lower the value, whereas the presence of heavy minerals may lead to higher values. Since iron minerals can have specific gravities in excess of 3.0, the results suggest that the quantity of iron minerals present in the samples is small, otherwise a higher specific gravity would have been expected. Dumbleton and Newill (1962) mentioned that the illitic tropical clays of Kenya and Uganda show specific gravity of 2.56 and 2.75 respectively. The specific gravity values obtained for the tropical clay soils of Dhaka are close to the values reported by Dumbleton and Newill (1962).

Table 5.6. Specific gravity values of three borehole samples

Location/ borehole no.	Sample no.	Depth (m)	Specific gravity
Borehole one/ Mirpur	$1D_1$	1.5-2.0	2.61
	$1D_2$	4.0-4.5	2.65
	$1D_3$	5.0-5.5	2.59
	$1D_4$	7.0-7.5	2.60
Borehole two/ Curzon Hall	$2D_1$	1.0-1.5	2.60
	$2D_2$	2.0-2.5	2.62
	$2D_3$	4.0-4.5	2.60
	$2D_4$	6.0-6.5	2.61
Borehole three/ Mirpur	$3D_1$	1.0-1.4	2.60
	$3D_2$	3.0-3.5	2.65
	$3D_3$	4.0-4.5	2.64
	$3D_4$	5.5-6.0	2.61

5.4.3 Atterberg Limits

Atterberg consistency limits of samples from the three boreholes were determined in accordance with B.S. 1377 (1990). Liquid Limit tests were found by using cone penetrometer and the plastic limits were found by the rolling thread method as described in B.S. 1377 (1990). The results obtained are listed in Table 5.7 with the derived plasticity index values.

5.4.3.1 Liquid Limit

It can be seen from Table 5.7 that the Liquid Limit values for natural (un-dried) soils of borehole one lie between 46% to 55% and air-dried samples showed a value of 41% to 49%. The Liquid Limit values for natural soils of borehole two were in the range of 46% to 56% and those for air-dried samples in the range of 42% to 51%. The natural soils of borehole three showed Liquid Limit values of 47% to 59% and air dried borehole three samples showed values ranging from 41% to 52%. The variations of Liquid Limit values with respect to depth for natural undried soils of three borehole samples are shown in figures 5.27, 5.28 and 5.29.

Table 5.7. Atterberg Limit values of three borehole samples

Location/ borehole no.	Sample no.	Depth (m)	LL (natural)	PL (natural)	PI (natural)	LL (air-dried)	PL (air-dried)	PI (air-dried)
Borehole one/ Mirpur	$1S_1$	1.3-1.8	55	24	31	49	24	26
	$1S_2$	2.5-3.0	51	23	28	46	22	24
	$1S_3$	4.0-4.5	54	21	32	48	22	26
	$1S_4$	5.4-5.8	50	21	29	47	20	27
	$1S_5$	6.5-7.0	46	24	23	42	24	18
	$1S_6$	8-8.4	46	24	22	41	23	20
Borehole two/ Curzon Hall	$2S_1$	2.0-2.5	56	24	31	51	19	31
	$2S_2$	4.0-4.5	51	23	29	46	20	26
	$2S_3$	5.5-6.0	52	21	31	48	21	28
	$2S_4$	7.5-8.0	46	19	27	42	18	24
Borehole three/ Mirpur	$3S_1$	3.0-3.5	59	23	37	52	22	30
	$3S_2$	5.5-6.0	56	21	35	50	20	30
	$3S_3$	6.5-7.0	50	19	31	46	18	28
	$3S_4$	8.0-8.4	47	17	30	41	16	25

Broadly a consistency of Liquid Limit values with small variations was observed at different depths and also at different sites. The small range of variations of the Liquid Limit values at different depths and also at different sites might be due to the particle size variations and type of clay minerals present in each sample. The difference between the consistency limit values of natural and air-dried samples might be due to the alteration of minerals and mineral structure (permanent changes) on drying (Fookes, 1997).

BS1377 (1990) mentioned that in low plasticity clays the Liquid Limit is less than 30%, in intermediate plasticity clays the Liquid Limit ranges from 35% to 50% and in the high plasticity clays the Liquid Limit is greater than 50%. The results obtained suggest that the tropical clay soil of Dhaka is intermediate to high plasticity clay. The values for all the samples of three boreholes are plotted in the Standard Plasticity Chart in the form of Liquid Limit versus Plasticity Index and is shown in figure 5.30. From the Plasticity Chart (figure 5.30) it is observed that all the plotted values lie above the 'A-line'. Some values are very close to the 'A-line'. In the British soil classification system the tropical clay soils of Dhaka can be characterized as an intermediate to high plasticity inorganic clay. These soils are classified as CI (Clay of intermediate plasticity) and CH (Clay of high plasticity) from their position on the Plasticity Chart.

Newill (1961) reported the Liquid Limit values from 65% to 107% for Sasumua Red Clay and from 56% to 84% for Kabete Red Clay from Kenya. He also noted that the removal of iron oxide from these soils showed a considerable increase of the Liquid Limit values. Grim (1962) pointed out that montmorillonites and illites have higher Liquid Limits whereas kaolinites generally have lower values. Grim (1962) also mentioned that there is a wide range of variations in Liquid Limit values for illites generally ranging from 60% to 90%, for kaolinites from 30% to 75%. He also noted that the mixing of illite minerals with other elements and minerals might reduce the Liquid Limit values. He further suggested that there is no single Liquid Limit value that is characteristic of a particular clay mineral. Indeed the range of values for a particular clay mineral can be used for comparison. For some natural mixtures of illite, he quoted the Liquid Limit values range from 52% to 62%.

The tropical clay soils of Dhaka consists of illite, kaolinite and contains quartz and feldspar as non-clay minerals. The obtained Liquid Limit values are lower than the values quoted by Grim (1962) for illitic minerals and closer to the values observed

by Newill (1961) for some tropical clays. The presence of kaolinite as well as iron oxide in the samples might reduce the Liquid Limit values below those expected for pure illite.

5.4.3.2 Plastic Limit

The observed Plastic Limit values for three borehole samples are listed in Table 5.7. It can be seen from Table 5.7 that the Plastic Limit values for natural soils of borehole one lie in between 21% to 24% and air-dried samples showed a value of 20% to 24%. The Plastic Limit values for natural soils of borehole two found are in the range of 19% to 24% and those for air dried samples found are in the range of 18% to 20%. The natural soils of borehole three showed Plastic Limit values of 17% to 23% and air dried borehole three samples showed values ranging from 16% to 22%. The variations of Plastic Limit values with respect to depth for natural soils of three borehole samples are shown in figures 5.27, 5.28 and 5.29. From Table 5.7 it can be seen that the range of variations between the Plastic Limit values at different depths and also at different sites is very small.

Grim (1962) pointed out that montmorillonites and illites have higher Plastic Limits, whereas kaolinites have generally lower values. The Plastic Limit values vary from about 48% to 97% for montmorillonite, from 21% to 26% for illites and from 30% to 37% for kaolinite (Grim, 1962). He also noted that for natural mixtures of illite, the Plastic Limit values ranged from 26% to 33%. Newill (1961) mentioned the Plastic Limit of 35% to 39% for some red tropical clays of Kenya. The observed Plastic Limit values are close to the values quoted by Grim (1962) for illitic minerals and also close to the values mentioned by Newill (1961). The X-ray diffraction results justified the presence of illite in these soils.

5.4.3.3 Plasticity Index

The Plasticity Index values of different samples from the three boreholes are shown in Table 5.7. It can be seen from this table that the Plasticity Index of borehole one samples lie between 22% to 32% for natural samples and between 18% to 27% for air-dried samples. The natural soil samples of borehole two showed Plasticity Index values ranging from 27% to 31% and air dried samples showed 24% to 31% plasticity values. Plasticity Index values of natural soils of borehole three lie between 30% to 37% and the air dried samples of the same borehole showed Plasticity Index values in between 25% to 30%. The observed values at different depths and also at different sites showed small variations. The variations with respect to depth for natural soils of three different boreholes are shown in figures 5.27 to 5.29. It can be seen from these figures that the clear trend of reduction in Plasticity Index with depth.

Newill (1961) reported that the Plasticity Index of Sasumua Clay ranges from 16% to 34% and of Kabete Clay ranges from 18% to 45%. The observed values are close to the values quoted by Newill (1961). Grim (1962) mentioned that the Plasticity Index values for kaolinites range from 1% to 40% with usual values of about 25% and for illites range from 23% to 50%. Montmorillonites have higher Plasticity Index value. The observed Plasticity Index values are consistent with high illitic content and the values are close to the values quoted by Grim (1962). X-ray diffraction results strongly supports the presence of illite mineral in the analyzed samples.

5.5 Summary

In this chapter mineralogy, fabric and some basic geotechnical parameters of the tropical clay soils of Dhaka were discussed. It was observed from the X-ray diffraction results that the tropical clay soils of Dhaka are composed of illite, kaolinite and some non clay minerals, mainly quartz and feldspar. The interference of the chlorite peak with kaolinite sometimes made it difficult to identify chlorite minerals. Although no quantification was possible from the X.R.D. technique used, in general it appeared that Illite is the dominant clay mineral in most of the samples. The absence of chlorite in some samples might be due to destruction of chlorite because of weathering. Chlorite is quite easily weathered under moderate condition.

Fabric of the tropical clay soils of Dhaka was evaluated by using Scanning Electron Microscopy (S.E.M.). It was observed from the Scanning Electron Micrographs that the tropical clay soils of Dhaka showed a random open microfabric of silt and clay. The randomly oriented clay platelets or clusters were intermixed with large silt size grains. From the E.D.X. spectra results it was suggested that most of the silt grains were coated with clay and iron. Several intra and inter granular spaces were observed throughout the microfabric of all the samples. The clay clusters and silt grains showed the presence of Si, Al, Fe and some K in E.D.X. The strong silicon peak justified the presence of quartz. Other peaks of Al and Fe were detected mainly due to scattered clay and iron coating. It was also observed that these elements (Si, Al, Fe and K) were randomly oriented throughout the specimen in between clay flakes and grains. Silica and iron compounds might be acted as a cementing materials and formed bonds between and within the grains. This physical linkage between particles might have an influence on the engineering behaviour of the tropical clay soils of Dhaka.

Some basic geotechnical parameters were also discussed, compared and evaluated with mineralogy in this chapter. Silts and clays constitute over 80% of the particles. The analyzed clay is a silt dominated clay which consists of 56% to 63% silt, 22% to 33% clay and 8% to 19% sand size particles. The borehole two samples showed highest amount of clay fractions and lowest amount of sand particles. The samples showed a small variation of silt and clay size fractions with respect to depth. The specific gravity of the analyzed samples lie between 2.59 to 2.65.

The Liquid Limit values of the tropical clay soils of Dhaka lie between 41% to 56%. The Plastic Limit values obtained ranged between 16% to 24% and the Plasticity Index values lie in between 18% to 37%. A close agreement was found between the values at different depths and also at different sites. Variations in the Liquid Limit values were observed between natural and air-dried samples due to the effect of drying. The values obtained are consistent with values for other tropical soils and close to the values quoted by Grim (1962) for illitic minerals. This is consistent with the X-ray diffraction results.

In the British soil classification system the tropical clay soils of Dhaka can be characterized as an intermediate to high plasticity inorganic clay (CI to CH).

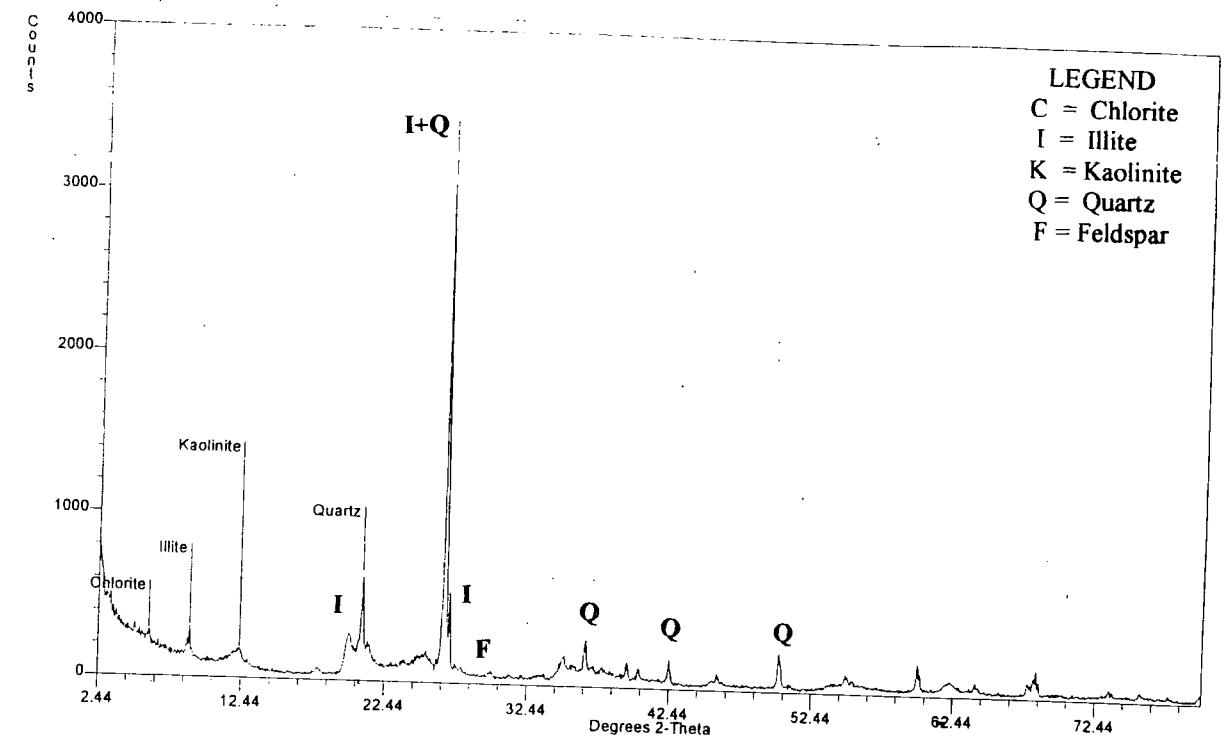

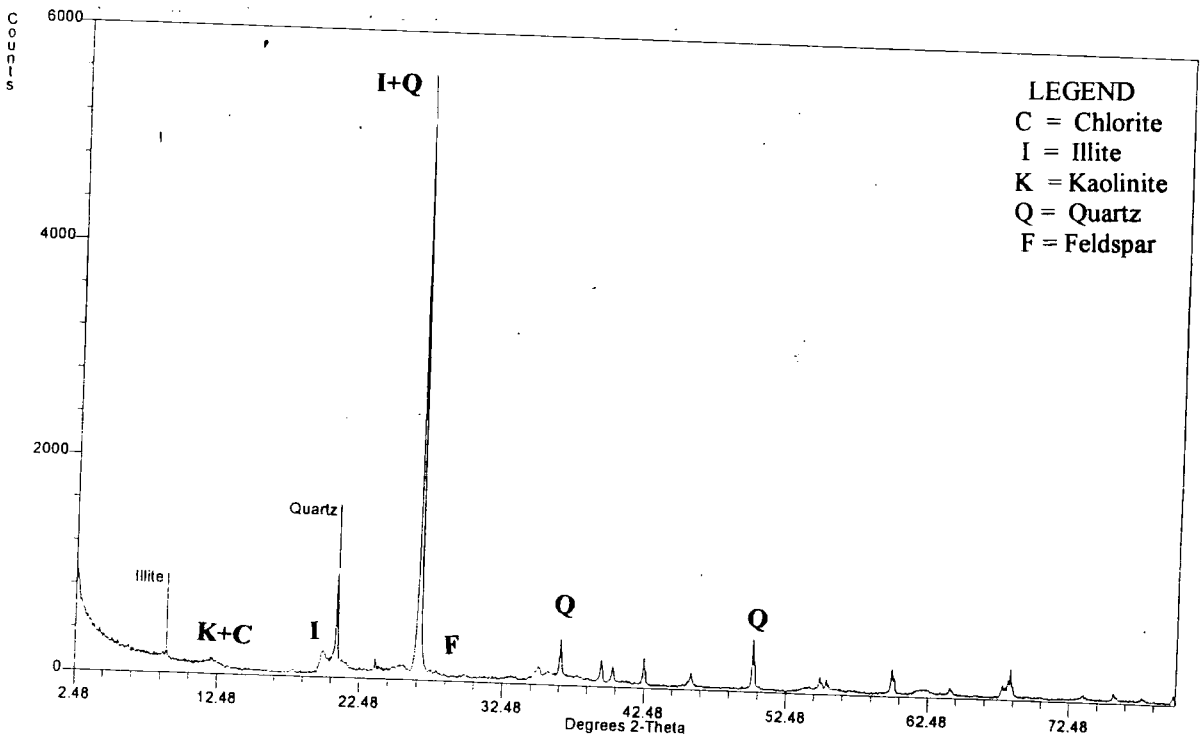

Fig. 5.1 X-ray diffractograms of samples $1S_1$ (above) and $1S_2$ (below)

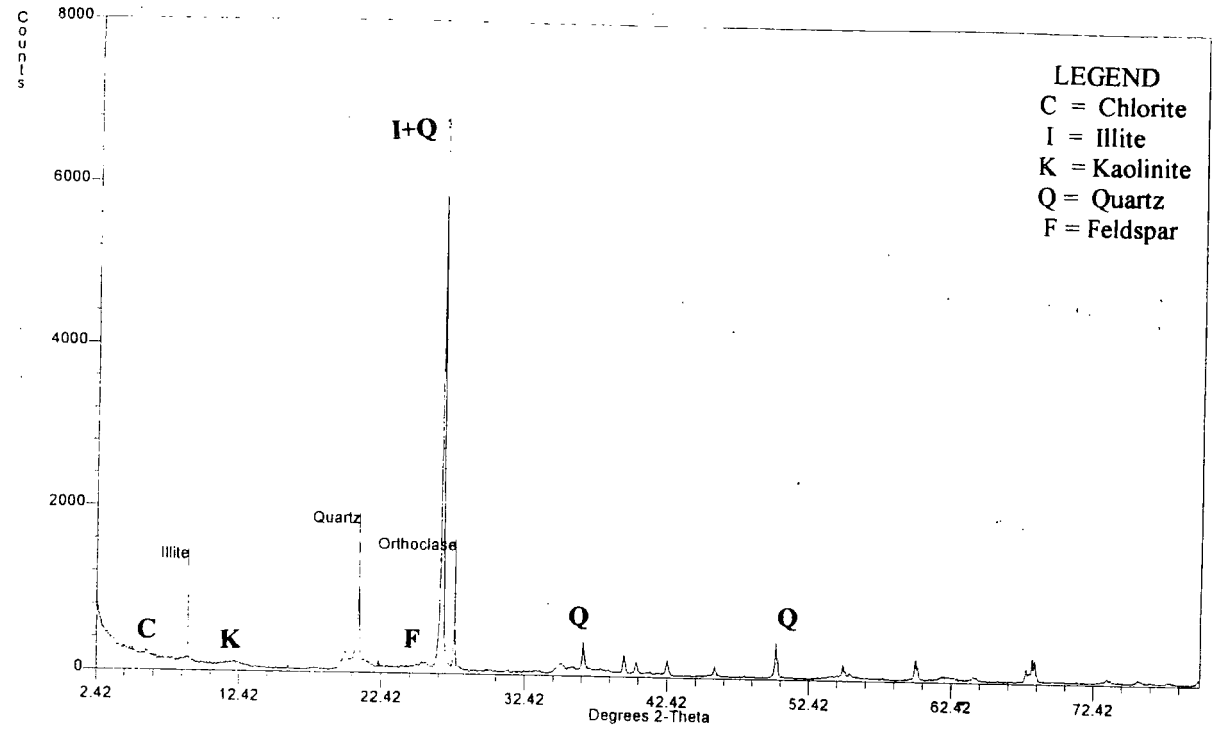

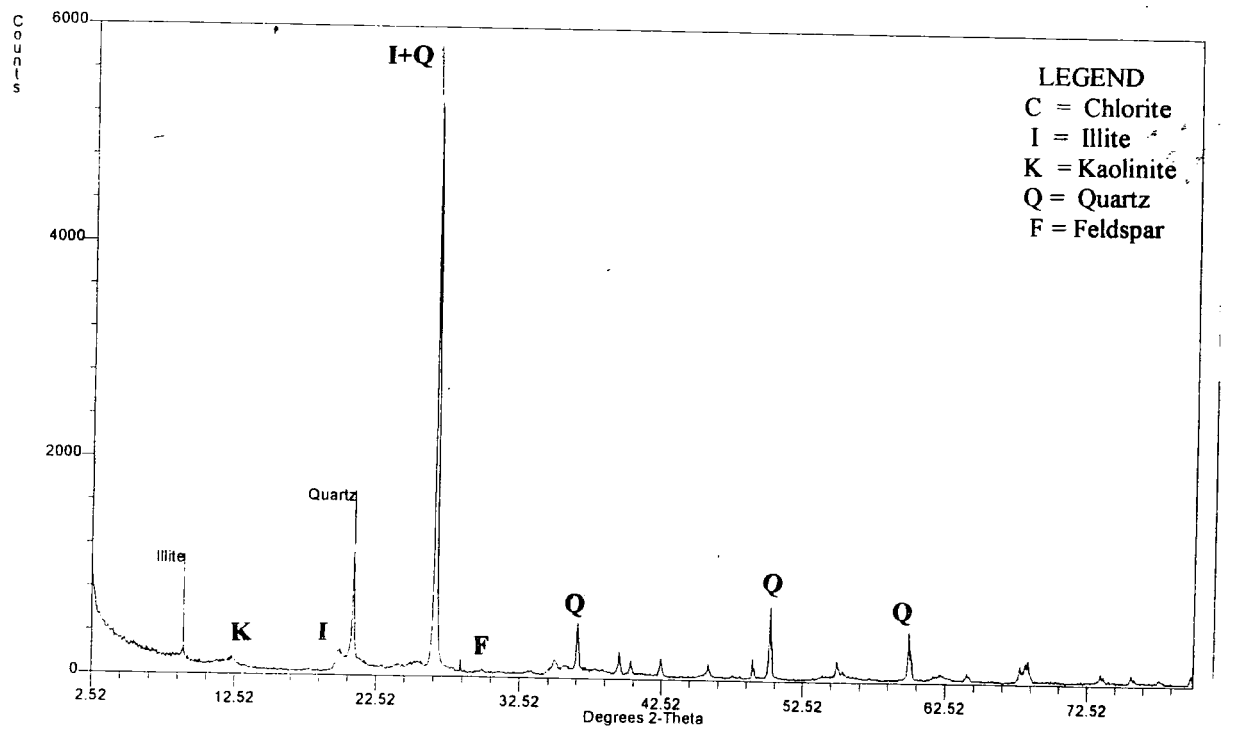

Fig. 5.2 X-ray diffractograms of samples $1S_3$ (above) and $1S_4$ (below)

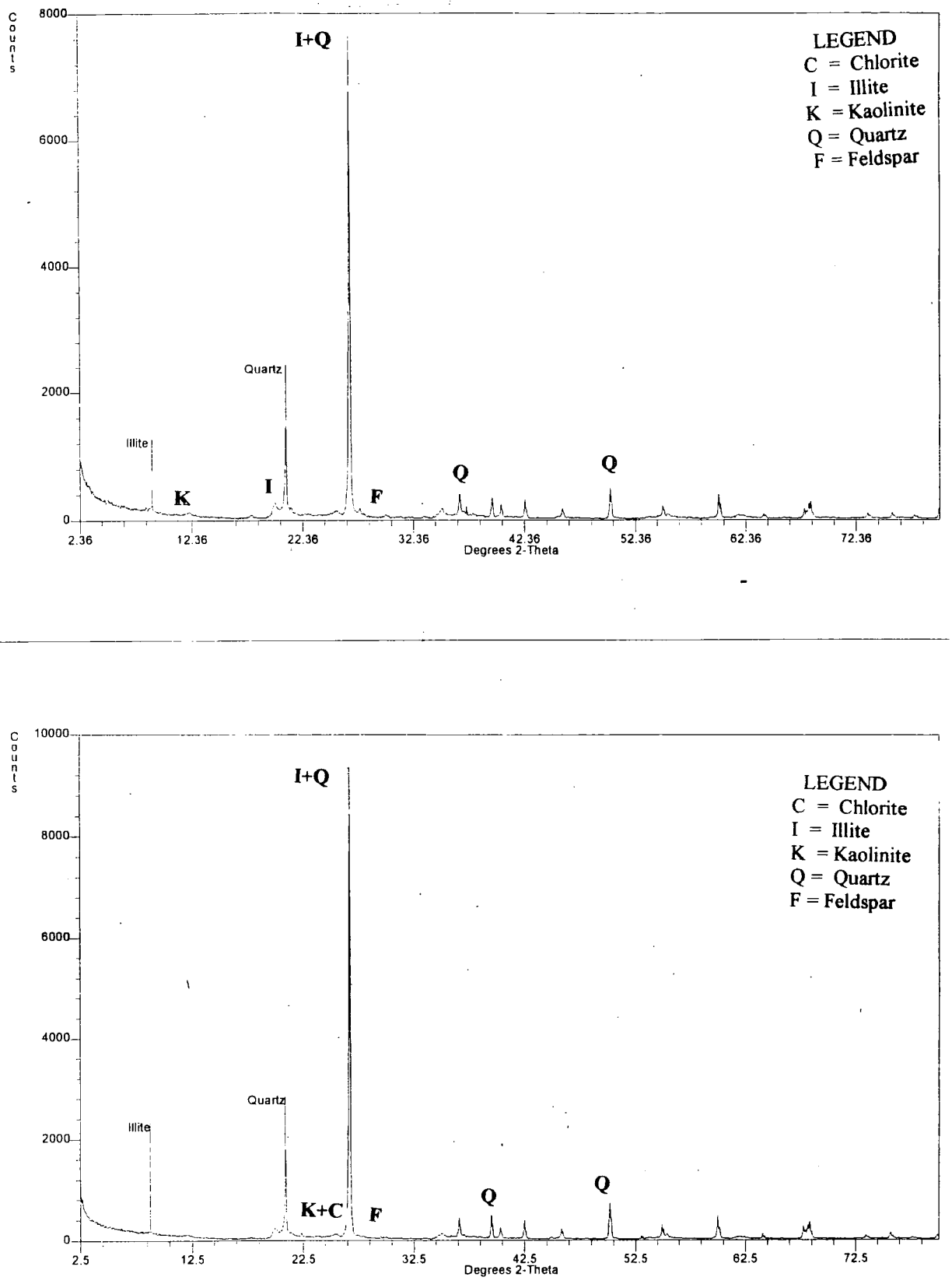

Fig. 5.3 X-ray diffractograms of samples $2S_1$ (above) and $2S_2$ (below)

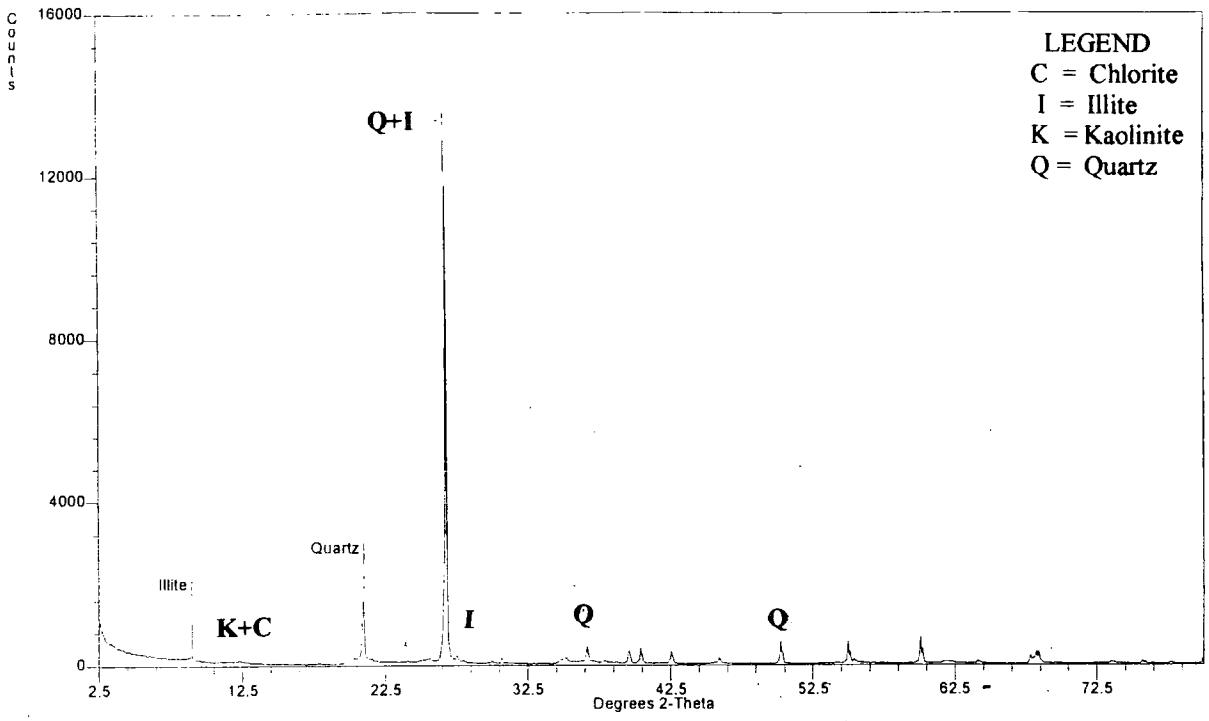

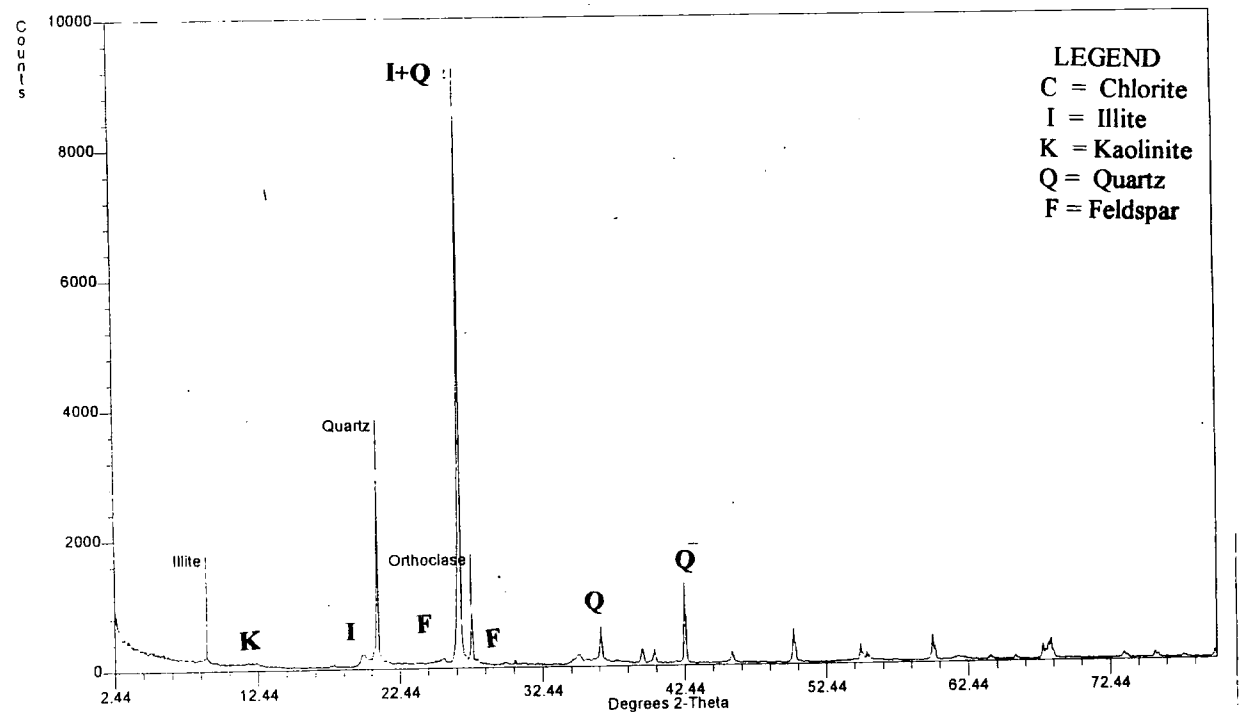

Fig. 5.4 X-ray diffractograms of samples $2S_3$ (above) and $2S_4$ (below)

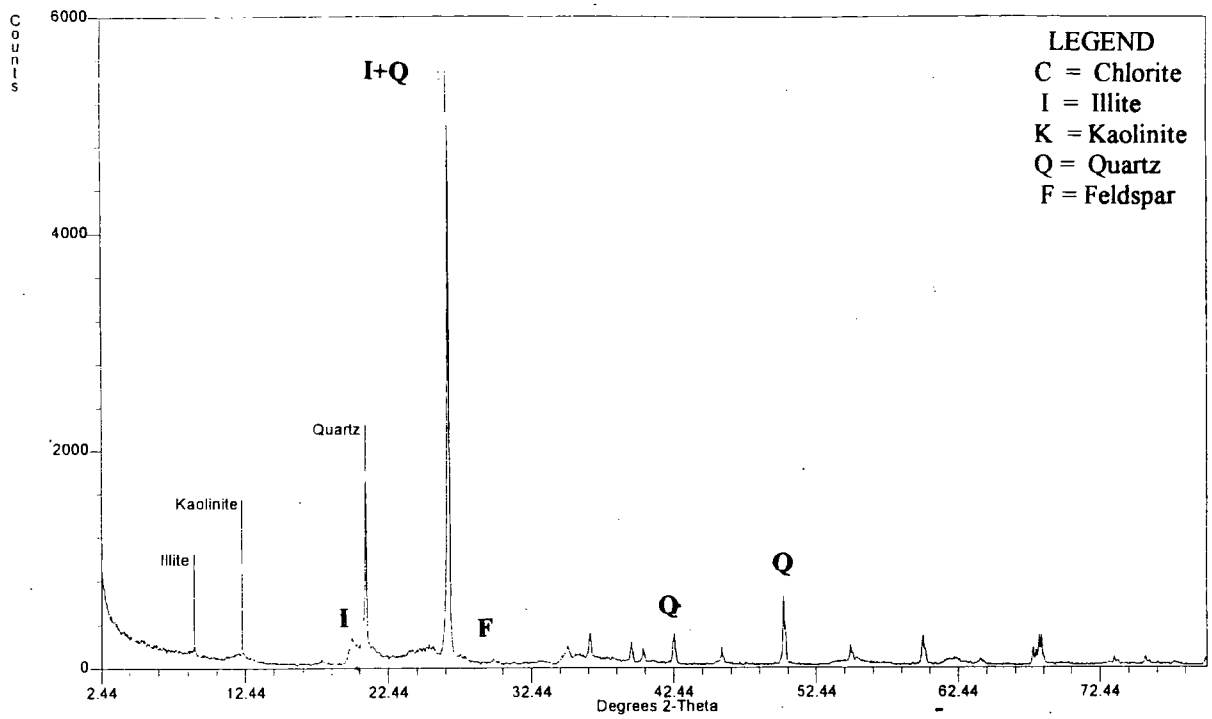

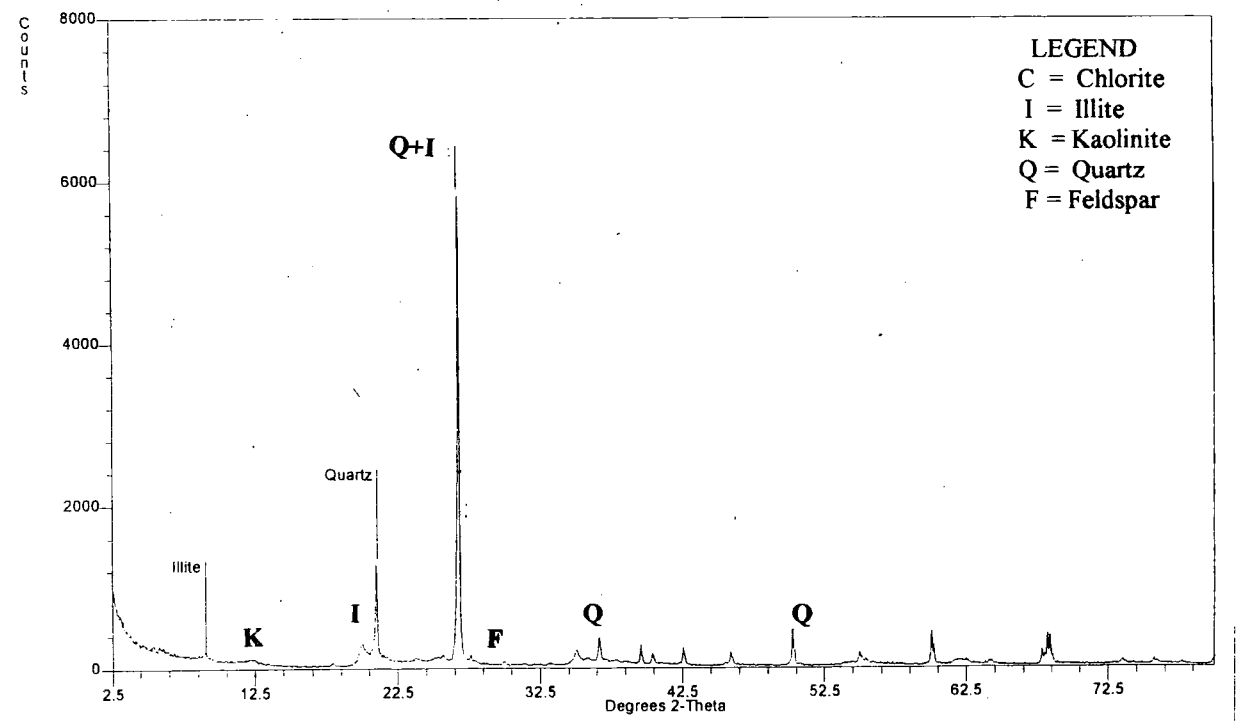

Fig. 5.5 X-ray diffractograms of samples $3S_1$ (above) and $3S_2$ (below)

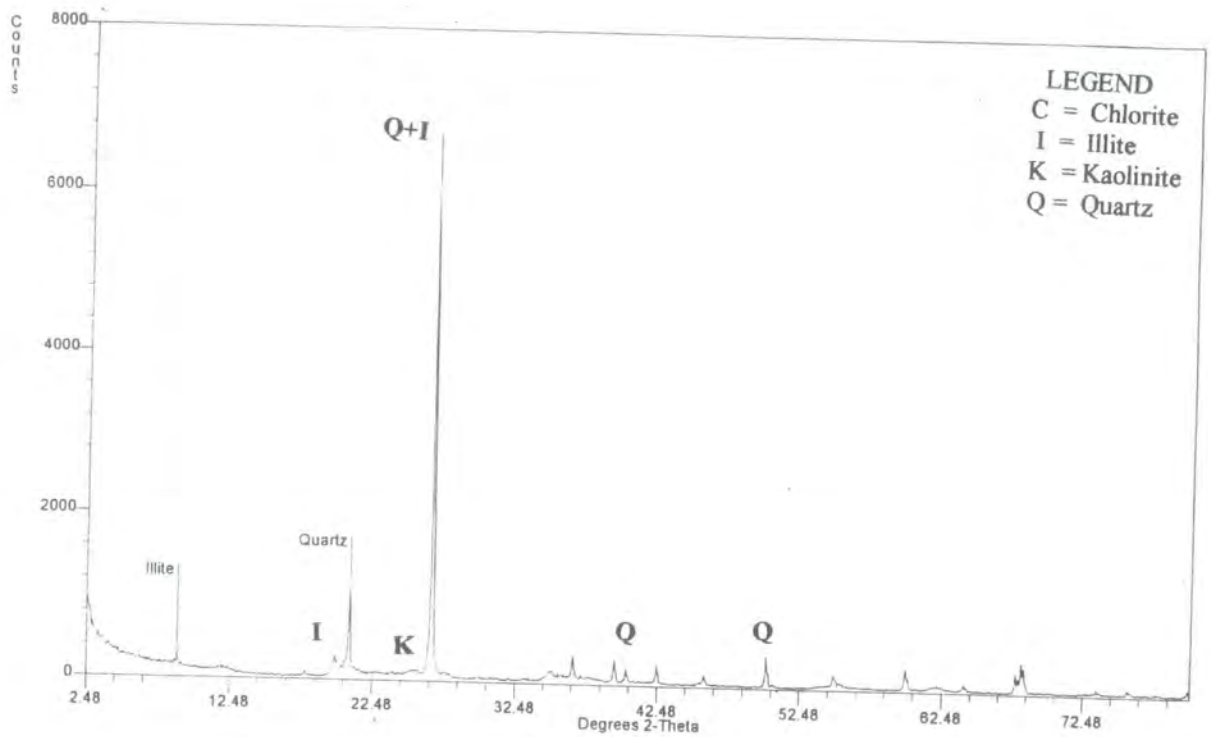

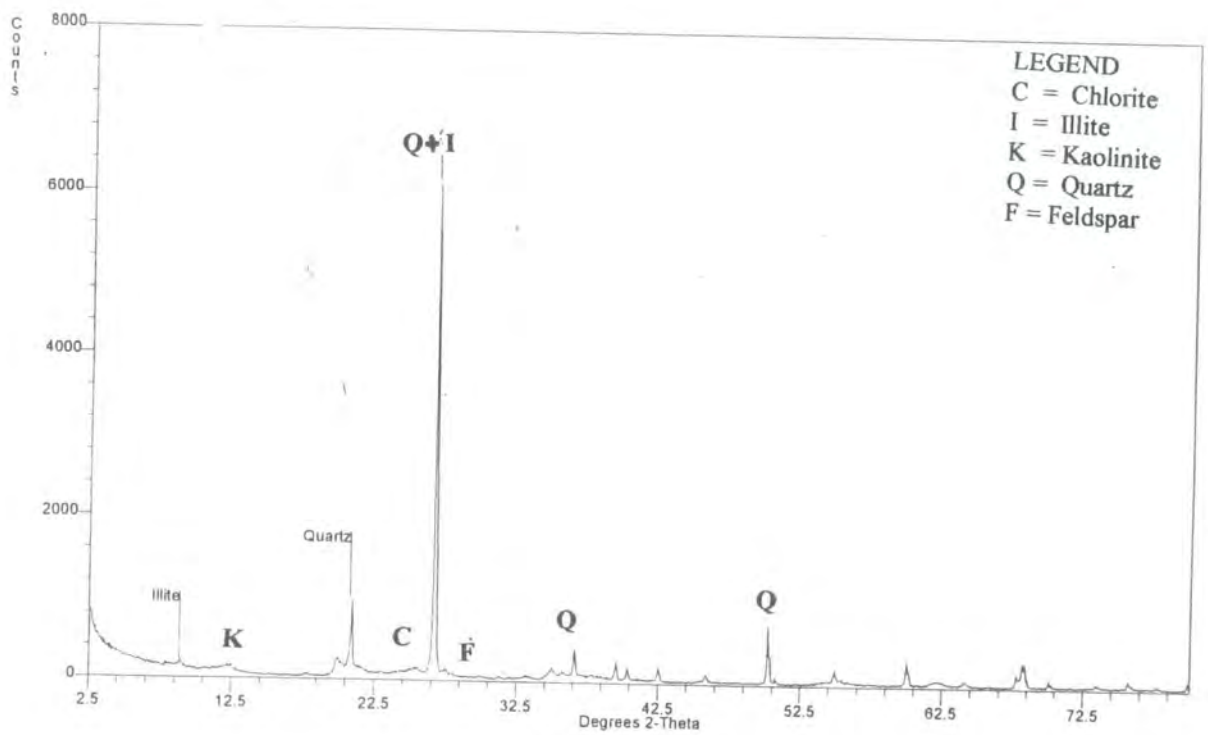

Fig. 5.6 X-ray diffractograms of samples $3S_3$ (above) and $3S_4$ (below)

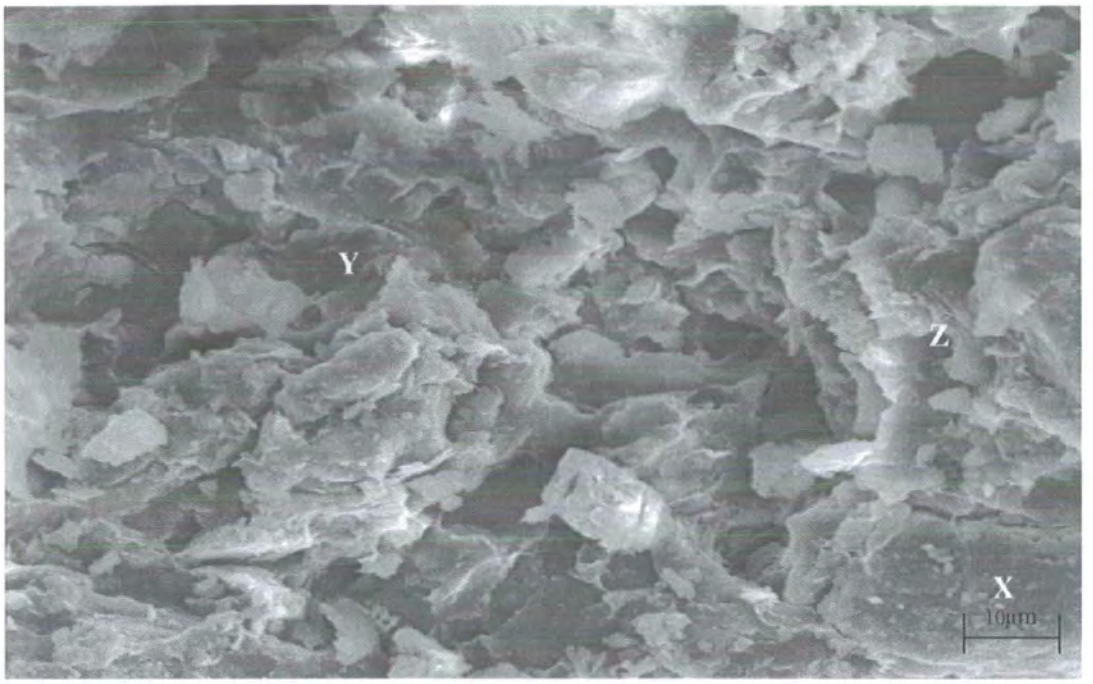

Fig. 5.7 Scanning electron micrograph of sample $1SEM_1$ (scale 10µm.)

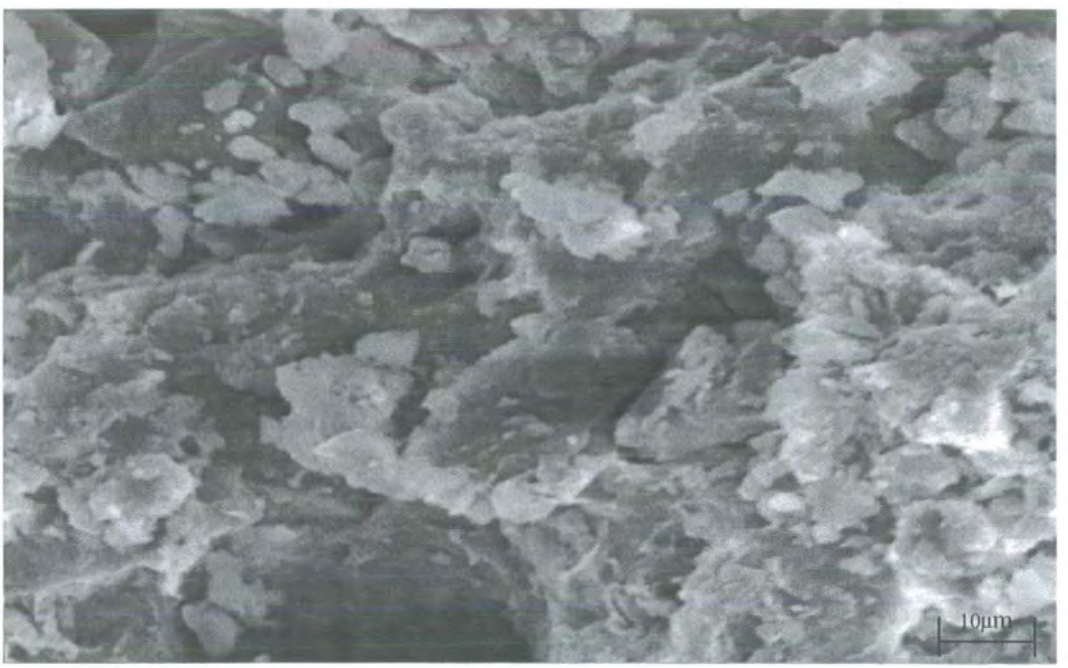

Fig. 5.8 Scanning electron micrograph (2^{nd} image) of sample $1SEM_1$ (scale 10µm.)

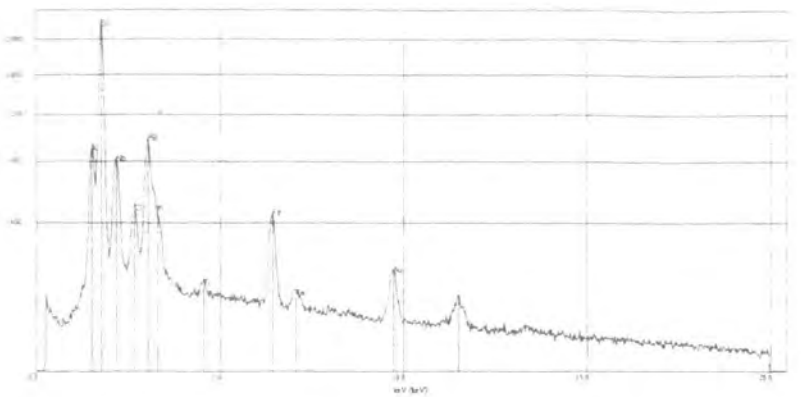

Fig. 5. 9 Energy dispersive X-ray spectrum (EDX) of area X of sample $1SEM_1$

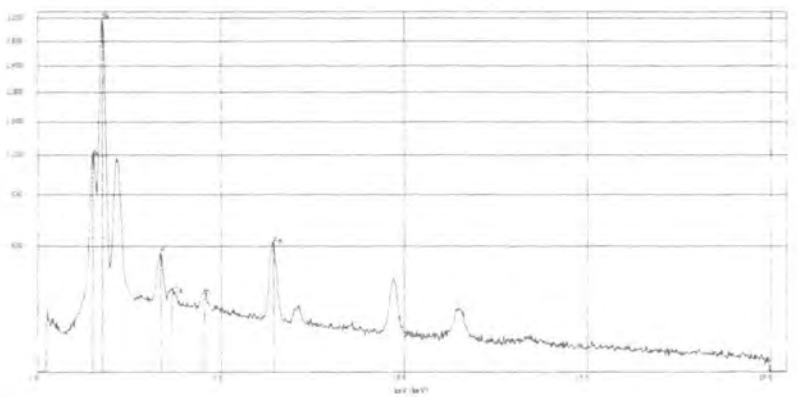

Fig. 5. 10 Energy dispersive X-ray spectrum (EDX) of area Y of sample $1SEM_1$

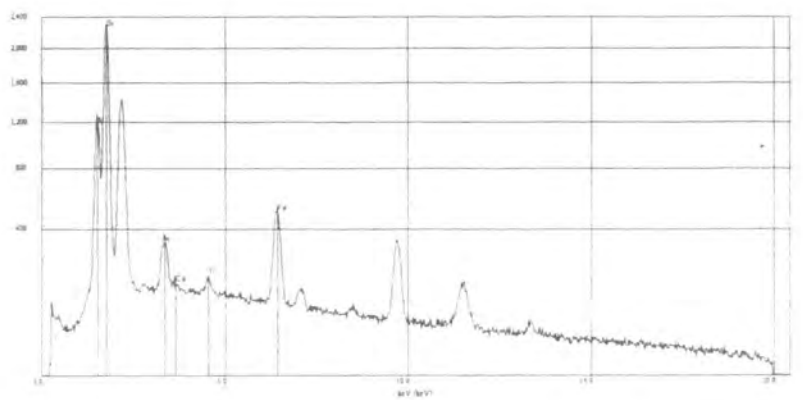

Fig. 5. 11 Energy dispersive X-ray spectrum (EDX) of area Z of sample $1SEM_1$

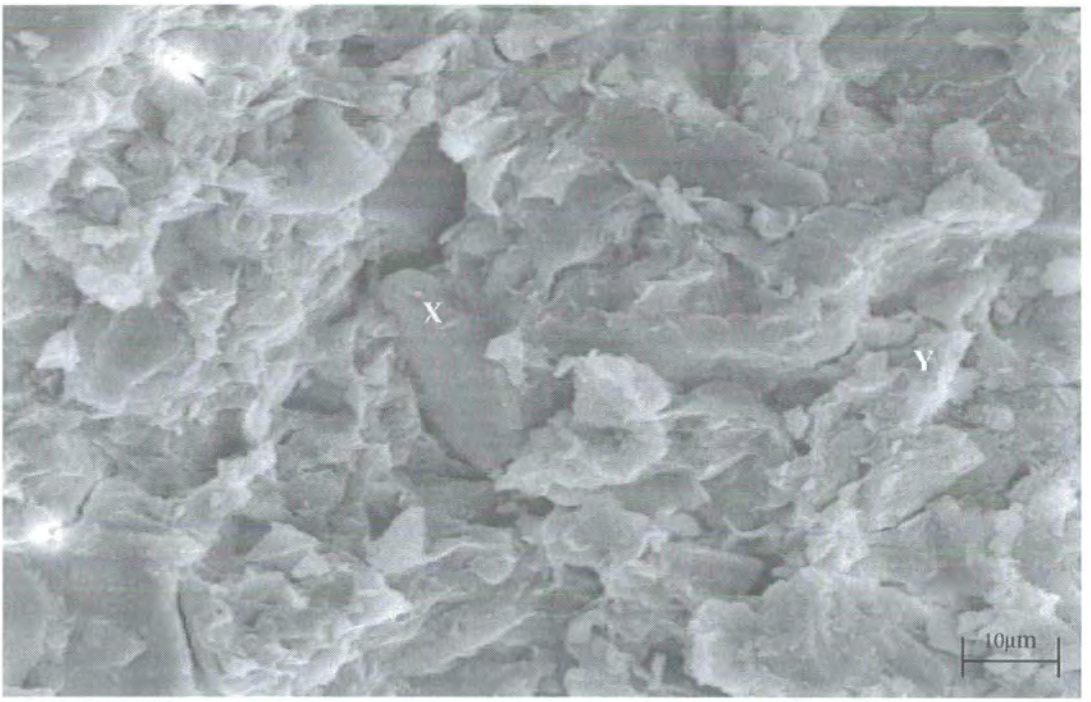

Fig. 5. 12 Scanning electron micrograph of sample $2SEM_1$ (scale 10μm.)

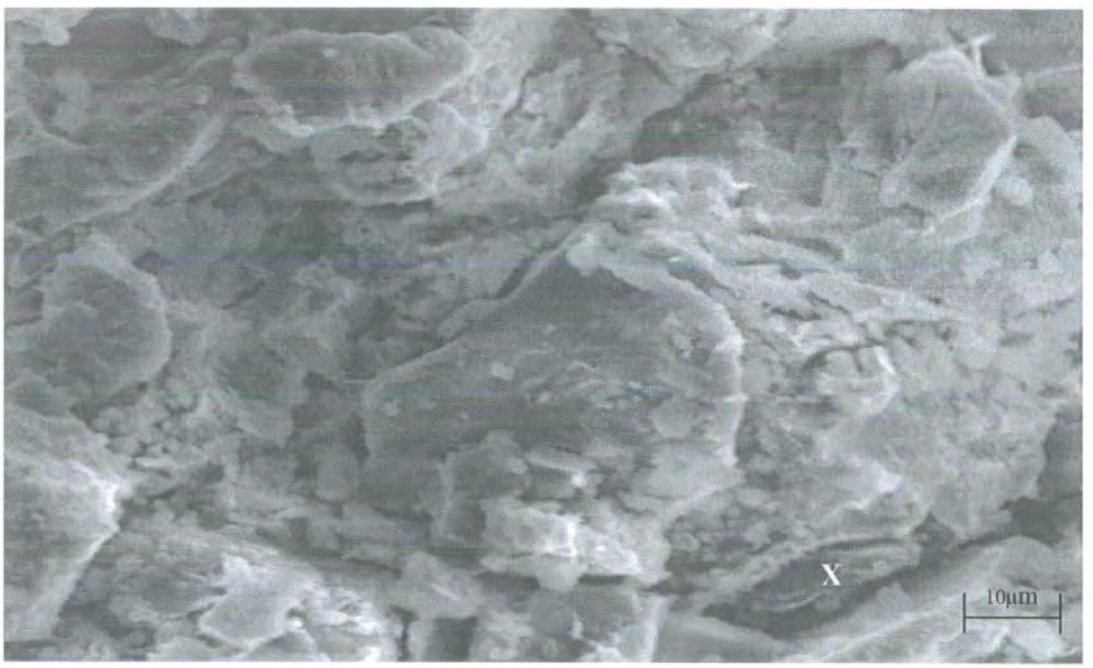

Fig. 5.13 Scanning electron micrograph $2SEM_2$ (scale 10μm.)

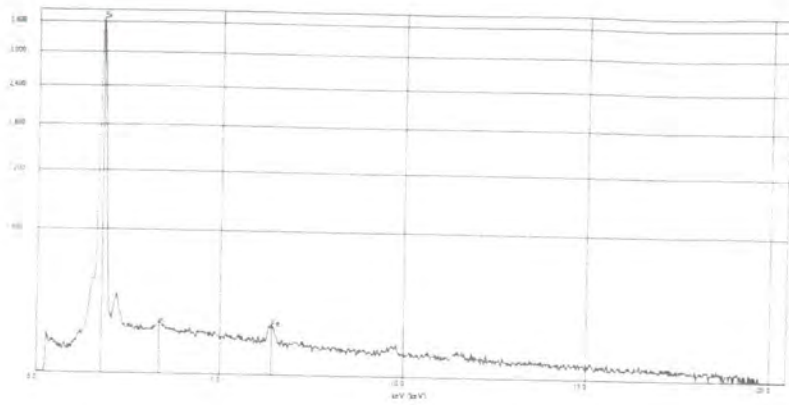

Fig. 5.14 Energy dispersive X-ray spectrum (EDX) of area X of sample $2SEM_1$

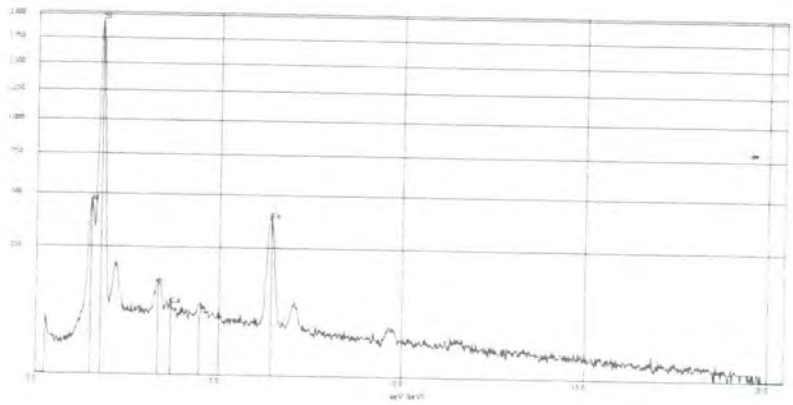

Fig. 5.15 Energy dispersive X-ray spectrum (EDX) of area Y of sample $2SEM_1$

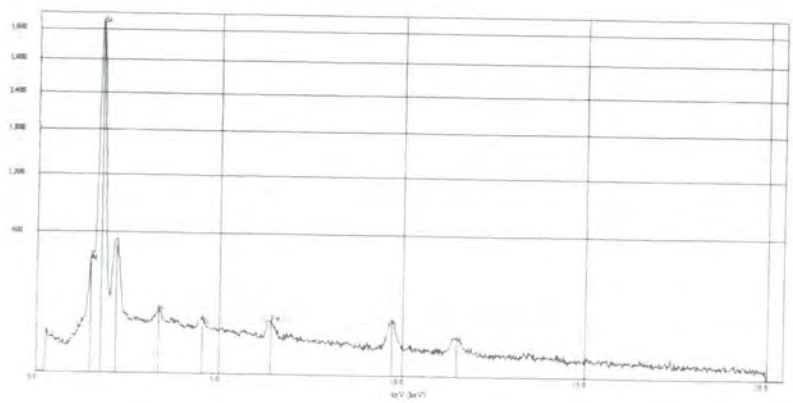

Fig. 5.16 Energy dispersive X-ray spectrum (EDX) of area X of sample $2SEM_2$

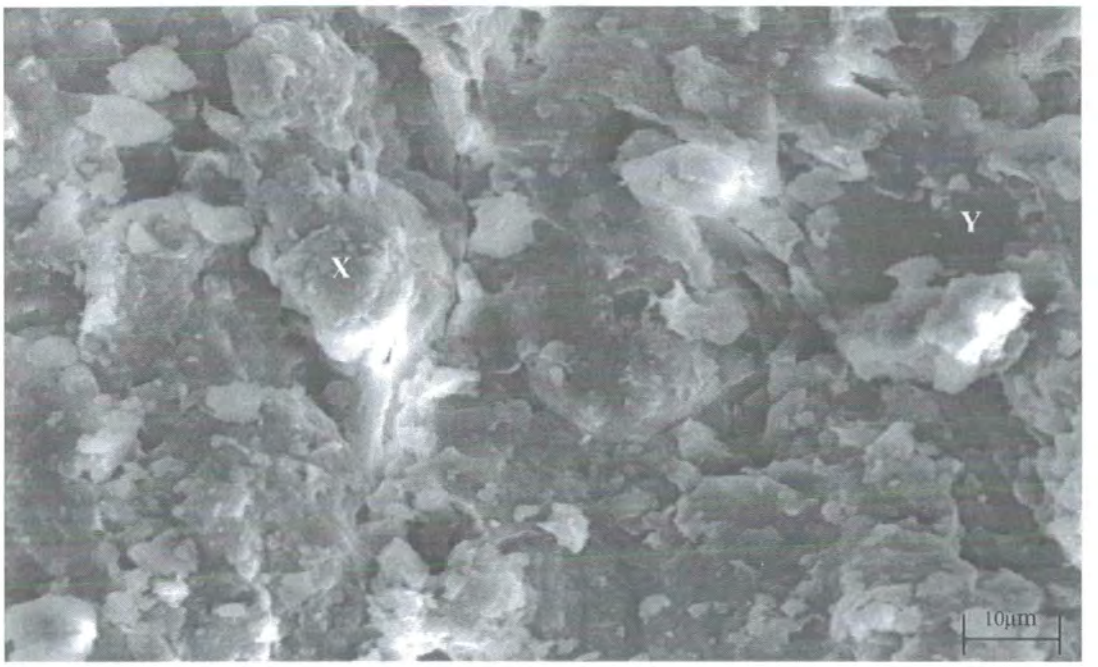

Fig. 5.17 Scanning electron micrograph of sample $3SEM_1$ (scale 10µm.)

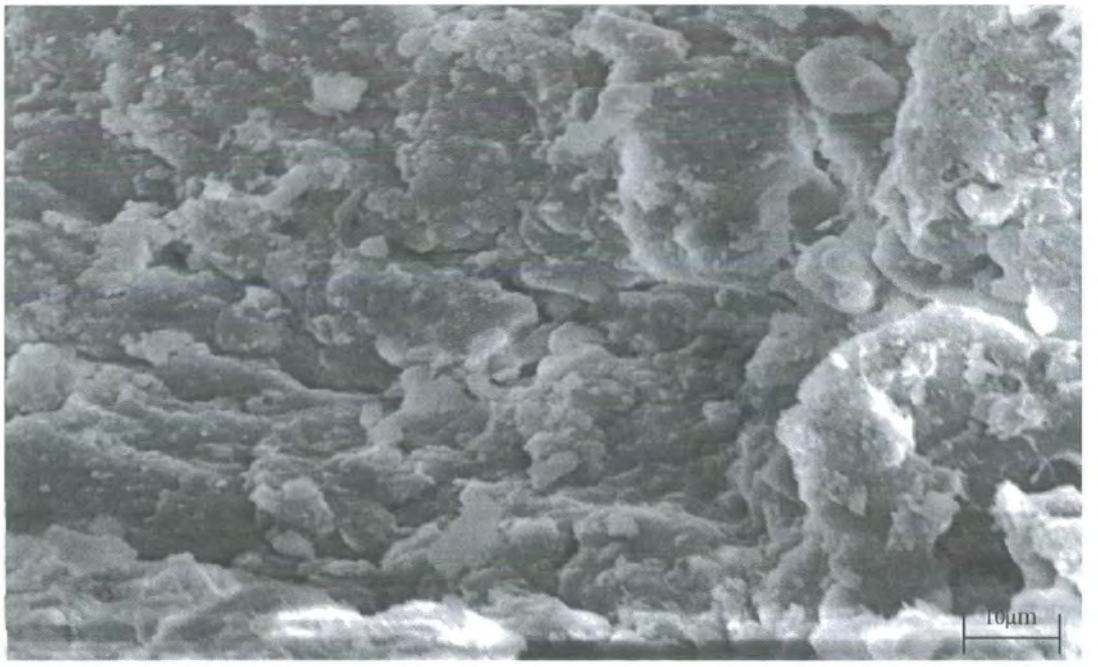

Fig. 5.18 Scanning electron micrograph (2^{nd} image) of sample $3SEM_1$ (scale 10µm.)

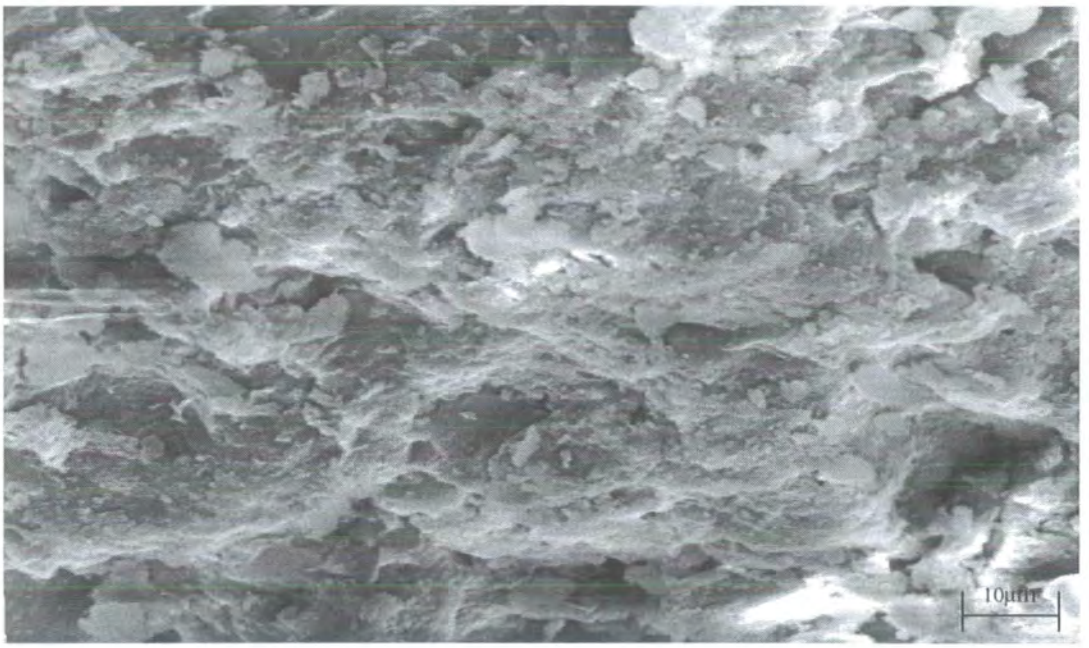

Fig. 5.19 Scanning electron micrograph (3rd image) of sample $3SEM_1$ (scale 10μm.)

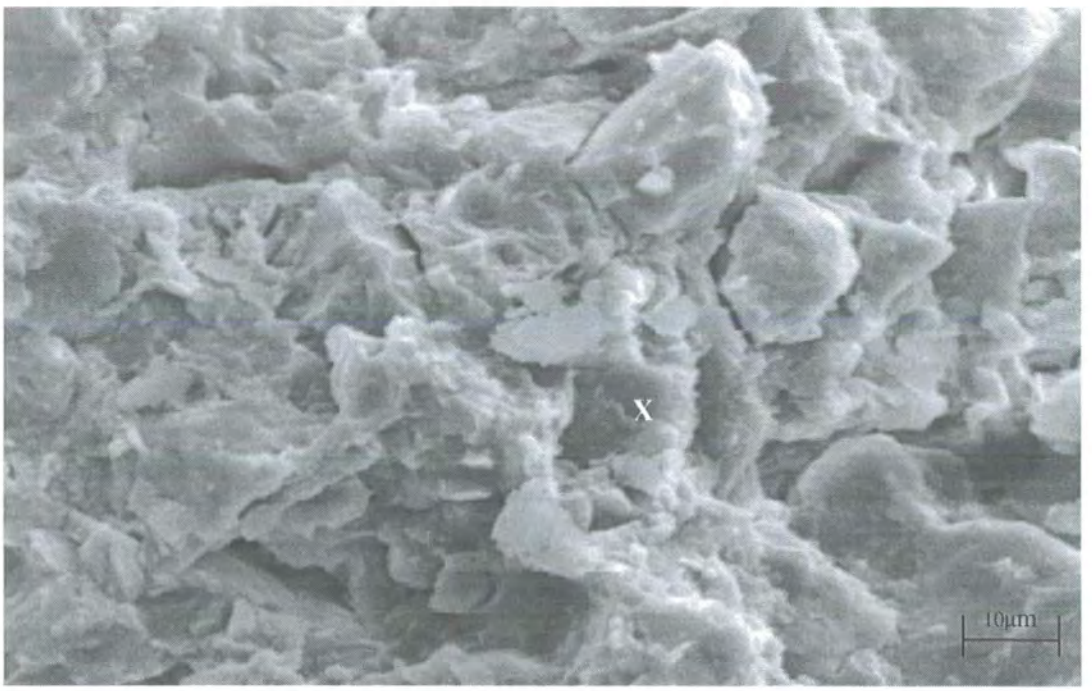

Fig. 5.20 Scanning electron micrograph of sample $3SEM_2$ (scale 10μm.)

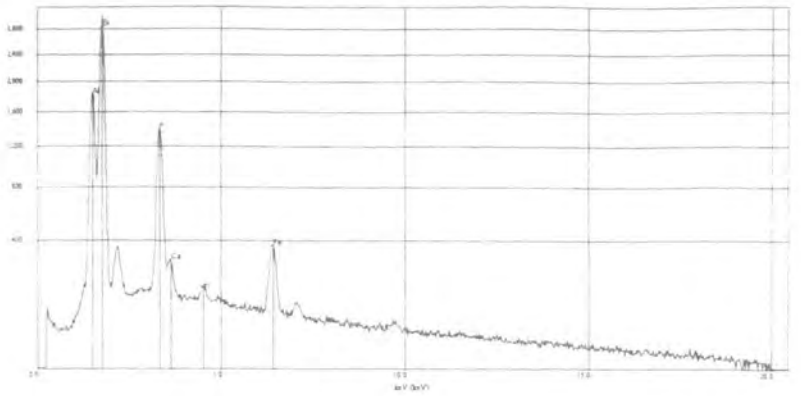

Fig.5. 21 Energy dispersive X-ray spectrum (EDX) of area X of sample $3SEM_1$

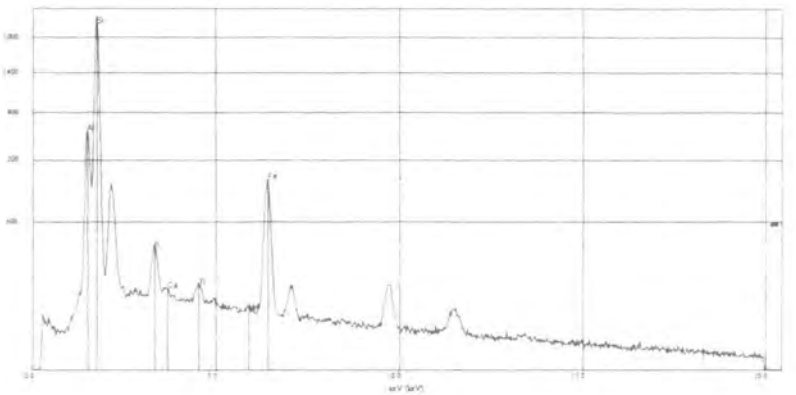

Fig.5. 22 Energy dispersive X-ray spectrum (EDX) of area Y of sample $3SEM_1$

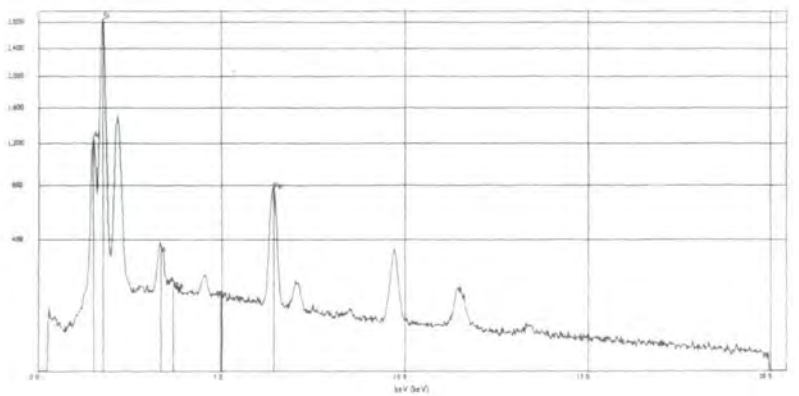

Fig.5. 23 Energy dispersive X-ray spectrum (EDX) of area X of sample $3SEM_2$

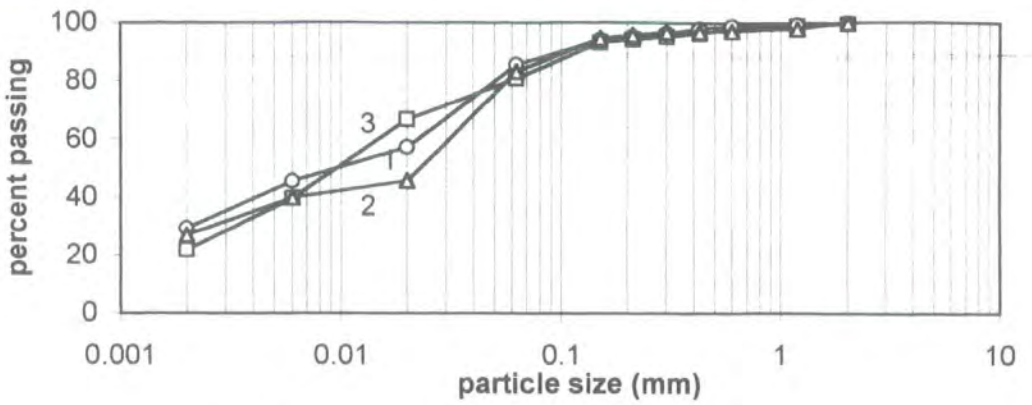

Fig.5.24 Particle size distribution of borehole one samples

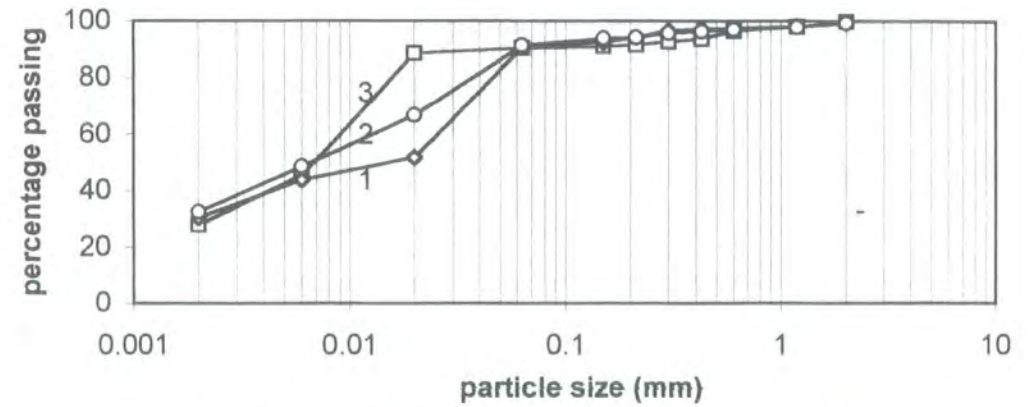

Fig.5.25 particle size distribution of borehole two samples

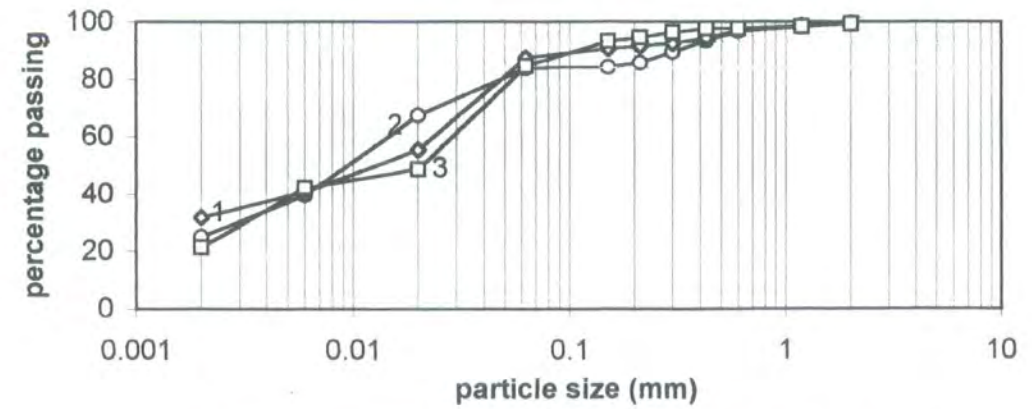

Fig.5.26 particle size distribution of borehole three samples

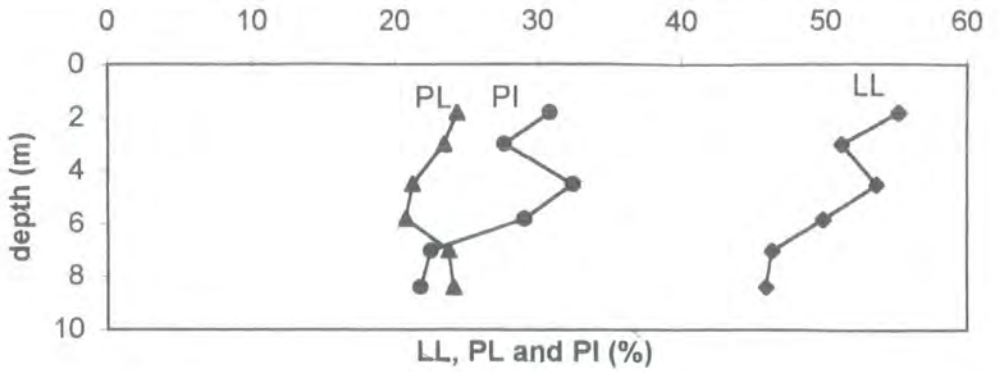

Fig.5.27 vertical variations of Atterberg consistency limits of natural samples of borehole one

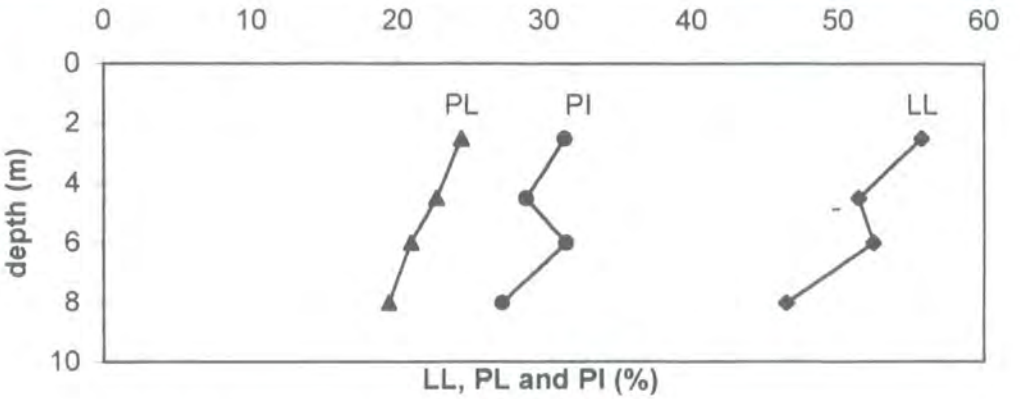

Fig.5.28 vertical variations of Atterberg consistency limits of natural samples borehole two

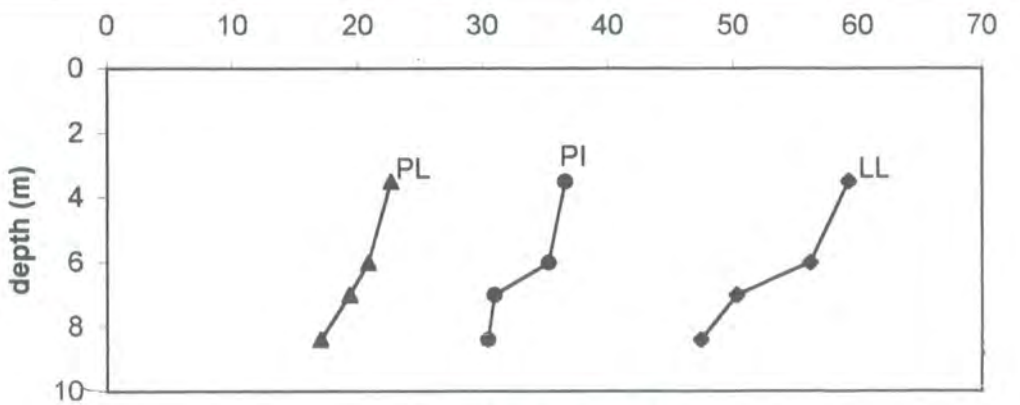

Fig.5.29 Vertical variations of Atterberg consistency limits of natural samples of borehole three

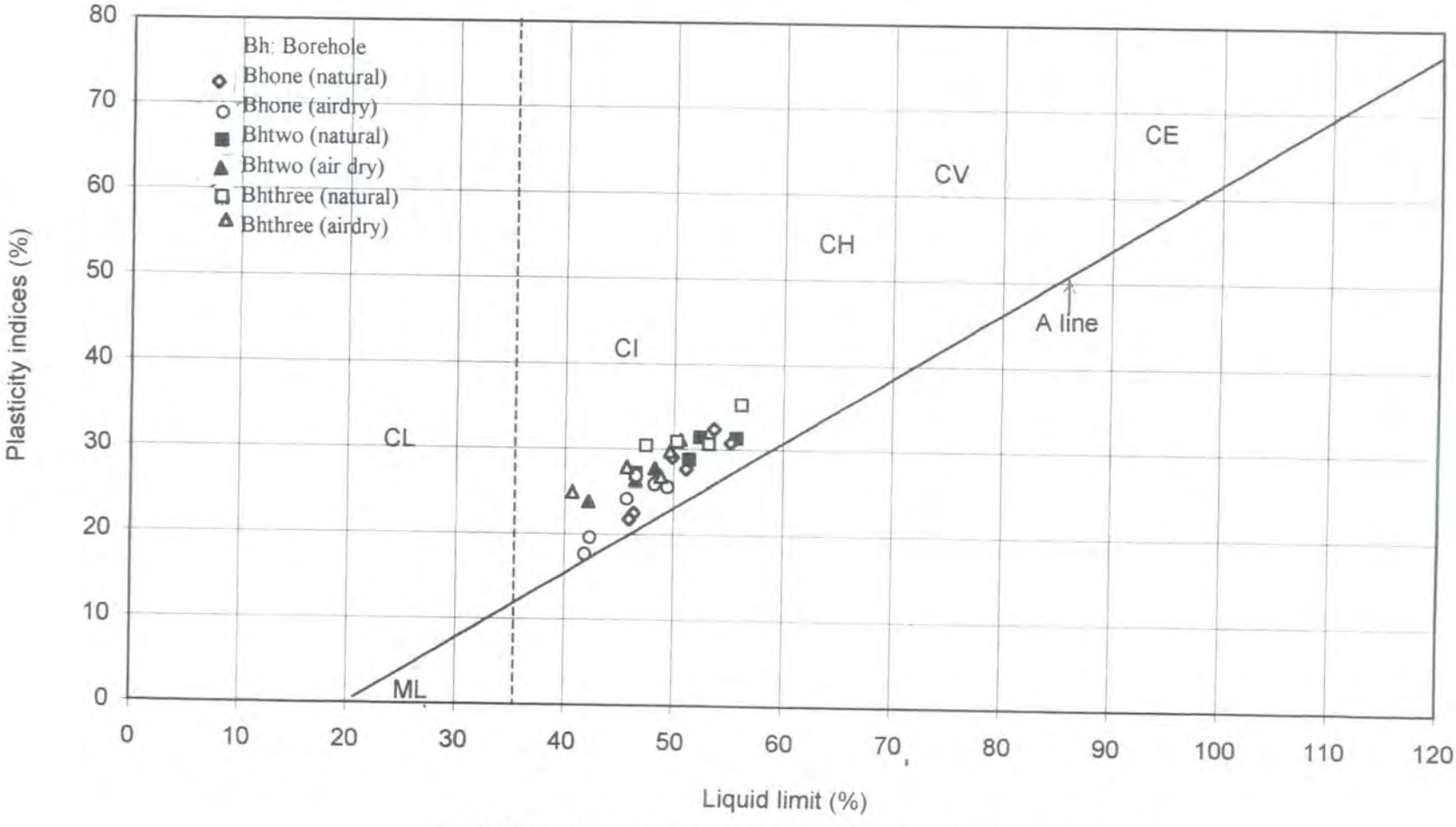

Fig. 5.30 Liquid limits and plasticity indices for the three boreholes

CHAPTER 6

CONSOLIDATION CHARACTERISTICS

6.1 Introduction

In this chapter the triaxial consolidation test results carried out on samples from three different boreholes are discussed. A limited number of Oedometer consolidation test results from borehole one are also discussed. The samples were collected from the same geological formation but at different depths.

In the case of triaxial consolidation, at the end of saturation stage, all the samples were isotropically consolidated in the Triaxial Cell with effective confining pressures ranging from 50 to 800 kPa. After the application of each effective

confining pressure the samples were allowed to drain for a minimum of 24 hours. Readings of pore water pressure at the mid-height of the specimen (as discussed in Chapter 4), drainage volume change and the time were recorded. The use of a mid-height pore water probe made it possible to relate volume change to p′ for a single increment test. It is assumed that the mean effective stress at the mid hight represents an average for the sample as a whole and can therefore be related to the overall volume change. The consolidation stage was taken to be completed when the degree of consolidation was greater than 95%.

Results are presented in terms of volume change versus time curves and void ratio versus p′ curves. Consolidation parameters –the values of the coefficient of consolidation (c_v), the values of the coefficient of volume compressibility (m_v) and the compression index (C_c) of some of the selected samples of three boreholes were determined. The coefficient of permeability (k) was calculated from the m_v and c_v values. The results are presented, compared and evaluated.

Oedometer consolidation tests were carried out in accordance with the British Standard BS.1377 (1990). The results are discussed in terms of void ratio versus log p′ curves. The apparent pre-consolidation pressures of some of the selected samples were observed and some m_v, c_v and C_c values obtained from Oedometer tests are also presented.

The triaxial samples are named by using letters and numbers. For example test 1cn50 means an isotropic triaxial consolidation test (c) carried out on natural samples (n) of borehole one (1), which was consolidated at a consolidation pressure of 50 kPa. Similarly 3cd400 means an isotropic triaxial consolidation test (c) carried out on destructured samples (d) of borehole three (3), which was consolidated at a consolidation pressure of 400 kPa. Oedometer samples are named in a similar way. For example test $1ON_1$ indicates an oedometer test (O) carried out on a natural

sample (N) of borehole one (1). The subscript at the end indicates the sample number. Sample details are listed in Table 6.1 and Table 6.2 (in section 6.3.1).

6.2 Consolidation characteristics

In this section triaxial consolidation characteristics for natural and destructured samples are discussed in terms of the volume change versus time curves, coefficient of consolidation (c_v), the coefficient of volume compressibility (m_v), compression index (C_c) and the coefficient of permeability (k). Oedometer consolidation test results are also evaluted.

6.2.1 Volume change versus time curves for triaxial consolidation

The volume change versus time graphs for natural samples from the three boreholes are shown in figures 6.1, 6.2 and 6.3 respectively and those of destructured samples from the three boreholes are shown in figures 6.4, 6.5 and 6.6 respectively. The volume change of all the samples during consolidation was recorded for at least 24 hours. It can be seen from these graphs that the volume decrease was greatest during the early consolidation of each sample. After that all the samples reached almost a steady condition.

It can be seen from figure 6.1 that the primary stage of consolidation for natural samples of borehole one (100-800 kPa) was completed within approximately 30 to 240 minutes (i.e. approximately from half an hour to four hours). After that the volume decrease became almost constant. It was also found that sample 1cn50 showed a very small amount of volume change. The highest amount of volume change was observed for sample 1cn600. Generally the decrease of volume of the samples increased with increasing confining pressures except for samples 1cn400

and 1cn800. These variations might be due to the natural variability of the samples, which were collected from different depths of the same borehole.

The destructured samples of borehole one in each case showed a greater amount of volume change than the natural samples (figure 6.4). This would be expected due to the destruction of the original structure in the destructured soils. The primary consolidation of the destructured samples of borehole one was completed within approximately 20 to 380 minutes. After that all the destructured samples reached almost a steady condition. It was also observed that the decrease of volume of the destructured samples also increased with increasing consolidation pressures.

The initial consolidation of the natural samples of borehole two was completed within approximately 25 minutes to 450 minutes (figure 6.2). At low confining pressures (50 to 300 kPa) the decrease of volume increased with increasing confining pressures and the primary consolidation for these samples was completed within less than 3 hours. Conversely the high confining pressure samples (400 to 800 kPa) did not show any regularity in terms of the decrease of volume with increasing confining pressure. These samples completed initial consolidation between approximately 150 minutes to 450 minutes. The decrease of volume of the destructured samples of borehole two increased with increasing confining pressures and the primary consolidation of these samples was completed within approximately less than 5 hours (figure 6.5). After that most of the destructured samples reached almost a steady condition.

From figure 6.3 it can be observed that the initial consolidation of the natural samples of borehole three was completed within approximately 20 minutes to 300 minutes. These samples broadly showed an increase of volume change with increasing confining pressure except for samples 3cn400 and 3cn500. Most of the natural samples of borehole three reached a constant value of volume change after 600 minutes. On the other hand, destructured samples of borehole three completed

initial consolidation in less than 8 hours and after that they reached almost a steady state condition (figure 6.6). It was also observed that destructured samples of borehole three in each case also showed a greater amount of volume change than the natural samples due to the destruction of original structure. The decrease of volume of the destructured samples of borehole three also increased with increasing confining pressures.

Grim (1962) noted that for montmorillonite clay the amount of consolidation decreased with increasing load and for kaolinitic and illitic clay, the consolidation increased with increasing pressure. Broadly similar reflections are also observed in this study, since these soils are dominated by illite and kaolinite type of minerals (as discussed in chapter 5). It was also observed from figures 6.1 to 6.3 that the largest amount of volume change (approximately 6 cm^3) was observed for the natural samples of borehole two. The maximum amount of volume change for natural samples of borehole one and three was found to be 3.5 cm^3 and 4.5 cm^3 respectively. The variation of the volume change with respect to time for different samples from the three boreholes might be due to the degrees of weathering and natural variability of the samples at different sites. The samples of borehole one and three were highly oxidized, more weathered and contained ferruginous nodules and iron concretions. In contrast, borehole two samples were less oxidized, less weathered and contained smaller amounts of iron concretions than the other boreholes. The amount of iron content could well have an influence on the volume change of the samples. The presence of more iron oxide in the shallower depth samples might also have reduced the volume change during consolidation especially at low confining pressures.
It should be noted here that the samples tested at low confining pressures came from shallower depths (see Table 6.1) and hence are likely to be more weathered than the samples tested at high confining pressures which came from lower depths.

6.3 Consolidation parameters

The triaxial consolidation parameters were calculated as described by Head (1998) and the values obtained are listed in Table 6.1. The void ratio versus p′ curves of the natural and destructured samples of three boreholes is also presented in figures 6.11-6.14. The Oedometer test results are presented in Table 6.2. The observed values are compared and evaluated with the work of other researchers.

6.3.1 Coefficient of consolidation (c_v)

The coefficient of consolidation for all the samples are shown in Table 6.1 and Table 6.2. In triaxial consolidation, c_v values for borehole one natural samples lie between 8 to 24 m^2/year and those for destructured soils lie between 5 to 8 m^2/year. The c_v values for natural samples of borehole two are in the range of 3 to 9 m^2/year and those of destructured samples lie between 2 to 7 m^2/year. The c_v values for natural samples of borehole three range from 3 to 6 m^2/year and those for destructured soils range from 2 to 3. The c_v values obtained from oedometer tests lie in between 1 to 4 m^2/year.

Lambe and Whitman (1969) quoted some typical values of coefficient of consolidation for inorganic soils. He mentioned a value of 0.1 to 1 m^2/year for high plasticity montmorillonite clay, 1-10 m^2/year for medium plasticity clay and 10-100 m^2/year for low plasticity clay. The results are consistent with the values 1-10 m^2/year for medium plasticity clay. It is interesting to note that the natural samples of each borehole showed higher c_v values than the destructured samples, which might be due to the presence of bonded structure in natural soils.

Grim (1962) pointed out that illite, chlorite and kaolinite would have somewhat similar consolidation characteristics, but consolidation properties of halloysite clays would be quite variable. The tropical clay soils of Dhaka (having illite and kaolinite)

showed a narrow range of coefficient of consolidation value and are consistent with the values for illite and kaolinite type of clay minerals.

Table 6.1 Results of triaxial consolidation parameters

Sample number	Depth (m)	Initial Void ratio	Coefficient of consolidation (c_v) m^2/year	Coefficient of volume compressibility (m_v) m^2/MN	Negative slope of NCL (λ)	Coefficient of permeability (k) m/sec
1cn50	1.22-1.37	0.616	24	0.04	0.58	$3.27x10^{-8}$
1cn200	1.52-1.68	0.429	13	0.07	0.45	$2.90x10^{-8}$
1cn400	5.33-5.79	0.526	9.92	0.06	0.40	$1.84x10^{-8}$
1cn600	8.38-8.83	0.452	8.42	0.07	0.40	$1.82x10^{-8}$
1cn800	9.6-10.0	0.481	8.85	0.06	0.42	$1.67x10^{-8}$
2cn100	1.32-1.47	0.410	6.23	0.15	0.50	$2.91x10^{-8}$
2cn200	1.50-1.65	0.402	8.05	0.11	0.44	$2.64x10^{-8}$
2cn400	4.13-4.33	0.440	9.52	0.08	0.45	$2.42x10^{-8}$
2cn600	5.45-5.65	0.482	5.19	0.05	0.41	$0.8x10^{-8}$
2cn800	6.09-6.40	0.493	3.49	0.07	0.38	$0.7x10^{-8}$
3cn50	0.97-1.37	0.461	6.06	0.24	0.60	$4.58x10^{-8}$
3cn200	1.52-1.98	0.443	4.96	0.14	0.48	$2.15x10^{-8}$
3cn400	2.74-3.20	0.412	3.38	0.14	0.41	$1.47x10^{-8}$
3cn600	4.26-4.72	0.445	5.03	0.07	0.40	$1.09x10^{-8}$
3cn800	5.48-5.94	0.439	5.47	0.06	0.37	$0.9x10^{-8}$
1cd50	1.22-1.37	0.616	8.57	0.33	0.52	$8.79x10^{-8}$
1cd200	1.52-1.68	0.429	7.74	0.17	0.47	$4.10x10^{-8}$
1cd400	5.33-5.79	0.525	5.71	0.17	0.45	$3.09x10^{-8}$
1cd600	8.38-8.83	0.453	5.58	0.13	0.43	$2.17x10^{-8}$
1cd800	9.6-10.0	0.481	5.45	0.11	0.40	$1.86x10^{-8}$
2cd100	1.32-1.47	0.411	4.21	0.36	0.60	$4.67x10^{-8}$
2cd200	1.50-1.65	0.403	6.23	0.24	0.48	$4.59x10^{-8}$
2cd400	4.13-4.33	0.440	6.66	0.15	0.42	$3.02x10^{-8}$
2cd600	5.45-5.65	0.482	3.69	0.43	0.42	$4.87x10^{-8}$
2cd800	6.09-6.40	0.494	2.44	0.15	0.38	$1.1x10^{-8}$
3cd50	0.97-1.37	0.461	3.58	0.66	0.60	$7.3x10^{-8}$
3cd200	1.52-1.98	0.443	3.28	0.33	0.56	$3.39 x10^{-8}$
3cd400	2.74-3.20	0.414	2.64	0.21	0.40	$1.72 x10^{-8}$
3cd600	4.26-4.72	0.446	3.28	0.21	0.38	$2.10 x10^{-8}$
3cd800	5.48-5.94	0.438	3.04	0.18	0.37	$1.66 x10^{-8}$

All the coefficients of consolidation values obtained are plotted against void ratio values in figure 6.7. It can be seen from figure 6.7 that the c_v value increased with increasing void ratio. A graph is also plotted to show the relationship of coefficient of consolidation with effective pressure in figure 6.8. It can be seen from this figure that the coefficient of consolidation showed a tendency to decrease with the increase of effective pressure. However, the trend is not very clear and it should be noted that the high value at low consolidation pressure was carried out on a sample with a larger void ratio (figure 6.8).

Table 6.2 Results of oedometer consolidation parameters

Sample no.	Depth (m)	Pressure (kPa)	Coefficient of consolidation (c_v) m^2/year	Coefficient of volume compressibility (m_v) m^2/MN	Compre-ssion index (C_c)	Apparent pre-consolidation pressure (p'_c) kPa
$1ON_1$	1.5-1.7	100	4.23	0.25		170
		200	1.86	0.18		
		400	1.19	0.21		
		800	1.42	0.13	0.2	
		1600	1.99	0.08		
$1ON_2$	4.0-4.3	100	2.35	0.37		190
		200	2.33	0.23		
		400	1.47	0.15		
		800	1.02	0.09	0.2	
		1600	1.20	0.06		
$1ON_3$	6.1-6.4	-	-	-		220
$1ON_4$	9.0-9.3	-	-	-		250

6.3.2 Coefficient of volume compressibility (m_v)

Coefficients of volume compressibility for all the triaxial consolidation samples were calculated for each pressure increment and the results obtained are listed in Table 6.1. The m_v values obtained from Oedometer tests are listed in Table 6.2. The

coefficient of volume compressibility (m_v) for triaxial consolidation of borehole one natural samples ranges from 0.04 to 0.07 m^2/MN and for destructured samples m_v values lie between 0.11 to 0.33 m^2/MN. The m_v values for natural samples of borehole two found are in the range of 0.05 to 0.15 m^2/MN and for destructured samples of the same borehole range between 0.15 to 0.43 m^2/MN. The m_v values for borehole three natural samples range from 0.06 to 0.24 m^2/MN and for destructured samples range from 0.18 to 0.66. In contrast, m_v values obtained from oedometer tests on borehole one samples lie between 0.06 to 0.37 m^2/MN. Lambe and Whitman (1969) mentioned some typical values of coefficient of volume compressibility (m_v) to classify soils on the basis of compressibility. He mentioned a m_v value of 0.10-0.30 m^2/MN for medium compressibility and 0.05-0.10 m^2/MN for low compressibility clays. The samples show a small range of variation in the coefficient of volume compressibility (m_v) values and the obtained results are compatible with the values quoted by Lambe and Whitman (1969) for the low to medium compressibility clays. One sample (test 1un50) at low confining pressure showed very low compressibility (<0.05 m^2/MN).

Hobbs et al. (1988) mentioned that values of the coefficient of volume compressibility (m_v) for tropical clay soils of west Java, Indonesia lie in the range 0.03 to 1.0 m^2/MN and for the high pressure tests between 0.01 and 0.43 m^2/MN. Carter and Bentley (1991) quoted a value of 0.05-0.1 m^2/MN for low compressibility very stiff tropical clay and a value of 0.1-0.3 m^2/MN for medium compressibility firm tropical red clays. Therefore the m_v values identified for the Dhaka soils are consistent with the values quoted by Hobbs et al. (1988) and Carter and Bentley (1991).

From Table 6.1 it is observed that the coefficient of volume compressibility (m_v) varies slightly with depth and the variation is not regular. It can be seen from figure 6.9 that m_v tends to decrease with increasing consolidation pressure. However, from

the observed results it was found difficult to establish any general relationship for m_v with void ratio (figure 6.10).

6.3.3 Void ratio versus p′ curves

For isotropic triaxial consolidation tests, void ratio is plotted against effective pressure (p′) (in log scale) from a single increment test for each sample. The e-log p′ curves of boreholes one, two and three are shown in figures 6.11 to 6.13 respectively. It can be seen from these figures that the void ratio values decreased in each case with increasing effective pressure. Although very small, the change of void ratio from start to the end of the test for a single increment is more in the destructured samples.

The void ratio versus log p′ curves for some selected samples of borehole one obtained from Oedometer tests are shown in figure 6.14. The apparent preconsolidation pressures were determined by using the Casagrande construction method. The measured apparent preconsolidation pressures are listed in Table 6.2. The value ranges from approximately 170 kPa to 250 kPa. This quasi-preconsolidation pressure developed in natural soils is due to the bonded structure of the soil. To interprete this behaviour a graph is plotted to see the variations of observed quasi-preconsolidation pressures for different samples of borehole one with respect to depth and to compare the results with the effective overburden pressures. It can be seen from figure 6.15 that the effective overburden pressure is much lower than the observed quasi-preconsolidation pressure. Stress history only does not explain such high values of quasi-preconsolidation pressure, as the overburden pressure is approximately half the value of quasi-preconsolidation pressure. The difference between the effective overburden pressure and the observed quasi-preconsolidation pressure increases with depth. The observed quasi-preconsolidation pressure also increases with depth. Therefore, it is unlikely that a

previous removal of soil, by erosion for instance, could be the cause of the quasi-preconsolidation pressures. It is more likely that the observed quasi-preconsolidation pressure is due to bonding.

6.3.4 Compression index (C_c)

In one dimensional cosolidation the compression index (C_c) is the slope of the linear portion of the e-log σ' plot and is dimensionless. In isotropic triaxial consolidation the gradient of the normal consolidation line (NCL) in v-log p′ is expressed by λ. In isotropic consolidation, C_c values were estimated based on observed λ values. The λ values of three borehole samples obtained from isotropic consolidation tests are listed in Table 6.1. The compression index values obtained from Oedometer tests are listed in Table 6.2. Based on λ values obtained (Table 6.1) the compression index value estimated from isotropic consolidation ranges from 0.2 to 0.3 and those obtained from Oedometer test is 0.2 (Table 6.2).

Head (1982) mentioned some typical values of C_c for different types of clays. He quoted a compression index value of 0.2 to 0.8 for medium to low plasticity clay and a C_c value of up to 2.6 for montmorillonite clay. Hobbs et al. (1988) mentioned a C_c value of 0.33 to 0.75 for tropical clay soils of west Java, Indonesia. The obtained results (0.2-0.3) are generally consistent with these values.

6.3.5 Coefficient of permeability (k)

The coefficient of permeability (k) values obtained are listed in Table 6.1. The coefficient of permeability of borehole one natural samples lies between 1.67×10^{-8} m/sec to 3.27×10^{-8}m/sec and those of destructured samples are in the range of 1.86×10^{-8}m/sec to 8.79×10^{-8}m/sec The k value for borehole two natural sample range

from 0.7 $x10^{-8}$m/sec to 2.91 $x10^{-8}$m/sec and that of destructured samples lie between 1.1 $x10^{-8}$m/sec to 4.87 $x10^{-8}$m/sec. The *k* value for borehole three natural sample ranges from 0.9 $x10^{-8}$m/sec to $4.58x10^{-8}$m/sec and for destructured samples range from $1.66x10^{-8}$m/sec to $7.3x10^{-8}$m/sec The results obtained suggest that the permeability of the analysed soils is very low, typical of weathered clays (Casagrande and Fadum, 1940).

Grim (1962) pointed out that permeability decreases with increasing mica (illite) and then the replacement of mica by kaolinite and also the replacement of kaolinite by montmorillonite makes it less permeable to almost impermeable. Grim (1962) also mentioned that in the case of quartz and mica (illite) permeability ranges from $4.2x10^{-6}$ m/sec to $5.8x10^{-6}$ m/sec and in the case of quartz and kaolinite permeability ranges from $2.5x10^{-8}$ to $9.5x10^{-8}$ m/sec. Hobbs et al. (1988) mentioned that the *k* value for the tropical red clay soils of west Java, Indonesia lie between $2.2x10^{-8}$ m/sec to $5.6x10^{-9}$ m/sec. The permeability values obtained are close to the values mentioned by Hobbs et al. (1988) and Grim (1962) for illite and kaolinite type of clays and are in agreement with the mineralogy of the samples.

The relationship between the coefficient of permeability and the consolidation pressure is shown in figure 6.16. It can be seen from this figure that permeability is dependent on the applied consolidation pressure and the value decreases with increasing consolidation pressure. Wu et al. (1993) also reported similar results for smectitic mudstone. The relationship between coefficient of permeability and void ratio is shown in figure 6.17. It is observed from figure 6.17 that the permeability value of the samples increases with increasing void ratios. Grim (1962) reported similar results for kaolinite and illite clay. Sridharan (1988) mentioned a linear relationship between void ratio and permeability for red tropical soils of Bangalore. A relationship was also plotted to see the variation of coefficient of permeability with the coefficient of consolidation and this relationship is shown in figure 6.18. It

can be seen from figure 6.18 that there may be a tendency for the permeability to increase with increasing value of coefficient of consolidation, but the relationship is not clearly defined.

6.4 Summary

In this chapter the consolidation characteristics of the tropical clay soils of Dhaka were discussed in terms of the coefficient of consolidation, coefficient of volume compressibility, compression index and the coefficient of permeability. These consolidation parameters were compared and evaluated with the work of other researchers. The identified values were also evaluated with respect to mineralogy. Volume change versus time curves, void ratio versus effective pressure curves for isotropic triaxial consolidation for a single increament and void ratio versus log p′ curves for Oedometer consolidation are also presented. Finally an attempt has been made to show the relationship of the consolidation parameters with the consolidation pressure and void ratio.

The soils showed a major reduction in volume initially with time and after a few hours they showed almost a constant volume with time. There were small variations between the samples at different sites. However, the initial consolidation of the natural samples was completed between approximately 20 minutes to 600 minutes with increasing consolidation pressure. Conversely, the initial consolidation of the destructured samples was completed between 20minutes to 480 minutes with increasing consolidation pressure. Generally the consolidation of the samples increased with increasing confining pressures. The destructured samples from the three boreholes in each case showed greater amount of volume change than the natural samples, which would be expected due to the destruction of original structure

in destructured soils. A quasi-preconsolidation pressure was observed in Oedometer tests, which is likely to be due to the bonded structure of the soils.

The coefficients of consolidation (C_V) values obtained are consistent with low to medium plasticity inorganic clay. The samples showed a narrow range of coefficient of consolidation value and they are consistent with that of a kaolinitic and illitic soil. It was observed that the c_v value increased with increasing void ratio. The samples also broadly showed a decrease of coefficient of consolidation with increasing effective pressure. The coefficient of volume compressibility (m_v) of the natural samples range between 0.04 to 0.24 m^2/MN and that of destructured samples lie between 0.11 to 0.66 m^2/MN. The results suggest that the compressibility of the soil is very low to medium. It was found that the m_v value decreased with increasing consolidation pressure. A compresssion index (C_C) value of 0.2 to 0.3 was observed for these soils.

The permeability of the soil was very low with a k value ranging from $0.7x10^{-8}$m/sec to $4.58x10^{-8}$m/sec for natural samples and a value of $1.1x10^{-8}$m/sec to $8.79x10^{-8}$ m/sec for destructured samples. The obtained values of *k* are consistent with that of kaolinitic and illitic soil and are in agreement with the mineralogy of the samples. It was observed that the coefficient of permeability of the samples decreased with increasing consolidation pressure. It was also found that k value of the samples increased with increasing void ratio and with increasing coefficient of consolidation.

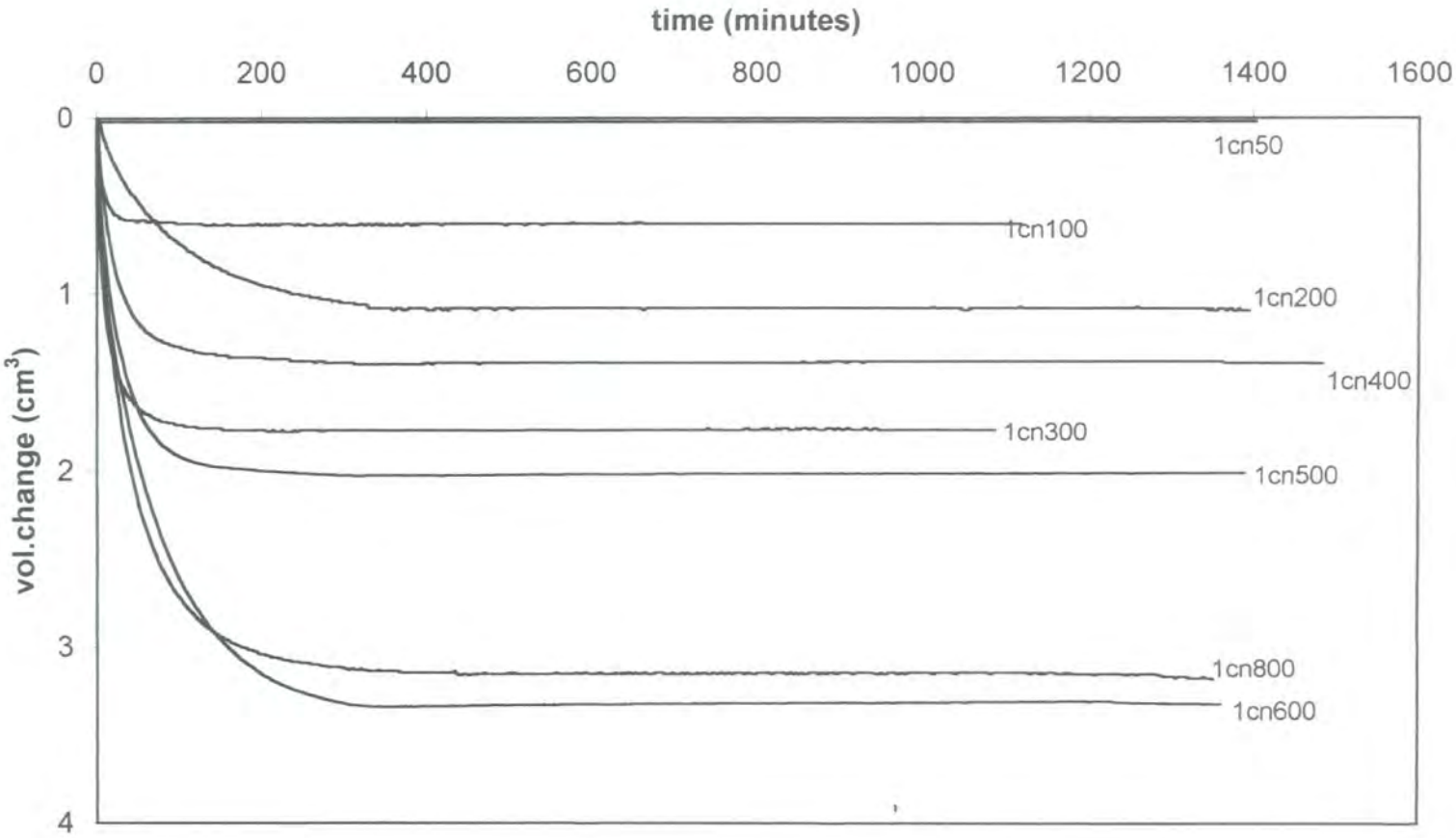

Fig. 6.1 Triaxial consolidation graphs of natural samples of borehole one

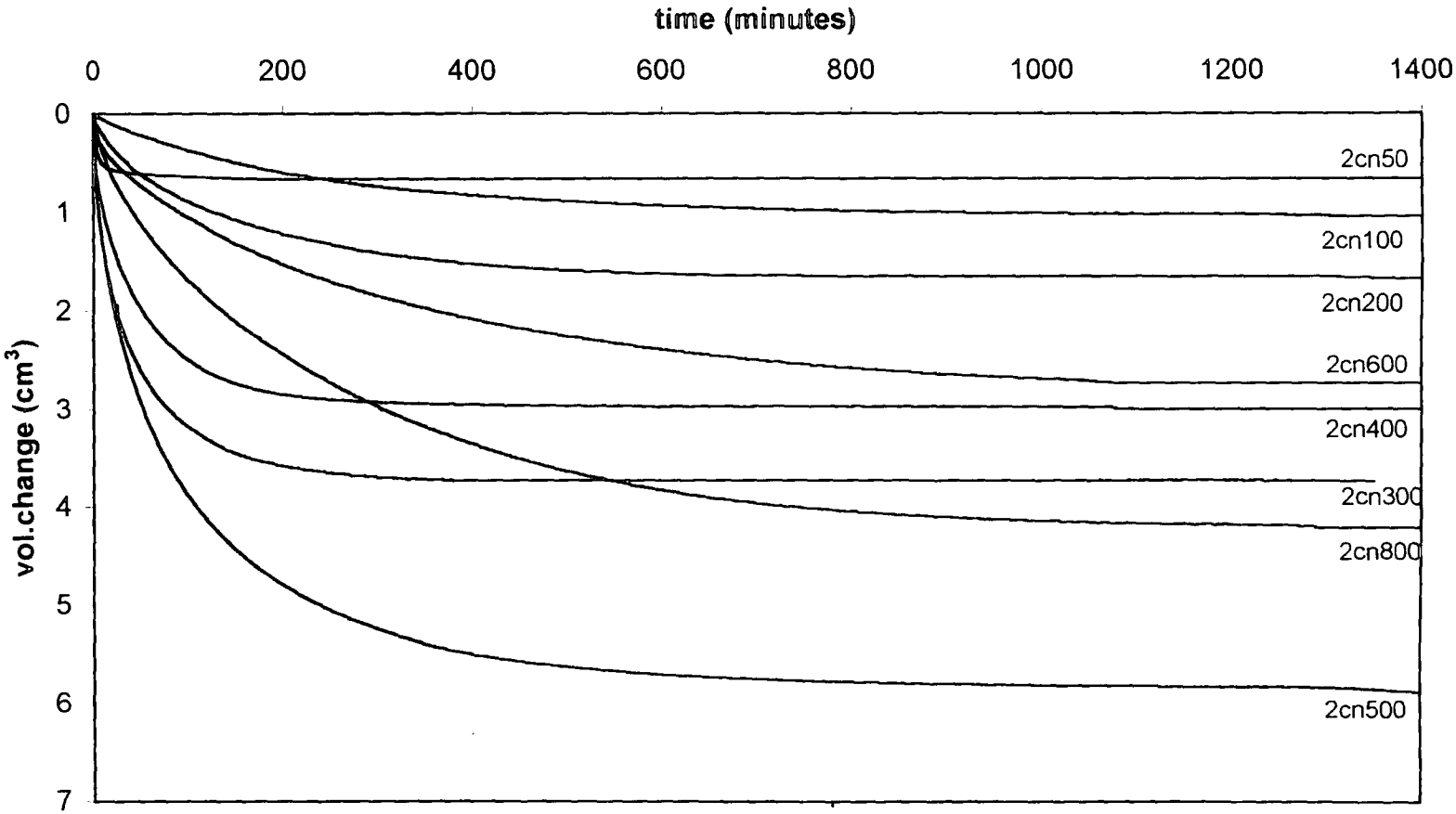

Fig.6.2 Triaxial consolidation graphs of natural samples of borehole two

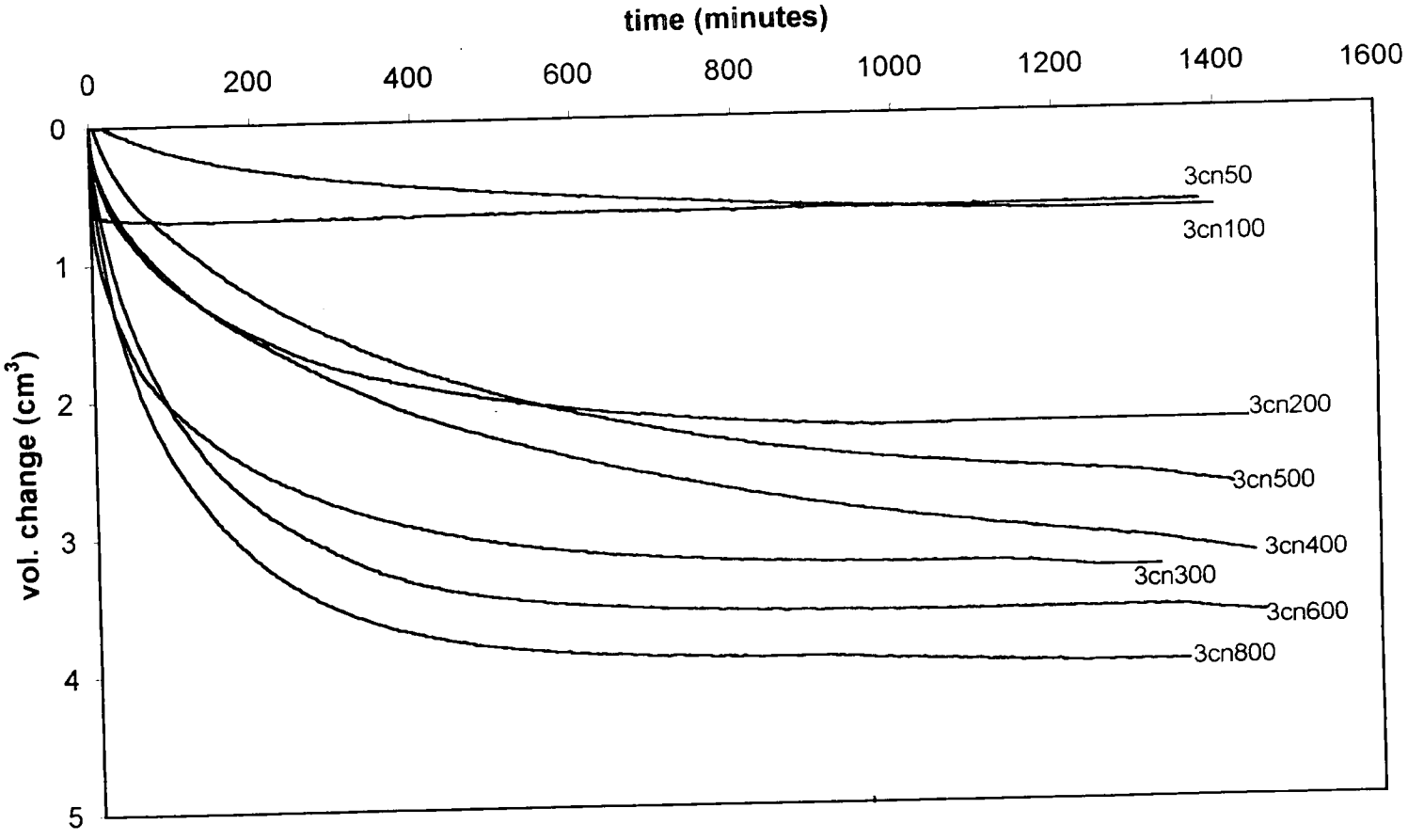

Fig. 6.3 Triaxial consolidation graphs of natural samples of borehole three

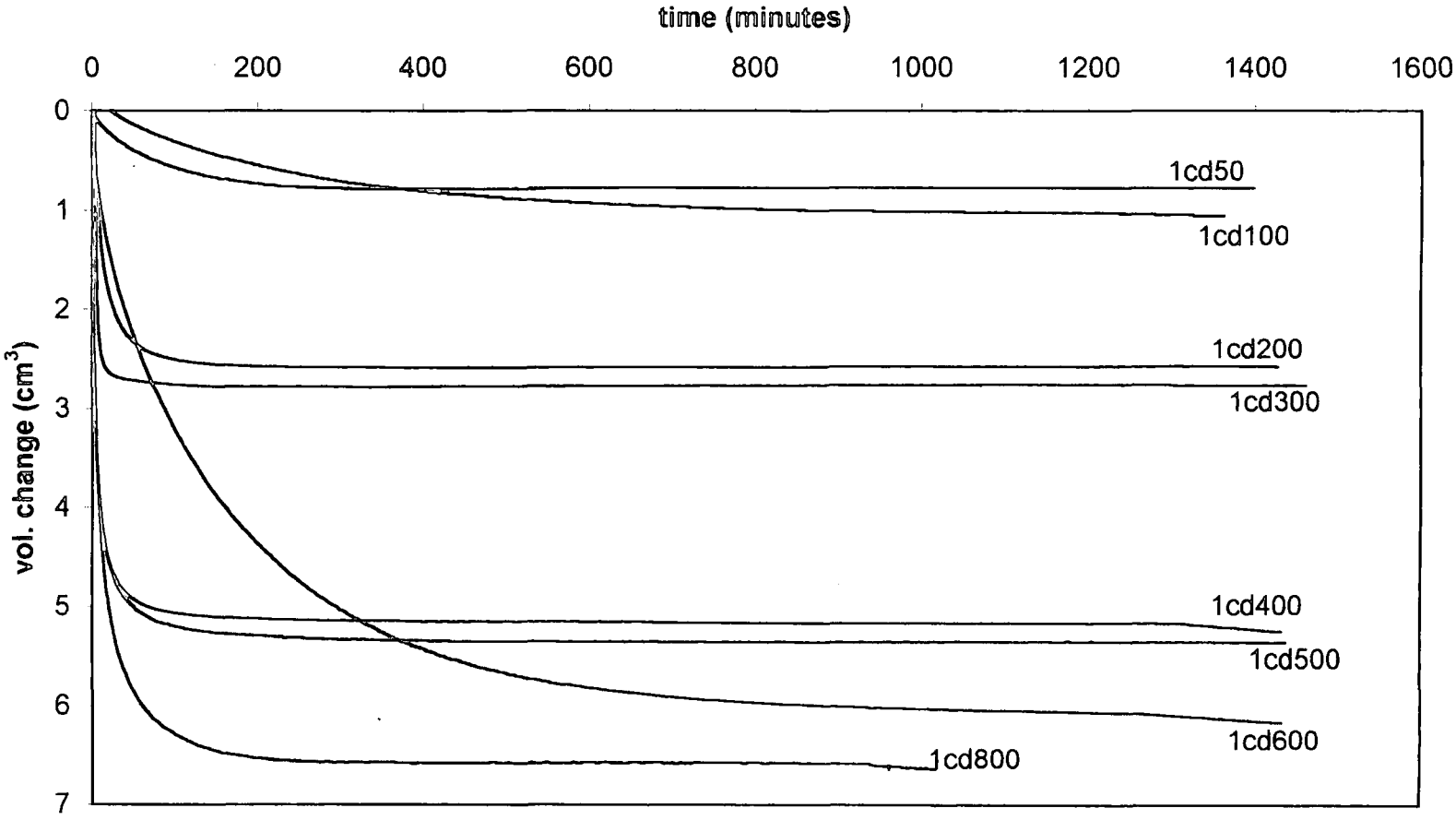

Fig. 6.4 Triaxial consolidation graphs for destructured samples of borehole one

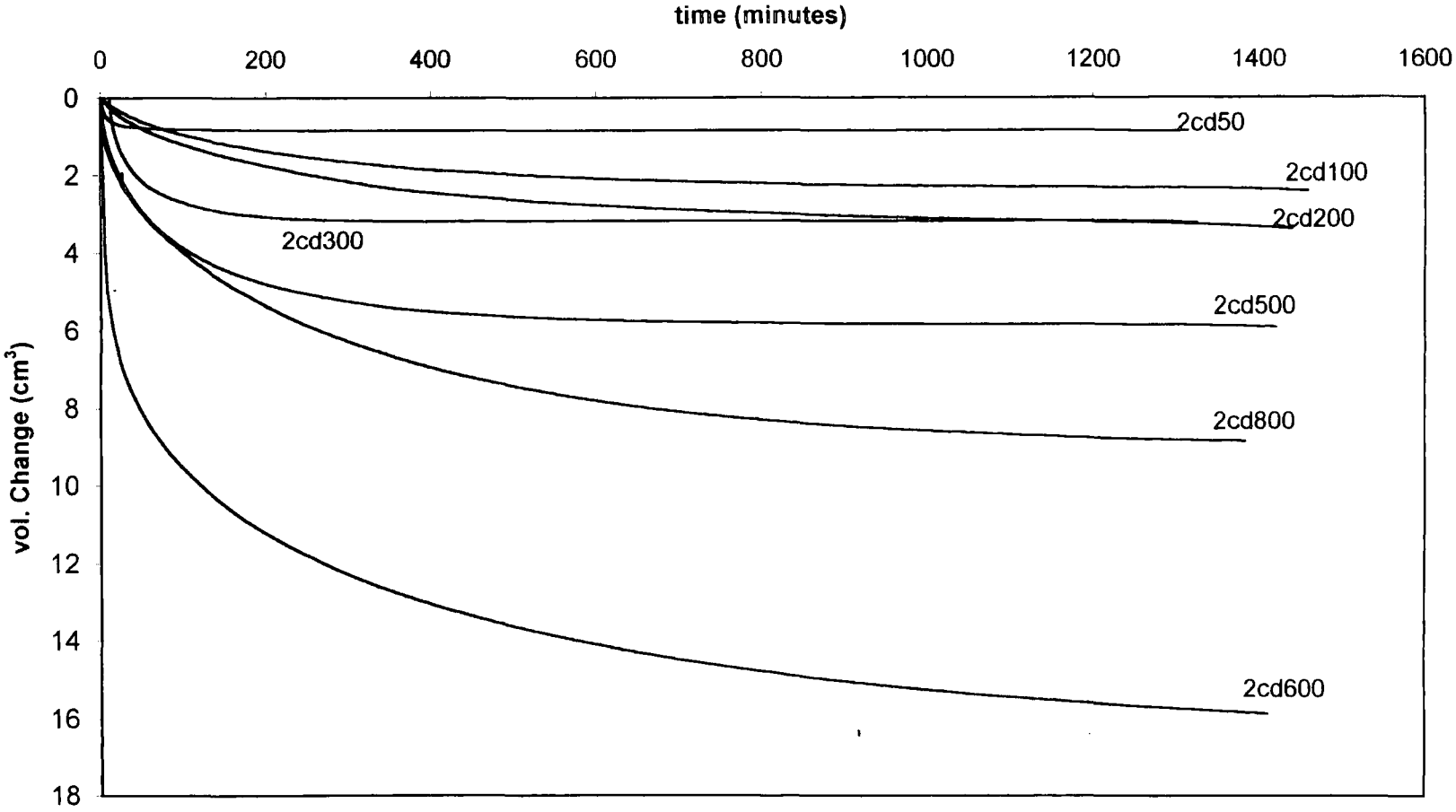

Fig. 6.5 Triaxial consolidation graphs for destructured samples of borehole two

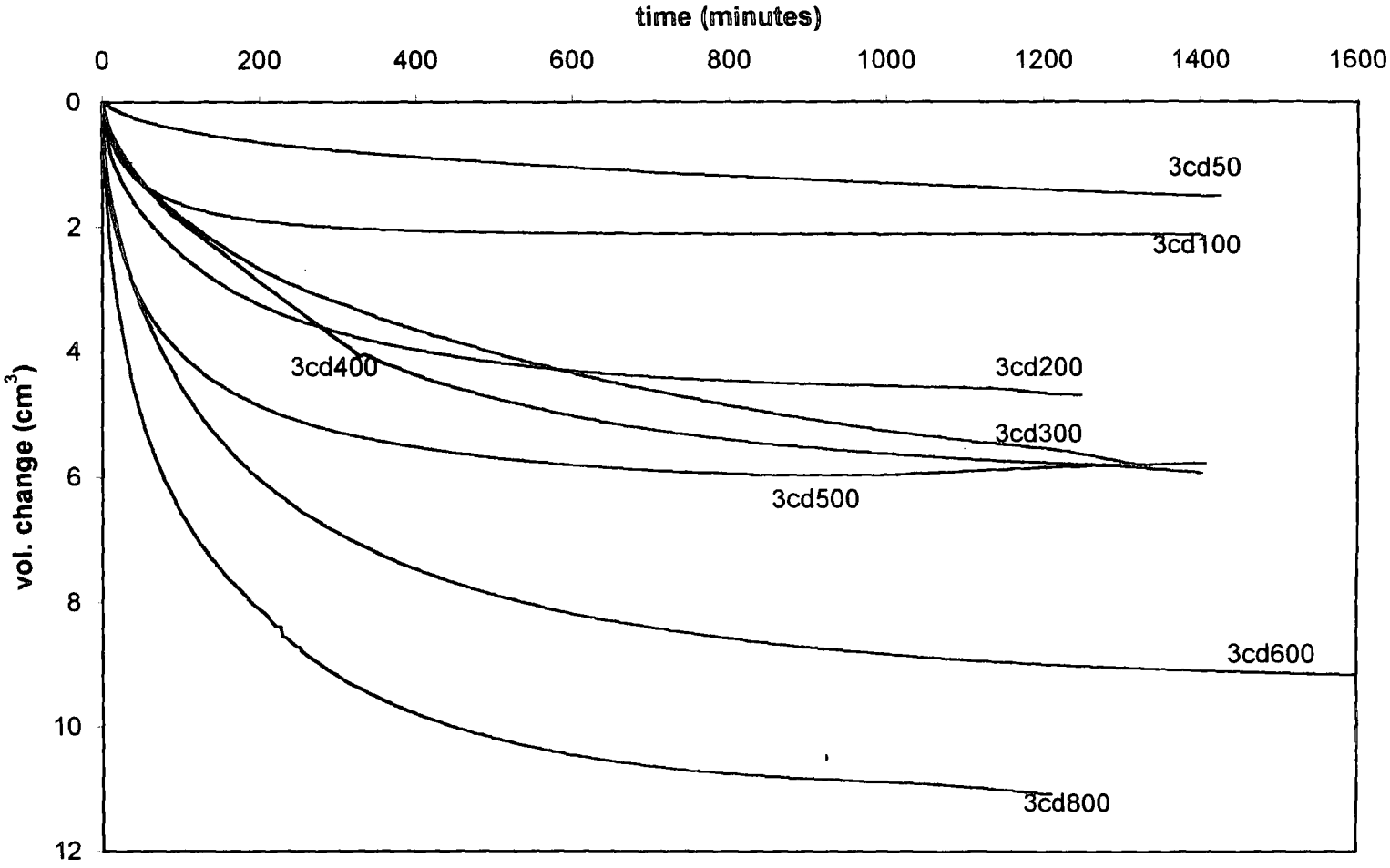

Fig. 6.6 Triaxial consolidation graphs for destructured samples of borehole three

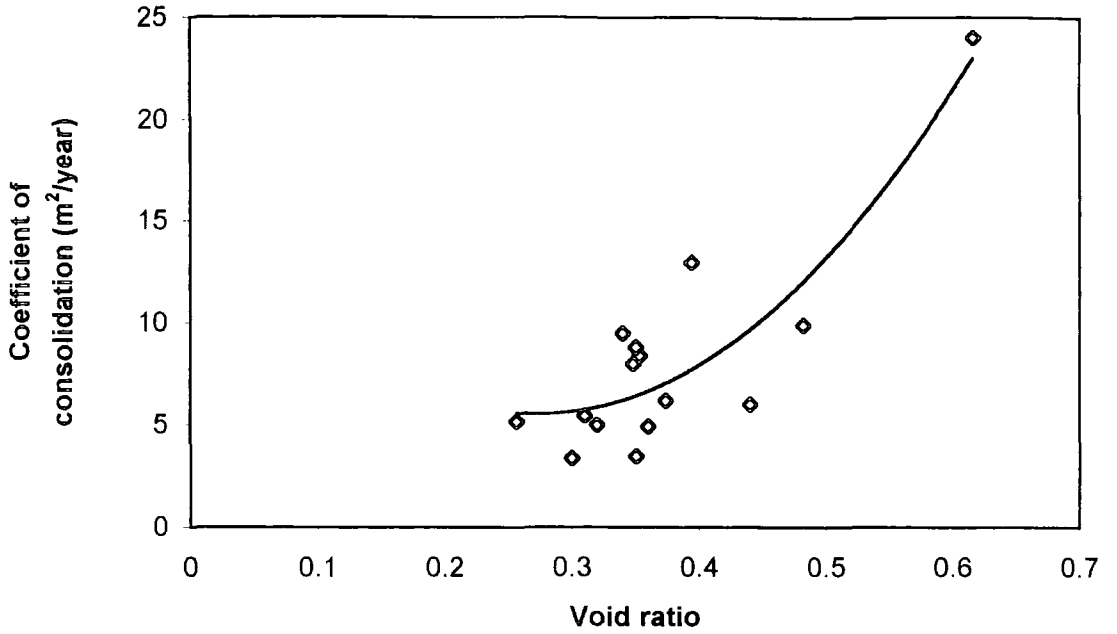

Fig.6.7 Relationship of void ratio versus coefficient of consolidation (Isotropic consolidation)

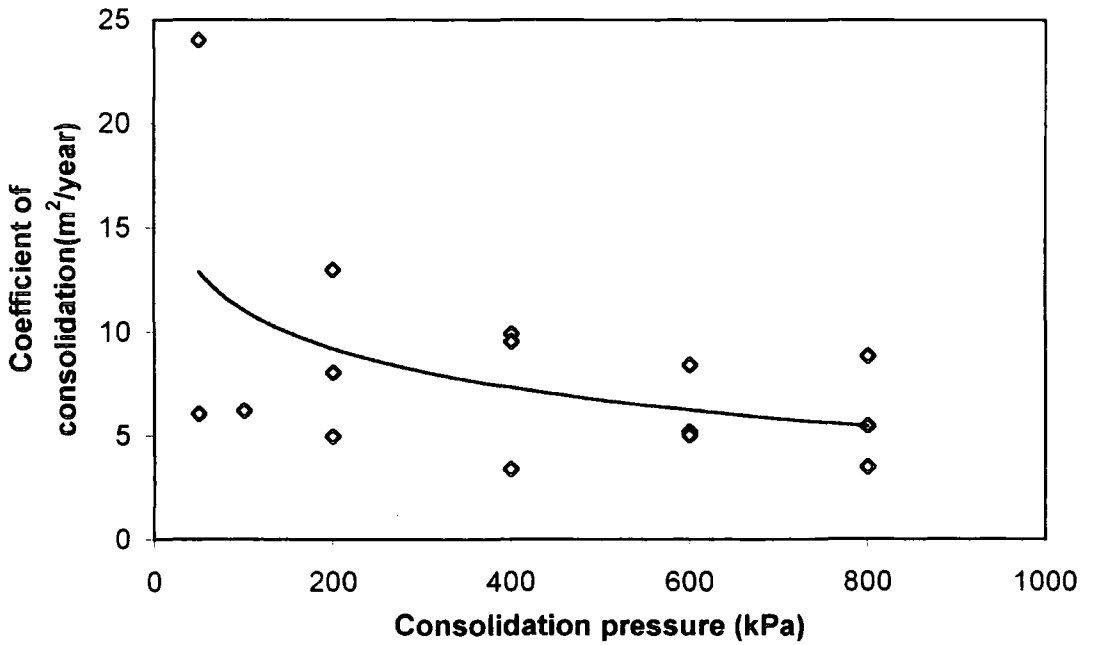

Fig.6.8 Relationship of coefficient of consolidation and effective pressure (Isotropic consolidation)

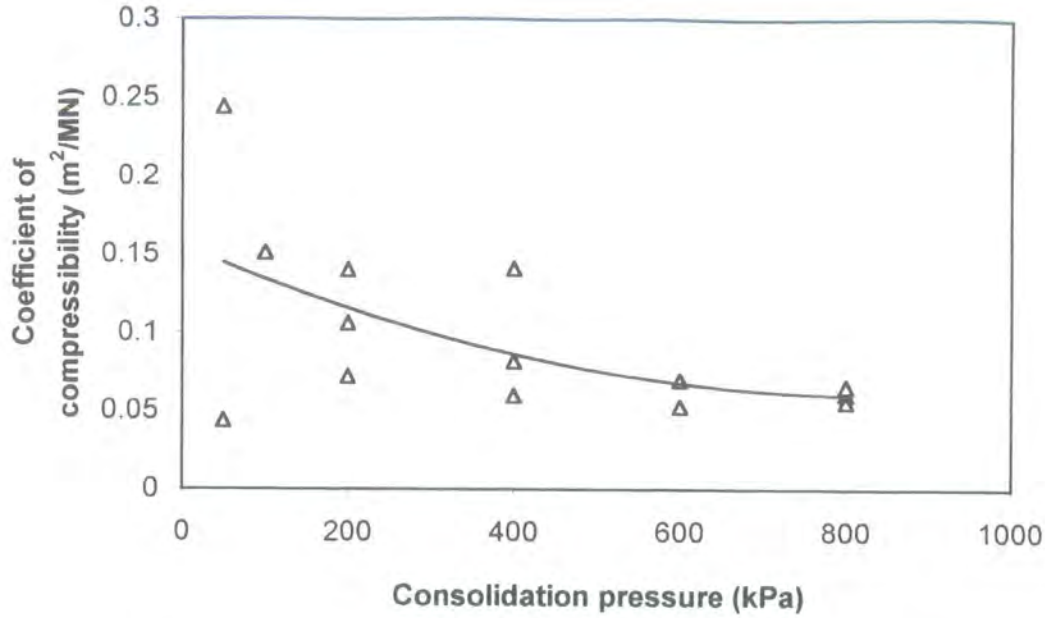

Fig. 6.9 Relationship of coefficient of volume compressibility and consolidation pressure (Isotropic consolidation)

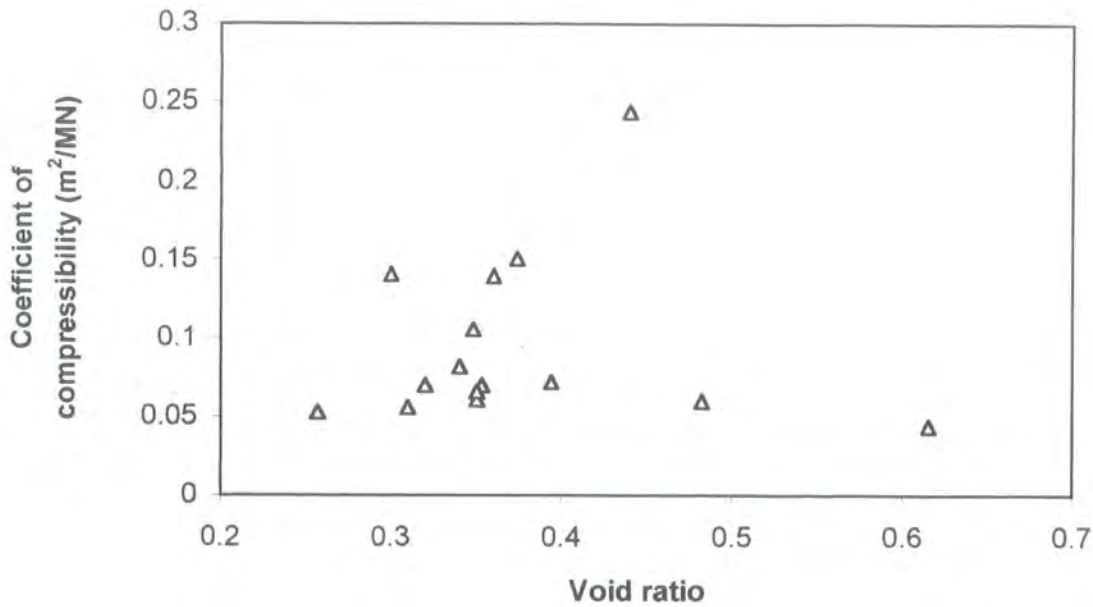

Fig. 6.10 Relationship between coefficient of compressibility and void ratio (Isotropic consolidation)

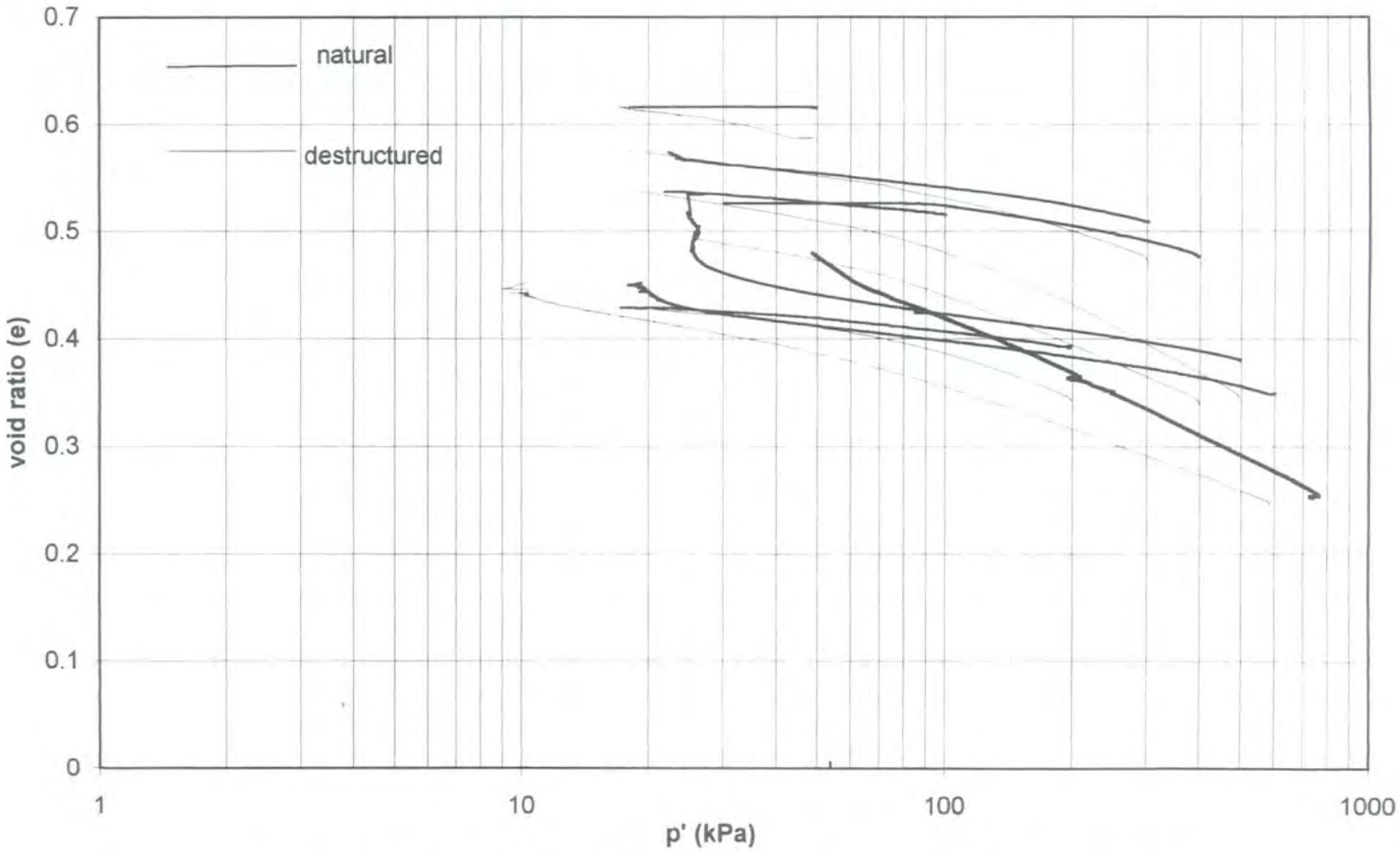

Fig.6.11 Comparison of e-p' curves for natural and destructured soils of borehole one

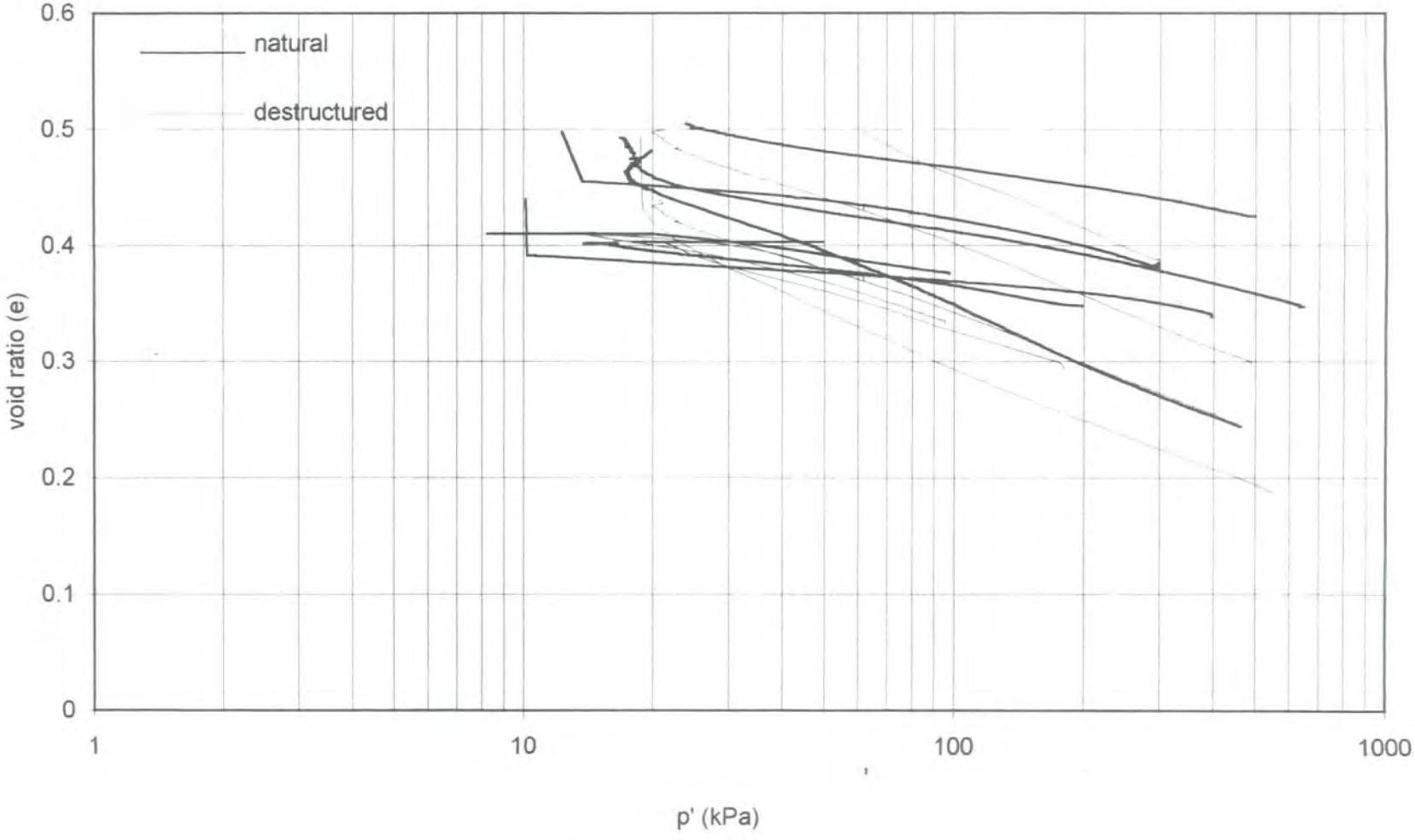

Fig.6.12 Comparison of e-p' curves for natural and destructured soils of borehole two

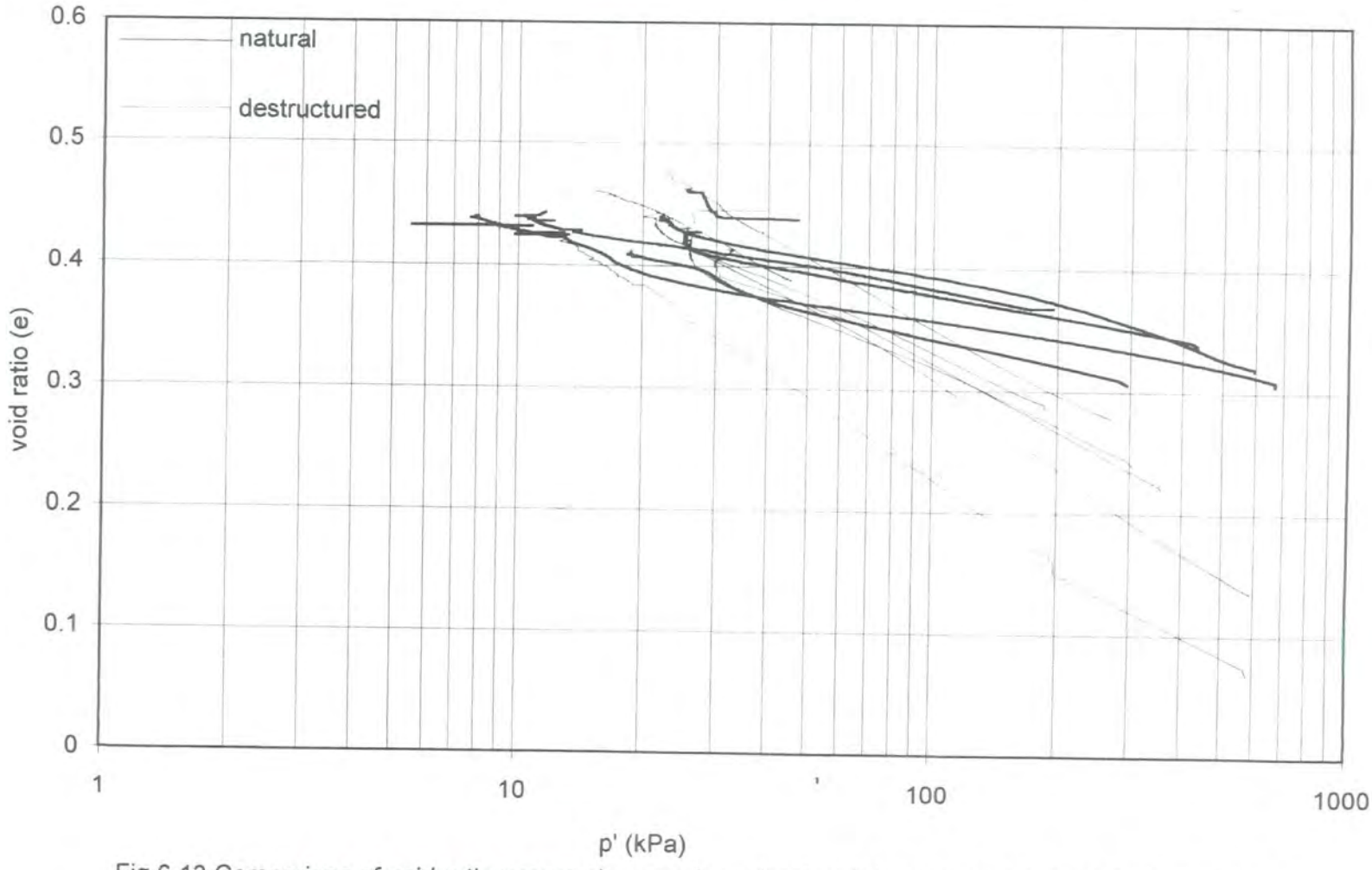

Fig.6.13 Comparison of void ratio versus p' curves for natural and destructured soils of borehole three

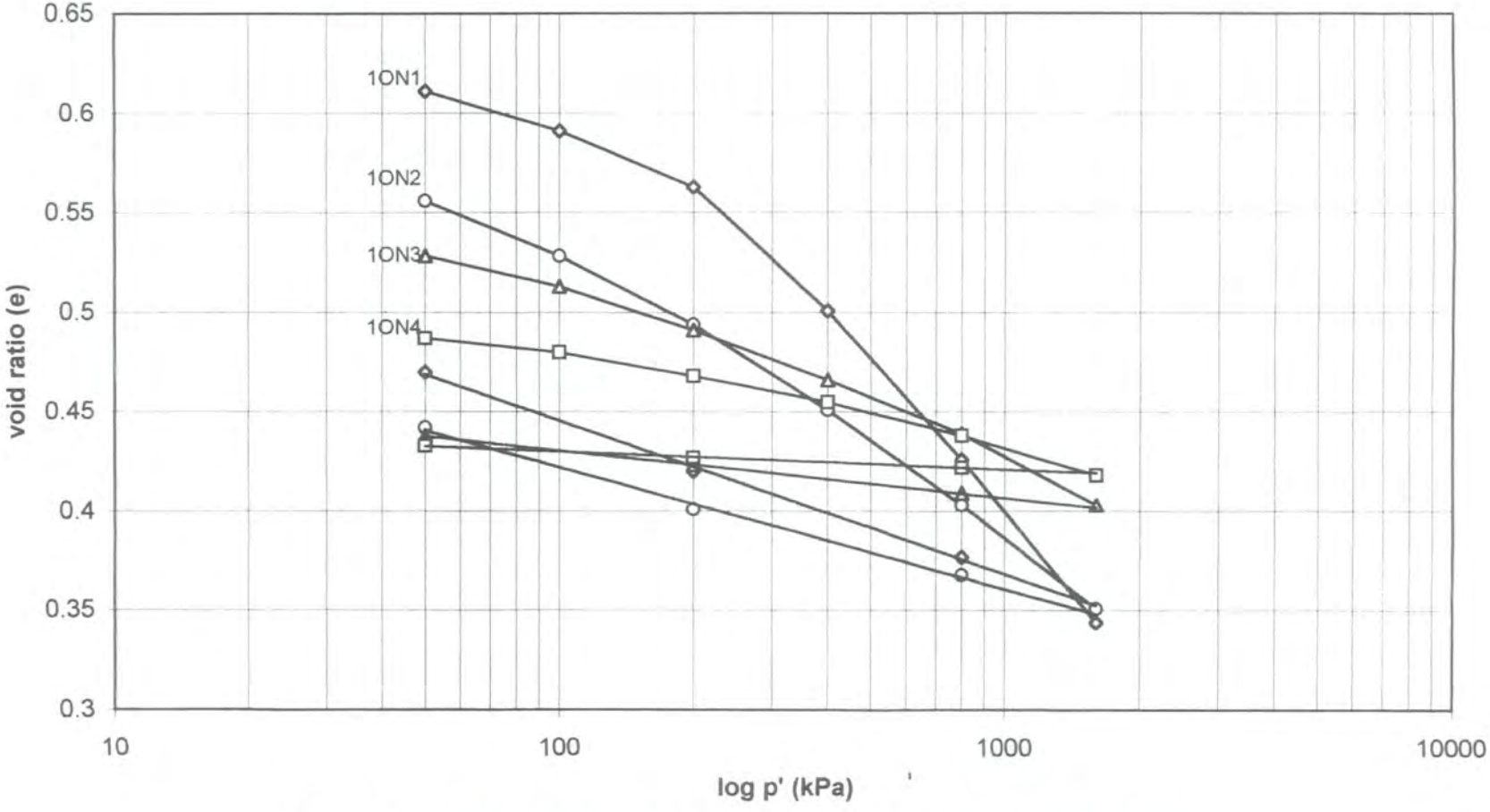

Fig. 6.14 void ratio versus log p' curves obtained from oedometer consolidation tests

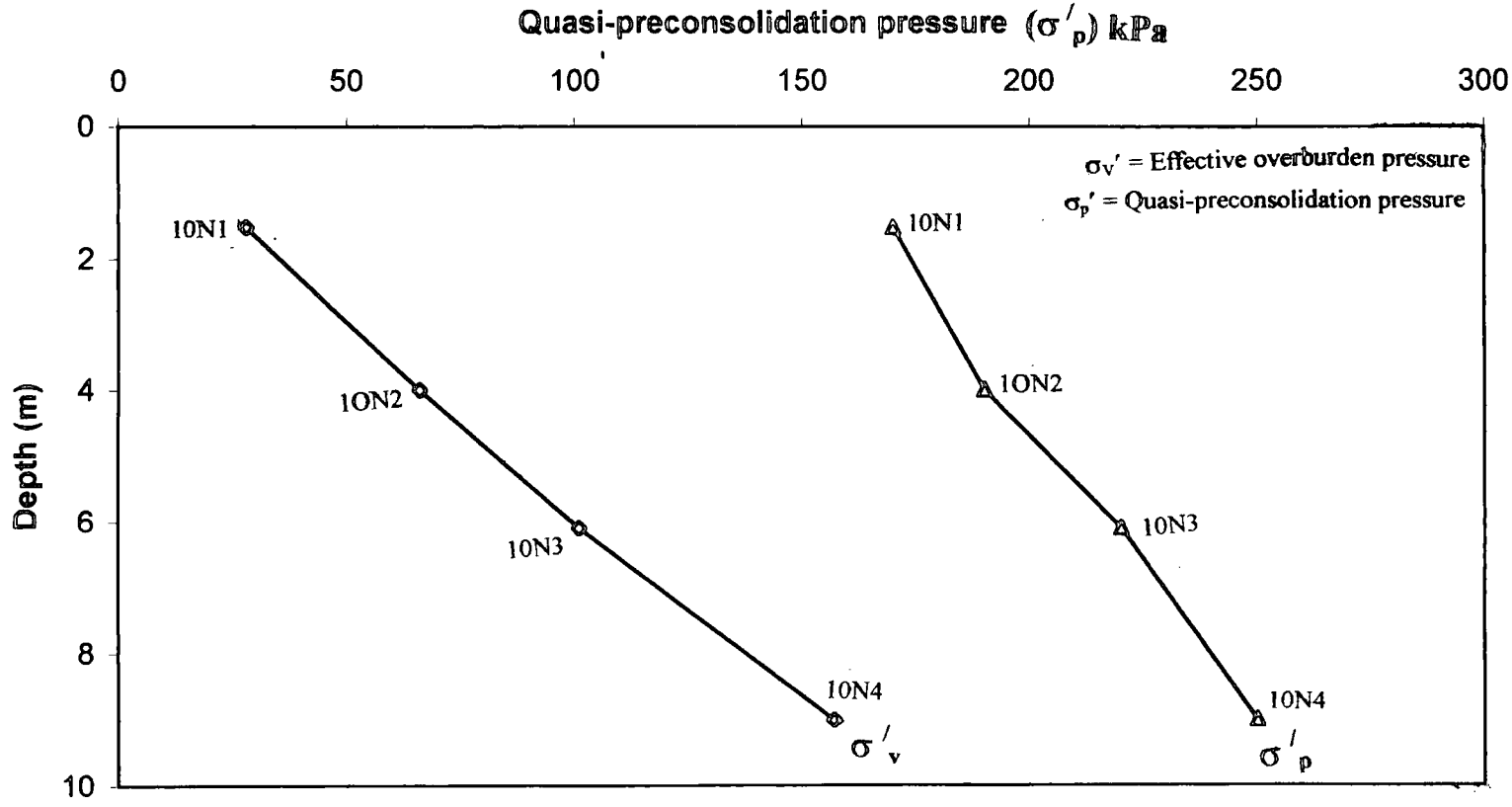

Fig.6.15 Variation of insitu overburden pressure and the quasi-preconsolidation pressure with depth for oedometer samples of borehole one

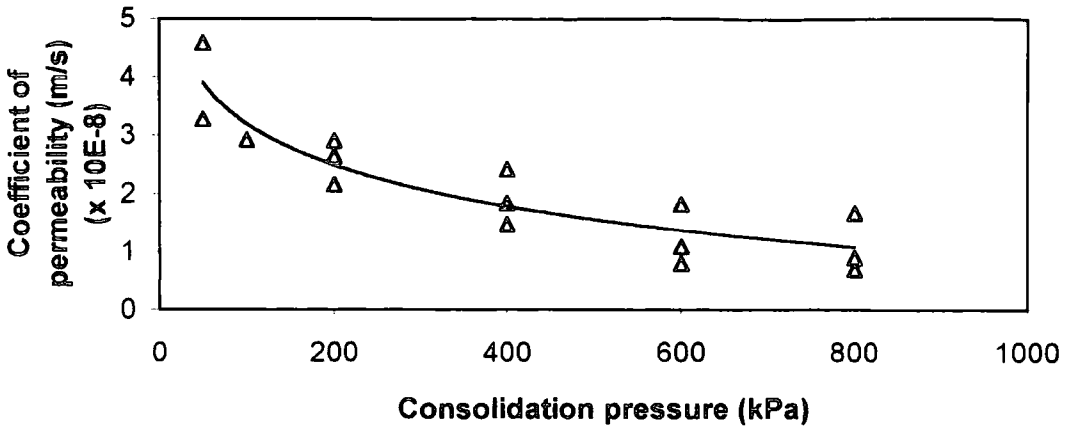

Fig.6.16 Relationship of coefficient of permeability and consolidation pressure

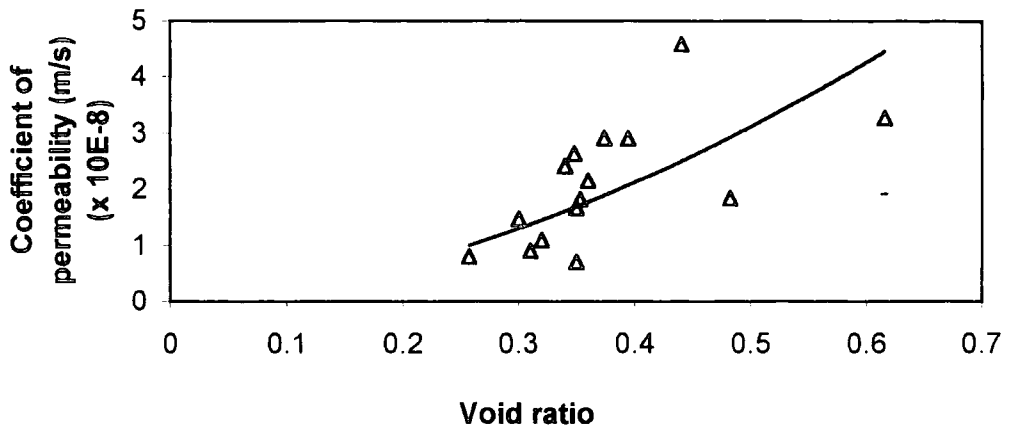

Fig. 6.17 Relationship of coefficient of permeability with void ratio

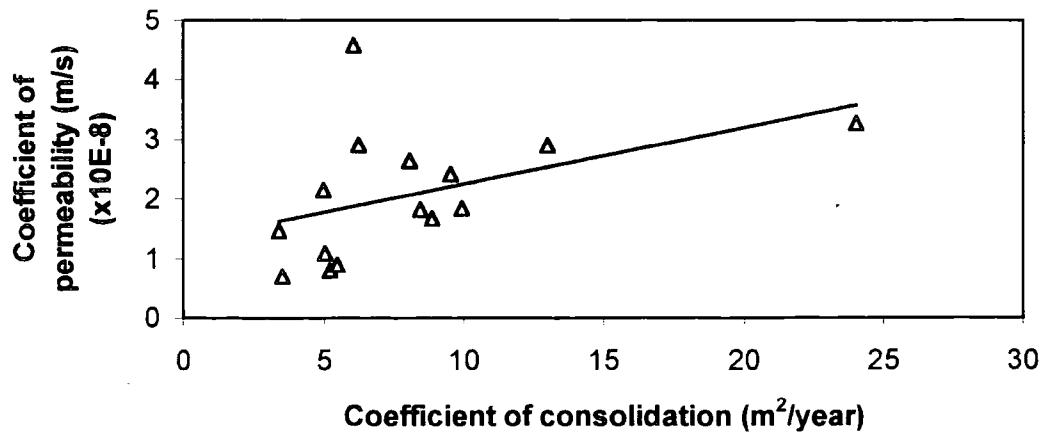

Fig. 6.18 Relationship between coefficient of permeability and coefficient of consolidation

CHAPTER 7

UNDRAINED TRIAXIAL TESTS

7.1 Introduction

This chapter describes in detail the results of all the consolidated undrained triaxial tests made on the tropical clay soils of Dhaka, Bangladesh. The samples were collected from two different boreholes of the same geological formation and their location is shown in figure 3.1 of chapter 3. Both natural and destructured samples were used to carry out the tests. Results are presented for boreholes one and two in terms of stress-strain curves, stress ratios, pore water pressures and stress paths in the q - p′ space. Critical state behaviour is also discussed.

Yield of the naturally bonded soil in the stress plane is evaluated and the failure surface is presented. Two yield points are identified from the loss of tangential stiffness curve during shearing as described by Malandraki and Toll (1996 & 2000). A final yield is also identified from the point of maximum curvature of the stress-strain curves. A comparison is made between the results of boreholes one and two. Comparisons are also made between undrained triaxial tests in both the natural state and in a destructured condition. Finally an attempt is made to define the important characteristics for developing a framework for the tropical clay soils of Dhaka.

7.2. Consolidated undrained triaxial tests on natural state tropical clay soils of Dhaka

The undrained behaviour of samples in the natural state from borehole one and two is discussed in this section. Stress-strain behaviour of these samples is carefully evaluated and stress paths are presented. The q/p′ ratio and the variation of excess pore water pressure (p.w.p.) with an increase in strain are also studied.

The position of all the identified yield points are shown in the stress space. The first loss of tangential stiffness is associated with the 'initial yield', which is defined from the log-log plot of tangential stiffness versus small strain graph (Malandraki and Toll, 1996 and 2000). The 'bond yield' is identified from the same graph at which a marked drop of tangential stiffness occurred (Malandraki and Toll, 2000). Small strain behaviour up to 2% strain are also evaluated with the help of tangential stiffness versus mean effective stress curves and the deviator stress versus p′ curves. All the results obtained are presented, compared and evaluated.

7.2.1 Testing details

Consolidated undrained triaxial tests with pore water pressure measurement were carried out on sixteen natural and sixteen destructured samples collected from two different boreholes (boreholes one and two). All samples were initially saturated and were subjected to isotropic consolidation (at a range of confining pressures from 50 kPa up to 800) before shearing. Testing details is discussed in section 4.6 of Chapter 4.

The detailed test information including test name, location, sample depth, void ratio, dry density, consolidation stress (i.e. effective confining pressure) for natural soils are listed in Tables.7.1 & 7.2 (in section 7.2) and that for destructured soils are listed in Tables 7.5 & 7.6 in section 7.3.

Table 7.1: Testing details of natural state soils of borehole one, Location: Mirpur

Test name	Depth (m)	Initial moisture content w %	Specific gravity G_s	Bulk density ρ (Mg/m^3)	Dry density ρ_d (Mg/m^3)	Initial void ratio e	Wet weight of sample (g)	Dry weight of sample (g)
1un50	1.22-1.37	18.8	2.61	1.918	1.614	0.616	165.39	139.18
1un100	1.37-1.52	18.4	2.60	2.003	1.691	0.537	172.64	145.78
1un200	4.72-5.08	14.4	2.64	2.113	1.847	0.429	182.19	159.20
1un300	5.68-5.85	17.6	2.65	1.979	1.683	0.574	170.62	145.09
1un400	6.90-7.15	17.2	2.59	1.989	1.697	0.526	171.45	146.25
1un500	7.16-7.62	17.1	2.61	1.992	1.701	0.535	171.73	146.61
1un600	8.68-8.83	17.3	2.60	2.101	1.791	0.452	181.11	154.33
1un800	9.6-10.0	15.6	2.62	2.044	1.770	0.481	176.31	152.55

7.2.2 Test name

All samples are named by using letters and numbers. The initial number indicates the borehole number and the number after the two letters in each case indicates the value of effective confining pressure at which the samples were consolidated before shearing. Two letters are used to designate each test. The first letter in each test indicates the type of shearing (undrained) and the second letter indicates the nature of the sample (natural or destructured). For example test 1un100 (in Table 7.1) indicates a test on a sample from borehole one, tested undrained in a natural state, which was consolidated at a confining pressure of 100 kPa before shearing. Similarly 2ud400 (in Table 7.6) means a test on a sample from borehole two, tested undrained in a destructured state, which was consolidated at a confining pressure of 400 kPa before shearing.

Table 7.2: Testing details of natural soils of borehole two

Location: Curzon Hall

Test name	Depth (m)	Initial moisture content w %	Specific gravity G_s	Bulk density ρ (Mg/m^3)	Dry density ρ_d (Mg/m^3)	Initial void ratio e	Wet weight of sample (g)	Dry weight of sample (g)
2un50	1.10-1.30	17.9	2.59	2.176	1.846	0.403	187.62	159.14
2un100	1.32-1.47	17.1	2.62	2.171	1.859	0.410	187.62	160.21
2un200	3.50-3.65	14.2	2.64	2.150	1.883	0.402	185.35	162.27
2un300	3.68-3.88	15.3	2.62	2.016	1.749	0.498	173.80	150.74
2un400	4.13-4.33	14.1	2.60	2.062	1.806	0.440	177.77	155.70
2un500	4.60-4.80	14.9	2.59	1.972	1.720	0.505	170.45	148.24
2un600	5.45-5.65	16.0	2.63	2.060	1.773	0.482	177.59	153.00
2un800	6.09-6.40	17.2	2.61	2.049	1.748	0.493	176.62	150.65

7.2.3 Results

7.2.3.1 Stress-strain curves (natural soils of borehole one and two)

The deviator stress versus axial strain curves for natural soils of borehole one are shown in figure 7.1 and those of borehole two are shown in figure 7.2. It can be seen from figures 7.1 and 7.2 that the stress strain curves show a maximum stress level in each case. After reaching the maximum stress level, a drop of deviator stress is observed in each case with increasing strain. It can be seen from figure 7.1 that at low effective confining pressures the maximum deviator stress points are not sharp except for the test 1un200 and they do not show a prominent peak. At very high effective confining pressures the samples show a broader peak at large strain. The maximum q points of borehole two samples are not sharp up to a confining pressure of 500 kPa (figure 7.2) but at higher confining pressures the samples show a more prominent peak. It can also be seen from these figures that the maximum deviator stress increases with increasing confining pressure. In many tests, the deviator stress decreases after the maximum point at almost a constant rate at very large strain.

The axial strains to attain maximum deviator stress for samples of borehole one are in the range 4% to 19% and those of borehole two samples lie in between approximately 8% to 26%. The lowest strain to attain the maximum deviator stress for borehole one samples is encountered for sample 1un200 and for borehole two samples is for sample 2un600. On the other hand, the highest value of strain at the maximum point is observed in 1un100 and 2un300. The maximum deviator stress and the corresponding values of axial strain, mean effective stress and the value of excess pore water pressure in each case are summarized in Table.7.3. It should be noted here that all the samples of the two boreholes are collected from the same geological formation but at different depths. Shallow depth samples are more weathered than those from greater depth.

Table 7.3: Summary of stress and strain parameters at maximum deviator stress

Sample number	Maximum deviator stress (q) kPa	Excess p.w.p. at maximum q (u) kPa	Axial strain at maximum q (ε_a%)	Mean effective stress (p') at maximum q kPa
1un50	181	-24	6.22	134
1un100	308	-62	19.47	253
1un200	361	-34	4.00	279
1un300	365	113	12.47	306
1un400	454	113	12.11	402
1un500	596	153	14.86	596
1un600	671	154	15.02	645
1un800	946	184	10.93	918
2un50	179	-63	20.52	167
2un100	284	-128	25.45	308
2un200	307	-19	10.13	314
2un300	280	85	26.35	296
2un400	366	171	9.26	345
2un500	461	113	20.34	529
2un600	553	143	7.67	636
2un800	577	223	7.94	714

7.2.3.2 Excess pore water pressure versus strain curves for natural soils of borehole one and two

The excess pore water pressures (p.w.p.) versus strain curves for natural state samples of borehole one and two are shown in figures 7.3 & 7.4 respectively. From these figures, it can be seen that the excess pore water pressure increased initially and reached a peak. After that it decreased with increasing strain. Tests at low confining pressures (50 to 200 kPa) initially showed low values of positive pore water pressures, followed by negative pore pressures at higher axial strains. No negative pore pressure was observed at higher confining pressures. The generation of negative excess p.w.p. values at low confining pressures (50-200 kPa) is due to a tendency to dilate during shearing. This dilation caused a decrease in pore water pressure and ultimately showed negative values (Atkinson and Bransby, 1978).

It can be seen from the excess pore water pressure versus axial strain graphs (figure 7.3 & 7.4) that there is a general trend between excess p.w.p. and confining pressure. The maximum positive excess pore water pressure values for borehole one samples lie between approximately 20 kPa to 280 kPa and those of borehole two samples lie between approximately 15 kPa to 250 kPa. The highest value of positive excess p.w.p. is observed in sample 1un500 and 2un800, whereas the lowest value was in sample 1un50 and 2un50 for natural soils of borehole one and two respectively. The excess p.w.p. values at maximum deviator stress in each case are listed in Table 7.3. These values lie in the range of –24 kPa to 184 kPa for borehole one samples and –19 kPa to 223 kPa for borehole two samples. In all samples excess pore water pressures have reached their maximum values at lower axial strains than the point at which maximum deviator stress occurred (figures 7.1,7.2,7.3 & 7.4).

By comparing the excess p.w.p. and strain (figure 7.3 & 7.4) curves, it is evident that at high confining pressures many samples tended towards a constant value of p.w.p. with increasing strain. It can be seen from figure 7.3 that the excess p.w.p. for tests 1un50 and 1un100 seem to reach a steady value at the end of the tests. This suggests that these two samples are very close to the critical state at larger strains (in excess of 20%). Other samples (1un300 to 1un800) at strains greater than 20% almost reach constant excess p.w.p. values at the end of the tests. Therefore these samples (1un300 to 1un800) might also have reached the critical state at very large strains (Atkinson, 1993). Test 1un200 showed a continuous change of excess p.w.p. values up to the end of the test and therefore this sample has not reached a critical state even at a very large strain.

It can also be seen from figure 7.4 that the samples of borehole two at low confining pressures (50-200 kPa) showed a continuous change of p.w.p. up to the end of the test and therefore these samples have not reached a steady state at the end of

shearing. But at high confining pressures (300-800 kPa), samples of borehole two tended towards a constant value of excess p.w.p. at very large strains and therefore, these samples might be very close to the critical state.

7.2.3.3 q/p′ ratio versus strain curves for natural soils of borehole one and two

Head (1998) pointed out that the maximum stress ratio (q/p′) value does not necessarily occur at the same strain as the peak deviator stress. The maximum stress ratio criterion is preferable to the peak stress ratio criterion in some ways because it can provide a better correlation of shear strength with other parameters, or between different types of tests. It is particularly useful for clays in which the deviator stress continues to increase at larger strains. Atkinson (1993) mentioned that soils are frictional materials and their strength increases with normal stress and so the stress ratio is more important than the shear stress alone.

The q/p′ ratio versus strain graphs is shown in figure 7.5 and 7.6. It is clear from figure 7.5 that the maximum q/p′ ratios for all samples of borehole one are developed at low strains ranging from 1.96% to 6.75%. The maximum q/p′ ratios for all samples of borehole two is observed at the strain range of 2.53% to 7.94% strains (figure 7.6).

The maximum q/p′ values for borehole one samples lie between 1.11 to 1.60 and those of borehole two samples lie in between 0.81 to 1.66. The highest and lowest maximum stress ratio values for borehole one samples are observed in samples 1un100 and 1un800 respectively and those of borehole two samples are observed in test 2un50 and 2un800 respectively. After reaching the maximum q/p′ values at low strains all samples of borehole one showed a tendency to drop continuously with

respect to strain and at more than 20% strain some of the samples reached almost a constant stress ratio state (figure 7.5). On the other hand, some of the borehole two samples reached a constant stress ratio state at strains greater than 22% (figure 7.6). A variation in the maximum q/p′ ratio value is observed with the increase of effective confining pressures for samples of both boreholes. In general, low confining pressure samples showed higher values of maximum q/p′ ratio value than the high confining pressure samples.

It is also observed that the maximum q/p′ ratio for natural soils of both boreholes occurs before the maximum deviator stress is reached, which occurs at higher strain.

7.2.3.4 Stress paths in q-p′ space for natural soils of borehole one and two

The effective stress paths in q-p′ space for a series of consolidated undrained triaxial compression tests on natural state samples of borehole one and two are shown in figures 7.7 and 7.8. The stress paths at low (50 to 200 kPa) confining pressures (figures 7.7 and 7.8) initially increase almost vertically and show a tendency to move towards the right. At higher confining pressures (300 to 800 kPa) each stress path at the beginning of each test, shows a tendency to move towards the left with an increase of deviator stress. The clear change of behaviour can also be observed in the excess p.w.p. versus strain curves as shown in figures 7.3 & 7.4.

With the increase of mean effective stress and deviator stress, each stress path shows a tendency to move towards the right when they are approaching the failure zone. In the failure zone, the stress paths stabilize for a while and show a tendency to move along the failure envelope. However the stress paths then curve sharply down to approach an ultimate state (possibly the critical state line, CSL). The values of mean effective stress at maximum deviator stress and the corresponding maximum

deviator stress for these stress paths are mentioned in Table 7.3. It can be seen from figures 7.7 and 7.8 that the deviator stress at failure in each case increases with increasing mean effective stress except for test 2un300 of borehole two. The mean effective stress values at failure also increase with the increase of effective confining pressure (initial mean effective stress) (figures 7.7 & 7.8).

7.2.3.5 Failure surface for natural state samples of borehole one and two

A failure envelope in terms of effective stress for a set of tests is plotted in the q-p′ space for the natural soils of each borehole. The failure envelopes of borehole one and two are shown in figures 7.9 and 7.10 respectively. It is clear that both show curved failure envelopes. These will later be compared with the failure envelopes for the destructured soils.

All natural samples of borehole one failed with the formation of shear planes. At low effective confining pressures the shear planes were indistinct but at high effective confining pressures the shear planes were prominent and distinct.

All natural samples of borehole two also failed with shear planes. At low effective confining pressures (50-200 kPa) shear planes were not distinct. For test 2un100 & 2un200 samples failed with a number of indistinct shear planes. However at high confining pressures (2un300-2un800) shear planes were more prominent and distinct and the samples failed with a definite single shear plane. Similar distinct polished shear planes were observed by Jardine et al. (1984) on London Clay.

The failure surface for the whole range of tests for natural soils of borehole one showed some curvature up to approximately p′=450 kPa (figure 7.9.). At p′>450 kPa the slope of the failure envelope is slightly reduced. The failure surface for natural

soils of borehole two showed a curvature up to approximately p'=400 kPa (figure 7.10.). The slope of the curve reduces steadily as p' increases (figure 7.10). It was observed earlier that the samples of both boreholes reached a maximum q/p' ratio before failure and continue shearing with a decrease of q/p' ratio up to the end of the test.

The curved nature of the failure surface in terms of effective stress for different types of various bonded natural materials has been reported by Vaughan (1988). Vaughan et al. (1988) also reported similar results for lateritic residual soil from basalt from Mauritius. Malandraki and Toll (1994 and 1996) also mentioned a curved bounding surface for artificially bonded soils.

7.2.3.6. Yield and tangential stiffness on natural state soils of borehole one and two

There are proposals in the literature for identifying yield in natural and artificial soils, which are discussed in chapter two. Based on the work of other researchers, an attempt is made to identify yield points for the tropical clay soils of Dhaka, Bangladesh. Two samples are selected initially to present the first and second yield points as described by Maccarini (1987) and Bressani (1990). A deviator stress versus strain curve is plotted for sample 1un50 and 1un400, both in natural and log-log scales. Fluctuations in the strain measurements make identification of yield points difficult at small strains, nevertheless it can be seen from figure 7.11 for sample 1un50, the first yield can be identified at q = 9 kPa and second yield at q = 40 kPa. Similar values are also observed in figure 7.12 to identify first and second yield points. At the low confining pressure for sample 1un50, a consistency is observed between the values of first and second yield points (figure 7.11 & 7.12) obtained from the two methods.

Figures 7.13 and 7.14 show the results for test 1un400. At the higher confining pressure for sample 1un400, first yield appears to occur around at q = 45 kPa in natural scale (figure 7.13), whereas the second yield is indicated at q = 150 kPa in natural scale. For this higher confining pressure, however it is clear that the fluctuations in the strain measurements make it difficult to come to any firm conclusions about the location of yield points in this case (figure 7.14). However, even at the log-log scale (figure 7.14) it is clear there is a change in stiffness at around 45 kPa (first yield) and some evidence of a change around 150 kPa (second yield).

Vaughan (1988) pointed out that tangential stiffness versus strain might give a clearer indication of yield. After that an improved method for identification of first and second yield was proposed by Toll and Malandraki (1993). They suggested that curves of E_{tan} against strain on log scales give a better indication of the yield points. Malandraki and Toll (1996) defined the first and second yield points for a weakly bonded soil. The term 'second yield' was used by Vaughan (1988) and Malandraki and Toll (1994, 1996). To avoid confusion between the term 'second yield' (as used by Vaughan; 1985 & 1988) and Y_2 (as used by Jardine et al. 1991, Jardine; 1992 and Smith et al. 1992), Malandraki and Toll (2000) introduced the term 'bond yield' to represent the point where a major change in tangential stiffness occurs between the first and final yield condition. This definition will be tested in this section to identify the 'first' and 'bond yield' points for the tropical clay soils of Dhaka, Bangladesh.

Tangential stiffness in terms of shear modulus (G_{tan}) versus axial strain graphs for samples 1un50-1un400 are shown in figures 7.15 to 7.19. The G_{tan} versus axial strain graphs for borehole two samples (2un50-2un400) are shown in figures 7.23 to 7.27. It can be seen from these figures that the tangential stiffness versus strain curves are non-linear and show a reduction of stiffness values with increasing strain in each case. The identified yield points are marked on these figures as described by

Malandraki and Toll (1996 and 2000). Shear modulus (G_{tan}) is used rather than Young's modulus (E_{tan}) since shear modulus is independent of variations in volume strain and gives a 'purer' measure of yield under shear, whereas Young's modulus will implicitly be affected by volume strains. However, Malandraki and Toll (2001) have shown that the yield points identified using G_{tan} correspond closely to the equivalent points defined in terms of E_{tan}. G_{tan} versus strain curves for borehole one samples at higher confining pressures (>400 kPa) are shown in figures 7.20 -7.22 and those of borehole two samples are shown in figures 7.28-7.30.

Malandraki and Toll (1996) mentioned that the loss of stiffness with increasing strain indicates the breaking down of bonds at smaller strain. Non-linear stiffness decay curve at smaller strain are also observed by Burland (1989), Hight et al. (1992), Clayton et al. (1992), Smith et al. (1992), Little and Hataf (1993), Allman & Atkinson (1992) and Toll and Malandraki (1993).

In figure 7.15, for sample 1un50 a first loss in tangential stiffness is found at 0.001% of strain (equivalent to q = 4 kPa) and a second loss at 0.10% strain (q = 51 kPa). These are similar to the values identified from the stress-strain curves in figures 7.11 and 7.12. All the identified yield points for natural samples of both boreholes with their corresponding values of q and ε_a are listed in Table 7.4. No values are listed for effective confining stresses above 500 kPa as no clear trend of yield points were observed at these higher pressures. Even at the lower pressure ranges, the identification of yield is sometimes tenuous.

Table: 7.4 First and bond yield points for natural soils of borehole one and two with corresponding values of deviator stress (q) and axial strain (ε_a)

Sample no.	Yield	q (kPa)	ε_a (%)
1un50	First yield	4	0.001
	Bond yield	51	0.10
1un100	First yield	8	0.002
	Bond yield	37	0.14
1un200	First yield	4	0.02
	Bond yield	68	0.06
1un300	First yield	10	0.019
	Bond yield	35	0.05
1un400	First yield	-	-
	Bond yield	37	0.015
1un500	First yield	-	-
	Bond yield	5	0.003
2un50	First yield	2	0.0004
	Bond yield (?)	41	0.003
2un100	First yield	15	0.0048
	Bond yield	34	0.019
2un200	First yield	3	0.002
	Bond yield	53	0.05
2un300	First yield	24	0.006
	Bond yield	110	0.15
2un400	First yield	19	0.002
	Bond yield	86	0.041

The identified first and bond yield points for these tests on natural samples of borehole one and two are plotted in the q versus p′ space as shown in figures 7.31 and 7.32. The failure surface is also shown in figures 7.31 & 7.32. It can be seen from figure 7.31 that the first yield surface of borehole one encloses a very small area in the stress space and for higher stresses it levels off parallel to the isotropic axis. The first yield surface of borehole two samples (figure 7.32) increases up to approximately p′ = 200 kPa and after that it levels off parallel to the p′ axis.

The bond yield surface in figures 7.31 and 7.32 occurs at higher deviator stress levels than the first yield surface. The failure surface in figure 7.31 and 7.32 is shown at a higher deviator stress levels than the bond yield surface. The bond yield surface of borehole one encloses an area with a stress level of q = 5 kPa to 68 kPa in the q- p′ space. On the other hand the bond yield surface for borehole two encloses an area with a stress level of q = 34-110 kPa. In can be seen from these figures that the bond yield surface occurs well below the failure surface and if there were a zone of coincidence (Zone 1 as defined by Malandraki and Toll, 1996) it would only be at very low stress levels (<20 kPa).

At p′ > 300 kPa, the bond yield surface of borehole one moved towards the isotropic axis. The bond yield surface of borehole one coincides with the isotropic axis at about 500 kPa, confirming the suggestion earlier that bond breakdown would occur in isotropic compression for tests at higher confining pressures. This is consistent with the observation that no clear yield can be observed in samples with effective confining stress > 500 kPa. The bond yield surface of borehole two maintains a parallelism with the p′ axis for p′ values around 200-400 kPa (figure 7.32). However, it is possible that this also curves down to the p′ axis between 400-500 kPa, since no clear yield is seen in samples tested at 500 kPa and higher. By this stage a major change in stiffness values has taken place due to breakdown of bonds. The complete destruction of bonds will occur at higher stresses and at larger strains.

An attempt is made to identify the final yield surface for the natural state soils of borehole one and two. The final yield is identified based on the point of maximum curvature on the deviator stress versus strain curves (as suggested by Malandraki and Toll, 1996). The identified final yield points are also plotted in the q-p′ space in figures 7.31 and 7.32 to represent the final yield surfaces of both boreholes. It can be seen from these figures that the final yield surfaces occur at higher deviator stress levels than the first and bond yield surfaces. The final yield surface nearly coincides

with the failure surface at lower mean effective stress levels. After that the final yield surface diverts from the failure surface at higher stresses (at p' greater than 200 kPa). After bond yield, the soil involves the combined influences of both the remaining bonding and the plastic strains. When the soil reached the final yield surface, it loses almost all of its stiffness due to bonding. After final yield, a soil's behaviour is controlled only by friction and failure occurs at much larger strains due to slippage of individual grains.

7.2.3.7. Small strain behaviour

Stiffness of a material largely determines the strains and displacements in structures, or in the ground, as they are loaded or unloaded. It governs displacements at working load (Atkinson, 1993). A reduction in stiffness is significant in soil dynamics, earthquake engineering, offshore engineering and in ground movement (Little & Hataf, 1993). Changes of stiffness due to dynamic loading are therefore important in design of structures. Small strain stiffness is required for analysis of the dynamic and small strain cyclic loading of soils (Viggiani and Atkinson, 1995). Scholey et al. (1995) mentioned that the importance of using the small strain stiffness of soils for foundation settlement studies has received widespread acceptance. They also noted that typically, foundation settlements cause axial strains within the deforming soil mass on the order of 10^{-1} to 10^{-2} %. Since the stress- strain behaviour of soils is non-linear, the modulus for use in settlement calculations should be derived from the small strain region of the stress strain curve at strains corresponding to those anticipated during foundation settlement. Yielding characteristics at smaller strain of a bonded soil can be explained by using stiffness data. Therefore an attempt was made to evaluate the tangential stiffness versus mean effective stress data at smaller strain (0.01 to 2%) to interpret the effects of bonding on soil behaviour.

7.2.3.7.1. Tangential stiffness versus mean effective stress (up to 2 % strain)

Tangential stiffness at smaller strain for the natural state samples of borehole one and two will be studied in this section. Individual contours for 0.01%, 0.1%, 0.2%, 0.3%, 0.5%, 1% and 2% of strain of borehole one samples are plotted with tangential stiffness versus p′ values in figure 7.33 and 7.34. Individual contours with increasing strain (0.01% to 2%) for borehole two samples are plotted in figure 7.35. It can be seen from these figures that the stiffness values for natural soils of both boreholes decrease with increasing strain. The G_{tan} values are highest for 0.01% contour and lowest for 2% contour. The reduction of stiffness values with increasing strain is due to the breakdown of the bonded structure of the soil (Malandraki & Toll, 1996). The major changes of stiffness values are observed for strain contours 0.01% to 0.1% where bond destruction is abrupt. For contours 0.01% to 0.2% of borehole one samples, a rapid increase of G_{tan} with p′ is observed for tests 1un50-1un200. The slope of the curve changes for the same contours for tests 1un300-1un500. It can be seen from figure 7.35 that the 0.01% strain contour of borehole two initially showed an increase up to p′ = 200 kPa and after that it curved down towards the p′ axis at higher stresses. The strain contours 0.1% to 2% of borehole two initially showed an increase of stiffness value up to p′ = 300 kPa. At p′ > 300 kPa the slope of the curve changes (figure 7.35). The bond yield of borehole one and two samples was observed in between 0.003%-0. 14% strain and 0.003-0.15% strain respectively. Strain contours for 1% to 2% of both boreholes are very close to the p′ axis where G_{tan} values are very low. This low value of G_{tan} indicates that the soil has already lost almost all of the stiffness due to breakdown of bonds (Malandraki and Toll, 1996). In this study a drop of tangential stiffness value from approximately 700 MPa at 0.01% strain to about approximately 10 MPa at 1% strain was observed for borehole one samples (figures 7.33 and 7.34). The borehole two samples showed a reduction of stiffness value from approximately 300 MPa at 0.01% strain to about 6 MPa at 2% strain (figure 7.35).

Burland (1989) reported a drop of secant stiffness value from 1700 kPa at 0.003% strain to about 150 kPa at 1% strain on London Clay. Atkinson et al. (1992) also mentioned a drop of tangential stiffness values from 56 MPa at 0.005% strain to 30 MPa at 0.05% strain. Similar types of results are also reported by Malandraki (1994), Malandraki & Toll (1996) and Smith et al. (1992). Smith et al. (1992) observed that the tangential stiffness curves are non-linear at small strain and stiffness values also decline with increasing strain. They also noted that stiffness values gradually diminish with increasing strain. Similar reflections are also observed in this study.

7.2.3.7.2. Deviator stress versus mean effective stress (up to 2% of strain) of the natural soils of borehole one and two

Small strain behaviour is also studied by reference to q vs. p′ space. Strain contours from 0.01% to 2% of borehole one and two are plotted in the q - p′ plane in figures 7.36 and 7.37 respectively. The failure surface is also plotted in the same figures. It can be seen from figure 7.36, q value increases with increasing strain up to approximately p′ = 250 kPa for borehole one samples. The slope of each contour curve decreases at higher stresses. For p′ greater than 250 kPa strain contours of borehole one gradually change direction with increasing mean effective stress and showing a bending towards the p′ axis. The lowest value of q occurs for 0.01% strain contour and the highest value for 2% strain contour. Strain contours 0.01% to 0.1% are close to the p′ axis. The initial loss in tangential stiffness was found to occur in between 0.001% to 0.02 % strain. Strain contours 0.3% to 2% are close to the failure surface (figure 7.36). At higher mean effective stress (greater than 425 kPa) these contours of borehole one showing a tendency to move towards the isotropic axis with a small drop of q value. Bond yield was found to occur in between 0.003% to 0.14% strain. At low mean effective stresses, the 2% strain contour is very close to the failure surface and at higher mean effective stress levels the distance between the two increases with increasing p′.

The derived strain contours for borehole two samples are close to linear up to p′ = 120 kPa (figure 7.37). After that the slope of each contour curve decreases at higher stresses. It can also be seen from figure 7.37 that the strain contours of borehole two gradually change direction with increasing strain. The lowest strain contours (0.01%-0. 3%) are close to the p′ axis and higher strain contours (0.5%-2%) are close to the failure surface. At p′ greater than 350 kPa, 0.01% to 0.5% strain contours of borehole two showed a tendency to move towards the p′ axis at higher mean effective stresses with a small drop of q value. The first yield points of borehole two was found to occur in between 0.0004% to 0.006% strain and the bond yield was observed at around 0.003-0.15% strain.

Jardine et al. (1984) observed the small strain contours in s′ vs. t plane and noted that with increasing strain, contours are close to failure line. They also reported a loss of stiffness values when the small strain contours approach the failure surface. Malandraki (1994) also reported similar results. The observed small strain behaviour is consistent with the results quoted by Jardine et al. (1984) and Malandraki (1994).

7.3. Consolidated undrained triaxial tests on destructured samples of borehole one and two

Destructured samples were prepared from the natural soils of the two boreholes and reformed with the same void ratio and dry density as the natural samples. The destructured sample preparation is described in chapter 3. Testing details of destructured samples of boreholes one and two are listed in tables 7.5 and 7.6 respectively. Destructured samples of each borehole were also named by using letters and numbers. For example, test 2ud100 means a test carried out on a sample of borehole two, undrained on a destructured sample which was consolidated at a confining pressure of 100 kPa.

Table 7.5: Testing details of destructured soils of borehole one, Location: Mirpur

Test name	Depth (m)	Initial moisture content w %	Specific gravity G_s	Bulk density ρ (Mg/m^3)	Dry density ρ_d (Mg/m^3)	Initial void ratio e	Wet weight of sample (g)	Dry weight of sample (g)
1ud50	1.22-1.37	18.8	2.61	1.919	1.616	0.616	165.42	139.25
1ud100	1.37-1.52	18.4	2.60	2.003	1.691	0.537	172.63	145.76
1ud200	4.72-5.08	14.4	2.64	2.113	1.847	0.429	182.16	159.22
1ud300	5.68-5.85	17.6	2.65	1.979	1.683	0.574	170.55	145.05
1ud400	6.90-7.15	17.2	2.59	1.991	1.698	0.525	171.63	146.40
1ud500	7.16-7.62	17.2	2.61	1.989	1.697	0.537	171.44	146.33
1ud600	8.68-8.83	17.4	2.60	2.100	1.789	0.453	181.05	154.24
1ud800	9.6-10.0	15.6	2.62	2.045	1.769	0.481	176.22	152.47

The behaviour of the destructured soils of both boreholes under undrained triaxial compression testing is presented in this section. Stress strain curves of destructured soils of borehole one and two are evaluated, stress paths are clarified, and the failure surface for destructured soils of each borehole is plotted on the q-p′ stress space. Tangential stiffness is discussed with the help of G_{tan} versus p′ curves. The strain contours up to 2% strain are presented in the q versus p′ space. Comparisons are made between the natural and destructured soils of each borehole.

Table 7.6: Testing details of destructured soils of borehole two

Location: Curzon Hall

Test name	Depth (m)	Initial moisture content w %	Specific gravity G_s	Bulk density ρ (Mg/m^3)	Dry density ρ_d (Mg/m^3)	Initial void ratio e	Wet weight of sample (g)	Dry weight of sample (g)
2ud50	1.10-1.30	17.9	2.59	2.179	1.840	0.404	186.80	158.58
2ud100	1.32-1.47	17.1	2.62	2.168	1.854	0.411	187.40	160.03
2ud200	3.50-3.65	14.2	2.64	2.150	1.878	0.403	185.07	162.08
2ud300	3.68-3.88	15.3	2.62	2.056	1.739	0.498	173.70	150.73
2ud400	4.13-4.33	14.2	2.60	2.057	1.802	0.440	177.22	155.32
2ud500	4.60-4.80	14.9	2.59	1.976	1.720	0.504	170.29	148.23
2ud600	5.45-5.65	16.1	2.63	2.060	1.774	0.482	177.58	153.00
2ud800	6.09-6.40	17.3	2.61	2.048	1.747	0.494	176.50	150.60

7.3.1 Stress strain curves of destructured soils of borehole one and two

The deviator stress versus strain curves for destructured soils of borehole one and two are shown in figures 7.38 and 7.39 respectively. The non-linear curve in each case reaches a maximum deviator stress at large strain. After that the value of q decreases with an increase of strain. It can be seen from figure 7.38, the maximum deviator stress of borehole one sample in each case increases with increasing confining pressures except for sample 1ud300. The maximum deviator stress for sample 1ud300 is slightly lower than the sample 1ud200 with increasing confining

pressure. It can also be seen from figure 7.38, at low confining pressures that the maximum q points are not sharp. However, at high confining pressures the maximum q points show a prominent peak.

The stress strain curves of borehole two samples showed a maximum point without any prominent peak (figure 7.39). The maximum deviator stress in each case of borehole two samples also increases with increasing confining pressure (figure 7.39). The strains to attain the maximum q value for samples of borehole one lie between 8% to 28%. The lowest strain to reach the maximum q value is encountered for sample 1ud800 and the highest value is observed in sample 1ud200. The variation of strains to reach the maximum q for destructured samples 1ud50-1ud500 is very small, except for sample 1ud300. These samples reached the maximum value at about 24% to 26% strain. However, the samples 1ud600-1ud800 reached a maximum q value at lower strains ranging from 8% to 12%. The strains to attain maximum q value for samples of borehole two lie between approximately 15% to 28%. The maximum deviator stress and the corresponding values of axial strain, mean effective stress and the excess pore water pressure for both boreholes are listed in Table 7.7.

Table: 7.7 Summary of different stress strain parameters at maximum deviator stress for destructured soils of borehole one and two

Sample number	Maximum deviator stress (q) kPa	Excess p.w.p. at maximum q (u) kPa	Axial strain at maximum q (εa%)	Mean effective stress (p′) at maximum q kPa
1ud50	96	-14	24.16	91
1ud100	290	-89	26.23	267
1ud200	396	-73	27.95	387
1ud300	256	122	14.31	262
1ud400	455	105	26.21	440
1ud500	476	89	26.96	504
1ud600	599	173	12.25	615
1ud800	892	254	8.46	837
2ud50	170	-60	27.78	160
2ud100	205	-49	27.53	205
2ud200	272	-50	23.64	306
2ud300	273	48	24.93	317
2ud400	343	163	18.23	338
2ud500	418	216	15.89	420
2ud600	476	139	19.78	612
2ud800	489	321	15.90	639

7.3.2. Excess pore water pressure versus strain curves for destructured samples of borehole one and two

The excess pore water pressures versus strain curves for destructured soils of borehole one and two are shown in figures 7.40 and 7.41 respectively. It can be seen from figure 7.40 that the excess pore water pressure (p.w.p.) increased first and reached a peak region where the excess p.w.p. is maximum. After that the excess p.w.p. value gradually decreased with increasing strain in each case. Test 1ud50-1ud200 of borehole one generated both positive and negative values of excess p.w.p. At low confining pressures for tests 1ud50-1ud200, the values of excess p.w.p. are initially positive and negative values are observed at higher strains. At high

confining pressures for tests 1ud300-1ud800 of borehole one, the excess p.w.p. values increased first and then gradually decreased with further straining.

The destructured samples of borehole two also developed both positive and negative excess p.w.p. at low confining pressures (tests 2ud50-2ud200) and only positive p.w.p. (tests 2ud300-2ud800) at high confining pressures (figure 7.41). No negative pore water pressure was generated at higher confining pressures for both boreholes (figures 7.40 & 7.41). The reasons for generation of negative excess p.w.p. values at low confining pressures (50-200 kPa) is due to the tendency for the samples to dilate during shearing.

At low confining pressures (1ud50-1ud200), the maximum positive excess p.w.p. values of borehole one lie in the range of approximately 20 kPa to 80 kPa and those of borehole two (2ud50-2ud200) lie in between 20 kPa to 50 kPa. At high confining pressures the excess p.w.p.values are in the range of approximately 150 kPa to 260 kPa for destructured soils of borehole one and approximately 50 kPa to 320 kPa for destructured soils of borehole two. The excess p.w.p. values at maximum deviator stress in each case are listed in Table 7.7. In all destructured samples of borehole one and two, excess pore water pressures reached their maximum value at much smaller strains than the point of maximum q. After that the excess p.w.p. values progressively decreased with an increase of strain.

It can be seen from figure 7.40 that the excess p.w.p. for tests 1ud300 and 1ud800 ultimately reached a constant value at strains in excess of 22%, which indicates that these two samples might have reached the critical state (Atkinson, 1993). Test 1ud50 also reaches a stable excess p.w.p. and therefore is probably very close to the critical state. It can also be seen from figure 7.40 that the excess p.w.p. for other destructured samples of borehole one seems to be decreasing continuously until the

end of the test. Therefore these samples have not reached the critical state at the end of shearing.

The excess p.w.p.values for borehole two samples at high confining pressures (for tests 2ud400-2ud800) initially reached a peak value and after that they move towards an almost constant value at higher strains (figure 7.41). Therefore these samples of borehole two might have reached the critical state at strains in excess of 20%. Other destructured samples of borehole two (for tests 2ud50-2ud300) have not reached the critical state at the end of shearing.

7.3.3 q/p′ ratio versus strain curves for destructured soils of two boreholes

The q/p′ ratio versus axial strain curves for destructured soils of both boreholes are shown in figures 7.42 and 7.43. It can be seen from figure 7.42 that the maximum q/p′ ratio for borehole one samples in each case is developed at strains ranging from 0.85% to 10.66%. The maximum stress ratio value for borehole two samples developed at axial strains of approximately 1-10%. The maximum stress ratio values of destructured soils of borehole one slightly decrease with the increase of effective confining pressure. The maximum q/p′ values of destructured soils of borehole one lie between 1.02 to 1.33 and those of borehole two lie between 0.78 to 1.35. It can be seen from figures 7.38 and 7.42 that the maximum q/p′ ratios for destructured soils of borehole one in each case occurs at lower strain than the maximum deviator stress which occurs at higher strain. Similar reflections are also observed for borehole two samples (figures 7.39 and 7.43).

It can also be seen from figures 7.42 that all destructured samples of borehole one show a tendency of continuous dropping of q/p′ values after reaching the maximum value. Some of the destructured samples of borehole one (tests 1ud100, 1ud500 and 1ud800) do eventually exhibit an almost constant stress ratio state above 24% strain. The destructured samples of borehole two especially at high confining pressures (for tests 2ud300-2ud600) showed a constant stress ratio state in excess of 20% strain. Similar type of results is also observed by Allman and Atkinson (1992) on the reconstituted Bothkennar Clay soil.

7.3.4. Stress paths in the q-p′ plane for destructured soils of borehole one and two

Effective stress paths for destructured soils of borehole one and two are shown in figures 7.44 and 7.45 respectively. At the beginning of each test each stress path of borehole one increases almost vertically and at high confining pressures shows a tendency to move towards the left with the increase of q. A sharp bending towards the right side is observed in all curves when they approach the failure zone. In the failure zone, the stress path curves of borehole one stabilize for a while and they tend to move along the failure surface.

It can be seen from figure 7.45 that the stress paths of borehole two samples for tests 2ud50-2ud200 initially show near verticallity with increasing q up to a certain level. After that each curve showed a tendency to move towards the left at high confining pressures with the increase of q values. Two samples (2ud600 and 2ud800) at very high confining pressures initially shows a tendency to move towards the left. A sharp bending towards the right is observed in all curves of borehole two when they are approaching the failure zone. In the failure zone, these stress paths of borehole two (figure 7.45) also stabilize for a while.

All destructured samples of borehole one and two failed by bulging. For test 1ud50 of borehole one, the sample failed by bulging without developing any shear plane. For tests 1ud100-1ud400 of borehole one, the samples failed by bulging and developed a number of small indistinct shear planes. For tests 1ud500-1ud800 of borehole one the shear planes were more prominent and distinct and they showed limited bulging. The destructured samples of borehole two up to confining pressures of 400 kPa failed by bulging and developed a number of indistinct shear planes. At very high confining pressures (500-800 kPa) the samples failed by bulging and produced distinctive shear planes. Hobbs et al. (1988) observed a barreling type of failure with multiple internal shear planes on remoulded red clay soils of Java, Indonesia.

7.4. Failure surface for destructured soils borehole one and two

The failure surfaces for the destructured soils of borehole one and two are defined by using the maximum stress ratio values plotted in the q versus p′ space. The plotted failure surface for a set of tests for destructured soils of borehole one and two is shown in figures 7.46 and 7.47 respectively. The failure surface is roughly linear. It is to be noted here that the samples reached the maximum stress ratio values before reaching the point of maximum q.

7.5. Small strain behaviour

7.5.1. Tangential stiffness for the destructured soils of borehole one and two (up to 2% strain)

Tangential stiffness at smaller strain for the destructured soils of borehole one and two is carefully studied in this section. Individual contours for 0.01% to 0.1% strain of borehole one and two are plotted simultaneously with the tangential stiffness versus p′ values in figures 7.48 and 7.50 respectively. Strain contours from 0.1% to 2% strain of borehole one and two are shown in figures 7.49 and 7.51 respectively. It can be seen from these figures that the G_{tan} values for destructured soils of both boreholes decrease with increasing strain. The highest values of G_{tan} are found at 0.01% strain and the lowest values of G_{tan} are found at 2% strain. The major changes of stiffness values are observed between strain contours for 0.01% to 0.1%.

The destructured soils of borehole one showed a drop of tangential stiffness value from approximately 180 MPa at 0.01% strain to about approximately 5 MPa at 1% strain (figures 7.48 & 7.49). The stiffness values of the destructured soils of borehole two dropped from a value of approximately 150 MPa at 0.01% to about 4 MPa at 2% strain (figures 7.50 & 7.51). Similar results are reported by Malandraki (1994) on the destructured artificial soils. Allman & Atkinson (1992) observed that the stiffness value of the reconstituted Bothkennar Clay gradually diminishes with p′.

7.5.2. Strain contours (up to 2% strain) for the destructured soils of borehole one and two

Strain contours up to 2% strain for the destructured soils of borehole one and two are plotted in q versus p′ space and shown in figures 7.52 and 7.53 respectively together with the appropriate failure surfaces. It can be seen from these figures that the q value increases with increasing strain. The lowest value of q occurs at 0.01% strain and highest value at 2% strain. The derived strain contours are straight lines, although these seems to be some curvature near the origin for borehole one. Lower strain contours (0.01% to 0.3%) are close to the p′ axis and higher strain contours (0.5% to 2%) are close to the failure surface. It can be seen from the strain contours of borehole one (figure 7.52), for all tests q value gradually increases with the increase of p′. At higher p′(p′ >200 kPa) the distance between the strain contours increases with increasing strain. The strain contours turn in direction from the p′ axis to the failure surface with increasing strain (figure 7.52). Similar reflections are also observed for borehole two samples as shown in figure 7.53. The strain contours of both boreholes showed a loss of stiffness values when the small strain contours approach the failure surface with increasing strain (figures 7.49 and 7.51). Similar results are also reported by Jardine et al. (1984) and Malandraki (1994).

7.6. Comparisons between the behaviour of the natural & destructured soils of borehole one and two under undrained compression

In this section, consolidated undrained triaxial test results carried out both on natural and destructured soils of borehole one and two are compared and evaluated. Comparisons are made between the stress strain curves, stress path results, v versus

p′ curves of the natural and destructured soils of both boreholes. The positions of the two failure surfaces for natural and destructured soils in the q-p′ space are also compared. Comparisons between the small strain contours and loss in tangential stiffness with increasing strain for natural and destructured soils are also discussed.

7.6.1. Comparisons between stress strain behaviour of natural and destructured soils of borehole one and two

The deviator stress versus strain curves for the natural and destructured soils of borehole one and two are shown in figures 7.54 and 7.55 respectively. It can be seen from these figures, natural state samples in all cases show higher values of maximum deviator stress than those of the destructured soils. At low confining pressures, both the natural and destructured samples of both boreholes did not show a prominent peak, but at high confining pressures both types of samples have shown a point where deviator stress is maximum. The destructured soils of both boreholes showed lower maximum deviator stress levels, lower stiffnesses and larger strains to reach maximum deviator stress than the natural samples due to the destruction of bonds.

In natural state samples of borehole one, the strains to attain the maximum deviator stress range between 4% to 19%, whereas destructured soils of the same borehole reached a maximum value of q between 8% to 28 % strains (figure 7.54). The natural samples of borehole two attained a maximum q value at axial strains of 8-26% and the destructured samples of the same borehole reached a maximum value in between 15%-28% strains. This variation in the stress strain curves of natural and destructured soils indicates that destructuring does reduce the strength, clearly indicating the presence of structure (bonding) in the natural material. Allman and Atkinson (1992), Hight et al. (1992) observed higher values of peak deviator stresses

of the intact samples of Bothkennar Clay soil than those of destructured and reconstituted samples at the same water content. Hight et al. (1992) also observed a variation of axial strain with depth to reach the maximum stress level as observed in this study. Leroueil and Vaughan (1990) pointed out that structuring increases strength and enlarges the stress domain and observed that destructured soils exhibit lower stress levels than the structured soils. Sridharan (1988) noted undisturbed tropical soil exhibits higher deviator stress level than that of the remoulded soils.

The derived stress paths for both the natural and destructured soils of borehole one and two are compared and shown in figures 7.56 and 7.57. At low confining pressures (50-100 kPa), the stress paths of natural soils of borehole one are characteristically concave towards the right hand side. Other natural samples of the same borehole (200-600 kPa) showed a tendency to move linearly towards the left (figure 7.56). At very high confining pressure (800 kPa) the initial part of the derived stress path is almost linear and vertical. In contrast, the initial part of all the destructured samples (low and high confining pressure) of borehole one is linear and vertical. With increasing confining pressures (300-600 kPa) the destructured samples showed a tendency to move towards left. All the natural and destructured samples showed a characteristic bending towards the right hand side when they approach the failure zone. This type of variation in the stress paths was also observed for natural and destructured soils of borehole two (figure 7.57). The derived stress paths for natural soils showed higher stress levels in the q-p′ space than those of the destructured soils (figure 7.56 and 7.57). This variation in the stress paths indicates the destructuring of clay (Clayton et al. 1992).

Differences in failure type were observed between the natural and destructured soils of two boreholes. The natural state soils of borehole one and two failed with a definite single shear plane, which indicates brittle failure of the samples. The destructured soils failed by bulging in a ductile manner. At low confining pressures

the destructured samples of both boreholes failed with prominent bulging and developed a number of small indistinct shear planes. At very high confining pressures they failed with small bulging and distinctive shear planes. Sridharan (1988) observed peak strength in intact tropical soil samples with brittle failure. The destructured samples as described by Leroueil et al. (1979) showed ductile failure.

7.6.2. Comparisons between the natural and destructured failure surfaces of borehole one and two

The failure surfaces for the natural and destructured soils of borehole one and two are shown in figures 7.58 and 7.59. The failure surface for natural soils exists at higher deviator stresses than the destructured failure surface in each case. It can be seen from figure 7.58 that the natural failure surface for borehole one samples is slightly curved. However, the destructured failure surface is roughly linear. The natural failure surface of borehole one (figure 7.58) showed a curvature up to approximately $p' = 450$ kPa. Above 450 kPa, the slope of the natural failure surface decreased slightly. The natural failure surface at p' greater than 450 kPa turned close to the destructured failure surface and showed a convergence of the two failure surfaces at approximately $p' = 600$ kPa (figure 7.58). That is, at higher stresses, the limiting stress ratios of the natural samples will be governed by that of the destructured soils.

It can also be seen from figure 7.59 that the natural failure surface for borehole two samples initially showed a curvature up to approximately $p' = 400$ kPa and after that the slope of the curve is slightly reduced with increasing p'. At approximately p' greater than 550 kPa the natural failure surface almost coincided with the destructured failure surface.

The curvature of the natural failure surface is due to the bonded structure of the soil. The variations of the shape of the two failure surfaces justify the presence of bonding in natural samples. The convergence of the two failure surfaces also indicates that the bonded structure of the soil is destroyed at higher stresses.

7.6.3. Comparison between the tangential stiffness versus mean effective stress for natural and destructured soils of borehole one and two (up to 2% strain)

Comparison between tangential stiffness with increasing strain for natural and destructured soils of borehole one and two are shown in figures 7.60 to 7.63. Strain contours for 0.01% to 0.1% for both boreholes are plotted in figures 7.60 and 7.62 with tangential stiffness versus p′ values for natural and destructured soils. G_{tan} versus p′ curves for natural and destructured soils of borehole one from 0.1% to 2 % strain are plotted in figure 7.61. The loss of stiffness with increasing strain for natural and destructured soils of borehole two for 0.2% to 2% strain are plotted in figure 7.63.

It can be seen from these figures that the natural soils always showed higher stiffness values than the destructured soils which is clear evidence for the existence of structure (bonding) in the natural soils. Clayton et al. (1992) also observed that undisturbed specimens show higher stiffness values than the reconstituted specimens. Jardine et al. (1984) mentioned that intact samples showed higher stiffness values than remoulded ones. Atkinson et al. (1993) also reported similar results. The highest G_{tan} value calculated for natural soils of borehole one is approximately 700 MPa for strain contour of 0.01% and 180 MPa for destructured

soils of the same strain contour (figure 7.60). The lowest G_{tan} value observed for natural soils is approximately 10 MPa for 1% strain contour and approximately 5 MPa for destructured soils of the same contour (figure 7.61). On the other hand, the highest stiffness value calculated for natural soil of borehole two is approximately 300 MPa at 0.01% strain and approximately 150 MPa for the destructured soils of the same strain contour (figure 7.62). The lowest value of G_{tan} observed for natural soils of borehole two is approximately 6 MPa at 2% strain and approximately 4 MPa for the destructured soils of the same strain contour (figure 7.63).

It can be seen from these figures that at 2% strain, G_{tan} values of both natural and destructured soils are very close to each other and these contours run very close to the p′ axis. The difference between the strain contours decreases with increasing strain. It is also observed that the major change of stiffness values is observed for strain contours 0.01% to 0.1% for the natural soils of both boreholes. Malandraki and Toll (1994) reported similar results and they also observed that bonded soils show higher stiffness values than the destructured material up to 1% strain. Similar reflections are also observed in this study.

7.6.4. Comparisons between strain contours (up to 2% strain) for natural and destructured soils of borehole one and two in the q versus p′ space

Deviator stress versus mean effective stress curves for natural and destructured soils of borehole one and two are plotted in figures 7.64 and 7.65 respectively. A comparison of strain contours from 0.01% to 2% strain for both natural & destructured soils are shown in these figures in the q -p′ space. The natural failure surface is also plotted in these figures. The strain contours marked by solid lines

represent the curves for natural soil and the contours marked by dotted lines represent the curves for destructured soils.

It can be seen from figure 7.64 that the natural strain contours of borehole one are curved after showing near linearity approximately up to p′ = 80 kPa. Conversely, destructured strain contours are straight (figure 7.64). The natural strain contours of borehole two are curved after showing linearity up to approximately p′ = 100 kPa (figure 7.65). At higher p′ values strain contours for natural samples of the two boreholes showed a tendency to move towards the p′ axis with a small drop of q value. The difference between the position of the natural and destructured strain contours increases with increasing strain. Therefore the bonded structure of the soil has a strong influence on the development of strain (Malandraki and Toll, 1994).

7.7. Critical state behaviour

In this section critical state behaviour of the tropical clay soils of Dhaka are discussed. At first results are presented for natural soils of borehole one and two and then the critical state condition for the destructured samples of the two boreholes are discussed. Finally based on all the observed results on natural and destructured soils an estimation was made to obtain the critical state parameters for these soils.

7.7.1 Critical state behaviour for natural soils of borehole one and two

From the q/p′ ratio versus strain graphs for natural soils of borehole one and two (figures 7.5 and 7.6) it was found difficult to get a single common ultimate stress ratio value for these soils. The values of maximum q/p′ ratio showed a range of

variations. The maximum q/p′ values obtained for borehole one samples lie between 1.11 to 1.60 and those of borehole two samples lie in between 0.81 to 1.66. It is interesting to see that (figure 7.5) the two natural samples of borehole one at low confining pressures (50 kPa and 100 kPa) show a similar ultimate stress ratio around 1.05, perhaps suggesting that this is the critical state stress ratio. Similarly three natural samples of borehole two (figure 7.6) at low confining pressures (50, 100 and 300 kPa) also suggesting a similar common ultimate stress value around 0.96. However, the samples at high confining pressures of both boreholes showed lower values with a wide range of variations. It is important to note here that the samples at low confining pressures do not form distinct shear surfaces, therefore it is possible that the ultimate stress ratio for these tests might represent the critical state. On the other hand, samples at high confining pressures form distinct surfaces and once that occurs only a narrow band of soil is being affected by shearing and the 'overall' stress ratio and volume change is no longer representative of the sample as a whole. It is therefore difficult to justify that these samples at high confining pressures truly reached the critical state. This makes it difficult to construct a single unique CSL for the natural soils from the two boreholes. Allman and Atkinson (1992) mentioned a value of M = 1.38 for the Bothkennar Clay and noted that few intact samples of Bothkennar soil reached a reasonably well defined constant ratio states at very large strains.

All the undrained results of natural soils of both boreholes are also presented in the v (specific volume) versus p′ space to see the change of specific volume with increasing mean effective stress. These results are also carefully evaluated in terms of critical state. The v versus p′ curves for natural soils of borehole one and two are shown in figures 7.66 and 7.67 respectively. Since the tests were undrained, the specific volume for each test remains constant with increasing mean effective stress throughout the test. By considering the starting and end points of each test it is difficult to construct a single critical state line for natural samples of both boreholes. However, if greatest consideration is given to the low stress tests (up to 300 kPa)

where it was observed that failure did not involve a single distinct shear plane, a trend in terms of changes in mean effective stress (p′) can be seen. For tests at 50, 100 and 200 kPa of both boreholes, p′ increases suggesting these samples start from a state that is denser than the critical state. The test at 300 kPa for both boreholes shows p′ decreasing, indicating a state looser than the critical state. This suggests the CSL would fall between the end points for these four tests. The tests at 400-800 kPa (figures 7.66 and 7.67) show an overall movement of an increase in p′, even though they are above the apparent CSL. This is probably due to the formation of distinct shear planes in these tests. Initially they do show a decrease in p′ consistent with the sketched CSL. The change in direction may represent the initiation of a distinct shear surface when the pore water pressures measured no longer indicate what is happening within the failure surface itself.

7.7.2 Critical state behaviour for destructured soils of borehole one and two

The destructured samples of borehole one and two did not show any single common stress ratio value. It can be seen from the stress ratio versus strain graphs of two boreholes (figure 7.42 and 7.43) that the maximum stress ratio value for destructured samples of borehole one lie between 1.02 to 1.33 and those of borehole two lie between 0.78 to 1.35.

It can be seen from figure 7.42 that the tests 1ud50, 1ud100, 1ud200, 1ud400 of borehole one show a ultimate stress ratio around 1.02, perhaps suggesting that this is the critical state stress ratio. The stress ratio value for test 1ud500 is also very close to the stress ratio value of 1.02 for other low confining pressure tests. However, the destructured samples of borehole two showed a wide range variations in the stress

ratio values. Therefore, it is clear that there is no single common value of ultimate stress ratio for destructured soils for either borehole.

The samples of both boreholes do not form distinct shear surfaces at low confining pressures, therefore the common stress ratio value obtained at low confining pressures might represent the critical state. The stress ratio values for higher confining pressure samples might not represent the critical state (although tests 1ud600 and 1ud800 showing a common stress ratio value) as they formed distinct shear surfaces. This wide range of variations of maximum stress ratio values suggesting that constructing a single critical state line is very difficult for these soils.

However, based on the observed specific volume (v) and mean effective stress (p′) values for different tests of both boreholes during shearing an attempt is made to evaluate the results in terms of critical state. The v versus p′ curves for destructured soils of borehole one and two are shown in figures 7.68 and 7.69 respectively. It was also found difficult to construct a single critical state line for the destructured soils of both boreholes. If greatest consideration is given to tests 1ud50, 1ud100, 1ud200 and 1ud300 where distinct shear surfaces were not observed, then a line can be drawn (figure 7.68) between 1ud50, 1ud100 and 1ud200 which show an increase in p′ during shear (indicating a state 'denser' than the CSL) and 1ud300 which showed a decrease in p′. Tests 1ud400 to 1ud800 initially show a decrease in p′ consistent with a move towards the sketched CSL. However, the path directions are then reversed, possibly due to the formation of distinct shear surfaces when the measured pore pressures no longer represent the values within the failure surface itself.

In borehole two, tests 2ud50-2ud200 show an increase in p′ during shear (indicating a state 'denser' than the CSL) and test 2ud300 initially showed a decrease in p′. Therefore, a highly tentative CSL can be drawn for the destructured soils of borehole

two as shown in figure 7.69. Other tests of borehole two (2ud400 to 2ud800) initially show a decrease in p′ and consistent with a move towards the CSL. The path directions are then reversed, which might be due to the formation of distinct shear surfaces when the measured pore pressures are not representative. Therefore, the critical state line defined as described above will not be representative.

7.7.3 Comparison between critical state behaviour of natural and destructured soils

The 'v' versus 'p'' curves for natural and destructured soils of borehole one and two are also compared and shown in figures 7.70 and 7.71. It can be seen from figure 7.70 that the natural samples of borehole one at low confining pressures (for tests 50-200 kPa) moved from left to right and high confining pressure samples moved initially from right to left and then moved again towards the right. It is also interesting to note that samples at low confining pressures (50-200 kPa) developed negative p.w.p. at large strain due to a tendency to dilate. These samples at low confining pressures do not form distinct shear surfaces and the common constant stress ratio value (as discussed earlier) of some of these soils (50-100 kPa) might represent the critical state. The destructured samples of borehole one at low confining pressures almost maintained the same trend.

On the other hand, the high confining pressure samples (400-800 kPa) initially moved towards the assumed critical state line due to a tendency to contract that produces positive pore water pressures. However, these samples at high confining pressures formed distinct shear surfaces and it is questionable that the samples of borehole one at high confining pressures truly reached the critical state. The fact that they change direction and move away from the CSL suggests that the formation of a

distinct shear surface affected their behaviour and the pore water pressures being measured were no longer representative of what was happening within the failure surface.

Again from figure 7.71, it can also be seen that the natural and destructured soils of borehole two at low confining pressures (50-200 kPa) also moved from left to right side with almost a constant specific volume. It was found difficult to establish a single critical state line for these soils. The constant stress ratio value (which is discussed earlier) of tests 50 and 100 kPa might represent the critical state as they did not form distinct shear surfaces. However, at high confining pressures (400-800 kPa) both the natural and destructured soils of borehole two showed a tendency to contract with increasing p′. That is they moved towards the assumed critical state line with a lower specific volume. However, as these soils at high confining pressures also formed distinct shear surfaces, it is difficult to establish with confidence that these samples reached the critical state at very large strains.

Atkinson (1993) pointed out that the critical state parameters for a particular soil are generally considered to be constant. The variation seen in the stress ratio values and also difficulties in defining the CSL from v versus p′ curves made it difficult to obtain typical critical state parameters for these soils. However, based on the all observed results on natural and destructured soils a rough estimation was made to obtain the critical state parameters for the tropical clay soils of Dhaka. The intrinsic critical state parameters M, λ and Γ for both boreholes are listed in Table 7.8 and compared with the other values as quoted by Atkinson (1993) and Allman and Atkinson (1992).

Table: 7.8 Comparison of obtained critical state parameters of borehole one and two samples with some typical soils

Soil	λ	Γ	M
London clay*	0.16	2.45	0.89
Kaolin clay*	0.19	3.14	1.00
Glacial till*	0.09	1.81	1.18
Bothkennar clay+	0.18	2.78	1.38
Tropical clay, Dhaka (borehole one)	0.07	1.88	1.02-1.05
Tropical clay, Dhaka (borehole two)	0.06	1.83	0.95-0.96

* Atkinson (1993), + Allman and Atkinson (1992)

Atkinson (1993) mentioned that the intrinsic critical state parameters (M, λ and Γ) depend principally on the nature of the soil and might vary due to differences in grading and mineralogy from sample to sample. The critical state values (λ, Γ) obtained for the tropical clay soils of Dhaka are lower than the quoted values for some typical sedimentary clays. The tropical clay soils of Dhaka are of different nature from the other sedimentary and glacial clays. The tropical clay soils of Dhaka are oxidized, coated with ferruginous cement and contain calcareous and iron nodules, and therefore it might be expected that the value of λ, which is related to the compressibility of the soil, would be lower than the other soils listed in Table 7.8.

7.8. Comparisons between the behaviour of the natural soils two boreholes

In this section comparisons are made between the stress-strain and yielding characteristics of the natural soils of boreholes one and two. The deviator stress versus strain curves for natural soils of boreholes one and two are shown in figure

7.72.The stress strain curves for natural soils of borehole one are marked by solid lines and those of borehole two are marked by dotted lines. It can be seen from this figure, that natural samples of borehole one in all cases show higher values of maximum deviator stress than those of borehole two. At low confining pressures natural samples of borehole one did not show a prominent peak except for sample 1un200,but at high confining pressures they showed a maximum deviator stress. The stress strain curves of natural samples of borehole two at low confining pressures occurred at a lower deviator stress level than for borehole one samples and did not show a prominent peak. At high confining pressures they also showed a lower maximum deviator stress level than the borehole one samples. Samples from both boreholes attained maximum deviator stress level at large strains. Borehole one samples reached the maximum deviator stress level at strains ranging from approximately 4% to 19%, whereas borehole two samples reached the maximum deviator stress level range between 8% to 26%.

The derived stress paths for natural samples of boreholes one and two are compared and shown in figure 7.73. The derived stress paths for both borehole samples are broadly similar in shape. It can be seen from figure 7.73 that borehole one samples showed higher deviator stress level than the borehole two samples in the q-p′ space.

A comparison is made between the identified first and bond yield surfaces for natural soils of boreholes one and two in figure 7.74. The identified first and bond yield surfaces for boreholes one and two are broadly similar in shape, although a small variation between the position of the two yield surface is observed. It is to be noted here that the natural samples of borehole one initially showed a tangential stiffness of approximately 700 MPa at 0.01% strain and those of borehole two showed a value of approximately 300 MPa at the same strain contour. This variation between the initial stiffness values of two boreholes might indicate that there is a variation in bonding between the two boreholes. This variation reflects the variation

of the level of structure present in natural soils. Natural variability of the level of structure is reported by Hight et al. (1992). They mentioned that variations in the level of structure relate to facies type, being highest in the mottled facies and least in the laminated facies for Bothkennar Clay.

It is to be noted here that all samples of boreholes one and two were collected from two different sites of the same geological formation. The natural variability of colour mottling, soil composition and degrees of weathering within the same geological formation in different areas of Dhaka is reported by Monsur (1995). The borehole one samples are mainly deep reddish to yellowish brown colour, highly oxidized, containing large amount of ferruginous and calcareous nodules with some iron concretions and are more weathered than the borehole two samples. In contrast, borehole two samples are mainly light yellowish brown to moderate reddish brown colour, occasionally bluish colour, less oxidized, containing very small amount of iron concretions and nodules and less weathered than the borehole one samples. It was discussed in Chapter 5 that the borehole two samples contain lower sand fraction and higher clay fraction than the borehole one samples. The lower strength of borehole two can be explained by the higher clay fraction and lower sand fraction compared to borehole one. Therefore, the site variability of the samples in terms of composition, degrees of weathering, variability of colour mottling and local facies variations might be responsible for the variations between the results of the two boreholes.

7.9. Comparisons between the stress strain behaviour of the destructured soils of borehole one and two.

The stress-strain behaviour of the destructured soils of boreholes one and two are discussed in this section. The deviator stress versus strain curves for destructured soils of borehole one and two are shown in figure 7.75. It can be seen from this figure, that destructured samples of borehole one in each case show higher values of maximum deviator stress than those of borehole two. The stress-strain curves of destructured soils of borehole one showed a maximum point without any prominent peak up to a confining pressure of 500 kPa. At very high confining pressures tests 1ud600 and 1ud800 showed a maximum stress level with an identifiable peak. Conversely, stress-strain curves of destructured soils of borehole two in each case are positioned at lower stress levels than those of borehole one and did not show a prominent peak up to a confining pressure of 500 kPa. At very high confining pressures for tests 2ud600 and 2ud800 they showed maximum points with identifiable peaks. Destructured samples of both boreholes attained maximum stress levels at large strains ranging from approximately 8% to 28%.

The derived stress paths for destructured samples of borehole one and two are compared and shown in figure 7.76. It can be seen from figure 7.76 that the destructured samples of borehole one showed higher deviator stress levels than the borehole two samples in the q-p′ space. Differences between the stress domain of the stress paths of the two boreholes can easily be seen in figure 7.76. The stress domain of borehole two in each case occurs at lower deviator stress level than that of borehole one. Destructured samples of both boreholes failed with bulging and produced number of indistinct shear planes at low confining pressures and distinct shear planes at high confining pressures.

The variations of the results of destructured soils of two boreholes might be due to the natural variability of the samples in terms of composition, degrees of weathering, colour mottling and local facies variations.

7.10 Framework for the Tropical clay soils of Dhaka, Bangladesh

An attempt is made to identify the important characteristics to develop a framework of behaviour for the tropical clay soils of Dhaka, Bangladesh.

7.10.1 Undrained characteristics to identify zones of behaviour

All the observed undrained characteristics based on bonding effects and stress history are combined to develop a framework for the tropical clay soils of Dhaka, Bangladesh. Data for borehole one is used to illustrate the concepts. Three main zones of behaviour can be identified from the relative positions of the failure surfaces and the yield surfaces (figure 7.77). The observed natural and destructured failure surfaces and the three yield surfaces are plotted in the q versus p′ space. It was observed that the failure surface for the natural soils coincides with the destructured failure surface at approximately $p' \cong 600$ kPa. Below this stress level the natural soils showed higher deviator stress levels than the destructured soils due to their bonded structure.

It can be seen from figure 7.77 that the trend of the natural failure surface and bond yield surface indicates that it might be possible that the bond yield surface coincides

with the natural failure surface at very low mean effective stress levels. The final yield surface at low confining pressure is very close to the natural failure surface. Malandraki and Toll (1996) defined a zone 1 where the bonds entirely control the soil's behaviour at failure i.e. the failure surface coincides with the bond yield surface. The observed results suggest that if there were a zone of coincidence (Zone 1), it would only be at very low stress levels (approximately p′ less than 20 kPa). It is not clearly observed in this study. However, an estimate for the zone boundary can be assumed between Zone 1 and Zone 2 (as shown in figure 7.77).

The second zone (zone 2) of behaviour is identified between a value of p′ at failure approximately less than 20 kPa to approximately 600 kPa (figure 7.77). Malandraki and Toll (1996) noted that in this second zone bonds only partially control the soil's behaviour at failure. In zone 2, the bond yield occurs at deviator stresses lower than at the natural failure surface. The bond yield surface in figure 7.77 meets the p′ axis at 500 kPa. This is consistent with the observations that no clear trend of yield points was identified at effective confining pressure of greater than 500 kPa. Malandraki and Toll (1996) pointed out that the soil's behaviour in zone 2 is governed partially by bonding and also by the consolidation pressure. It can be seen from figures 7.33 and 7.34 that the slope of the tangential stiffness decreased to a lower value with increasing p′ in zone 2.

It can be seen from figure 7.77 that the natural failure surface exists at higher deviator stresses than the destructured failure surface due to the effect of bonding. The slope of the natural failure surface decreased slightly with increasing p′ in zone 2 and drops towards the destructured failure surface. The coincidence of the two failure surfaces indicates that the bonds are destroyed at this stress level. In Zone 2, final yield surface is very close to the natural failure surface.

Malandraki and Toll (2000) discussed that the zone boundaries rotate with effective stress path. The rotation of the stress path also has a direct influence on the size of the three zones of behaviour for the bonded soil. This suggests that the shape of the zone boundary between Zone 2 and 3 coincides with the effective stress path direction. For undrained tests, it is likely that the boundary will follow the shape of the stress paths for tests in this region of stress space. The upper limit of Zone 2 will be the coincidence point of the two failure surfaces. It can be seen from figure 7.7 that the stress paths at very high effective confining pressures showed very gentle inclinations due to bond destruction. By considering the gently changing inclinations of the last stress path (as shown in figure 7.7) and the slope of the stress paths 1un600 and 1un800, a Zone boundary can be drawn between Zone 2 and Zone 3 as shown in figure 7.77. This indicates that natural samples consolidated to isotropic effective stresses below 600 kPa would still show some evidence of bonding at failure (e.g. 1un600) whereas those above this threshold would not.

In the third zone (zone 3), the natural failure surface coincides with the destructured failure surface (reaching failure above $p' = 600$ kPa). Malandraki and Toll (1996) pointed out that in this zone the soil's behaviour at failure is independent of bonding and its behaviour is governed by that of the destructured materials, which is reflected in this study. This can be justified by the undrained stress paths as shown in figure 7.7. It can be seen from figures 7.7 and 7.77 that the undrained stress paths at consolidation stresses of p'_0 above 600 kPa do not exceed the destructured failure surface. However, figure 7.77 shows a difference in behaviour compared to Malandraki and Toll's (1996) model. It would be expected that a sample that had passed through the bond yield surface during isotropic consolidation would not demonstrate any bonded behaviour at failure. However the boundary between zones 2 and 3 (i.e. the point of total breakdown of bonds at failure) appears to occur at a higher stress level than indicated by the point at which the bond yield surface meets with the isotropic axis. This point, which would define the transition between zones

3 and 4 in Malandraki and Toll's (1996) model, actually occurs at p′ ≅ 500 kPa, much lower than the zones 2 and 3 boundary at p′ ≅ 600 kPa.

This indicates a flaw in Malandraki and Toll's (1996) model when applied to the tropical soils of Dhaka. The data for these soils suggest that even though they pass through yield in isotropic compression above 500 kPa, that the bonding is not totally destroyed. A higher isotropic stress level of p′ ≅ 600 kPa is needed before there is no evidence of bonding at failure.

7.11. Summary

In this chapter the undrained mechanical behaviour of the tropical clay soils of Dhaka from two different sites was discussed. A comparison has been made between the undrained triaxial test results of natural and destructured soils. Comparisons have also been made between the results of two boreholes. Finally a framework for the tropical clay soils of Dhaka, Bangladesh is discussed.

It was observed that the destructured samples in each case showed lower maximum deviator stresses, lower stiffnesses and larger strains to reach maximum deviator stress than the natural samples due to the breakdown of bonds. This is clear evidence that the natural samples do demonstrate the existence of structure (bonding).

At low confining pressures samples of both boreholes initially showed peak positive values of excess p.w.p. followed by negative values at higher strains due to the tendency to dilate of the samples. No negative pore pressures were observed at high confining pressures. For both boreholes, only some samples at low confining

pressures reached the critical state at very large strains approximately in excess of 20%. High confining pressure samples may not have reached the critical state due to the formation of distinct shear surfaces. It was found difficult to construct a single critical state line for these soils.

The samples showed a wide range of variations in ultimate stress ratio values. Few samples showed a common stress ratio value for different tests. Nevertheless values of the critical state stress ratio M were estimated to be 1.05 for borehole one and 0.96 for borehole two.

The derived stress paths for natural soils always showed higher stress level in the q-p′ space than the destructured samples. This variation in the stress paths indicates the destructuring of clay. The failure surface for natural soils is positioned at higher stress level in the q-p′ space than the destructured failure surface. The variations of the shape of the two failure surfaces justify the presence of bonding in natural samples. The natural failure surface initially showed a curvature with the increase of p′ up to approximately p′ = 400-450 kPa and after that the slope of the natural failure surface moved towards the destructured failure surface. The natural and destructured failure surfaces coincided at higher stresses due to complete destruction of bonds. At higher stresses both the natural and destructured soils showed similar stress ratios.

Undrained tangential stiffnesses were measured and small strain contours were evaluated. A drop of stiffness values with increasing strain was observed. The natural soils showed higher stiffness values than the destructured soils due to the presence of bonding in the natural soils. The difference between the stiffness values of the natural and destructured soils decreased with increasing strain. The maximum difference of stiffness values between the natural and destructured soils was observed at 0.01% strain. At 2% strain stiffness values of the two soils were very

close to each other. A significant difference between the strain contours of natural and destructured soils was also observed in the q-p′ space. The strain contours were seen to be curved for the natural soils but linear for the destructured soils.

Two yield surfaces were found to occur for natural tropical clay soils of Dhaka below the final yield surface under undrained shearing. The first yield surface was found to occur at low deviator stress levels showing a small change in stiffness. A bond yield surface was identified between the first and final yield surfaces. It was found that the bond yield surface occurs well below the failure surface. The final yield surface at very low confining pressure runs very close to the failure surface and then diverges at higher stresses. When the soil reaches the final yield surface, it loses almost all of its stiffness due to bonding.

Although the samples were collected from the same geological formation, a variation between the results of two boreholes was observed. These variations might be due to the natural variability of the samples at different sites in terms of composition, local facies variations and degrees of weathering.

From the observed undrained characteristics, three zones of behaviour could be identified for the tropical clay soils of Dhaka. It was observed that strain and stiffness development is directly related to the zones of behaviour. The observed undrained results suggest that if there were a zone of coincidence between bond yield and failure (Zone 1), it would only be at very low stress levels (approximately p′ less than 20 kPa). It is not clearly observed in this study. The Zone 2 is identified between a value of p′ at failure from less than 20 kPa to 600 kPa. In this zone the bond yield surface meets with the p′ axis at 500 kPa. This is consistent with the observation of no clear trend of yield points above 500 kPa. In Zone 3, the coincidence of the natural and destructured failure surfaces was observed at

approximately $p' \cong 600$ kPa. This means that at this stress level the soil's behaviour at failure is independent of bonding.

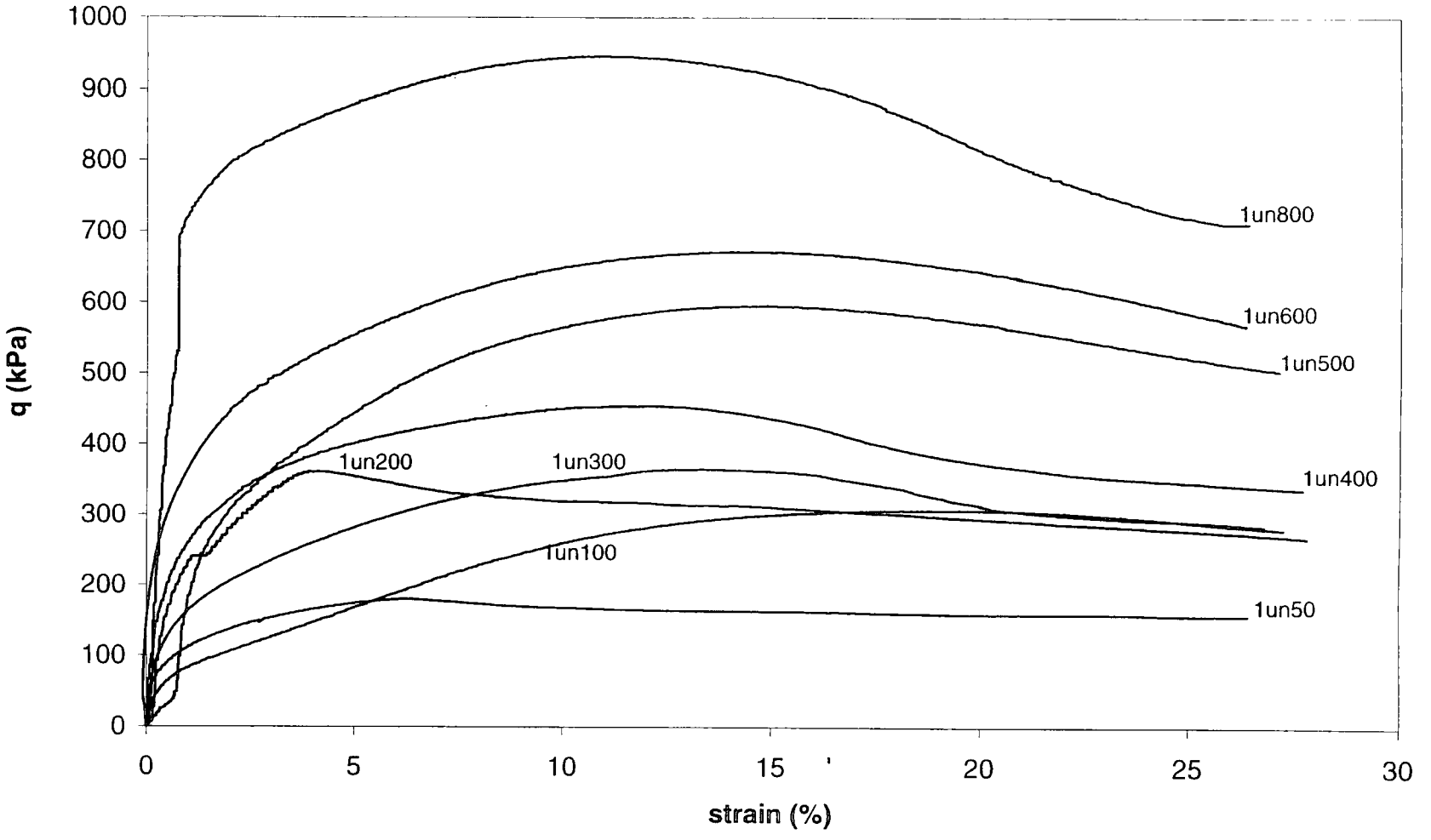

Fig. 7.1 Deviator stress vs. axial strain curves of natural soils of borehole one

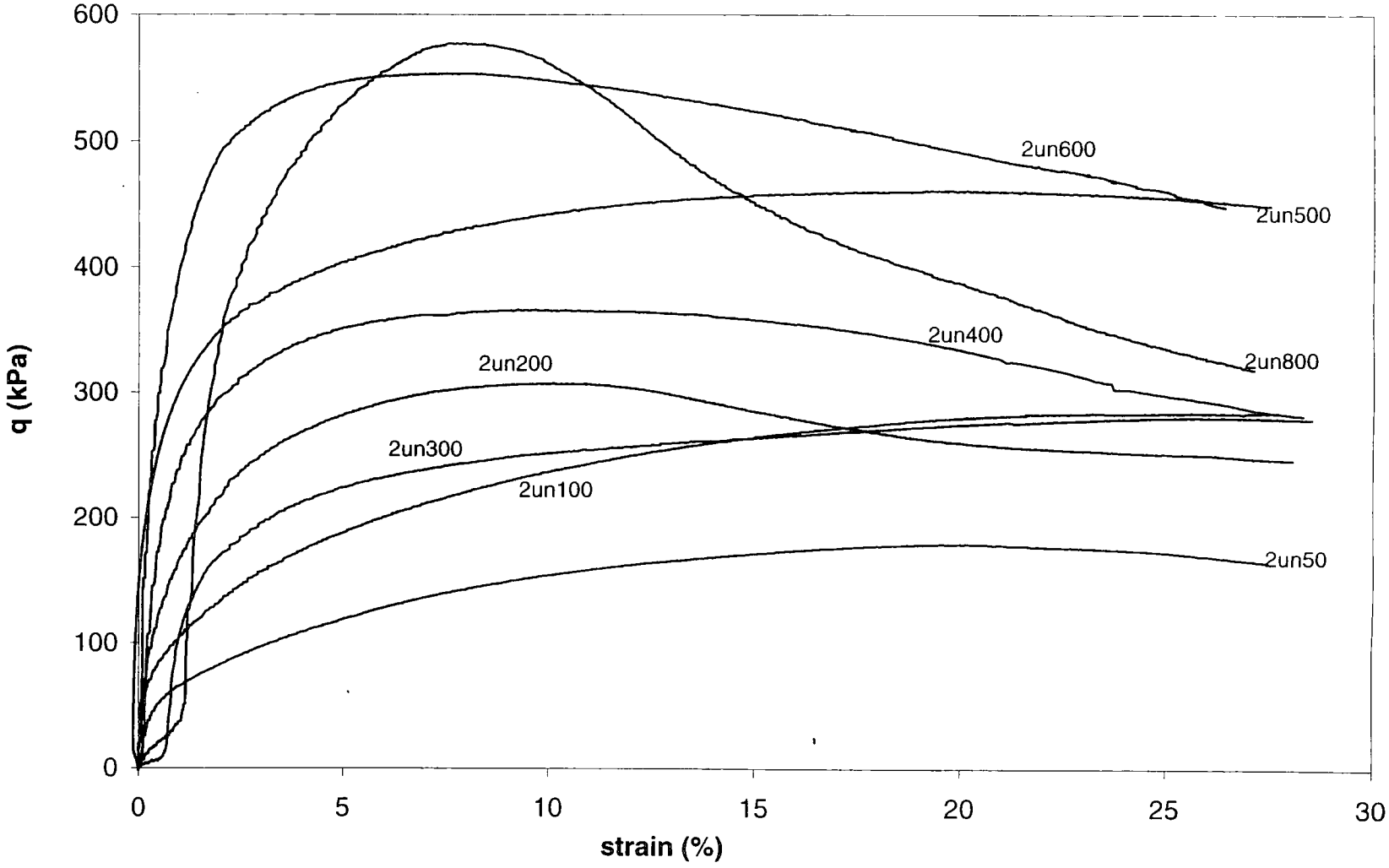

Fig.7.2 Deviator stress versus axial strain curves of natural soils of borehole two

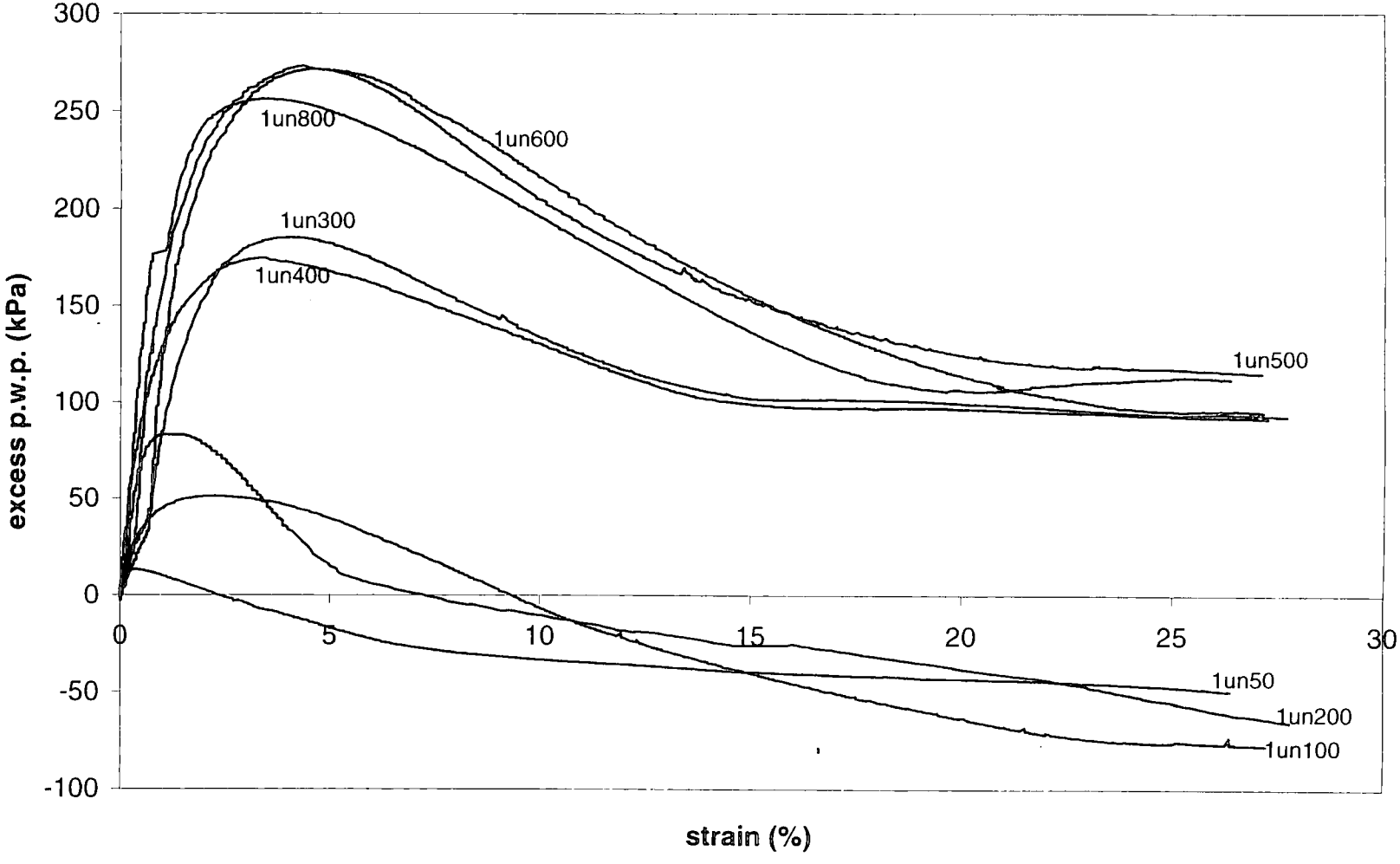

Fig. 7.3 Excess pore water pressure versus axial strain curves for natural soils of borehole one

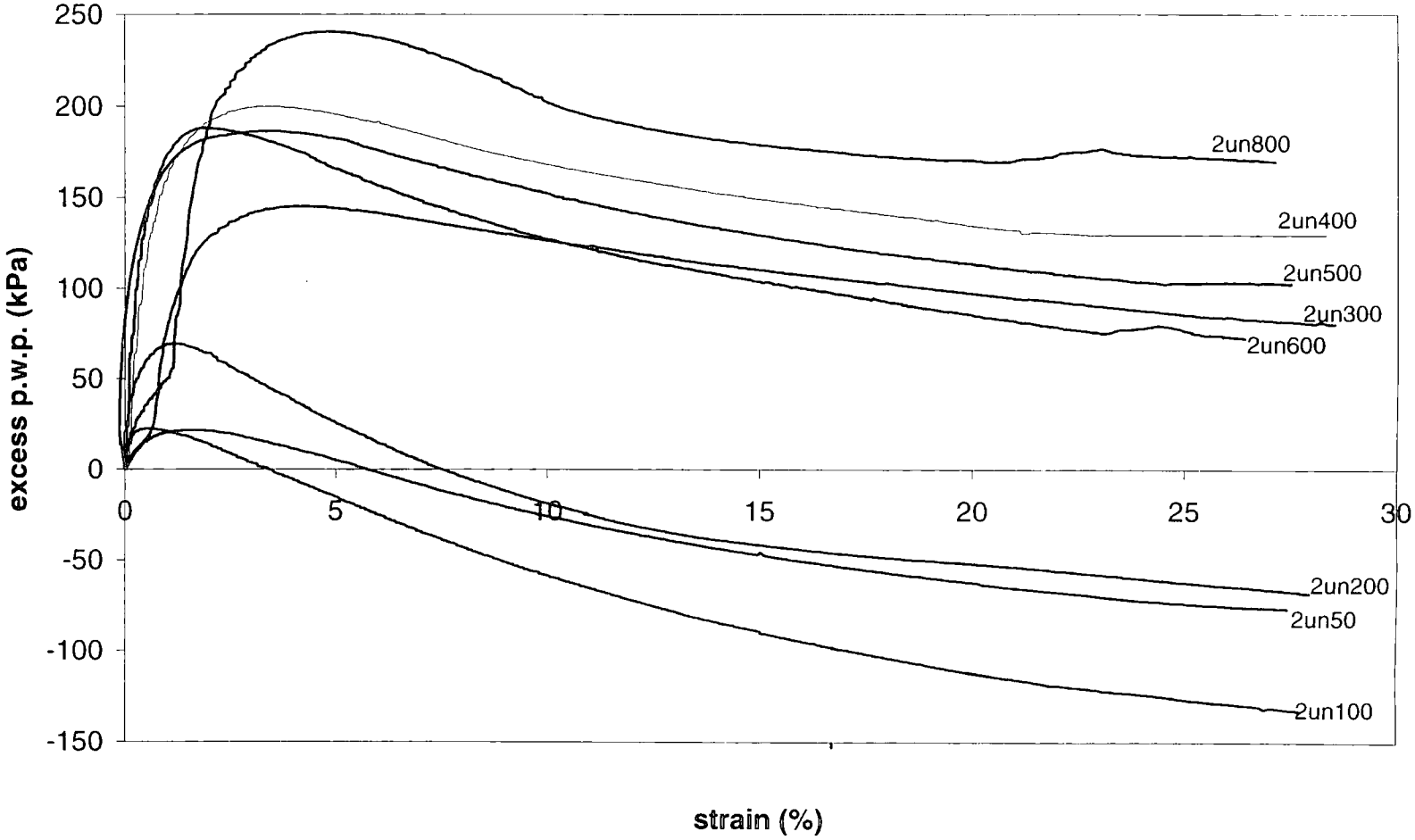

Fig. 7.4 Excess pore water pressure versus axial strain curves of natural soils of borehole two

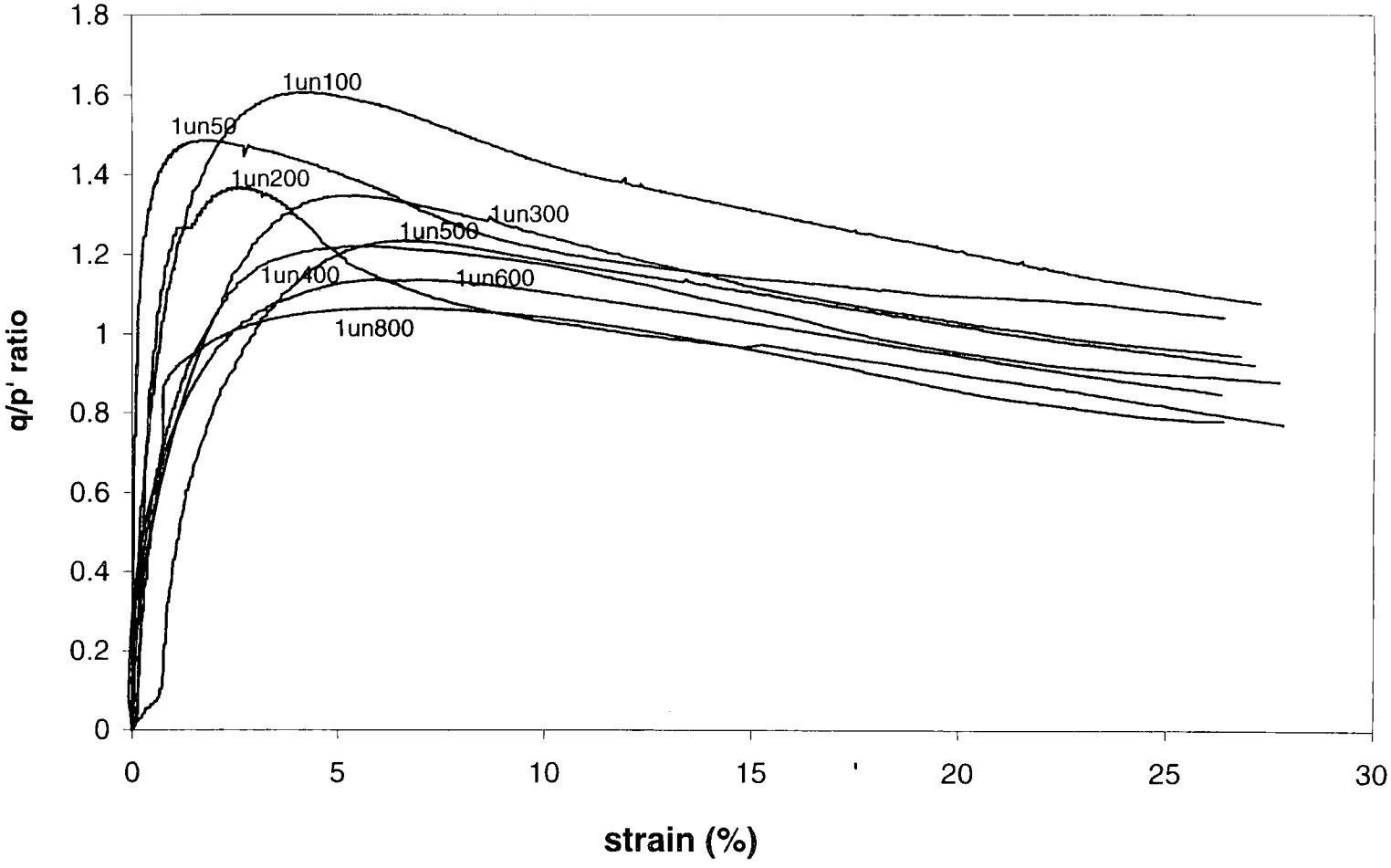

Fig.7.5 q/p' ratio versus axial strain graphs for natural soils of borehole one

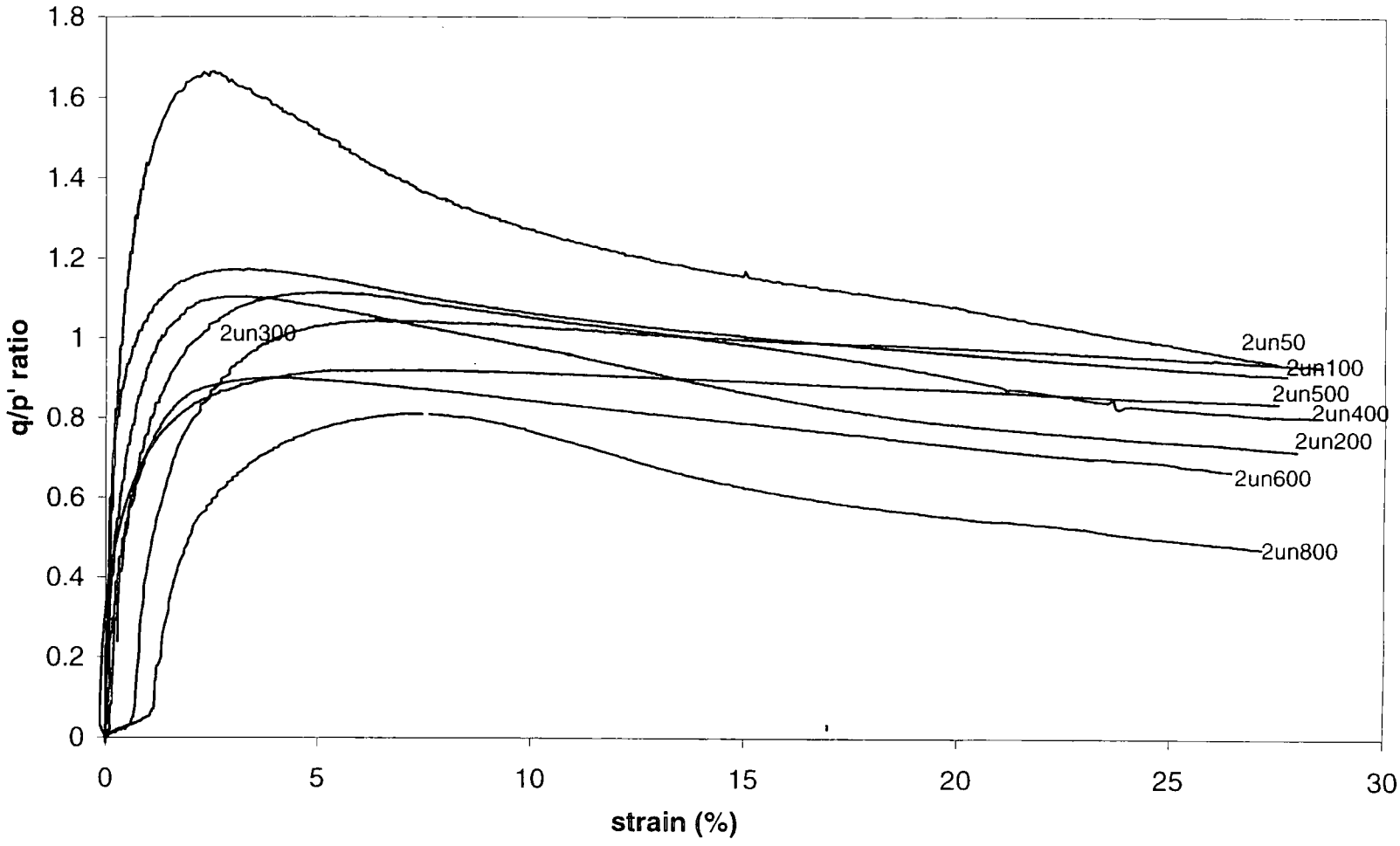

Fig.7.6 q/p' ratio versus axial strain curves of natural soils of borehole two

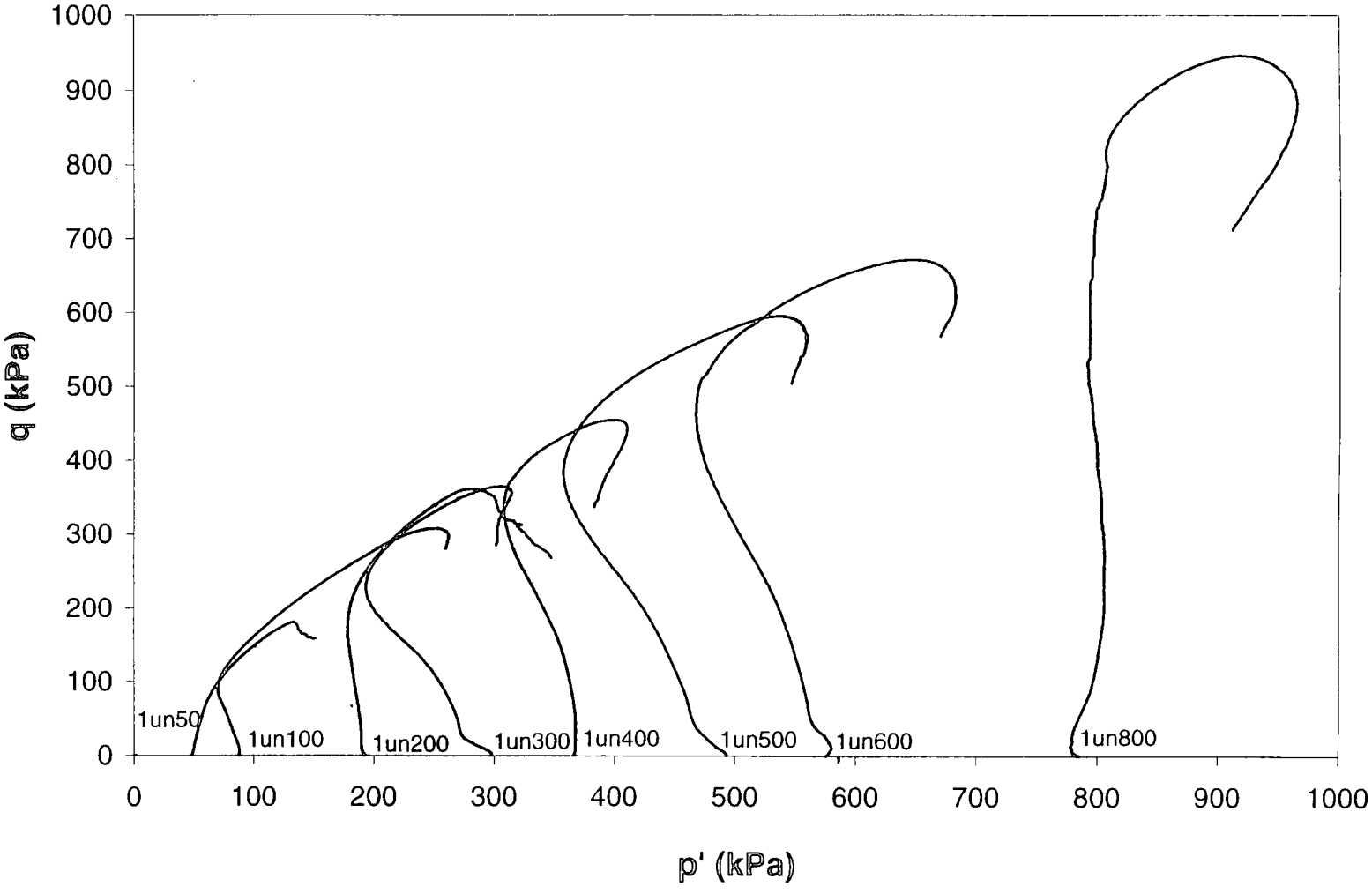

Fig.7.7 Stress paths derived from a series of triaxial tests on natural soils of borehole one

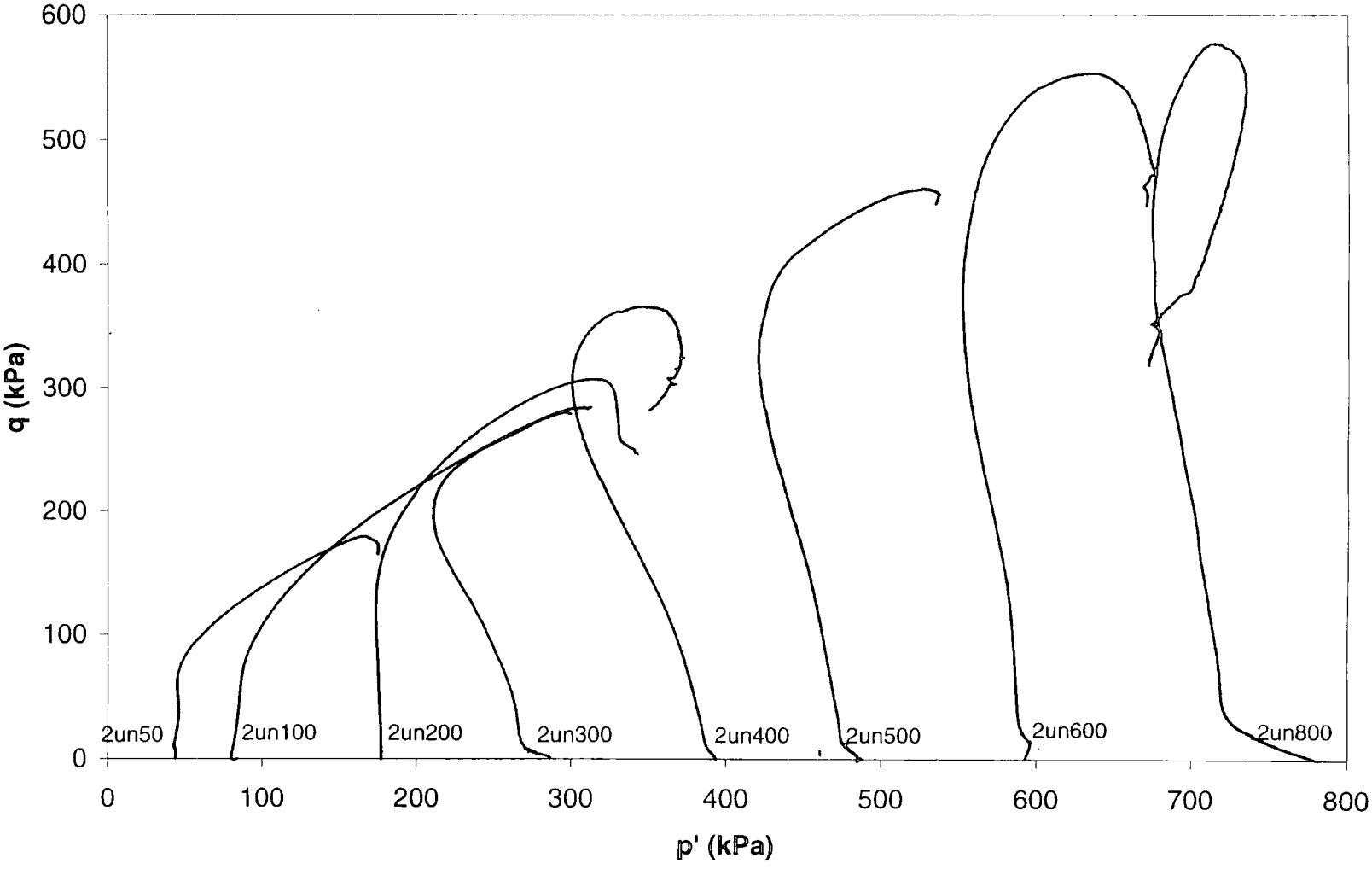

Fig.7.8 Stress paths derived from a series of triaxial tests on natural soils of borhole two

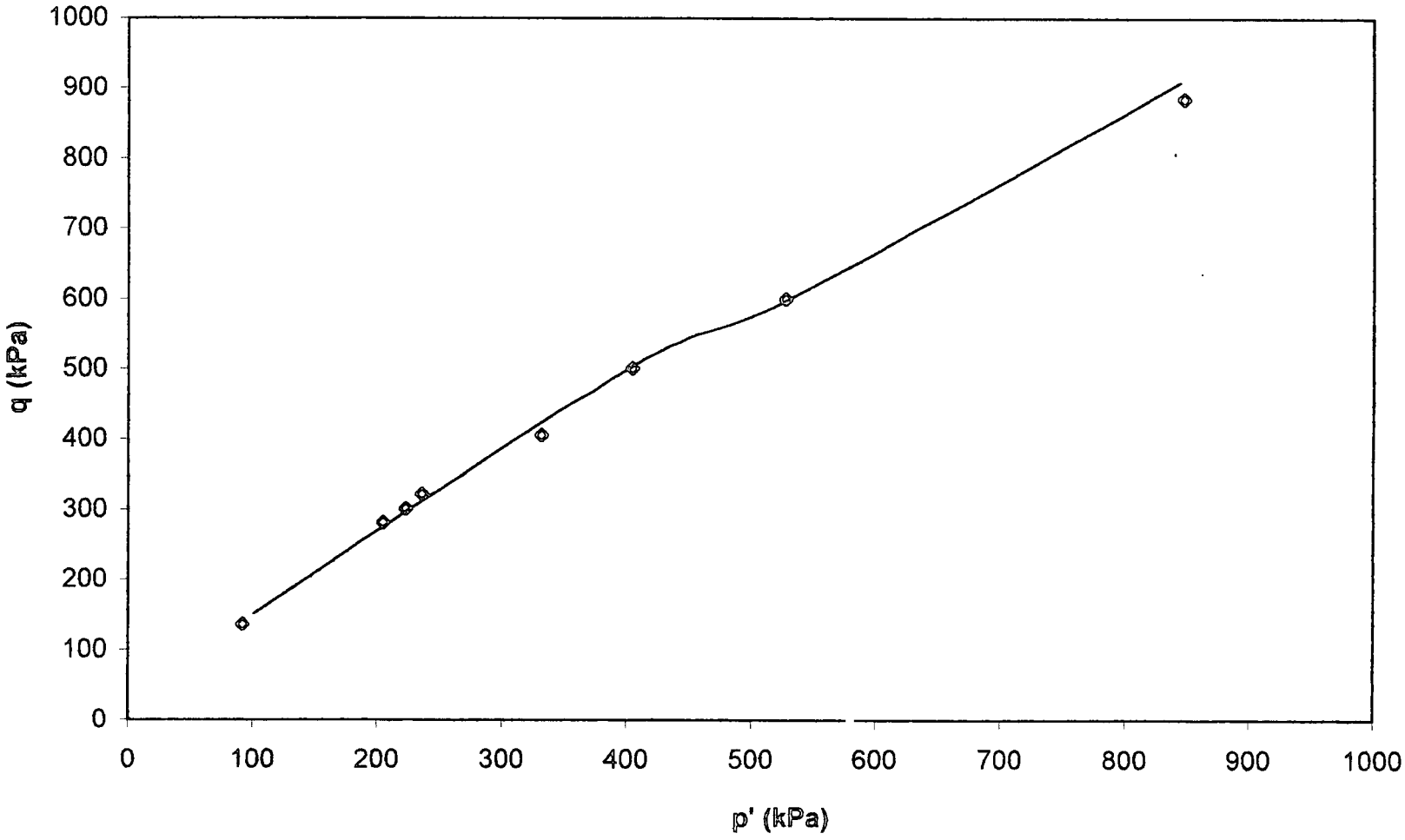

Fig. 7.9 Failure surface for natural soils of borehole one

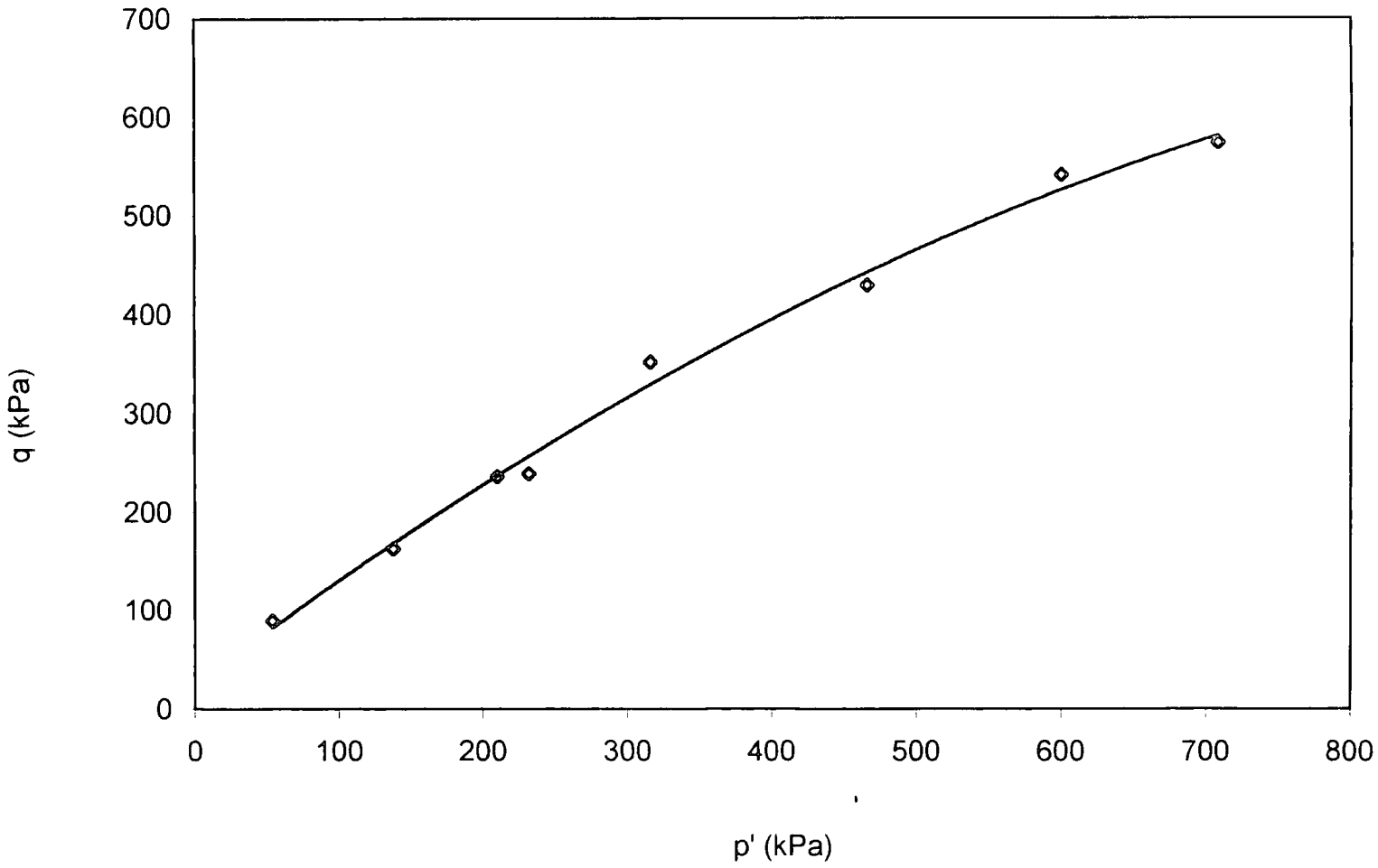

Fig.7.10 Failure surface for natural soils of borehole two

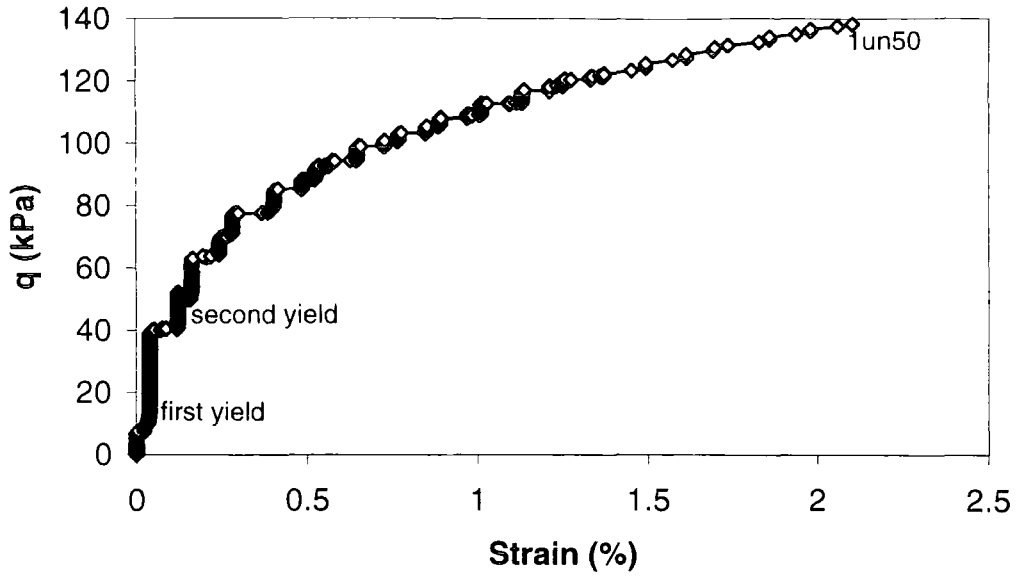

Fig.7.11 Stress strain curve for 1un50 showing first and second yield points plotted on natural scale

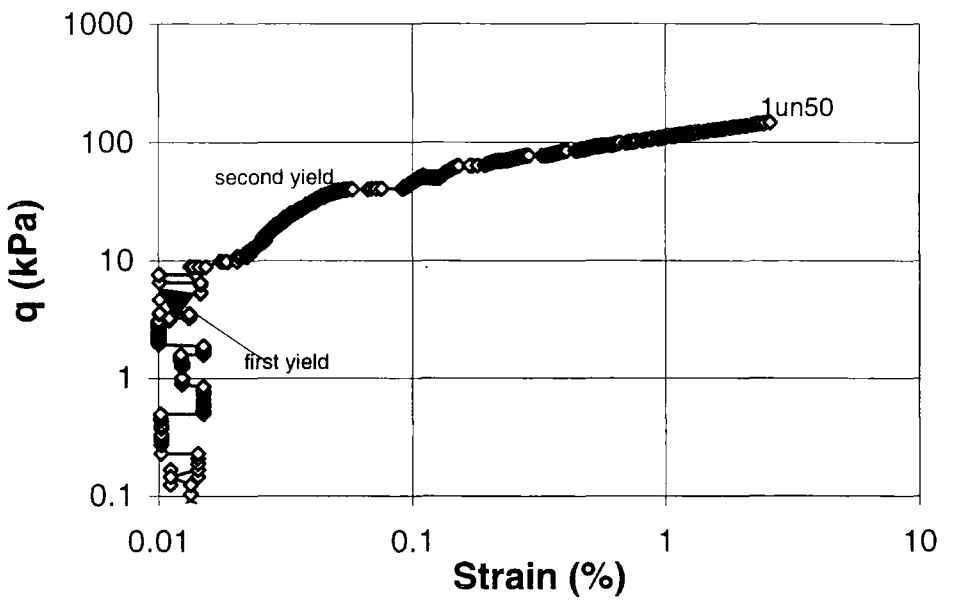

Fig.7.12 Stress strain curve for 1un50 showing first and second yield points plotted on log-log scale

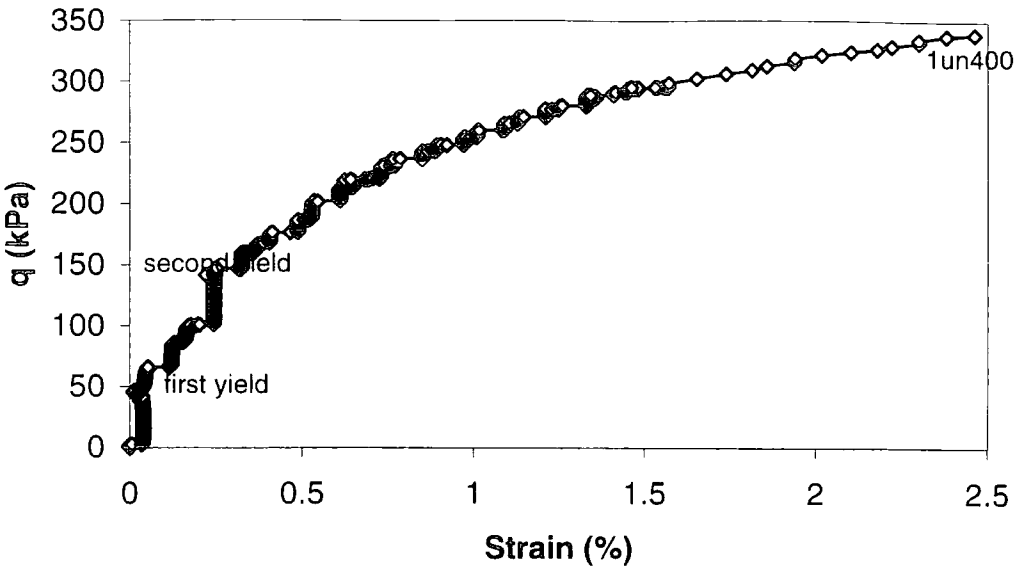

Fig.7.13 Stress strain curve for 1un400 showing first and second yield points plotted on natural scale

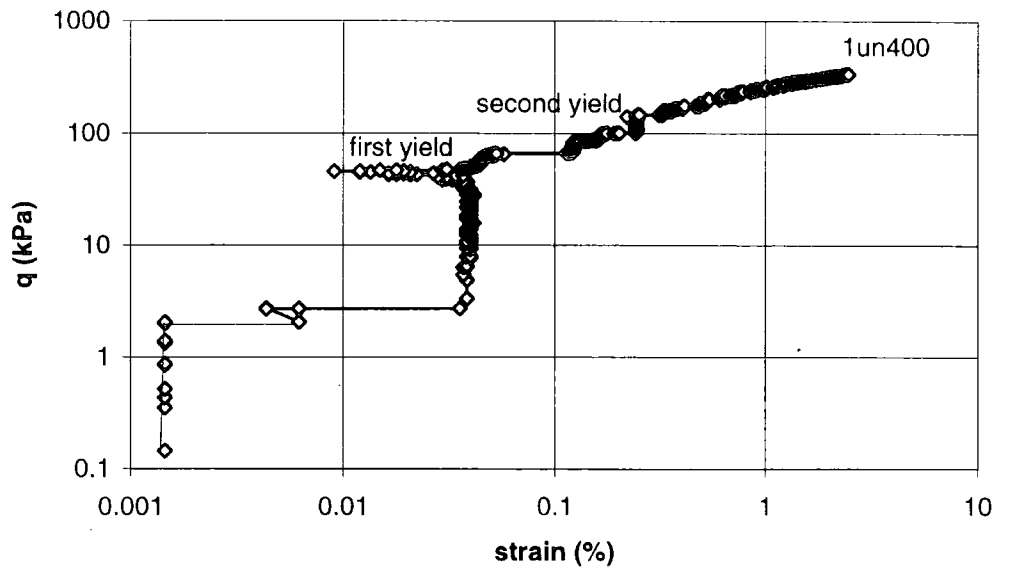

Fig.7.14 Stress strain curve for 1un400 showing first and second yield points plotted on log-log scale

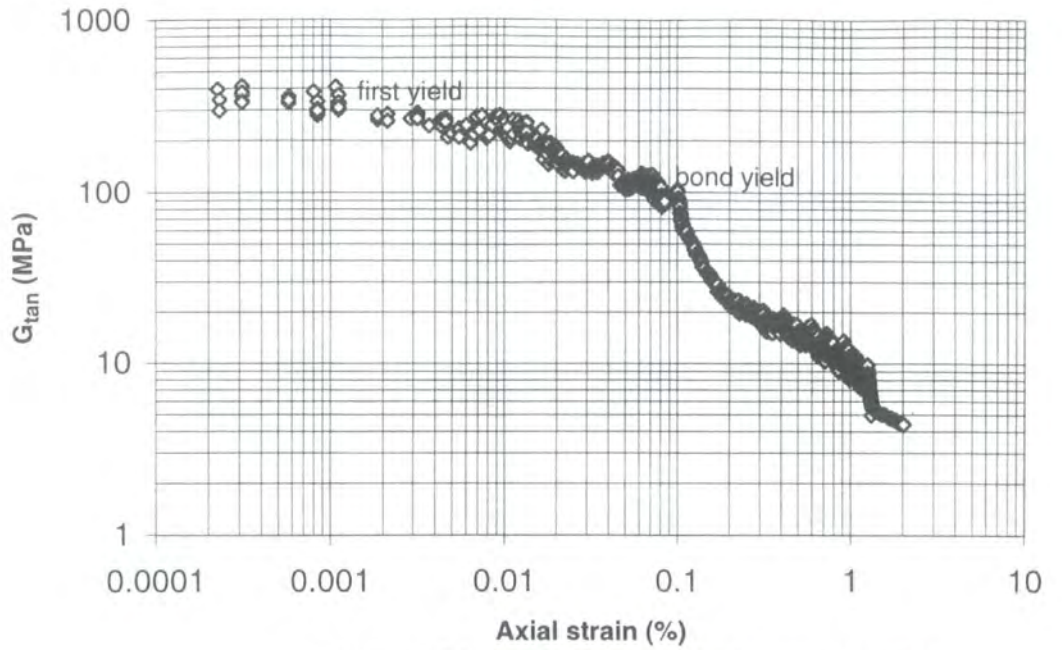

Fig.7.15 First and bond yield for test 1un50

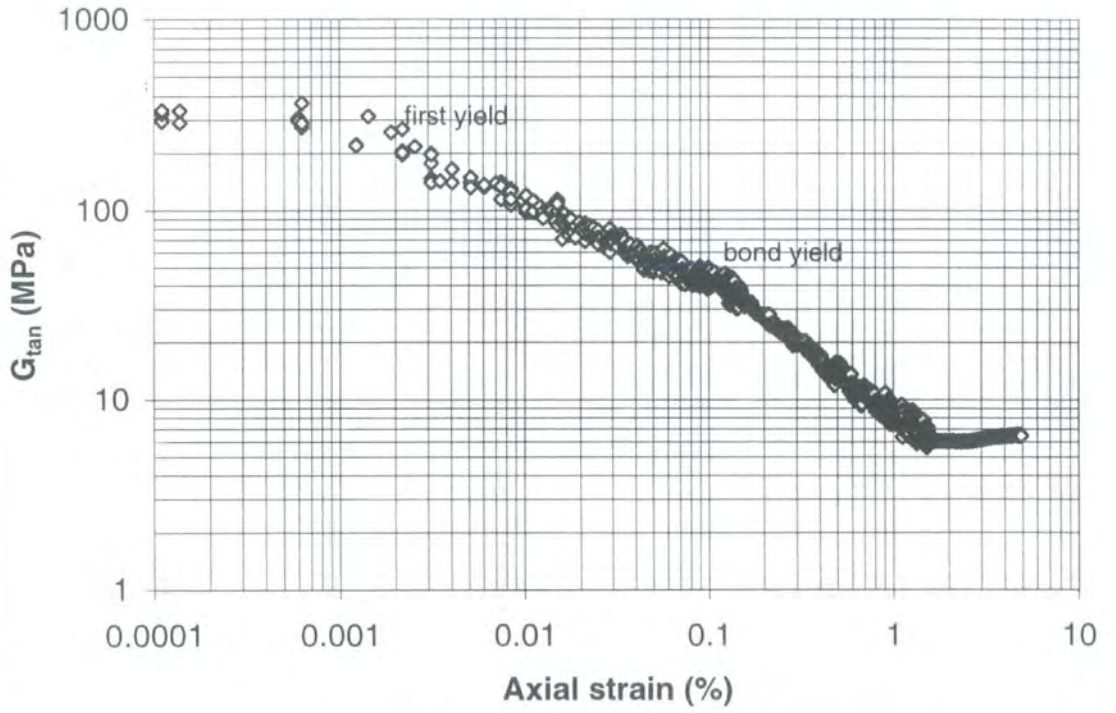

Fig.7.16 First and bond yield for test 1un100

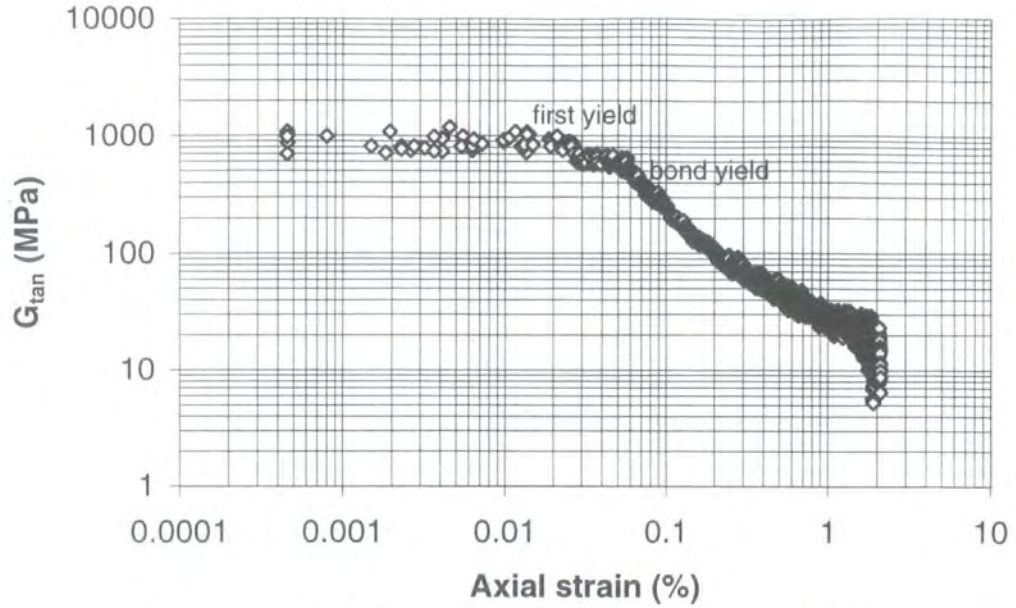

Fig.7.17 First and bond yield for test 1un200

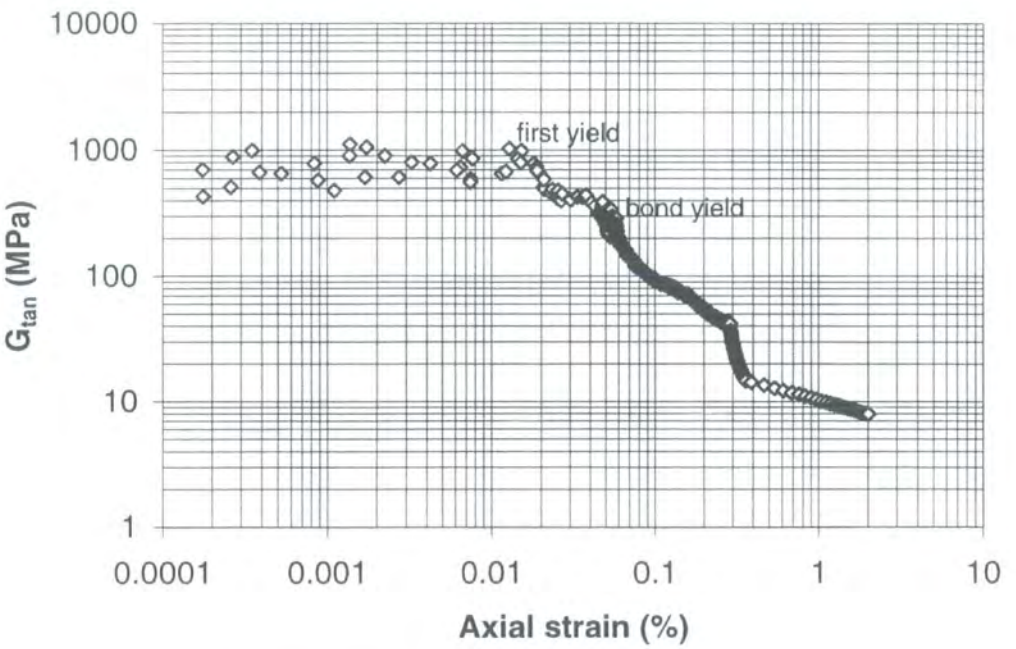

Fig.7.18 First and bond yield for test 1un300

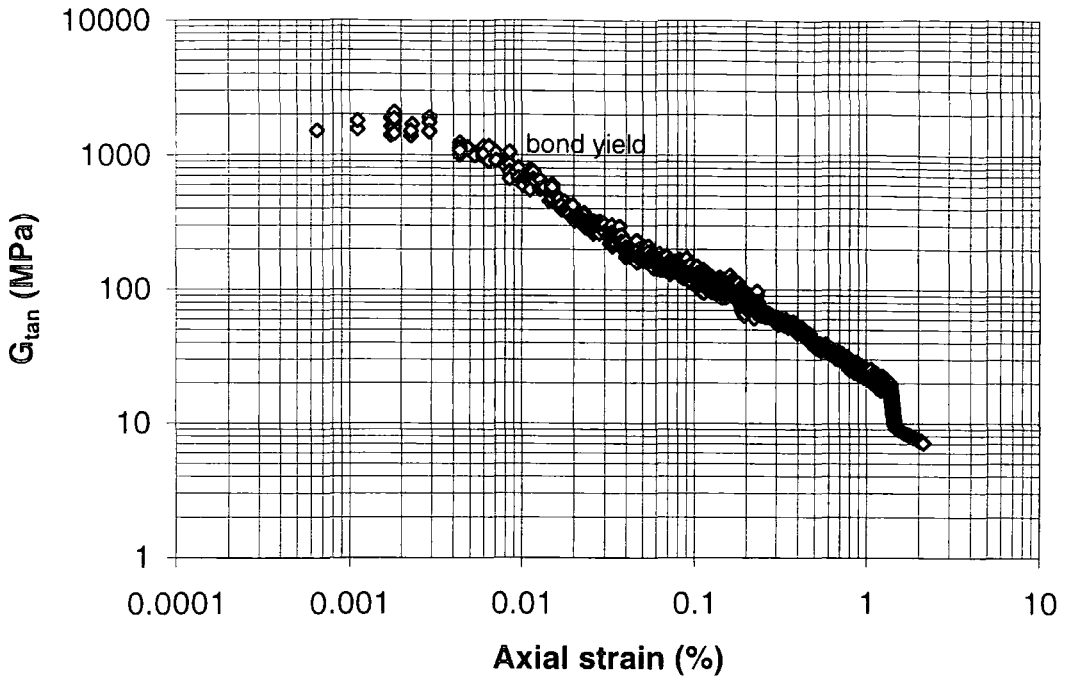

Fig.7.19 Bond yield for test 1un400

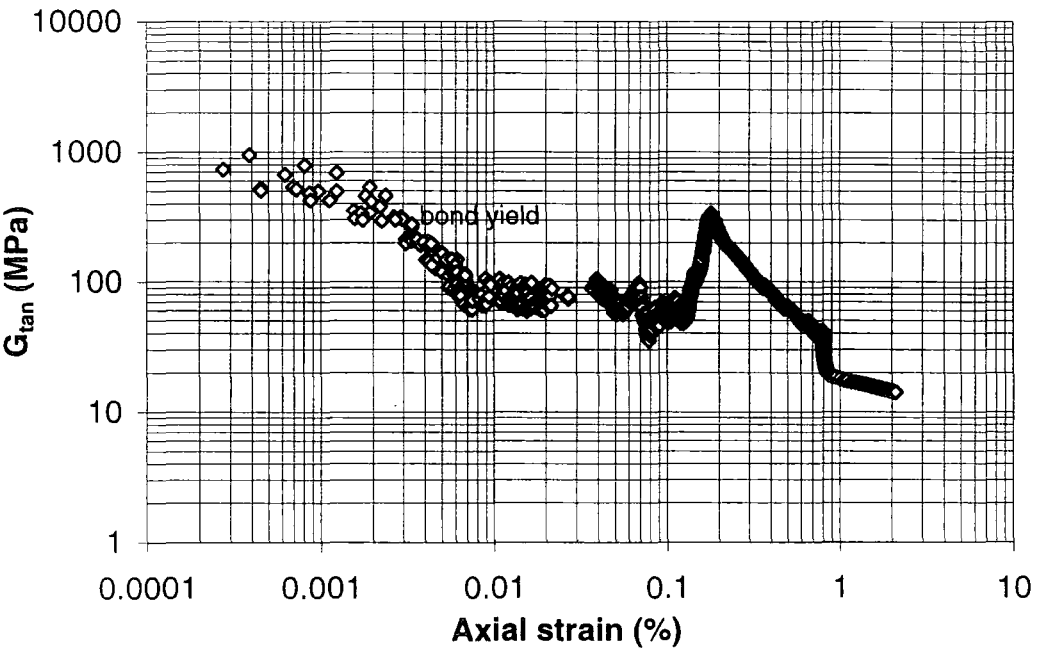

Fig.7.20 stiffness versus strain for test 1un500

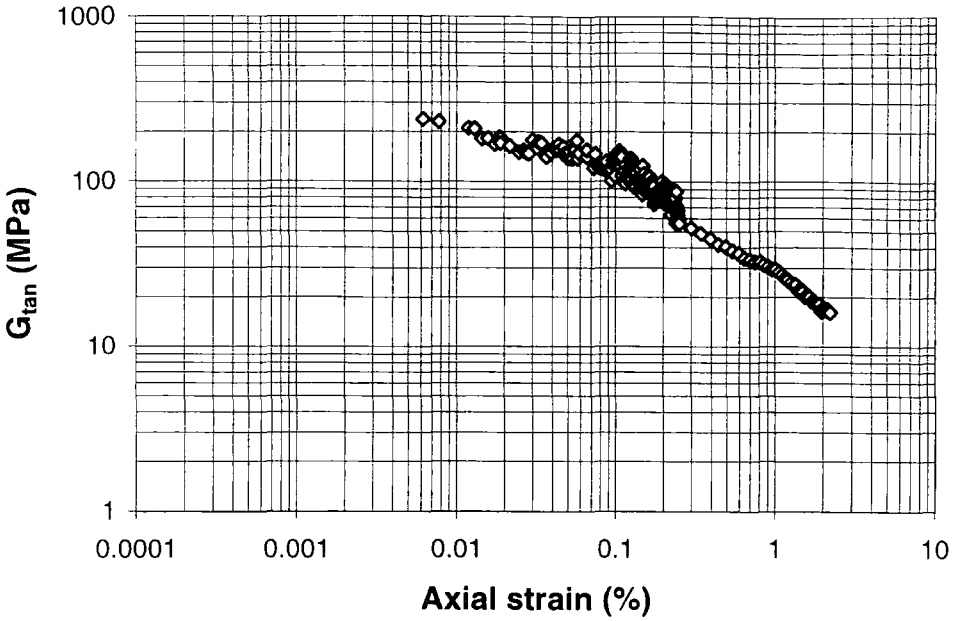

Fig.7.21 Stiffness versus strain for test 1un600

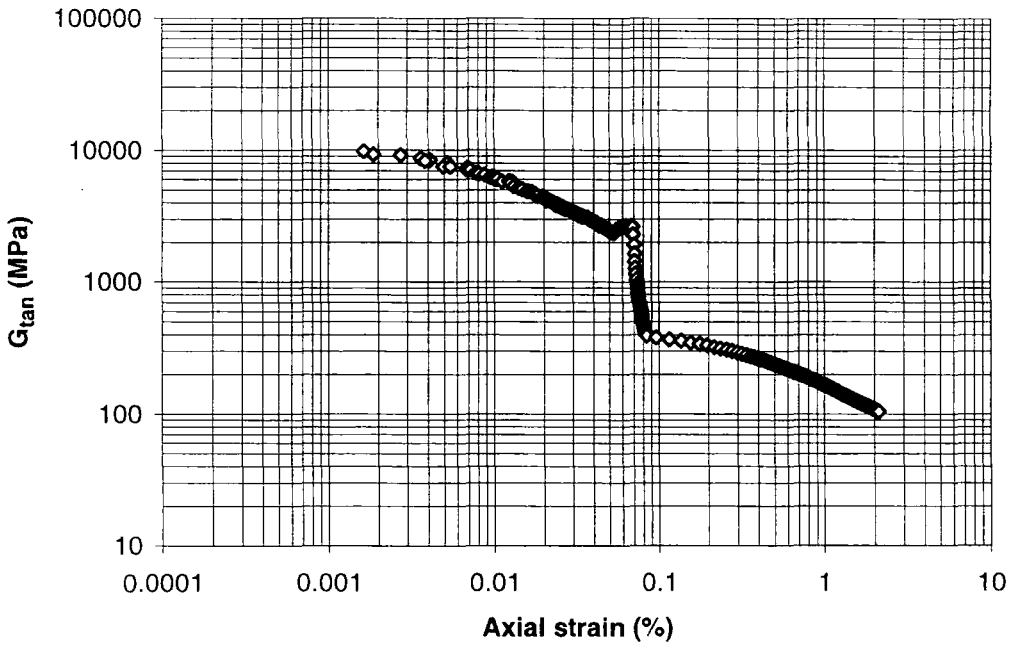

Fig.7.22 Stiffness versus strain for test 1un800

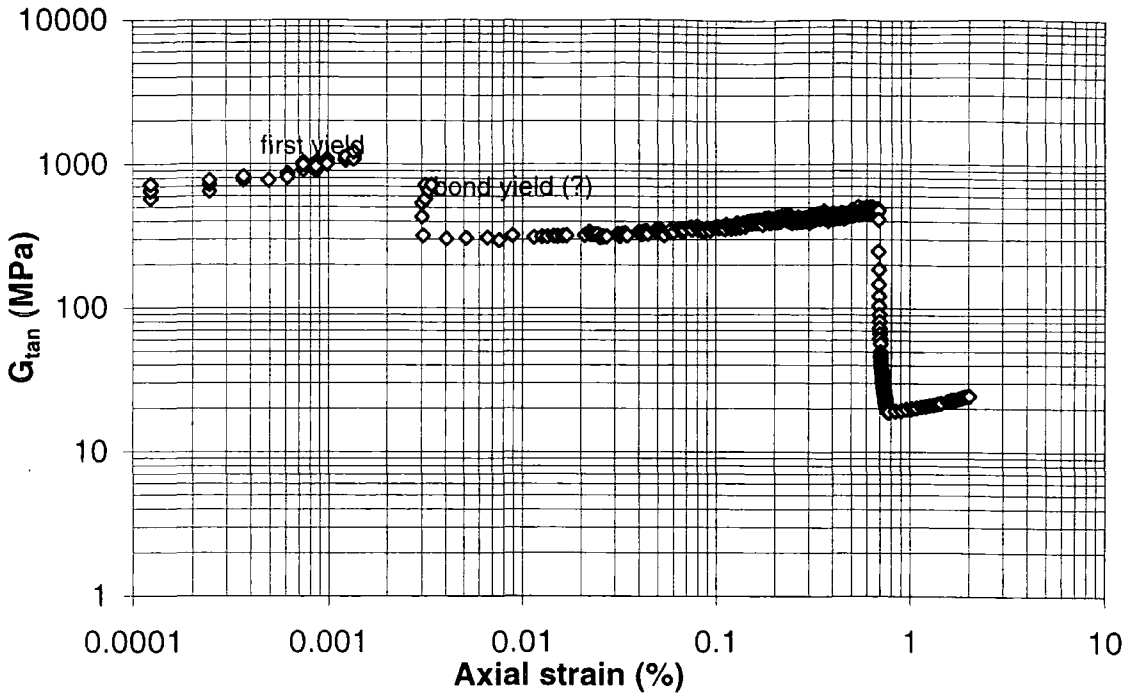

Fig.7.23 First and bond yield for test 2un50

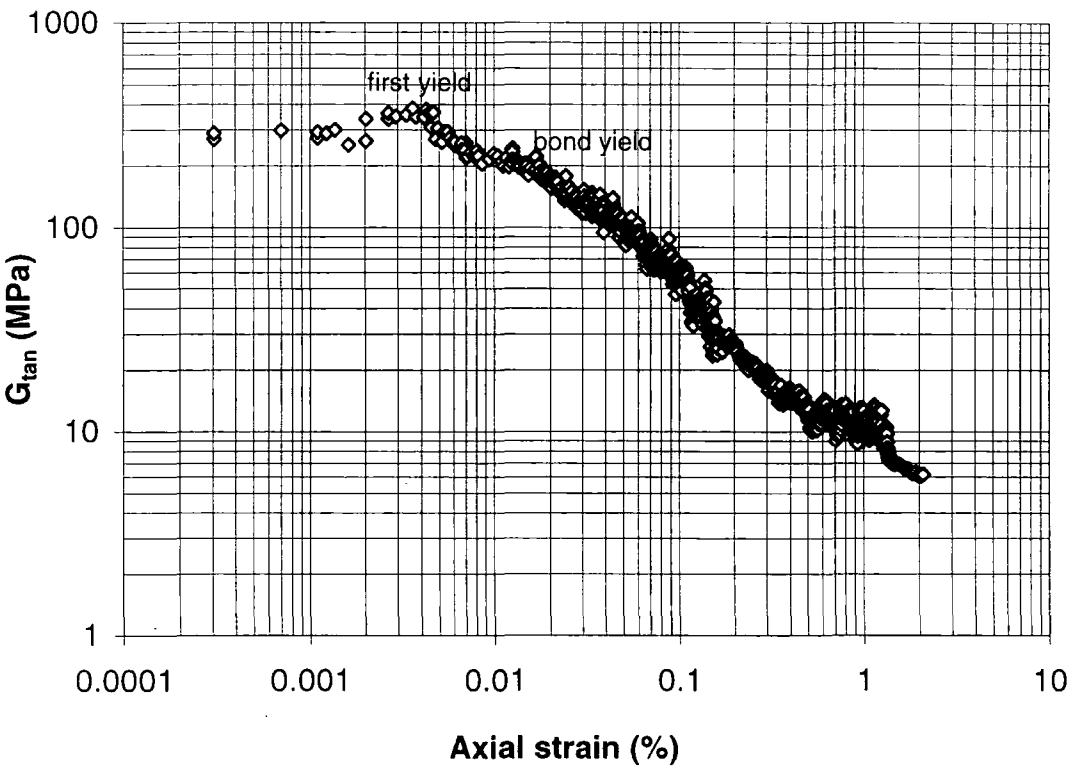

Fig. 7.24 First and bond yield for test 2un100

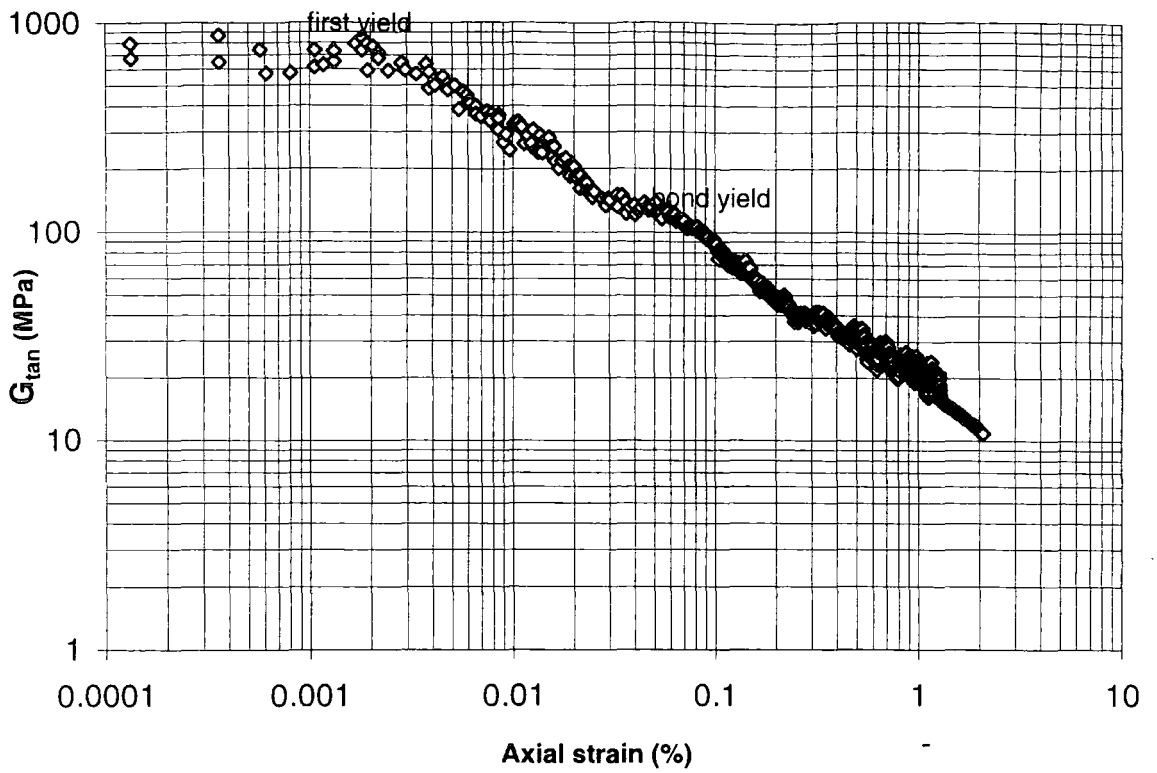

Fig.7.25 First and bond yield for test 2un200

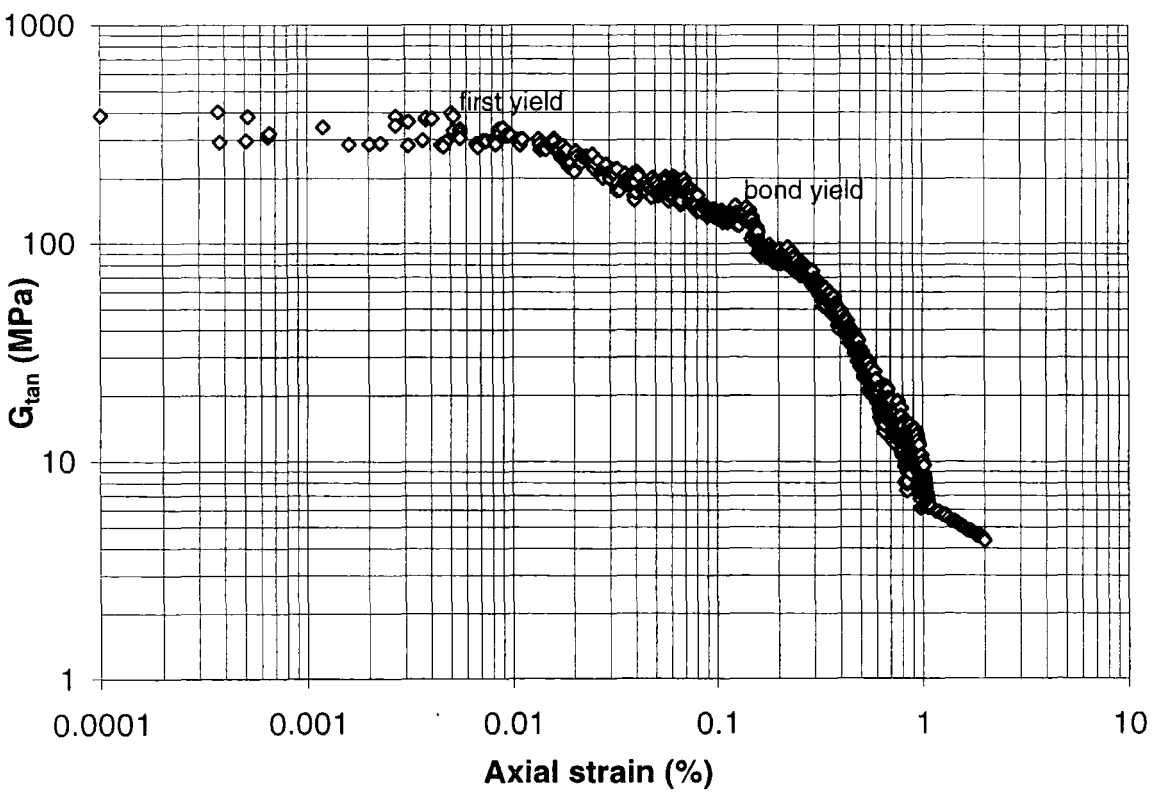

Fig.7.26 First and bond yield for test 2un300

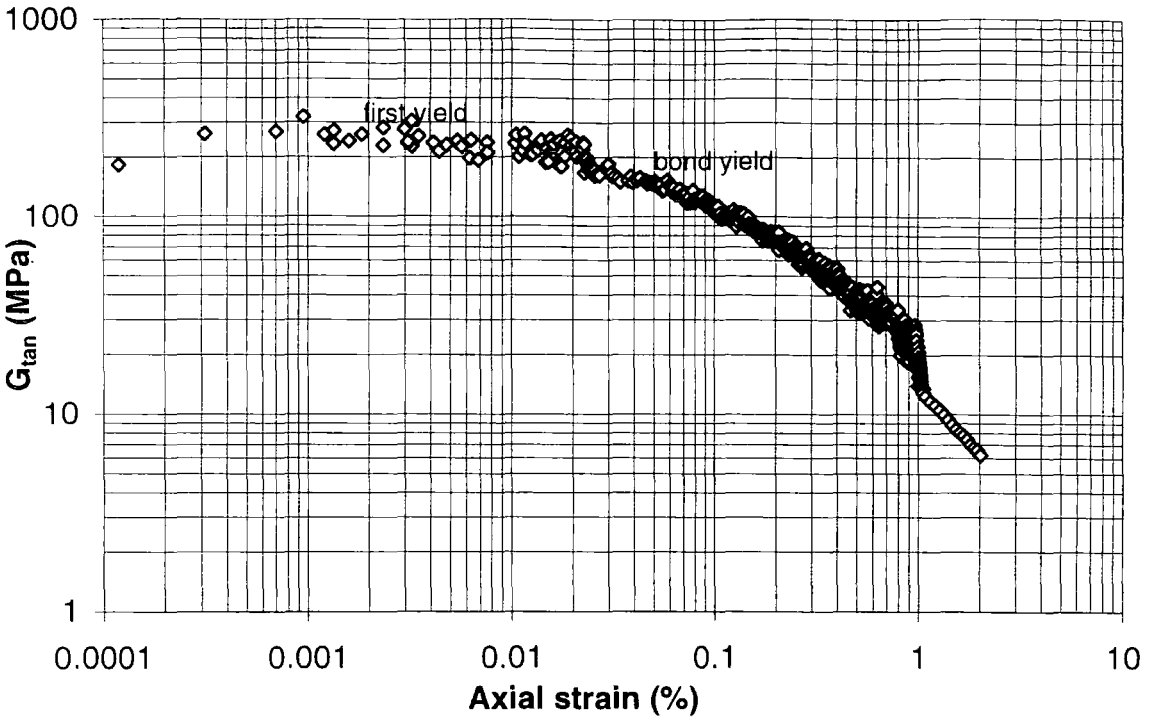

Fig.7.27 First and bond yield for test 2un400

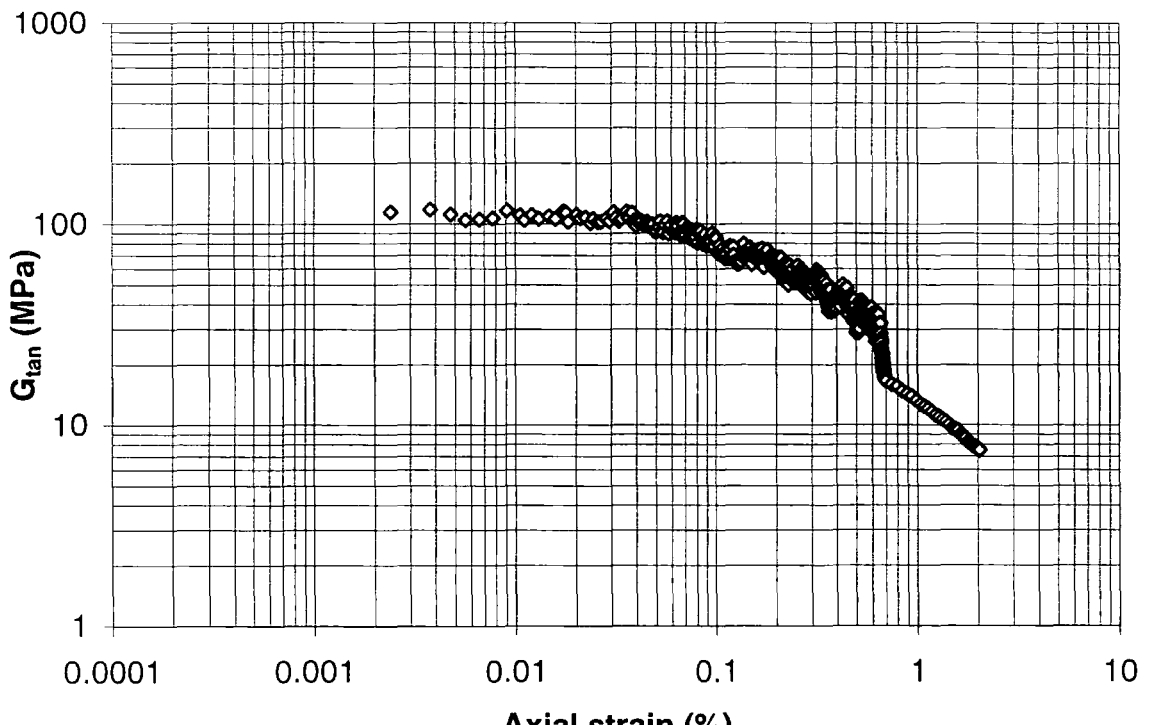

Fig.7.28 Stiffness versus strain for test 2un500

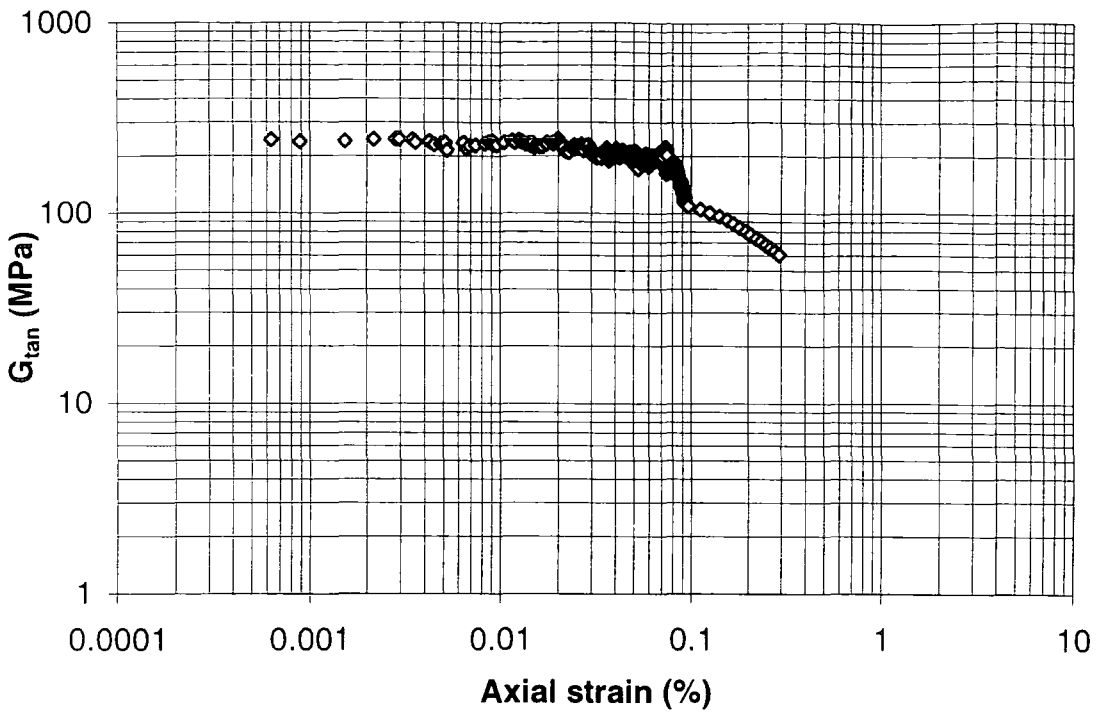

Fig.7.29 Stiffness versus strain for test 2un600

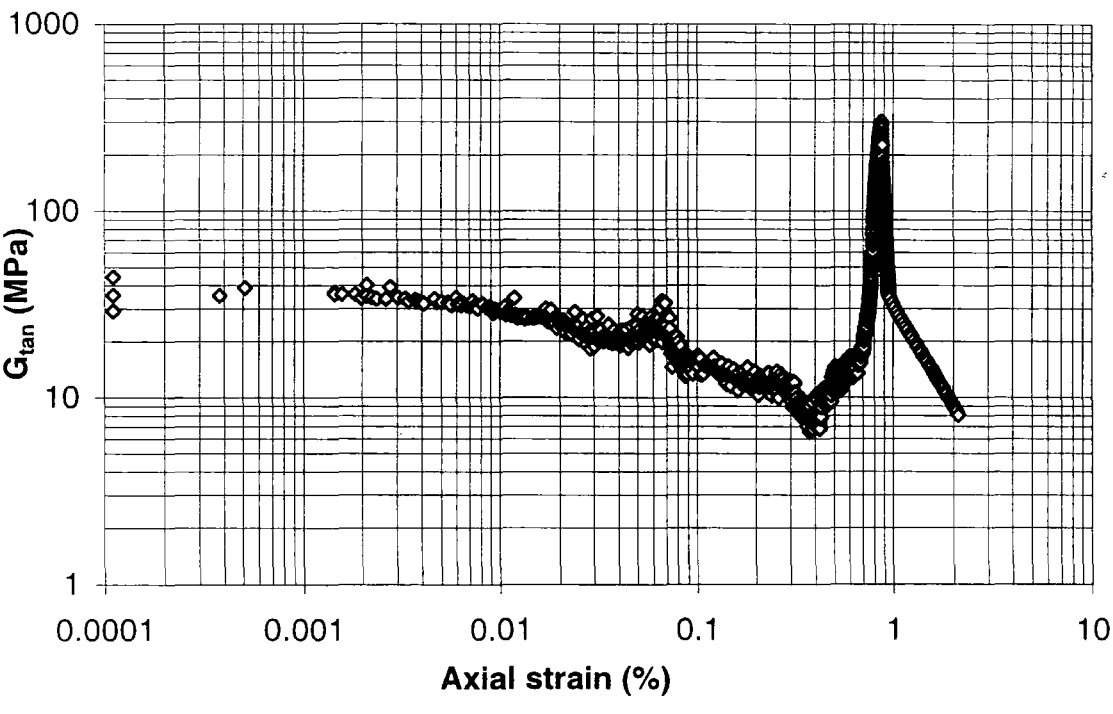

Fig.7.30 Stiffness versus strain for test 2un800

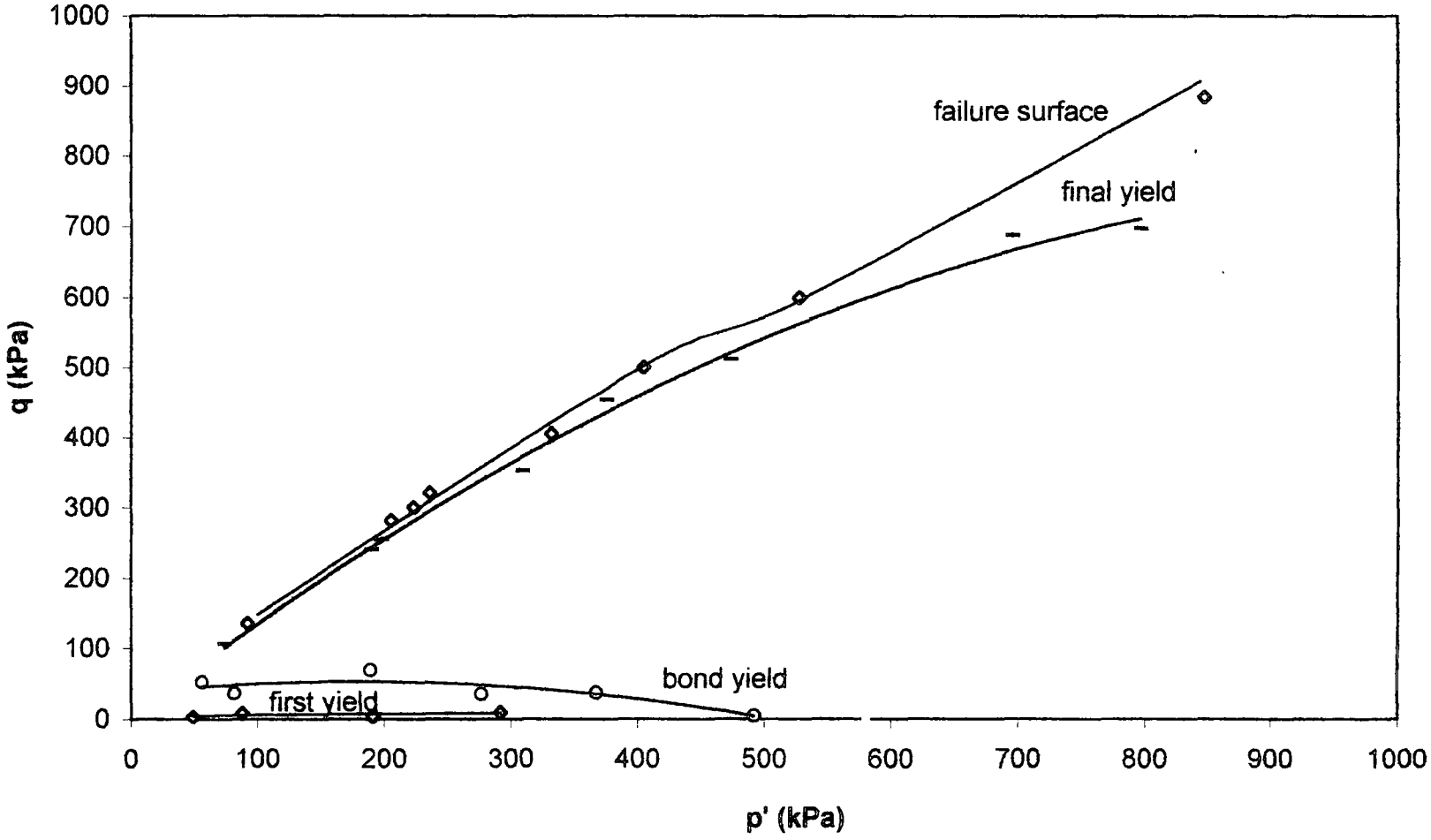

Fig. 7.31 Three yield surfaces and failure surface for natural soils of borehole one

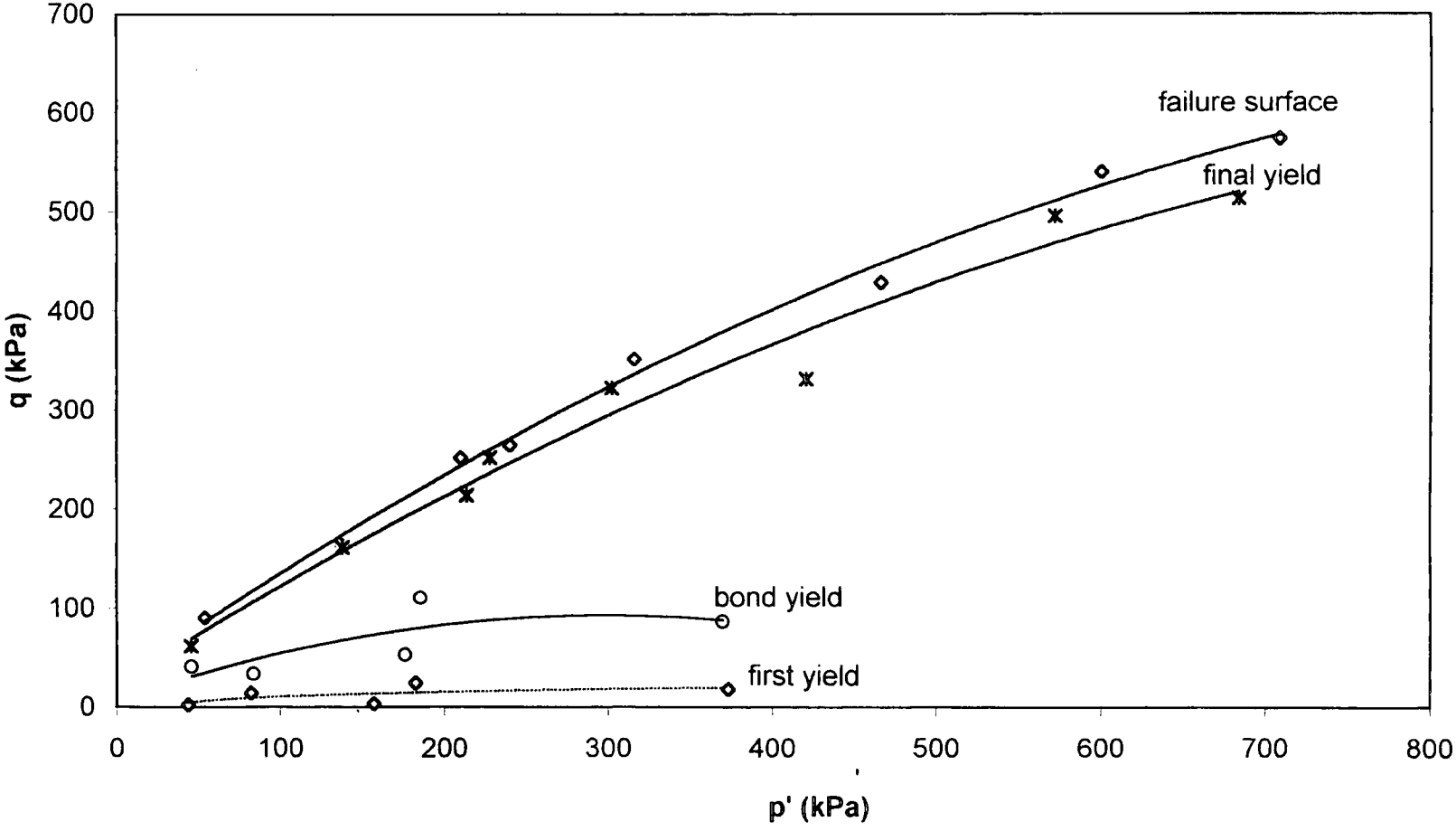

Fig.7.32 Failure surface and three yield surfaces for natural soils of borehole two

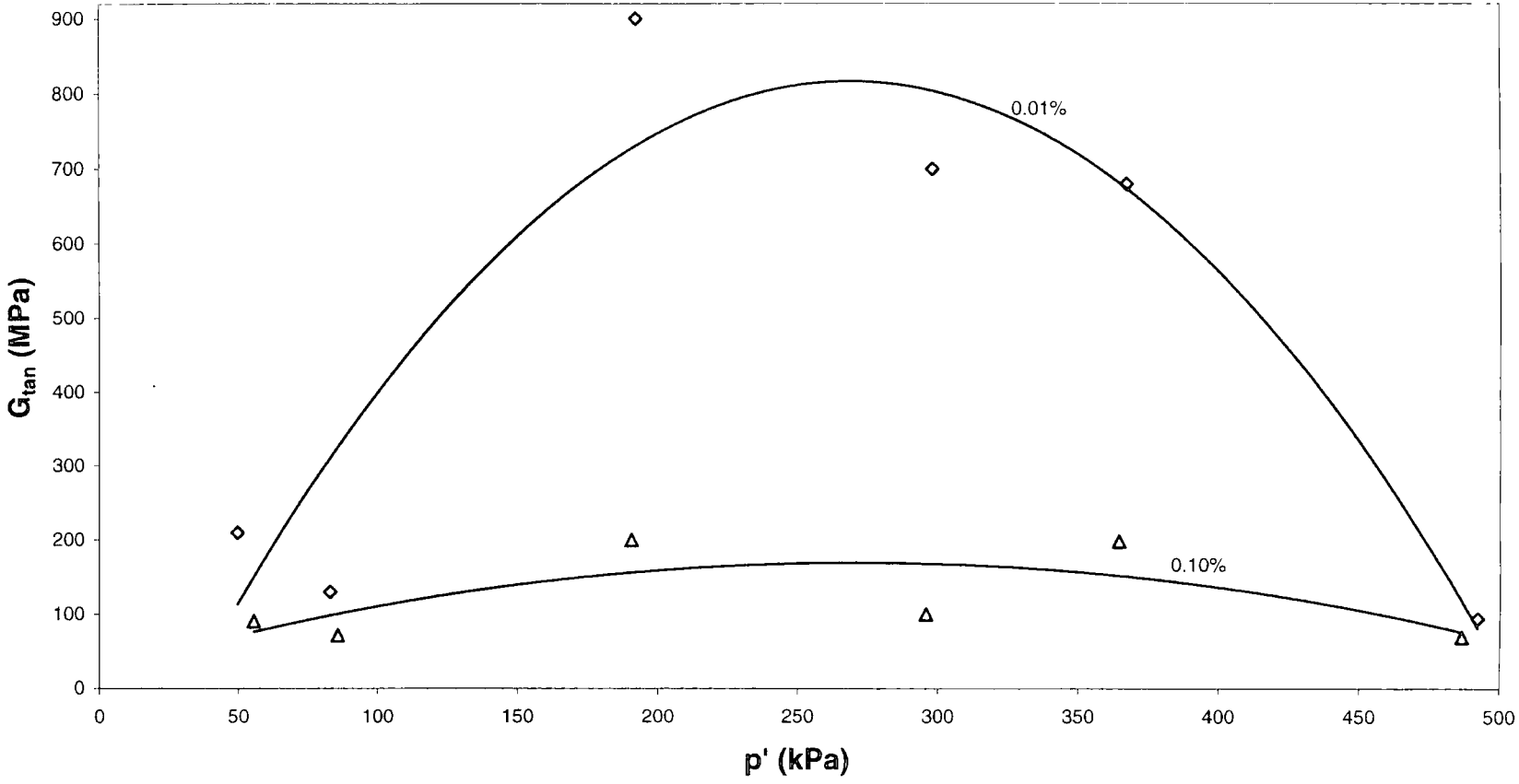

Fig.7.33: Loss in stiffness with increasing strain (from 0.01% to 0.1%) for natural soils of borehole one

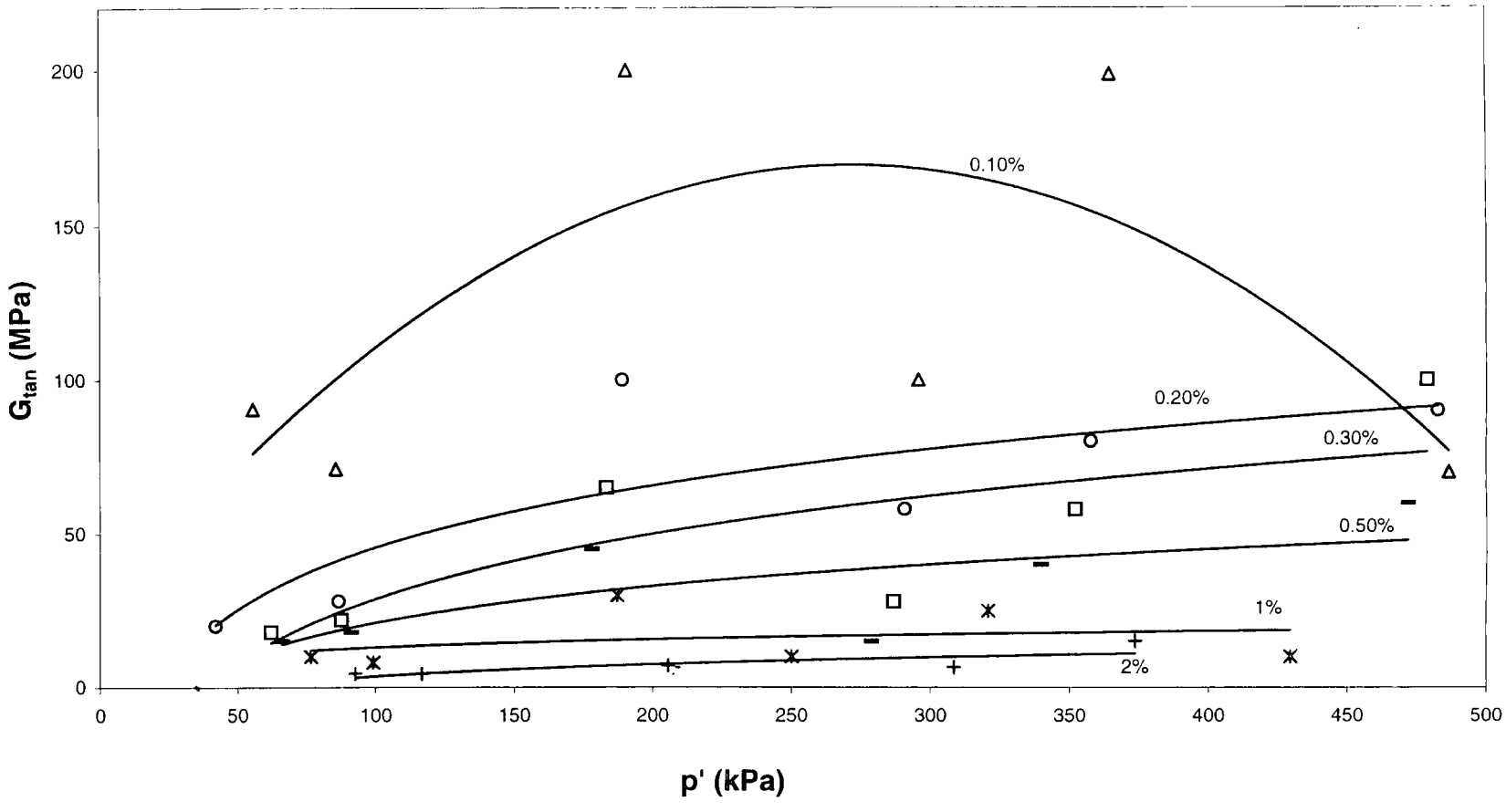

Fig. 7.34 Loss in stiffness with increasing strain (from 0.1% to 2%) for natural soils of borehole one

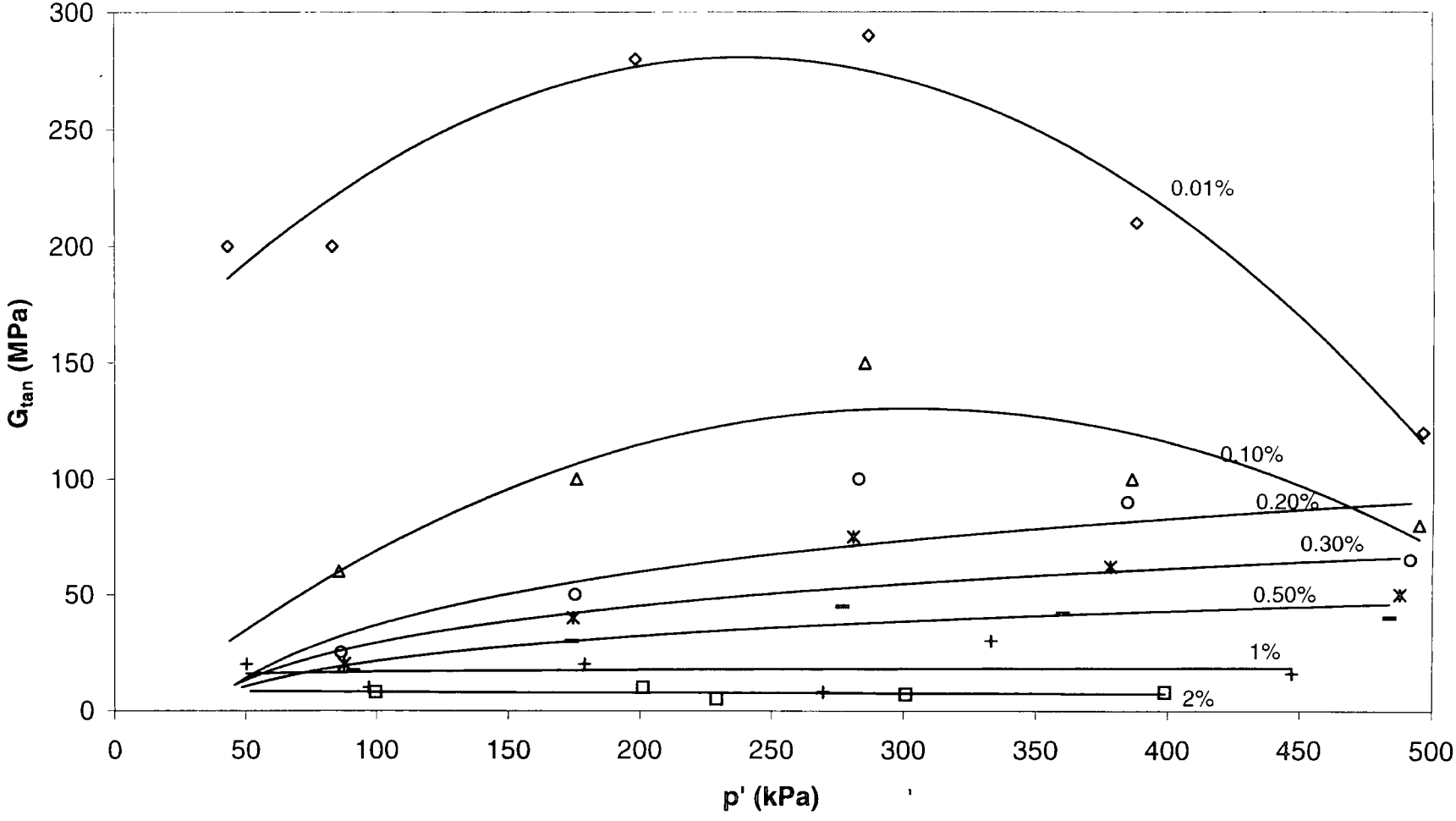

Fig.7.35 Loss of stiffness with increasing strain (0.01% to 2%) for natural soils of borehole two

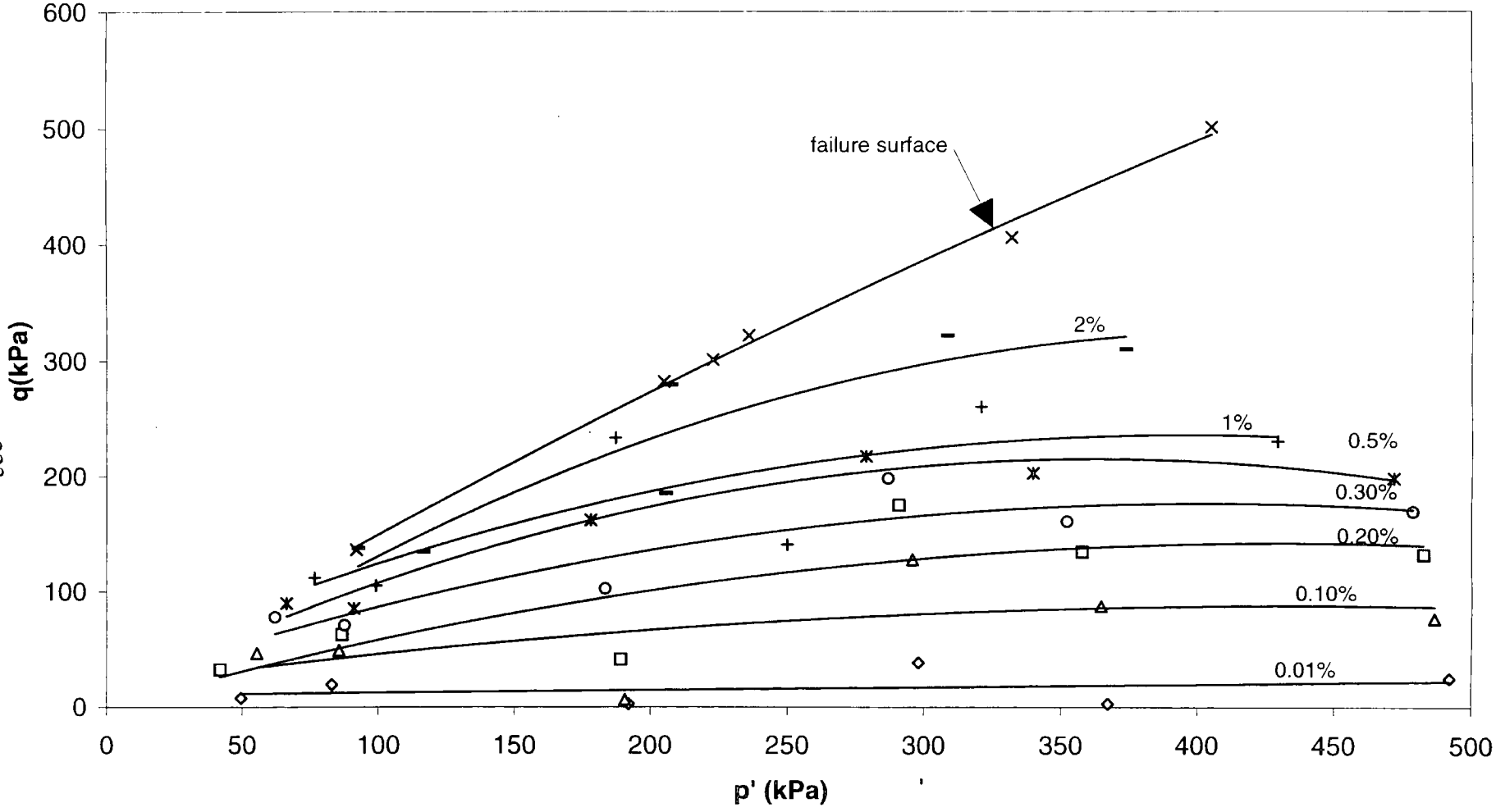

Fig. 7.36 Strain contours of natural soils of borehole one from 0.01% to 2% strain

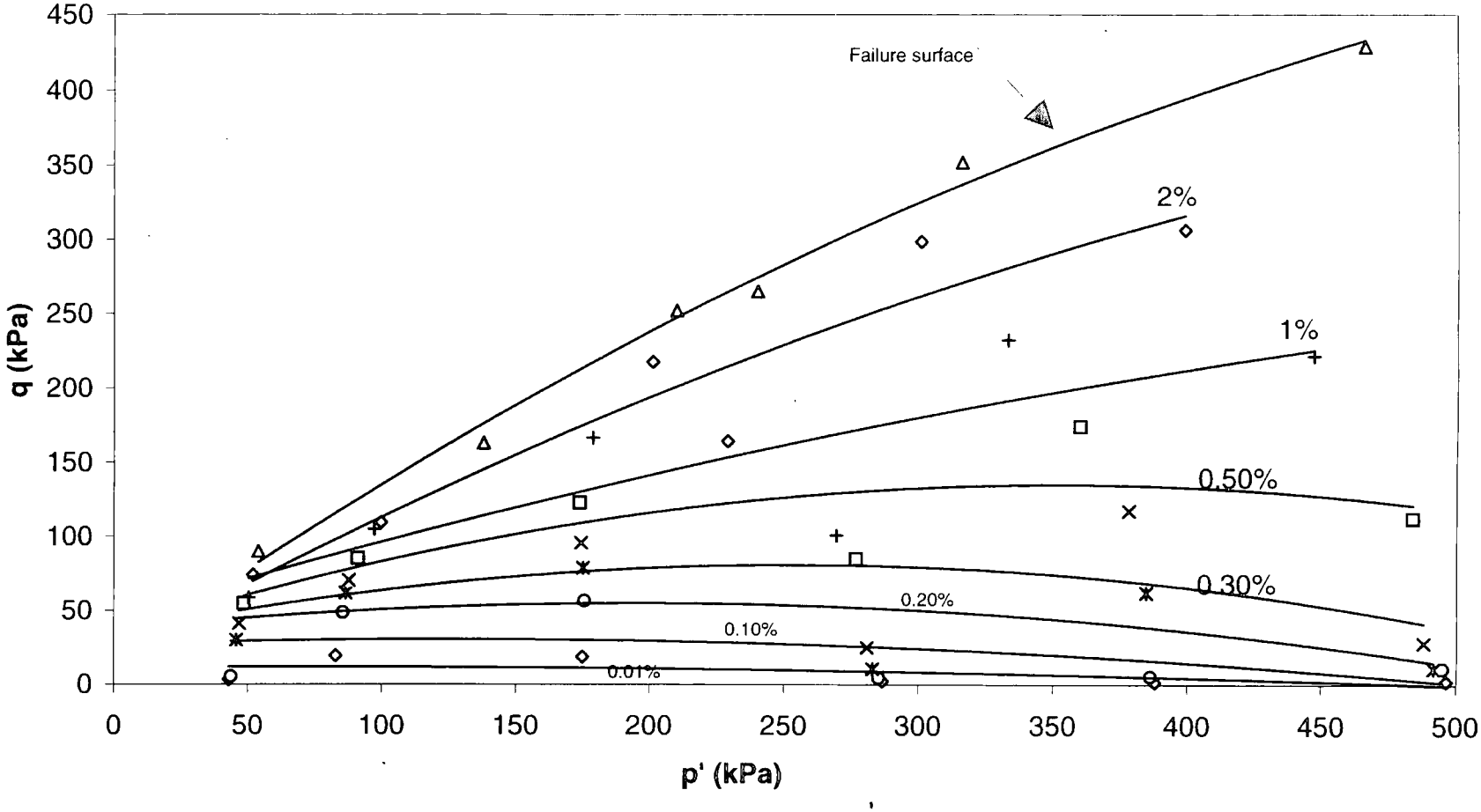

Fig.7.37 Failure surface and strain contours (from 0.01% to 2%) for natural soils of borehole two

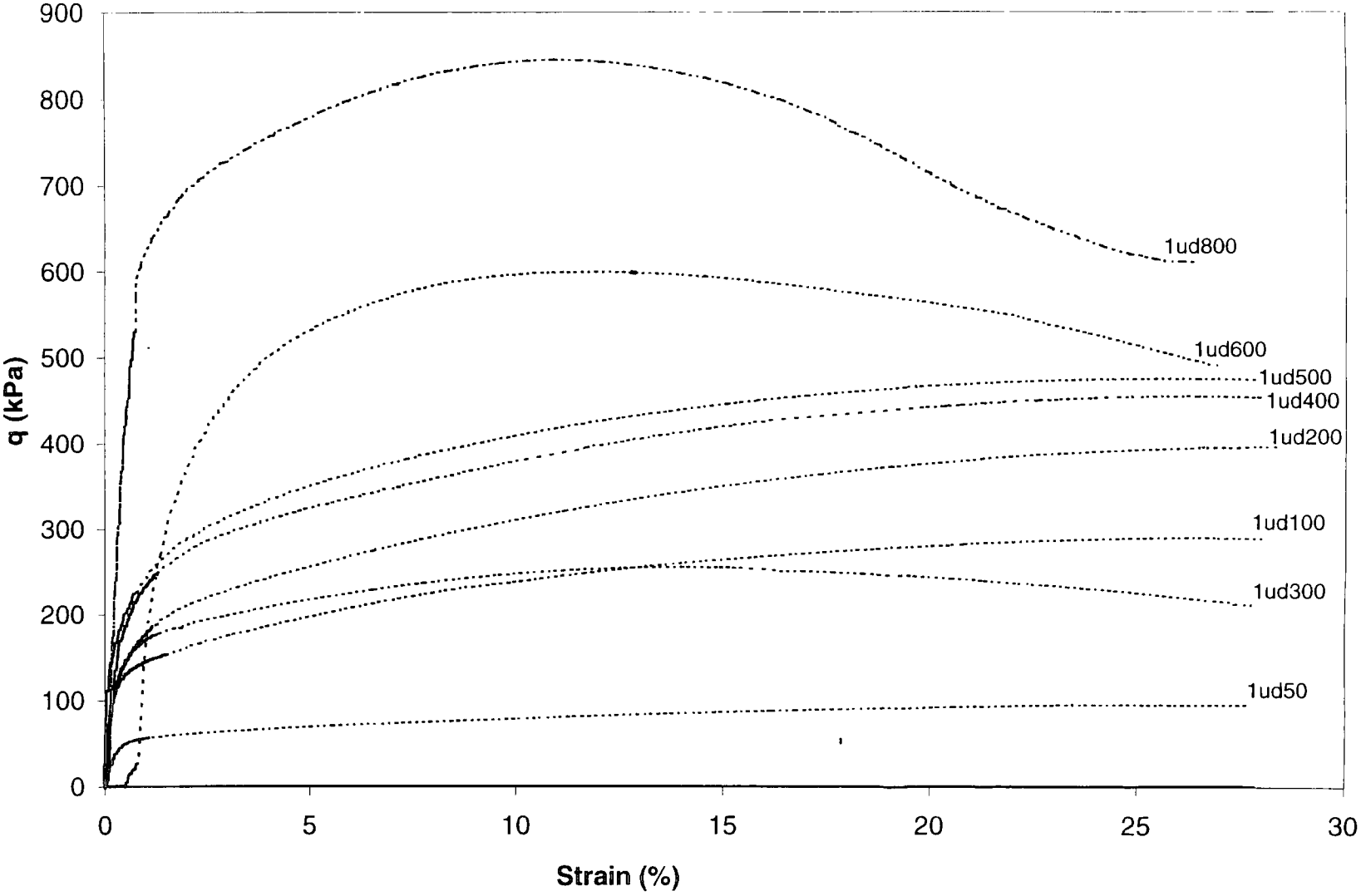

Fig. 7.38 Deviator stress versus axial strain curves for destructured soils of borehole one

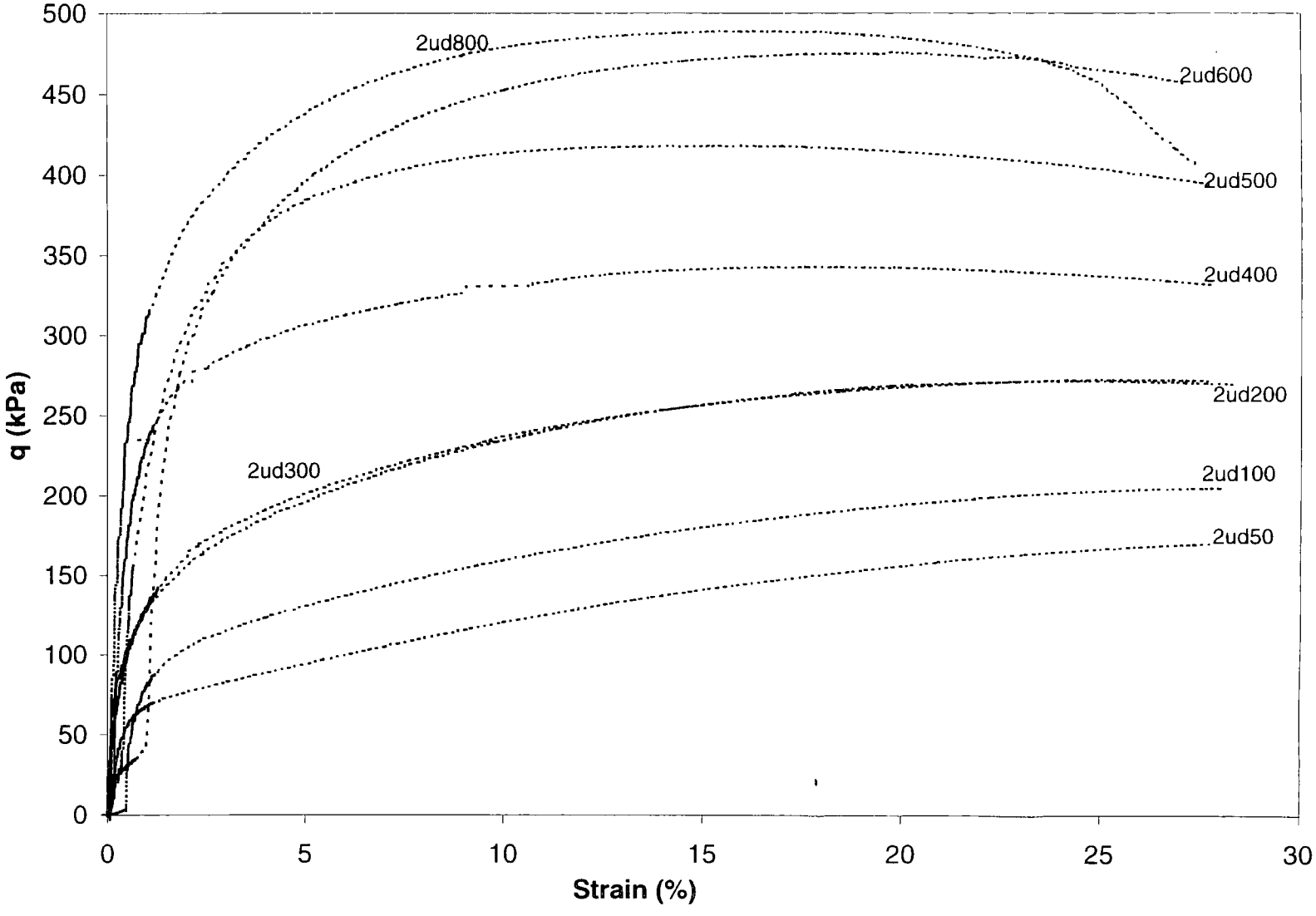

Fig. 7.39 Deviator stress versus axial strain curves for destructured soils of borehole two

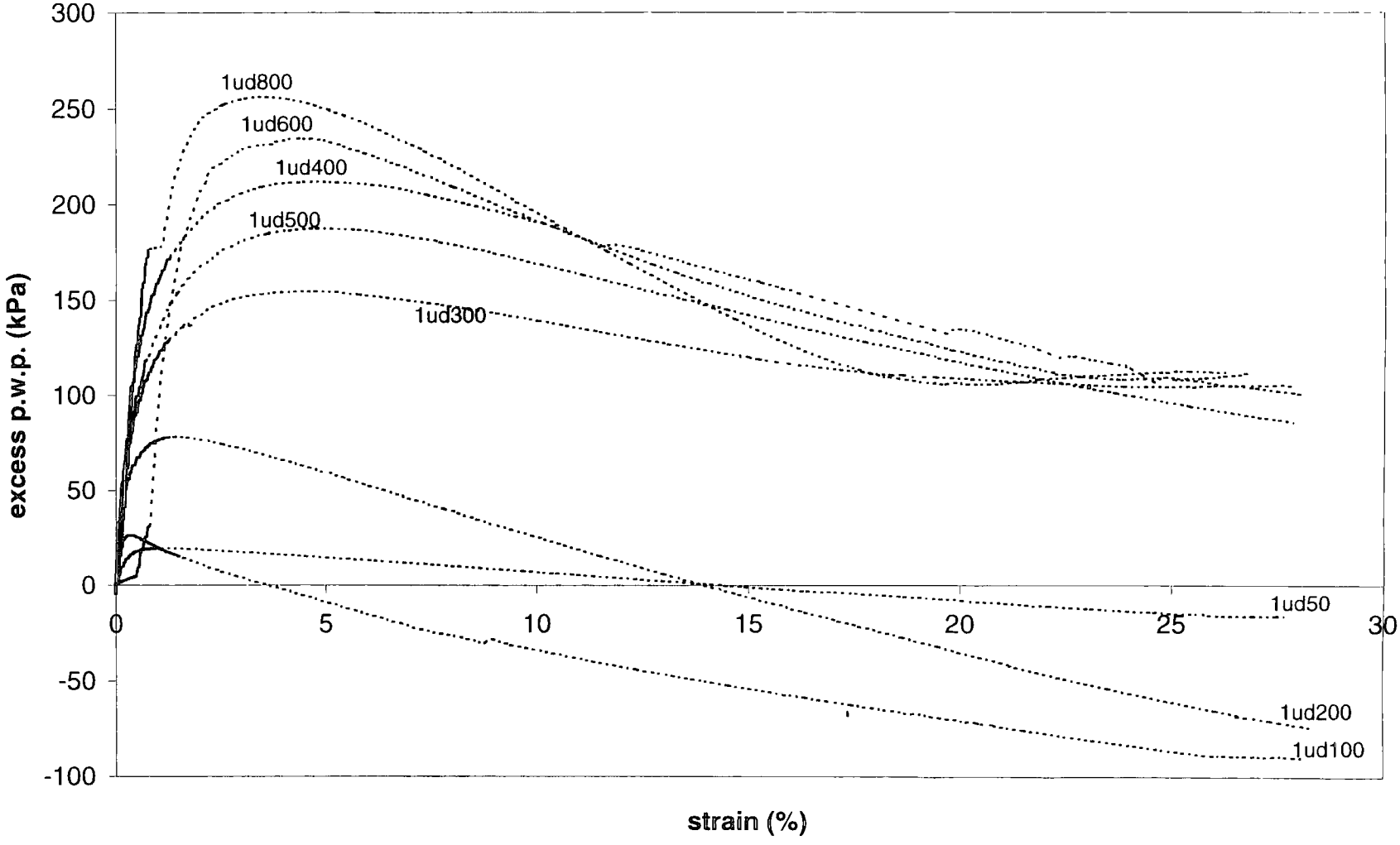

Fig. 7.40 Excess pore water pressure versus axial strain curves for destructured soils of borehole one

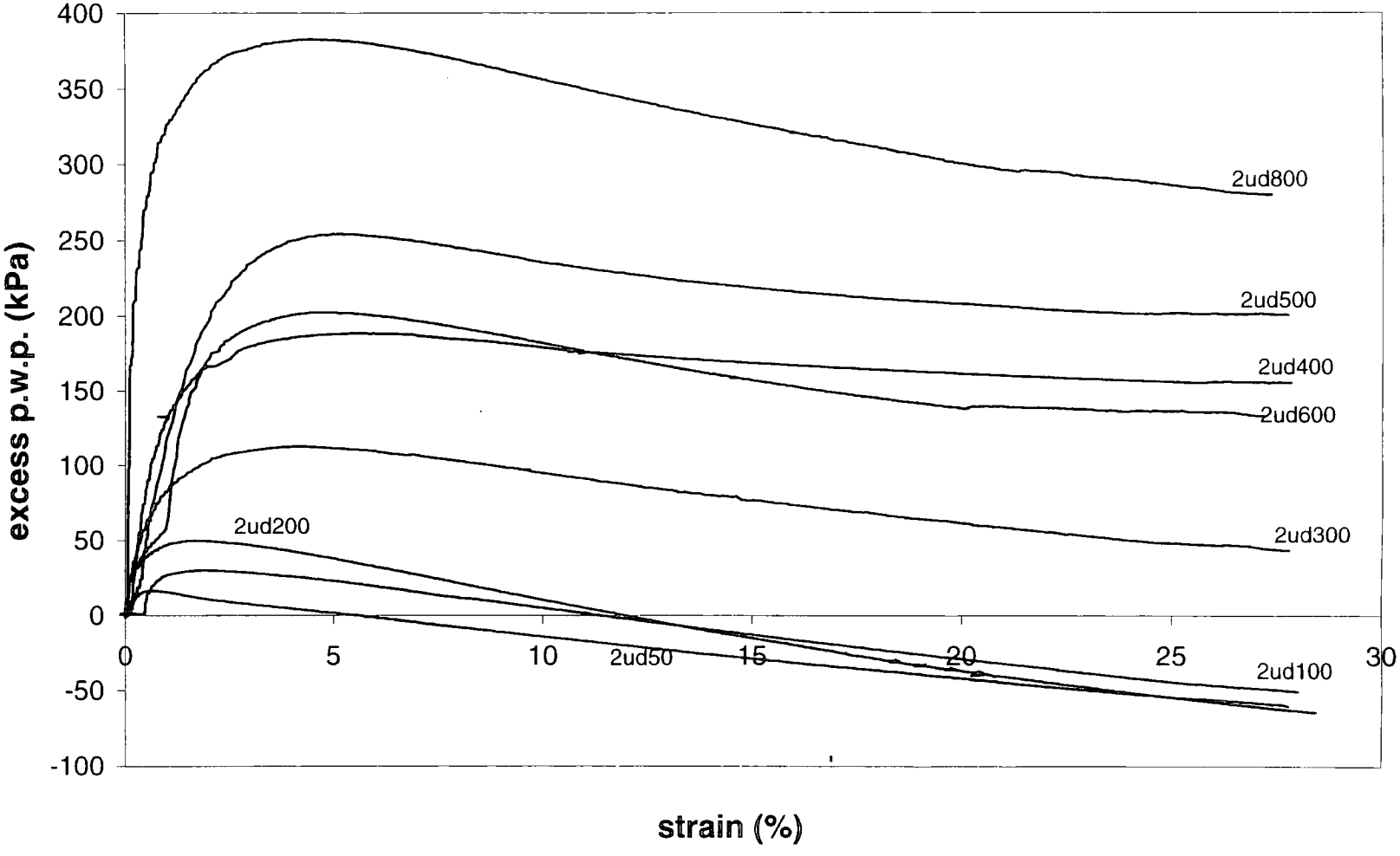

Fig.7.41 . Excess pore water pressure versus axial strain curves for destructured soils of borehole two

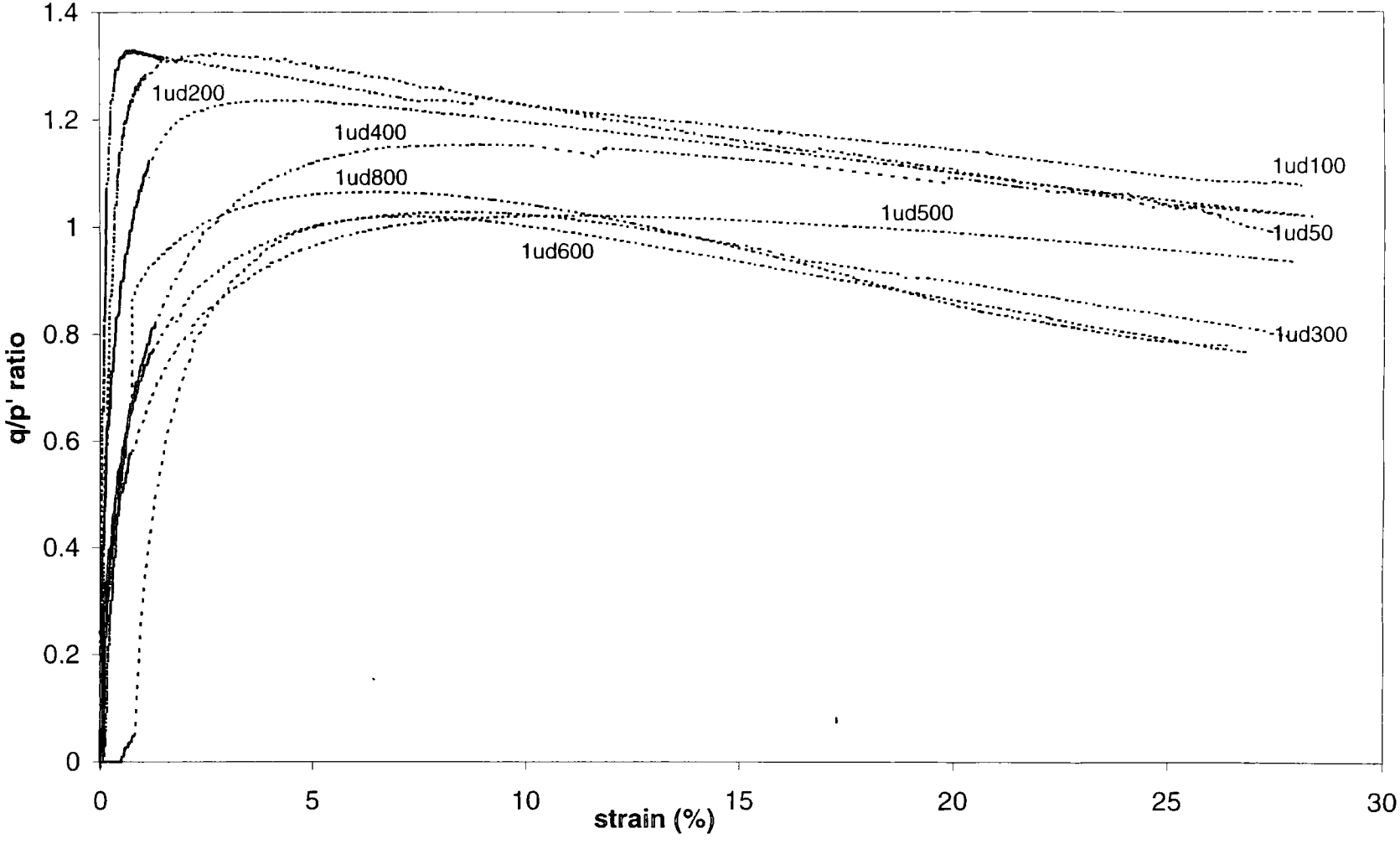

Fig.7.4.2 q/p' ratio versus axial strain graphs for destructured soils of borehole one

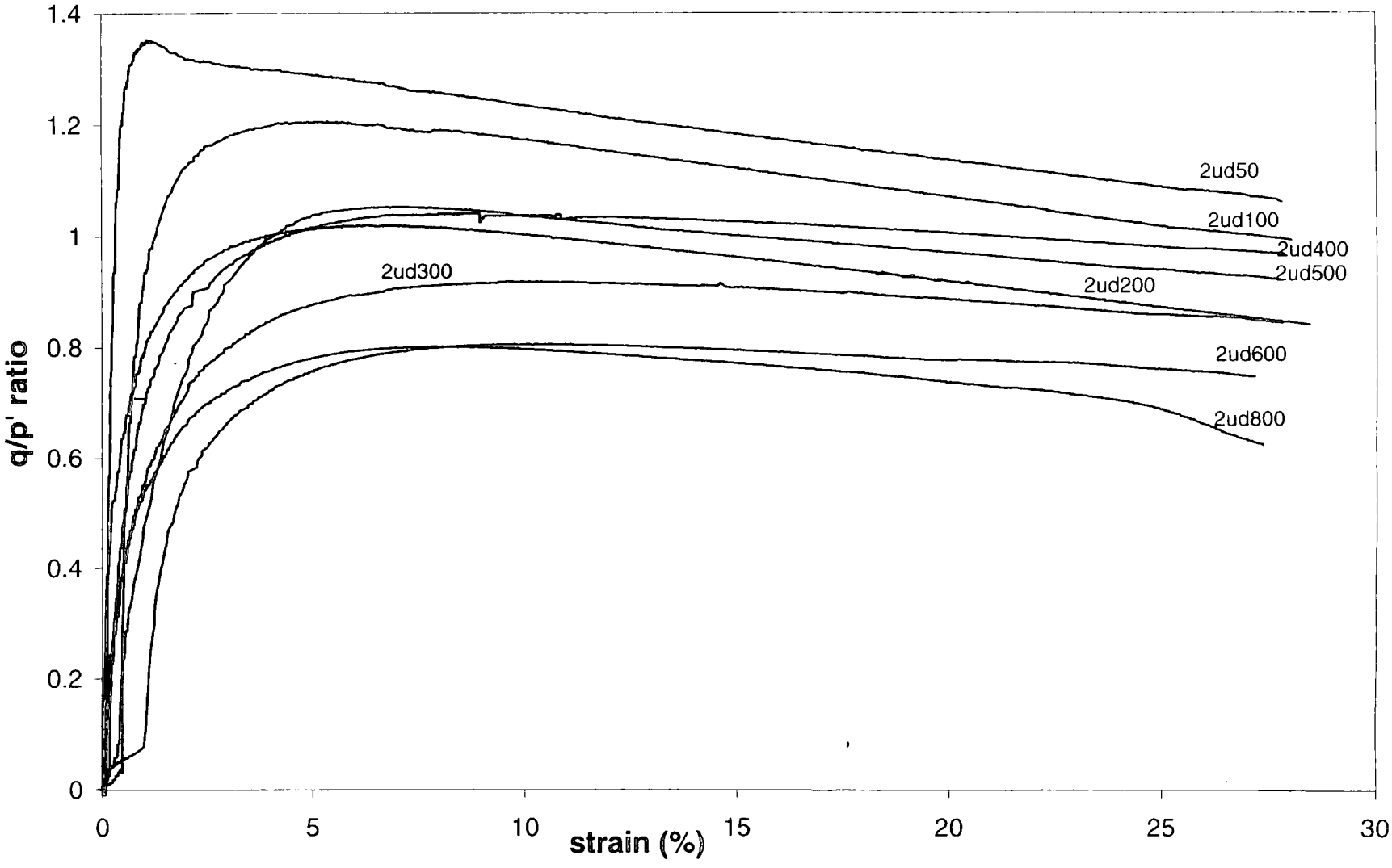

Fig.7.43 q/p' ratio versus axial strain curves of destructured soils of borehole two

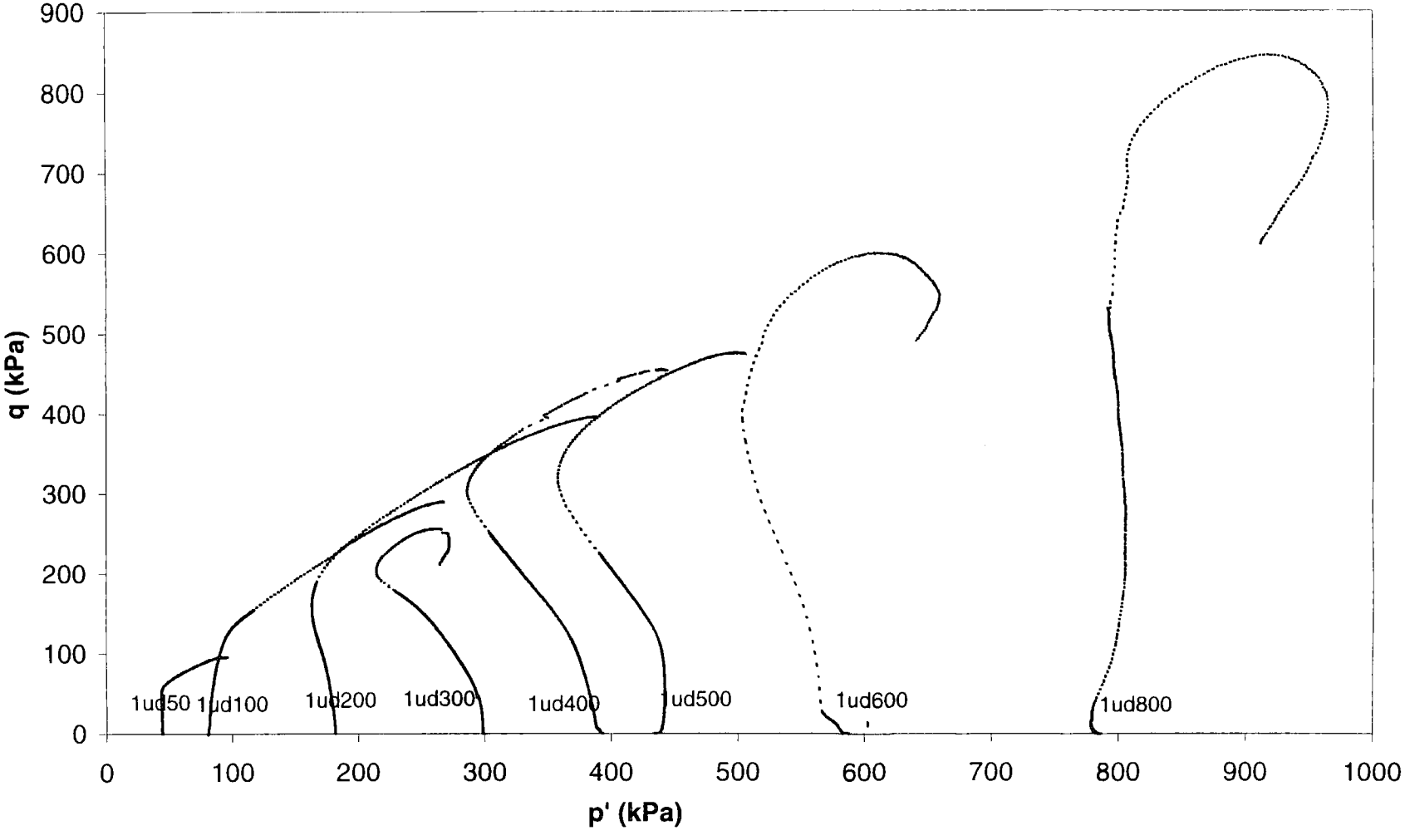

Fig. 7.44 Stress paths derived from a series of triaxial tests on destructured soils of borehole one

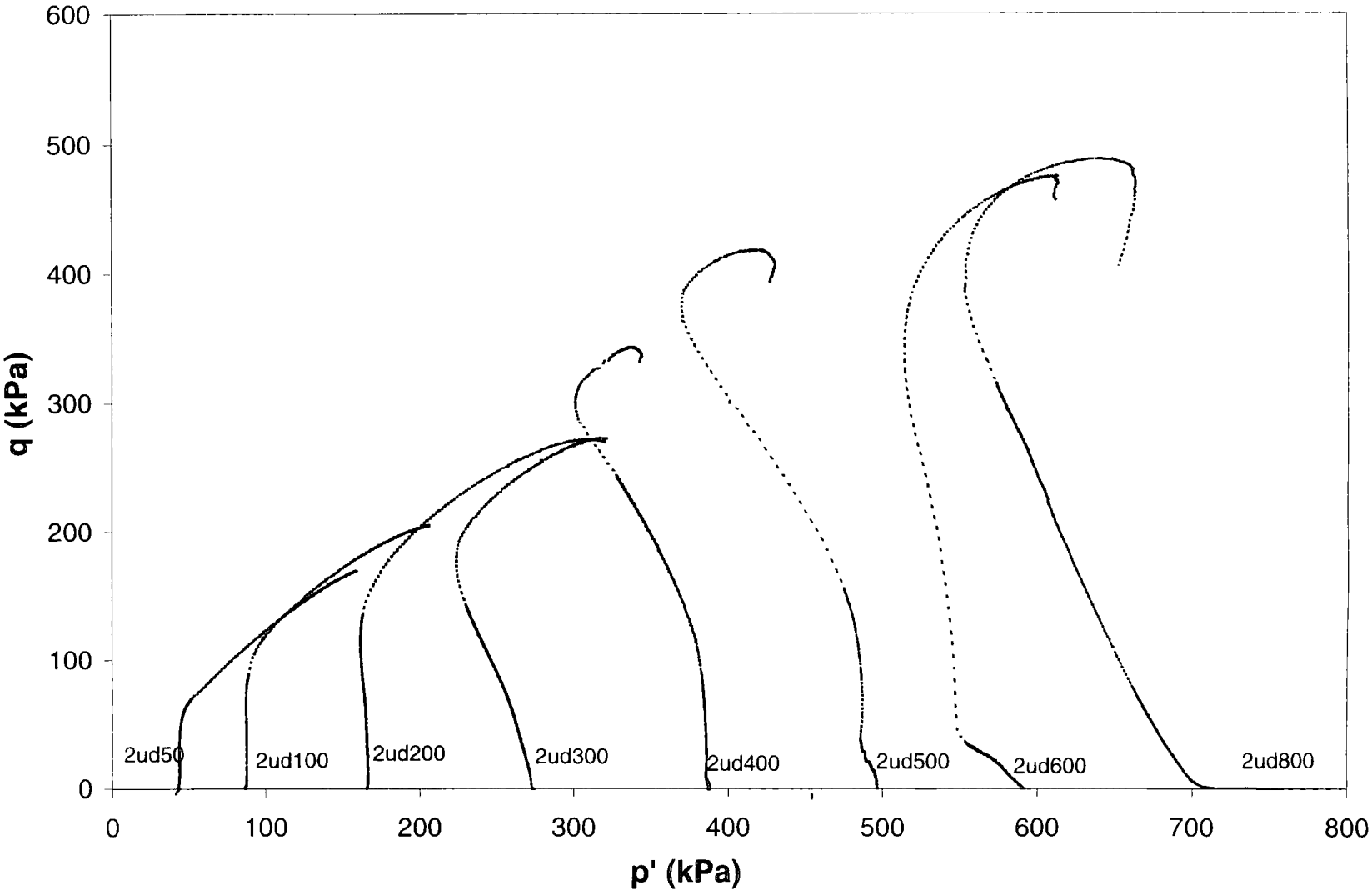

Fig.7.45 Stress paths derived from a series of triaxial tests on destructured samples of borehole two

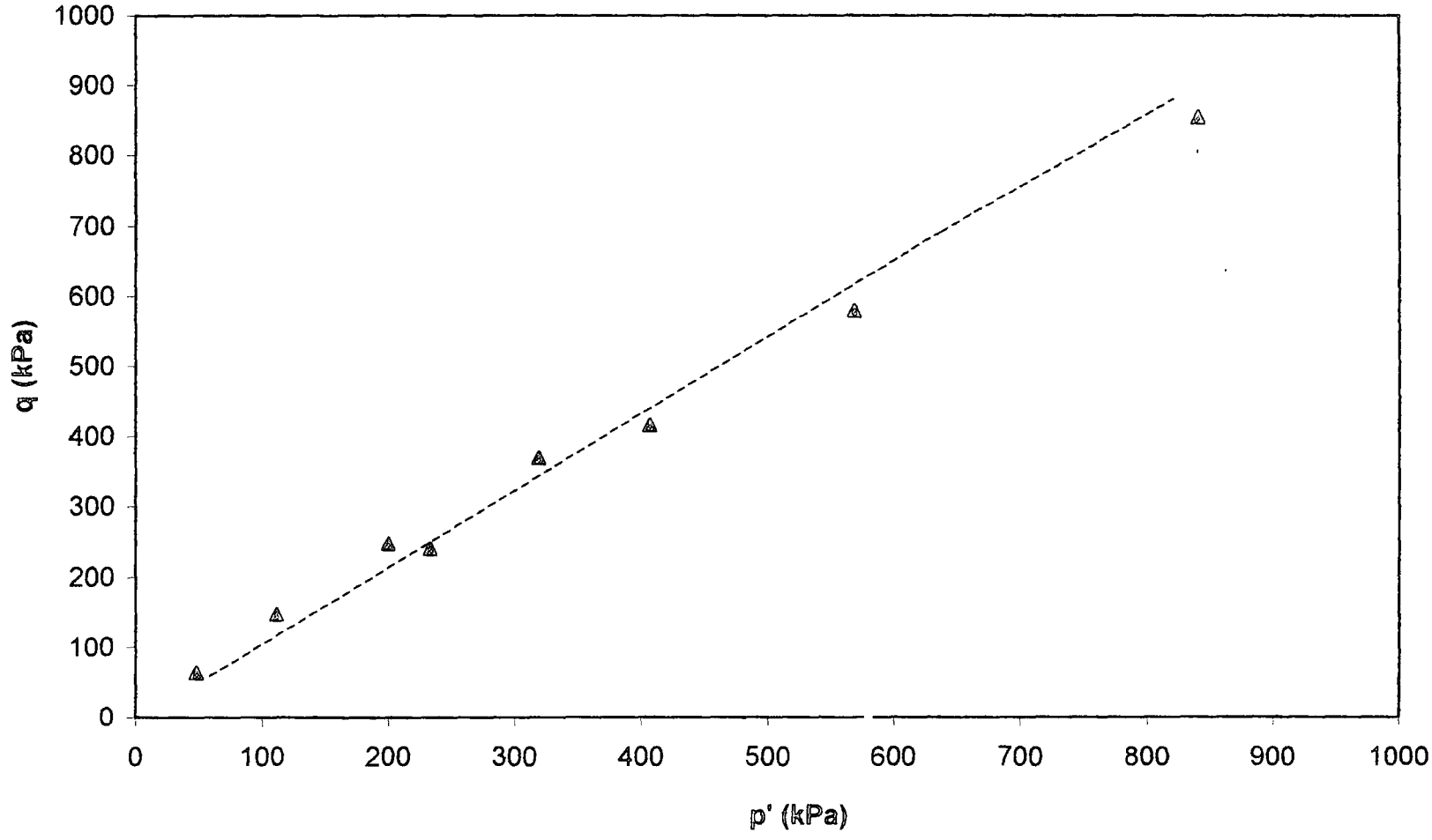

Fig. 7.46 Failure surface for destructured soils of borehole one

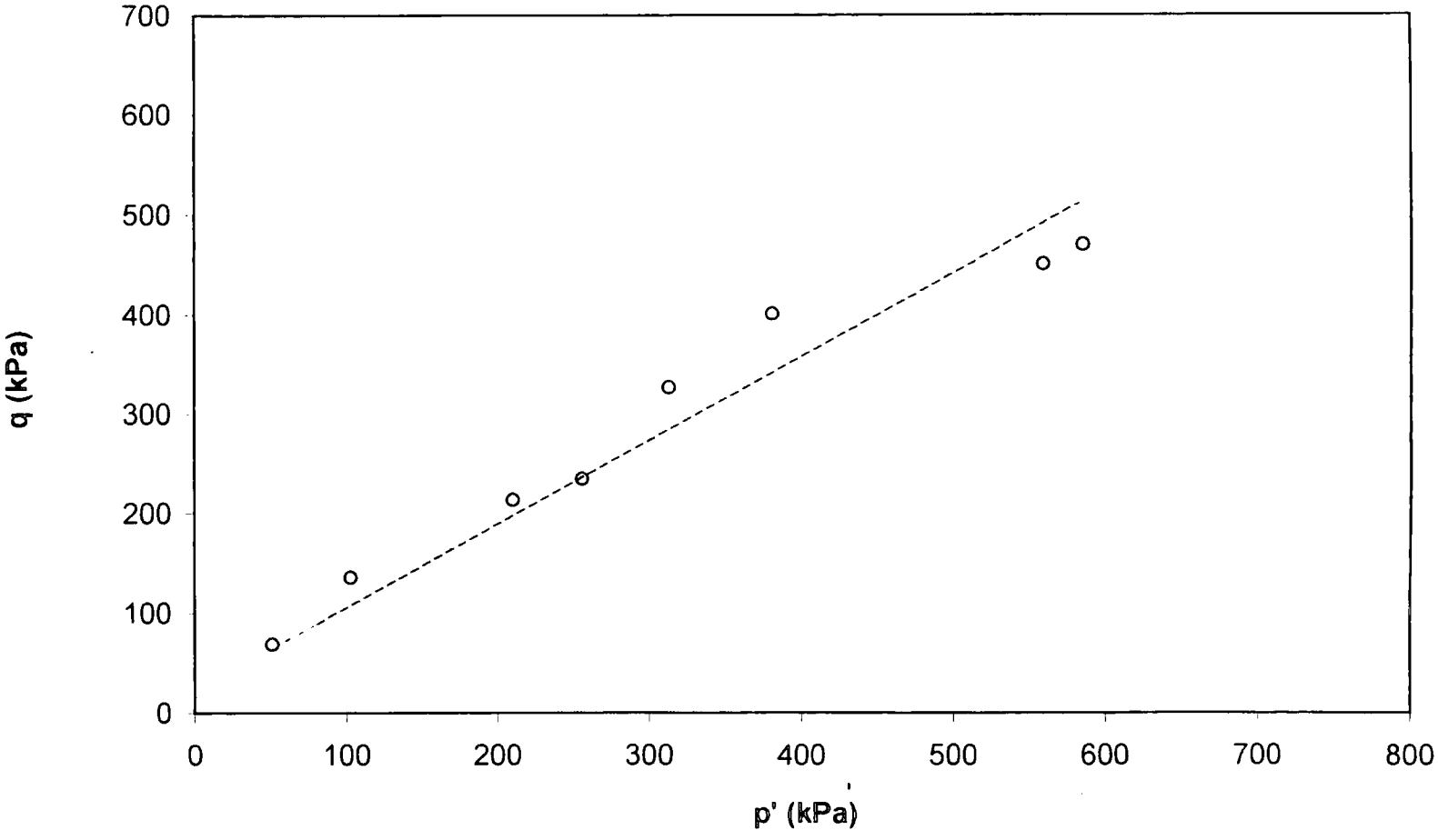

Fig.7.47 Failure surface for destructured soils of borehole two

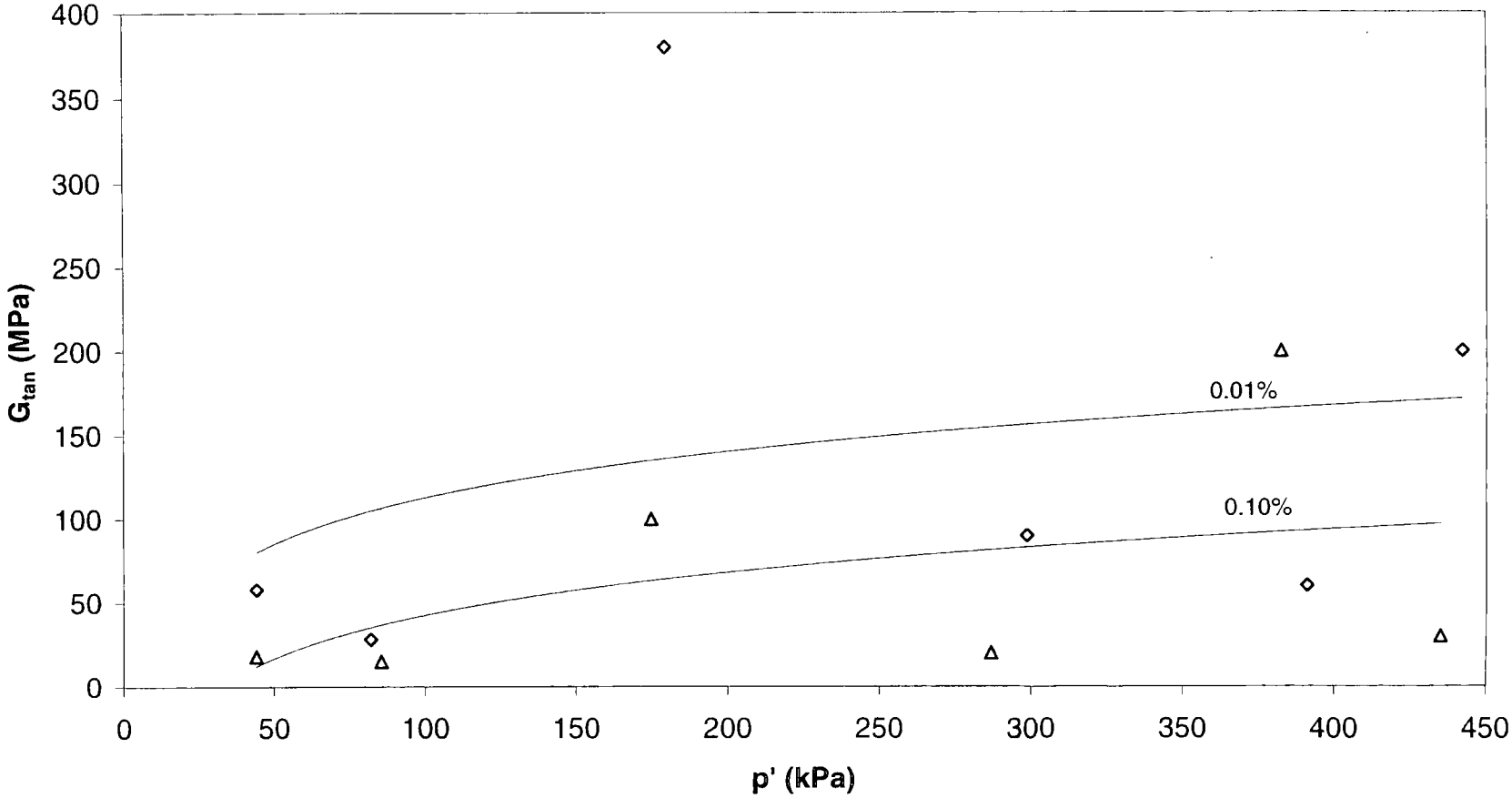

Fig. 7.48 Loss in stiffness with increasing strain from 0.01% to 0.1% strain for destructured soils of borehole one

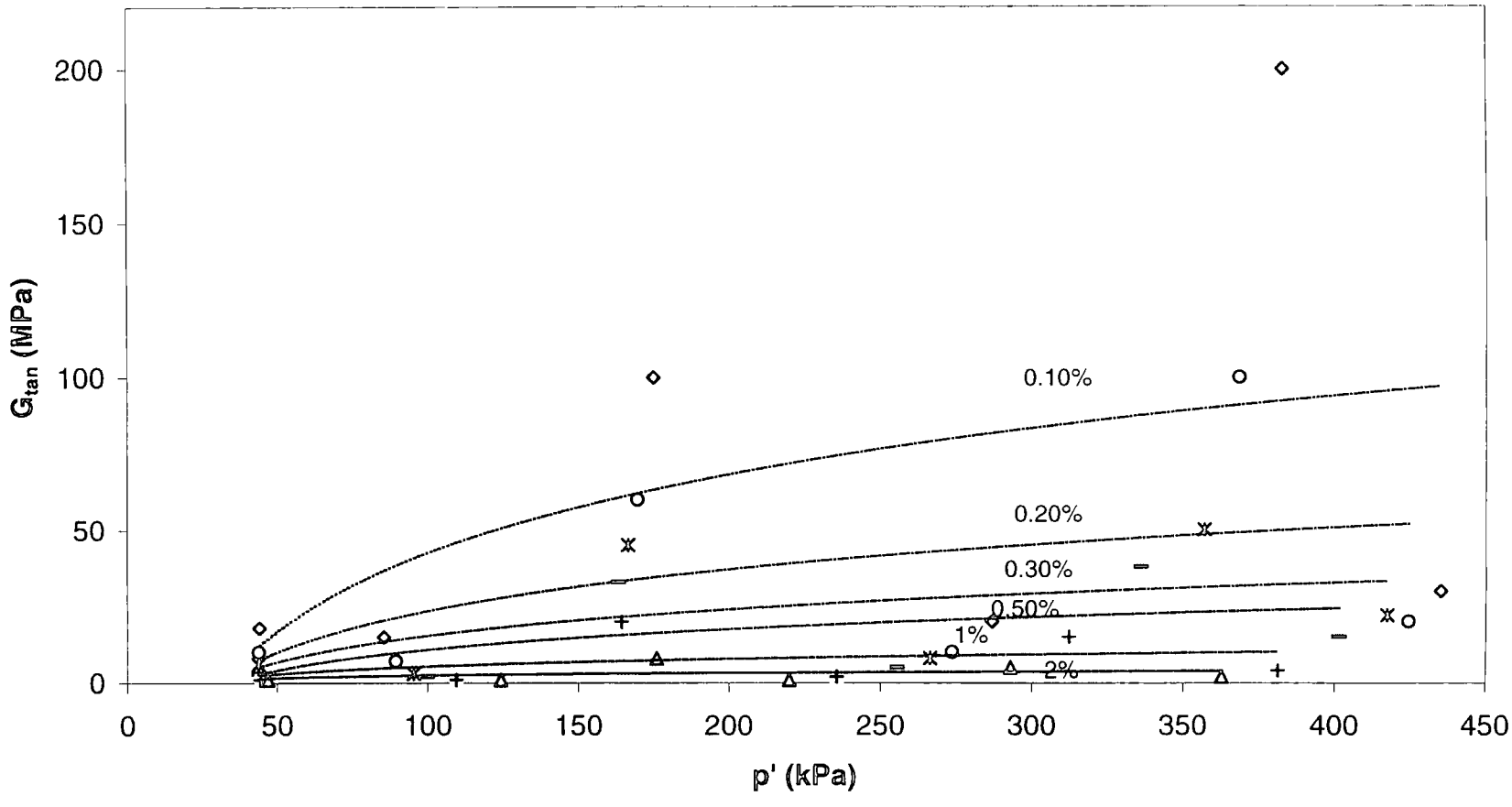

Fig.7. 49 Loss in stiffness with increasing strain from 0.1% to 2% strain for destructured soils of borehole one

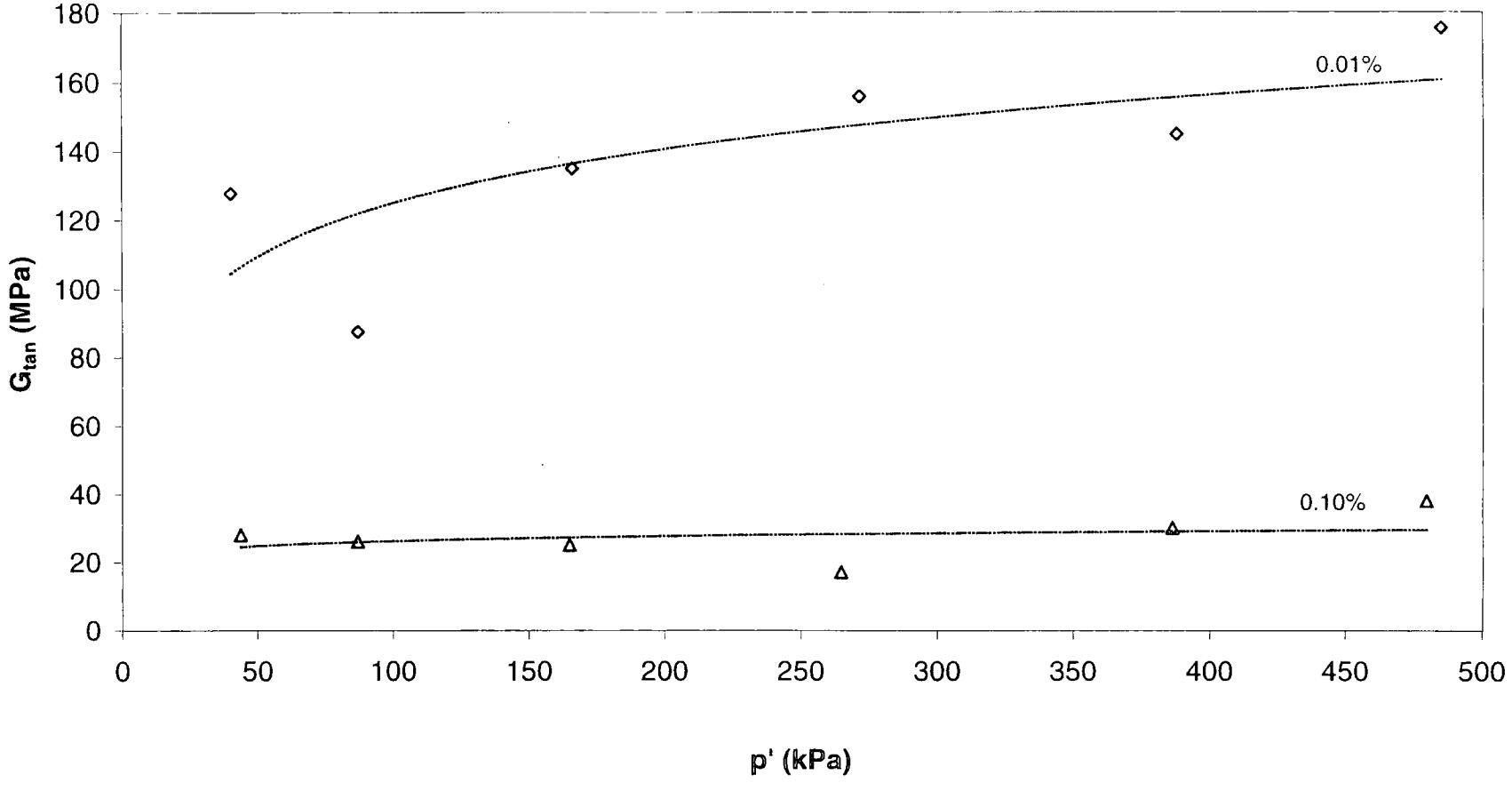

Fig.7.50 Loss of stiffness with increasing strain (0.01%-0.1%) for destructured soils of borehole two

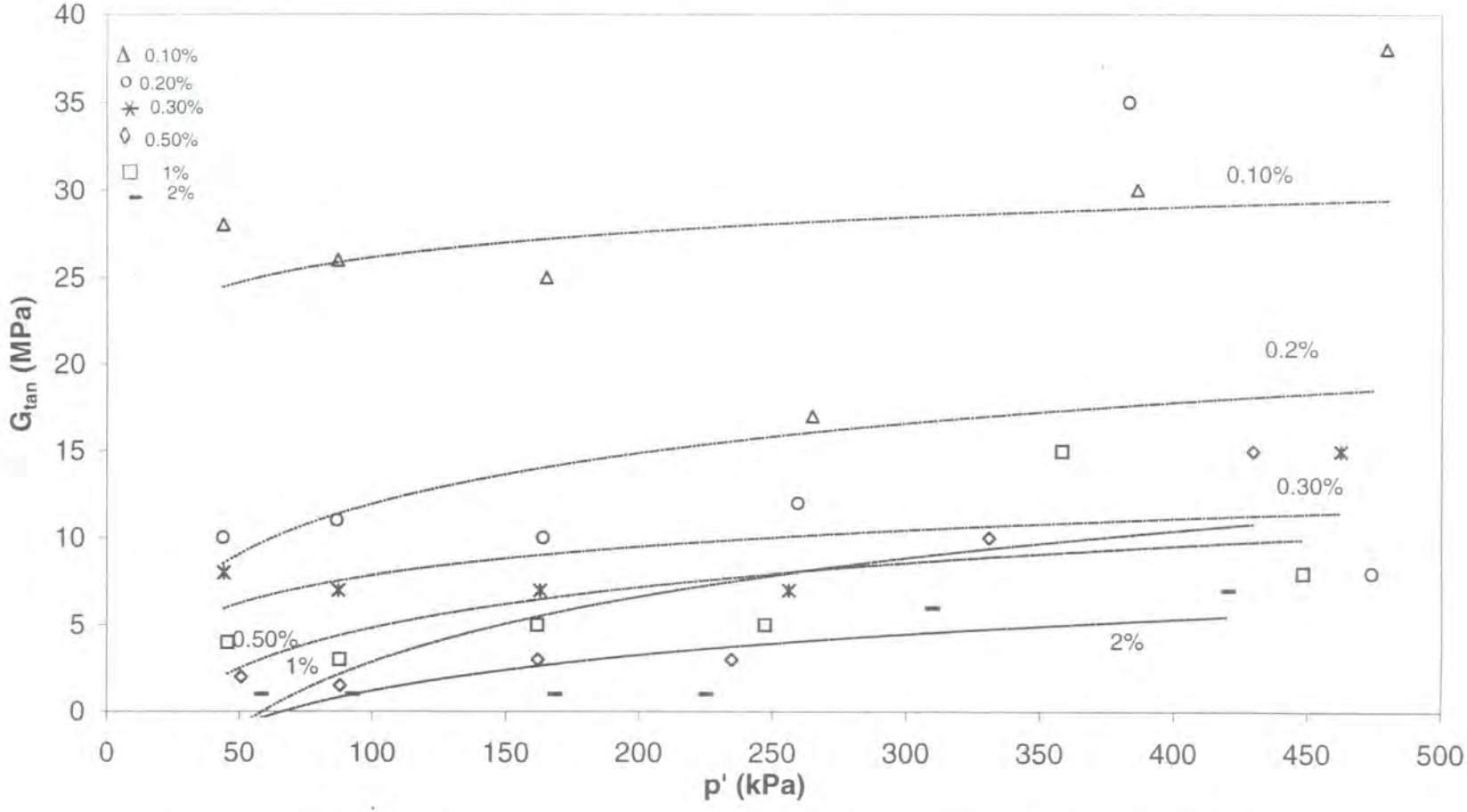

Fig.7.5*1* Loss of stiffness with increasing strain (0.1% to,2% strain) for destructured soils of borehole two

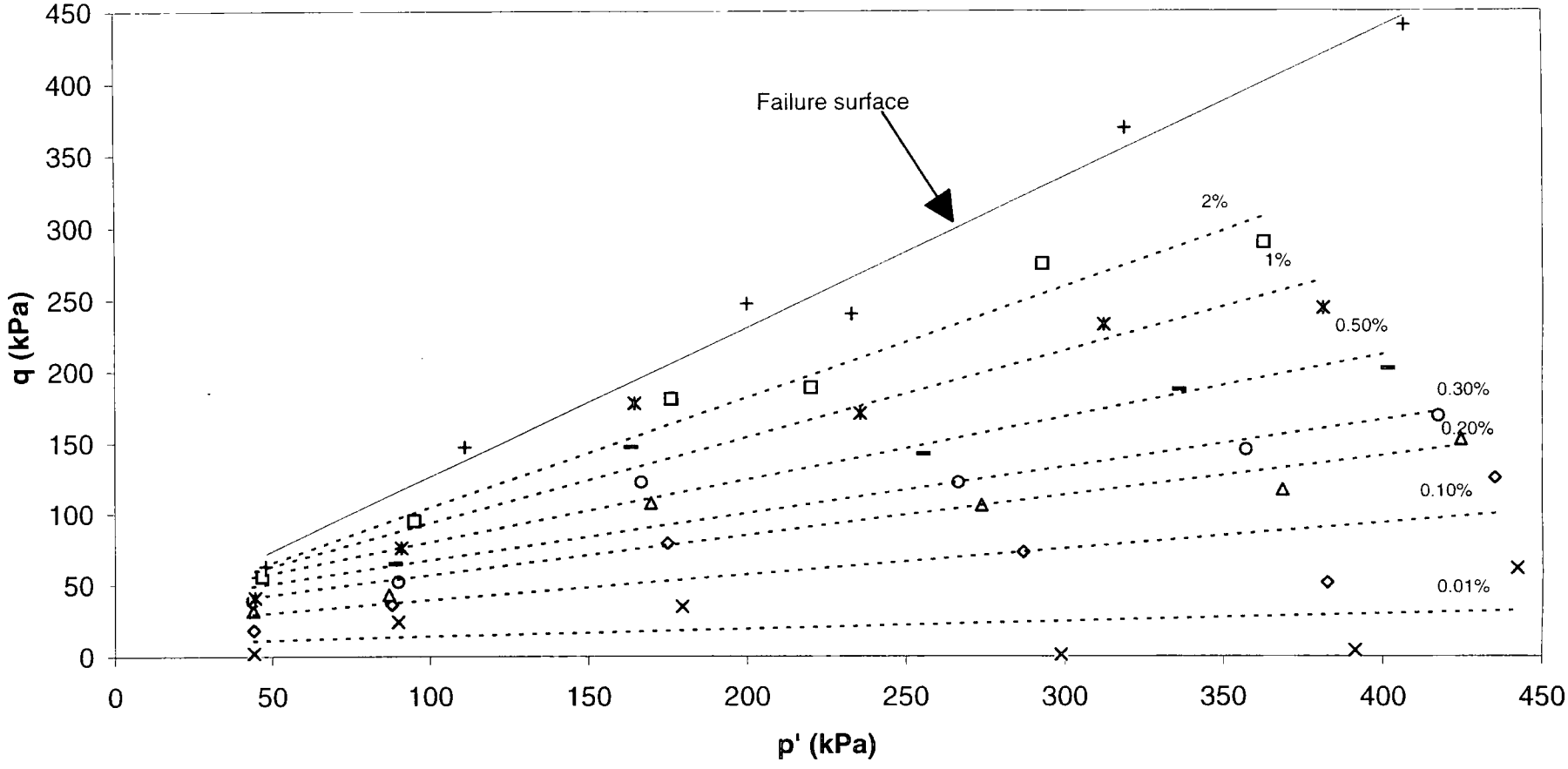

Fig. 7.52 Failure surface and strain contours (up to 2%) for the destructured soils of borehole one

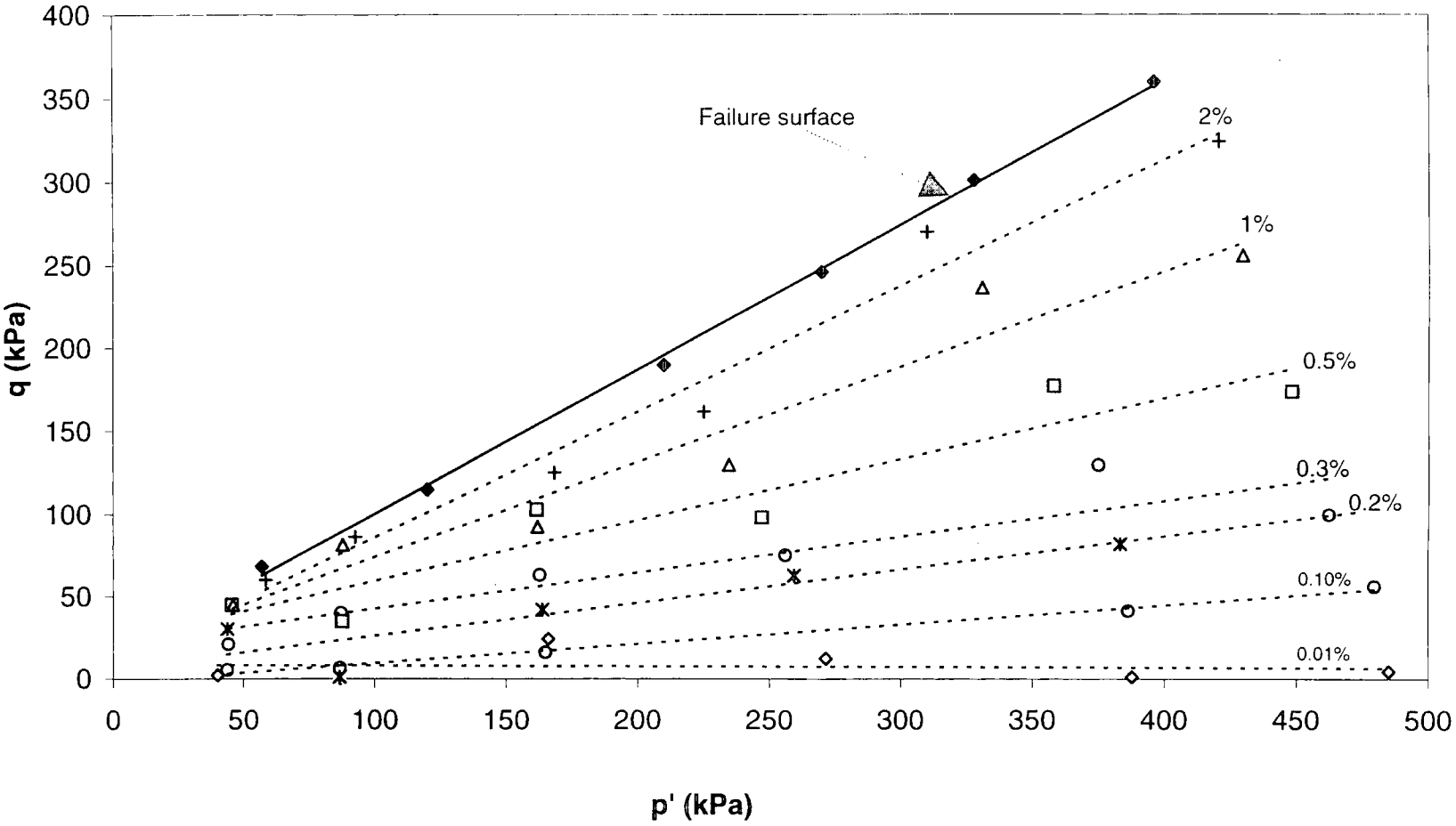

Fig.7.53 Failure surface & strain contours (up to 2%) for destructured soils of borehole two

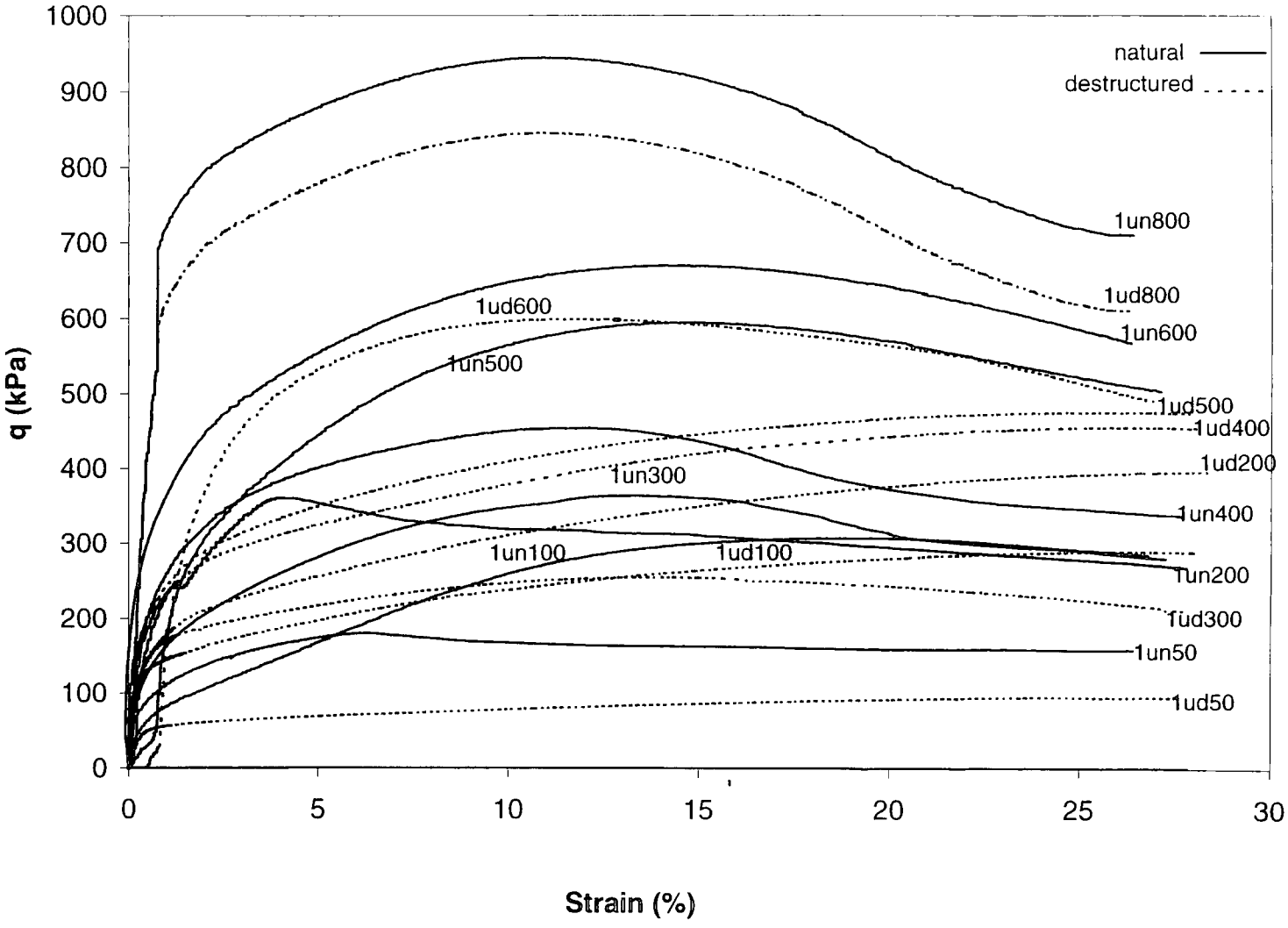

Fig.7.54 Comparison of deviator stress versus axial strain curves for natural & destructured soils of borehole one

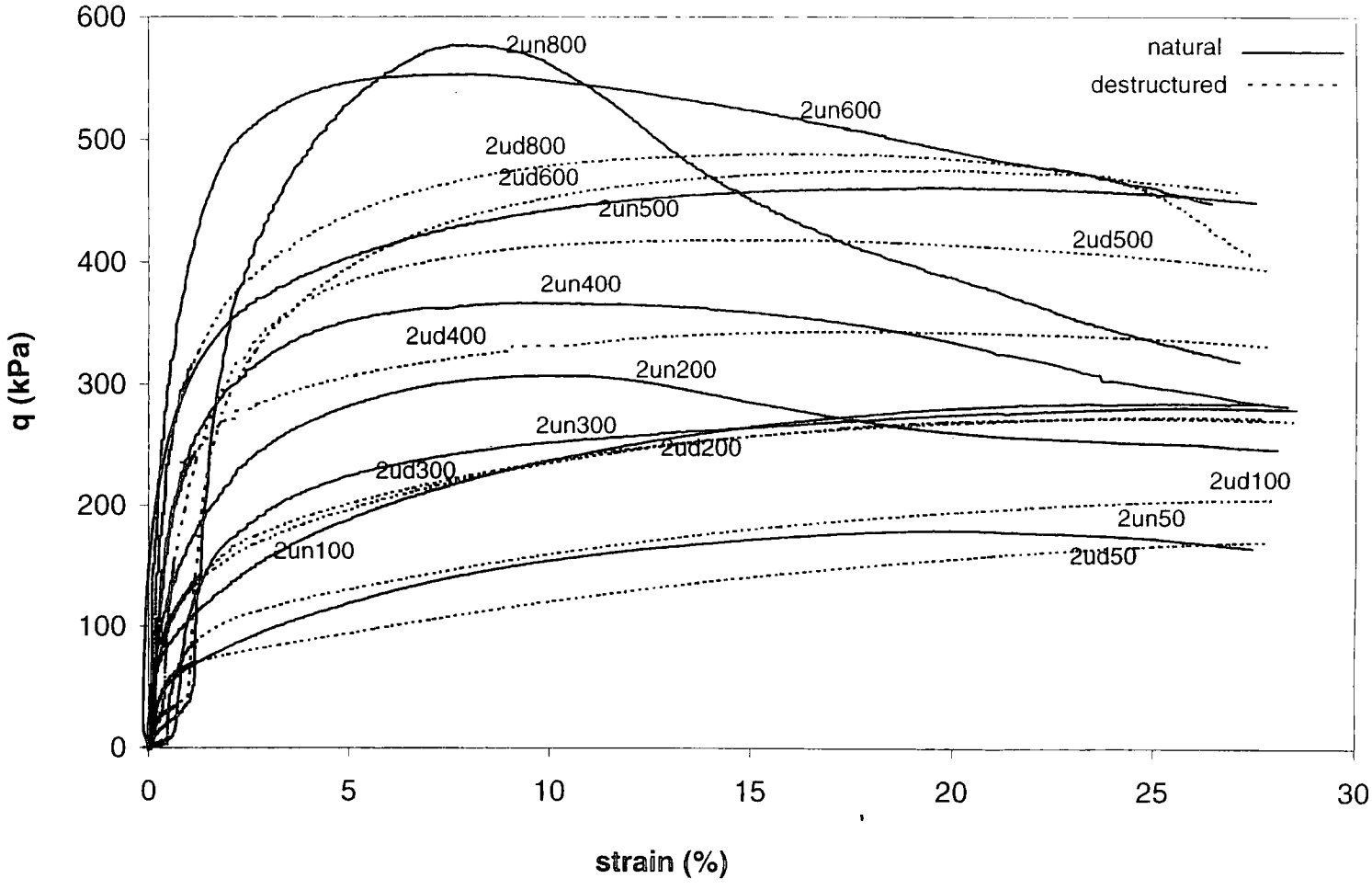

Fig.7.55 Comparison of deviator stress versus axial strain curves for natural & destructured soils of borehole two

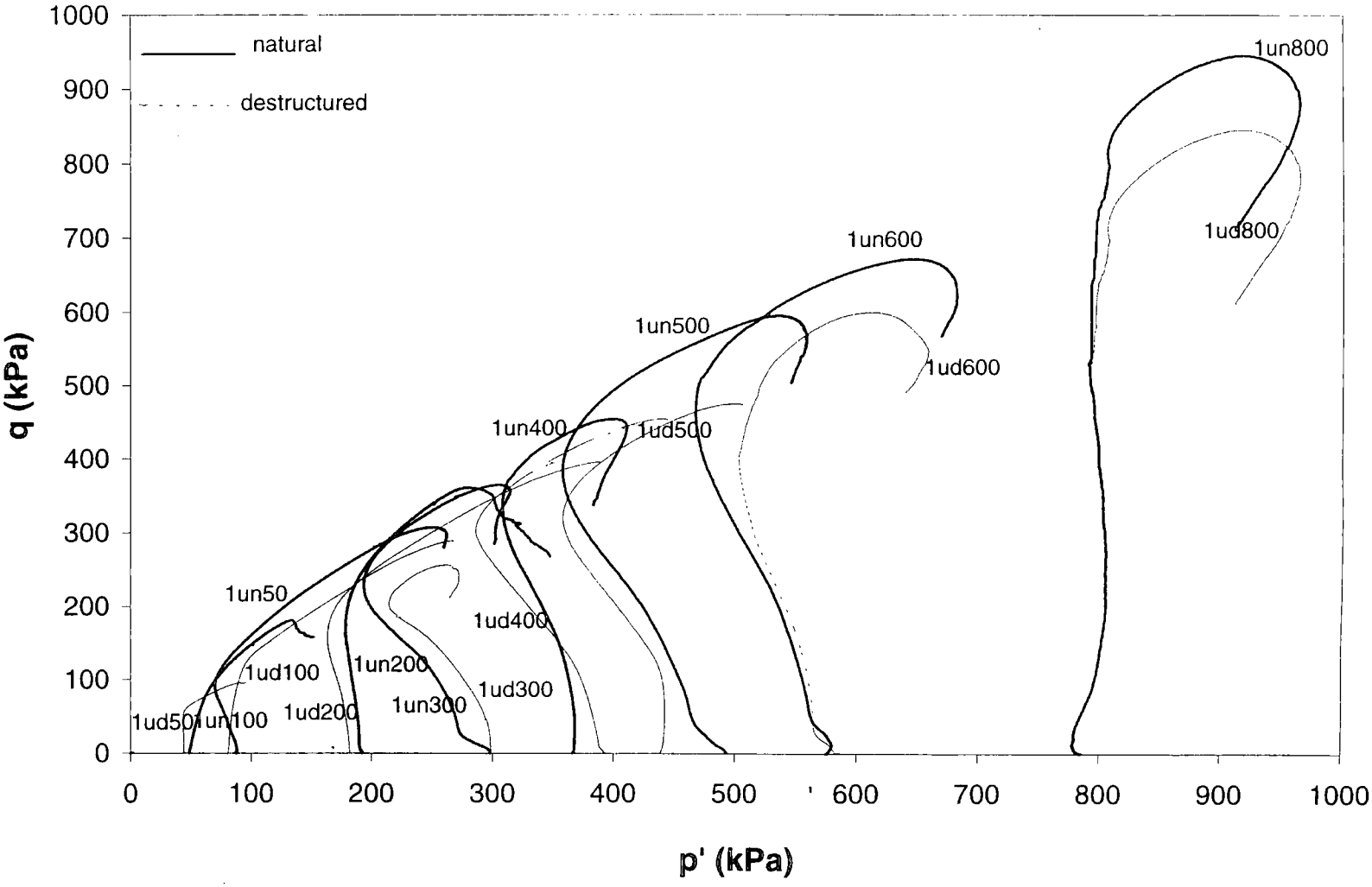

Fig.7.56 Comparison of Stress paths derived from a series of triaxial tests on natural & destructured soils of borehole one

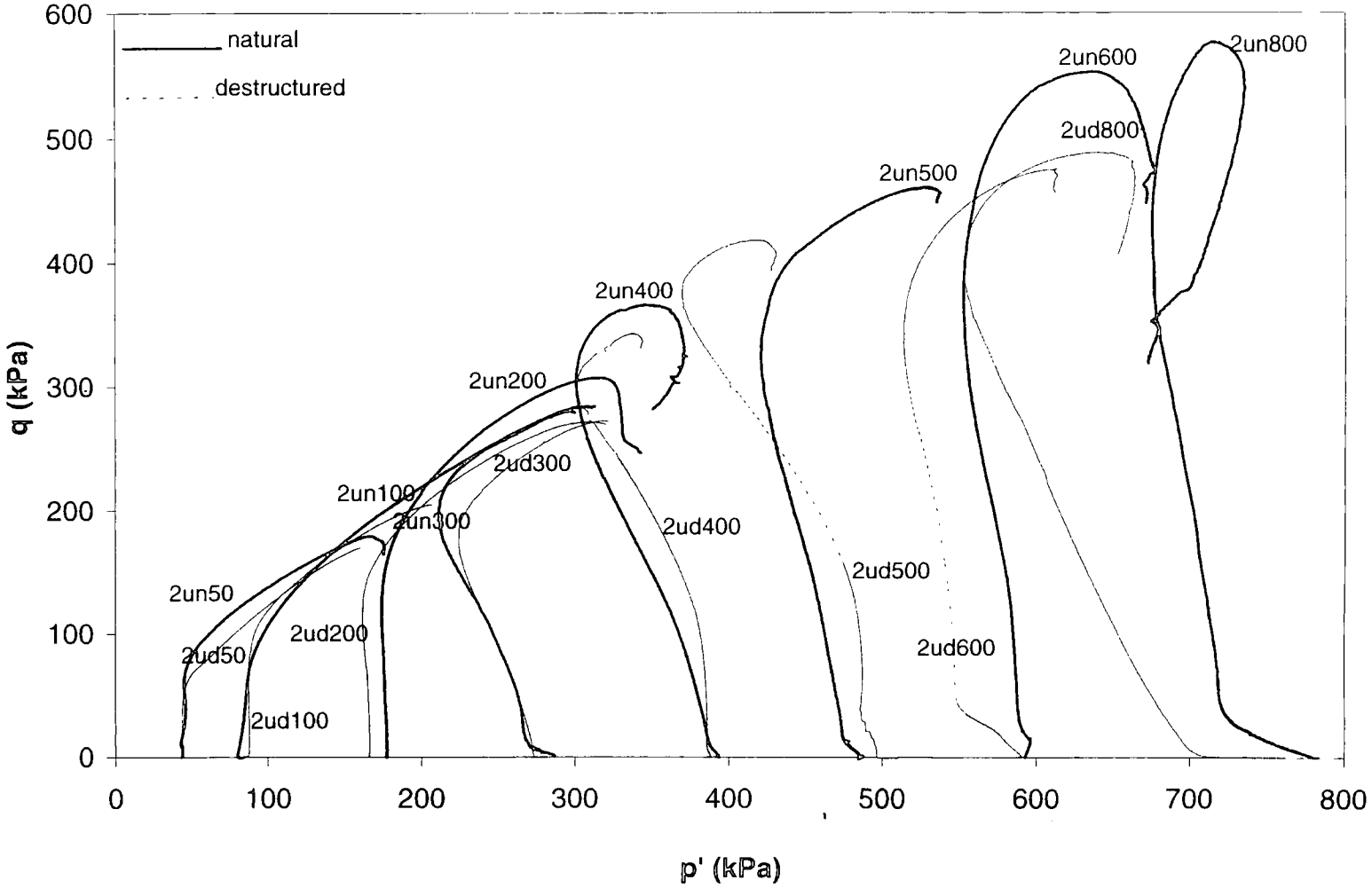

Fig.7.57 Comparison of stress paths derived from a series of triaxial tests on natural & destructured samples of borehole two

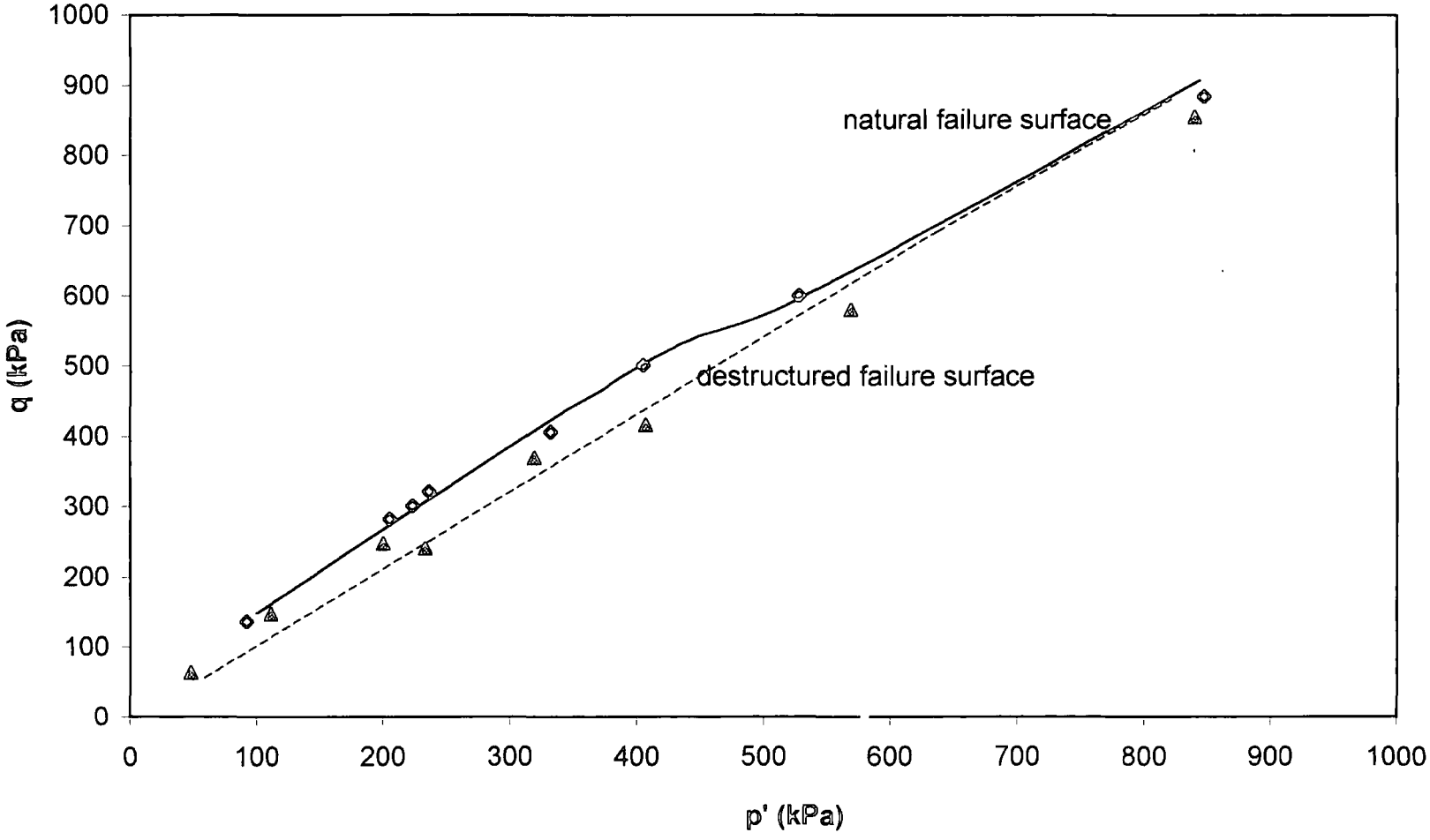

Fig. 7.58 Comparison of failure surfaces for natural and destructured soils of borehole one

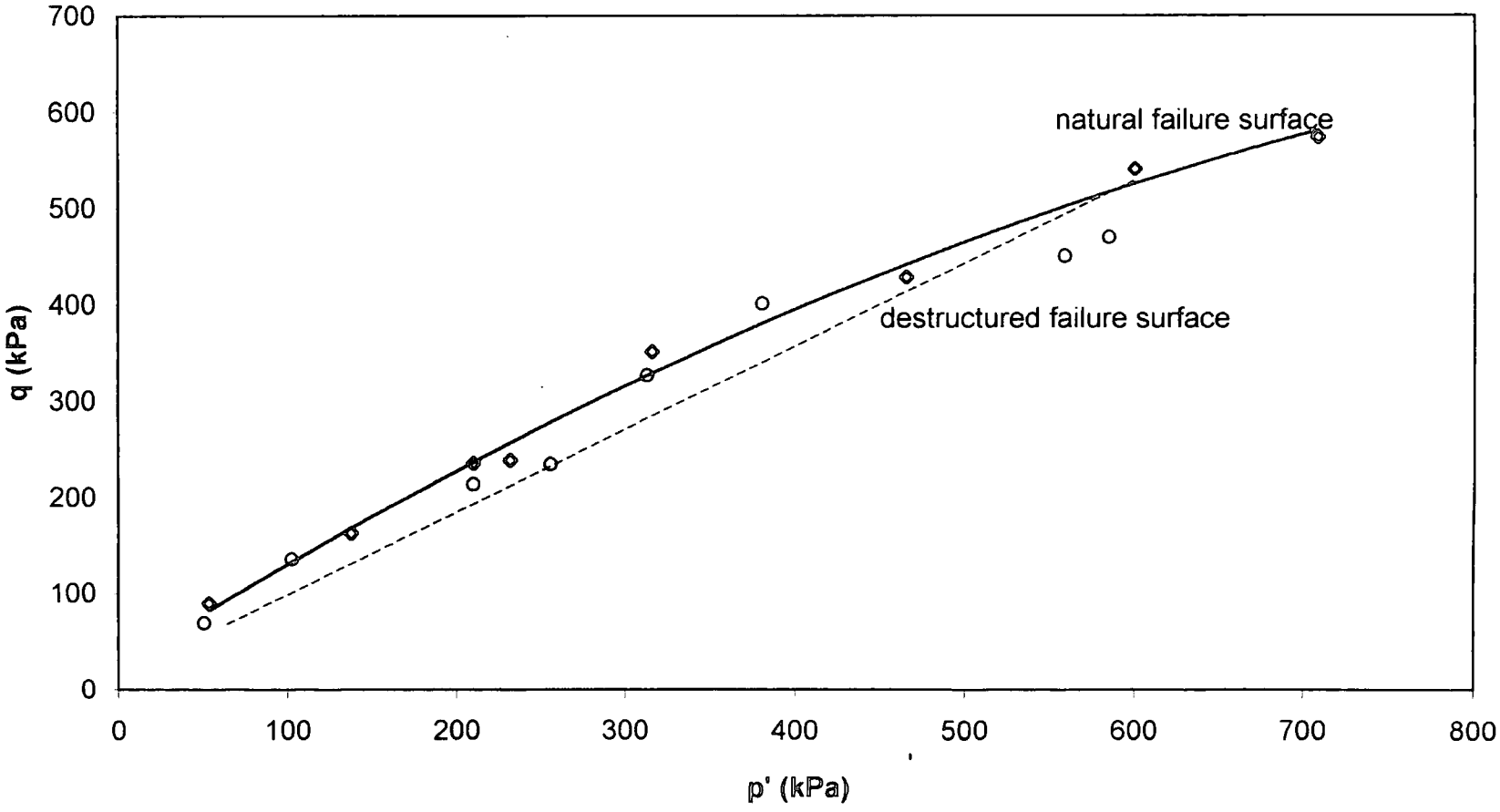

Fig.7.59 Comparison of failure surfaces for natural and destructured soils of borehole two

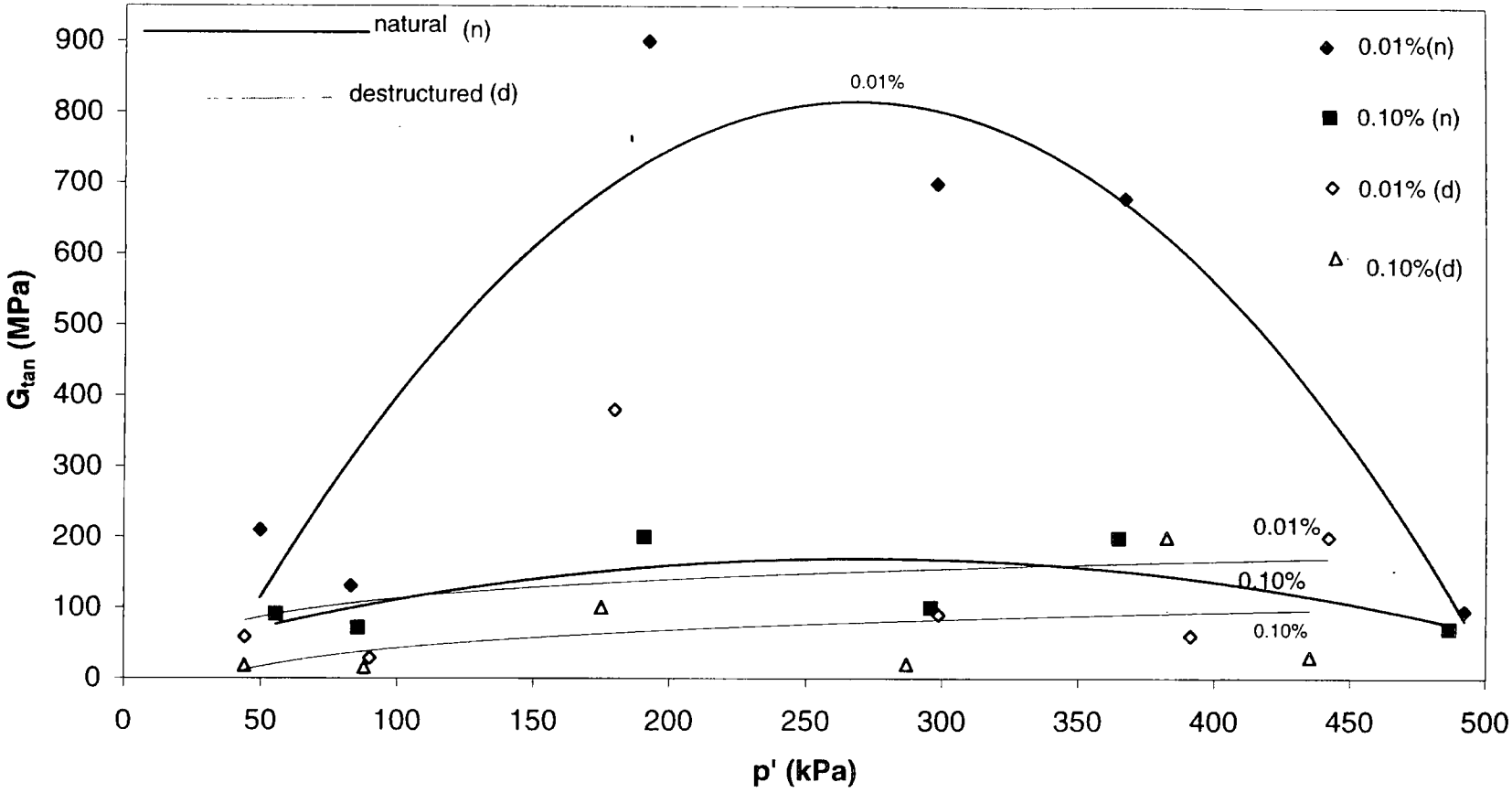

Fig.7.60 Comparison between stiffness values with increasing strain from 0.01% to 0.1% strain for natural & destructured soils of borehole one

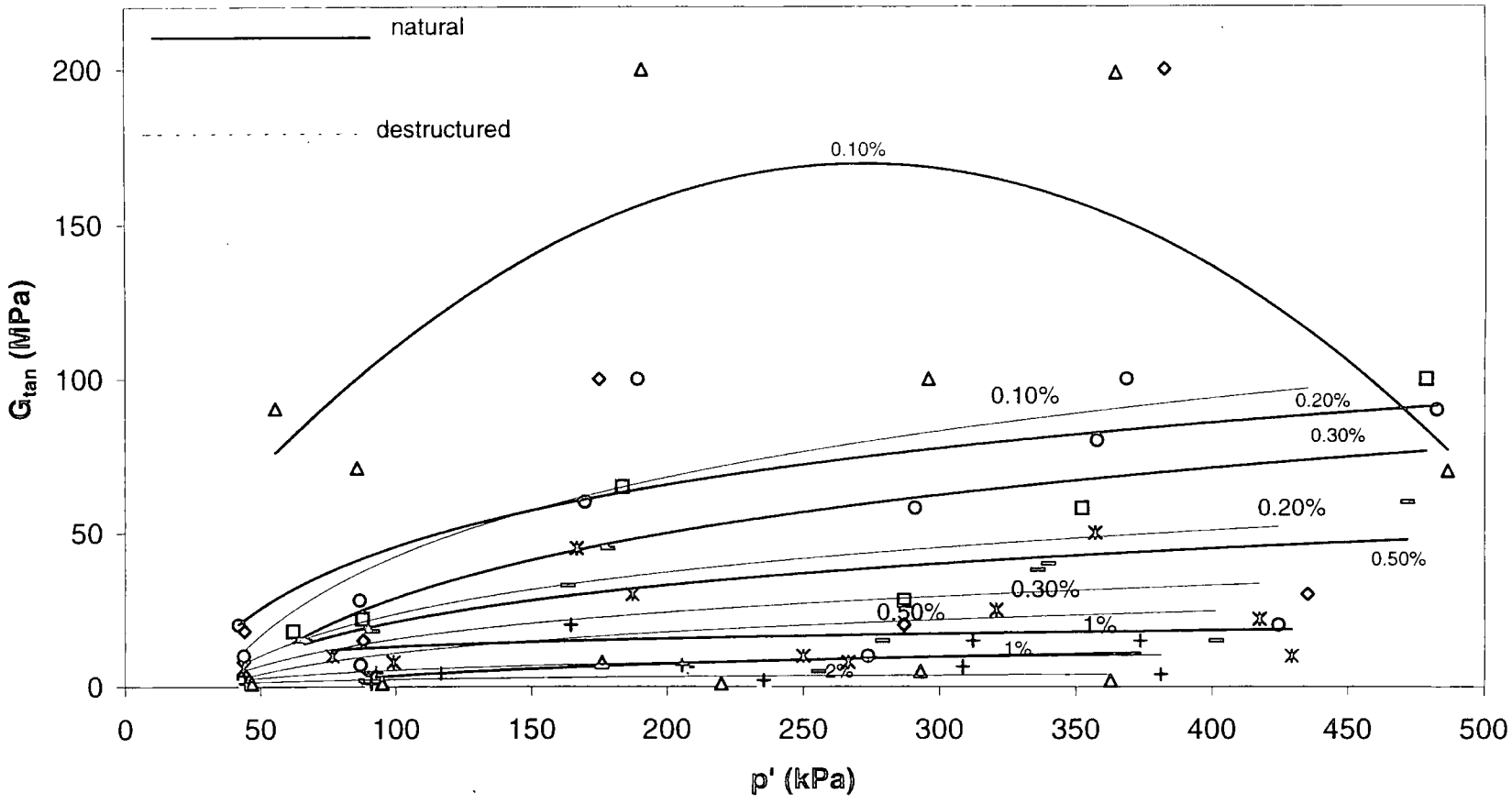

Fig.7.61 Comparison between stiffness with increasing strain from 0.1% to 2% strain for natural & destructured soils of borehole one

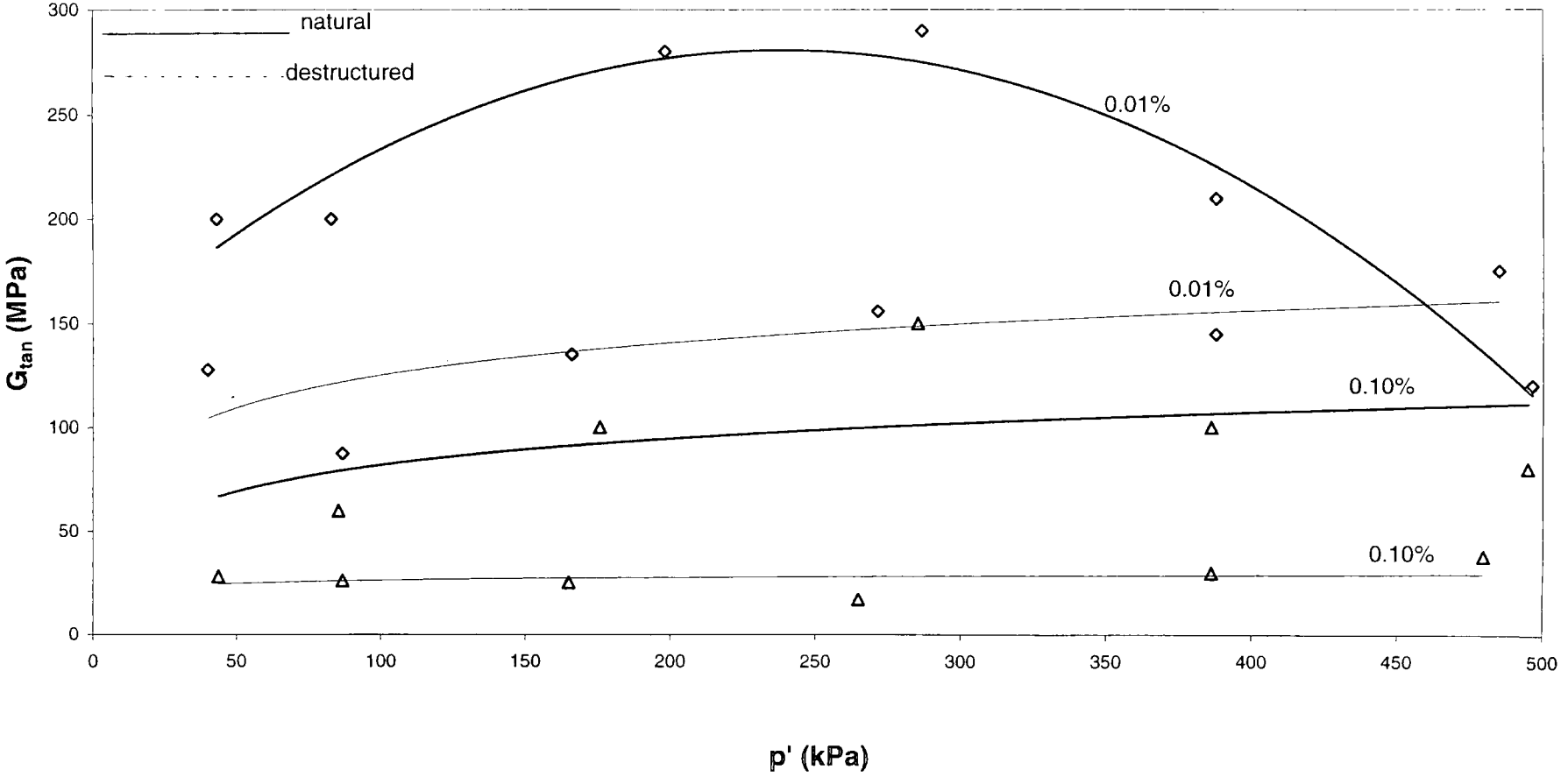

Fig.7.62 Comparison between stiffness versus strain (0.01%-0.1%) for natural and destructured soils of borehole two

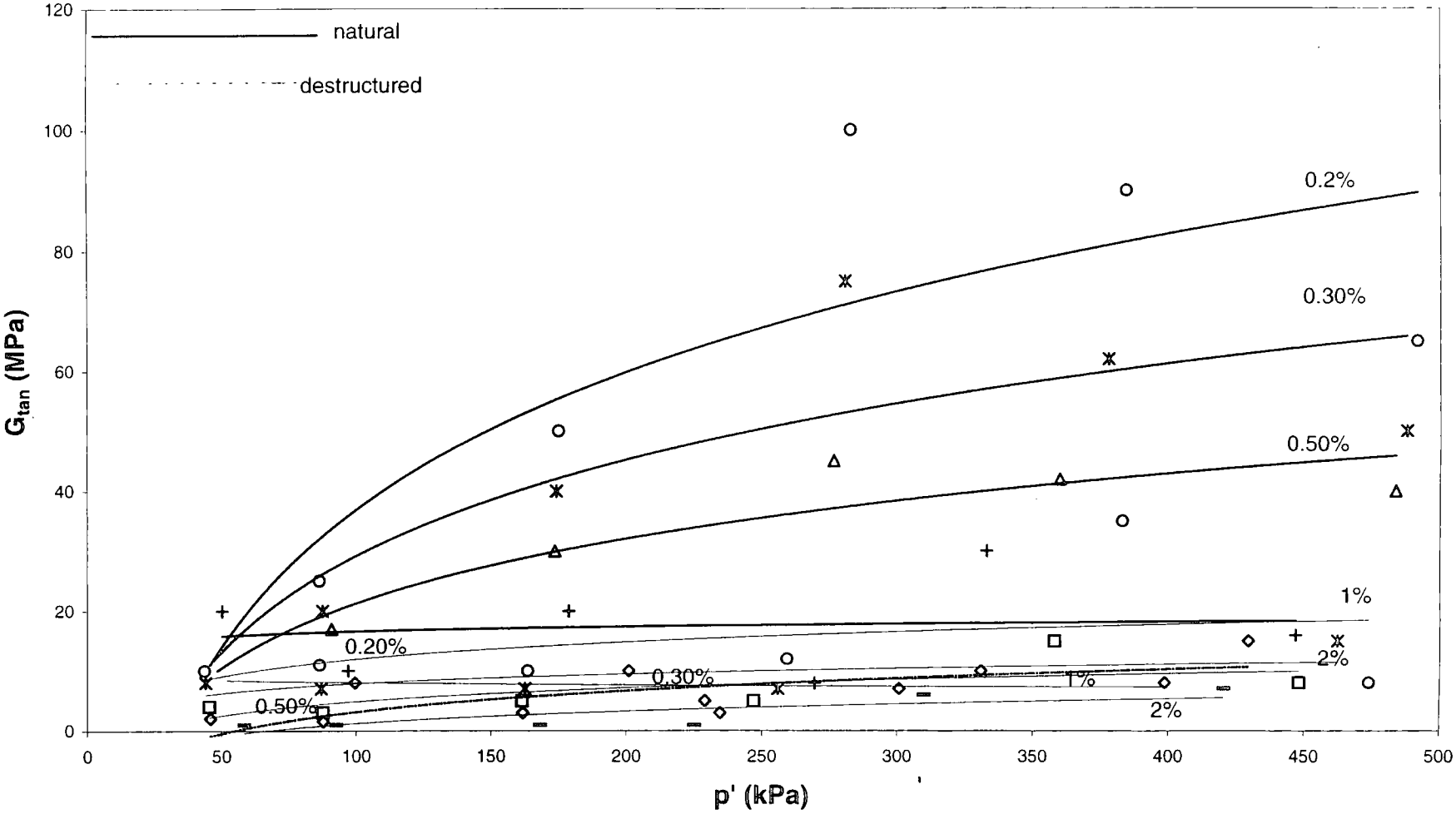

Fig.7.63 Comparison between stiffness versus strain (0.2% to 2% strain) for natural and destructured soils of borehole two

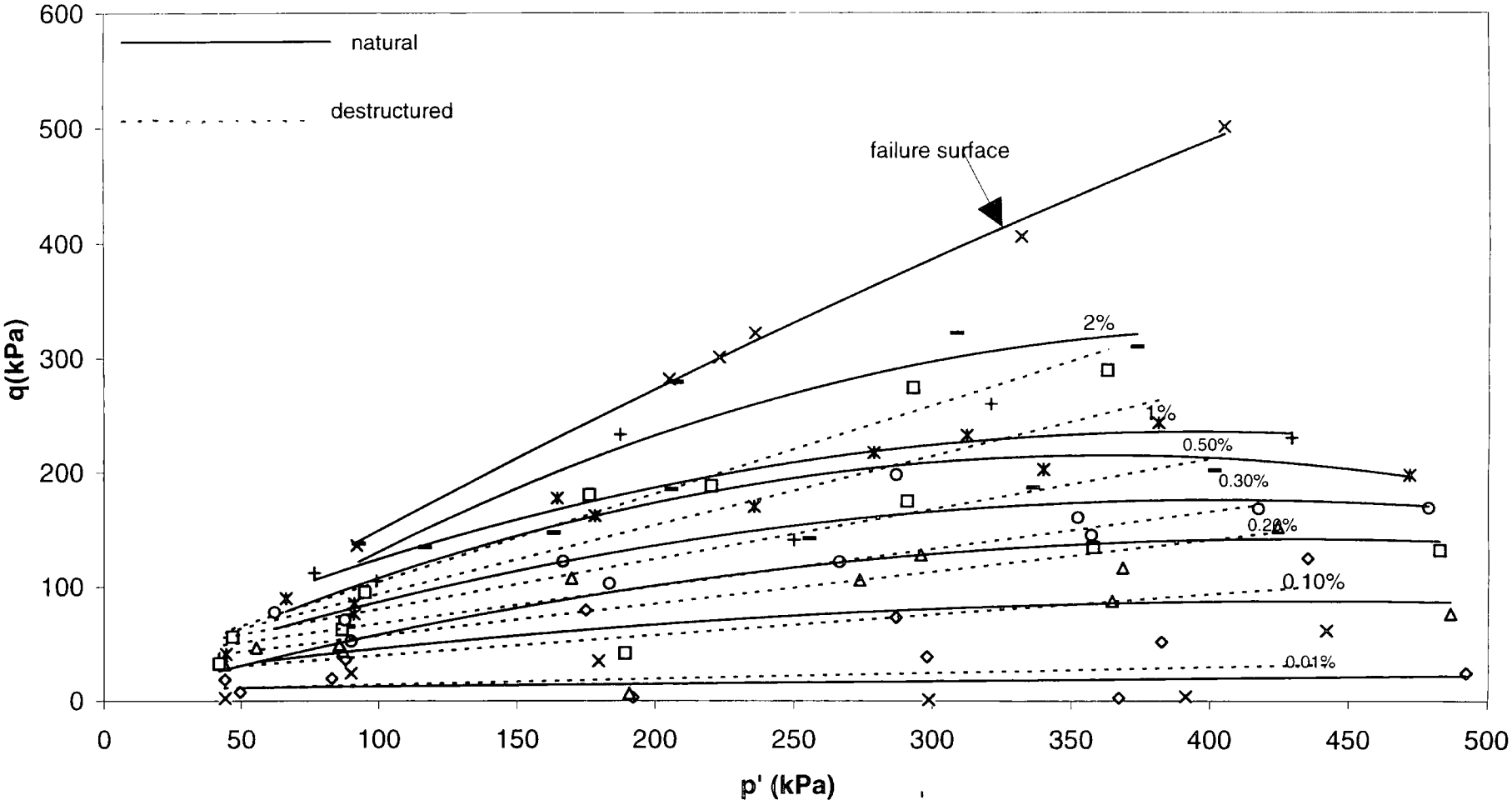

Fig.7.64 Comparison between strain contours (up to 2% strain) for the natural & destructured soils of borehole one

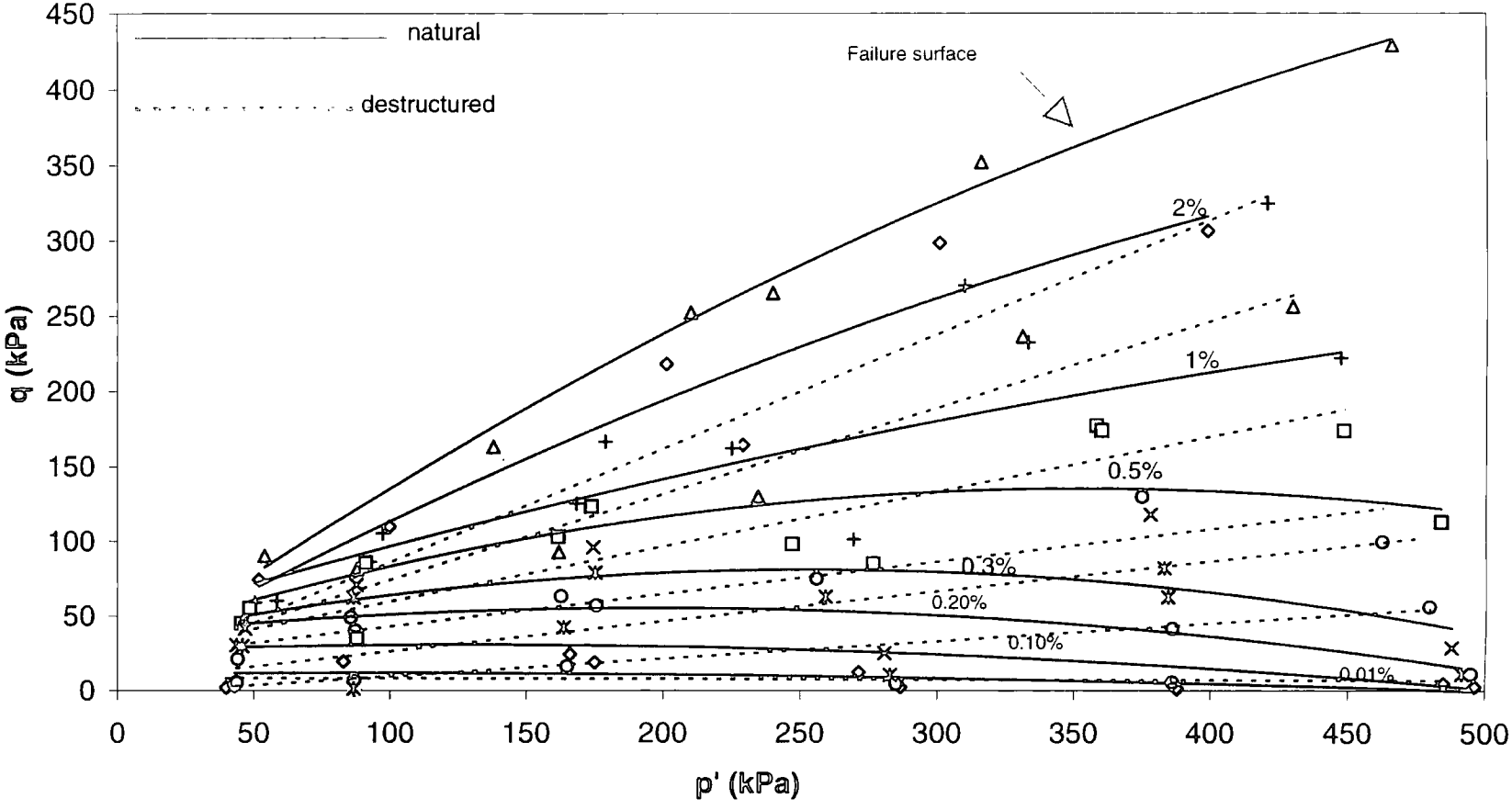

Fig.7.65 Comparison between strain contours (from 0.01% to 2%) for natural & destructured soils of borehole two

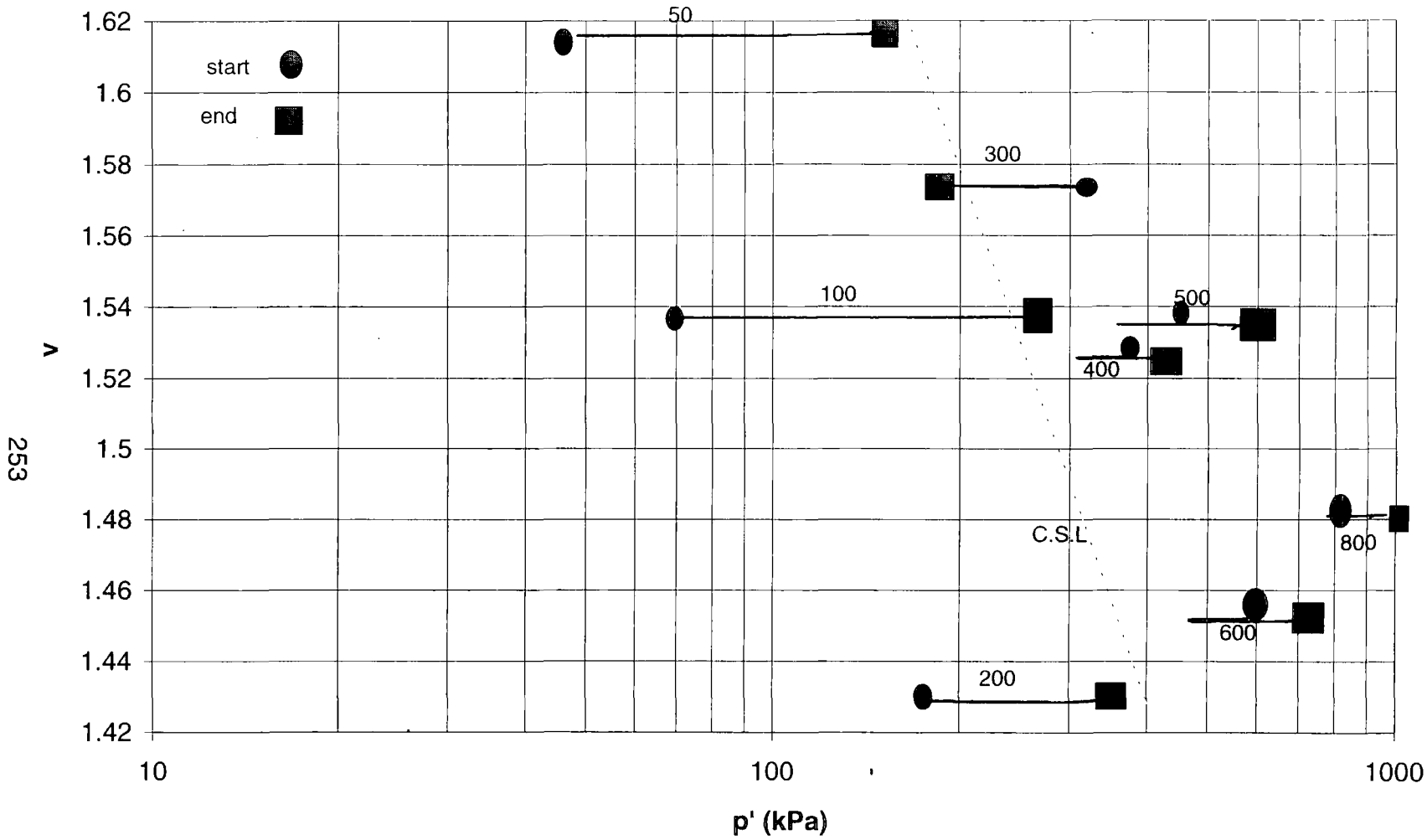

Fig.7.66 Specific volume vs. p' for natural soils of borehole one

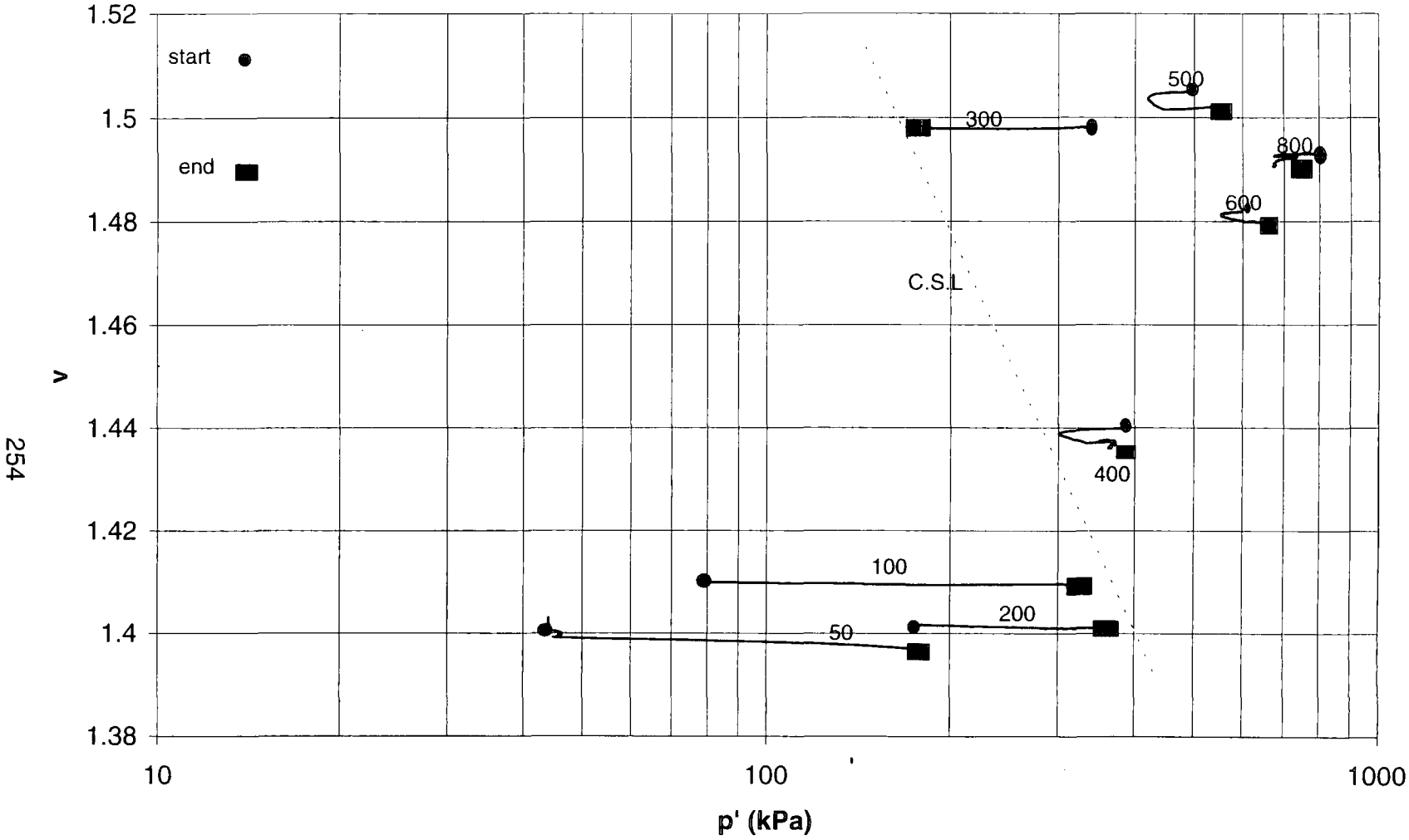

Fig.7.67 Specific volume vs. p' for natural soils of borehole two

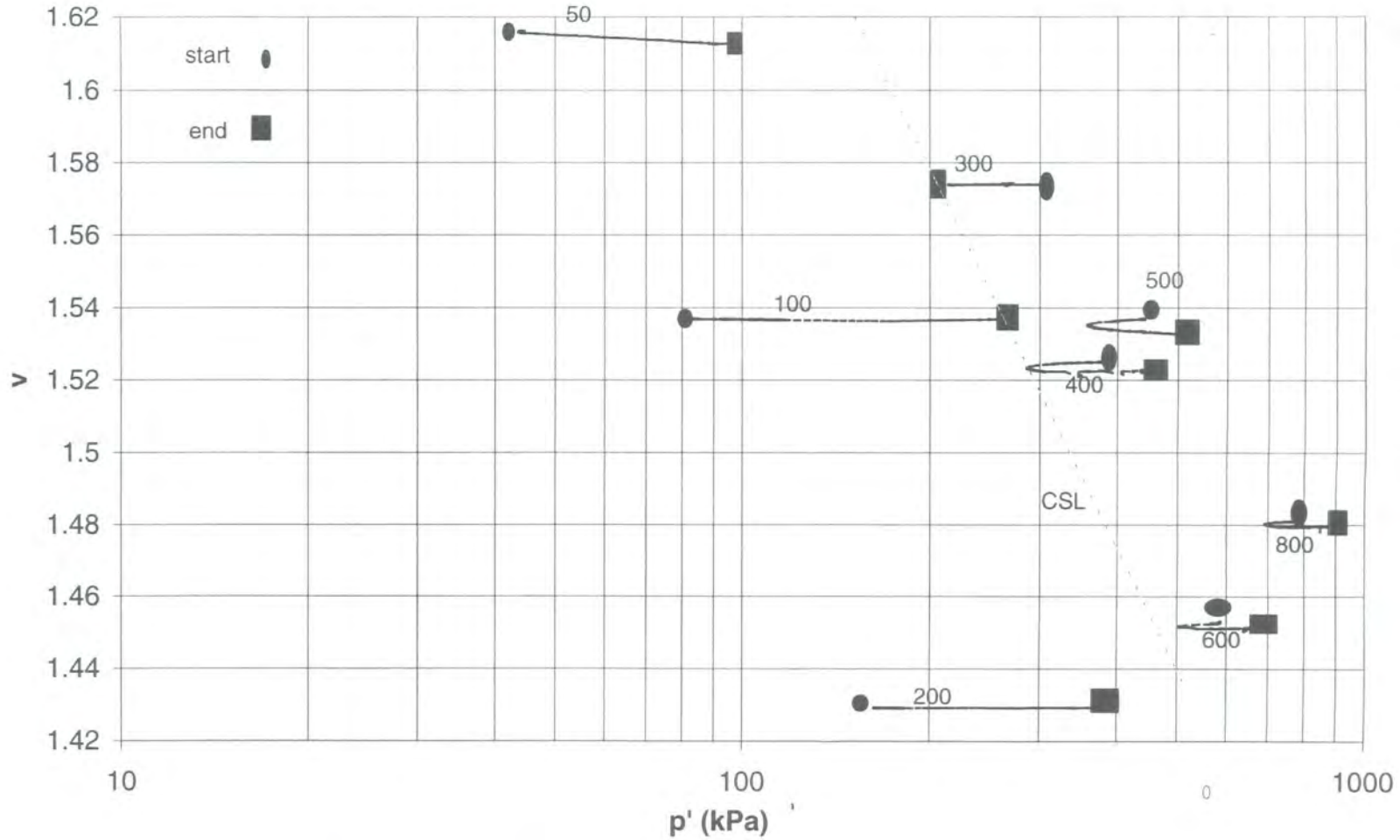

Fig.7.68 Specific volume vs. p' for destructured soils of borehole one

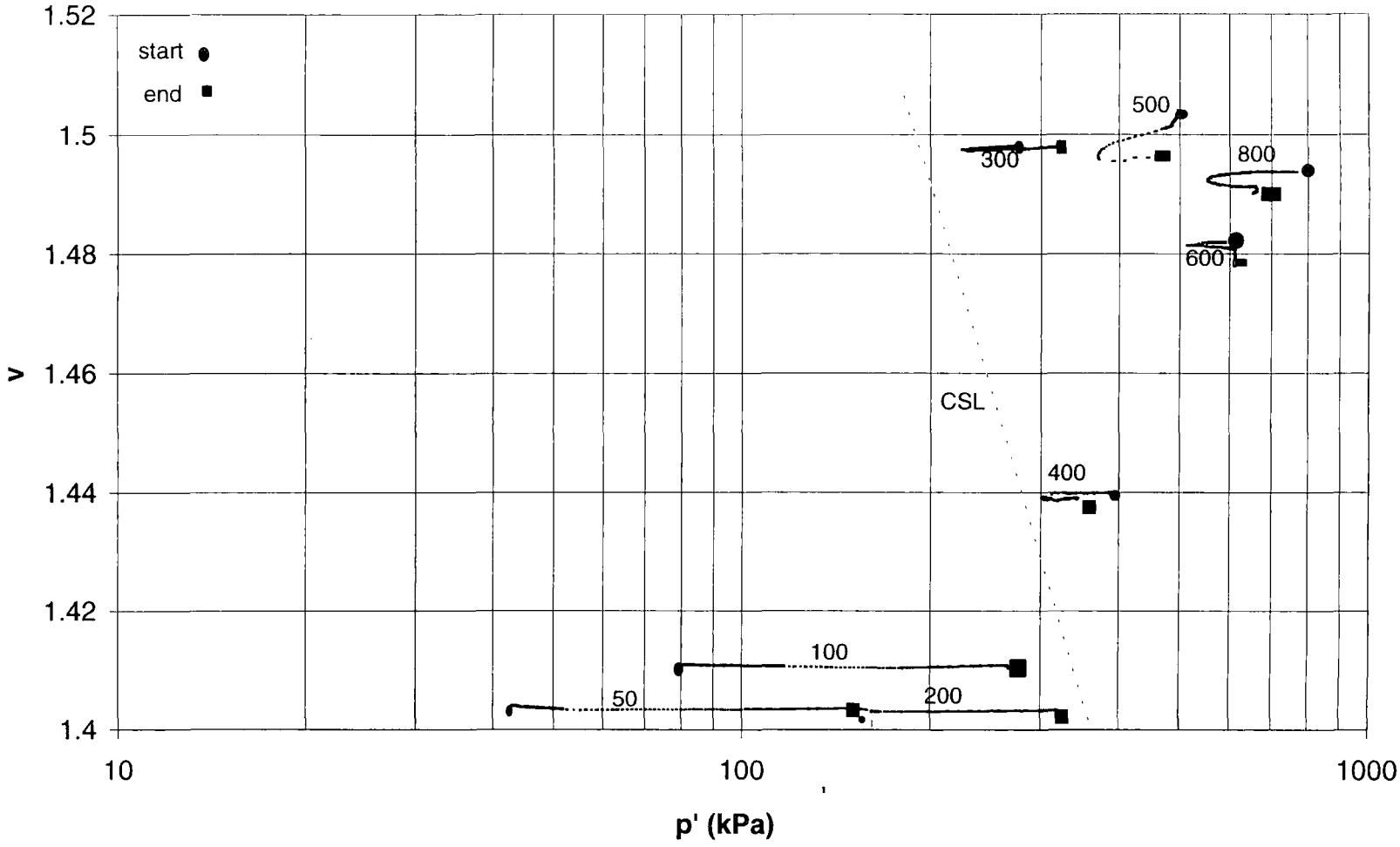

Fig.7.69 Specific volume vs. p' for destructured soils of borehole two

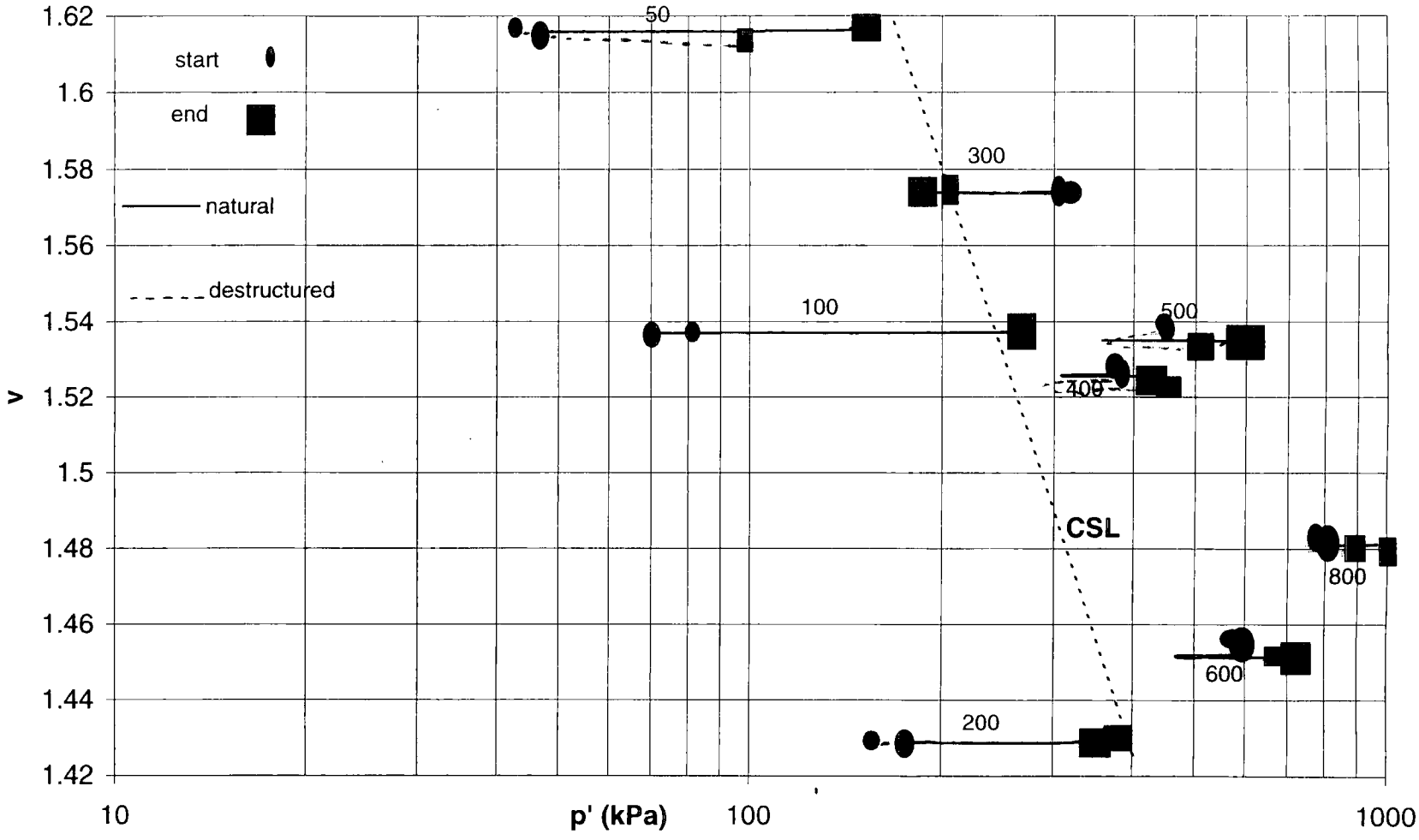

Fig.7.70 Comparison between specific volume vs. p' for natural and destructured soils of borehole one

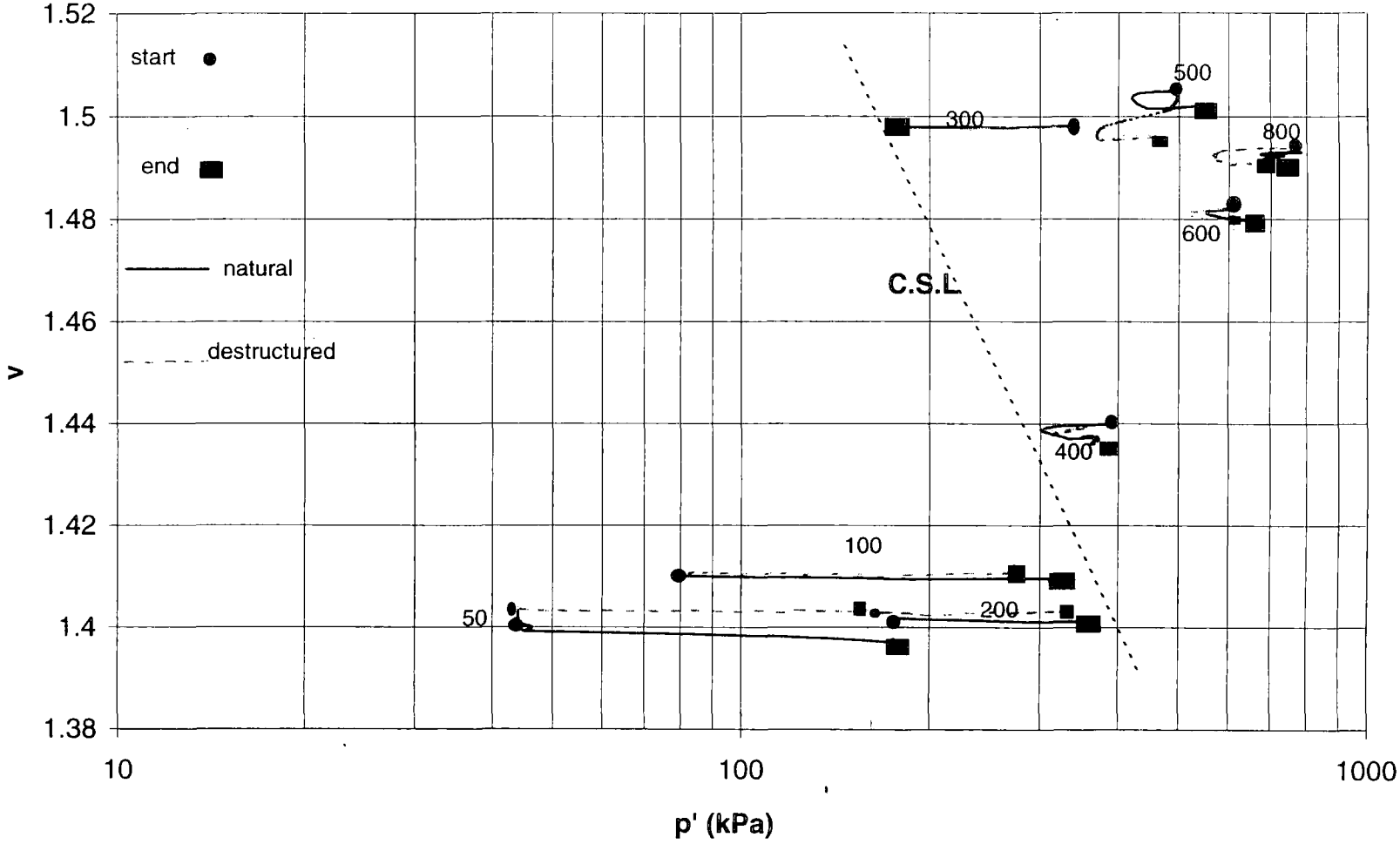

Fig.7.71 Comparison between specific volume vs. p' for natural and destructured soils of borehole two

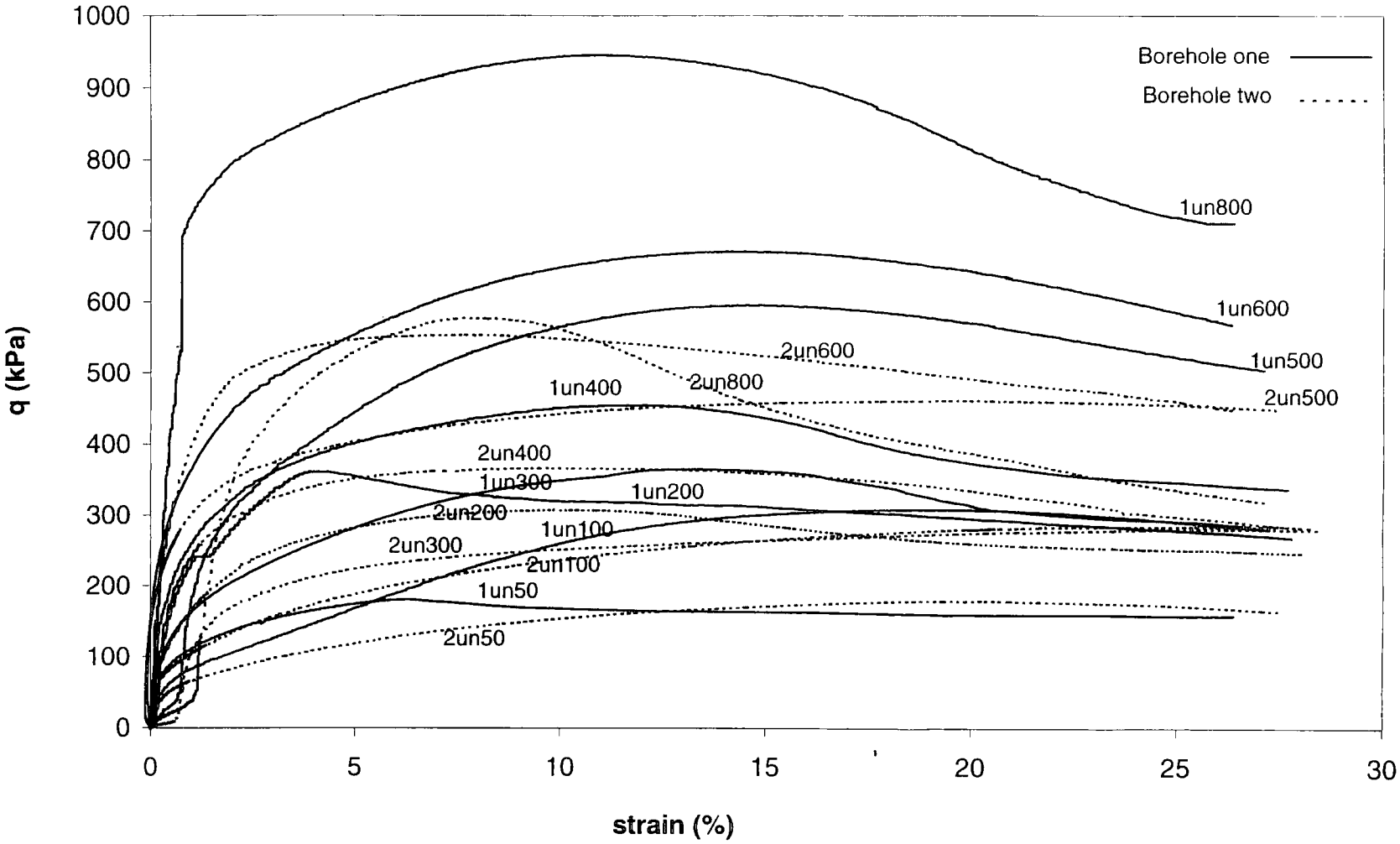

Fig.7.72 Comparison of deviator stress versus axial strain curves of natural soils of borehole one & two

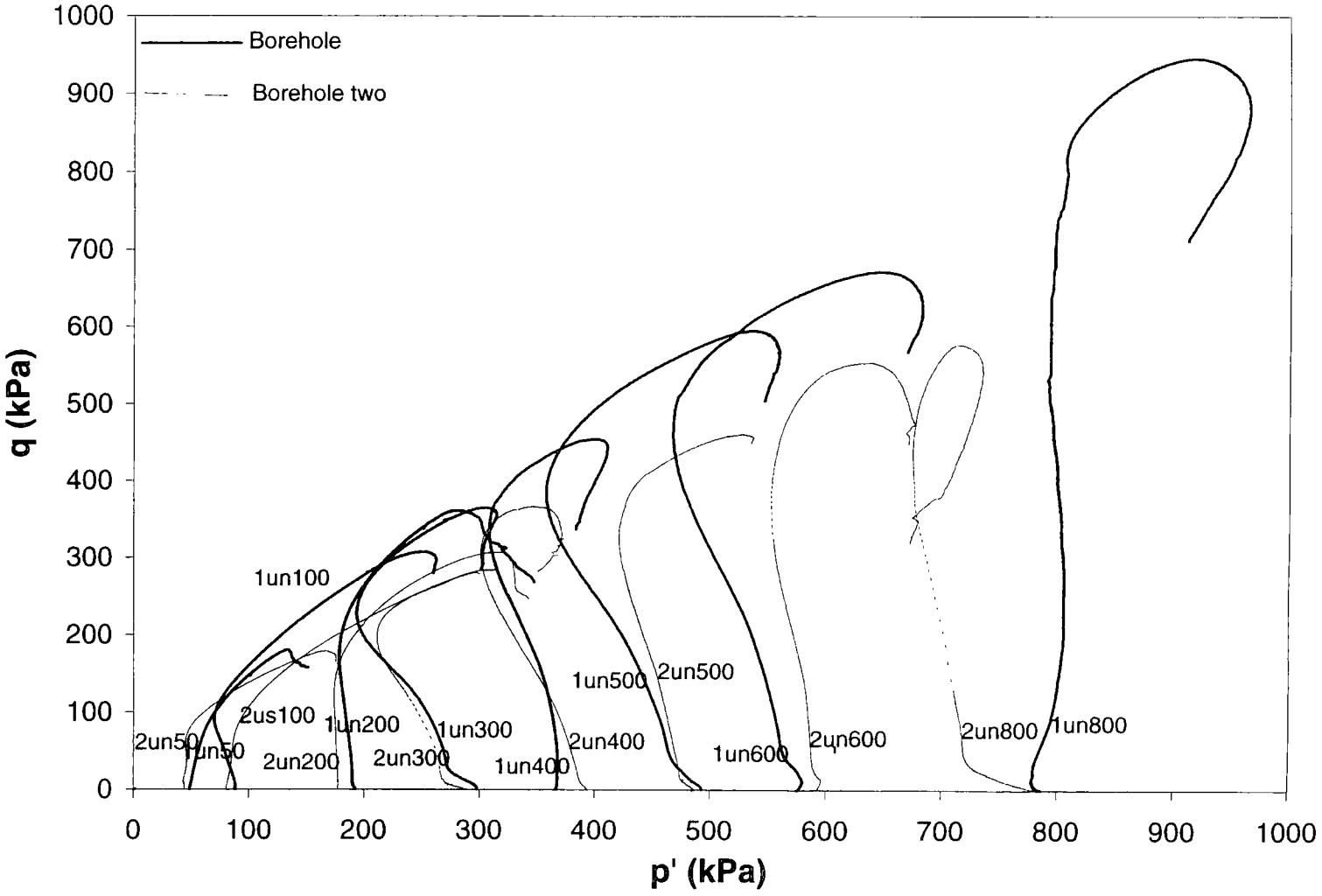

Fig. 7.73 Comparison of stress paths derived from natural state samples of borehole one and two

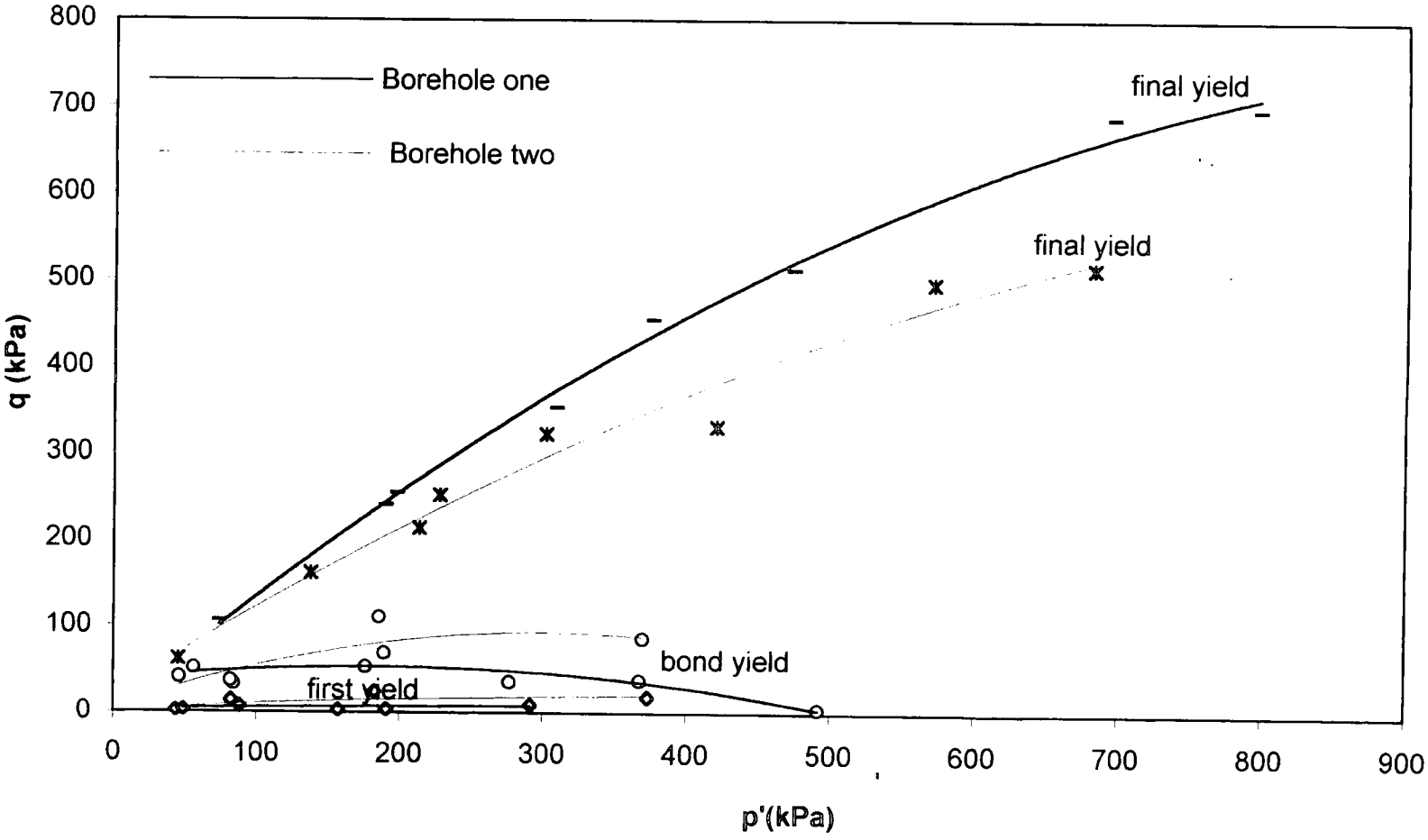

Fig. 7.74 Comparison between three yield surfaces for natural soils of borehole one and two

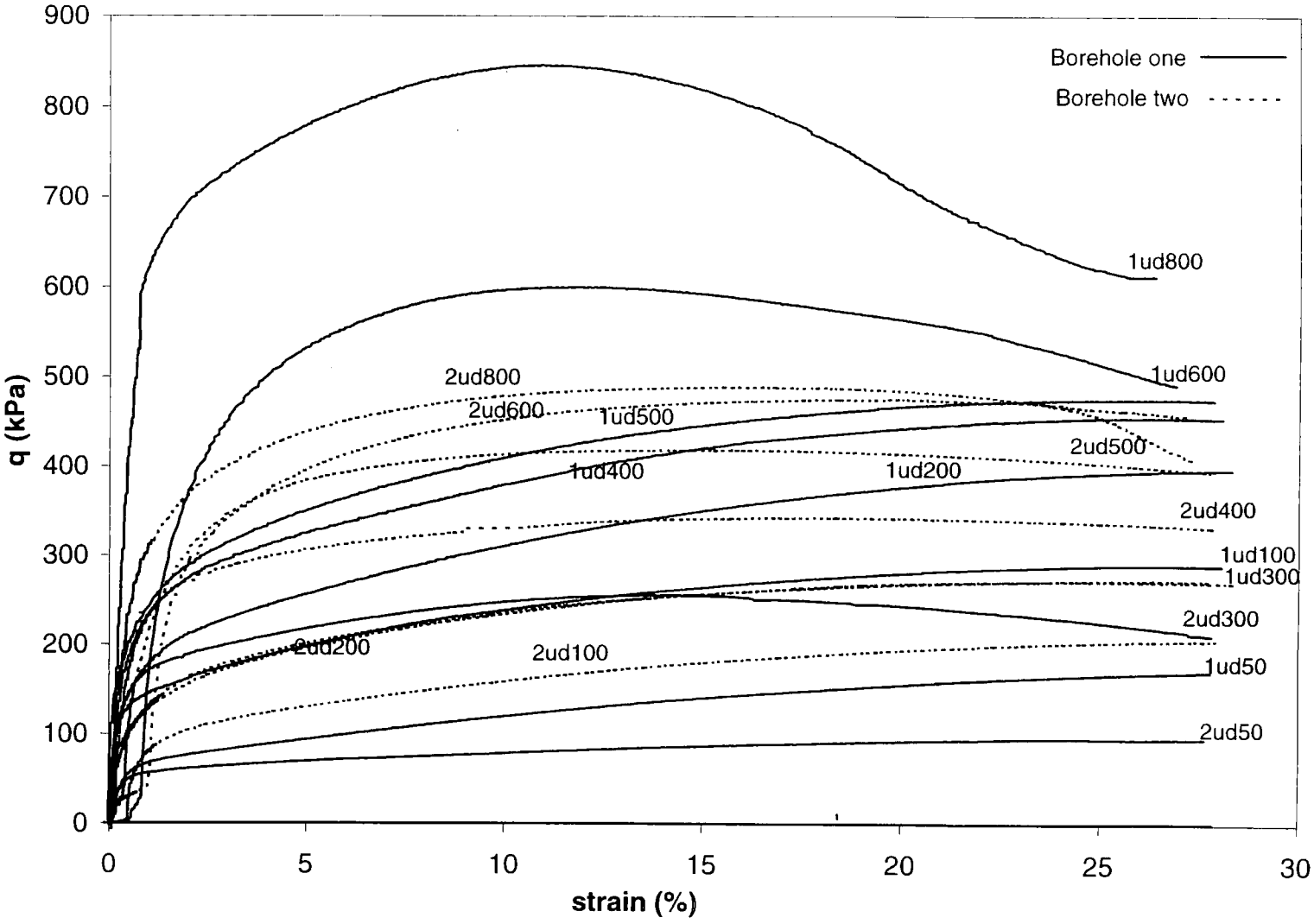

Fig.7.75 Comparison of deviator stress versus axial strain curves for destructured soils of borehole one & two

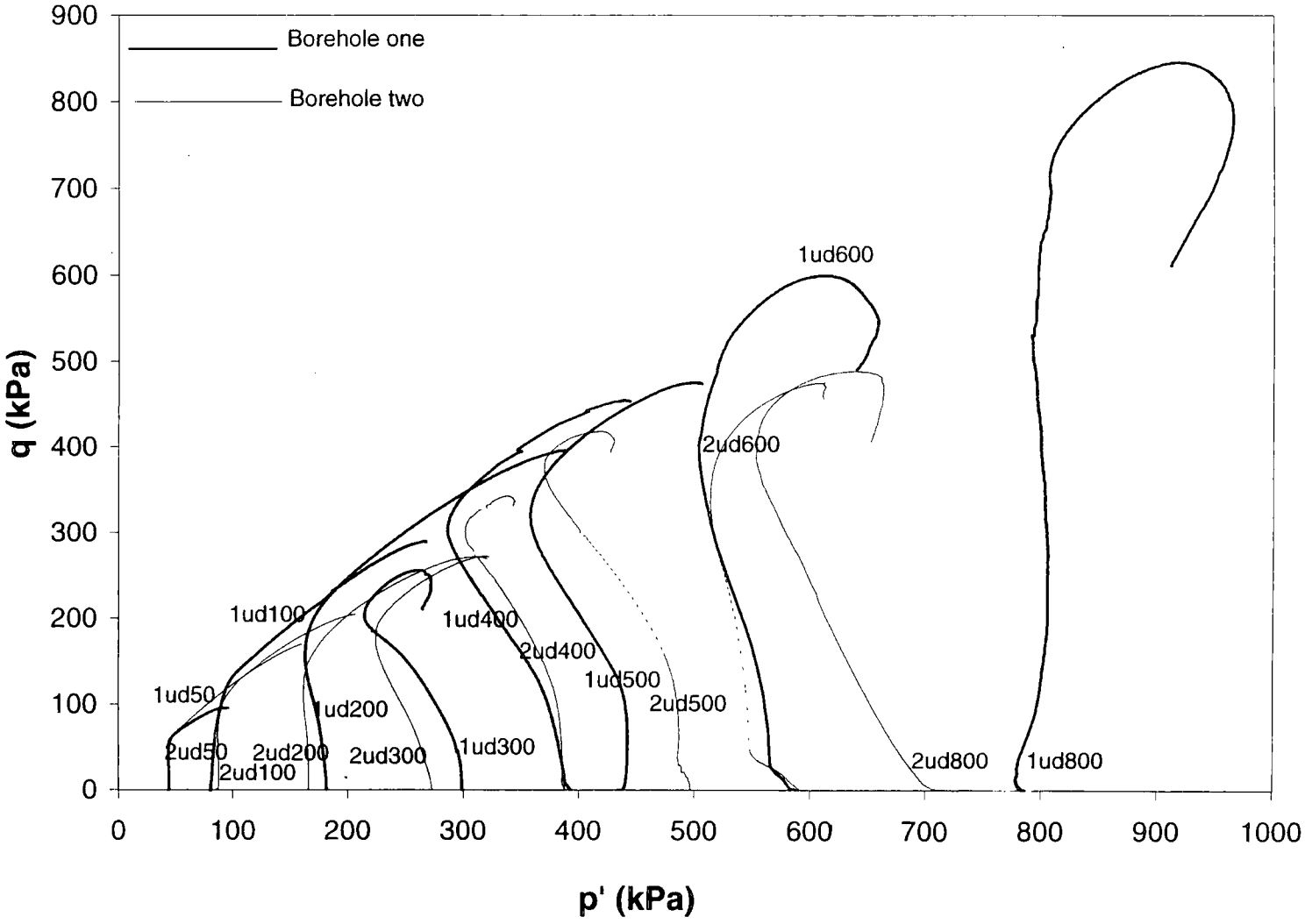

Fig.7.76 Comparison of stress paths derived from a series of triaxial tests on destructured soils of borehole one and two

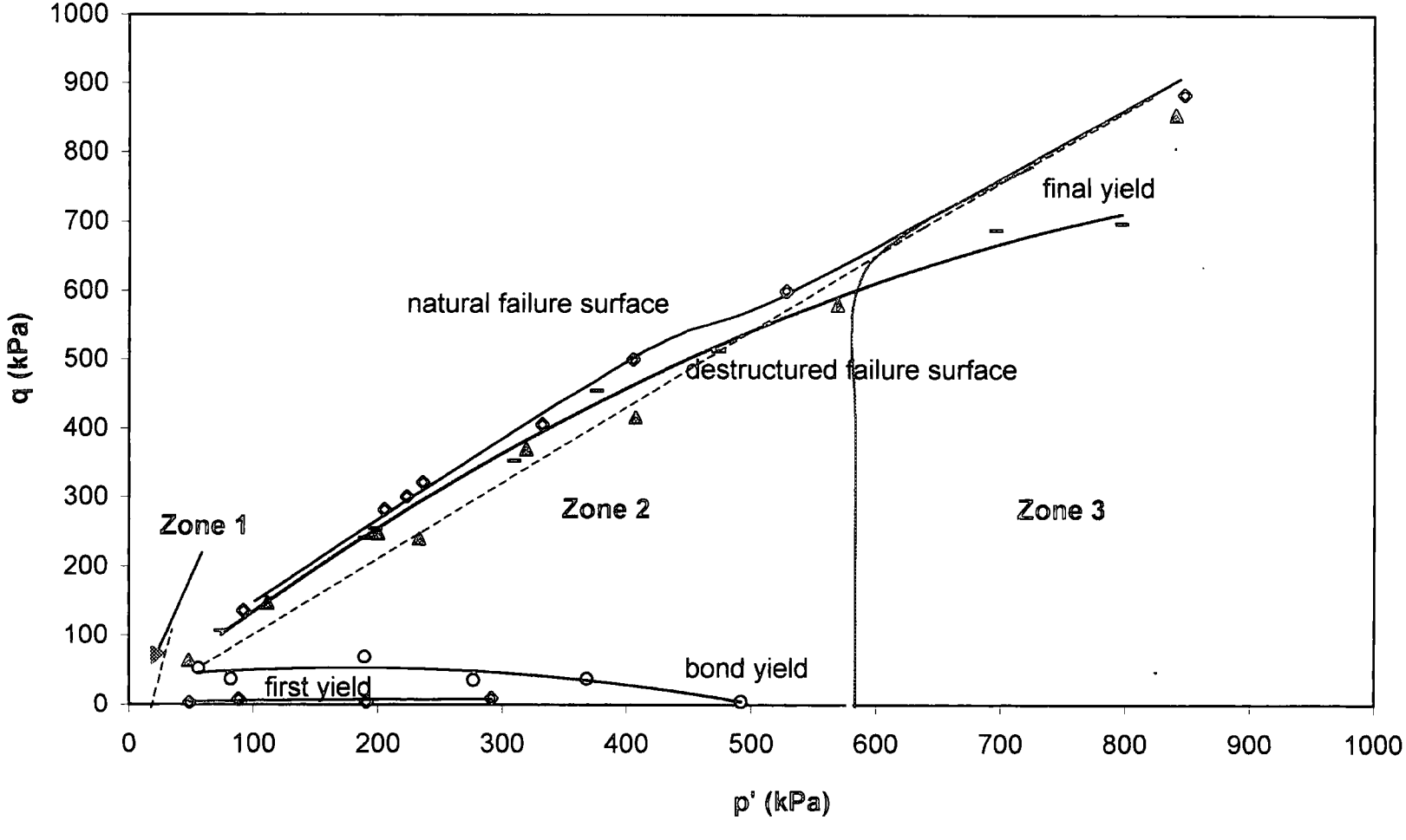

Fig. 7.77 Zones of behaviour for borehole one samples under undrained shearing

CHAPTER 8

DRAINED TRIAXIAL TESTS

8.1 Introduction

This chapter describes in detail the results of all the consolidated drained triaxial tests made on the tropical clay soils of Dhaka, Bangladesh. The samples were collected from borehole three of the same geological formation from which samples of other boreholes were collected and the location is shown in figure 3.1 of Chapter 3. Both natural and destructured samples were used to carry out the drained tests.

8.2 Consolidated drained triaxial tests on natural tropical clay soils of Dhaka.

The drained behaviour of natural state samples of borehole three is discussed in this section. Stress strain behaviour of these samples is carefully evaluated. The volumetric strain curves with an increase in axial strain are also studied. The drained stress paths are identified from the deviator stress versus mean effective stress curves.

Tangential stiffness in terms of shear modulus (G_{tan}) and yielding behaviour of the tropical clay are also evaluated. The first and bond yield points are identified as described by Malandraki and Toll (1996 & 2000). The positions of the identified yield points are shown in the q-p′ space. Smaller strain behaviour up to 2% strain is also discussed. All the results are presented, compared and evaluated.

Critical state behaviour is discussed. A comparison is made between the results of natural and destructured soils of borehole three. Finally an attempt is made to define the important characteristics for developing a framework for the tropical clay soils of Dhaka.

8.2.1 Testing details

Consolidated drained triaxial tests were carried out on seven natural and seven destructured samples collected from borehole three. The detailed test information including test name, location, sample depth, void ratio, dry density, consolidation stress are listed in Table 8.1. All samples were initially saturated and were subjected to isotropic consolidation before shearing. Samples were consolidated at a range of confining pressures from 50 kPa up to 800 kPa before shearing. Each test on average

took 5-6 days to complete. The seven tests carried out on natural samples of borehole three were taken from different depths and had consolidation pressures ranging from 50 to 800 kPa. The same effective confining pressures were applied to the seven destructured samples prepared from the natural samples of the same borehole to get a clear picture of behaviour. Testing details are discussed in section 4.6 of Chapter 4.

The samples of borehole three were named by using numbers and letters. The initial number indicates the borehole number and the number after the two letters in each case indicates the value of effective confining pressures at which the samples were consolidated before shearing. Two letters are used to designate each test. The first letter in each test indicates the type of shearing (drained) and the second letter indicates the nature of the sample (natural or destructured).

Table 8.1: Testing details of natural soils of borehole three Location: Mirpur

Test name	Depth (m)	Initial moisture content w %	Specific gravity G_s	Bulk density ρ (Mg/m^3)	Dry density ρ_d (Mg/m^3)	Initial void ratio e	Wet weight of sample (g)	Dry weight of sample (g)
3dn50	0.97-1.37	15.8	2.60	2.059	1.779	0.461	177.33	153.15
3dn200	1.52-1.98	14.0	2.62	2.070	1.820	0.443	178.22	156.29
3dn300	3.13-3.59	14.7	2.60	2.009	1.739	0.482	172.98	150.78
3dn400	3.74-4.20	13.7	2.65	2.130	1.870	0.412	183.96	171.20
3dn500	5.65-6.11	13.0	2.63	2.084	1.842	0.428	179.74	163.97
3dn600	6.26-6.72	13.1	2.62	2.051	1.810	0.445	177.23	160.03
3dn800	7.48-7.94	13.6	2.61	2.061	1.810	0.439	177.39	156.18

For example test 3dn200 (in Table 8.1) indicates a sample from borehole three tested in a drained condition in a natural state, consolidated at a confining pressure of 200 kPa before shearing. Similarly 3dd500 (in Table 8.4) indicates a test on a sample from borehole three, tested drained in a destructured state, which was consolidated at a confining pressure of 500 kPa before shearing. All other tests are named similarly.

8.2.2 Interpretation of results

8.2.2.1 Stress strain curves (natural soils of borehole three)

The drained deviator stress versus axial strain curves for the natural soils of borehole three are shown in figure 8.1. It can be seen from figure 8.1 that the curves show a maximum stress level in each case. After reaching the maximum stress level, a decrease of deviator stress with increasing strain is observed in each case. At high effective confining pressures (400-800 kPa) the peak in deviator stress is more distinct and sharp. On the other hand (in figure 8.1) at low effective confining pressures (50-200 kPa) the maximum deviator stress points are not sharp and they do not show a prominent peak. It can also be seen from figure 8.1 that the maximum deviator stress increases with increasing confining pressure.

The axial strains to attain maximum deviator stress for these samples lie between approximately 8% to 16%. The lowest strain to attain the maximum deviator stress is encountered for sample 3dn800 and the highest value is for 3dn200. The maximum deviator stress and the corresponding values of axial strain, mean effective stress and the value of volumetric strain in each case are summarized in Table 8.2. It is important to note here that two samples (tests 3dn400 and 3dn500) showed some bedding error at the beginning of the test. This initial bedding error for these two samples appeared due to membrane penetration. The membrane penetration caused

the position of the pivot of the internal strain gauge to move introducing an error at low strains.

Table: 8.2. Summary of stress and strain parameters at maximum deviator stress

Sample number	Maximum deviator stress (q) kPa	Volumetric strain (ε_v%) at maximum q	Axial strain at maximum q (ε_a%)	Mean effective stress (p') at maximum q kPa
3dn50	117	-0.19	13.34	88
3dn200	303	0.42	15.89	300
3dn300	339	0.72	15.20	400
3dn400	677	0.62	12.42	624
3dn500	737	0.55	11.96	744
3dn600	844	0.60	8.94	880
3dn800	903	0.98	8.45	1100

8.2.2.2 Volumetric strain versus strain curves for natural soils of borehole three

The volumetric strain versus axial strain curves for the natural soils of borehole three are shown in figure 8.2. It is important to note here that a positive volumetric strain was taken as contraction and a decrease in value was taken as dilation of the sample. It can be seen from figure 8.2, that the samples initially showed a contraction because of reduction in volume during drained shearing. After attaining a maximum contraction, the volumetric strain of each sample stabilized for a while and then started to show dilation at larger strains. The amount of contraction and dilation varied from sample to sample. The highest amount of contraction and lowest dilation were observed in sample 3dn800. The lowest contraction and maximum dilation were seen in sample 3dn50.

It can be seen from figure 8.2 that the volumetric strain values for tests 3dn50 and 3dn200 seem to be decreasing continuously because of dilation until the end of the test. Therefore, these samples did not reach a steady state condition at the end of shearing. However, volumetric strain data for tests 3dn400, 3dn500 and 3dn800 show that at strain greater than 25%, volumetric strain values reach almost a steady value at the end of the tests. Therefore these samples (3dn400 to 3dn800) might be very close to the critical state at very large strain. Tests 3dn300 and 3dn600 initially showed a contraction and then tended towards an almost constant volumetric strain value at the end of the tests, perhaps suggesting that they might have approached a critical state condition. These curves are replotted with the deviator stress versus axial strain curves in figures 8.3 and 8.4 to compare the overall behaviour of the deviator stress versus axial strain with the volumetric strain versus axial strain curves. It can be seen from these two figures that the shape of the volumetric strain versus axial strain curves reflects approximately the same shape of deviator stress versus axial strain curves.

8.2.2.3 Derivation of drained stress paths in q-p′ space for natural soils of borehole three

Effective stress paths in q-p′ space for the series of consolidated drained triaxial compression tests on natural soils of borehole three are plotted in figure 8.5. The derived stress paths are straight lines at a slope of 3:1, since they are drained tests. With the increase of mean effective stress and deviator stress the stress paths for tests 3dn50, 3dn200 and 3dn400 in figure 8.5, moved up to the failure point and then moved back down again along the same stress path towards an ultimate state, possibly the critical state line. However, the stress paths for tests 3dn300 and 3dn600 showed only a small drop post-failure, as could be seen in the stress-strain curves

(fig.8.1). The maximum deviator stress and the corresponding mean effective stress values for these stress paths are listed in Table 8.2.

All natural samples of borehole three failed with the formation of shear surfaces. At low effective confining pressures (50-200 kPa) the samples showed brittle failure with a number of indistinct shear planes. At effective confining pressures of 300 to 600 kPa the samples showed brittle failure with number of distinct shear planes. Test 3dn800 showed a prominent and distinct single shear plane with some bulging. A possible critical state line is shown in figure 8.5. The problem of defining critical state line will be discussed in section 8.5.1.

8.2.2.4.Failure surface for natural soils of borehole three

The failure surface is identified by using maximum stress ratio criteria plotted in the q versus p′ space as shown in figure 8.6. By considering the failure line for the whole range of tests it was found that the observed failure line is slightly curved. It can be seen from figure 8.6 that the failure surface initially showed a curvature up to approximately p′ = 300 kPa. For p′ greater than 300 kPa the slope of the curve reduces steadily as p′ increases. Similar curved failure surfaces for bonded soils have also been reported by Vaughan (1988) and Malandraki and Toll (1994).

It is important to note here that the failure envelope between tests 3dn300 and 3dn400 showed a clear change of behaviour. This will be explained later in figure 8.32 in section 8.5.1.

8.2.2.5. Stiffness and yielding characteristics

Tangential stiffness in terms of shear modulus (G_{tan}) versus axial strain graphs for samples 3dn50 to 3dn300 are shown in figures 8.7 to 8.9. It can be seen from these figures that tangential stiffness versus strain curves are non-linear and showed a reduction of stiffness values with increasing strain in each case. The loss of stiffness with increasing strain is related to the breakdown of bonds (Malandraki and Toll, 1996). The variation of small strain data probably reflects to some extent the variability at the level of structure (Hight et al., 1992) in natural soils. The identified first and bond yield points for tests 3dn50, 3dn200 and 3dn300 as marked in figures 8.7 to 8.9 are described by Malandraki and Toll (1996 and 2000). It can be seen from these figures that two identifiable drops of stiffness values occurred in each case. The first identifiable drop of stiffness is considered as first yield and the second significant drop is considered as bond yield where the soil loses most of its stiffness values. A variation in the position of first and bond yield points is due to the degree of cementation as described by Hight and Higgins (1995). G_{tan} versus strain curves for other samples of borehole three (3dn400-3dn800) at high confining pressures are shown in figures 8.10 to 8.13. No clear yield points are observed at these confining pressures. This suggests that bond destruction has occurred during application of the very high isotropic confining pressures (400 kPa or greater) on natural samples of borehole three.

The identified first and bond yield points for tests 3dn50 to 3dn300 with their corresponding values of deviator stress and axial strain are listed in Table 8.3.

Table: 8.3 First and bond yield points for natural soils of borehole three with corresponding values of q and ε_a %

Sample no.	Yield	q (kPa)	$\varepsilon_{a\,(\%)}$
3dn50	First yield	6	0.0025
	Bond yield	12	0.010
3dn200	First yield	26	0.015
	Bond yield	39	0.028
3dn300	First yield	14	0.007
	Bond yield	29	0.025

The identified first and bond yield points for these tests are plotted in figure 8.14 in the q-p′ space. The failure surface is also shown in this figure. The first yield surface occurred at approximately 0.0025% to 0.015% strain and the bond yield at approximately 0.01% to 0.028% strain. The first yield surface occurred at low deviator stress level and enclosed a small area with q = 6 to 26 kPa in the q- p′ space. The first yield surface in figure 8.14 increased up to approximately p′ = 200 kPa. For p′ greater than 200 kPa this surface curved down towards the p′ axis. It is expected that the first yield surface will meet the p′ axis at higher stresses.

The identified bond yield surface shown in figure 8.14 is located at higher deviator stress levels than the first yield surface in the q- p′ space and is consistent with the bond yield surface as described by Malandraki and Toll (2000). This bond yield surface enclosed an area approximately with q = 12 kPa to 39 kPa in the q- p′ space where major loss of stiffness occurred. The bond yield surface appears to curve down towards the isotropic axis before p′ = 400 kPa, confirming the suggestion earlier that bond breakdown would occur in isotropic compression for tests at higher confining pressures, as no yield would be seen during shear.

The final yield surface for natural soils of borehole three was identified by using the point of maximum curvature of the stress strain curve and is shown in figure 8.14. The final yield surface plotted in the q versus p′ space occurred at higher deviator stress levels than the first and bond yield surfaces and is positioned below the failure surface. At low mean effective stress (approximately p′ less than 100 kPa) the final yield surface is very close to the failure surface and the distance between the two surfaces increased with increasing mean effective stress. After bond yield, the soil behaviour involves the combined influences of both the remaining bonding and the plastic strains. When the soil reached the final yield surface, it loses almost all of its stiffness due to bonding and failure occurs at much larger strains due to slippage of individual grains.

8.2.3 Small strain behaviour (up to 2% strain)

8.2.3.1 Tangential stiffness versus mean effective stress for natural soils of borehole three

G_{tan} versus p′ curves are plotted with increasing strain (from 0.01% to 1% strain) in figure 8.15 to show the loss of stiffness during drained shearing. The small strain contours showed a decrease of stiffness values with increasing strain. G_{tan} values are highest for 0.01% strain contour and lowest for 1 % strain contour (figure 8.15). The reduction of stiffness values with increasing strain is due to the breakdown of the bonded structure of the soil (Malandraki and Toll, 1996). It can be seen from these figures that the major loss of stiffness values occurred for strain contours 0.01% to 0.2% where bond destruction is greatest. First yield for natural soils of borehole three occurred between 0.0025% and 0.015% strain. The quick destruction of some

bonds at very low strain made it sometimes difficult to identify the first yield accurately. After 0.2% strain loss in stiffness is less pronounced. The bond yield for these samples occurred at approximately 0.01% to 0.028% strain where the major loss of stiffness occurred. The lower G_{tan} values at 1% strain indicates that the soil has already lost most of the stiffness due to breakdown of bonds as described by Malandraki and Toll (1996). The natural strain contours shown in figure 8.15 showed a drop of tangential stiffness values from approximately 250 MPa at 0.01% strain to approximately 12 MPa at 1% strain. The drop of stiffness values with increasing strain is also reported by Burland (1989), Atkinson et al. (1993) and Malandraki and Toll (1996).

8.2.3.2 Strain contours (up to 2% strain) for natural soils of borehole three

Small strain contours (up to 2% strain) for natural soils of borehole three are plotted in q versus p′ space and shown in figures 8.16. The failure surface is also plotted in the same figure. It can be seen from this figure that deviator stress value for each strain contour increased with increasing strain up to approximately p′ = 200 kPa. For p′ greater than 200 kPa, strain contours gradually changed direction with increasing mean effective stress and showing a bending towards the p′ axis.

It is also observed that small strain contours with increasing strain move close to the failure line. Jardine et al. (1984) observed that strain contours with increasing strain approach the failure line. They also observed that soil losses its stiffness when approaching the failure surface as observed in this study. Malandraki (1994) also reported similar results. It can be seen from this figure that the 0.01% strain contour is very close to the p′ axis and the 2% strain contour is very close to the failure surface at low p′ values. The first and bond yield of these soils occurred

approximately between 0.0025% to 0.015% strain and 0.01% to 0.028% strain respectively.

8.3 Consolidated drained triaxial tests on destructured soils of borehole three

Destructured samples were prepared from the natural samples of the same borehole with the same void ratio and dry density. Testing details of destructured samples of borehole three are given in Table 8.4.

The drained stress strain behaviour of the destructured soils of borehole three is carefully evaluated. The volumetric strain curves with an increase in strain are also analyzed. Drained stress paths are plotted in the q versus p′ space. Small strain contours (up to 2% strain) are plotted in the q versus p′ plane. Loss in tangential stiffness with increasing strain for destructured soils is also discussed. Finally comparisons are made between the results of natural and destructured soils of borehole three.

Table: 8.4 Testing details of destructured soils of borehole three
Location: Mirpur

Test name	Depth (m)	Initial moisture content w %	Specific gravity G_s	Bulk density ρ (Mg/m^3)	Dry density ρ_d (Mg/m^3)	Initial void ratio e	Wet weight of sample (g)	Dry weight of sample (g)
3dd50	0.97-1.37	15.8	2.60	2.059	1.779	0.461	177.20	153.02
3dd200	1.52-1.98	14.0	2.62	2.070	1.820	0.443	177.99	156.03
3dd300	3.13-3.59	14.7	2.60	2.008	1.737	0.482	173.12	150.89
3dd400	3.74-4.20	13.7	2.65	2.130	1.870	0.414	183.52	170.79
3dd500	5.65-6.11	13.0	2.63	2.084	1.842	0.429	180.12	163.73
3dd600	6.26-6.72	13.2	2.62	2.051	1.810	0.446	176.91	159.74
3dd800	7.48-7.94	13.6	2.61	2.061	1.810	0.438	177.32	156.32

8.3.1 Stress strain curves for destructured soils

Drained stress strain curves for destructured soils of borehole three are shown in figure 8.17. It can be seen from figure 8.17 that the curves show a maximum deviator stress level in each case. After reaching the maximum deviator stress level, a decrease of deviator stress with increasing strain is observed in each case. At low effective confining pressures (3dd50 to 3dd200 kPa) the maximum deviator stress points are not sharp and they do not show a prominent peak and reached almost a steady state at very large strain (approximately greater than 20%). Stress strain curves for other tests (3dd300 to 3dd600 kPa) showed a peak at large strain. The stress strain curves for tests 3dd400, 3dd600 and 3dd800 showed a broad peak. These three samples initially exhibited a maximum deviator stress level and then the

deviator stress decreased from its maximum value at strain greater than approximately 20%. It can also be seen from figure 8.17 that the maximum deviator stress increased with increasing confining pressure.

The axial strains to attain maximum deviator stress for these samples lie between approximately 15% and 24%. The lowest strain to attain the maximum deviator stress was encountered for test 3dd400 and the highest strain for test 3dd50. The maximum deviator stress and the corresponding values of axial strain, mean effective stress and the value of volumetric strain in each case are summarized in Table 8.5.

Table: 8.5 Summary of stress and strain parameters at maximum deviator stress for destructured soils

Sample number	Maximum deviator stress (q) kPa	Volumetric strain (ε_v %) at maximum q	Axial strain at maximum q (ε_a%)	Mean effective stress (p′) at maximum q kPa
3dd50	93	0.97	24.33	79
3dd200	288	1.02	22.66	294
3dd300	342	1.82	18.04	412
3dd400	452	1.57	15.46	550
3dd500	541	1.31	23.18	679
3dd600	661	1.93	20.30	819
3dd800	764	2.28	17.93	1030

8.3.2.Volumetric strain versus axial strain curves for destructured soils of borehole three

The volumetric strain versus axial strain curves for destructured soils are shown in figure 8.18. It can be seen from figure 8.18 that the destructured samples showed contraction only (i.e. a reduction in volume) during drained shearing. This is in contrast to the natural samples where dilation was also observed.

It can be seen from figure 8.18 that most of the destructured samples tended towards a steady value of volumetric strain at very large strain, perhaps suggesting that they might approach the critical state condition. Test 3dd800 showed a continuous change of volumetric strain up to the end of the test. Therefore, this sample did not approach the critical state condition. It can also be seen from figure 8.18 that the amount of contraction varied from sample to sample. The highest amount of contraction was observed for sample 3dd800 and the lowest amount of contraction for test 3dd50. These curves are replotted with the deviator stress versus axial strain curves in figures 8.19 and 8.20 to compare the overall shape of the deviator stress versus axial strain with the volumetric strain versus axial strain curves. The shape of the volumetric strain versus axial strain curves reflects approximately the same shape of deviator stress versus axial strain curves.

8.3.3.Derivation of drained stress paths in q-p′ space for destructured soils of borehole three

Effective stress paths for a series of consolidated drained triaxial compression tests on destructured soils of borehole three are shown in figure 8.21. Since the tests were drained, the derived stress paths are straight lines at a slope 3:1. It can be seen from figure 8.21 that the stress path for tests 3dd50, 3dd200 and 3dd300 show only a small drop in stress post-failure. The failure surface for destructured soils of

borehole three is defined by using the maximum q/p′ ratio values plotted in the q versus p′ space and is shown in figure 8.22. The failure surface is roughly linear and appears to suggest a cohesion intercept at p′ = 0 kPa.

All destructured samples failed with the formation of shear surfaces and by bulging. At low effective confining pressures (50-300 kPa) the samples showed ductile failure and small amounts of bulging with a number of indistinct shear planes. The samples for tests 3dd400-3dd600 failed with a number of distinct shear planes and bulging. At high effective confining pressure of 800 kPa the sample failed with distinct shear planes and prominent bulging. A possible critical state line is shown in figure 8.21. The problem of defining critical state line will be discussed later in section 8.5.2.

8.3.4. Small strain behaviour

8.3.4.1. Tangential stiffness with increasing strain (up to 2%) for destructured soils of borehole three

The losses of tangential stiffness with increasing strains (from 0.01% to 1% strain) during drained shearing for destructured soils are shown in figure 8.23. Highest values of G_{tan} are observed for 0.01% strain contour and lowest for 1% strain contour. The 1% strain contour runs very close to the p′ axis where stiffness values are very low. The destructured soils showed a decrease of stiffness value from approximately 100 MPa at 0.01% strain to about 8MPa at 1% strain.

8.3.4.2. Strain contours up to 2% strain for destructured soils of borehole three

Small strain contours (from 0.01% to 2% strain) for destructured soils of borehole three are plotted in the q versus p′ space and shown in figure 8.24. The failure surface is also plotted in figure 8.24. It can be seen from figure 8.24 that these strain contours are linear and deviator stress for each strain contour increased with increasing mean effective stress. At higher p′ (p′ > 200 kPa) the distance between the strain contours increases with increasing strain. It can also be seen from this figure that the 0.01% strain contour is very close to the p′ axis and the 2% strain contour is close to the failure surface. The strain contours turn in direction from the p′ axis to the failure surface with increasing strain.

8.4. Comparisons between the behaviour of the natural and destructured soils of borehole three

The behaviour of the natural and destructured soils under drained triaxial compression are compared and evaluated. Comparisons are made between the deviator stress versus axial strain, volumetric strain and versus axial strain and between the stress paths of the natural and destructured soils. Loss of tangential stiffness with increasing strain and small strain contours in the q-p′ space is also compared. Comparisons between the positions of two failure surfaces in the q- p′ space are discussed.

8.4.1.Comparisons between stress strain behaviour of natural and destructured soils of borehole three

Deviator stress versus axial strain curves for natural and destructured soils under drained triaxial compression tests are shown in figure 8.25. It can be seen from figure 8.25 that the natural state curves exhibit higher maximum deviator stress than the destructured curves in each case. At low confining pressures (50 to 200 kPa), both the natural and destructured soils did not show a prominent peak, but at high confining pressures (400 to 800kPa) both types of samples show a maximum deviator stress level with an identifiable peak. Bishop et al. (1965) reported similar test results. The destructured soils in each case showed lower maximum deviator stress levels, lower stiffnesses and larger strains to reach maximum deviator stress than the natural samples. In natural samples, the axial strains to attain maximum deviator stress ranged from 8% to 16%. Conversely, the destructured soils attained a maximum deviator stress value at axial strains of 15% to 24%. These variations in the deviator stress versus axial strain curves indicate that there is bonding in the natural samples that gives higher strength and stiffness. Leroueil and Vaughan (1990), Clayton et al. (1992) and Allman and Atkinson (1992) reported similar results when comparing natural and destructured test data.

The volumetric strain versus axial strain curves for natural and destructured soils of borehole three are also compared and shown in figure 8.26. It can be seen from this figure that most of the natural samples initially showed contraction and then small amounts of dilation at very large strain. The amount of contraction and dilation varied from sample to sample. Conversely, the destructured samples showed only contraction until the end of shearing.

Differences in failure type were observed between the natural and destructured samples. All natural samples at low confining pressures showed brittle failure with number of indistinct shear planes and at high confining pressures shear plane is prominent and distinct. The destructured samples failed with bulging in a ductile manner. At low confining pressures destructured samples showed small bulging with a number of indistinct shear planes and at high confining pressures they failed with distinct shear planes and prominent bulging.

The two failure surfaces for natural and destructured soils are shown in figure 8.27. The failure surface for natural soils shown in figure 8.27 exists at higher deviator stresses than the destructured failure surface. Differences in the two failure surfaces are due to the presence of bonding in natural soils. The failure surface for natural soils progressively increased with the increase of p′ up to a value of approximately >300 kPa (figure 8.27). After that the slope of the natural failure surface reduces steadily as p′ increases. It is discussed in section 8.5.1 that the variations between the very loose and very dense samples (between tests 300 and 400 kPa) showed a clear change of behaviour in the failure envelope.

8.4.2. Comparisons between the tangential stiffness versus mean effective stress for natural and destructured soils (up to 2% strain)

Comparisons between stiffness values for natural and destructured soils are shown in figures 8.28 & 8.29. Natural and destructured strain contours with tangential stiffness versus p′ curves for 0.01% to 1% strain are plotted in these figures. The natural strain contours in each case showed higher values of G_{tan} than the destructured soils, which indicates that the natural soils are structured. The highest value of G_{tan} calculated for natural soil is approximately 250 MPa at 0.01% strain and approximately 80 MPa for destructured soils of the same strain contour. The

lowest value of G_{tan} observed for natural soil is approximately 12 MPa at 1% strain contour and approximately 8 MPa for destructured soil at the same strain contour.

8.4.3 Comparisons between small strain contours (up to 2%) for natural and destructured soils of borehole three

Strain contours (up to 2% strain) for natural and destructured soils are compared in the q versus p′ space and shown in figures 8.30 and 8.31. It can be seen from these figures that for natural soils the deviator stress increased with increasing strain approximately up to p′= 200 kPa. At p′ greater than 200 kPa natural strain contours turned down towards the p′ axis with increasing mean effective stress. Conversely, the deviator stress for destructured strain contours increased with increasing mean effective stress and they are roughly linear.

It is important to note here that although both the natural and destructured samples were tested at the same void ratios but they showed clear differences in their behaviour. The difference in position between the natural and destructured strain contours shown in figures 8.30 and 8.31 is due to the presence of bonds in the natural samples. Therefore, bonded structure of the soil has a strong influence on the development of strain. Similar results were also reported by Jardine et al. (1984) and Malandraki and Toll (1994).

8.5 Critical state behaviour

In this section critical state behaviour of borehole three samples under drained shearing are discussed. At first results are presented for natural soils of borehole three and then the critical state condition for the destructured samples of the same borehole is discussed. Finally based on the all observed results on natural and destructured soils an estimation was made to obtain the critical state parameters for these soils.

8.5.1 Critical state condition for natural soils under drained shearing

An attempt is made to identify the critical state condition under drained shearing. From the derived stress paths as shown in figure 8.5 in q- p′ space, an attempt is made to interpret the critical state stress ratios for the natural soils of borehole three. Based on the observed stress paths in q- p′ space, it was found very difficult to establish with confidence the ultimate points for these tests. The stress strain curves (figure 8.1) for tests 3dn50, 3dn200 and 3dn300 show a reasonably stable deviator stress values at the end of the tests, perhaps suggesting they had reached a stable ultimate state. However, it can be seen from figure 8.5 that the end points for these three tests indicate a cohesion intercept. This would not be expected for a critical state condition. The validity of the data for tests 3dn400, 3dn500 and 3dn600 at very large strain is questionable (as they formed shear surfaces). Tests 3dn300 and 3dn800 also formed distinct shear surfaces and they might not represent the true critical state condition at the end of shearing. Therefore, it is very hard to justify the true ultimate points for these tests to identify the critical state conditions. However, a possible CSL is sketched in figure 8.5 but it is very tenuous.

All the results of natural soils of borehole three are also plotted in the v-p′ space to see the change of specific volume with increasing mean effective stress in figure 8.32. It can be seen from this figure that the tests 3dn50 and 3dn200 of borehole three after an initial decrease in specific volume showed a dilation up to the end of the tests. It can also be seen from this figure that the specific volume for tests 3dn400, 3dn500 and 3dn600 initially showed a reduction of specific volume due to contraction of the sample and then an increase in specific volume due to dilation of the sample with increasing mean effective stress. Two tests (3dn300 and 3dn800) showed contraction with increasing p′. These two samples showed almost zero rate of volume change at the end of the tests, perhaps suggesting that they reached the critical state. Other tests did not approach the true critical state condition. Similar reflections were observed in the volumetric strain versus axial strain curves as shown in figure 8.2.

It is interesting to note here that the borehole three samples at low confining pressure (3dn50-3dn200 kPa) showed brittle failure with a number of indistinct shear planes. High confining pressure samples (3dn300-3dn800 kPa) formed distinct shear surfaces and once that occurs only a narrow band of soil is being affected by shearing and the overall stress ratio and volume change is no longer representative of the sample as a whole. Two tests 3dn300 and 3dn800 showed constant rate of volume change at the end of shearing but they form distinct shear surfaces at the time of failure. It is therefore difficult to justify that these two tests 3dn300 and 3dn800 approached a true critical state condition. In this circumstance, it is possible to conclude that in drained shearing on natural samples of borehole three, no test approached a true critical state condition. Smith et al. (1992) observed that in drained shearing on a group of Bothkennar soils, no test approached a true critical state condition. They also proposed a tentative critical state line (CSL) based on the end points of different tests.

From the observed results as shown in figure 8.32, it is very difficult to construct a single critical state line for these soils. A tentative drained critical state line is drawn as shown in figure 8.32, which in general, separates those tests showing contraction (i.e. loose of critical state) from those demonstrating dilation (i.e. dense of critical state). However, as no tests on natural samples of borehole three approached a true critical state condition, the validity of the critical state line drawn is questionable. It can also be seen from this figure that test 3dn300 is very loose and contractive and the test 3dn400 is very dense and dilative. The variations between the very loose and very dense samples (tests 3dn300 and 3dn400) could explain the very clear change of behaviour in the failure envelope (figure 8.6).

8.5.2. Critical state condition for destructured soils under drained shearing.

From the derived stress paths as shown in figure 8.21 in q- p′ space, an attempt is made to interpret the critical state condition for the destructured soils of borehole three. It can be seen from figure 8.21 that the failure points and end points for tests 3dd50, 3dd200, 3dd300 and 3dd500 are very close. It was found very difficult to establish with confidence the ultimate points for these tests in q- p′ space. The validity of the data for tests 3dd300-3dd600 at very large strain is questionable (as they formed distinct shear surfaces). It is therefore very hard to justify that these samples (3dd300-3dd600) truly reached the critical state at very large strain. Since tests 3dd50 and 3dd200 did not form distinct shear surfaces it might be possible that these two samples might approach the critical state at very large strains. Tests 3dd800 also formed distinct shear surfaces and might not represent the true critical state condition at the end of shearing. However, a possible CSL is sketched in figure 8.21 but this is tenuous, due to the difficulties involved in assessing a critical state condition in samples that form shear surfaces.

The critical state condition for destructured soils of borehole three under drained shearing is also investigated in the v-p′ space. The test paths in v-p′ space for different tests on destructured samples under drained shearing are shown in figure 8.33. It can be seen from figure 8.33 that the tests 3dd50 and 3dd200 mainly showed decrease in specific volume due to contraction of the samples. Both tests showed an almost steady value of 'v' near the end of the tests, although 3dd50 showed a very small amount of dilation at the end of shearing. Towards the end of these tests, they show a tendency for an increase in p′ suggesting they could fall below the critical state line. All other destructured samples showed contraction throughout. Tests 3dd300 and 3dd400 showed almost zero rate of volume change at the end of shearing, perhaps suggesting that they also reached the critical state. Other tests (3dd500, 3dd600 and 3dd800) did not approach a true critical state condition. However, for tests 3dd300-3dd800 they all show a reduction in p′ at the end of the tests suggesting that they might fall above the critical state line.

It was discussed earlier that the destructured samples of borehole three at low confining pressures (3dd50-3dd200 kPa) showed ductile failure with indistinct shear planes and at high confining pressures (3dd300-3dd800 kPa) they failed with distinct shear planes and bulging. As the high confining pressure samples formed distinct shear surfaces, the volume change and the overall stress ratio of these samples is no longer representative. It is therefore difficult to rely on the data at very large strain and hard to justify that these samples at high confining pressures truly reached the critical state. On the other hand, as the tests 3dd50 and 3dd200 did not form distinct shear surfaces and they showed almost zero rate of volume change at the end of shearing, therefore it is likely that only these two samples approached a true critical state condition.

From the observed results as shown in figure 8.33, it is difficult to construct a single representative critical state line for these soils. However, a tentative critical state line is drawn as shown in figure 8.33 that separates those tests that show a movement to the right (3dd50 and 3dd200) from those that show a movement to the left (3dd300-3dd800), although the denser sample 3dd400 still falls below the line as drawn even though it shows a movement to the left. Again questions must arise regarding the validity of the critical state line drawn. As only two samples at low confining pressures (3dd50 and 3dd200) approached a critical state condition and others did not truly reach the critical state then the validity of the drawn critical state line is questionable. Defining the critical state line in this way will not be representative. The critical state condition for the destructured soils will be compared now with the critical state condition of the natural soils.

8.5.3 Comparison of critical state condition of natural and destructured soils

The test paths in v-p′ space for natural and destructured soils under drained shearing are also compared and shown in figure 8.34. A significant difference between the natural and destructured test paths in v-p′ space can be clearly seen in this figure. Most of the natural samples initially showed contraction and then dilation and the destructured samples generally showed only contraction. Based on all the natural and destructured test paths in v-p′ space, it is difficult to construct a single critical state line for these soils. However, based on the end points of maximum number of tests, a tentative critical state line (CSL) can be drawn as shown in figure 8.34. It is important to note here that most of the natural and destructured samples at high confining pressures formed distinct shear surfaces and once that occurs only a narrow band of soil is being affected by shearing and the overall stress ratio and volume change of the sample is no longer representative. Therefore, it is very difficult to rely on the data at very large strains.

The critical state line drawn does separate two types of behaviour. For tests at 50 and 200 kPa, tests in the natural state show strong dilation and in the destructured state they show a tendency to move to the right (increase in p′). This suggests that the specific volume state for these samples falls below (denser than) the critical state. Conversely tests at 300 and 800 kPa show contraction in both the natural and destructured state suggesting they are above (looser than) the critical state. However, the test results for 400, 500 and 600 kPa do show anomalies compared with what might be expected. Although the tests at 400 kPa fall below the CSL, the destructured test still show contraction although it might be expected that it would dilate to achieve a critical state. Similarly, the natural state tests at 500 and 600 kPa show dilation, even though they fall above the sketched CSL and it might be expected that they would contract. Clearly the volumetric behaviour is more complex than would be predicted by the critical state model. This may be due to the formation of shear surfaces, as has been discussed, when shear takes place with a narrow band and the volume changes are no longer representative of the sample as a whole.

Difficulties in defining the CSL from the v versus p′ curves made it difficult to obtain typical critical state parameters for these soils under drained shearing. However, based on the all observed results on natural and destructured soils a rough estimation was made to obtain the critical state parameters for these soils. The M value was estimated from the slope of the critical state line drawn in figures 8.5 and 8.21. The approximate critical state parameters obtained are listed in Table 8.6 and these values can be compared with the values quoted by Atkinson (1993) and Allman and Atkinson (1992) as mentioned in section 7.7.3 of Chapter 7.

Table: 8.6 Critical state parameters of borehole three samples

Soil	λ	Γ	M
Tropical clay, Dhaka (borehole three)	0.05	1.75	0.84

Atkinson (1993) mentioned that the critical state parameters for a particular soil are generally considered to be constant. As only a limited number of tests approached a true critical state condition, the quoted values might not be representative.

8.6. Comparison between failure surfaces of three boreholes

By taking the natural variability of the samples at different sites into account, a comparison is made between the natural failure surfaces obtained from three borehole samples under undrained and drained shearing in figure 8.35. A closer agreement was found between the undrained and drained failure surfaces at low confining pressures. A significant difference between the two undrained natural failure surfaces was observed at high confining pressures. The lower strength of borehole two was explained in Chapter 7 to be due to the higher clay fraction and lower sand fraction compared to borehole one. Although some natural variability in terms of composition, degrees of weathering, colour mottling and local facies variations is inevitable between the samples of different boreholes, the variation between the undrained (boreholes one and two) and drained (borehole three) failure surfaces at high confining pressures might be due to the changes in stress path direction and the type of shearing. The undrained stress paths follow very different stress paths than the drained tests due to generation of excess p.w.p. changes during shear. The generation of excess p.w.p. changes from low to high confining pressures also varies. As a result rotation of stress paths in undrained shearing was observed. The rotation of stress path gives different failure surfaces (Malandraki and Toll, 2000). Malandraki and Toll (2000) also pointed out that the differences in failure

surface might well be due to differences in volumetric strain behaviour. Therefore, the failure surface of natural soils is affected at high confining pressures by stress path direction and the type of shearing. Malandraki and Toll (2000) observed a close agreement between the undrained and drained failure surfaces for the case where small excess p.w.p. changes were generated during shear. Coop and Atkinson (1993) also reported undrained and drained test results on cemented carbonate sands and noted that the soil's peak shear strength state is affected by the direction of the stress path, the drainage condition and the initial confining pressure.

8.7. Drained characteristics to identify zones of behaviour

Based on all the observed drained characteristics a graph is plotted in figure 8.36 to show the zones of behaviour for the tropical clay soils of Dhaka, Bangladesh. The identified yield surfaces and the natural and destructured failure surfaces are plotted in the q versus p′ space. Three zones of behaviour could be identified from the relative positions of the failure surfaces and the yield surfaces as shown in figure 8.36. It was observed that the failure surface for the natural soils coincides with the destructured failure surface at approximately $p' \cong 1100$ kPa. Below this stress level the natural soils showed higher stress levels than the destructured soils due to their bonded structure.

It can be seen from figure 8.36 that the trend of the bond yield surface and the natural failure surface indicates that they could only coincide at very low mean effective stress levels (near zero). The final yield surface at low confining pressure is also very close to the failure surface of natural soils. Therefore, it might be possible that if there were a zone of coincidence between bond yield and failure (Zone 1), it would only be at very low stress levels (p′ less than 5 kPa). Zone 1 is not clearly

observed in this study. However, a zone boundary can be assumed between Zone 1 and Zone 2 as shown in figure 8.36.

The second zone (Zone 2) of behaviour can be identified between a value of p′ at failure less than 5 kPa to approximately 1100 kPa (figure 8.36). It can be seen from figure 8.36 that the bond yield surface in Zone 2 occurred at lower deviator stresses than the final yield surface and the natural failure surface. The bond yield surface curved down and showed a tendency to meet with the p′ axis below 400 kPa. This is consistent with the observations that no clear trend of yield points was identified at effective confining pressure of 400 kPa and greater.

It can also be seen from figure 8.36 that the natural failure surface exists at higher deviator stresses than the destructured failure surface due to the presence of bonding in the natural soils. In Zone 2, the slope of the natural failure surface decreased slightly with increasing p′ and then meets the destructured failure surface. The final yield surface in Zone 2 is also very close to the natural failure surface.

Malandraki and Toll (2000) showed that the rotation of the stress path has a direct influence on the size of the three zones of behaviour for the bonded soil. The shape of the zone boundary between Zone 2 and 3 will be consistent with the effective stress path direction. It can be seen from figure 8.5 and 8.36 that the drained stress paths (3dn50 to 3dn600) for natural soils failed on the natural failure surface and the stress path 3dn800 failed on the destructured failure surface. As the stress paths at very high mean effective stress level is on the destructured failure surface, it means that the stress path is now entering in zone 3. The upper limit of the Zone 2 will be at the coincidence point of the two failure surfaces. A Zone boundary can be assumed between Zone 2 and Zone 3 as shown in figure 8.36, which rises at slope 3:1 from the initial stress state.

It is clear that the drained behaviour for samples from borehole three broadly shows the same features as the undrained tests on borehole one samples. The bond yield surface shown in figure 8.36 appears to meet the isotropic axis at $p' \cong 400$ kPa, at an isotropic stress level well below the zone 2 and 3 boundary ($p' \cong 750$ kPa). Again, this indicates that bonding is still present even after the bond yield surface showed a tendency to meet with the isotropic axis at approximately $p' \cong 400$ kPa.

8.8 Summary

In this chapter the drained stress-strain behaviour of the tropical clay soils of Dhaka was discussed in terms of stress-strain curves, stress paths and volumetric strains. Stiffness and yielding characteristics were discussed. A comparison has been made between the drained test results of natural and destructured soils. Finally drained characteristics to identify zones of behaviour for the tropical clay soils of Dhaka, Bangladesh are discussed.

At low confining pressures both the natural and destructured soils of borehole three did not show a prominent peak, but at high confining pressures both types of samples showed a maximum deviator stress level with an identifiable peak. The destructured samples in each case showed lower maximum deviator stress levels, lower stiffness and larger strains to reach maximum deviator stress than the natural samples, which is due to breakdown of bonds. Leroueil and Vaughan (1990) pointed out that the change of properties, which results from destructuring, is an indication of the initial presence of structure. Therefore, there is clear evidence that the natural soils are bonded.

It was found that the natural samples initially showed a contraction and then dilation at very large strain. Conversely, the destructured samples only showed contraction until the end of shearing. It was observed that the specific volume for tests at 50 and 200 kPa in both natural and destructured state, falls below (denser than) the critical state. Conversely the specific volume for two tests at 300 kPa and 800 kPa which show contraction in both the natural and destructured state, falls above (looser than) the critical state. Other tests (400, 500 and 600 kPa) do show anomalies in defining the critical state.

A significant difference between the natural and destructured failure surfaces was observed due to the presence of bonds in natural soils. The natural failure surface initially showed a curvature with the increase of p′ up to approximately p′ > 300 kPa and after that the slope of the natural failure surface reduces steadily as p′ increases. A clear difference between the very loose and very dense samples showed a clear change of behaviour in the failure envelope.

Tangential stiffness and small strain contours were also evaluated. A loss of stiffness values was observed when the small strain contours approached the failure surface with increasing strain. It was observed that tangential stiffness values decreased with increasing strain. The natural strain contours in each case showed higher stiffness values than the destructured soils due to the presence of bonded structure of the natural soils. The highest value of G_{tan} calculated for natural soil is approximately 250 MPa at 0.01% strain and approximately 80 MPa for destructured soils of the same strain contour. At 1% strain stiffness values of the two soils were close to each other.

Two yield surfaces were found to occur for natural tropical clay soils of Dhaka below the final yield surface and the failure surface under drained shearing. The

bond yield surface appears to curve down towards the isotropic axis before p′ ≅ 400kPa, confirming that bond breakdown would occur in isotropic compression for tests at higher confining pressures, as no yield would be seen during shear.

A distinctive difference between the natural failure surfaces of three boreholes was observed under undrained and drained shearing. The failure surface might be affected by the rotation of the stress path and the type of shearing.

From the observed drained characteristics, broadly three zones of behaviour could be identified for the tropical clay soils of Dhaka.The observed drained results suggest that if there were a zone of coincidence between bond yield and failure surface (Zone 1), it would only be at very low stress levels (p′ less than 5 kPa). It is not clearly observed in this study. The Zone 2 is identified between a value of p′ at failure from less than 5 kPa to approximately 1100 kPa. In this zone the bond yield surface showed a tendency to meet with the p′ axis below 400 kPa. This is consistent with the observation of no clear trend of yield points at 400kPa or greater. In zone 3, the coincidence of the natural and destructured failure surfaces was observed at approximately p′ ≅ 1100 kPa.

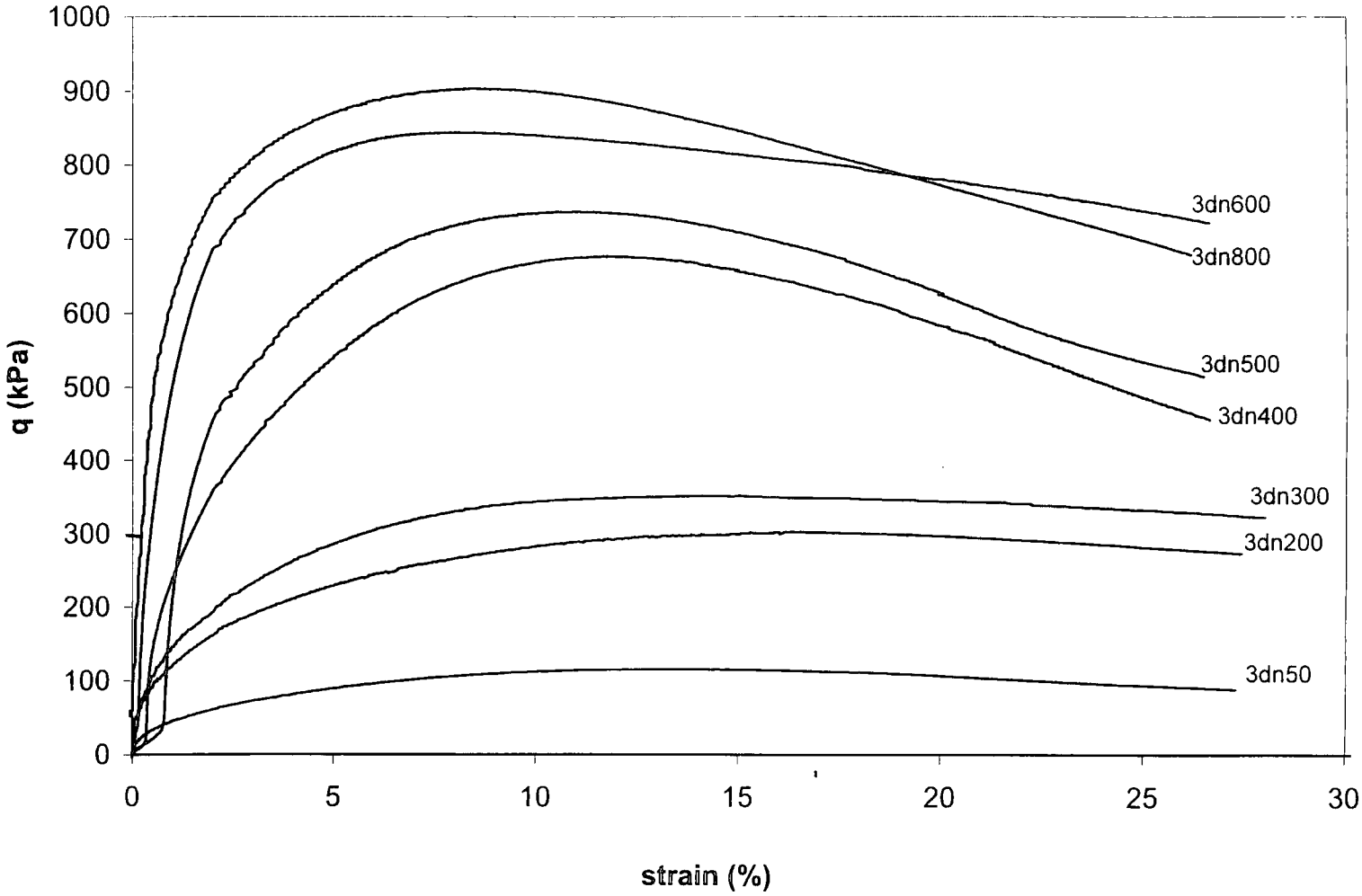

Fig. 8.1 Deviator stress versus axial strain curves for natural soils of borehole three

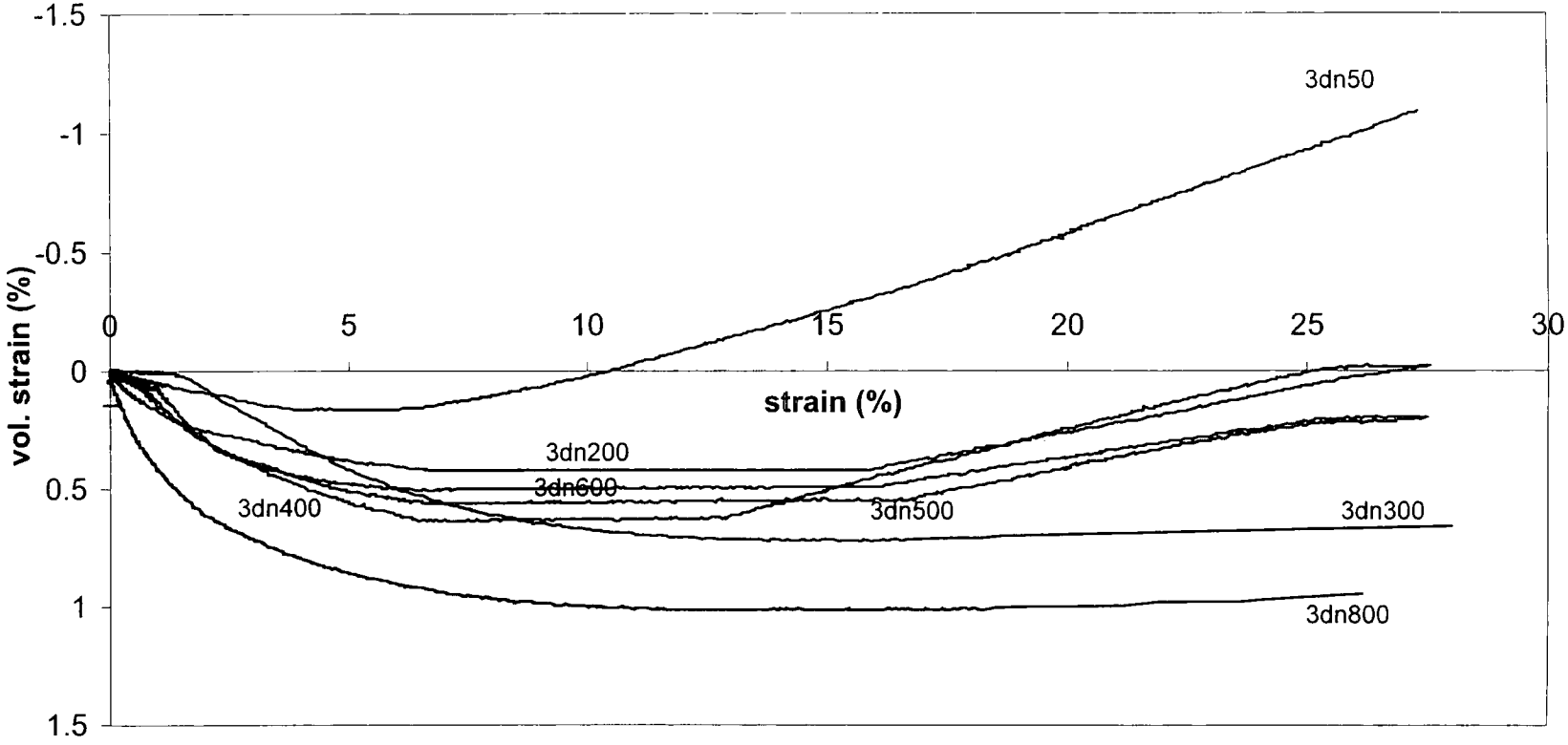

Fig.8.2 Volumetric strain versus axial strain for natural soils of borehole three

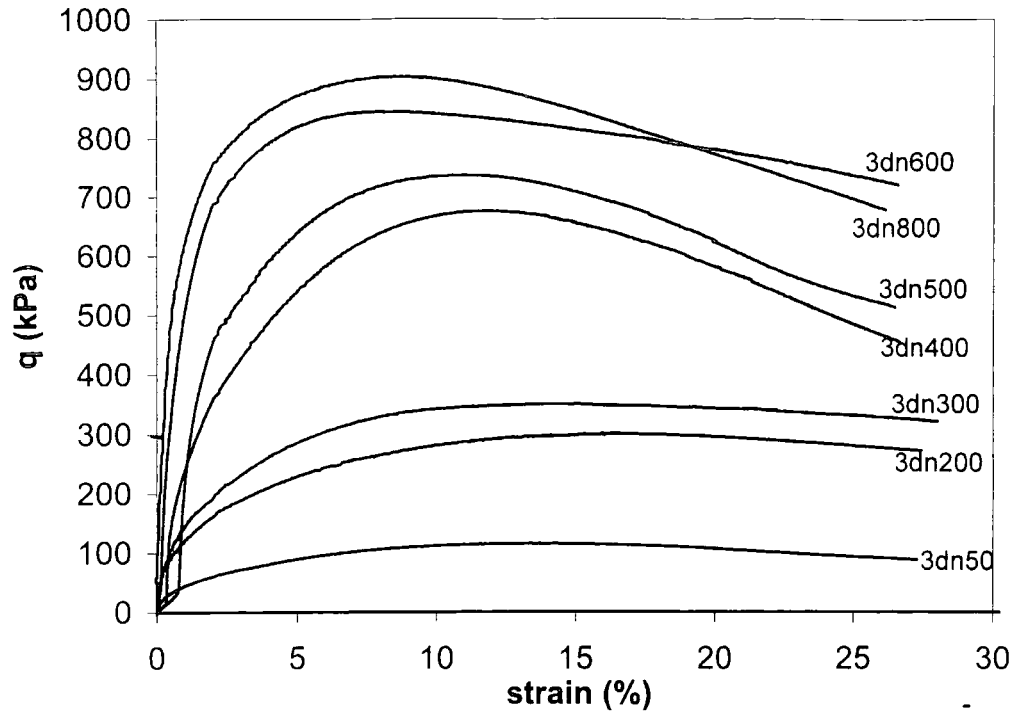

Fig. 8.3 Deviator stress versus axial strain curves for natural soils of borehole three

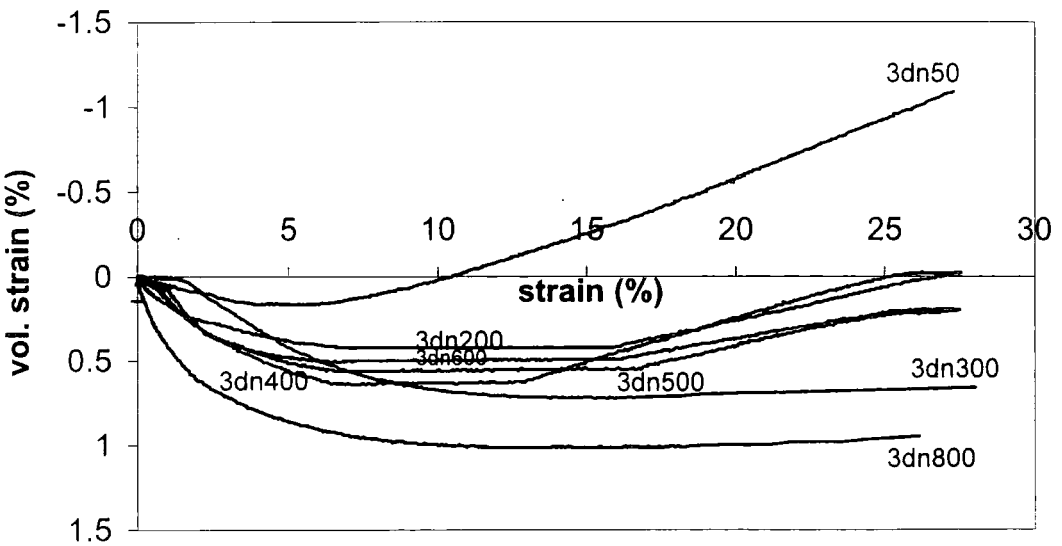

Fig.8.4 Volumetric strain versus axial strain for natural soils of borehole three

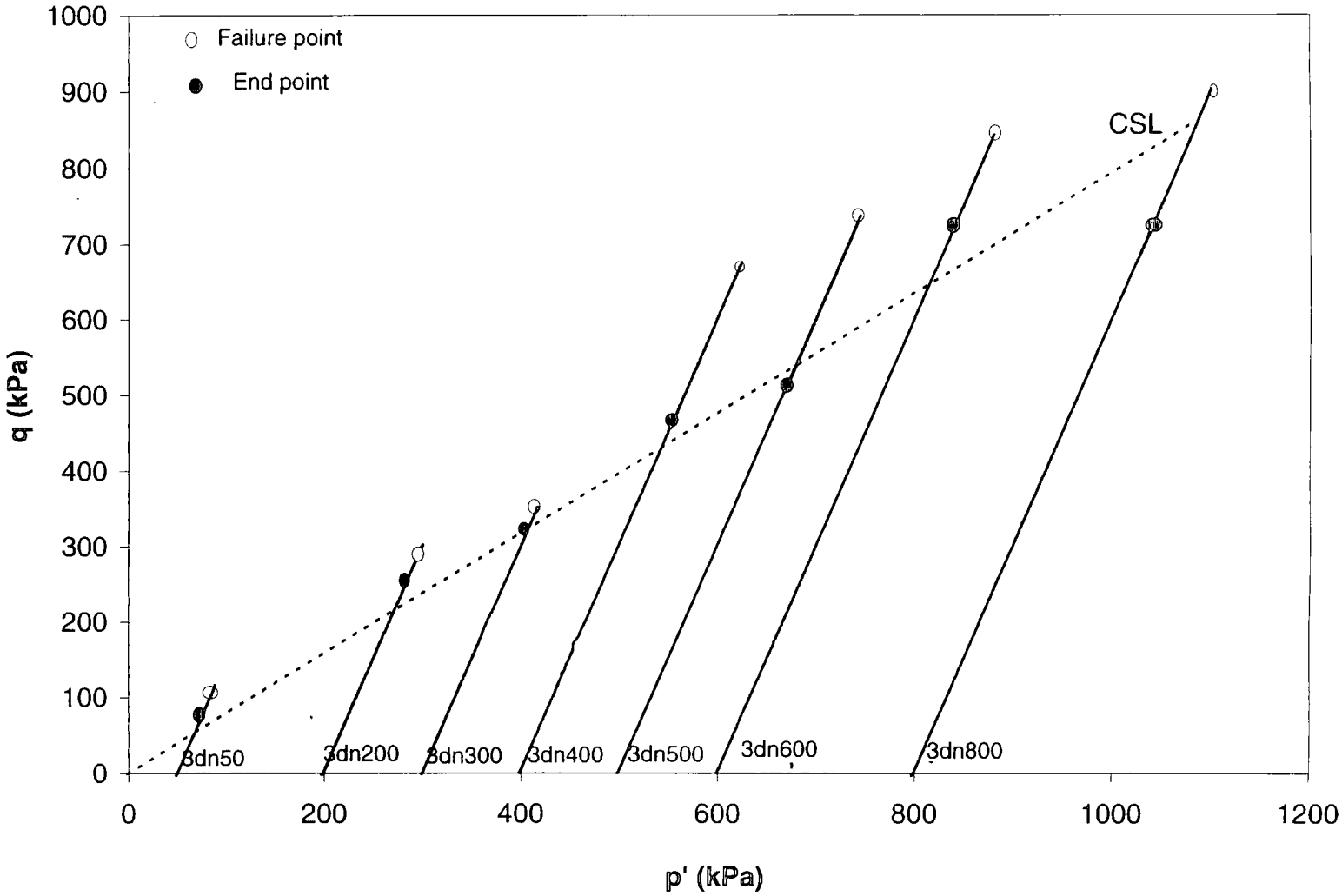

Fig.8.5 Stress paths derived from a series of drained tests on natural soils of borehole three

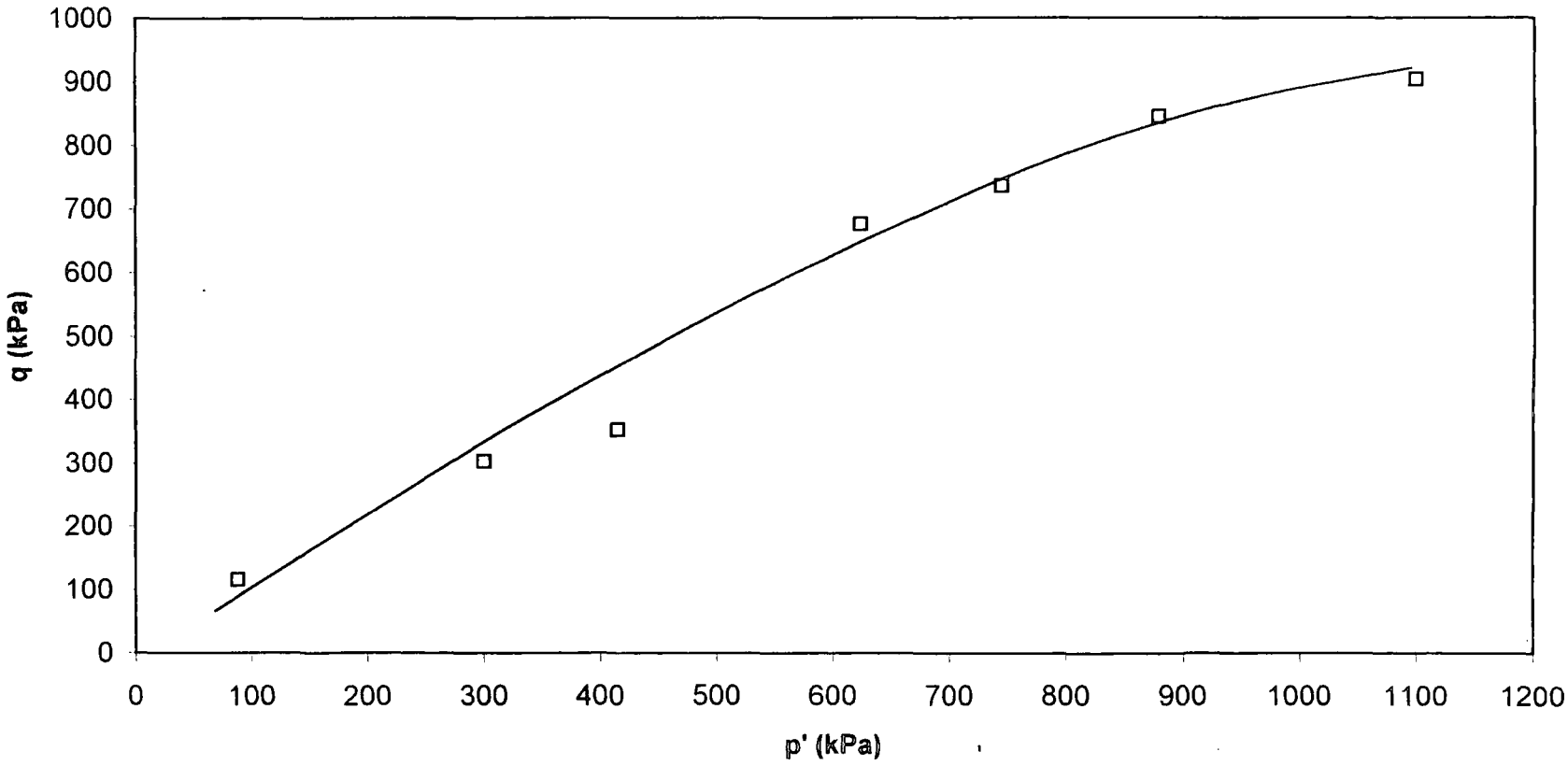

Fig. 8.6 Failure surface for natural soils of borehole three

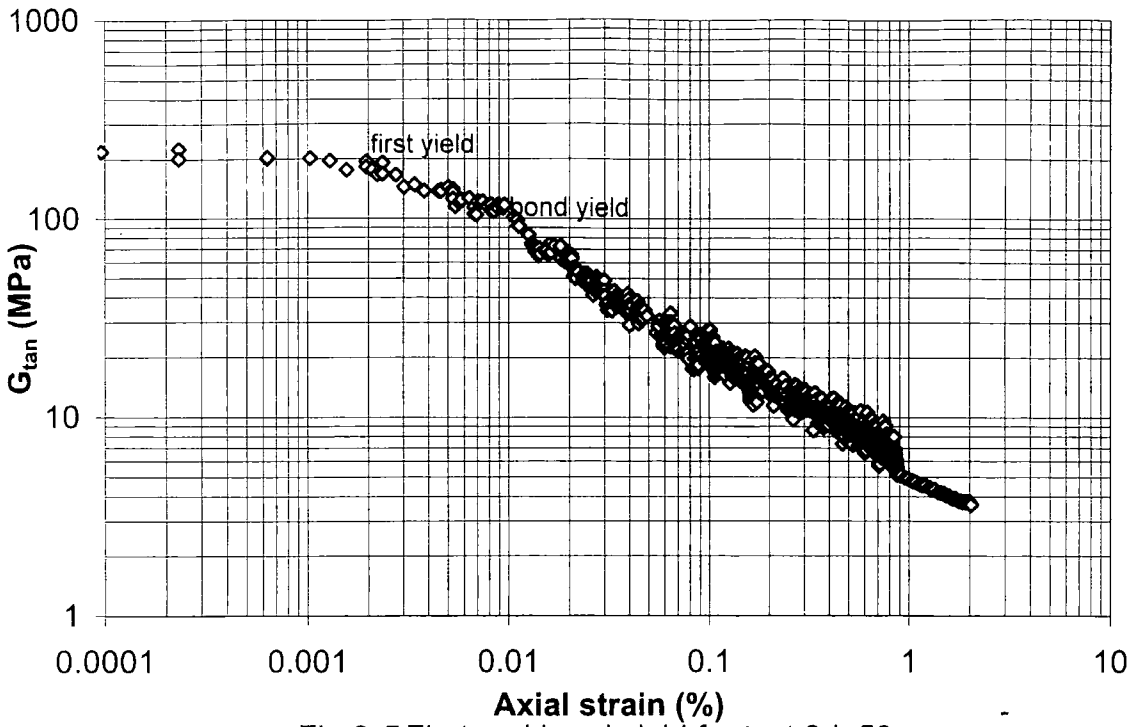

Fig.8.7 First and bond yield for test 3dn50

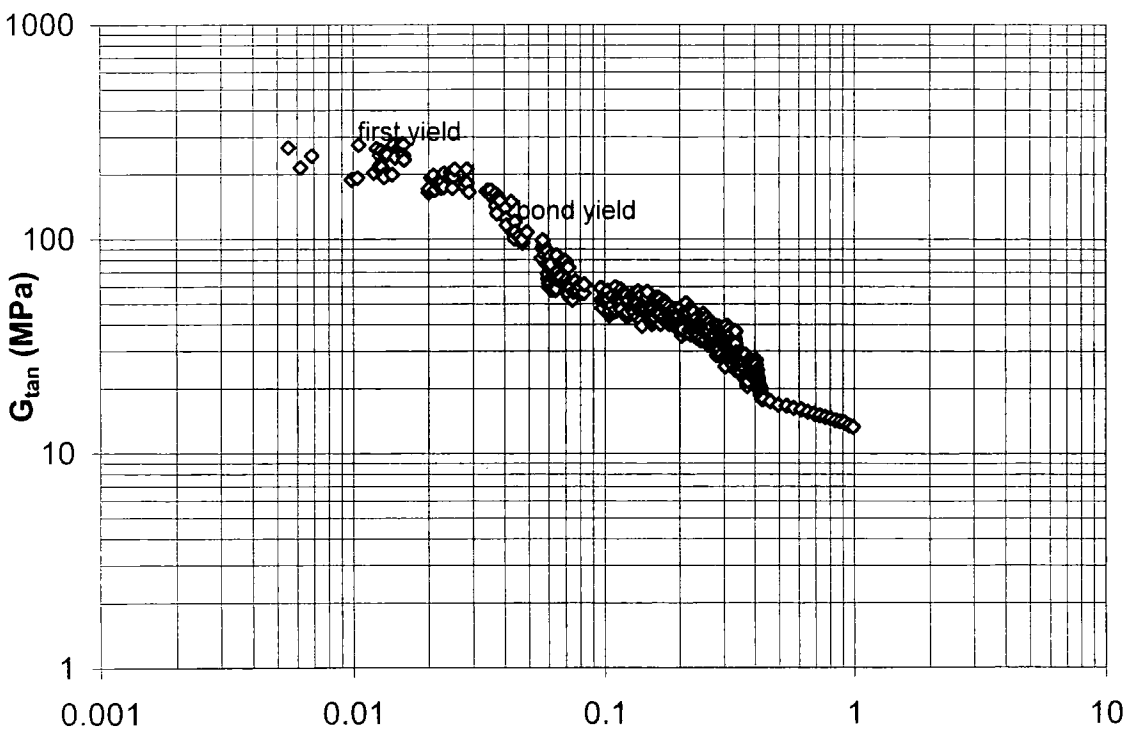

Fig.8.8 First ond bond yield for test 3dn200

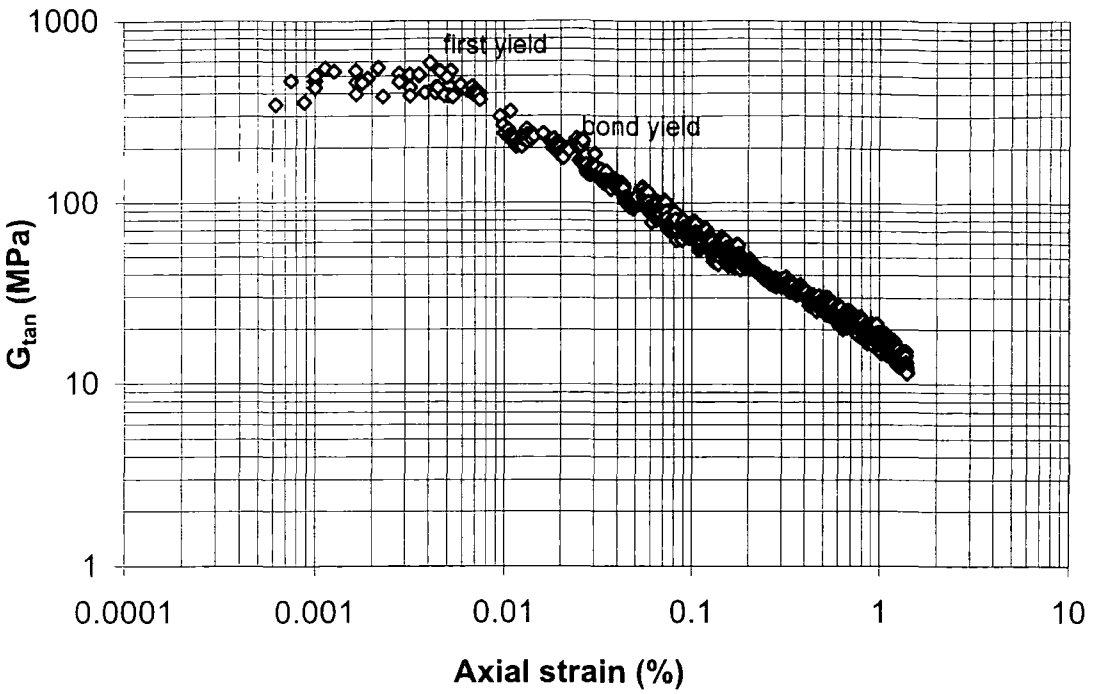

Fig.8.9. First and bond yield for test 3dn300

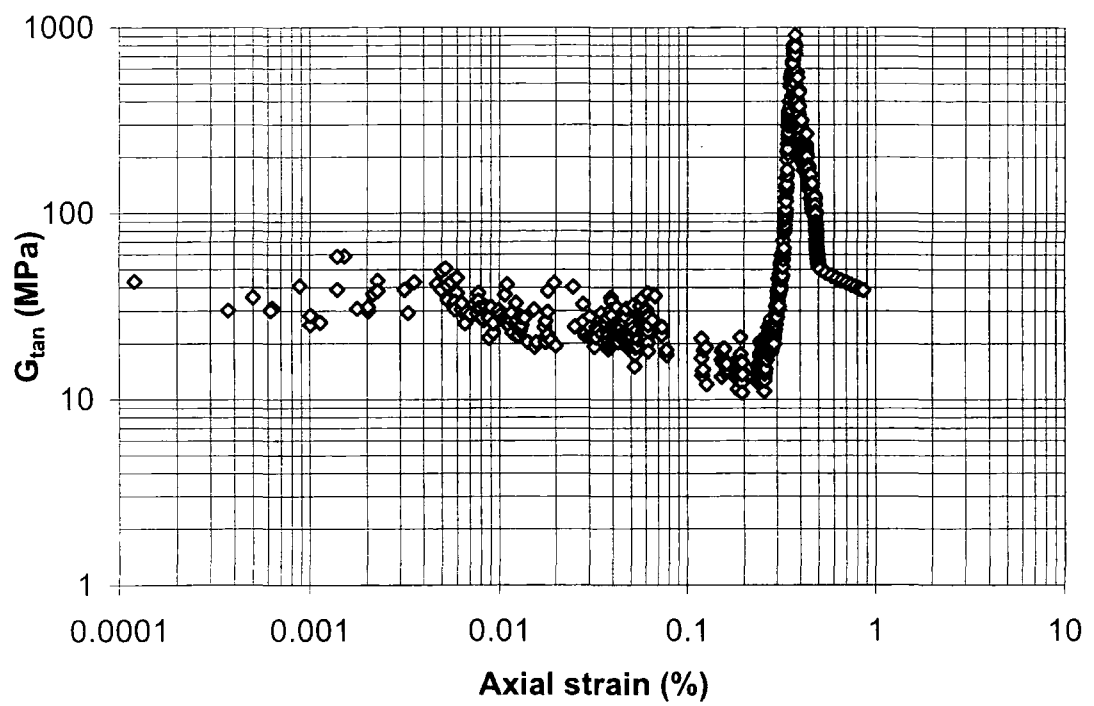

Fig.8.10 Stiffness versus axial strain for test 3dn400

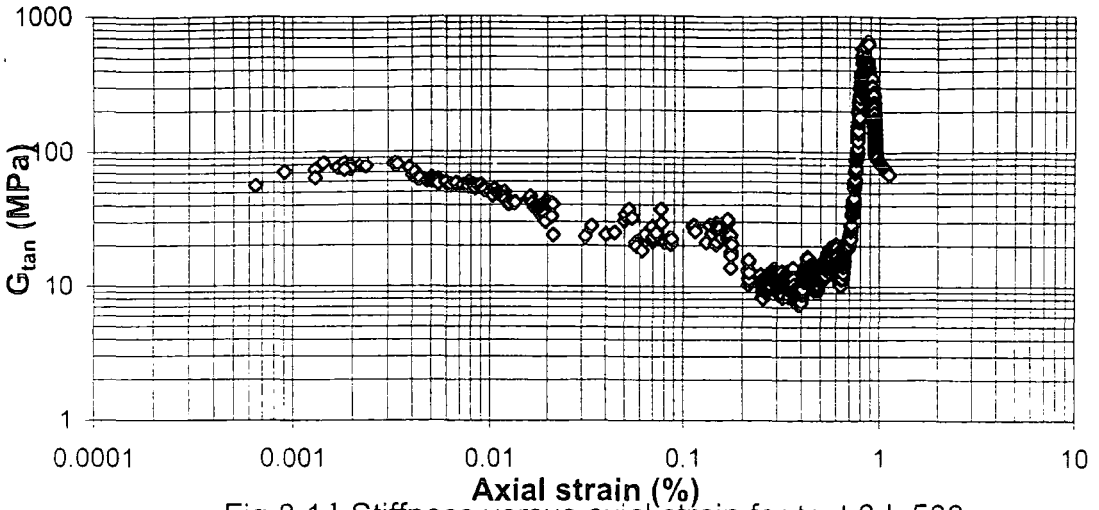

Fig.8.1.1 Stiffness versus axial strain for test 3dn500

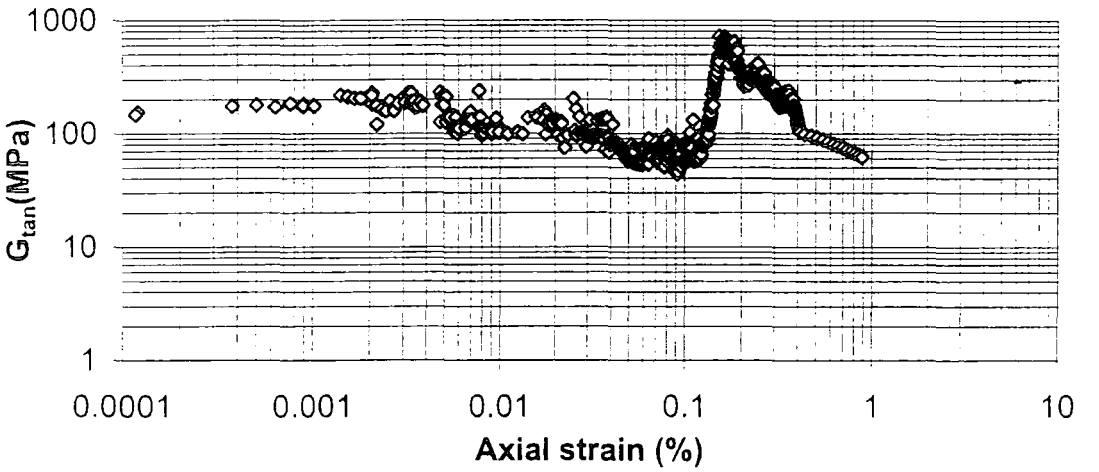

Fig.8.1 2Stiffness versus axial strain for test 3dn600

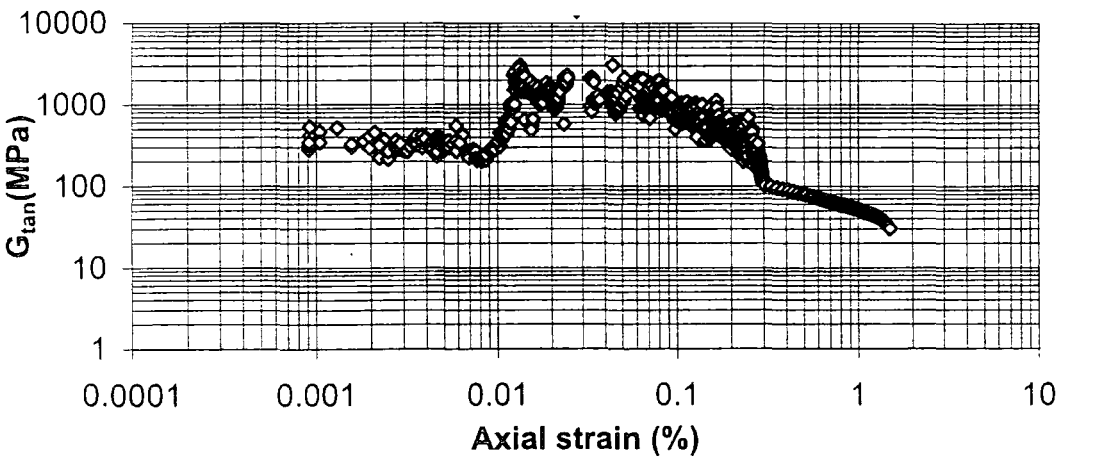

Fig.8.1 3 Stiffness versus axial strain for test 3dn800

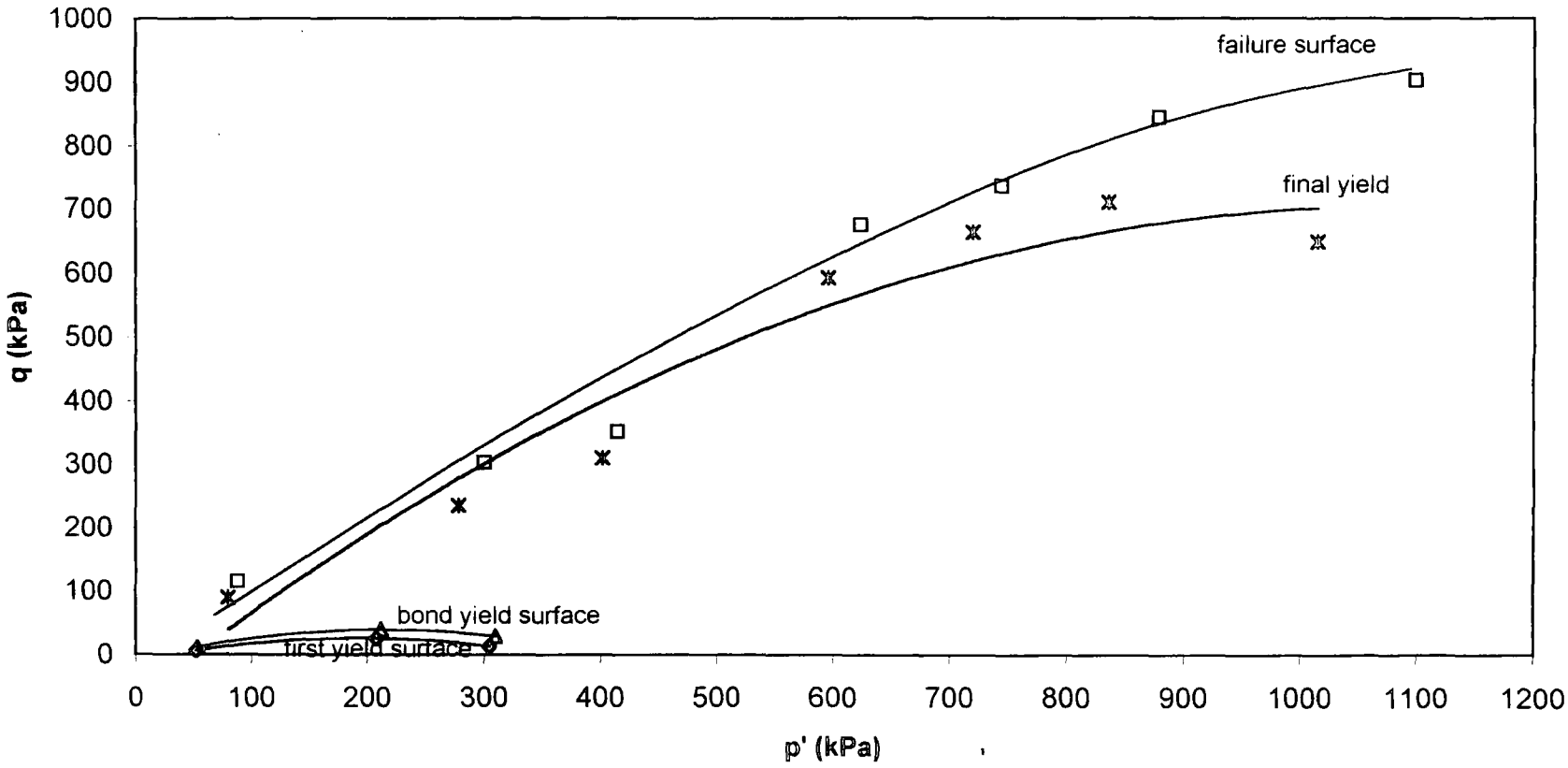

Fig. 8.14 Failure surface and three yield surfaces for natural soils of borehole three

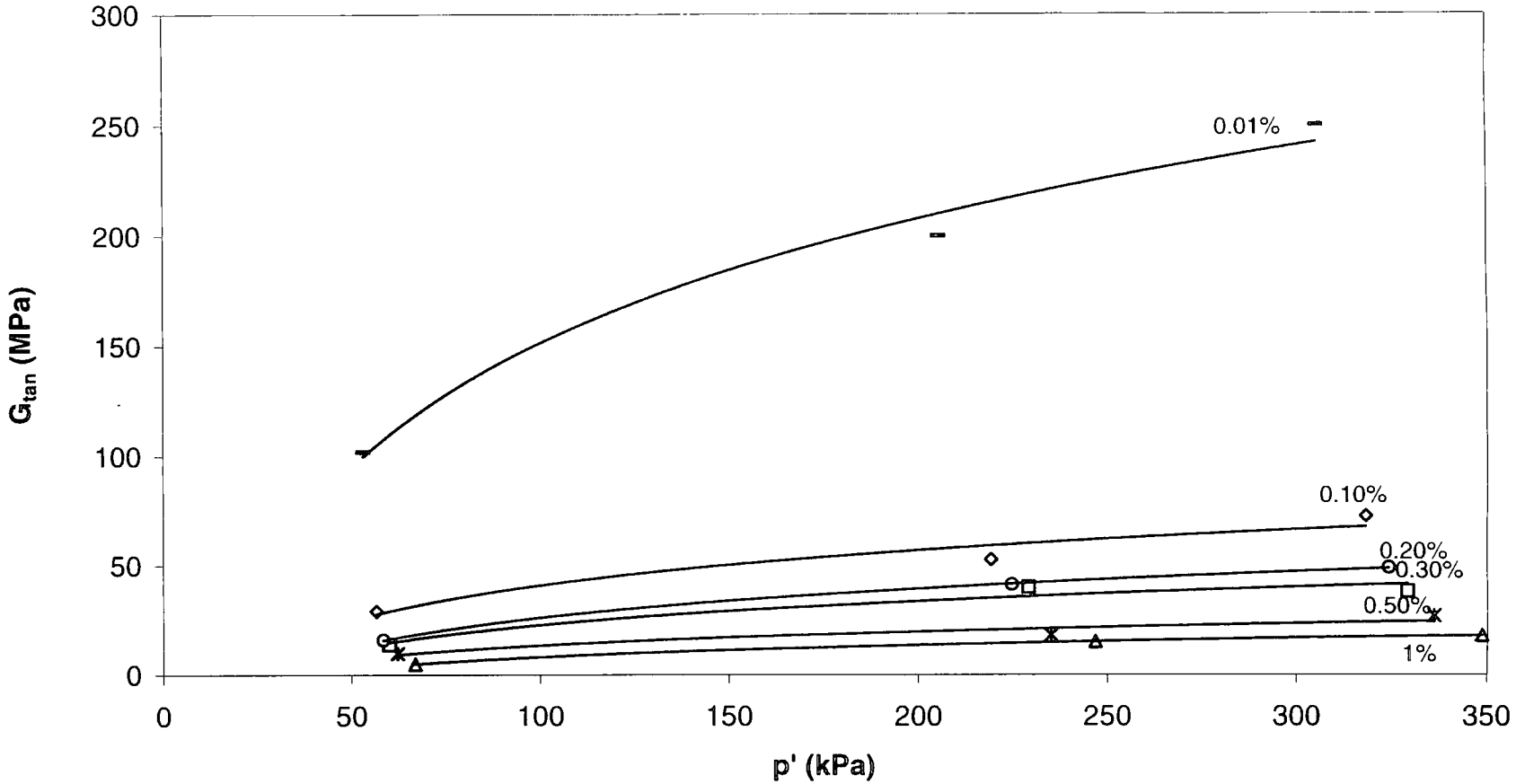

Fig.8.15 Loss in stiffness with increasing strain (from 0.01% to 1%) for natural soils of borehole three

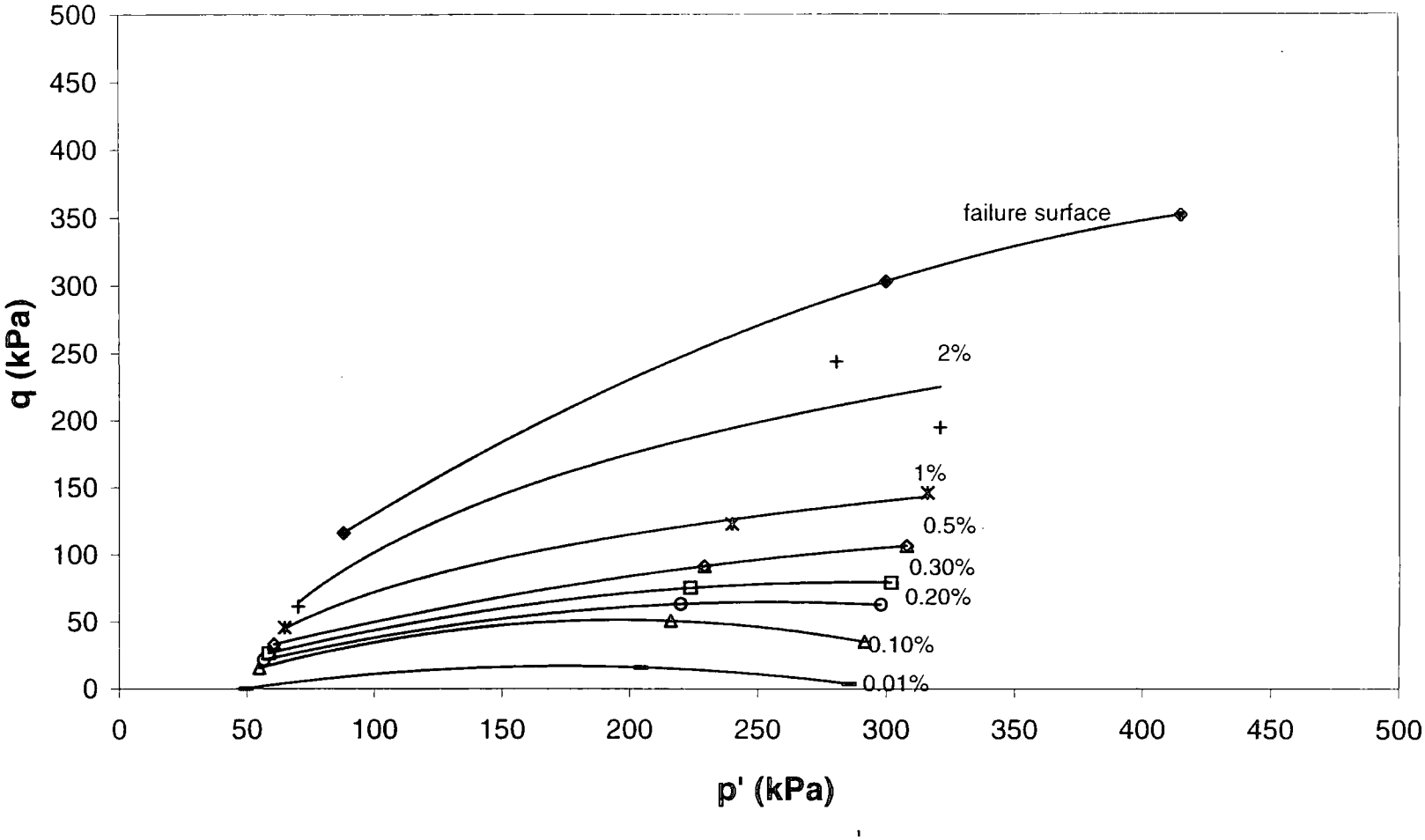

Fig.8.16 Small strain contours (0.01% to 2%) for natural soil of borehole three

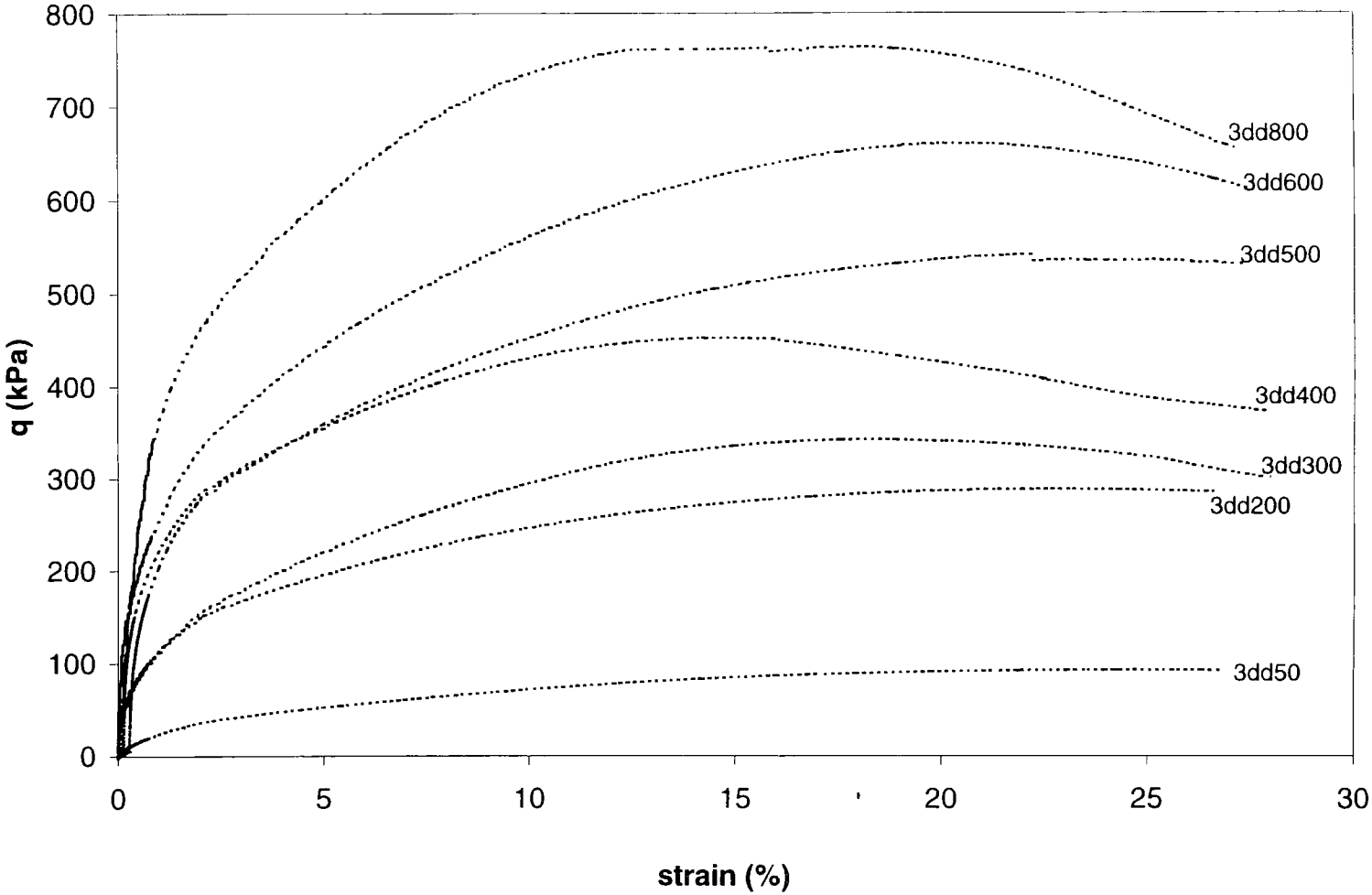

Fig. 8.17 Deviator stress versus axial strain curves for destructured soils of borehole three

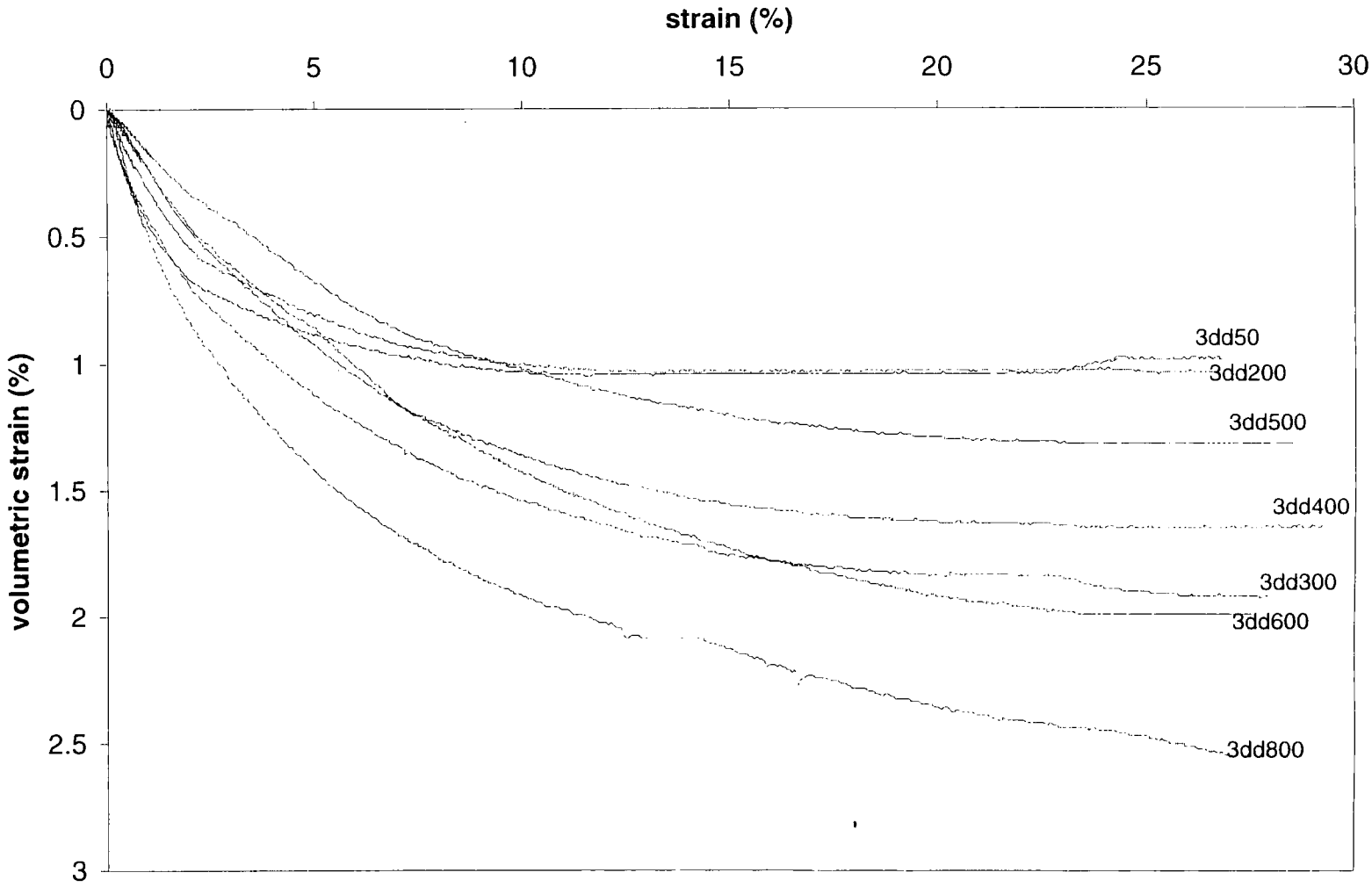

Fig. 8.18 Volumetric strain versus axial strain curves for destructured soils of borehole three

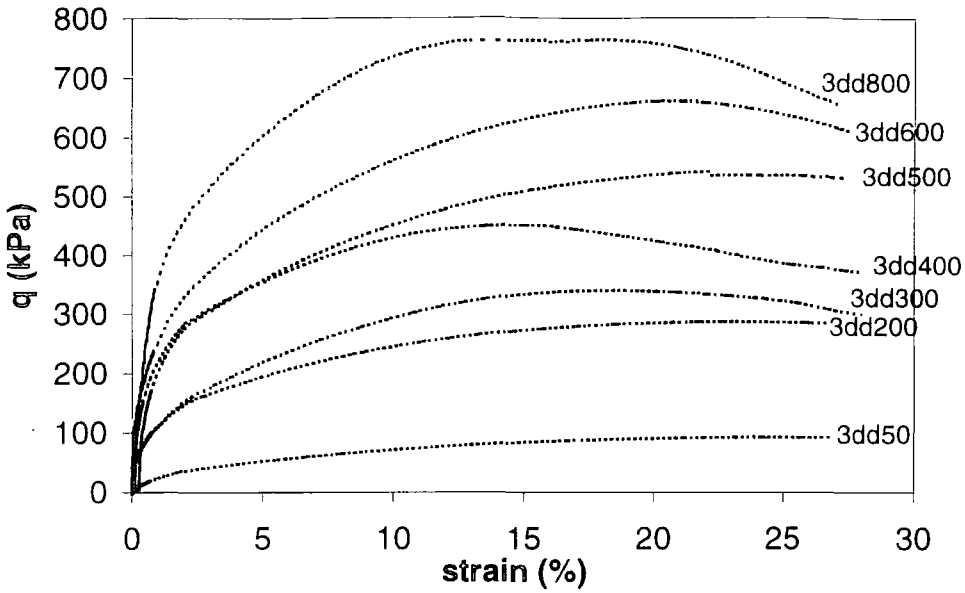

Fig.8.19 Deviator stress versus axial strain curves for destructured soils of borehole three

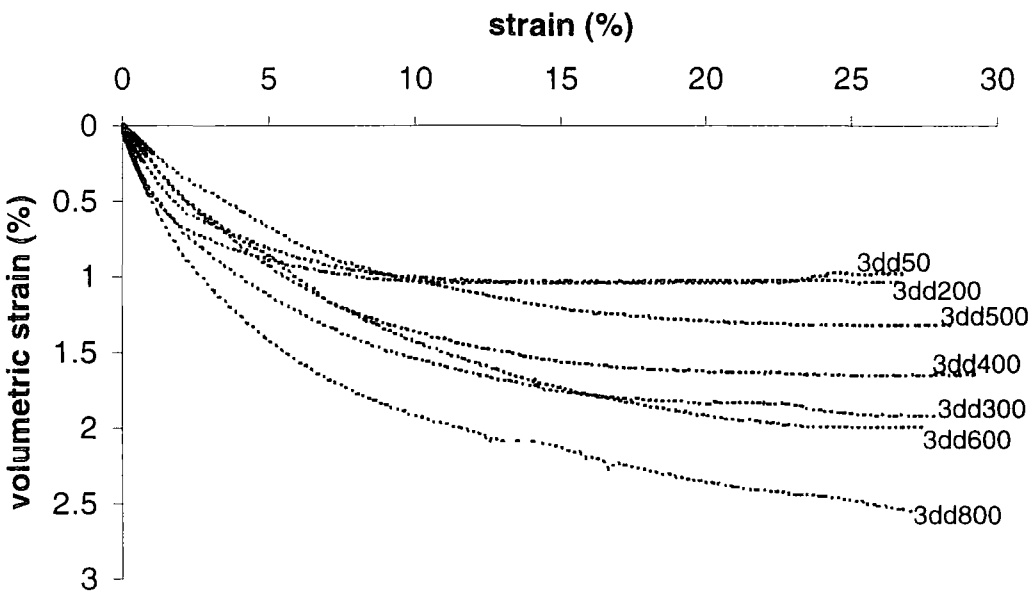

Fig.8.20 Volumetric strain versus axial strain curves for destructured soils of borehole three

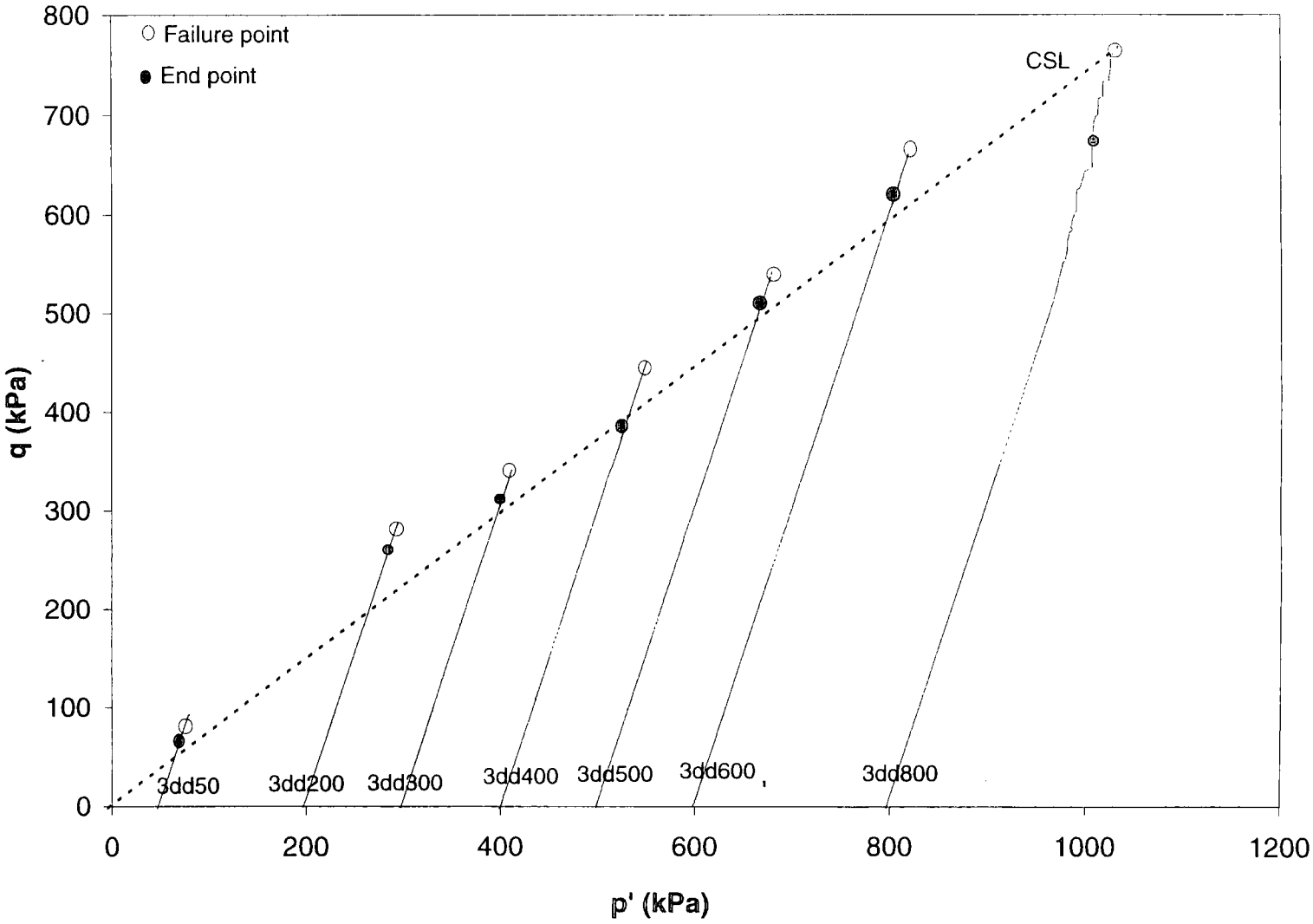

Fig. 8.21 Stress paths derived from a series of drained tests on destructured soils of borehole three

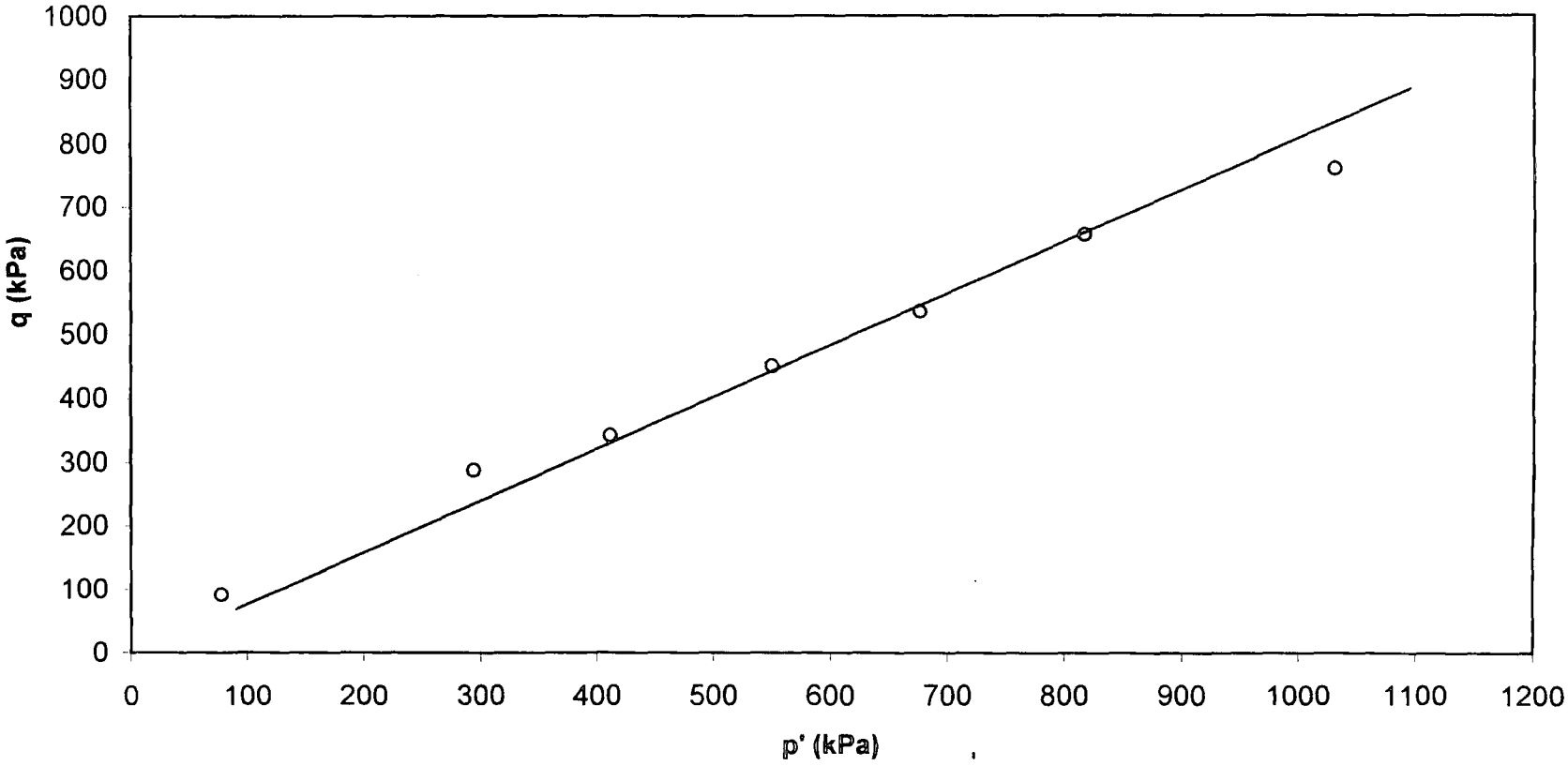

Fig. 8.22 Failure surface for destructured soils of borehole three

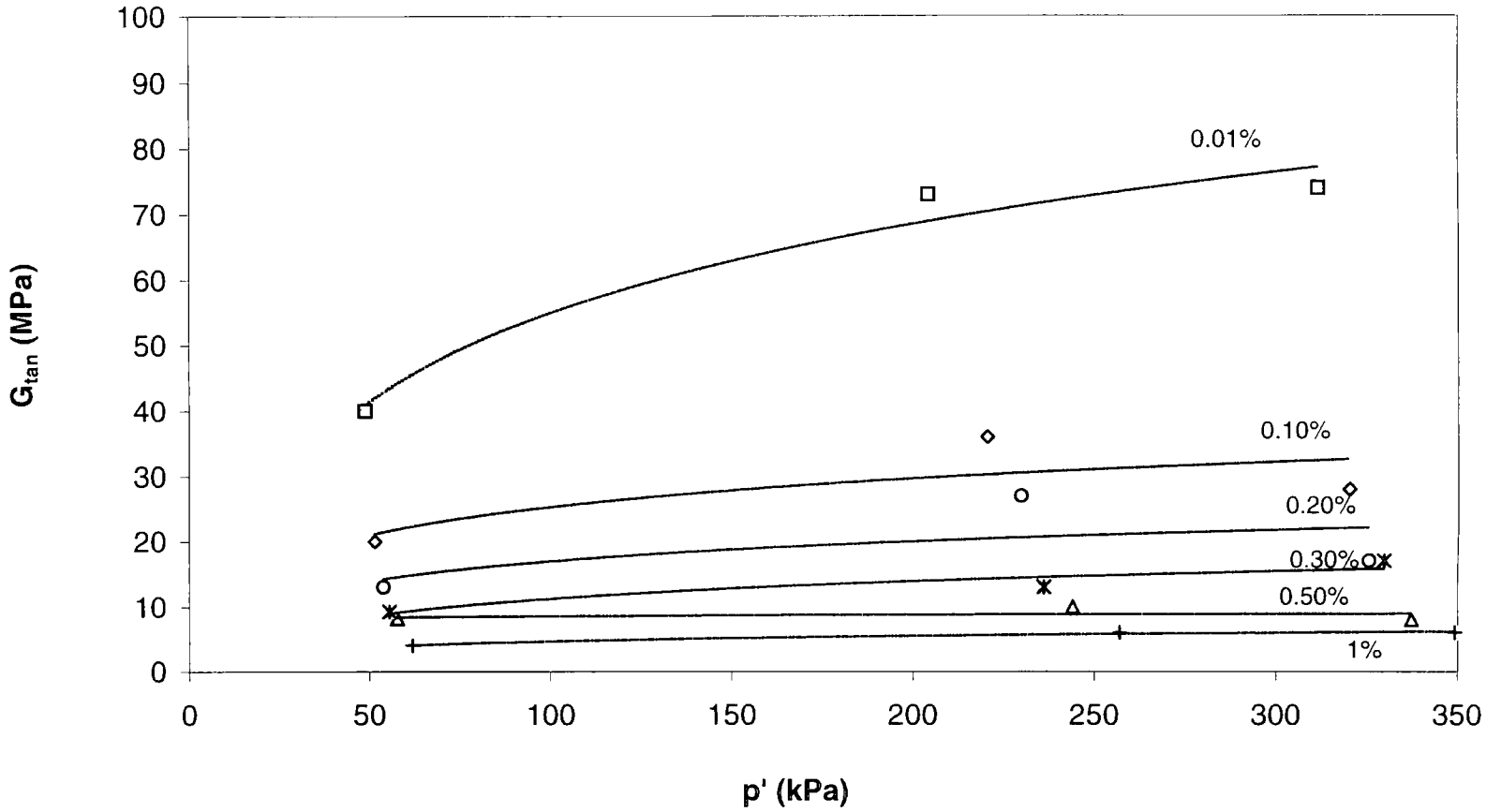

Fig.8.23 Loss in stiffness with increasing strain (0.01% to 1%) for destructured soils of borehole three

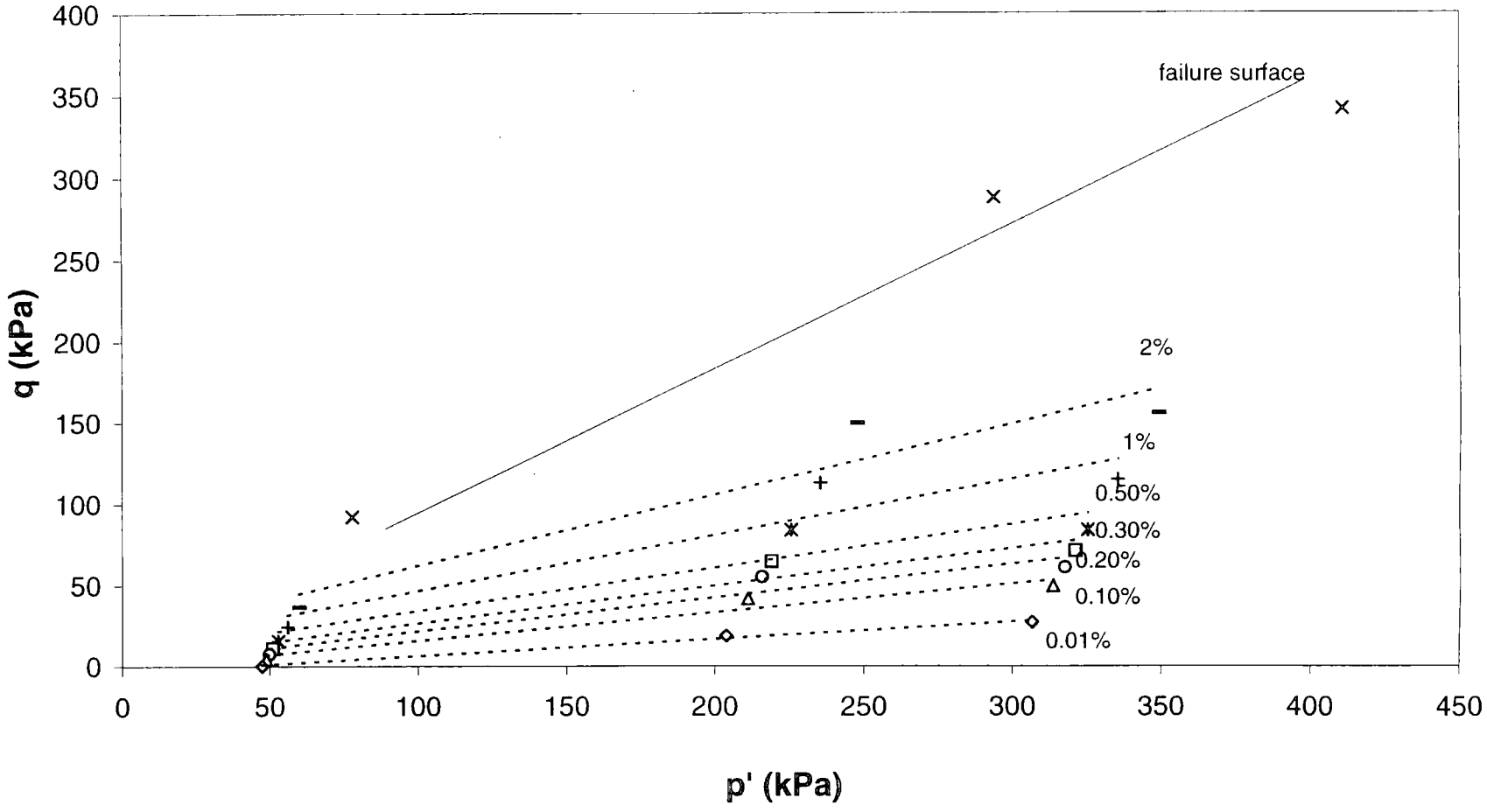

Fig.8.24 Small strain contours (from 0.01% to 2%) for destructured soils of borehole three

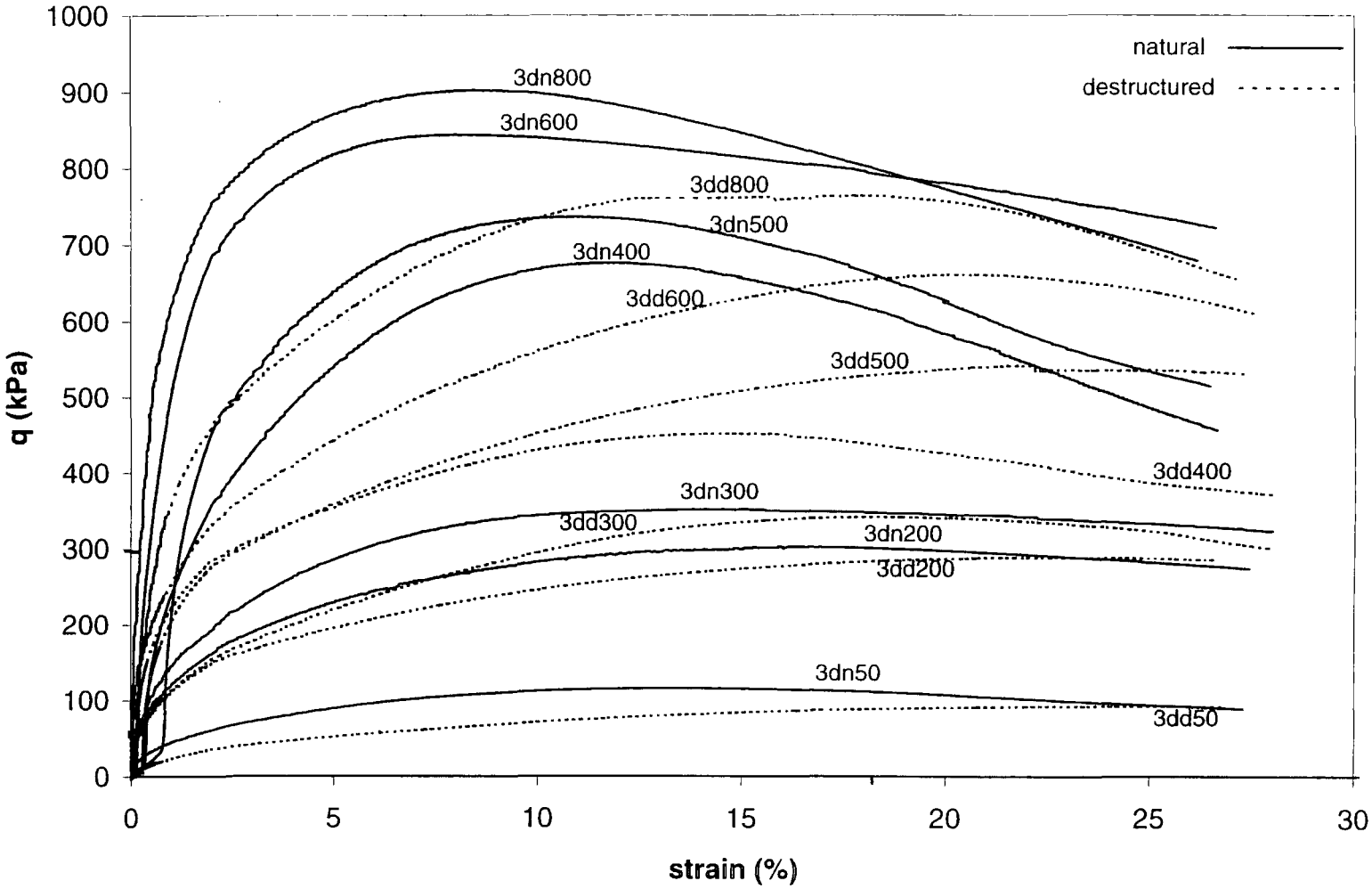

Fig. 8.25 Comparison of deviator stress versus axial strain curves for natural & destructured soils of borehole three

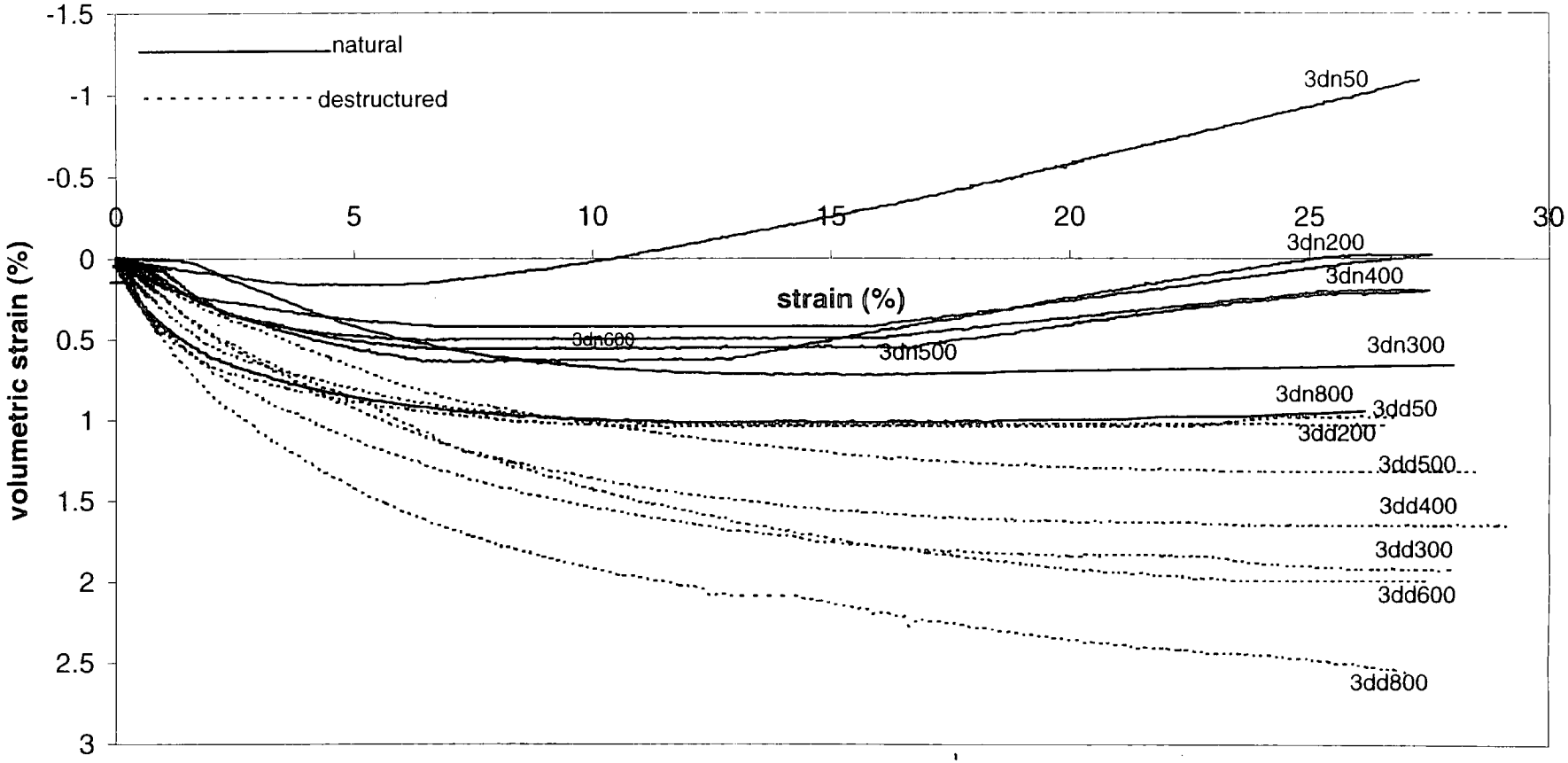

Fig.8.26 Comparison of volumetric strain versus axial strain curves for natural & destructured soils of borehole three

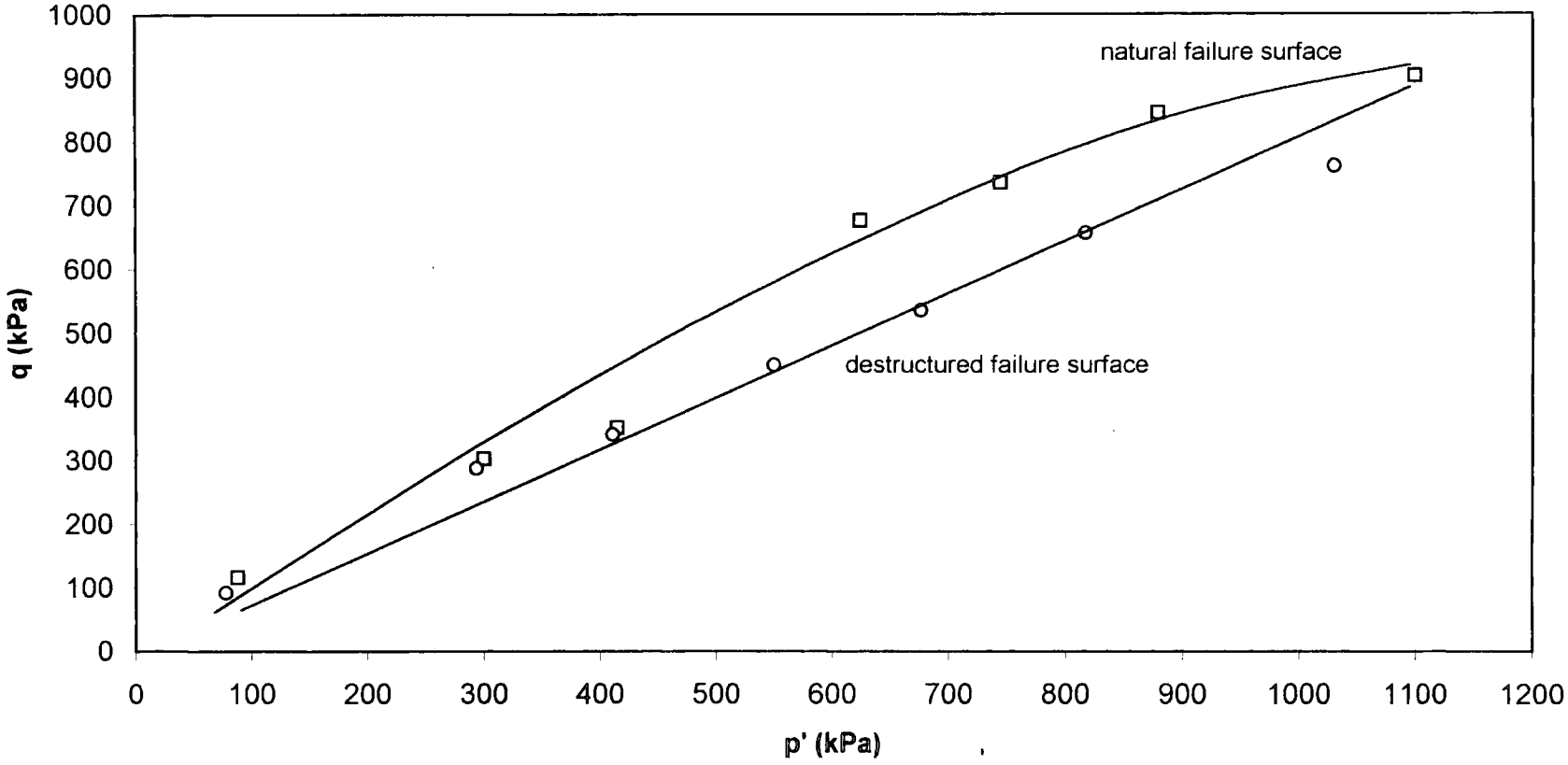

Fig. 8.27 Comparison of failure surfaces for natural and destructured soils of borehole three

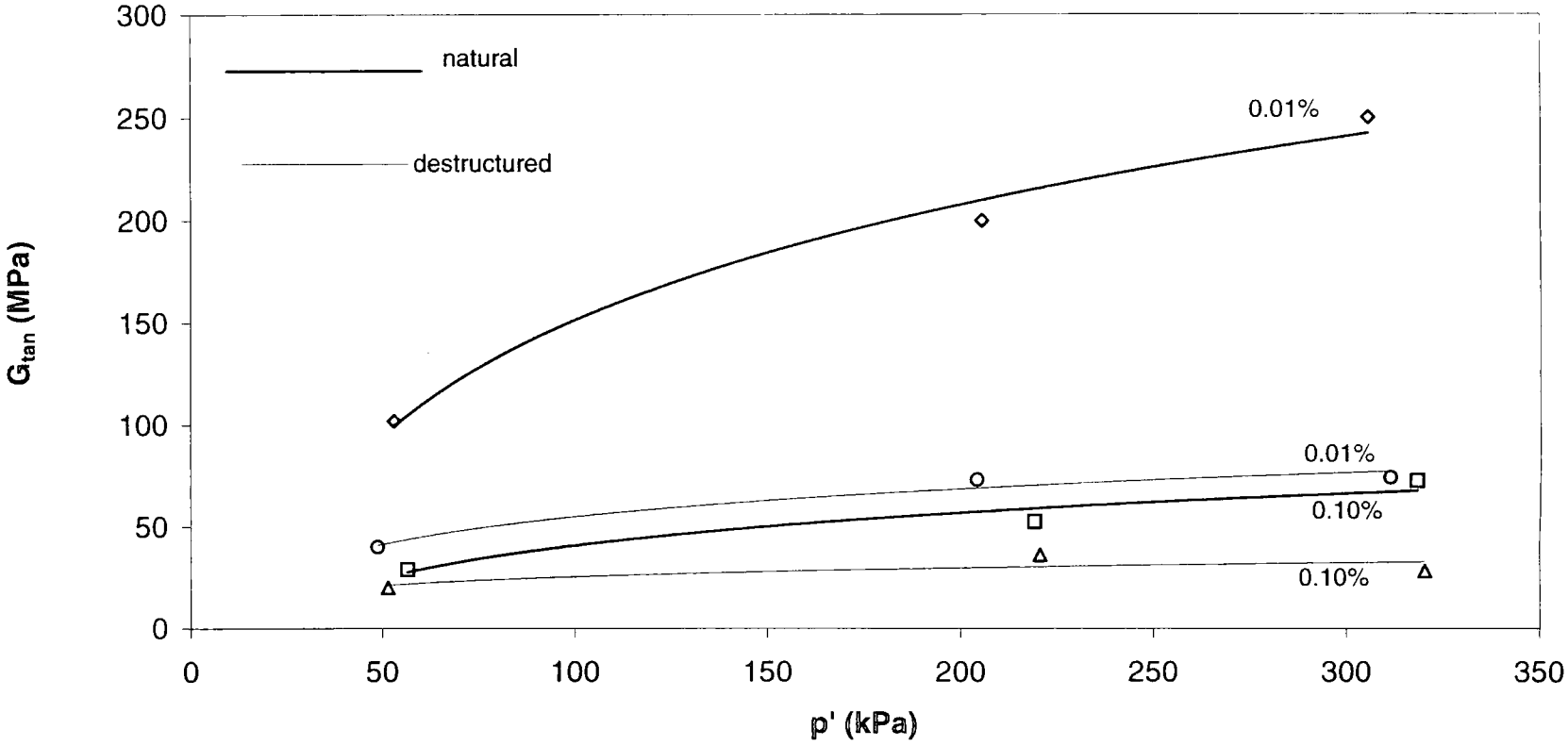

Fig. 8.28 Comparison between stiffness versus p' (0.01% to 0.1%) for natural and destructured soils of borehole three

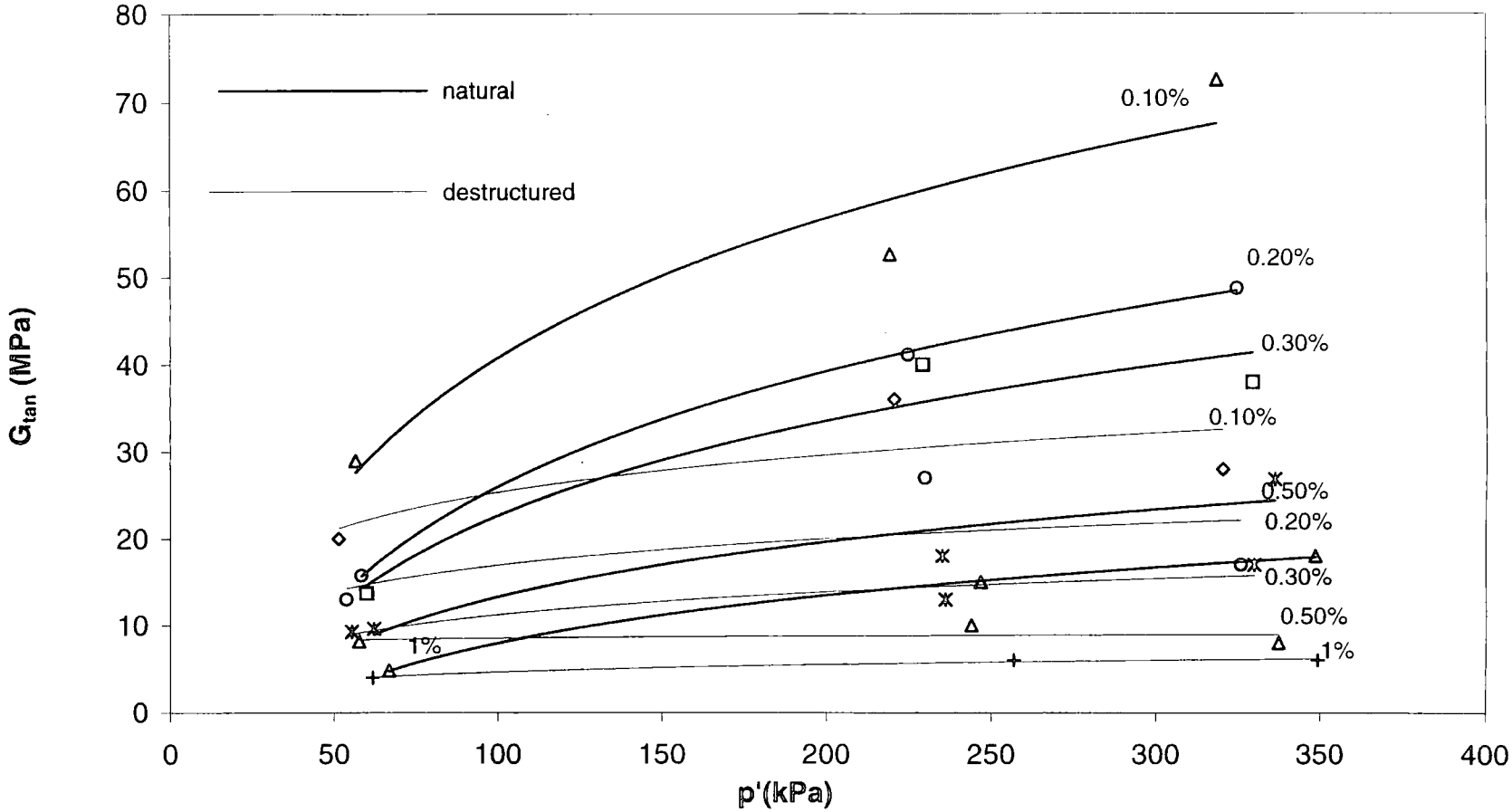

Fig. 8.29 Comparison between stiffness vs. p' (0.1% to 1%) for natural & destructured soils of borehole three

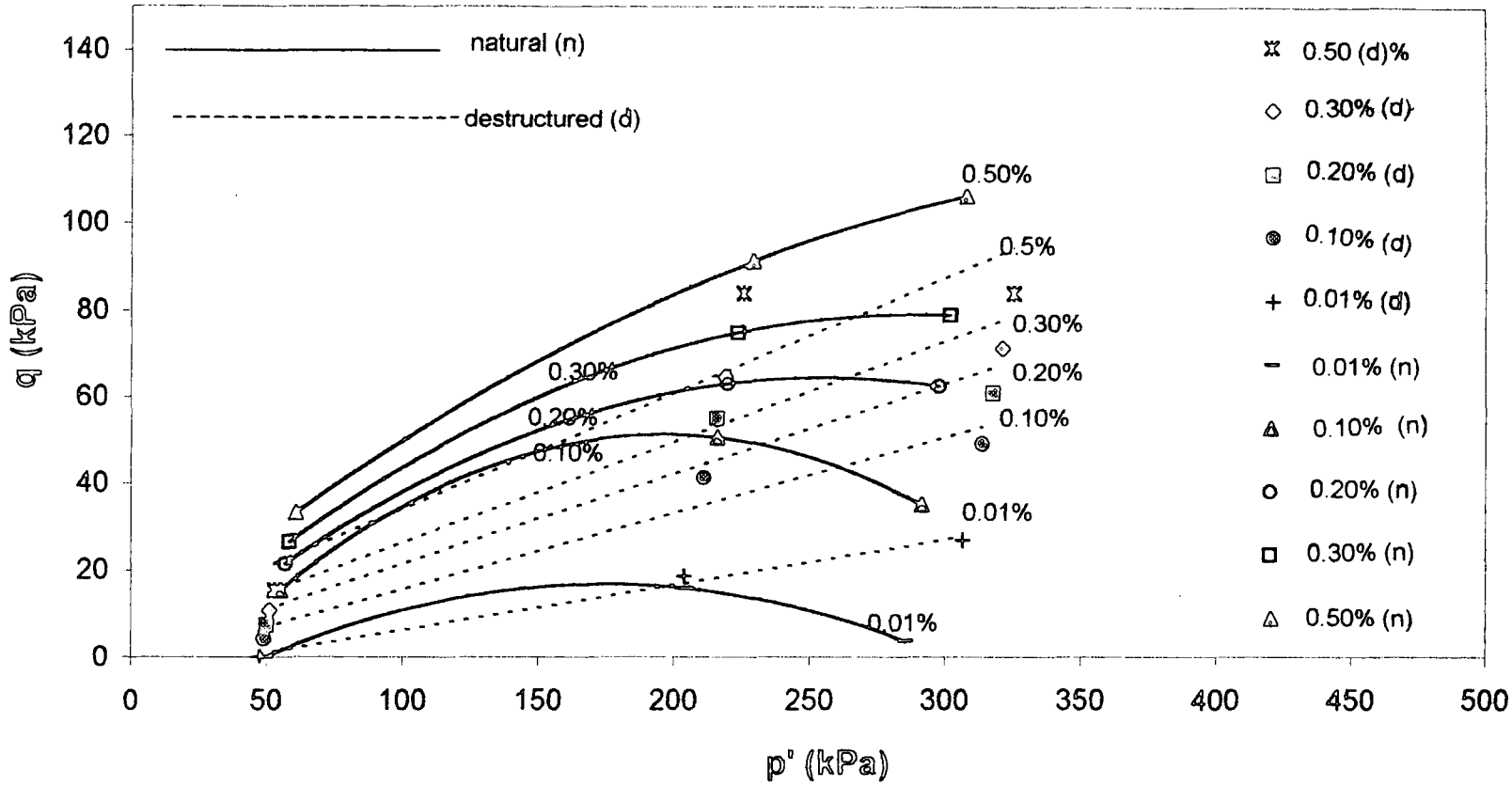

Fig.8.30 Comparison of small strain contours (0.01% to 0.5%) for natural & destructured soils of borehole three

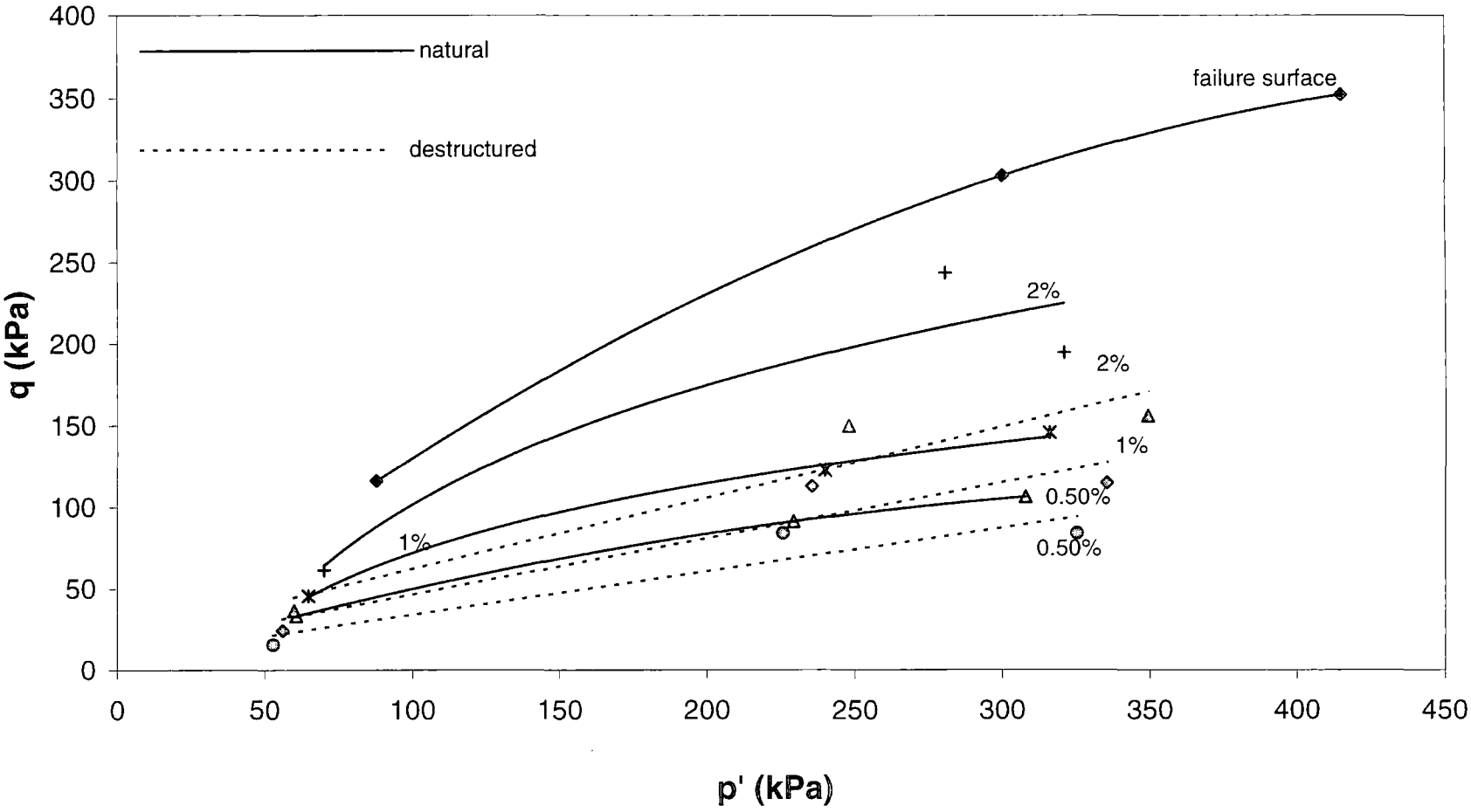

Fig.8.31 Comparison of small strain contours (from 0.5% to 2%) for natural & destructured soils of borehole three

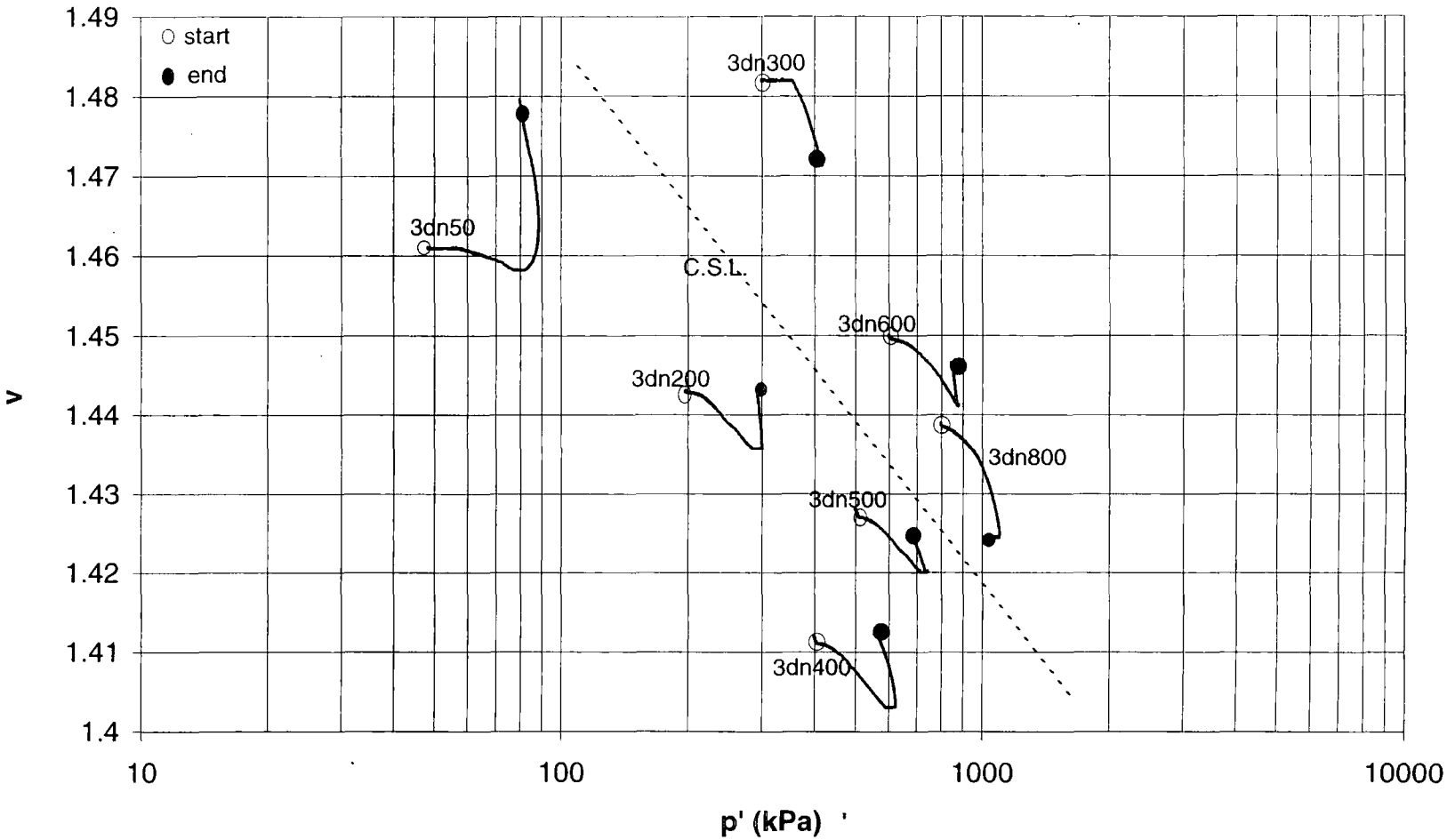

Fig.8.32 Specific volume vs. p' for natural soils of borehole three

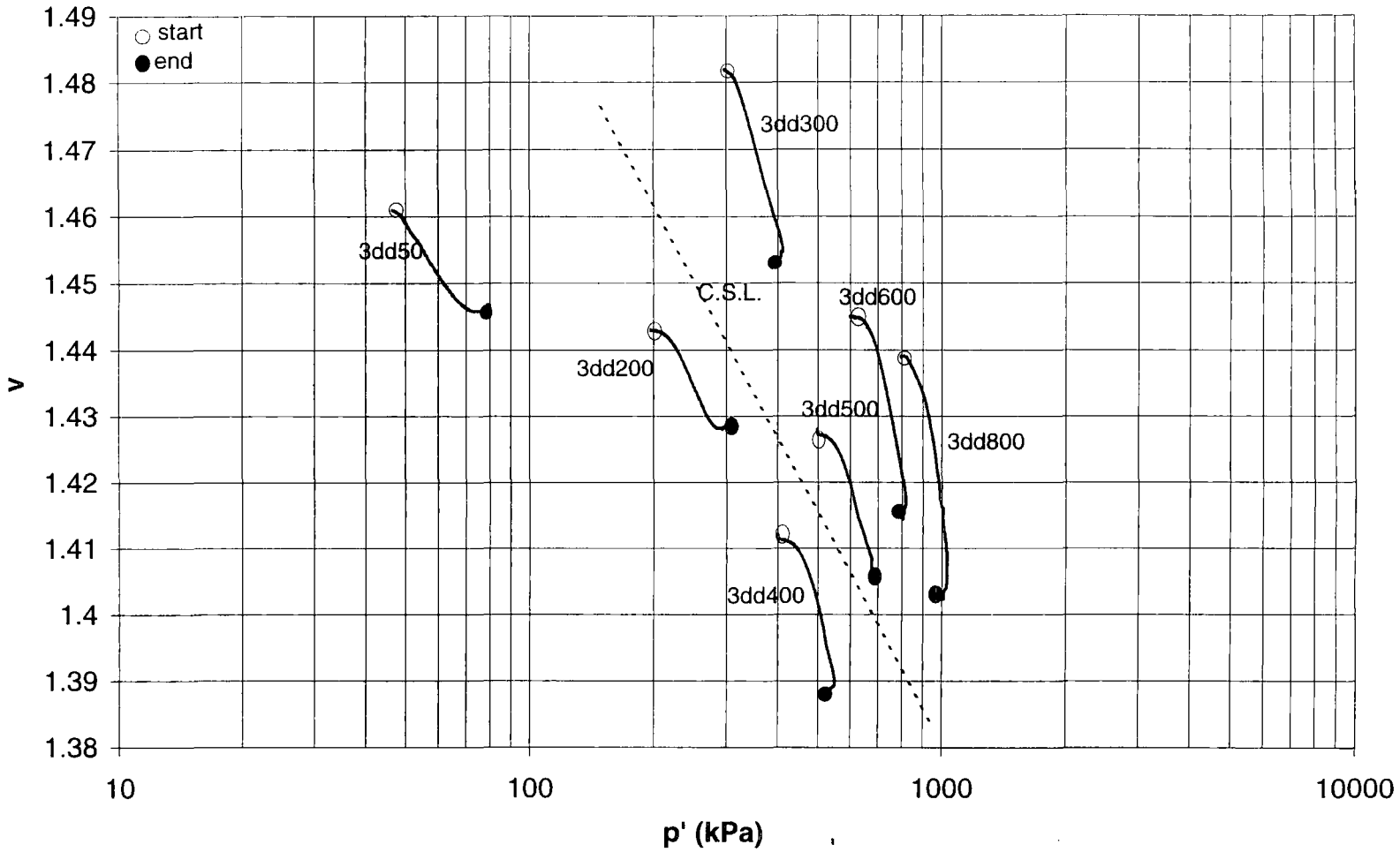

Fig.8.33 Specific volume vs. p' for destructured soils of borehole three

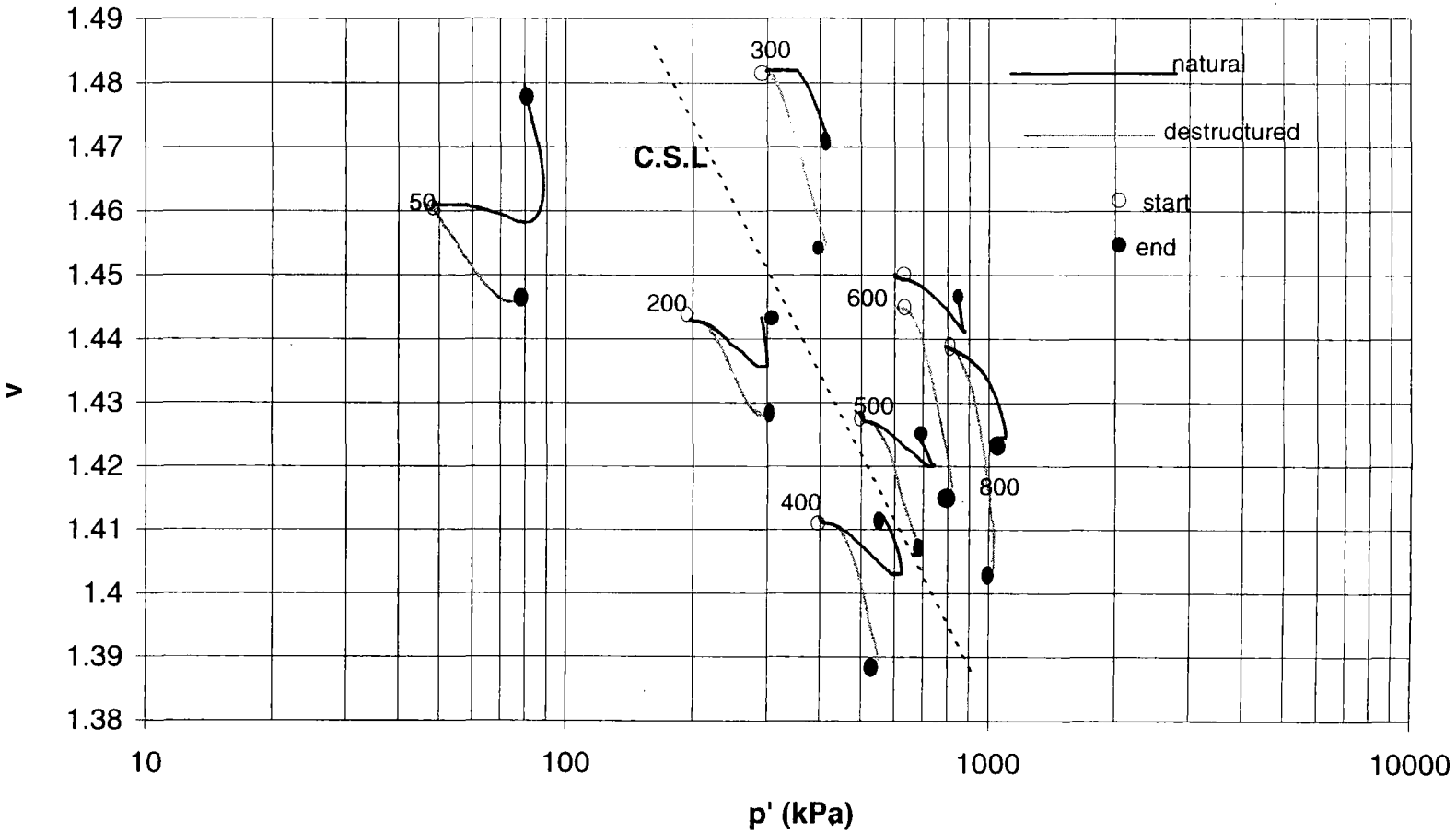

Fig.8.34 Comparison between v vs. p' for natural and destructured soils of borehole three

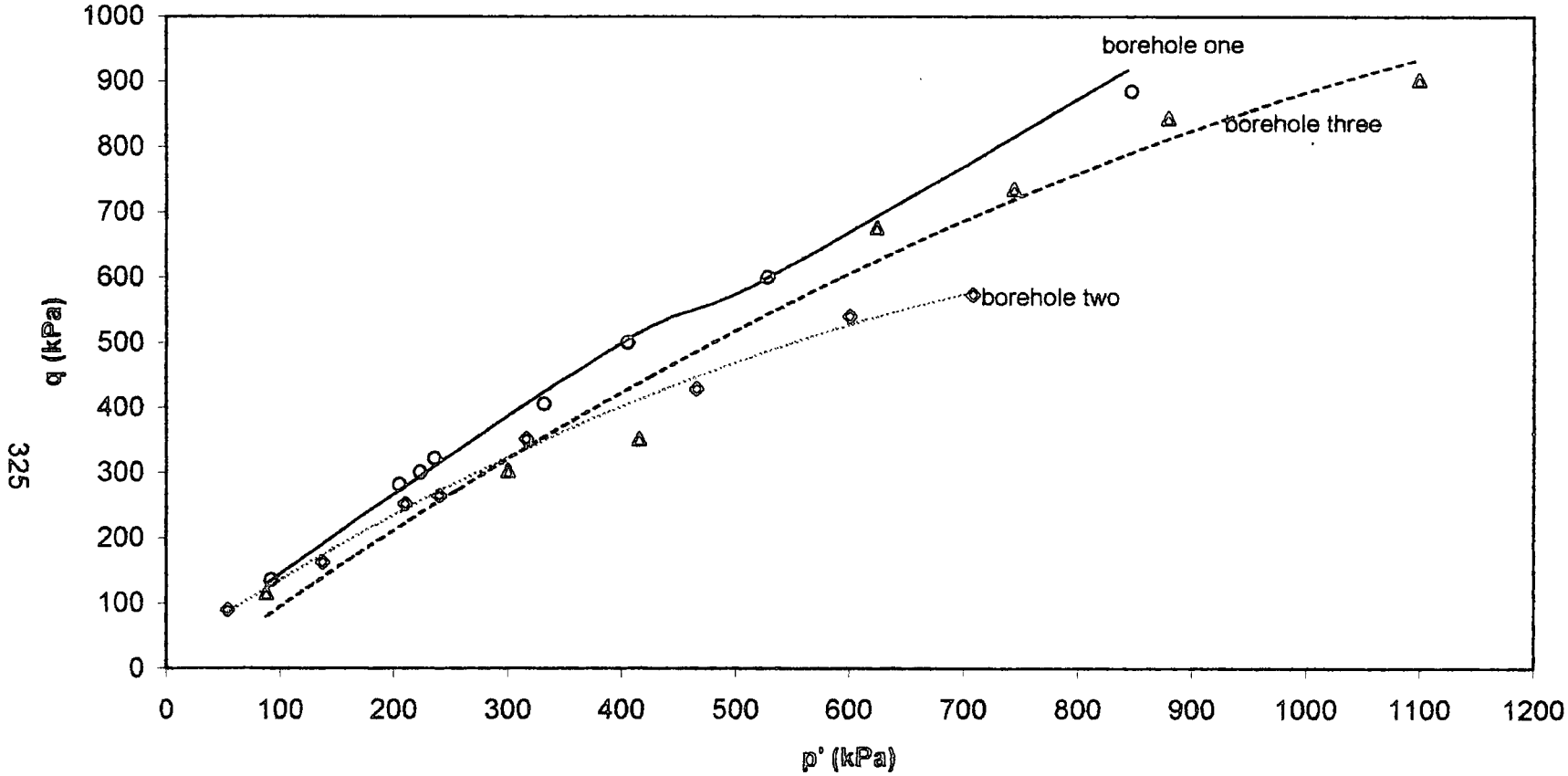

Fig.8.35 Comparison of failure surfaces for natural soils of boreholes one, two and three

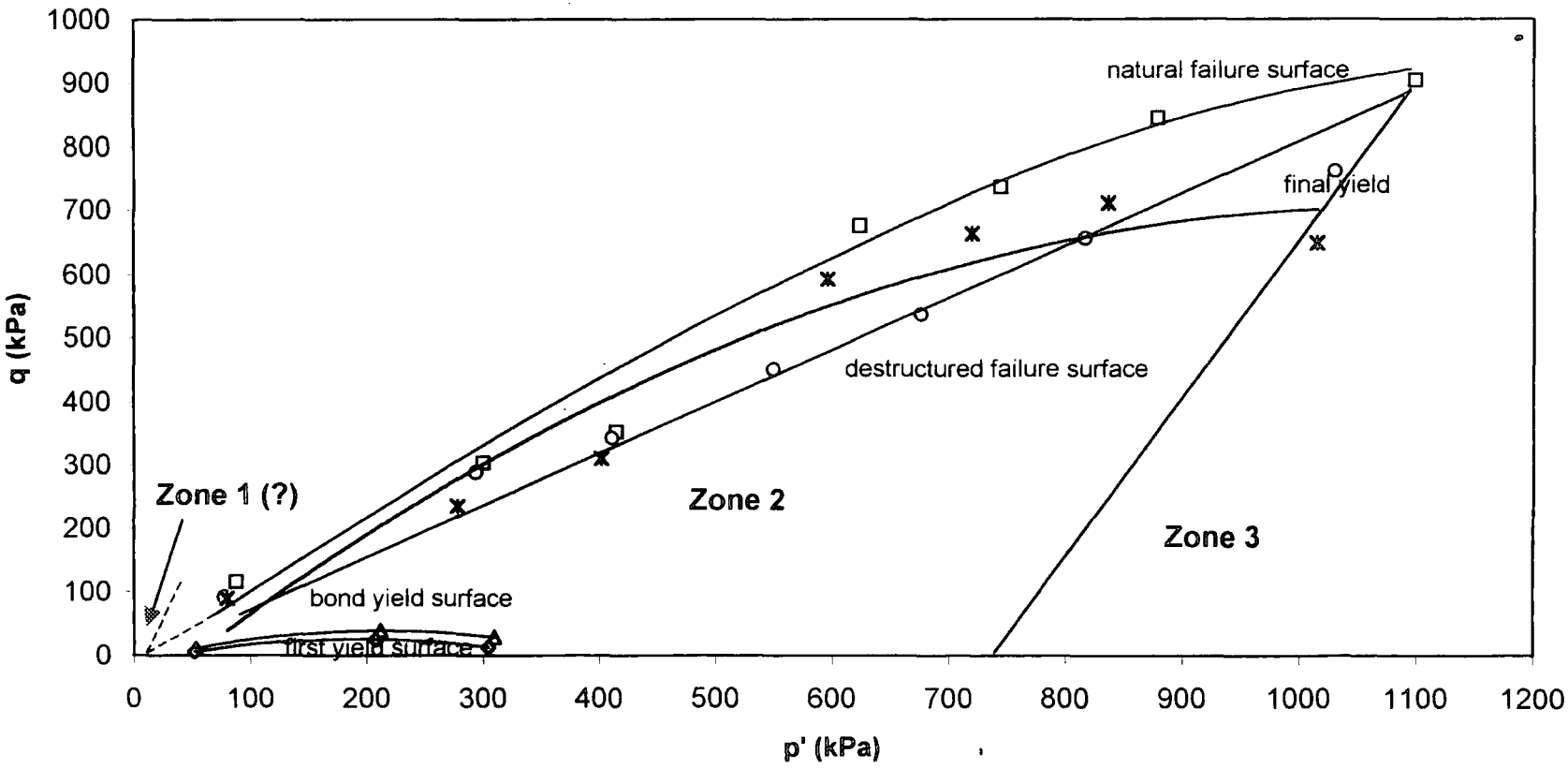

Fig.8.36 zones of behaviour for borehole three samples under drained shearing

CHAPTER 9

CONCLUSIONS

In this chapter, the major findings of this research work are discussed. Some suggestions for further research to study the behaviour of the red tropical clay soils of Dhaka are presented.

9.1 Conclusions

On the basis of all the experimental results, the following conclusions may be summarized:

The tropical clay soils of Dhaka are composed of illite, kaolinite, chlorite and some non clay minerals mainly quartz and feldspar. In general, it appeared that illite is the

dominant clay mineral in most of the samples. The soils showed a random open microfabric of silt and clay. The randomly oriented clay platelets or clusters were intermixed with large silt sized grains. It was observed that most of the silt grains were coated with clay and iron. Several intra- and inter- granular spaces were observed throughout the microfabric in all the samples. It was also observed that aluminosilicates, iron compounds and silica may form bonds between and within the grains. E.D.X. spectra confirmed the presence of these elements (K, Al, Si and Fe) on the analysed soils. These elements were observed throughout the specimen in-between clay flakes and grains.

The tropical clay soils of Dhaka are silt dominated clays which consists of 56% to 63% silt, 22% to 33% clay and 8% to 19% sand size particles. The specific gravity of the samples lie between 2.59 to 2.65. A small variation of silt and clay size fractions was also observed with respect to depth. The tropical clay soils of Dhaka can be characterized as an intermediate to high plasticity inorganic clay. The Liquid Limit values lie between 41% to 56%. The Plastic Limit values obtained ranged between 15% to 24% and the Plasticity Index values lie in between 17% to 37%. The values obtained are consistent with the values for other tropical soils and close to the values quoted by Grim (1962) for illitic minerals. Variations in the Liquid Limit values were observed between natural and airdried samples due to the effect of drying.

From the isotropic consolidation characteristics, it was observed that generally the amount of consolidation of the samples increased with increasing confining pressures. Destructured samples (in which the original structure had been destroyed) in each case showed greater amount of volume change than the natural samples, which is a clear indication of structure (bonding) in the natural samples.

The coefficient of consolidation (c_v) values for the tropical clay soils of Dhaka are consistent with values for low to medium plasticity inorganic clay and also consistent with those of kaolinitic and illitic soils. It was also observed that the c_v values increased with increasing void ratio. The samples also broadly showed a decrease of c_v value with increasing effective pressure. The measured coefficient of volume compressibility (m_v) of the natural samples ranged between 0.04 to 0.24 m^2/ MN and that of destructured samples lie between 0.11 to 0.66 m^2/MN. The results suggest that the compressibility of the soil is very low to medium. The measured value of the slope of the isotropic normal consolidation line (λ) ranged between 0.37 to 0.6. A compression index (Cc) value of 0.2 to 0.3 was estimated for these soils. The permeability of the analysed soils is very low with k ranging from 0.7×10^{-8} m/sec to 8.79×10^{-8} m/sec. The estimated values of k are consistent with that of kaolinitic and illitic soil and are in agreement with the mineralogy of the samples.

From the limited number of Oedometer test results, an apparent preconsolidation pressure of 170 kPa to 250 kPa was estimated for the natural soils. It was also observed that the observed apparent or quasi-preconsolidation pressure increases with depth. The quasi-preconsolidation pressure observed in Oedometer tests is likely to be due to the bonded structure of the soils.

All the observed undrained and drained characteristics on the natural and destructured samples suggest that the tropical clay soils of Dhaka are bonded. Bonding increases strength in these soils and bonding has an influence on the development of strain and stiffness. Natural samples always showed higher deviator stresses, higher stiffnesses and lower strains to reach maximum deviator stress than the destructured samples due to the initial presence of bonding in the natural soils.

Undrained triaxial tests were carried out on samples for borehole one (Mirpur) and borehole two (Curzon Hall). In undrained shearing at low confining pressures, samples of both boreholes initially showed peak positive values of excess p.w.p. followed by negative values at higher strains due to the tendency to dilate of the samples. No negative pore pressures were observed at high confining pressures. Only some samples of boreholes one and two at low confining pressures reach the critical state at very large strains (approximately in excess of 20%). High confining pressure samples may not have reached the critical state due to the formation of distinct shear surfaces. The samples of boreholes one and two showed a wide range of variation in ultimate stress ratio values. Few samples showed a common stress ratio value for different tests. Nevertheless values of the critical state stress ratio M were estimated to be 1.05 for borehole one and 0.96 for borehole two. A critical state value of $\lambda = 0.06$ were estimated for both borehole samples and a value of $\Gamma = 1.90$ for borehole one and $\Gamma = 1.84$ for borehole two samples were estimated under undrained shearing. However, due to the difficulties in identifying when a critical state had been achieved, these values are tenuous.

Drained triaxial tests were carried out on samples from borehole three (Mirpur). From the drained test results, it was observed that the natural samples of borehole three initially showed contraction and then dilation at very large strains. Conversely, the destructured samples only showed contraction, right through until the end of shearing. It was observed that under drained shearing, only two destructured samples approached a true critical state condition. However, it was observed that the specific volume for tests at 50 and 200 kPa in both natural and destructured state, falls below (denser than) the critical state. Conversely the specific volume for two tests at 300 kPa and 800 kPa which show contraction in both the natural and destructured state, falls above (looser than) the critical state. Other tests of borehole three (400, 500 and 600 kPa) do show anomalies in defining the critical state. Based on the drained test results, critical state values of $M = 0.84$, $\lambda = 0.05$ and $\Gamma = 1.75$ were estimated for

borehole three samples. As only a limited number of tests approached a true critical state condition, these values might not be representative and are questionable.

It was observed that the failure surface for natural soils is positioned at higher stress levels in the q-p′ space than the destructured failure surface. A significant difference between the natural and destructured failure surfaces was observed in all the three boreholes due to the presence of bonds in natural soils. The natural and destructured failure surfaces for boreholes one and two coincided approximately at $p' \cong 550\text{-}600$ kPa due to the complete destruction of bonds. At $p' > 550\text{-}600$ kPa both the natural and destructured soils of boreholes one and two showed similar stress ratios. The failure surface of borehole three showed a convergence at $p' \cong 1100$ kPa. A distinctive difference between the natural failure surfaces of three boreholes was observed under undrained and drained shearing. The failure surface might be affected by the rotation of the stress path and the type of shearing.

Differences in failure type were observed between the natural and destructured soils of the three boreholes. The natural soils failed with a definite single or multiple shear planes and showed brittle failure. Conversely, the destructured samples of these three boreholes failed by bulging in a ductile manner.

Tangential stiffnesses were measured and small strain contours were evaluated from the undrained and drained shearing. The natural soils showed higher stiffness values than the destructured soils due to the presence of bonding in natural soils. It was also observed that the difference between the stiffness values of natural and destructured soils decreased with increasing strain. A significant difference between the strain contours of natural and destructured soils was also observed in the q-p′ space.
Tangential stiffness versus axial strain graphs are used to identify yield points at smaller strain. It was observed that due to bond breakdown stiffness values gradually

decreased with increasing strain and the soil undergoes yield. Although identification of yield points in some samples is tenuous, two yield points could be identified for these soils at low confining pressures. It was also observed that bond breakdown would occur in isotropic compression for tests at higher confining pressures, as no clear trend of yield points would be seen during shear. Two yield surfaces could be defined in the stress space below the final yield surface for these soils. The 'first yield' surface was found to occur at low deviator stress levels showing a small change in stiffness. A 'bond yield' surface was identified between the first and final yield surfaces. It was observed that the bond yield surface occurs well below the failure surface. The final yield surface at very low confining pressure runs very close to the failure surface and then diverges at higher stresses. When the soil reaches the final yield surface, it looses almost all of its stiffness due to bonding. After final yield, a soil's behaviour is controlled only by friction.

Undrained and drained characteristics suggest that three zones of behaviour could be identified for the tropical clay soils of Dhaka. It was observed that strain and stiffness development is directly related to the zones of behaviour. A zone of coincidence (Zone 1) between the bond yield and failure surfaces is not clearly observed in this study. If it does exist, it would only be at very low stress levels (less than 5-20 kPa).

In the case of undrained shearing, zone 2 is identified for the range of values of p′ at failure from less than 20 kPa to 600 kPa. In this second zone bond yield occurs before failure and the natural soils showed higher stress ratio values than those of the destructured soils. The final yield surface in zone 2 is very close to the natural failure surface. Zone 3 is identified when the two failure surfaces under undrained shearing coincides approximately at $p' \cong 600$ kPa due to complete destruction of bonds. The soil's behaviour in Zone 3 is independent of bonding and the final yield surface in Zone 3 diverges from the natural failure surface. Under drained shearing,

Zone 2 is identified between a value of p′ at failure from less than 5 kPa to approximately 1100 kPa. The coincidence of the natural and destructured failure surfaces under drained shearing was observed at approximately p′ ≅ 1100 kPa.

9.2 Future recommendations

This research approach highlights the importance of mineralogy, fabric and the presence of bonding and their influence on the engineering behaviour of the tropical clay soils of Dhaka, Bangladesh. From this study it seems that several aspects of these soils need further investigation.

The observed mineralogy is not conclusive. Halloysite is a common mineral present in many tropical soils. However, no halloysite is identified in this study. It is important to note here that kaolinite generally transformed to halloysite and vice versa. The problems of halloysite identification and its distinction from kaolinite have been discussed by Gillot (1987). As the present investigation to evaluate mineralogy had some limitations because of the accessibility of the X.R.D. techniques, it needs further investigation. In addition, Infrared spectroscopy analysis might be helpful to identify hydrated halloysite.

In this study samples were sheared at an initial effective confining pressure starting from 50 kPa. Bond yield surface did not show any coincidence with the natural failure surface and the final yield surface at very low mean effective stress levels. Due to this reason for these soils, Zone 1 is not clearly identified in this study. This also needs further investigation.

The behaviour of these soils can also be studied with changes in stress path during shear to see the influence of stress paths on the yield of the bonded structure and failure surface. Initially the behaviour of these soils could be studied by following a constant p′ path and then the stress path can be changed to a constant q path. The behaviour can also studied by following initially a constant σ'_1 path then the stress path can be changed to constant σ'_3 path or constant p′ shearing paths at different stress levels. Stiffness, yield of the bonds and failure surfaces can then be examined for each individual stress path followed in the stress space during shear to clarify the influences of the different shearing paths on the soil's behaviour.

Tropical red clay soils are also exposed in the Madhupur Tract, the Barind Tract and the Lalmai Hill areas of Bangladesh. In the present study samples were used only from the Dhaka Metropolitan area. There is scope to repeat the work and to apply this framework in other regions of the country where similar type of soils are exposed before any final conclusions could be drawn for the expected behaviour of the tropical soils of Bangladesh.

REFERENCES

Alam, M.K., Hasan, A.K.M.S., Khan, M.R. and Whitney, J.W. (1990)
Geological Map of Bangladesh. Geological Survey of Bangladesh.

Alam, M.K. and Khan, M.R. (1980)
Madhupur clay and its probable scope of economic uses. Seminar issue, Petroleum and Mineral Resources of Bangladesh.

Allman, M.A. and Atkinson, J.H. (1992)
Mechanical properties of reconstituted Bothkennar soil. Geotechnique, vol. 42, no. 2, pp.289-301.

Anon (1990)

Tropical residual soils, Engineering Group of the Geological Society Working Party Report, QJEG, vol. 23, no 1, pp. 1-101.

Atkinson, J.H. (1990)

Discussion of session 1.2. Proceedings of the Conference on Engineering Geology of Weak Rock, Leeds, (eds Cripps et al.), pp. 150 Rotterdam, Balkema

Atkinson, J.H.(1993)

The mechanics of soils and foundations. McGraw and Hill book Company, England.

Atkinson, J.H. & Bransby, P.L. (1978)

The mechanics of soils. McGraw and Hill book company Ltd. England.

Atkinson, J.H., Coop, M.R., Stallebrass, S.E. and Viggiani, G.(1993)

Measurement of stiffness of soils and weak rocks in laboratory tests. Conference proceedings on The Engineering Geology of Weak Rock, Leeds, (eds Cripps et al.), pp. 21-27, Rotterdam, Balkema.

Bakr, M.A.(1977)

Quaternary geomorphic evolution of the Brahmaputra-Noakhali area, Comilla and Noakhali districts, Bangladesh Records of the Geological Survey of Bangladesh, vol.1, part 2, pp. 1-48.

Bishop, A.W., Webb, D.L. and Lewin, P.I. (1965)
Undisturbed samples of London clay from the Ashford Common Shaft: Strength-effective stress relationship, Geotechnique, vol. 15, no.1, pp. 1-31.

Blight, G.E. (1988)
Construction in tropical soils. Proceedings of the 2nd international conference on Geomechanics in Tropical Soils, Singapore, vol. 2.pp.449-467.

Bressani, L.A. (1990)
Experimental properties of bonded soils. PhD thesis, University of London.

Bressani, L.A. and Vaughan, P.R. (1989)
Damage to soil structure during triaxial testing. 12 th International Conference on Soil Mechanics and Foundation Engineering, RIO., PP. 1-4.

British Standard B. S. 1377 (1990)
British standard methods of test for soils for civil Engineering purposes. British standards Institution, London.

Burland, J.B. (1989)
Ninth Laurits Bjerrum Memorial Lecture: 'Small is beautiful'-the stiffness of soils at small strains. Canadian Geotechnical Journal, vol. 26, pp. 499-516.

Carter, M. & Bentley, S.P. (1991)

Correlations of soil properties. Pentech press limited, London.

Casagrande & Fadum (1940)

Notes on soil testing for engineering purposes. Harvard University, Graduate School of Engineering Publication 268.

Clayton, C.R.I., Hight, D.W. and Hopper, R.J. (1992)

Progressing destructuring of Bothkennar clay: Implications for sampling and reconsolidation procedures. Geotechnique, vol. 42, no.2, pp. 219-239.

Collins, K. and McGown, A. (1974)

The form and function of microfabric features in a variety of natural soils. Geotechnique, vol. 24, no. 2, pp. 223-253.

Cook, J.R. and Newill, D. (1988)

The field description and identification of tropical residual soils. Proceedings of the 2nd international conference on Geomechanics in Tropical Soils, Singapore, vol. 1.pp.3-10.

Coop, M.R. and Atkinson, J.H. (1993)

The mechanics of cemented carbonate sands. Geotechnique, vol. 43, no. 1, pp. 53-67.

Duchaufour, p. (1982)

Pedology Pedogenesis and Classification (English Edition Trans. T.R.Paton) George Allen and Unwin, London.

Dumbleton, M.J. & Newill, D.D. (1962)

A study of properties of 19 tropical clay soil and the relation of these properties with the mineralogical constitution of the soils. Transport and road research Laboratory report no. LN 44, PP.1-14.

Fookes, P.G. (1997)' (Ed.)

Tropical residual soils. The Geological society publishing house, U.K.

Gens, A. & Nova, R. (1993)

Conceptual bases for a constitutive model for bonded soils and weak rocks. Proceedings of an international symposium on the geotechnical engineering of hard soils-soft rocks, Athens (eds A. Anagnostopoulos, F. Schlosser, N. Kalteziotis & R. Frank), Rotterdam, Balkema, pp. 485-494,

Gidigasu, M.D. (1976)

Laterite Soil Engineering, Elsevier, Amsterdam.

Gillott, J.E.(1987)

Clay in Engineering Geology. Elsevier Science Publishers B.V. The Netherlands

Grim, R.E. (1962)

Applied Clay Mineralogy. McGraw Hill, New York.

Head, K.H. (1982)

Manual of soil laboratory testing, vol.2, Pentech press, London.

Head, K.H. (1998)

Manual of soil laboratory testing. Vol.3, second edition, John Wiley & Sons, England.

Hight, D.W. (1982)

A simple piezometer probe for the routine measurement of pore pressure in triaxial tests on saturated soils. Technical note, Geotechnique, vol. 32, pp. 397-401.

Hight, D.W., Bond, A.J. and Legge, J.D. (1992)

Characterization of the Bothkennar clay: an overview. Geotechnique, vol. 42, no. 2, pp.303-347.

Hight, D.W., & Higgins, K.G.(1995)

An approach to the prediction of ground movements in engineering practice: background and application. Proceedings of the International Symposium on Pre-Failure Deformation Characteristics of Geomaterials, Hokkaido, Japan, (eds Shibuya, S., Mitachi, T and Miura, S), Rotterdam, Balkema, vol. 2, pp. 855-885.

Hobbs, P.R.N., Culshaw, M.G., Northmore, K.J., Rachlan, A.and Entwisle, D.C. (1988),

Preliminary consolidation and triaxial strength test results for some undisturbed tropical red clay soils from Java, Indonesia. Proceedings of the 2nd international conference on Geomechanics in Tropical Soils, Singapore, vol.1, pp. 149-155.

Islam, M.A.(1974)

On the Madhupur clay. Journal of Bngladesh National Geographic Association, vol. 2, no.1 and 2.

Jardine, R.J. (1992)

Some observations on the kinematic nature of soil stiffness. Soils and Foundations, vol. 32, pp.111-124.

Jardine, R.J., St. John, H.D., Hight, D.W. and Potts, D.M. (1991)

Some practical applications of a non-linear ground model. Proceedings of the 10 th European Conference on Soil Mechanics, Florence, vol. 1, pp. 223-228.

Jardine, R.J., Symes, M.J. and Burland, J.B.(1984)

The measurement of soil stiffness in the triaxial apparatus. Geotechnique, vol. 34, no. 3, pp. 323-340.

Lambe, T.W. & Whitman, R.V. (1969)
Soil Mechanics. John Wiley & Sons, New York.

Leddra, M.J., Jones, M.E. & Goldsmith, A.S. (1993)
Compaction and shear deformation of a weakly-cemented, high porosity sedimentary rock. Conference proceedings on The Engineering Geology of Weak Rock, Leeds, (eds Cripps et al.), pp. 45-54, Rotterdam, Balkema.

Leroueil, S., Tavenas, F., Brucy, F., La Rochelle, P., and Roy, M. (1979)
Behaviour of destructured natural clays. J. of the Geotechnical Engineering Division, American Society of Civil Engineers, 105 (GT6), PP. 759-778.

Leroueil, S. and Vaughan, P.R. (1990)
The general and congruent effects on structure in natural soils and weak rocks. Geotechnique, vol. 40, no. 3, pp. 467-488.

Little, J.A. & Hataf, N. (1990) Some monotonic and cyclic properties of weathered undisturbed and reconstituted Keuper Marl. Conference on The Engineering Geology of the Weak Rock, Leeds, PP. 55-64.

Maccarini, M. (1987)
Laboratory studies of a weakly bonded artificial soil. PhD thesis. University of London.

Malandraki, V. (1994)

The engineering behaviour of a weakly bonded artificial soil. PhD thesis, University of Durham

Malandraki, V. & Toll, D.G.(1994)

Yielding of a weakly bonded artificial soil. Proceedings of the International Symposium on pre-Failure Deformation Characteristics of Geomaterials, Hokkaido, Japan, (eds Shibuya, S., Mitachi, T and Miura, S), Rotterdam, Balkema, vol. 1, pp. 315-320.

Malandraki, V. & Toll, D.G. (1996)

The definition of yield for bonded materials. Geotechnical and Geological Engineering, vol. 14, no. 1, pp. 67-82.

Malandraki, V. & Toll, D.G.(2000)

Drained probing triaxial tests on a weakly bonded artificial soil. Geotechnique, vol.50, no.2, pp. 141-151.

Malandraki, V. & Toll, D.G. (2001)

Triaxial tests on weakly bonded soil with changes in stress path. Journal of Geotechnical and Geoenvironmental Engineering, vol. 127, no. 3, March, 2001, pp. 282-291.

Monsur M.H. (1990)

Stratigraphical and paleomagnetical studies of some Quaternary deposits of the Bengal Basin, Bangladesh. PhD thesis (unpub.), Free University, Brussels, Belgium.

Monsur M.H. (1995)

An introduction to The Quaternary Geology of Bangladesh. City press and publications, Dhaka.

Newill, D. (1961)

A laboratory investigation of two red clays from Kenya. Geotechnique, vol. 11, pp. 302-318.

Paul, M. A., Peacock, J.D. & Wood, B.F. (1992)

The engineering geology of the Carse clay of the national soft clay research site, Bothkennar. Geotechnique, vol. 42, no. 2, pp. 183-198.

Rao, S.M., Sridharan, A. And Chandrakaran, S. (1988)

The role of iron oxide in tropical soil properties. Proceedings of the 2nd international conference on Geomechanics in Tropical Soils, Singapore, vol. 1, pp.43-48.

Sabba Rao, K.S., Sivapullaiah, P.V. and Padmanabha, J.R. (1988).

Influence of climate on the properties of tropical soils. Proceedings of the 2nd international conference on Geomechanics in Tropical Soils, Singapore, pp. 49-54.

Sangrey, D.A. (1972)

Naturally cemented sensitive soils. Geotechnique 22, vol. 1, pp. 139-152.

Scholey, G.K., Frost, D., Diego, C.F. Presti, Lo and Jamiolkowski (1995)

A reiview of instrumentation for measuring small strains during triaxial testing of soil specimens. Geotechnical Testing Journal, GTJODJ, vol. 18, no.2, pp. 137-156.

Smith, D.M.A.(1985)

Suggested modus operandi for research into natural lateritic soil. Proceedings of the 1st international conference on Geomechanics in Tropical Lateritic and Saprolitic Soils, vol.3, pp. 300-306.

Smith, P.R., Jardine, R.J. and Hight, D.W. (1992)

The yielding of Bothkennar clay. Geotechnique, vol. 42, no.2, pp.257-274.

Sridharan, A. (1988)

Engineering properties of tropical soils. Proceedings of the 2nd international conference on Geomechanics in Tropical Soils, Singapore, vol. 2, pp. 527-540.

Taylor, D.W. (1972)

Fundamentals of Soil Mechanics. John Wiley & Sons, New York

Taylor, R.N.& Coop, M.R. (1993)

Stress path testing of Boom clay from Mol, Belgium. Conference proceedings on The Engineering Geology of Weak Rock, Leeds, (eds Cripps et al.), pp. 77-82, Rotterdam, Balkema.

Toll, D.G. (1993)

A computer control system for stress path triaxial testing. 5 th International Conference on Civil and Structural Engineering Computing, Edinburgh, pp. 107-113.

Toll, D.G. & Malandraki, V. (1993)

Triaxial testing of a weakly bonded soil. Proceedings of an international symposium on the geotechnical engineering of hard soils-soft rocks, Athens (eds A. Anagnostopoulos, F. Schlosser, N. Kalteziotis & R. Frank) vol. 1, pp. 817-824, Rotterdam, Balkema.

Uriel, R.S. and Serrano, A.A. (1973)

Geotechnical properties of two collapsible soils of low bulk density at the site of two dams in Canary Islands, Spain. Proceedings of the 8 th International Conference on Soil Mechanics and Foundation Engineering, Moscow, vol. 2.2, pp. 257-264.

Vargas, M. (1953)

Some engineering properties of residual clay soils occurring in southern Brazil. Proceedings of the 3rd International Conference on Soil Mechanics and Foundation Engineering, Switzerland, vol. 1, pp. 84-90

Vargas, M. (1988)

Characterization, identification and classification of tropical soils. Proceedings of the 2nd international conference on Geomechanics in Tropical Soils, Singapore, pp. 71-75.

Vaughan, P.R. (1985)

Mechanical and hydraulic properties of in situ residual soils. Proceedings of the 1 st International conference on Geomechanics in Tropical Lateritic and Saprolitic Soils. General report, vol. 3, Brazil, pp. 231-263.

Vaughan, P.R. (1988)

Characterising the mechanical properties of in situ residual soil. Proceedings of the 2nd international conference on Geomechanics in Tropical Soils, Singapore, vol. 2, pp. 469-487.

Vaughan, P.R. and Kwan, C.W. (1984)

Weathering, structure and in-situ stress in residual soil. Geotechnique, vol. 34, no. 1, pp. 43-59.

Vaughan, P.R., Maccarini, M. and Mokhtar, S.M. (1988)

Indexing the engineering properties of residual soil. Quaterly Journal of Engineering Geology, vol. 21, pp. 69-84.

Viggiani, G. and Atkinson, J.H. (1995)

Stiffness of fine grained soil at very small strains. Geotechnique, no.2, pp. 249-265.

Wesley, L.D. (1973)

Some basic engineering properties of halloysite and allophane claya in Java, Indonesia. Geotechnique, vol. 23, pp. 471-494.

Wesley, L.D. (1974)

Discussion on structural behaviour of residual soils of the continually wet highlands of Papua New Guinea. Geotechnique, vol. 24, no. 1, pp. 101-105.

Wesley, L.D. (1988)

Engineering classification of residual soils. Proceedings of the 2nd international conference on Geomechanics in Tropical Soils, Singapore, vol. 1, pp. 77-84.

Wu, B., Marsden, J.R.& Hudson, J.A. (1993)

Undrained mechanical behaviour of mudstone. Conference proceedings on The Engineering Geology of Weak Rock, Leeds, (eds Cripps et al.), Rotterdam, Balkema, pp. 87-94.